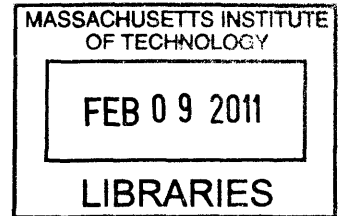


Dynamic Simulation of Nuclear Hydrogen Production Systems

by

Patricio D. Ramírez Muñoz



Submitted to the Department of Chemical Engineering
in partial fulfillment of the requirements for the degree of

ARCHIVES

Doctor of Philosophy in Chemical Engineering

at the

MASSACHUSETTS INSTITUTE OF TECHNOLOGY

September 2010

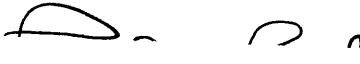
© Massachusetts Institute of Technology 2010. All rights reserved.

Author


Department of Chemical Engineering

Aug 10, 2010

Certified by


Paul I. Barton
Lammot du Pont Professor of Chemical Engineering
Thesis Supervisor

Accepted by

William M. Deen
Professor of Chemical Engineering
Chairman, Committee on Graduate Theses

Dynamic Simulation of Nuclear Hydrogen Production Systems

by

Patricio D. Ramírez Muñoz

Submitted to the Department of Chemical Engineering
on October 15, 2010, in partial fulfillment of the
requirements for the degree of
Doctor of Philosophy in Chemical Engineering

Abstract

Nuclear hydrogen production processes have been proposed as a solution to rising CO₂ emissions and low fuel yields in the production of liquid transportation fuels. In these processes, the heat of a nuclear reactor is used to run the chemical reactions in a hydrogen plant. The resulting system is tightly interconnected and operates at very high temperature and pressure, which can lead to operational disruptions and accidents. For this reason, computational studies validating the safe operation of the system are required by regulatory authorities. In the past, safety studies have been conducted by using legacy codes, such as RELAP and MELCOR, and their focus has been the operation of nuclear power plants.

However, traditional legacy codes are not appropriate to simulate nuclear hydrogen production. The simulation of a nuclear reactor itself is already complex because it involves simulating reactor kinetics and transport phenomena. To that complexity, nuclear hydrogen production adds the need to simulate chemical reactions in the hydrogen plant. These chemical reactions cannot be represented easily in legacy codes because these codes lack the flexibility, speed and accuracy required to simulate them. Therefore, only a limited number of studies on the safety of these systems exist.

Instead of using legacy codes, this thesis proposes using equation-based simulators developed by the chemical engineering community to model and study the safety of a nuclear hydrogen production plant. Equation-based simulators were designed to be flexible, extensible and fast because they have to simulate a vast range of processes from the chemical industry. Thus, they provide a good platform for the simulation of nuclear hydrogen production systems. This thesis explains the models used for the different parts in the nuclear hydrogen production plant, and then presents the response of this plant model to different accident scenarios.

The first contribution of this thesis is a novel equation-based model for the heat transfer loop connecting a nuclear reactor and a hydrogen production plant. This heat transfer loop uses helium as the heat transfer fluid, which makes simulating its behavior difficult because of the need to model gas dynamics. To resolve this, three models for gas dynamics and two set of coupling conditions for boundary variables

were tested in JACOBIAN, an equation-based simulator. The three models for gas dynamics in combination with a novel approach to set coupling conditions for boundary variables were able to represent the interesting time scales accurately in transient scenarios. The accuracy and computational speed of these simulations outperformed those produced by a reference model created in RELAP, a legacy code.

The second contribution is a model of a nuclear hydrogen production plant using high-temperature steam electrolysis to produce hydrogen. This model was created to study the effect of potential accidents on the nuclear reactor. It included detailed models of the nuclear reactor and heat transfer loop, and a partial model of the electrolysis plant. The nuclear reactor was modeled as a pebble bed modular reactor, which is one of the safest designs available. The reactor was connected to the hydrogen production plant using the heat transfer loop model already developed in this thesis. The hydrogen production plant was partially represented as a steam superheater in the heat transfer loop.

The third contribution is the demonstration of the safety characteristics of the nuclear hydrogen production plant by subjecting the plant model to three accident scenarios. The scenarios involved disruptions in the hydrogen plant or in the heat transfer loop, and all of them—directly or indirectly—lead to a loss of heat sink capacity for the nuclear reactor. This resulted in an increase of the nuclear reactor core temperature, which was quickly moderated by the fission power reduction at the fuel pebbles and by the safe design of the nuclear reactor. As a consequence, the maximum temperature reached in the core was always less than the fuel melting point and the reactor was always in a safe condition. The heat transfer loop could suffer the rupture of a pipe in one of the scenarios, and design modifications to address this were suggested.

This thesis' results partially prove that nuclear hydrogen production plants could be safe, and simultaneously, that equation-based simulators are good platforms to demonstrate the safety of these plants. Developing these models and tests further will help guarantee the safety of the plant and obtain regulatory and public approval for this new nuclear application.

Thesis Supervisor: Paul I. Barton

Title: Lammot du Pont Professor of Chemical Engineering

Acknowledgments

Thank you, Corrinne Fogg, for your love and support during the PhD; the journey was rough, but you always had a smile in your face. I could not have made it without such a wonderful wife.

Professor Paul Barton, I appreciated and enjoyed having you as my advisor. You not only taught me about dynamic systems, but also attention to detail and the highest professional standards. I know I was not the easiest student, so thank you for your patience and financial support all these years.

Professor Kazimi and Professor Green, thank you for being part of my thesis committee and for your time reviewing my work. Your help was fundamental to learn about nuclear systems and how to be a better scientific communicator. My gratitude also goes to Professor Jensen and the Chemical Engineering Department at MIT for educating me and for providing financial support at different times during my studies. Finally, my work would not have been possible without the help of gifted researchers: Dr. Memmott (MIT), Dr. Hejzlar (MIT), Dr. Sherman (SNRL), Dr. Herring (INL) and Dr. Davis (INL), Dr. Vilim (ANL).

Many thanks to my labmates in the Barton group for their friendship and academic advice; working with you helped me grow a great deal. Dr. Ajay Selot, your technical guidance and lessons made me a better researcher; listening to your point of view in different topics from economics to human nature made a better person—thank you. Professor Alexander Mitsos, thank you for your constant encouragement and strategies to do good research; you believed in me more than I did. Dr. Cha Kun Lee, I appreciated your friendship and your teaching me DSL despite the fact that you were extremely busy finishing your thesis. Dr. Derya Ozyurt, thank you for starting the project that was the foundation of my thesis and for sharing with me your knowledge about nuclear hydrogen production systems. Professor George Bollas, I am grateful to you for being my project colleague and for shouldering the project responsibilities with me. Geoff Oxberry, thank you for your discussions about how to best present my work to professors and for making the lab environment welcoming.

Matt Stuber, I am indebted to you for your fashion advice and car advice—everything was spot on. I enjoyed working with all the exceptional researchers in the lab: Achim Wechsung, Spencer Schaber, Yang Chen, Professor Thomas Adams II, Mehmet Yunt, Yang Chen, Xiang Li, Richard Lakerveld, Kamil Khan, Ruth Misener, Vibhu Prakash Saxena, Earl Solis, John Tolsma, Brian Simpson, Joe Scott, Audun Aspelund, Lars Hellemo, and Emre Armagan.

Thank you to all my friends in Boston and in Chile for the great times together and the encouragement all these years. In particular, I would like to extend my sincere gratitude to Joel Yuen, for the great discussions and the fine cooking; you are a truly renaissance man and my hero. Arman Haidari, I enjoyed our conversations about running and school. Biz Bose, thank you for the motivation and help to get the job I wanted. Surasak Chunsriviro, our table tennis matches were delightful. Ian Hoag, doing adventure racing with an ex-Navy SEAL is one of the best training experiences I could have ever had. Professor Luis Rademacher, your example motivated me to come to MIT and your support helped me get there. Cristian Bawlitza, you have been a wonderful friend all these years—thank you.

Thank you to all the staff members of the Chemical Engineering and Nuclear Engineering departments; you not only made my life infinitely easier, but also you cheered me on every single time. In particular, I would like to thank Suzanne Maguire, Katie Lewis, Christine Preston, Barbara Balkwill, Rebecca Hailu, Craig Abernethy, Carolyn Carrington, Melanie Miller, Alina Haverty, Jean Belbin, and Fran Miles.

I'm indebted to Kathy Neumueller, Julie Cook, Hernan Saenz, and to the people at Bain & Co. in Dallas. You let me spend a summer at your great office and gave me the opportunity to come back as a full-time employee after finishing my PhD. This gave me extra motivation to finish my studies.

Finally, thank you Darío Ramírez and Alejandra Muñoz, I could not be here without you. My achievements are only the result of being raised by a great family. Thank you, Paula Ramírez, for being there all these years to share your PhD experience with your brother. Blanca and Ana, I'm sorry I didn't spend as much time as I wanted with you; I will make up for that in the coming years.

Contents

1	Introduction	15
2	Background	19
2.1	Nuclear energy to aid fuel production	19
2.1.1	Current transportation energy challenges	20
2.1.2	New nuclear applications for hydrogen and heat	23
2.1.3	Nuclear hydrogen production can make the biggest impact . .	28
2.2	The need for new computational models	30
2.2.1	Legacy codes lack simulation features	31
2.2.2	Equation-based simulators are a good alternative	32
2.3	Nuclear hydrogen plant used in this thesis	36
2.3.1	PBMR and PCU Operation	37
2.3.2	HTSE	39
2.3.3	Heat transfer loop	40
3	Dynamic simulation of a heat transfer loop for alternative nuclear reactor applications	43
3.1	Introduction	43
3.2	Using equation-based languages for the simulation of novel nuclear applications	46
3.2.1	Equation-based simulators provide flexibility, speed and accuracy	46
3.2.2	Simulation challenges in equation-based simulators are minimal and mostly related to initial conditions	48

3.3	Modeling the heat transfer loop	50
3.3.1	Dynamic models in JACOBIAN	51
3.3.2	RELAP model for comparison	61
3.4	Model Performance Evaluation	62
3.4.1	Test 1: Feasibility and steady-state profiles	62
3.4.2	Test 2: Dynamic simulation profiles	64
3.4.3	Test 3: Computational time	71
3.5	Conclusions	71
4	Transient analysis of a nuclear hydrogen production facility	75
4.1	Introduction	75
4.2	Definition of the system	77
4.3	Dynamic model of a nuclear hydrogen production system	80
4.3.1	Equation-based simulators as a simulation platform	81
4.3.2	Nuclear reactor model	82
4.3.3	Heat Transfer Loop Model	87
4.4	Transient simulations	88
4.4.1	Loss of heat sink accident	89
4.4.2	Loss of flow in the heat transfer loop	93
4.4.3	Leak in the heat transfer loop	95
4.5	Conclusion	98
5	Conclusions	101
A	Discretization of Gas Dynamic Equations	105
A.1	Discretization of the continuity equation	107
A.2	Discretization of the momentum equation	109
A.3	Discretization of the energy equation	115
B	JACOBIAN code	119

List of Figures

2-1	Using alternative feedstocks to produce liquid fuels increases CO ₂ -eq emissions [28].	21
2-2	Equation-based simulation languages allow the variables and equations describing physical and chemical phenomena to be declared explicitly [5].	34
2-3	The nuclear hydrogen production used in this thesis is a combination of technologies in development.	37
2-4	The design of fuel pebbles for PBRs avoids meltdowns by having a high fusion point (2000°C) and decreases the possibility of radiation spread [26].	39
2-5	The SOEC cell disassociates superheated steam into hydrogen and oxygen [36].	41
2-6	A HTSE plant is designed to be built in modular form [42].	41
2-7	Heat transfer loop [8].	42
3-1	Nuclear hydrogen production is an example of novel nuclear applications. The design of the heat transfer loop requires special attention.	45
3-2	Discretizing the gas dynamics equations using combination of standard grid and a staggered grid makes the solution of the system more stable.	54
3-3	One approach to set the boundary variables; it uses P_{In} as suggested in the literature [27].	57
3-4	Alternative approach to set the boundary conditions for a gas dynamics model; it replaces the specification on P_{In} with $P_{Aux,1}$	59

3-5	RELAP model used to benchmark JACOBIAN models.	62
3-6	Heat transfer loop's pressure profiles at steady state in JACOBIAN match RELAP's profiles with small differences.	64
3-7	Heat transfer loop's temperature profiles at steady state in JACOBIAN match RELAP's profiles with small differences.	65
3-8	The heat transfer loop's total helium mass decreases in RELAP after introducing 50% decrease in PHX's cold stream inlet flowrate.	66
3-9	Pressure of helium in the loop at the end of the PHX after a 50% decrease in PHX's cold stream flowrate. RELAP simulation reaches a lower pressure than that in JACOBIAN simulations because of RELAP's numerical error in mass conservation; however, RELAP and JACOBIAN models respond with the same speed to the step change.	67
3-10	Temperature of helium in the loop at the end of the PHX after a 50% decrease in PHX's cold stream flowrate. RELAP simulation reaches a lower temperature than that in JACOBIAN simulations because of RELAP's numerical error in mass conservation; however, RELAP and JACOBIAN models respond with the same speed to the step change.	68
3-11	Pressure of helium in loop at the outlet of the compressor; the time scale of the response to a change in the compressor is similar again in the four models, but it differs during the first second of the transient. RELAP's numerical errors in mass conservation affect the final steady state.	69
3-12	Temperature of helium in loop at the outlet of the compressor; the response to a change in the compressor is similar again in the four models, but it differs during the first second of the transient. RELAP's numerical errors in mass conservation again affect the final steady state.	69
3-13	The RELAP model's pressure profile presents oscillations during the first 0.5 s of the transient because of pressure wave effects in the helium. The simplifications used in the JACOBIAN models distort or eliminate these oscillations.	70

3-14	The RELAP model's temperature profile presents oscillations during the first 0.5 s of the transient because of pressure wave effects in the helium. The simplifications used in the JACOBIAN models distort or eliminate these oscillations.	70
3-15	Heat transfer loop simulations in JACOBIAN are more than 10 times faster than corresponding simulations in RELAP.	72
4-1	Nuclear hydrogen production system studied; the units surrounded by the dashed line will be simulated in this study.	78
4-2	The PBMR is safe, modular, and economical, and it can produce the high-temperature heat needed to run hydrogen production plants. . .	79
4-3	After a loss of heat sink accident, the temperature in the cold leg of the heat transfer loop increases more than 330°C.	90
4-4	Increased temperature in cold pipe after loss of heat sink accident decreases pipe's stress resistance from over 10 ⁵ hrs to less than 1 hr. .	91
4-5	After a loss of heat sink accident, the helium entering the core is hotter, but its temperature is lower at the outlet.	92
4-6	After a loss of heat sink accident, the average temperature in the fuel slightly increases, which leads to a reduction in the reactor power. . .	92
4-7	After a loss of flow in the heat transfer loop, the helium temperature around the loop stays within specifications.	94
4-8	After a loss of flow in the heat transfer loop, the temperature of helium at the core inlet increases. The core response reduces the temperature at the core outlet.	94
4-9	After a loss of flow in the heat transfer loop, the core reacts safely by reducing the fission power.	95
4-10	After a leak accident in the heat transfer loop, the temperature of helium along the loop stays within specifications.	96

4-11	After a leak accident in the heat transfer loop, the temperature at the core inlet slightly increases, which results in a minor temperature decrease at the core outlet.	97
4-12	After a leak accident in the heat transfer loop, the heat transfer loop still can remove a significant amount of heat from the nuclear reactor coolant. This results in a power reduction of 24 MWth.	98
A-1	A combination of standard grid and a staggered grid is used to discretize the gas dynamics equations.	106
A-2	i^{th} control volume in the standard grid.	108
A-3	i^{th} control volume in the standard grid.	109
A-4	i^{th} control volume in the staggered grid.	110
A-5	i^{th} control volume in the staggered grid.	110
A-6	i^{th} control volume in the staggered grid with a change in section. . . .	111
A-7	i^{th} control volume in the staggered grid.	114
A-8	i^{th} control volume in the standard grid.	116

List of Tables

2.1	High-temperature gas reactors have been developed since the 1960s; the current ones being developed today are at the commercial scale [10, 65].	29
2.2	Four different nuclear hydrogen production programs are in development [10].	29

Chapter 1

Introduction

Replacing crude oil with more local and more affordable feedstocks, and decreasing CO₂ emissions are the most important problems that the U.S. needs to tackle regarding transportation fuels [12]. Oil is fundamental for transportation in the U.S.; it accounts for 95% all the energy used in this sector. Yet its sourcing is increasingly more complex; two thirds of oil is imported mostly from politically unstable regions, and the availability of cheap-to-process light crude oil is decreasing [13]. This has resulted in high prices [6] and an oil supply chain with a higher risk of disruption. At the same time, the processing of oil into liquid fuels and the combustion of these fuels emits large amounts of CO₂; thus, increasing the CO₂ concentration in the atmosphere. This higher CO₂ concentration is believed to affect the climate and catastrophic consequences have been projected.

To produce liquid fuels from alternative feedstocks and decrease CO₂ emissions simultaneously, it appears beneficial to use new nuclear applications to generate heat and hydrogen to support these novel production processes. Affordable and more local feedstocks such as oil sands, coal and biomass can be good replacements for crude oil in liquid fuel production. Unfortunately, their processing into liquid fuels requires large amounts of hydrogen and heat, which are currently generated by consuming natural gas or the same feedstock. This results in emissions of considerable amounts of CO₂ in the supply chain (*fuel chain*), which can more than double the total emissions of the fuel chain. Also, when the feedstock itself is consumed to run operations,

low fuel yields are achieved. CO₂ emissions and low yields can be avoided by using nuclear energy, which can provide the necessary hydrogen and heat. Several new nuclear applications to support liquid fuel production processes have been proposed, and special reactors are in development for these purposes.

Demonstrating the safety of these new nuclear applications with computational simulations is fundamental to obtaining regulatory approval. Producing hydrogen by using thermal power from a nuclear reactor requires a tight coupling between the reactor and the hydrogen production plant. Using heat from a nuclear reactor to support a liquid fuels production plant also requires tight coupling. These systems will operate at extreme conditions that can cause operational upsets and affect the nuclear reactor. Validating that the reactor and system will behave safely during this and other extreme upsets is required to obtain approval from authorities. This is achieved in part by studying the system with computational simulations, which allow different combinations of conditions to be tested without risking real accidents. Computational simulations have been used extensively to study nuclear reactors in power plants, and different legacy codes exist for this (e.g., RELAP [52], MELCOR [14]).

However, legacy codes do not have enough flexibility, speed and accuracy to simulate these new nuclear applications. The simulation of nuclear reactors is already complex because it involves simulating reactor kinetics and transport phenomena. To that complexity, new nuclear applications add the need to simulate chemical reactions in the hydrogen plant or in the liquid fuels plant. Chemical reactions cannot be represented easily in legacy codes because these codes lack the flexibility, speed and accuracy to simulate them. Some efforts have been made to modify legacy codes to represent chemical reactions, but they involve large teams of scientists. This situation has resulted in a limited number of studies on the safety of these systems.

This thesis proposes using equation-based simulators to model the new nuclear applications and illustrates this by creating and simulating models for a nuclear hydrogen production plant. Equation-based simulators were created to simulate a large range of process in the chemical industry. Thus, they are specifically designed to be extensible, flexible and fast, and can provide the platform needed to model new

nuclear applications. From all the proposed nuclear applications, nuclear hydrogen production is the one that can have the biggest impact. Therefore, nuclear hydrogen production was used as the case study and high temperature steam electrolysis was chosen as the specific method of production.

The specific contributions of this thesis are:

- a set of models to represent a nuclear reactor coupled to a hydrogen production plant,
- a new method to set the boundary conditions in a closed heat transfer loop using gas as the heat transfer fluid, and
- the simulation of three new possible accident scenarios encountered in a hydrogen production plant.

This thesis is structured in five chapters. Chapter 2 explains how new nuclear applications—in particular nuclear hydrogen production—can help solve problems in the production of fuels for the transportation sector. It also explains the computational difficulties in simulating the new nuclear applications and how equation-based simulators can be an appropriate platform. Chapter 3 explains how to simulate correctly a heat transfer loop connecting a nuclear plant and a hydrogen plant. Chapter 4 presents the dynamic models for the nuclear reactor, the heat transfer loop and part of the hydrogen plant. These models are used to represent and analyze three possible accident scenarios caused by upsets in the hydrogen production plant or the heat transfer loop. Chapter 5 presents the final conclusions and recommendations.

Chapter 2

Background

This chapter explains the problems associated with fuel production processes from alternative feedstocks in the U.S. It details how nuclear energy can help solve these problems by providing heat and hydrogen for the new facilities needed. It also describes the challenges in the simulation of these new nuclear applications and how equation-based simulators can provide a good platform to replace/supplement legacy codes. It finally specifies the nuclear hydrogen plant used as a case study: a pebble-bed reactor coupled to a high-temperature electrolysis plant.

2.1 Nuclear energy to aid fuel production

One of the key priorities for the transportation sector in the U.S. is to replace/reduce crude oil in the production of liquid transportation fuels. To do this, alternative feedstocks have been proposed and studied: oil sands, coal, biomass and natural gas [28, 12]. These alternative feedstocks are advantageous because they can be produced locally or in politically stable countries, and because they are either cheaper or cleaner. However, the pathways to transform them into liquid fuels require large amounts of heat and hydrogen, which are generated by consuming natural gas or the same feedstock. This results in the emission of large quantities of CO_2 and low fuel yields. Using nuclear energy to produce the heat and hydrogen needed can eliminate the high CO_2 emissions and increase fuel yields; thus, paving the way to replace crude oil

with alternative feedstocks. This section explains the problems in the production of liquid fuels using alternative feedstocks and details how nuclear energy can help with heat and hydrogen production. At the same time, this section explains that nuclear hydrogen production will be the focus of this thesis because this application might have the biggest impact in the future.

2.1.1 Current transportation energy challenges

Transforming alternative feedstocks (e.g., oil sands, coal, biomass and natural gas) into liquid transportation fuels requires a supply chain (*fuel chain*) with several steps: *extraction/production*, *conversion/refining* and *transportation/distribution* [28]. Unfortunately, these fuel chains are very energy intensive and can consume more than five times the energy needed by the fuel chain for crude oil. This also results in corresponding large CO₂ emissions, as the CO₂ emissions are approximately proportional to the energy used in each step. The energy demand and emissions vary depending on the process and feedstock used, but are caused mainly by the production of process heat and hydrogen.

1. *Light crude oil*. Production of liquid transportation fuels from light crude oil (e.g., Arab light crude) already requires large amounts of energy, which results in fuel chain emissions of 143 g CO₂ equivalent per mile driven in a SUV (g CO₂-eq/mile in SUV) or 39% of the CO₂ emitted by burning the fuel itself [28]. In particular, refineries are the largest energy consumers in the U.S. and most of this energy is used to generate heat and hydrogen. High-temperature heat (500–700°C) is required for several operations, distillation and thermal cracking being the major demands. This heat input accounts for 10% of the energy in the final fuel. The total heat input required to process the crude oil consumption in the U.S. is 142 GWth or about 50% of the nuclear capacity installed in the U.S [12]. Hydrogen is also widely used at different process steps, hydrotreating and hydrocracking being the most important ones. Refineries use approximately 4 million tonnes of hydrogen per year [64], which makes them also the largest

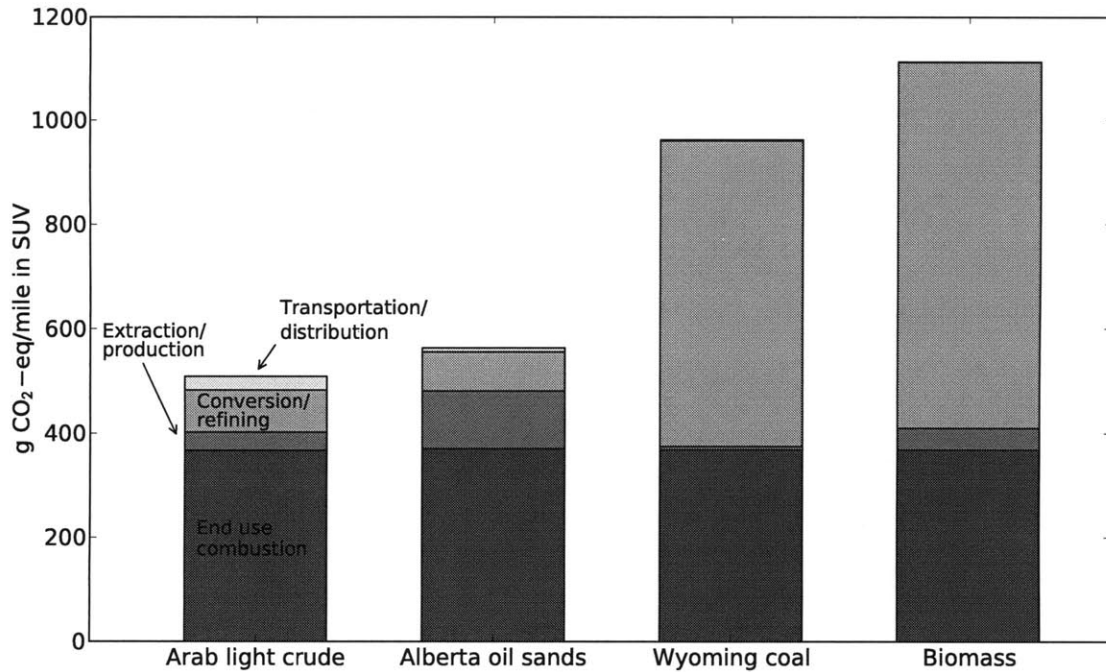


Figure 2-1: Using alternative feedstocks to produce liquid fuels increases CO₂-eq emissions [28].

consumers of hydrogen in the U.S.

2. *Heavier crudes and oil sands.* As heavier forms of crude oil are used for the production of liquid transportation fuels, the processing becomes more complex and results in higher energy consumption and higher CO₂ emissions. For example, the fuel chain for Alberta oil sands emits 193 g CO₂-eq/mile in SUV or 52% of the CO₂ emitted when burning the fuel (Fig. 2-1) [28, 31]. These emissions correspond to 35% more than the emissions generated in the processing of light crude.

In the case of oil sands, the higher CO₂ emissions and energy requirements are explained by the increased intensity of the mining, extraction and upgrading processes. The mining of oil sands in open pits uses large quantities of fuel to operate the equipment (e.g., shovels) and to move oil sands to extraction facilities by hydrotransport pipelines. The extraction of oil sands requires large quantities of steam to decrease their viscosity and separate the bitumen from solids. For example, in situ thermal extraction requires around 1.0 Mcf of

natural gas per barrel of bitumen [34], which corresponds to approximately 17% of the energy in the bitumen. Finally, upgrading the bitumen produces syncrude that can be processed by traditional refineries. This stage involves additional steps of distillation, cracking and hydrotreating, which need large amounts of heat and hydrogen. Most of this heat and hydrogen are currently produced from natural gas, and the requirements are about 0.1 and 0.4 Mcf of natural gas per barrel of bitumen, respectively [34].

3. *Coal*. Coal, a local and abundant feedstock in the U.S. (e.g., Wyoming Coal), can also be used to produce liquid transportation fuels by the Fischer-Tropsch process. However, this fuel chain requires much more energy than the fuel chain for crude oil, and its emissions are 594 g CO₂-eq/mile in SUV or 3.2 times more (Fig. 2-1). Most of the CO₂ emissions and energy consumption are associated with the production of hydrogen from CO and H₂O in the water gas shift (WGS) reaction: $\text{CO} + \text{H}_2\text{O} \leftrightarrow \text{CO}_2 + \text{H}_2$. Additionally, this step results in very low yields in the conversion of coal into fuel, as CO is produced by the gasification of coal. Only 30% of the carbon in the coal input to the process ends in the final liquid fuel [7].
4. *Biomass*. The two most important ways to produce liquid transportation fuels from biomass are the production of ethanol by fermenting biomass-derived sugars and the production of hydrocarbon fuels by gasification and the Fischer-Tropsch process.

The production of ethanol by fermentation is an energy-intensive process. For example, producing a gallon of ethanol from corn starch requires 120% of the energy value in the ethanol gallon, and generates a corresponding amount of CO₂-eq emissions [61]. A large part of the energy is used to produce process heat for separation steps. Currently this heat is mostly generated by burning natural gas, which results in large CO₂ emissions. In addition, the fermentation process itself generates CO₂, as yeast produces two molecules of ethanol and two of CO₂ per molecule of glucose.

A more efficient way to produce liquid fuels based on biomass is using gasification and the Fischer-Tropsch process to produce liquid fuels, because this process can use the biomass constituents as feedstock. This process works similarly to the one used for coal described previously. Here again, using the feedstock to produce hydrogen in the WGS reaction accounts for a large part of the CO₂ emissions, energy used and low conversion yields. The fuel chain emissions in this case are 746 g-CO₂-eq/mile SUV or 4.2 times more than the emissions for the light crude oil fuel chain (Fig. 2-1) [28]. These extra emissions are accounted for by the energy used for cultivating, harvesting and transporting biomass. On the other hand, such a fuel chain could be CO₂ neutral if all the energy comes from biomass or renewable sources.

Additionally in this case, it is crucial to increase the conversion yield of biomass into liquid fuels by finding alternative means of hydrogen production. Not only is it expensive and energy intensive to produce and collect biomass, but also the area that can be used to supply the biomass is limited in size. For example, one study used 17.25 miles as the average haul from the field to the plant [28]. Therefore, low conversion yields severely limit the output of a single facility. As the production of hydrogen for the Fischer-Tropsch process is the biggest factor decreasing the conversion yield, using alternative hydrogen sources can increase the output substantially.

2.1.2 New nuclear applications for hydrogen and heat

As explained above, transforming alternative feedstocks into liquid transportation fuels requires large amounts of energy to produce the hydrogen and heat needed for the processes. Producing this hydrogen and heat with conventional approaches results in high costs, high CO₂ emissions and low conversion yields, which makes it hard to use alternative feedstocks for liquid transportation fuels. However, producing the hydrogen and heat with cheaper and cleaner substitutes could solve this problem. Nuclear energy is one of the possible substitutes and extensive applications of it to

liquid transportation fuel production have been analyzed [12]. This section reviews how nuclear energy can be used to produce hydrogen – nuclear hydrogen production – and how it can provide heat for different liquid fuel production processes.

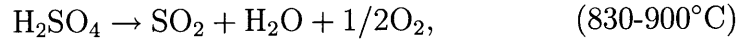
Nuclear hydrogen production

Most hydrogen production involves significant emissions of CO₂ because it relies on fossil fuels. Coupling a very high-temperature nuclear reactor to a hydrogen production plant could provide carbon neutral and inexpensive hydrogen. Two hydrogen production technologies are being developed to do this: high-temperature steam electrolysis (HTSE) and the sulphur-iodine (SI) cycle [63]. These two technologies, their applications and their benefits are explained in this section.

HTSE can produce hydrogen with no CO₂ emissions and approximately double the efficiency of traditional electrolysis. This process uses part of the heat from a high-temperature nuclear reactor to produce superheated steam with temperature in the range of 800-900°C. The rest of the high-temperature heat from the nuclear reactor is used to produce electricity using a Brayton cycle. This electricity is then used in the solid oxide electrolysis cells to produce hydrogen and oxygen from the superheated steam [63]. The use of high-temperature heat to produce electricity results in increased power cycle efficiency over previous power plants. In addition, the operation of the electrolysis cell at high temperatures enables a reduction in the electrical power needed for the electrolysis reactions. The combination of these two factors achieves thermal efficiencies in the production of hydrogen of 45% to 55% [63, 18]. This greatly exceeds efficiencies of 27% achieved by current electrolyzer technologies using electricity from earlier generations of power plants.

The SI cycle can also produce hydrogen from the heat produced by a nuclear reactor without CO₂ emissions and at high efficiency. This cycle was developed by General Atomics in the 1970s [63] and involves the dissociation of water by using

three chemical reactions:



These reactions have been demonstrated in the laboratory and progress has been made in scale up [10]. All the reagent in these reactions is recycled, which means that only hydrogen and oxygen are the final output of the system. In this case, the high-temperature reactor is mainly used to provide high-temperature heat for the second reaction. The thermal efficiency of this process has been estimated between 45% and 55% [63].

Hydrogen produced with either of these two nuclear hydrogen production technologies could be used in different liquid transportation fuel processes to reduce emissions or increase efficiency:

- *Crude oil refining.* In the U.S., displacing the use of natural gas for hydrogen production in refining processes would decrease CO₂ emissions by 10–15% and would require 35–41 GWth of nuclear reactor capacity. In the U.S. in 2003, the 145 active refineries required 4.08 million tonnes of hydrogen for hydrotreating, hydrocracking and other processes [64]. Almost all of this hydrogen was produced by using natural gas steam reforming, and this process accounted for 10–15% of the CO₂ emissions [62, 48]. These emissions could be avoided by using hydrogen produced by nuclear hydrogen production plants using HTSE or SI. It is estimated that 60–70,000 tonnes of hydrogen per year can be produced from a 600 MWth high-temperature nuclear reactor [12]. Then, the nuclear capacity required supply all the refineries in the U.S. corresponds to 35–41 GWth. This corresponds to approximately 11–13% of the current installed nuclear capacity in the U.S., as the average power cycle efficiency of this capacity is 32% [1].

- *Oil sands upgrading.* Incorporating nuclear hydrogen production for the upgrading of Alberta oil sands could decrease CO₂ emissions in the extraction/production step by 35%. Upgrading one barrel of bitumen of Alberta oil sands requires 2.4 kg of hydrogen on average [44]. As the production of 1 kg of hydrogen from natural gas generates 11.9 kg CO₂-eq [50], the upgrading of one barrel of bitumen generates 28 kg CO₂. Overall, the production of one barrel of bitumen emits about 81 kg CO₂-eq [34], which means emissions would decrease by 35% in this step.

Replacing all the hydrogen used for upgrading with hydrogen produced with nuclear means would require 5.1–6.0 GWth of nuclear power. In 2007, the production rate of bitumen in Alberta was approximately 700 thousand barrels per day. Thus, the corresponding requirement for hydrogen was about 0.6 million tonnes of hydrogen per day. As 60–70,000 ton-H₂/yr need 600 MWth of nuclear power for its production, satisfying this hydrogen demand would need 5.1–6.0 GWth of nuclear power.

- *Converting coal to liquids or biomass to liquids.* CO₂ emissions in a coal-to-liquids facility could be reduced by 49% by using nuclear hydrogen production. In a traditional coal-to-liquids facility, only 30% of the carbon in the coal is incorporated into the final liquid fuel [7]. Most of the remaining 70% ends as CO₂ in the WGS reaction and accounts for nearly all the CO₂ emissions. Nuclear hydrogen can replace the WGS reaction to provide hydrogen for the Fischer-Tropsch process, and this would result in 66% of the carbon in coal being incorporated in the final fuel. Therefore, emissions could be reduced by 49%. A coal-to-liquids facility processing 19 thousand tons of coal per day would require 0.5 thousand tons of hydrogen per day [7]. This rate of hydrogen can be produced by a nuclear hydrogen facility with 1.7 GWth of power. Using nuclear hydrogen production to support a biomass-to-liquids facility would have a similar effect. This is crucial in the case of biomass as the production rate of the facility is limited by the area of land that can supply the facility. Thus,

doubling the carbon conversion yield would allow a single facility to double its output and achieve economies of scale.

Nuclear heat integration

Nuclear reactors can also be used to provide heat for liquid fuel production processes and reduce CO₂ emissions. This will require a customized design for heat integration, as the different steps in each process use different amounts of heat at different temperatures. Using nuclear reactors to produce heat for industrial applications – including ethanol production – has been already tried successfully in other parts of the world. This section will describe some potential uses of nuclear heat in liquid fuel production processes.

1. *Refineries.* The heat needed to supply refineries in the U.S. would require a nuclear capacity of 142 GWth. Most of the heat used in refineries is used in distillation and thermal cracking, and it accounts for 10% of the heat content in the final liquid fuel. The total fuel output from refineries is equivalent to 20 million barrels of oil per day; then, the nuclear capacity required in this case is 142 GWth [12]. The heat provided should be at 600–700°C, which would require designing specific equipment to transfer the heat at such high temperatures.
2. *Oil sands extraction and upgrading.* In the case of oil sands, heat could be used to produce steam to extract bitumen in situ, or to separate it from solid residues [11]. In the case of extraction in situ, one pebble bed modular reactor of 250 MWth could support the production of 50 thousand barrels of bitumen per day. Other process designs are going even further by suggesting the idea of nuclear underground refining, where high-temperature heat is used to distill the bitumen in situ [12]. A process like this would avoid all the CO₂ emissions associated with producing the high-temperature heat from natural gas and it would require a 600 MWth reactor to produce 50 thousand barrels of oil per day.
3. *Ethanol production from corn.* Using low-temperature steam from nuclear re-

actors could reduce by 50% the fossil fuel use in starch-based ethanol refineries. 50% of the energy consumed in traditional ethanol refineries is used to produce steam with low temperature and pressure. The same kind of steam is produced by nuclear power plants as a by-product, and it can be easily transported for a distance of about one mile. Thus, using the steam from a nuclear power plant in an ethanol refinery is feasible, would reduce emissions and would add value to the power production in the nuclear plant. Producing 2.4 million barrels of ethanol per year would need 80 MWth of steam [12].

2.1.3 Nuclear hydrogen production can make the biggest impact

As demonstrated, nuclear hydrogen production and nuclear heat coupling can both reduce CO₂ emissions and increase feedstock conversion yields. From these two new nuclear energy applications, it is nuclear hydrogen production that can make the biggest impact in the near future. Some of the reasons for this are that nuclear hydrogen production could reduce more than 1% of CO₂ emissions in the U.S., and that its development has made significant progress. At the same time, its application could be highly standardized, contrasting the customized integration required for heat coupling projects. Furthermore, nuclear heat coupling has not been developed much. For all these reasons, this thesis will focus on nuclear hydrogen production.

The development of nuclear hydrogen production has made significant progress. Seven high-temperature gas reactors have already been built—only two of them are operational—and five more will be built by 2020 (Table 2.1) [10]. In particular Japan and China have made considerable progress. They own the two operational reactors (the 30-MW HTTR and 10-MW HTR-10, respectively) and are developing larger versions of them (the 300-MW GTHTR300 and the 250-MW HTR-PM, respectively) [10, 65]. All these reactors are also being designed to be passively safe, which will help gain public acceptability. In addition, these reactors could be used for hydrogen production, and research efforts are also being developed in this direction (Table 2.2)

[10].

Table 2.1: High-temperature gas reactors have been developed since the 1960s; the current ones being developed today are at the commercial scale [10, 65].

Reactor	Location	Power (MWth)	He temperature in/out (°C)	Core	Operation years
Dragon	UK	20	350/750	Cylindrical	1965-1975
Peach Bottom	USA	115	377/750	Cylindrical	1967-1974
AVR	Germany	46	270/950	Pebble bed	1968-1988
Fort St Vrain	USA	842	400/775	Hexagonal	1976-1989
THTR	Germany	750	270/750	Pebble bed	1985-1989
HTTR	Japan	30	395/950	Hexagonal	1998-Present
HTR-10	China	10	250-300/700-950	Pebble bed	2000-Present
PBMR	SA	500	350/950	Pebble bed	In development
ANTARES	France	600	400/850	Hexagonal	In development
GT-MHR	USA/Russia	550-600	490/950	Hexagonal	In development
HTR-PM	China	250	250/750	Pebble bed	In development
GTHTR300	Japan	600	589/850	Hexagonal	In development

Table 2.2: Four different nuclear hydrogen production programs are in development [10].

Company	JAEA	GA	PBMR/Westinghouse	AREVA NP
Country	Japan	USA	SA/USA	France
Reactor	GTHTR300	MHR-GT	PBMR	ANTARES
Power	600	550-600	500	600
PCS	Brayton	Brayton	Rankine	Rankine
HPP	SI	HTE/SI	HyS/HTE	HTE/SI
Cycle configuration	Direct PCS, series indirect HPP	Direct PCS, parallel indirect HPP	Indirect, series HPP and PCS	Indirect, parallel HPP and PCS
IHX	Helical coil S&T	Single-stage PCHE	Two stage PCHE	PCS: helical coil S&T Process: PCHE or fin plate

In addition, nuclear hydrogen production would operate as a standard standalone plant, avoiding the customized integration required by nuclear heat coupling. The hydrogen transfer is the only point of contact between a nuclear hydrogen plant supporting a fuel production plant. As hydrogen can be stored in limited quantities, the operation of the nuclear hydrogen plant is relatively independent from its fuel counterpart. Therefore, a standard modular nuclear hydrogen plant could be used to assist a large variety of fuel plants. This would make the manufacturing and deployment of nuclear hydrogen plants cheaper and faster. On the other hand, nuclear

heat coupling requires a customized integration with the fuel plant, which will make the adoption of this technology much slower.

Moreover, nuclear heat coupling has not been developed significantly. Research exploring the use of nuclear heat in refineries has not been reported yet [12]. Also, only preliminary studies have been on the use of nuclear heat to extract bitumen from oil sands [12, 11]. The development of these topics would require large multidisciplinary teams with understanding of materials, chemistry and nuclear engineering. This author does not know of such a team yet.

2.2 The need for new computational models

New nuclear applications for fuel production, such as nuclear hydrogen production, will need to demonstrate safe operation by going through a rigorous assessment, similar to the one used for nuclear power plants. This assessment involves understanding how the plant behaves during normal operation and how it responds to possible equipment failures and disruptions. In particular, the assessment will help validate the limits for the important process variables, the design of the safety procedures and the specifications for the different materials and equipment used [56]. Positive results in this assessment are fundamental to obtain a license for the reactor, because they will help guarantee the public health and safety.

The scenarios used to validate new nuclear applications will include adapted versions of the ones used for nuclear power plants and new ones depending on the chemical processes used. Scenarios including operational disruptions will comprise the decrease/increase of heat removal by the secondary system, decrease in the reactor coolant system flowrate, reactivity and power disruptions anomalies, radioactive release from a subsystem, etc. Normal operation scenarios will involve studying the procedures for the normal operational transients that the plant will experience such as start-up, shutdown and re-start.

In the case of nuclear power plants, these scenarios are studied using computer simulation codes that can model the associated physical phenomena. The leading ones

in the U.S. are MELCOR, MAAP4 and RELAP5 [57]. MELCOR and RELAP5 are used by regulatory agencies and research institutions to evaluate hypothetical severe accident events such as a station blackout or the potential for steam generator tube rupture. MAAP4 is the severe accident code most widely used by nuclear utilities and vendors because of its short run time and reduced requirements for code expertise.

However, the simulation of new nuclear applications for fuel production is more complex than the simulation of a nuclear power plant and new codes are required for this. Legacy codes lack the extensibility, flexibility and speed required to simulate chemical reactions that appear in a new nuclear application such as nuclear hydrogen production. This problem can be solved by using equation-based simulators, which are simulation platforms designed by chemical engineers to model a large variety of chemical processes. This section explains the main reasons why legacy codes, such as RELAP5, struggle to simulate nuclear hydrogen production. At the same time, this section explains how equation-based simulators can be a good platform to simulate this new kind of nuclear system.

2.2.1 Legacy codes lack simulation features

Legacy codes have been extensively used to demonstrate the safety of nuclear power plants. However, they lack the extensibility, flexibility, speed and accuracy required to represent new nuclear applications such as nuclear hydrogen production.

New nuclear applications are complex systems and their simulation requires models of a variety of physical and chemical phenomena. In the case of nuclear hydrogen production using HTSE or the SI cycle, these phenomena comprise many complex chemical reactions and unit operations. HTSE involves electrolysis cells with temperature gradients, mass transfer and steam electrolysis reactions at the cells electrodes. The SI process involves electrolyte solutions and highly corrosive chemical reactions at high-temperature: Bunsen reaction, sulfuric acid decomposition, and HI decomposition. The dynamics all of these phenomena need to be represented in order to understand the behavior of the hydrogen production plant and how it can affect the nuclear reactor.

However, legacy codes are not designed to model these chemical and physical phenomena. Legacy codes have been created to model accidents in the reactor accurately and specifically. For example, MELCOR, MAAP4 and RELAP5 can represent - with precision - the behavior of the reactor primary loop, the fission reactions in the core, and the core thermodynamics [57]. Yet, these codes do not have the necessary routines to represent the chemical reactions and processes in new nuclear applications such as hydrogen production. Nor do they have algorithms that can efficiently simulate stiff chemical reactions, which are difficult to simulate and can slow down the code's performance.

At the same time, legacy codes are hard to modify to incorporate chemical reactions. In these codes, the equations representing the reactor physics and the solution methods for these equations are tightly coupled. Additionally, these codes are collections of capabilities that have evolved and grown over the years. For example, MELCOR was initially design to be a risk assessment tool; now, it is a dynamic simulation tool [57]. This means that adding new chemical reactions and new unit operations to legacy codes requires a deep understanding of their architecture. Some research groups have attempted this, but their efforts involved years of work and large and specialized teams [43].

2.2.2 Equation-based simulators are a good alternative

Equation-based simulators used in the chemical industry are an alternative platform to legacy codes for the simulation of new nuclear applications. Chemical engineers have to deal with a large number of vastly different processes, which involve chemical reactions, different unit operations, complex thermodynamic models and heat and mass transfer phenomena. To design and optimize these processes, they often use equation-based simulators, which are general-purpose modeling environments for dynamic and steady-state simulation. Such simulators provide a high-level simulation language for the user to describe processes in terms of equations and variables. These simulators and their supporting mathematical theory have been developed for more than 30 years and some examples of them are JACOBIAN [35], Aspen Custom

Modeler [53], and gPROMS [41]. They have been developed to be extensible, flexible, fast and accurate, and this combination of features makes them ideal to simulate new nuclear applications such as nuclear hydrogen production.

The extensibility, flexibility, speed and accuracy of equation-based simulators are achieved by decoupling the description of the physical system from the numerical methods employed to simulate this system. This is a key difference between these simulators and legacy codes, where the definition of the model is tightly coupled to its solution algorithm. On the one hand, a description of the physical system is made by declaring the model, which corresponds to representing all the unit operations individually with equations and variables. These unit operations models can be coded from scratch in the simulation language or they can be imported from a library. The ability to create new unit operation models is very important in the development of new nuclear reactor applications, as the systems have not been completely defined and are constantly changing with the results of new experimental data. On the other hand, the solution of the model is done automatically by powerful general-purpose algorithms. These algorithms assemble all the equations of the model in one single system and then solve this system directly fast and accurately by automatically identifying and exploiting problem structure such as block decomposition. Model declaration and the model solution are explained in the following.

Model declaration—flexibility

Equation-based simulation languages are declarative, which means the user only needs to input the model as a set of differential-algebraic equations (DAEs) [5]. These languages can represent any physical or chemical system as a combination of DAEs:

$$\begin{aligned}\mathbf{f}(\mathbf{x}(t), \dot{\mathbf{x}}(t), \mathbf{y}(t), t) &= \mathbf{0} \\ \mathbf{g}(\mathbf{x}(t), \mathbf{y}(t), t) &= \mathbf{0}\end{aligned}$$

where $\mathbf{x}(t) \in \mathbb{R}^{n_x}$ and $\dot{\mathbf{x}} \in \mathbb{R}^{n_x}$ represent the differential variables (those whose time derivatives appear explicitly in the model) and the time derivatives of these variables,

```

MODEL Vessel_With_Safety_Valve

PARAMETER
  Vessel_Volume,R          AS REAL
  Set_Press, Reseat_Press  AS REAL
  Valve_Const              AS REAL

VARIABLE
  Flow_In, Flow_Out,
  Relief_Flow              AS Molar_Flowrate
  Holdup                   AS Moles
  Temp                     AS Temperature
  Press, Press_In          AS Pressure

STREAM
  Inlet  : Flow_In, Press_In  AS MainStream
  Outlet : Flow_Out, Press    AS MainStream
  Relief : Relief_Flow, Press AS MainStream

SELECTOR
  Valve_Flag              AS (Closed,Open)

EQUATION

  # Mass balance
  $Holdup = Flow_In - Flow_Out - Relief_Flow ;

  # Equation of state (perfect gas)
  Press*Vessel_Volume = R*Holdup*Temp ;

  # Safety relief valve with hysteresis
  CASE Valve_Flag OF
    WHEN Closed :Relief_Flow = 0 ;
                  SWITCH TO Open IF Press >= Set_Press ;
    WHEN Open   :Relief_Flow = Valve_Const*Press/Temp^0.5 ;
                  SWITCH TO Closed IF Press <= Reseat_Press ;
  END # CASE

END # Vessel_With_Safety_Valve

```

Figure 2-2: Equation-based simulation languages allow the variables and equations describing physical and chemical phenomena to be declared explicitly [5].

respectively. $\mathbf{y} \in \mathbb{R}^{n_y}$ correspond to the algebraic variables. $\mathbf{f} : \mathbb{R}^{n_x} \times \mathbb{R}^{n_x} \times \mathbb{R}^{n_y} \times \mathbb{R} \rightarrow \mathbb{R}^{n_x}$ are the differential equations, and $\mathbf{g} : \mathbb{R}^{n_x} \times \mathbb{R}^{n_y} \times \mathbb{R} \rightarrow \mathbb{R}^{n_y}$ are the algebraic equations. The purpose is to specify the functional form of a model (e.g., a system of equations), and not a series of statements to be executed in a sequence (Fig. 2-2). The process model so defined is completely decoupled from the numerical methods used to solve it, which allows the user to focus solely on the model.

Furthermore, equation-based simulation languages use hierarchical decomposition, which greatly simplifies the coding of large models [5]. Hierarchical decomposition allows building models in levels—in the same way one would build a real plant. For example, a first level of simple models can represent basic units (e.g., pipes, heat exchangers, chemical reactors). A second level connects models from the first to

represent subsystems (e.g., heat transfer loop). Finally, a third level could connect all the subsystems to assemble a plant model. With this approach, lower-level models can be easily tested and corrected, avoiding hard-to-find errors in higher-level models.

In sum, equation declaration and hierarchical decomposition allow equation-based simulation languages to represent the details of new nuclear applications in a simple and intuitive way.

Model solution—speed and accuracy

Equally important, equation-based simulators find solutions to simulations quickly and accurately. To solve simulations quickly, they assemble all the model equations into one single equation system, which is solved simultaneously by general-purpose codes for root finding and fast numerical integration. They also automatically exploit the characteristics of the equation system (e.g., sparsity, analytical derivatives, and block decomposition) to accelerate the solution process and solve 100,000s of equations in minutes. To be accurate, they use error control based on theoretical guarantees for accuracy and stability, and these estimates are controlled automatically [4]. These features are made possible by powerful algorithms: implicit predictor-corrector methods for integration [3], automatic differentiation algorithms [16] and algorithms for sparse linear algebra [9]. These algorithms are explained here.

The best equation-based simulators use implicit predictor-corrector methods to integrate the system of equations numerically. They are implicit methods that use an explicit method to calculate an initial guess for the solution of the system of equations at each time step. The implicit methods normally used are multi-step methods, and, in particular, variable step size, variable order Backward Differentiation Formula (BDF) methods are used [15]. These methods are very stable and can solve stiff problems such as the simulation of complex systems of chemical reactions. Additionally, the step size used in the integration is controlled by the truncation error rather than the stability. Thus, the integrator can take larger time steps when the system of equations is stiff and the fast modes of the transient have decayed. This results in a faster solution of the simulation.

Automatic differentiation algorithms calculate the Jacobian (matrix of partial derivatives) of the equations analytically. These algorithms increase the speed and accuracy of the solution, because predictor-corrector methods work more efficiently with an analytical Jacobian instead of a numerical one. At the same time, these automatic algorithms avoid the tedious and prone-to-error task of deriving the analytical Jacobian manually. For these reasons, automatic differentiation algorithms are extensively used in equation-based languages [16, 54]

Algorithms for sparse linear algebra take advantage of the sparsity of an equation system to solve it faster. Normally, systems with more than about 20 equations will have only a few variables appearing in each equation. This creates a very sparse system, whose Jacobian will have mostly zeros. Using this information in numerical Jacobian evaluations and while solving a system's linear equations greatly increases the solution speed of the equation system.

2.3 Nuclear hydrogen plant used in this thesis

The goal of this thesis is to study the safety of a nuclear hydrogen production plant by simulating this plant's operation in an equation-based simulator. The plant selected for this is a combination of well-developed technologies: two modular pebble bed reactors (MPBR), a power conversion unit (PCU) using the Brayton cycle, a heat transfer loop, and a HTSE facility (Fig. 2-3). In this process, the nuclear reactor produces 500 MWth of high-temperature heat for the PCU and for the HTSE process. The PCU uses 450 MWth to produce the electricity needed in the electrolysis cell of the HTSE unit. The remaining 50 MWth of heat is transferred from the nuclear reactors to the HTSE unit by the heat transfer loop, and it is used to produce superheated steam (800-900°C). This steam is fed to the electrolysis cell where it is decomposed into oxygen and hydrogen; this reaction occurs at high temperature, which increases the efficiency of the electrolysis. The oxygen is recuperated and the hydrogen/water stream is sent to a steam separator, to be recover hydrogen.

The specific design for the MPBR and PCU was adapted from the pebble bed

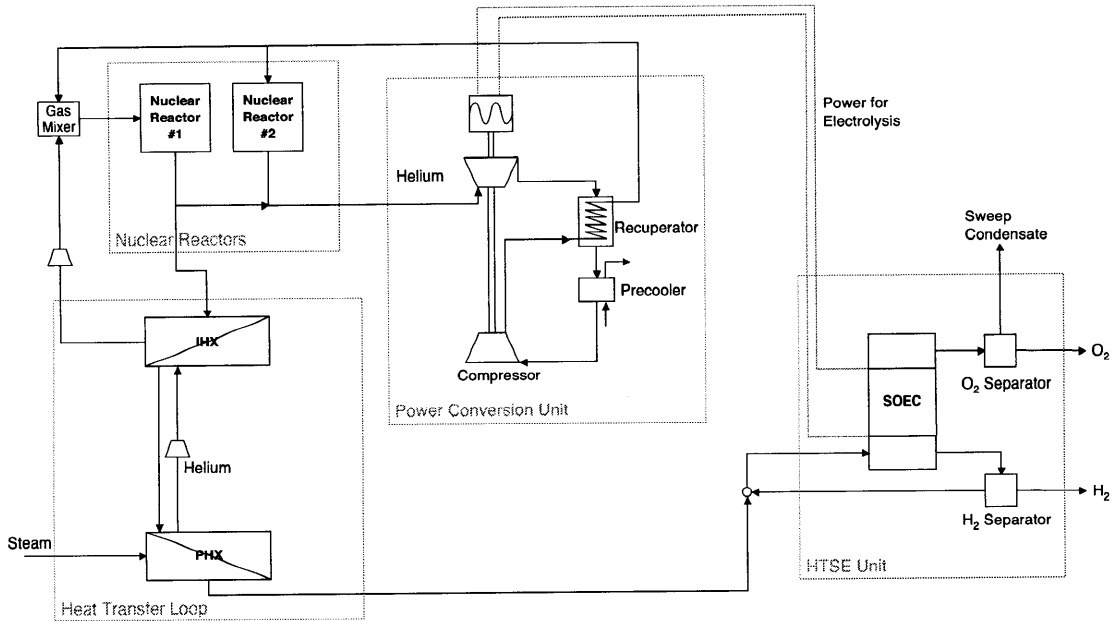


Figure 2-3: The nuclear hydrogen production used in this thesis is a combination of technologies in development.

reactor research at MIT [60, 23]. The HTSE facility and the heat transfer loop are modeled after ones developed at INL [32, 8]. This section explains how each of these components work.

2.3.1 PBMR and PCU Operation

As explained before, nuclear hydrogen production requires very high-temperature heat (over 750°C) and electricity and different reactors/PCU combinations have been studied for this (Tables 2.1, 2.2). From these technologies, the modular pebble bed reactor technology is most promising and the one chosen for this study. Pebble bed reactors (PBR) are an attractive choice because their design provides excellent economics and safety. Also, good progress has been made in their development: Germany built two PBRs in the 1970s and 1980s, China built a 10-MWth PBR as a test and is developing a nuclear plant with two 250-MWth PBRs, and South Africa is developing a 268-MWth PBR.

In particular, this study will use the design developed at MIT called the “Modular

Pebble Bed Reactor”. (MPBR) coupled to a helium Brayton cycle [60]. This design has a capacity of 250 MWth, it is based on the South African PBR and it exploits modularity to decrease production and construction costs. Two MPBRs are used in the nuclear hydrogen production plant (Fig. 2-3), which is a similar modular configuration to the new PBR project developed in China [65]. Some of the key features of the MPBR to achieve safety and good economics are the fuel pebbles used in the core, the primary coolant system and the Brayton cycle used in the PCU. These features are explained in the following.

The core in the MPBR uses fuel pebbles to simplify the reactor operation. The MPBR’s fuel system is composed of 360,000 6-cm-diameter graphite pebbles containing the uranium fuel in microspheres (Fig. 2-4). These pebbles can be introduced at the top of the reactor and extracted at the bottom during operation. This online refueling capability avoids the breaks needed to refuel normal reactors, increasing the uptime and economics.

Additionally, the MPBR’s fuel is designed to avoid meltdowns passively and to have a lower possibility of radiation spread. To avoid meltdowns, these reactors use fuel particles with low uranium density that cannot melt down during operational upsets or accidents. The fuel particles are designed to operate at temperatures over 1000°C, where a temperature increase results in the Doppler broadening of the fuel isotope’s resonance-absorption line. As a consequence, the fission rate decreases—negative reactivity—because U-238 can attach more neutrons and less neutrons are available for the fission of U-235. The negative reactivity limits the maximum temperature the fuel can reach to 1600°C, which is well below the fusion point of the fuel (2000°C). In addition, the fuel particles are designed to feature high retention capability of fission products (Fig. 2-4), which decreases radiation spread in the case of an accident.

The coolant loop in the pebble bed reactor uses helium to decrease reactor maintenance and to decrease the possibility of radiation spread even further. Helium is an inert gas and does not corrode the components in the nuclear reactor coolant system, as water does in water-cooled reactors. Using helium, thus, avoids the cost of replac-

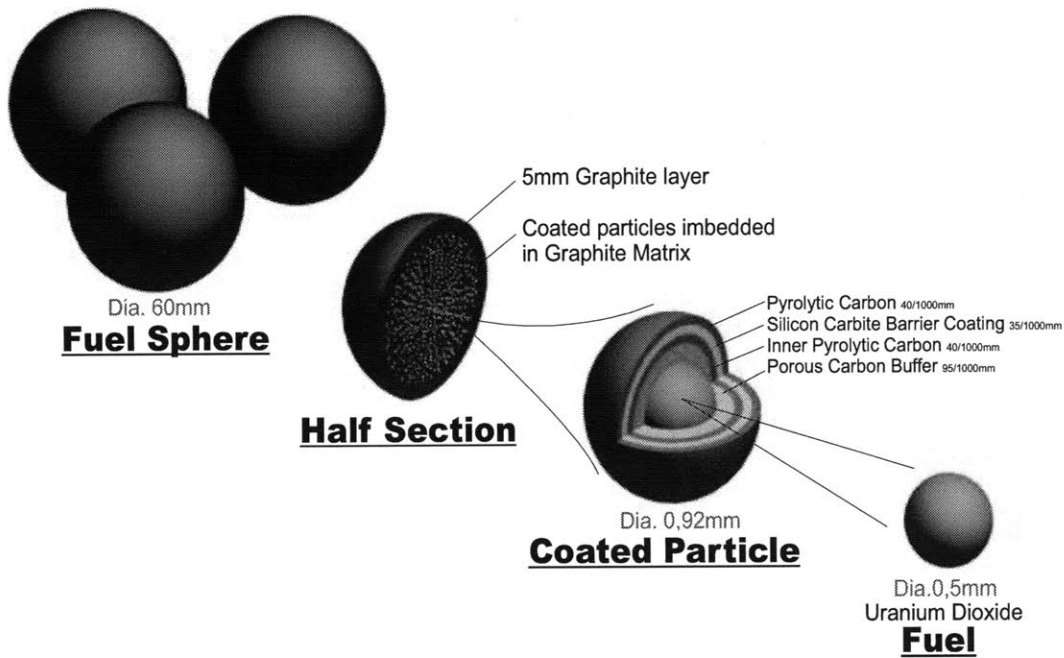


Figure 2-4: The design of fuel pebbles for PBRs avoids meltdowns by having a high fusion point (2000°C) and decreases the possibility of radiation spread [26].

ing degraded components and stopping the plant for this kind of maintenance. At the same time, helium is not transmuted to radioactive elements, which helps reduce even further the possibility of radiation dissemination in the case of an accident.

The PCU coupled to the MPBRs uses a Brayton cycle to achieve high efficiency in the production of electricity. Water-cooled reactors such as PWRs use a Rankine cycle to produce electricity, which achieves approximately 32% of power cycle efficiency. The PCU considered in this thesis, uses a Brayton cycle with helium as a coolant instead, which can achieve power cycle efficiencies of about 45%. This PCU is composed of a turbine, a compressor, a generator, a recuperator and a heater.

2.3.2 HTSE

As mentioned before, high-temperature steam electrolysis (HTSE) is an efficient way to generate hydrogen from water. One of the leading technologies being developed to do this is the solid oxide electrolysis cell (SOEC), which is based on ceramic fuel cell technology. This technology is being developed by the Idaho National Labora-

tory (INL) in collaboration with Ceramatec [8]. INL has made a lot of progress in improving cell performance and reducing cell degradation [51]. For these reasons this technology has been selected for this thesis.

The HTSE unit generates hydrogen and oxygen from water by using high-temperature heat from the nuclear reactor and electricity produced in the PCU. First, water is heated by recovered heat from product streams, and later is superheated in the process heat exchanger (PHX) (Fig. 2-3). Then, the superheated steam goes into the electrolysis cell, where the voltage applied to the cell splits water molecules into H_2 and O^{2-} at the cathode (Fig. 2-5). The O^{2-} so generated migrates through the ion-conducting solid electrolyte to the porous anode to produce O_2 . As a result, the electrolysis cell dissociates the superheated steam and separates the products at the same time. The use of superheated steam allows the use of a lower voltage than the voltage needed in conventional electrolyzers, and it increases the speed of the reactions in the system.

It is important to note that the ceramic materials are very sensitive to thermal gradients, so temperature increases in the cells need to be gradual to avoid them. In the case of the cell tested at INL, the rate of temperature increase is $1^\circ\text{C}/\text{min}$. This point has to be taken into account when planning start-up and shutdown procedures.

The HTSE unit is built in a modular form. Its minimal constituent is the SOEC (10 cm x 10 cm x 3 mm). These cells are arranged in stacks of 500 cells, which then are arranged in 40 stack modules, which are finally laid out in containers containing eight modules each (Fig. 2-6). Approximately 63 of these eight-module containers would be required for the system considered in this study [42].

2.3.3 Heat transfer loop

The heat transfer loop transfers 50 MWth of heat from the nuclear reactor to the HTSE unit over a distance of 90 m. In this way, the heat transfer loop couples the nuclear reactor with the HTSE unit and, at the same time, provides safe physical separation between them. A detailed design of this loop has been developed at INL [8], and it will be the base for the loop used in this thesis.

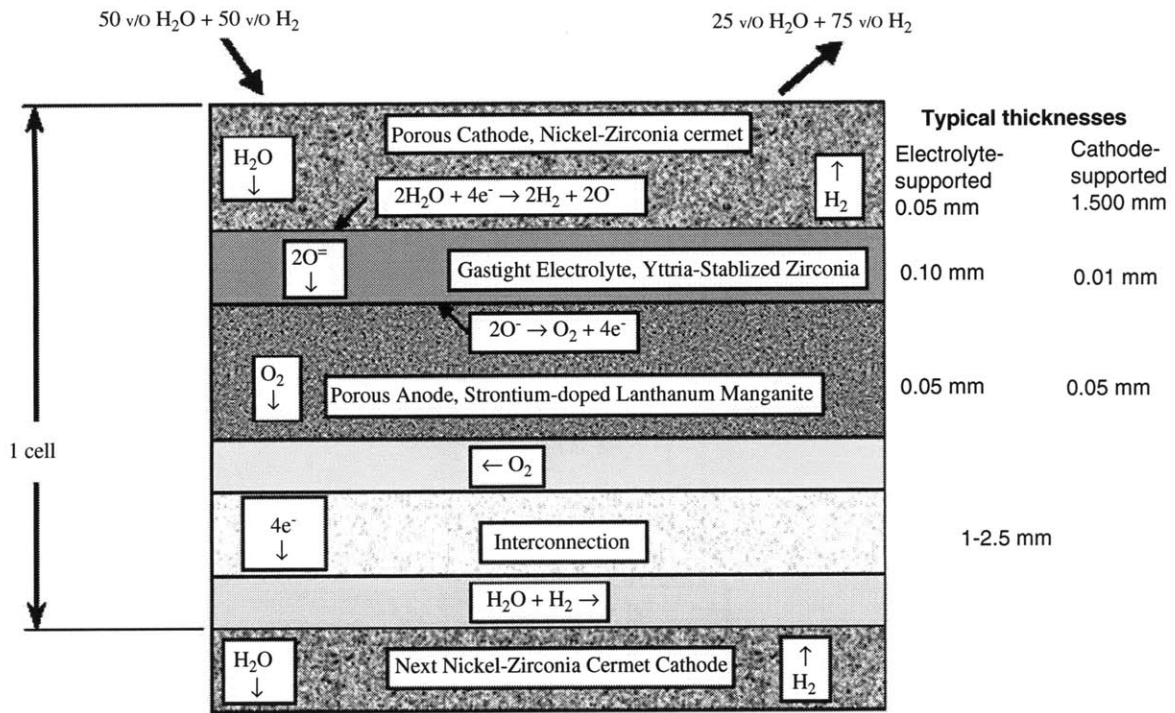


Figure 2-5: The SOEC cell disassociates superheated steam into hydrogen and oxygen [36].

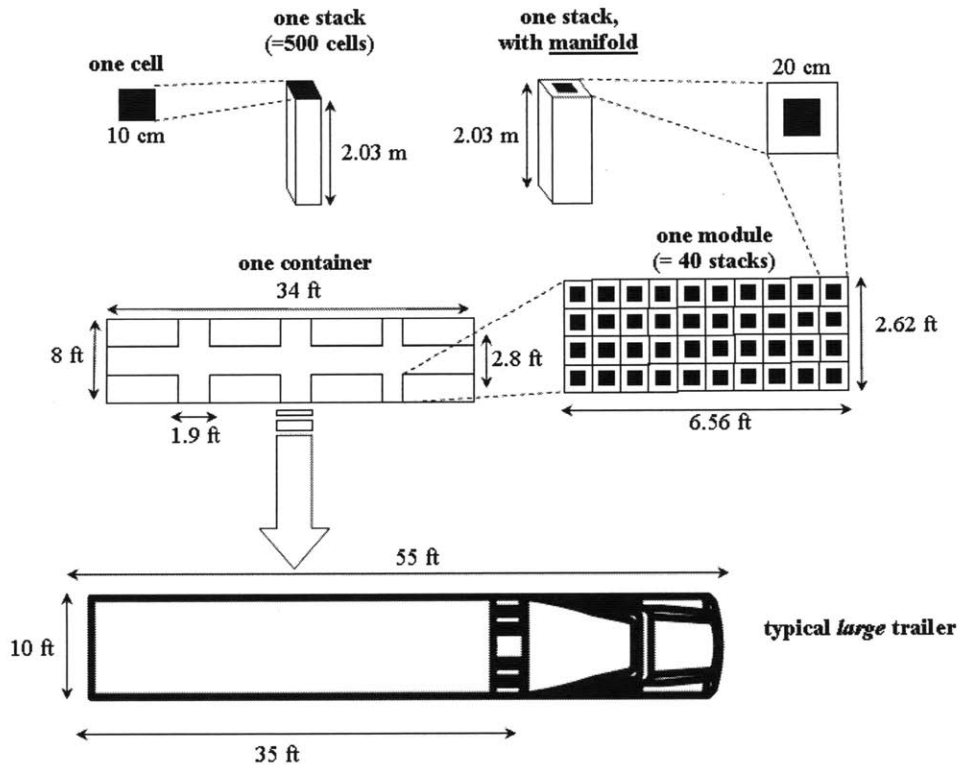


Figure 2-6: A HTSE plant is designed to be built in modular form [42].

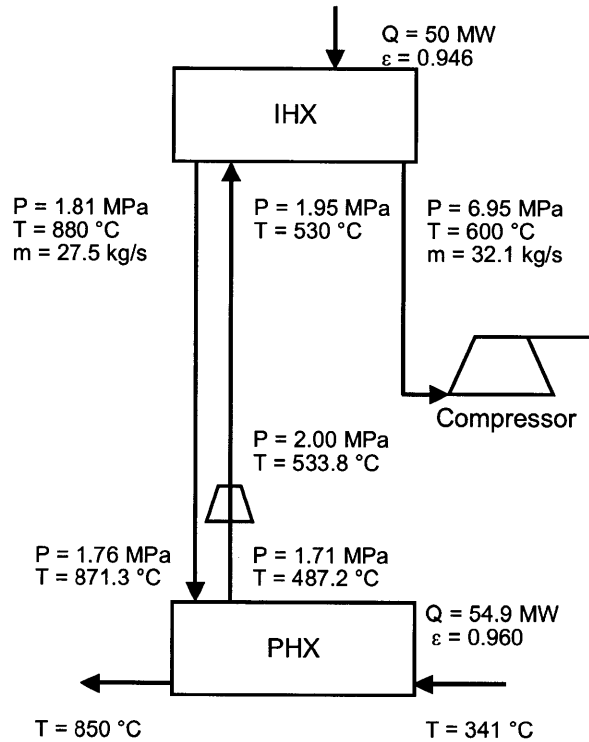


Figure 2-7: Heat transfer loop [8].

The heat transfer loop uses helium at 2 MPa and is composed of an intermediate heat exchanger (IHX), a hot leg, a process heat exchanger (PHX), a cold leg and a compressor. The IHX transfers 50 MWth from the nuclear reactor coolant at 900°C to the helium in the loop, which reaches 880°C (Fig. 2-3). Its design is based on the printed circuit heat exchanger (PCHE) technology developed at Heatric [8]. It is connected by the hot leg to the process heat exchanger (PHX), where steam is superheated to feed the electrolysis cells. The PHX is a tube-in-shell heat exchanger and the helium flows on the shell side. At the end of it, the colder helium (487.2°C) is pressurized by a compressor and then taken back to the IHX by the cold leg (Fig. 2-7).

Chapter 3

Dynamic simulation of a heat transfer loop for alternative nuclear reactor applications

3.1 Introduction

Using nuclear reactors as an energy source is an attractive alternative to reduce CO₂ emissions in energy-intensive chemical processes (e.g., oil refining, biofuels production). These processes need carbon-based fuels to provide energy and chemicals for plant operation, thus generating large amounts of CO₂. Using a nuclear reactor for these support tasks can eliminate the CO₂ emissions, and several new processes have been proposed for this [12, 2].

For example, nuclear reactors could be used for hydrogen production, which is fundamental for oil refining and other processes. Hydrogen production is currently based on steam methane reforming and releases 60 Mt of CO₂ per year in the U.S., or almost 1% of the total CO₂ emissions [55, 1]. This process could be replaced by a high-temperature nuclear reactor coupled to a hydrogen production plant [63]. In this system, the nuclear reactor provides heat and power to a solid oxide electrolysis cell (SOEC) to run high-temperature electrolysis reactions. Heat is transferred to the

SOEC by a heat transfer loop, which also provides safe separation between the nuclear reactor and the chemical plant. The rest of the heat generated by the nuclear reactor is used by the power conversion unit (PCU) to produce electricity, which powers the electrolysis in the SOEC (Fig. 3-1).

Safety and operability of these new nuclear reactor applications need to be demonstrated; in particular, the connection between the reactor and the chemical plant (the heat transfer loop) requires special attention. These new applications involve extreme conditions (e.g., high temperatures (900°C), high pressures (7 MPa), exothermic chemical reactions, and corrosive chemicals) that could cause accidents, make operation more difficult, and require exotic materials of construction. To ensure safety, the system design should prevent or isolate operational disruptions that might affect the nuclear reactor (e.g., loss of heat sink capacity, accidents). To ensure operability, the system design should be demonstrated to perform well during operational transients (e.g., start-up, shut-down, re-start). One of the key elements to achieve these goals is the heat transfer loop connecting the nuclear reactor and the chemical plant (Fig. 3-1). This loop is a new piece of engineering and presents several design challenges. It will incorporate new technologies and materials to handle the extreme conditions, and it will isolate the nuclear reactor from the chemical plant. Careful study of its performance will pave the road for the new nuclear applications.

The response of novel nuclear systems to accidents will be simulated and studied with equation-based dynamic simulators. As mentioned above, a novel system must behave safely during upsets and operational transients, and computational simulations of the system can provide some a priori assurance of this. Usually, nuclear reactor designs are tested by computational simulations in legacy simulation codes (e.g., RELAP [52]). Unfortunately, these codes cannot simulate the chemical plant because they lack flexibility, computational speed and adequate algorithms to represent chemical reactions. These problems can be overcome by using equation-based dynamic simulators from the chemical engineering field (e.g., JACOBIAN [35], Aspen Custom Modeler [53], gPROMS [41]). These simulators can easily simulate chemical reactions and they have already been used to simulate the nuclear reactor and PCU

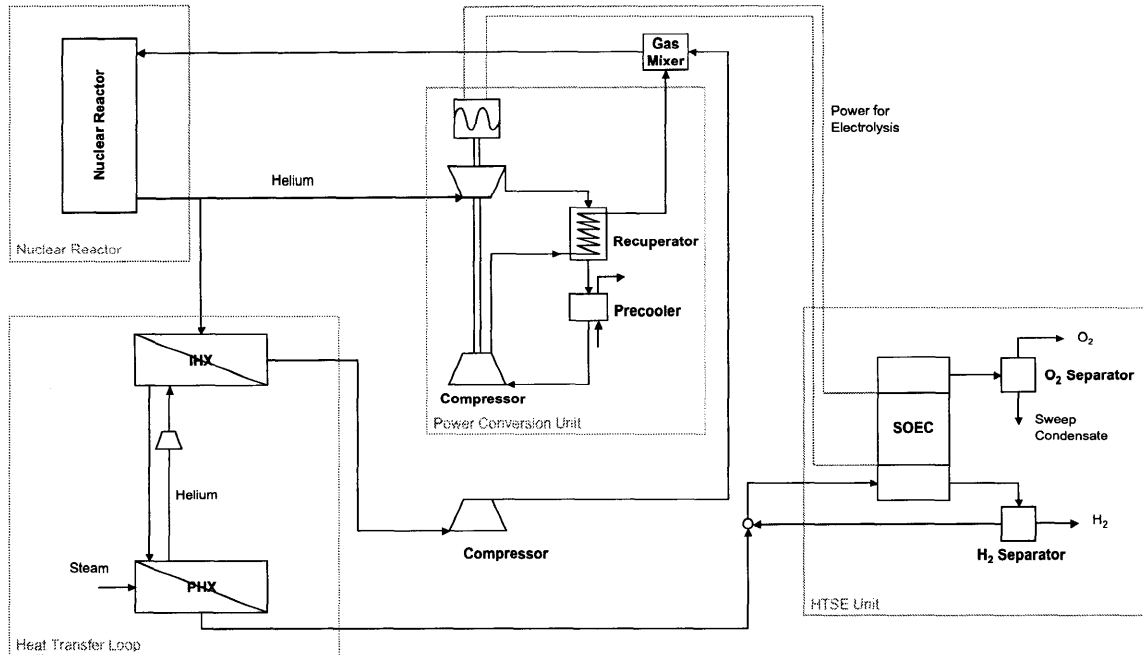


Figure 3-1: Nuclear hydrogen production is an example of novel nuclear applications. The design of the heat transfer loop requires special attention.

[24].

However, the dynamics of the heat transfer loop have not yet been studied in equation-based simulators and its simulation is technically challenging. Several studies have investigated the loop's operating point at steady state [63, 8, 38], but the work on the transient simulation front is not as well developed [59]. In addition, the use of equation-based simulators is not widespread in the nuclear engineering community, which makes finding similar studies even harder. At the same time, the simulation of the heat transfer loop using helium as a heat transfer fluid is difficult, because simulating gas dynamics rigorously involves a complex set of hyperbolic equations [25]. These equations normally require complex algorithms for their numerical integration and it is not clear if equation-based simulators can solve them accurately and efficiently [17].

This chapter, then, proposes a set of models to represent the dynamics of a heat transfer loop in equation-based simulators successfully. First, it explains equation-based simulators and their advantages. Second, it presents a description of the heat

transfer loop, six models to simulate the loop in equation-based simulators, and a reference model created in a legacy code (RELAP). Finally, recommendations concerning the best models are made by evaluating their performance and advantages.

3.2 Using equation-based languages for the simulation of novel nuclear applications

Chemical engineers have to deal routinely with a large number of vastly different processes, which involve chemical reactions, and heat and mass transfer phenomena. To design and optimize these processes, the use of equation-based simulators has become widespread; these simulators are general-purpose-modeling environments for dynamic and steady-state simulation. Such simulators provide a high-level simulation language for the user to describe process models in terms of equations and variables [5]. Then, they solve the equations automatically by using powerful general-purpose numerical algorithms. These simulators and their supporting mathematical theory have been developed over more than 30 years and some examples of them are JACOBIAN [35], Aspen Custom Modeler [53], and gPROMS [41].

Equation-based simulators are ideal to simulate nuclear reactors coupled to chemical plants because they are flexible, extensible, computationally fast and accurate. On the other hand, their use does present some challenges, for formulating large systems of equations that are mathematically correct is not easy. Yet they make these challenges less burdensome by providing error-checking algorithms to address them.

3.2.1 Equation-based simulators provide flexibility, speed and accuracy

Equation-based simulators come with simulation languages that are declarative and hierarchical, which makes them able to incorporate new user-defined models and different processes easily. They also have powerful general-purpose numerical algorithms to simulate any new models, which allow them to solve simulations quickly

and accurately.

A declarative language means the user only needs to input the model as differential-algebraic equations (DAEs) [5]. These languages can represent any physical or chemical system as a system of DAEs [3]:

$$\begin{aligned}\mathbf{f}(\mathbf{x}(t), \dot{\mathbf{x}}(t), \mathbf{y}(t), t) &= \mathbf{0} \\ \mathbf{g}(\mathbf{x}(t), \mathbf{y}(t), t) &= \mathbf{0}\end{aligned}$$

where $\mathbf{x}(t) \in \mathbb{R}^{n_x}$ and $\dot{\mathbf{x}}(t) \in \mathbb{R}^{n_x}$ represent the differential variables (those whose time derivatives appear explicitly in the model) and the time derivatives of these variables, respectively. $\mathbf{y}(t) \in \mathbb{R}^{n_y}$ correspond to the algebraic variables. $\mathbf{f} : \mathbb{R}^{n_x} \times \mathbb{R}^{n_x} \times \mathbb{R}^{n_y} \times \mathbb{R} \rightarrow \mathbb{R}^{n_x}$ are the differential equations, and $\mathbf{g} : \mathbb{R}^{n_x} \times \mathbb{R}^{n_y} \times \mathbb{R} \rightarrow \mathbb{R}^{n_y}$ are the algebraic equations. Although this formulation of DAEs is not the most general one, it is enough to represent most physical and chemical systems. The philosophy of an equation-based simulator is that the process model so defined is completely decoupled from the numerical methods used to solve it, which allows the user focus solely on the model formulation.

Furthermore, declarative simulation languages support hierarchical model decomposition, which greatly simplifies the coding of large models [5]. It allows building models in levels in the same way one would conceptualize a real plant. For example, a first level of simple models can represent basic units (e.g., pipes, heat exchangers, chemical reactors). A second level uses models from the first to represent subsystems (e.g., heat transfer loop). Finally, a third level could incorporate all the subsystems to assemble a plant-wide model. With this approach, lower-level models can be easily tested and corrected in isolation, avoiding hard-to-find errors in higher-level models.

Equally important, equation-based simulators find solutions to simulations quickly and accurately. They assemble the equations from all the different models in one single equation system, which is solved simultaneously by general-purpose codes for root finding and implicit numerical integration. They also exploit the characteristics of the equation system (e.g., sparsity, block decomposition) to accelerate the simulations

and solve 100,000s of equations in minutes. They are accurate too, because their error control is based on theoretical guarantees for consistency and stability, and the error can be controlled automatically.

3.2.2 Simulation challenges in equation-based simulators are minimal and mostly related to initial conditions

Equation-based simulators' flexibility, extensibility and accuracy come from using large DAE systems to represent models and from solving these systems simultaneously. However, this approach forces the user to define the system of equations, initial conditions, and parameters correctly, which is hard to accomplish for large and complex models. To address this difficulty, equation-based simulators use automatic error-checking algorithms to help the user find errors.

These automatic error-checking algorithms help verify that the system of equations is properly posed. As the number of unit operations and the number of equations in a model grow, the user finds it harder to detect missing or unnecessary equations. To assist with this task, algorithms examine the degrees of freedom of the system. This ensures the number of equations (neq) and the number of unknown variables (nev) are equal. Furthermore, sometimes a system with $neq = nev$ might have inconsistent equations (e.g., linearly dependent equations) that can render the equation system infeasible. This problem can often be resolved by algorithms that analyze the structural singularity of the system of equations and reveal the equations with conflicting information [40].

In addition, error-checking algorithms test whether the formulated initial conditions are consistent. Not having consistent initial conditions can lead to failed simulations or results that are nonsense. Normally, finding consistent initial conditions for a simulation is a straightforward task; consider the following system of equations

[30]:

$$\dot{x}_1 = x_1 + x_2 + y, \quad (3.1)$$

$$\dot{x}_2 = x_1 - x_2 - y, \quad (3.2)$$

$$0 = x_1 + 2x_2 - y. \quad (3.3)$$

In this example, $\dot{x}_1(0)$, $\dot{x}_2(0)$, $y(0)$, $x_1(0)$ and $x_2(0)$ are the initial values needed to start the numerical integration for dynamic simulation at $t = 0$. It is simple to calculate them: any two of these variables are assigned initial values by the user and the remaining three are calculated from solving the system of equations at $t = 0$. Equation-based simulators do this automatically, thus guaranteeing that the initial condition of the simulation is consistent.

In a few cases though, error-checking algorithms can struggle to find a consistent set of initial conditions. Consider the system [30]:

$$\dot{x}_1 = x_1 + x_2 + y, \quad (3.4)$$

$$\dot{x}_2 = x_1 - x_2 - y, \quad (3.5)$$

$$0 = x_1 + 2x_2, \quad (3.6)$$

which has a similar form to the system of Eqs. (3.1)-(3.3). However, one cannot assign arbitrary values to any pair of the unknowns as before, because Eq. (3.6) imposes a very strong restriction. For example, one cannot set both $x_1(0)$ and $x_2(0)$ because they are related by Eq. (3.6). The issue is caused by an additional nonredundant “hidden” constraint derived by differentiating Eq. (3.6) with respect to time:

$$0 = \dot{x}_1 + 2\dot{x}_2. \quad (3.7)$$

So, in fact there are four equations relating the initial values of the five variables. One realizes that only one variable can be set by the user before solving for consistent initial conditions. This type of problem is referred to informally as a “high-index

problem,” In general, DAEs are categorized according to their “index” [3] and DAEs with index greater than one will exhibit the following two features:

1. Additional “hidden” constraints on consistent initial conditions, as in the second example above.
2. Dependence of the solution on first and higher-order derivatives of the forcing functions.

In addition, error-controlled numerical integration of DAEs with index greater than one is not possible with standard codes, and correct numerical integration is only possible with highly-specialized algorithms specific to certain problem structures. The first example above is index 1, whereas the second example is index 2.

On the other hand, DAEs of index 1 can be solved reliably with standard codes, and the issue with additional hidden constraints on consistent initial conditions only occurs rarely. Moreover, most models in practical applications are index 1, with higher-index problems arising from modeling errors (which can be corrected) or modeling approximations (which can be relaxed). Since most equation-based simulators only support consistent initialization and numerical integration of index 1 DAEs, they apply an automatic structural analysis to detect high-index problems with the purpose of screening out DAEs with index greater than one. The first example above would pass this test, whereas the second example above would fail the test. Some simulators can provide additional feedback that Eq. (3.6) is causing the high-index problem.

3.3 Modeling the heat transfer loop

Since equation-based simulators are good environments to simulate new nuclear applications, the next step is to use them to model the heat transfer loop. We chose to model a heat transfer loop engineered at the Idaho National Laboratory (INL) [8], because of its well-thought-out design. This heat transfer loop consists of an intermediate heat exchanger (IHX), a process heat exchanger (PHX), a hot leg, a cold leg,

and a compressor (Fig. 3-1). It transfers 50 MWth from the nuclear reactor to the chemical plant, and it has to withstand very high temperatures (up to 900°C) and high pressures (up to 7 MPa) [8]. These challenging conditions require brand new design with new materials and new pieces of equipment.

Researchers at INL determined the following equipment characteristics for the heat transfer loop:

1. The IHX is a compact heat exchanger made of Alloy 617 with 786,560 semi-circular channels of 1.5 mm in diameter. The length of the IHX was 0.988 m and its width was 1.44 m.
2. The PHX is a tube-in-shell heat exchanger with 3,500 circular tubes, and each tube has an internal diameter of 10 mm. High-temperature helium flows on the inside of the tubes and the steam flows on the outside. The length of the exchanger is 8.66 m and its material is Alloy 800.
3. The hot leg and cold leg are pipes of 90 m in length with internal diameters of 0.44 m and 0.41 m, thickness-to-diameter ratio of 0.117 and 0.114, and insulation thickness 59 mm and 58 mm, respectively. Both of them are made of Alloy 800.
4. The compressor should be able to produce a pressure differential of at least 0.4 MPa.

These specifications were used to build the dynamic models for the loop in JACOBIAN—one of the best equation-based simulators available [35]. To confirm the simulation results of this model, a similar model was created using RELAP—a legacy code [8].

3.3.1 Dynamic models in JACOBIAN

The models created in JACOBIAN must contain equations for each physical phenomena considered in the loop. This was done by creating individual models containing these equations for the different parts of the loop: pipes, heat exchangers, and compressor:

1. *Pipe model.* As a first approximation, radial variations inside the pipe can be neglected, and one-dimensional models can be used to represent the gas dynamics. Three models were used for this task, and they were derived from the *Navier-Stokes* equations. The *Navier-Stokes* equations are a realistic approach to represent gas dynamics [25]; they consider mass, momentum and energy balances and they include viscosity, friction and heat transfer effects. However, in the case of pipes filled with helium, kinetic and viscosity terms in the energy equations, and viscosity terms in the momentum equation are negligible. Eliminating those terms produces the following system of equations, which will be termed the *Full Dynamics* model:

$$\text{Continuity} \quad \frac{\partial \rho}{\partial t} = -\frac{\partial \phi}{\partial x}, \quad (3.8)$$

$$\text{Momentum} \quad \frac{\partial \phi}{\partial t} = -\frac{\partial P}{\partial x} - \frac{\partial}{\partial x} \frac{\phi^2}{\rho} - \frac{2f|\phi|\phi}{D\rho}, \quad (3.9)$$

$$\text{Energy} \quad \frac{\partial \psi}{\partial t} = -\frac{\partial}{\partial x} \phi h - \frac{4U(T - T_{Ext})}{D}, \quad (3.10)$$

$$\text{Physical Properties} \quad \psi = \rho h - P, \quad (3.11)$$

$$h = h_{form} + \frac{C_P}{M} (T - T_{stand}), \quad (3.12)$$

$$P = \frac{R_C \rho T}{M}. \quad (3.13)$$

Here ρ is the helium density, ϕ is the mass flux, P is the pressure, ψ is the internal energy, h is the enthalpy, T is the gas temperature, and T_{Ext} is the temperature surrounding the pipe. The parameters are the friction factor f , the diameter of the pipe D , the heat transfer coefficient U , the universal constant R_C , the enthalpy of formation for helium h_{form} , the heat capacity at constant pressure C_P , molecular weight M , and the standard temperature T_{stand} . Note that these equations are actually partial differential-algebraic equations (PDAEs), which can also be categorized according to their index and can exhibit similar issues with consistent initial conditions [29]. On semi-discretization of the spatial derivatives in PDAEs using the method of lines [47] a system of DAEs results.

Simplified versions of these equations were also used, in order to find faster alternative models. The *Full Dynamics* model can represent the fast time scales of gas dynamics, which means some changes in the variables can travel with the speed of sound. This makes the integration of such a model inefficient and inaccurate, because very small time steps are needed to track the variables correctly and artificial oscillations might appear depending on the spatial discretization employed. Fortunately, these fast time scales can be excluded, since the velocity in the loop is below the speed of sound and fast-moving effects become less important. In addition, those time scales are not relevant to the goal of this study, as we are interested in the longer time scale (over 0.5 s) behavior of the coupled system. To eliminate the fast phenomena, we formulated simpler models for the differential equations: the *Zero Mach Number Limit* model and the *Quasi-Steady State (QSS) Approximation* model.

The *Zero Mach Number Limit* model eliminates the accumulation term in the momentum equation [17]:

$$\text{Continuity} \quad \frac{\partial \rho}{\partial t} = -\frac{\partial \phi}{\partial x}, \quad (3.14)$$

$$\text{Momentum} \quad 0 = -\frac{\partial P}{\partial x} - \frac{\partial}{\partial x} \frac{\phi^2}{\rho} - \frac{2f|\phi|\phi}{D\rho}, \quad (3.15)$$

$$\text{Energy} \quad \frac{\partial \psi}{\partial t} = -\frac{\partial}{\partial x} \phi h - \frac{4U(T - T_{Ext})}{D}. \quad (3.16)$$

The *QSS Approximation* model additionally eliminates the accumulation term in the continuity equation:

$$\text{Continuity} \quad 0 = -\frac{\partial \phi}{\partial x}, \quad (3.17)$$

$$\text{Momentum} \quad 0 = -\frac{\partial P}{\partial x} - \frac{\partial}{\partial x} \frac{\phi^2}{\rho} - \frac{2f|\phi|\phi}{D\rho}, \quad (3.18)$$

$$\text{Energy} \quad \frac{\partial \psi}{\partial t} = -\frac{\partial}{\partial x} \phi h - \frac{4U(T - T_{Ext})}{D}. \quad (3.19)$$

The equations in the different models were discretized using a control volume method with a combination of a standard grid and a staggered grid (Fig. (A-1)).

The standard grid divides each section of the loop (cold leg, hot leg, PHX, IHX) into control volumes, which are used to calculate ρ , P , ψ , h and T . The staggered grid divides the loop into control volumes too, but it centers these control volumes at the faces of the control volumes in the standard grid. This grid is used to calculate the flowrate variable F , which replaces the mass flux variable ϕ in the discretized equations ($F = \phi A$; A is the total cross sectional area in pipes or heat exchangers). F is used instead of ϕ because the equations produced in this way are simpler to write and do not lose accuracy. Using this combination of grids generates a system of equations that is more stable to integrate [39]. This approach has been used to simulate gas dynamics in the past [24, 49]. The heat transfer coefficient at each control volume in the standard grid were calculated using the Dittus-Boelter equation according to the specifications from Davis et al. [8].

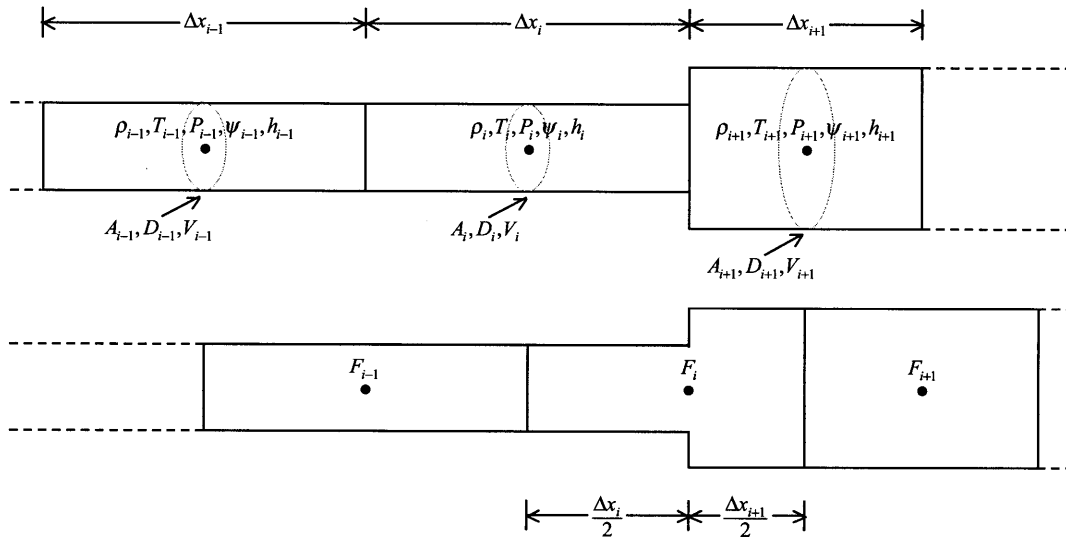


Figure 3-2: Discretizing the gas dynamics equations using combination of standard grid and a staggered grid makes the solution of the system more stable.

The discretized equations are written for the case of a change in cross sectional area in the loop, which is the most difficult case to simulate. The equations so written can also represent the case of constant cross sectional area in the loop. The list of equations is:

- Continuity

$$\Delta x_i A_i \dot{\rho}_i = F_{i-1} - F_i \quad i = 2 \dots N. \quad (3.20)$$

- Momentum

$$\begin{aligned} & \left(\frac{\Delta x_i}{2} + \frac{\Delta x_{i+1}}{2} \right) \dot{F}_i = \\ & - \left(P_{i+1} A_{i+1} - \frac{P_i \frac{\Delta x_{i+1}}{2} + P_{i+1} \frac{\Delta x_i}{2}}{\frac{\Delta x_i}{2} + \frac{\Delta x_{i+1}}{2}} (A_{i+1} - A_i) - P_i A_i \right) \\ & - \left(\frac{\left(\frac{F_i + F_{i+1}}{2} \right)^2}{\rho_{i+1} A_{i+1}} - \frac{\left(\frac{F_{i-1} + F_i}{2} \right)^2}{\rho_i A_i} \right) \\ & - \left(\frac{2f_i}{D_i} \frac{F_i^2}{\rho_i A_i} \frac{\Delta x_i}{2} + \frac{2f_{i+1}}{D_{i+1}} \frac{F_i^2}{\rho_{i+1} A_{i+1}} \frac{\Delta x_{i+1}}{2} \right) \\ & i = 2 \dots N - 1. \end{aligned} \quad (3.21)$$

- Energy

$$\Delta x_i A_i \dot{\psi}_i = - (F_i h_i - F_{i-1} h_{i-1}) - \frac{4U_i}{D_i} (T_i - T_{Ext,i}) \Delta x_i A_i \quad i = 2 \dots N. \quad (3.22)$$

- Algebraic equations

$$\psi_i = \rho_i h_i - P_i \quad i = 1 \dots N, \quad (3.23)$$

$$h_i = h_{form} + \frac{Cp}{M} (T_i - T_{stand}) \quad i = 1 \dots N, \quad (3.24)$$

$$P_i = \frac{R_C \rho_i T_i}{M} \quad i = 1 \dots N. \quad (3.25)$$

Analogous discretizations were used for the *Zero Mach Number Limit* model and for the *QSS Approximation* model.

2. *Compressor model.* At this time, our focus is on the thermal behavior of the heat transfer loop and not on the compressor dynamics. Therefore, the compressor

was represented by a simple adiabatic equation (Eq. (3.26)). In addition, the compressor equations included a mass conservation equation (Eq. (3.27)). This equation forces the mass flow entering the compressor to be the same as that leaving it:

$$\left(\frac{P_{In}}{P_{Out}}\right)^{\gamma-1} = \left(\frac{T_{In}}{T_{Out}}\right)^{\gamma}, \quad (3.26)$$

$$A_{In}\phi_{In} = A_{Out}\phi_{Out}. \quad (3.27)$$

These equations not only define the compressor, but they also define the coupling conditions for the boundary variables of the previous pipe model when used to model the loop. Two combinations of boundary conditions were used to write the coupling conditions.

The first combination of boundary conditions consists of the pressure and temperature at the left boundary and the pressure at the right boundary (P_{In} , T_{In} , P_{Out}) (Fig. 3-3). The pressure as a boundary condition at the left is normally used in the simulation of fluid dynamics [27]. In this case, the flow in the compressor was regulated by specifying the pressure differential in the compressor ($\Delta P(t)$). This approach was used for the loop and for the external pipes in heat exchangers. In addition, two extra control volumes were inserted after the compressor to model the effects of the change in cross sectional area at the compressor. These control volumes are frictionless, adiabatic and short (1 cm); therefore, they do not alter the simulation.

The differential equations that represent these coupling conditions are:

$$\Delta x_{Aux} A_N \dot{\rho}_{Aux,1} = (F_{In} - F_{Aux,1}), \quad (3.28)$$

$$\Delta x_{Aux} A_N \dot{\rho}_{Aux,2} = (F_{Aux,1} - F_{Aux,2}), \quad (3.29)$$

$$\Delta x_1 A_1 \dot{\rho}_1 = (F_{Aux,2} - F_1), \quad (3.30)$$

$$\frac{\Delta x_{Aux}}{2} \dot{F}_{In} = - (P_{Aux,1} A_N - P_{In} A_N)$$

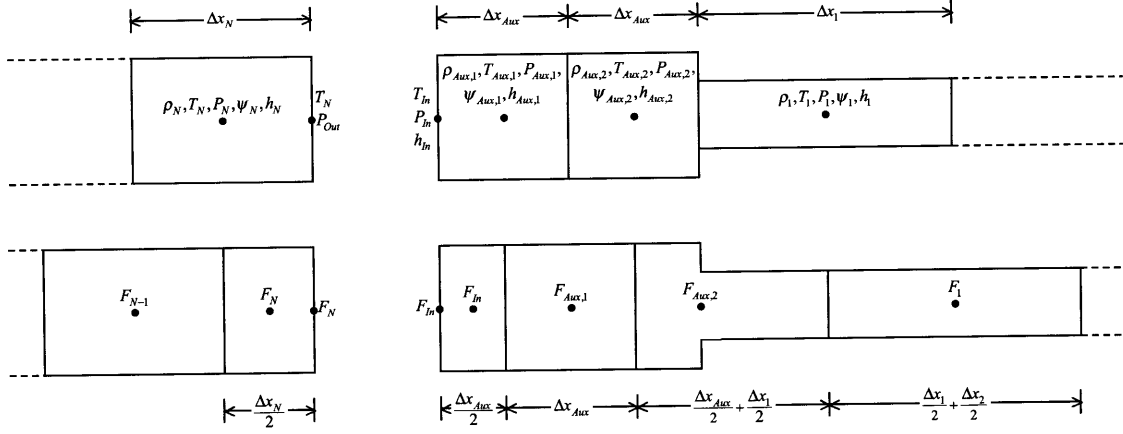


Figure 3-3: One approach to set the boundary variables; it uses P_{In} as suggested in the literature [27].

$$- \left(\frac{\left(\frac{F_{In} + F_{Aux,1}}{2} \right)^2}{\rho_{Aux,1} A_N} - \frac{F_{In}^2}{\rho_{Aux,1} A_N} \right), \quad (3.31)$$

$$\begin{aligned} \Delta x_{Aux} \dot{F}_{Aux,1} = & - (P_{Aux,2} A_N - P_{Aux,1} A_N) \\ & - \left(\frac{\left(\frac{F_{Aux,1} + F_{Aux,2}}{2} \right)^2}{\rho_{Aux,2} A_N} - \frac{\left(\frac{F_{In} + F_{Aux,1}}{2} \right)^2}{\rho_{Aux,1} A_N} \right), \end{aligned} \quad (3.32)$$

$$\begin{aligned} \left(\frac{\Delta x_{Aux,1}}{2} + \frac{\Delta x_1}{2} \right) \dot{F}_{Aux,2} = & - P_1 A_1 + \frac{P_{Aux,2} \frac{\Delta x_1}{2} + P_1 \frac{\Delta x_{Aux}}{2}}{\frac{\Delta x_{Aux}}{2} + \frac{\Delta x_1}{2}} (A_1 - A_N) \\ & + P_{Aux,2} A_N \\ & - \left(\frac{\left(\frac{F_{Aux,2} + F_1}{2} \right)^2}{\rho_1 A_1} - \frac{\left(\frac{F_{Aux,1} + F_{Aux,2}}{2} \right)^2}{\rho_{Aux,2} A_N} \right) \\ & - \frac{2f_1 F_{Aux,2}^2 \Delta x_1}{D_1 \rho_1 A_1 2}, \end{aligned} \quad (3.33)$$

$$\begin{aligned} \left(\frac{\Delta x_1}{2} + \frac{\Delta x_2}{2} \right) \dot{F}_1 = & - \left(P_2 A_2 - \frac{P_1 \frac{\Delta x_2}{2} + P_2 \frac{\Delta x_1}{2}}{\frac{\Delta x_1}{2} + \frac{\Delta x_2}{2}} (A_2 - A_1) - P_1 A_1 \right) \\ & - \left(\frac{\left(\frac{F_1 + F_2}{2} \right)^2}{\rho_2 A_2} - \frac{\left(\frac{F_{Aux,2} + F_1}{2} \right)^2}{\rho_1 A_1} \right) \\ & - \frac{2f_1 F_1^2 \Delta x_1}{D_1 \rho_1 A_1 2} - \frac{2f_2 F_1^2 \Delta x_2}{D_2 \rho_2 A_2 2}, \end{aligned} \quad (3.34)$$

$$\begin{aligned} \frac{\Delta x_N}{2} \dot{F}_N &= - (P_{Out} A_N - P_N A_N) \\ &\quad - \left(\frac{F_N^2}{\rho_N A_N} - \frac{\left(\frac{F_{N-1} + F_N}{2} \right)^2}{\rho_N A_N} \right) \\ &\quad - \frac{2f_N}{D_N} \frac{F_N^2}{\rho_N A_N} \frac{\Delta x_N}{2}, \end{aligned} \quad (3.35)$$

$$\Delta x_{Aux} A_N \dot{\psi}_{Aux,1} = - (F_{Aux,1} h_{Aux,1} - F_{In} h_{In}), \quad (3.36)$$

$$\Delta x_{Aux} A_N \dot{\psi}_{Aux,2} = - (F_{Aux,2} h_{Aux,2} - F_{Aux,1} h_{Aux,1}), \quad (3.37)$$

$$\Delta x_1 A_1 \dot{\psi}_1 = - (F_1 h_1 - F_{Aux,2} h_{Aux,2}). \quad (3.38)$$

The algebraic equations that represent these coupling conditions are:

$$h_{In} = h_{form} + \frac{Cp}{M} (T_{In} - T_{stand}), \quad (3.39)$$

$$F_{In} = F_N, \quad (3.40)$$

$$\Delta P(t) = P_{In} - P_{Out}, \quad (3.41)$$

$$\left(\frac{T_{In}}{T_N} \right)^\gamma = \left(\frac{P_{In}}{P_{Out}} \right)^{\gamma-1}. \quad (3.42)$$

The second combination of boundary conditions used was similar, but it transformed the differential variable F_{In} into an algebraic variable by eliminating its corresponding control volume in the staggered grid. In addition, P_{In} was replaced by $P_{Aux,1}$ as boundary condition (Fig. 3-4). This combination of coupling conditions was used only in the loop.

The differential equations that represent these coupling conditions are:

$$\Delta x_{Aux} A_N \dot{\rho}_{Aux,1} = (F_{In} - F_{Aux,1}), \quad (3.43)$$

$$\Delta x_{Aux} A_N \dot{\rho}_{Aux,2} = (F_{Aux,1} - F_{Aux,2}), \quad (3.44)$$

$$\Delta x_1 A_1 \dot{\rho}_1 = (F_{Aux,2} - F_1), \quad (3.45)$$

$$\left(\Delta x_{Aux} + \frac{\Delta x_{Aux}}{2} \right) \dot{F}_{Aux,1} = - (P_{Aux,2} A_N - P_{Aux,1} A_N)$$

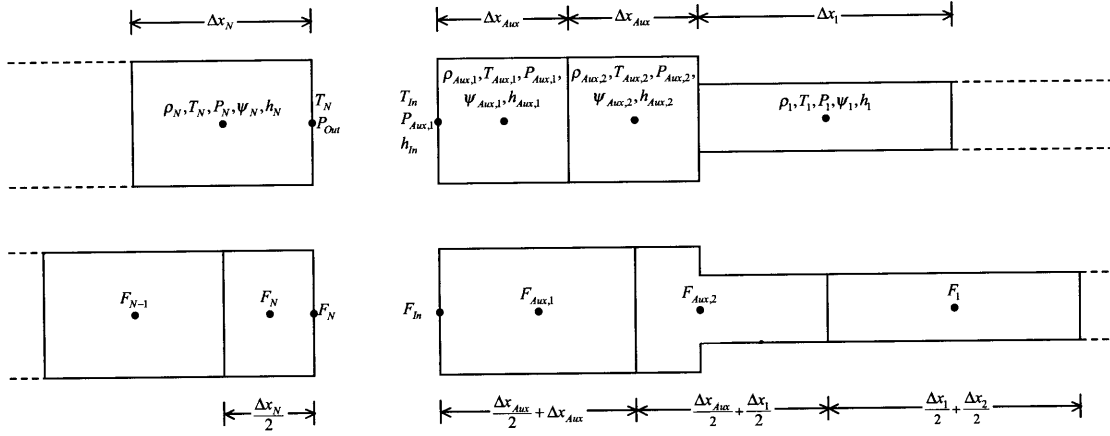


Figure 3-4: Alternative approach to set the boundary conditions for a gas dynamics model; it replaces the specification on P_{In} with $P_{Aux,1}$.

$$- \left(\frac{\left(\frac{F_{Aux,1} + F_{Aux,2}}{2} \right)^2}{\rho_{Aux,2} A_N} - \frac{F_{In}^2}{\rho_{Aux,1} A_N} \right), \quad (3.46)$$

$$\begin{aligned} \left(\frac{\Delta x_{Aux}}{2} + \frac{\Delta x_1}{2} \right) \dot{F}_{Aux,2} = & - P_1 A_1 + \frac{P_{Aux,2} \frac{\Delta x_1}{2} + P_1 \frac{\Delta x_{Aux}}{2}}{\frac{\Delta x_{Aux}}{2} + \frac{\Delta x_1}{2}} (A_1 - A_N) \\ & + P_{Aux,2} A_N \\ & - \left(\frac{\left(\frac{F_{Aux,2} + F_1}{2} \right)^2}{\rho_1 A_1} - \frac{\left(\frac{F_{Aux,1} + F_{Aux,2}}{2} \right)^2}{\rho_{Aux,2} A_N} \right) \\ & - \frac{2f_1 F_{Aux,2}^2 \Delta x_1}{D_1 \rho_1 A_1 2}, \end{aligned} \quad (3.47)$$

$$\begin{aligned} \left(\frac{\Delta x_1}{2} + \frac{\Delta x_2}{2} \right) \dot{F}_1 = & - \left(P_2 A_2 - \frac{P_1 \frac{\Delta x_2}{2} + P_2 \frac{\Delta x_1}{2}}{\frac{\Delta x_1}{2} + \frac{\Delta x_2}{2}} (A_2 - A_1) - P_1 A_1 \right) \\ & - \left(\frac{\left(\frac{F_1 + F_2}{2} \right)^2}{\rho_2 A_2} - \frac{\left(\frac{F_{Aux,2} + F_1}{2} \right)^2}{\rho_1 A_1} \right) \\ & - \frac{2f_1 F_1^2 \Delta x_1}{D_1 \rho_1 A_1 2} - \frac{2f_2 F_1^2 \Delta x_2}{D_2 \rho_2 A_2 2}, \end{aligned} \quad (3.48)$$

$$\begin{aligned} \frac{\Delta x_N}{2} \dot{F}_N = & - (P_{Out} A_N - P_N A_N) \\ & - \left(\frac{F_N^2}{\rho_N A_N} - \frac{\left(\frac{F_{N-1} + F_N}{2} \right)^2}{\rho_N A_N} \right) \end{aligned}$$

$$-\frac{2f_N}{D_N} \frac{F_N^2}{\rho_N A_N} \frac{\Delta x_N}{2}, \quad (3.49)$$

$$\Delta x_{Aux} A_N \dot{\psi}_{Aux,1} = - (F_{Aux,1} h_{Aux,1} - F_{In} h_{In}), \quad (3.50)$$

$$\Delta x_{Aux} A_N \dot{\psi}_{Aux,2} = - (F_{Aux,2} h_{Aux,2} - F_{Aux,1} h_{Aux,1}), \quad (3.51)$$

$$\Delta x_1 A_1 \dot{\psi}_1 = - (F_1 h_1 - F_{Aux,2} h_{Aux,2}). \quad (3.52)$$

The algebraic equations that represent these coupling conditions are:

$$h_{In} = h_{form} + \frac{C_p}{M} (T_{In} - T_{stand}), \quad (3.53)$$

$$F_{In} = F_N, \quad (3.54)$$

$$\Delta P(t) = P_{Aux,1} - P_{Out}, \quad (3.55)$$

$$\left(\frac{T_{In}}{T_N} \right)^\gamma = \left(\frac{P_{Aux,1}}{P_{Out}} \right)^{\gamma-1}. \quad (3.56)$$

Analogous coupling conditions were used for the *Zero Mach Number Limit* model and for the *QSS Approximation* model. In the case of the *QSS Approximation* model, the equation forcing mass conservation at the compressor (Eq. (3.54)) can be derived from the continuity equations, which produces an under determined system of equations. To eliminate this issue an equation forcing mass conservation was implemented: $\sum_{i=1}^N \rho_i A_i \Delta x_i = M(t)$, where $M(t)$ is the total mass of helium in the loop. This new user-specified variable, $M(t)$, is constant in most of the simulations, except in the case when helium leaks in the loop are simulated.

The combination of the three gas dynamics models and the two sets of boundary conditions led to six possible models for the heat transfer loop.

3. *Heat exchanger model.* The heat exchangers are represented by a thermal model for the metal structure (Eq. (3.57)) and by two pipe models—as the ones mentioned above. The thermal model accounts for the thermal inertia of the heat exchanger and considers conduction in the axial direction. This model assumes

that heat losses are negligible. The equations in this model are discretized using a control volume formulation and a centered difference scheme. Each one of the control volumes has two corresponding control volumes in the pipe models (a hot pipe and a cold pipe) for the heat exchange.

$$c_{Metal}\rho_{Metal}\frac{\partial T_{Metal}}{\partial t} = \frac{\partial}{\partial x} \left(k \frac{\partial T_{Metal}}{\partial x} \right) + Q_{ToColdPipe} - Q_{FromHotPipe} \quad (3.57)$$

After creating the individual modules for all these units, they were assembled to create a model of the full heat transfer loop. Six different heat transfer loop models were created from the combination of three types of pipe models and two combinations of boundary conditions. In these models, the IHX and PHX models used 40 control volumes for the discretization, and the hot and cold legs connecting the heat exchangers used 10. The models so built consisted of 1,550 equations and variables.

3.3.2 RELAP model for comparison

We created a similar model for the heat transfer loop in RELAP [52], in order to have a good reference for comparison with the equation-based model. RELAP is a powerful simulator used to study thermal hydraulics and accidents in nuclear reactors. Because it cannot include chemical reactions easily, it cannot simulate a nuclear reactor coupled to a chemical plant. However, its basic elements are more than enough to represent the heat transfer loop studied in this chapter (Fig. 3-5). In particular, the heat transfer loop can be represented by a combination of heat structures, pipe components and junction components. The compressor is represented as a junction, whose flowrate is specified directly. A similar heat transfer loop model in RELAP had already been created by Davis et al. [8]; this model used molten salt as the heat transfer fluid. This model was used as a base for the RELAP model in this study.

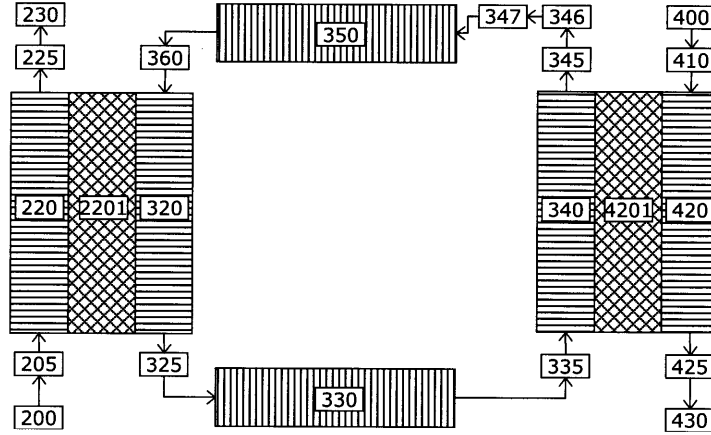


Figure 3-5: RELAP model used to benchmark JACOBIAN models.

3.4 Model Performance Evaluation

The heat transfer loop models from the previous section were tested for feasibility, accuracy and speed. The goal of running these tests is to find the models that can provide an accurate simulation of the heat transfer loop over the interesting time scales (greater than 0.5 s).

3.4.1 Test 1: Feasibility and steady-state profiles

The first step to evaluate the models is to show that the corresponding systems of equations are consistent and that the models can match the designed operating point. To do the former we used the error-checking tools included in JACOBIAN, and to do the latter we compared JACOBIAN's steady-state profiles to RELAP's.

JACOBIAN's error-checking tools revealed that for the loop Eqs. (3.28)-(3.42) were an incorrect choice of coupling conditions, whereas Eqs. (3.43)-(3.56) were the right one. As mentioned before, consistent initial conditions are needed to start numerical integration of this kind of model and to produce reliable results. Unfortunately, using Eqs. (3.28)-(3.42) as coupling conditions for the loop created an inconsistent system of equations for the calculation of initial conditions. This meant that one of the equations was inconsistent and incompatible with the rest of the system. On the other hand, using Eqs. (3.43)-(3.56) as boundary conditions for the loop

did not create this problem.

A high-index problem with a hidden constraint explains the issue caused by using Eqs. (3.28)-(3.42) as coupling conditions for the loop. The system of equations for the loop created by the combination of the semi-discretized version of the *Full Dynamics* model (Eqs. (3.20)-(3.25)) and the coupling conditions (Eqs. (3.28)-(3.42)) can be written as a semi-explicit DAE system:

$$\dot{\mathbf{x}}(t) = \mathbf{f}(\mathbf{x}(t), \mathbf{y}(t), t), \quad (3.58)$$

$$\mathbf{g}(\mathbf{x}(t), \mathbf{y}(t), t) = \mathbf{0}. \quad (3.59)$$

A semi-explicit DAE system is index 1 if and only if $\frac{\partial \mathbf{g}}{\partial \mathbf{y}}$ is nonsingular. Closer examination shows that the equation forcing mass conservation (Eq. (3.40)) at the compressor is the one conflicting with the rest of the equations:

$$F_{In} = F_N.$$

In this case, F_{In} and F_N are both differential variables on the grid shown in Fig. 3-3, which means that $\frac{\partial \mathbf{g}}{\partial \mathbf{y}}$ has a zero row from Eq. (3.40). Therefore, the system of equations for the loop is high-index and cannot be solved with standard codes.

On the other hand, using Eqs. (3.43)-(3.56) as coupling conditions does not generate this problem. When using Eqs. (3.43)-(3.56) as coupling conditions on the grid shown in Fig. 3-4, the equation forcing mass conservation does not create a high-index problem because F_{In} is an algebraic variable and not a differential one. Then, $\frac{\partial \mathbf{g}}{\partial \mathbf{y}}$ is nonsingular and the system of equations for the loop is index 1. Consequently, only the JACOBIAN models using this set of coupling conditions are used in the following tests.

Next, we simulated the plant's designed steady-state operating point using the JACOBIAN and RELAP models and we confirmed that the resulting variable profiles matched. The operating point has been calculated by Davis et al. [8] using lumped models. It consists of a heat transfer loop operating at a pressure of 2.0 MPa, with

a flow of 27.5 kg/s, a maximum temperature of 885°C at the outlet of the IHX and a minimum temperature of 460°C at the outlet of the PHX. The hot stream in the IHX–nuclear reactor coolant–enters at 900°C and 7.0 MPa, and leaves at 6.95 MPa. The cold stream of the PHX–steam–enters at 341°C and 1.0 MPa and leaves at 850°C. We implemented these conditions in the JACOBIAN and RELAP models.

Under these conditions, the pressure and temperature profiles calculated by RELAP and JACOBIAN agreed with some small differences (Figs. 3-6 and 3-7). These differences appear because JACOBIAN models and the RELAP model use different equations to represent the physical properties of helium and the heat structures in the loop (friction factors, heat transfer factors, and equation of state for helium). Overall, RELAP’s and JACOBIAN’s steady-states profiles are similar enough that they can be used as a starting point for the comparison of their dynamic behavior.

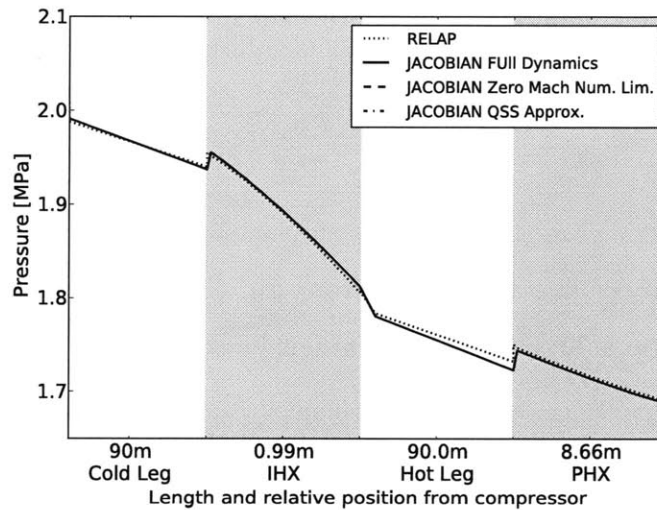


Figure 3-6: Heat transfer loop’s pressure profiles at steady state in JACOBIAN match RELAP’s profiles with small differences.

3.4.2 Test 2: Dynamic simulation profiles

The next step is to understand if JACOBIAN models can reproduce the dynamics of the heat transfer loop accurately. In particular, we are interested in understanding how fast the models respond to changes in the system. To do this, we simulated the models at the operating points calculated in the previous section, and then we

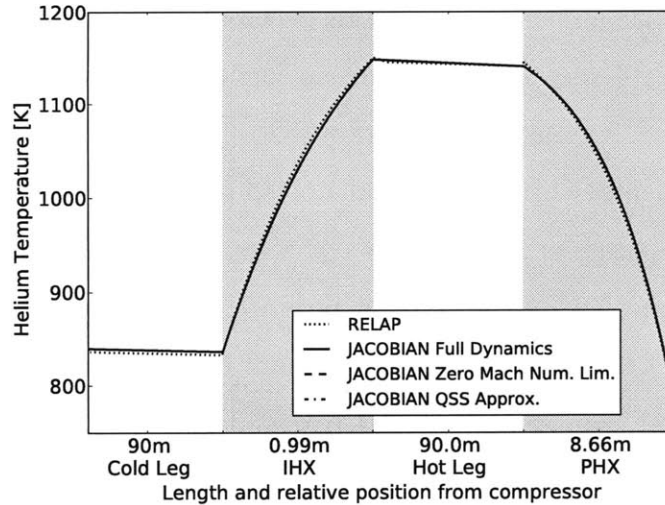


Figure 3-7: Heat transfer loop's temperature profiles at steady state in JACOBIAN match RELAP's profiles with small differences.

introduced fast changes in some variables. The first transient was a linear decrease in the PHX's inlet pressure over 0.2 s that produced a 50% decrease in cold stream flowrate, to simulate a heat sink capacity loss in the chemical plant. The second transient was a linear increase in the pressure differential at the compressor over 0.2 s that generated a 10% increase in the loop's gas flow, to study how the sudden change in pressure propagates around the loop.

A 50% decrease in the PHX's cold stream flowrate can illustrate how the heat transfer loop responds to disruptions in the chemical plant. The chemical plant behavior can have unexpected consequences for the nuclear reactor; understanding how the loop performs in these situations will help guarantee the safety of the system. In particular, process disruptions in the chemical plant will produce a loss of its heat sink capacity and this might lead to an increase in the nuclear reactor temperature. One way to illustrate this loss of heat sink capacity is to decrease the flowrate in the PHX's cold stream. This was represented by using a linear decrease in pressure at the inlet of the PHX that produced a 50% decrease in the flowrate, and it was implemented in the JACOBIAN and RELAP models. The time span of the pressure change was 0.2 s.

To compare the models' dynamic responses in JACOBIAN and RELAP, scaled

profiles of temperature and pressure had to be used (Figs. 3-9 and 3-10). RELAP is designed to simulate very fast transients in nuclear reactors and it does not use rigorous error control for mass conservation [52]. Thus, the mass in the loop can change during transients, which produces distorted pressure and temperature profiles that cannot be compared to JACOBIAN's profiles. For example, after introducing a 50% decrease in the PHX's cold stream flowrate, the mass in the loop decreased almost 4% (Fig. 3-8). In this simulation, the total helium mass at $t = 0$ s is greater in the RELAP model than in the JACOBIAN models (Fig. 3-8) because this model requires additional control volumes to connect the different components in the loop (i.e., to connect the cold leg to the IHX).

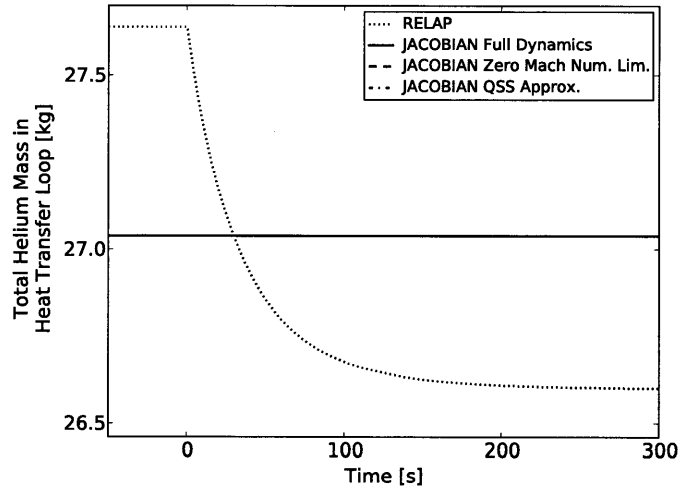


Figure 3-8: The heat transfer loop's total helium mass decreases in RELAP after introducing 50% decrease in PHX's cold stream inlet flowrate.

The three JACOBIAN models and the RELAP model responded in the same time scale to the 50% decrease in the PHX's cold stream flowrate, but their final steady states differed. To study this response we tracked the pressure and temperature of helium in the heat transfer loop at the outlet of the PHX. This point is the closest to the cold stream's inlet and it should experience the largest and fastest temperature change. Thus, it can show how quickly the system can respond when the linear pressure change is introduced at $t = 0.0$ s. The scaled pressure and temperature profiles (Figs. 3-9 and 3-10) at this point are almost identical for the three JACOBIAN

models and for the RELAP model. At the same time, these profiles are smooth, in contrast to the fast linear change originally introduced. This occurs because the heat conduction between the two PHX streams introduces a lag in the heat transfer. However, the final temperature and pressure at this point after 300 s in the RELAP model's result were lower from those in the JACOBIAN models' results. This is explained by the loss of helium mass in RELAP.

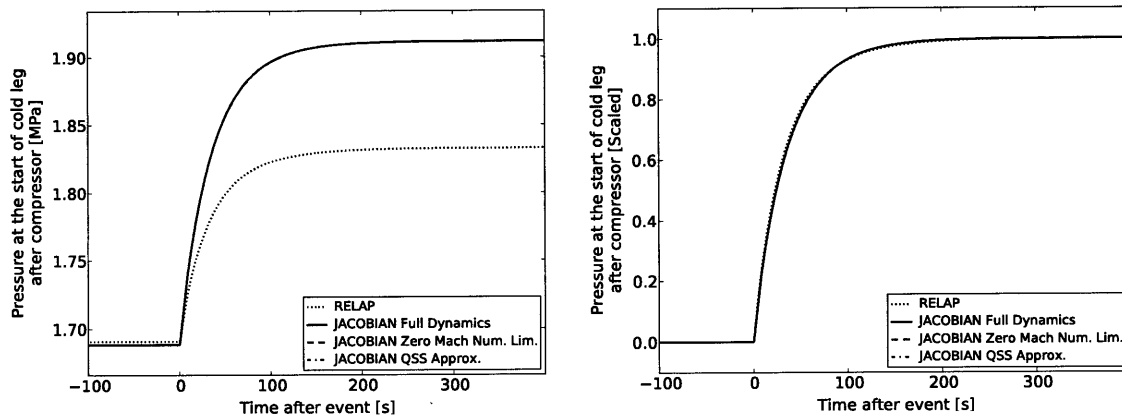


Figure 3-9: Pressure of helium in the loop at the end of the PHX after a 50% decrease in PHX's cold stream flowrate. RELAP simulation reaches a lower pressure than that in JACOBIAN simulations because of RELAP's numerical error in mass conservation; however, RELAP and JACOBIAN models respond with the same speed to the step change.

A more demanding scenario is to introduce an increase of 10% in the flowrate inside the heat transfer loop. Introducing such a change can show the differences in the responses of the different models more clearly, because it directly changes the conditions of the gas inside the heat transfer loop. Additionally, this kind of change does not face the smoothing effects of intermediate units (i.e., PHX) as in the previous scenario. The change in flowrate at the compressor was represented as a linear increase in $\Delta P(t)$ in the JACOBIAN models and as a linear increase in the flowrate in the RELAP model. The time span of the change was 0.2 s, pressure and temperature of helium were tracked at the outlet of the compressor.

A step change in the variables would be an even more demanding scenario. This was not used because JACOBIAN models are simplified representations of gas dy-

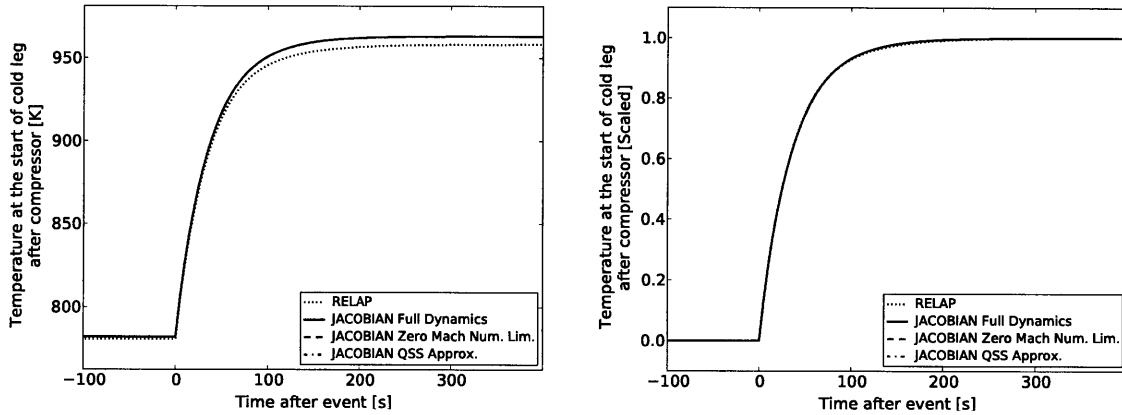


Figure 3-10: Temperature of helium in the loop at the end of the PHX after a 50% decrease in PHX's cold stream flowrate. RELAP simulation reaches a lower temperature than that in JACOBIAN simulations because of RELAP's numerical error in mass conservation; however, RELAP and JACOBIAN models respond with the same speed to the step change.

namics and lack the features to track fast pressure waves generated in such a scenario. Thus, the simulation of a step change in pressure makes the simulator fail or produces results that are physically incorrect. However, this is not an issue because strict step changes in pressure are not expected as accidents and because JACOBIAN models are designed to represent slower transients (those with a time span of over 1.0 s).

The increase of 10% in the flowrate of the heat transfer loop produces pressure and temperature profiles that change with similar time scales in all the models. Yet again, the the final steady state generated by the RELAP simulation differs from those produced by the JACOBIAN simulations because of the numerical errors in RELAP (Figs. 3-11 and 3-12). The pressure takes 53 s to achieve 90% of its final increase and the temperature takes 60 s to do the same.

However, the models perform differently during the first second after the change in pressure/flowrate is introduced (Figs. 3-13 and 3-14). The RELAP model's profiles for pressure and temperature present oscillations which result from RELAP's ability to simulate pressure waves in the gas. The JACOBIAN *Full Dynamics* model produces small and distorted oscillations. This occurs because the method of lines used to represent to the partial differential equations is not enough to track the pressure

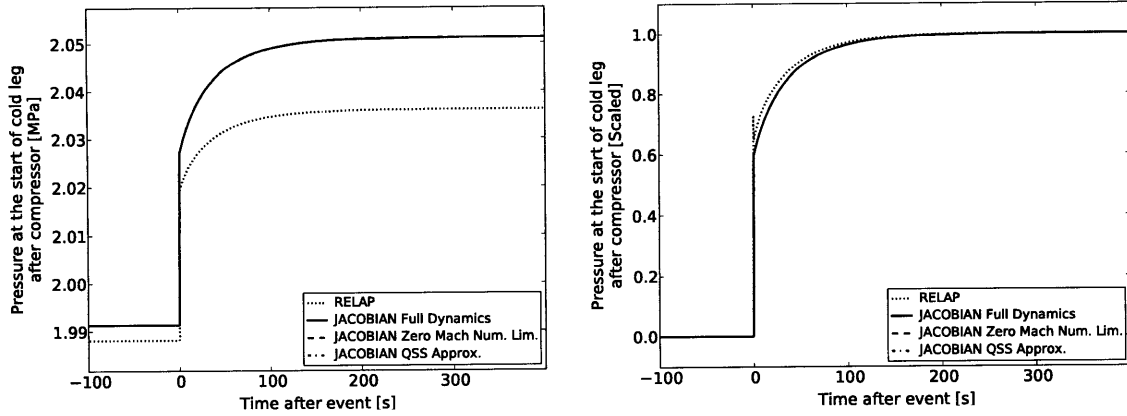


Figure 3-11: Pressure of helium in loop at the outlet of the compressor; the time scale of the response to a change in the compressor is similar again in the four models, but it differs during the first second of the transient. RELAP’s numerical errors in mass conservation affect the final steady state.

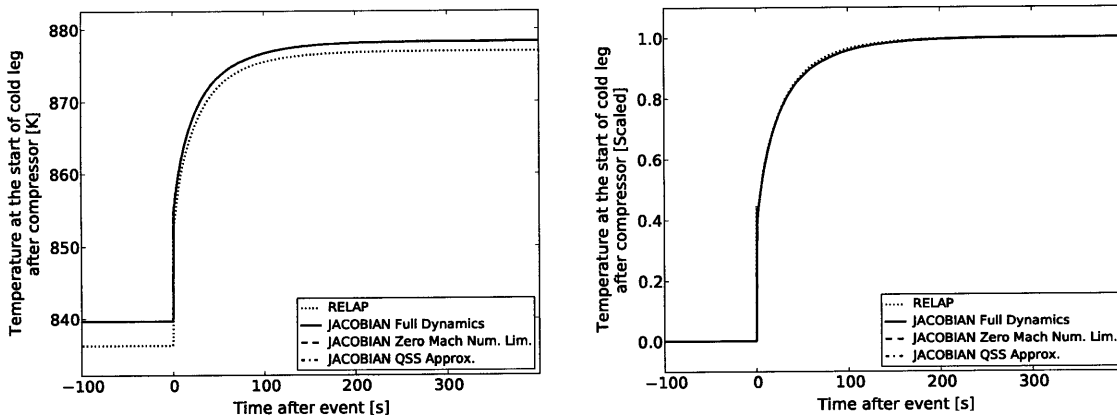


Figure 3-12: Temperature of helium in loop at the outlet of the compressor; the response to a change in the compressor is similar again in the four models, but it differs during the first second of the transient. RELAP’s numerical errors in mass conservation again affect the final steady state.

waves in the gas. On the other hand, the JACOBIAN *Zero Mach Number Limit* model and the *QSS Approximation* model produce a profiles without oscillations in pressure and temperature. These models eliminate the fast time scales in the gas dynamics that create the oscillations, but they are still accurate after 0.5 s.

From this analysis, the *Zero Mach Number Limit* model and the *QSS Approximation* model emerge as the best JACOBIAN models to simulate the heat transfer loop. As mentioned earlier, the purpose of formulating these models is to create a model of a nuclear reactor coupled to a hydrogen production plant. Such a model will allow

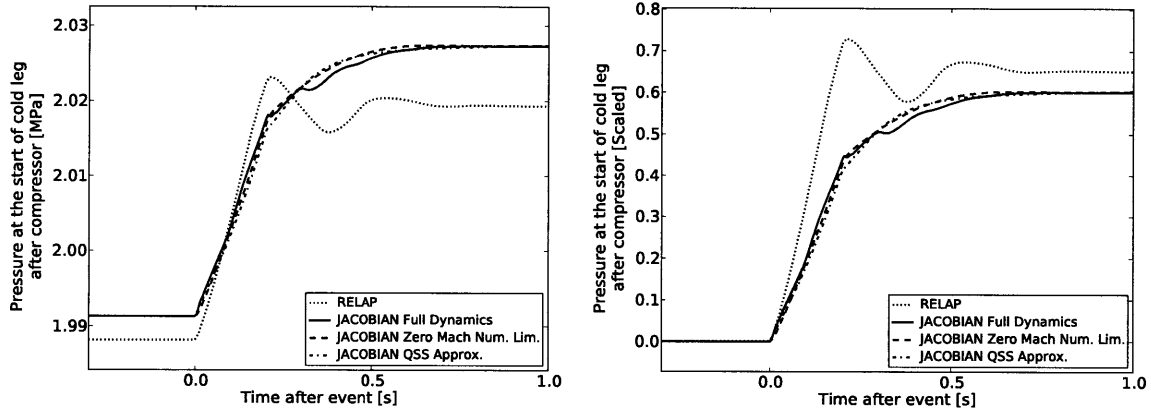


Figure 3-13: The RELAP model’s pressure profile presents oscillations during the first 0.5 s of the transient because of pressure wave effects in the helium. The simplifications used in the JACOBIAN models distort or eliminate these oscillations.

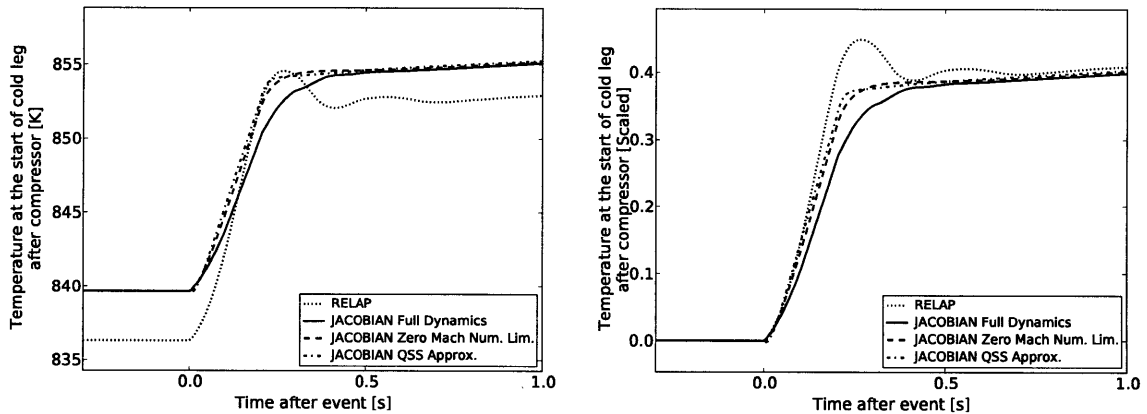


Figure 3-14: The RELAP model’s temperature profile presents oscillations during the first 0.5 s of the transient because of pressure wave effects in the helium. The simplifications used in the JACOBIAN models distort or eliminate these oscillations.

simulating scenarios such as system start-up or the system behavior after a disruption in the chemical plant. These scenarios happen over time-scales of more than 1.0 s, and the behavior of the model before this time is not so relevant. Then a good heat transfer loop model is a model that behaves reasonably well during the first second of the transient and is accurate afterwards. The *Zero Mach Number Limit* model and the *QSS Approximation* model satisfy these conditions.

3.4.3 Test 3: Computational time

Tests so far have shown two of the JACOBIAN models to be feasible and accurate in the relevant time scales; CPU times required for simulations show that they are fast too. Simulating 160 s of simulation time for the step change in the compressor (10 s before step change and 150 s after it) can be more to 25 times faster in JACOBIAN than in RELAP. The *Full Dynamics* model takes 3 min and 25 s, the *Zero Mach Number Limit* model takes 3 min and 20 s, and the *QSS Approximation* model takes 3 min 7 s. In contrast, the RELAP model takes 86 min and 55 s (Fig. 3-15). The simulations were run using JACOBIAN v. 4.0 and RELAP v. 2.3.6 on a Windows virtual machine supported by VMWare Fusion v. 2.6 on Mac OS X v. 10.5.8. The system used was an Apple MacBook with 2.0 GHz Intel Core 2 Duo processors and 4 GB of memory.

These performance difference is explained by how RELAP and JACOBIAN were designed. On the one hand, RELAP was designed to simulate light-water reactor coolant systems, and it is particularly good at simulating two-phase systems. In order to do this, RELAP involves complex tailored numerical schemes, which increase calculation time. On the other hand, JACOBIAN is flexible and allows simulating only the necessary models. In addition, JACOBIAN uses state-of-the-art stiff numerical integration algorithms. The combination of all these characteristics makes JACOBIAN faster.

3.5 Conclusions

The proposed models in this chapter show that it is possible to simulate the heat transfer loop in an equation-based simulator such as JACOBIAN. The models represented the loop's steady state at the designed operating point and they simulated the loop's dynamics during different transient scenarios. They did all this with similar accuracy as the models in RELAP (during relevant time scales), but additionally they were faster and better at mass conservation.

The proposed models and this study are limited and can be improved, yet their

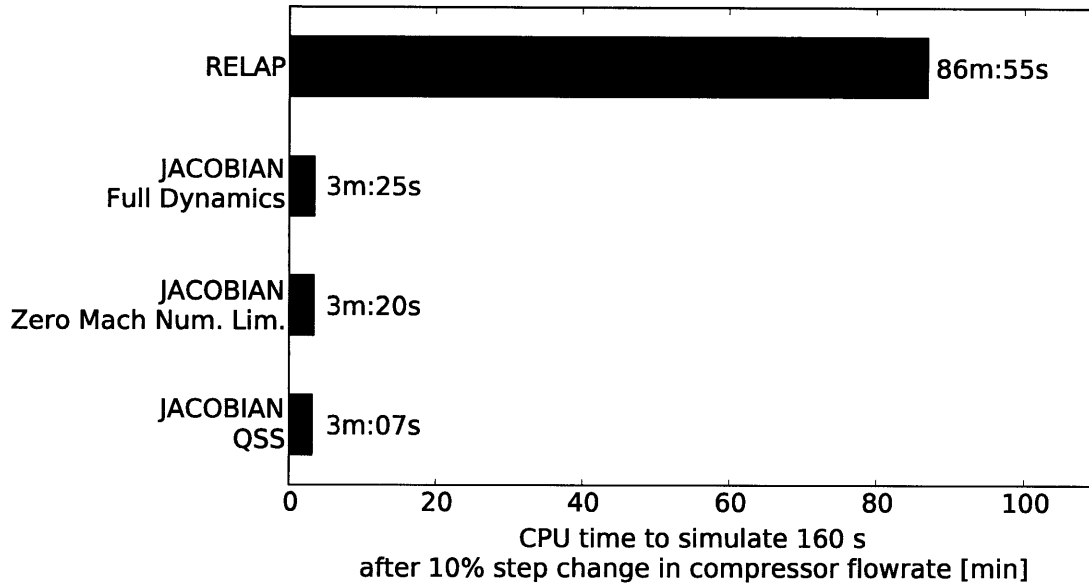


Figure 3-15: Heat transfer loop simulations in JACOBIAN are more than 10 times faster than corresponding simulations in RELAP.

implications are still valid. First, it is hard to show that JACOBIAN models will agree with RELAP models in all situations, and our set of test scenarios was restricted. Nevertheless, we believe that the scenarios simulated using fast changes in key variables give a good estimate of the model’s behavior. Second, a more sophisticated compressor model could make the simulation more realistic. However, this is not necessary for this study, as this work’s main goal was to show that gas dynamics over relevant time scales can be simulated effectively and we achieved that. Third, a different finite difference scheme could be used to discretize the partial derivatives in space. This would help to better track the waves and transients during the first 0.5 s after a change in the system is introduced in the *Full Dynamics* model.

Creating these models has a long-term goal, which is to propose equation-based simulators as an approach to simulate alternative nuclear applications. Equation-based simulators can comfortably incorporate these new processes, because they are modular, extendable and flexible platforms. They can also be easily audited by regulators, because they are open and declarative modelling environments. They are also faster and more precise than legacy codes because of the fast and accurate

algorithms they use for integration. For these reasons, equation-based simulators are a good choice to prove the safety and reliability of new nuclear applications, and hopefully their use will be included in future developments.

Chapter 4

Transient analysis of a nuclear hydrogen production facility

4.1 Introduction

As explained in Chapter 2, nuclear hydrogen production is a promising alternative to reduce CO₂ emissions associated to hydrogen production using traditional methods. Hydrogen is a very important commodity used for oil refining and chemicals production. Currently, its production releases 1% of the CO₂ produced in the U.S. because steam methane reforming is the predominant technology. These emissions can be eliminated by powering hydrogen production from water with a nuclear reactor. This system consists of a nuclear reactor, a heat transfer loop and a chemical plant. The nuclear reactor generates heat and electricity, and the heat transfer loop supplies heat to the chemical plant. The chemical plant uses the heat and electricity to split water into H₂ and O₂. To split water, two chemical processes are being considered: high-temperature steam electrolysis (HTSE) and the Sulfur-Iodine (SI) cycle [63]. Both processes operate at high temperature, which helps them deliver efficiencies of over 45%.

In particular, HTSE can achieve high operating efficiencies and its underlying technology has made considerable progress. High-temperature electrolysis is the decomposition of steam at high temperatures (>850°C) using solid oxide electrolysis

cells (SOECs). Operating at high temperatures offers thermodynamic advantages and the electrical demand is reduced [63]. Also, at high temperatures the kinetics of the reactions are faster [20]. These factors allow for a higher thermal-to-hydrogen conversion efficiency than that achieved with traditional electrolysis methods. This efficiency is defined as the ratio of energy content of the hydrogen produced (heating value) over the thermal energy input from the reactor (as heat or electricity). This efficiency has been projected to be 45% to 55% [63, 18], which will allow competitive hydrogen production costs to be achieved [19]. The Idaho National Laboratory (INL) has made a lot of progress in this area, and the efficiency and reliability of the cells has increased over the years [51].

Showing the safety of such a system with computational simulations is fundamental to obtain regulatory approval. The system comprising the HTSE plant, heat transfer loop and nuclear reactor operates at extreme conditions that can cause operational upsets and affect the nuclear reactor. For example, the system will lose its heat sink capacity if the HTSE plant suddenly shuts down, and this will perturb the temperature of the coolant in the nuclear reactor. Verification that the reactor and system will behave safely during this and other extreme upsets is required to obtain approval from authorities. This can be achieved by studying the system with computational simulations, which allow different combinations of conditions to be tested without risking real accidents. Computational simulations of nuclear reactors in power plants have been used extensively and different legacy codes exist for this (e.g., RELAP [52], MELCOR [14]); nuclear hydrogen production needs to undergo similar rigorous tests.

However, the complexity of nuclear hydrogen production systems has made it difficult to make progress with the simulation of accident scenarios. The simulation of nuclear reactors is already complex because it involves simulating reactor kinetics and transport phenomena. In the case of nuclear hydrogen production using HTSE, it is necessary to also simulate the chemical reactions happening in the hydrogen plant. Chemical reactions cannot be represented easily in legacy codes because these codes were not designed to incorporate them. Some efforts have been made to modify

legacy codes to represent chemical reactions, but they involve large teams of scientists [43]. This situation has resulted in a limited number of studies on the safety of these systems [43, 58].

This chapter makes progress in the study of accident scenarios in nuclear hydrogen production systems by using more flexible and powerful simulation codes: equation-based simulators. Equation-based simulators support very flexible modeling languages that allow the representation of diverse phenomena, and can be used to model nuclear hydrogen production systems easily. At the same time, they are powerful simulation codes and their use can increase the computational speed of the safety studies. In this work, we study three potential accidents and their effects on the core: a loss of heat sink at the HTSE, a loss of flow in the heat transfer loop, and a leak in the heat transfer loop.

This chapter first describes the nuclear hydrogen production system modeled; then it describes the models used to represent it. Finally, it explains the different transients studied and presents results on how the system responds.

4.2 Definition of the system

The nuclear hydrogen production facility considered in this study comprises two nuclear reactors, a power conversion unit (PCU), a heat transfer loop and a HTSE plant (Fig. 4-1). The nuclear reactors are modular, can produce the high-temperature heat needed for hydrogen production (900°C), and each of them produces 250 MWth. Fifty MWth of the heat produced by nuclear reactor #1 is delivered by the heat transfer loop to the HTSE plant. This provides the heat necessary to maintain a high-temperature environment in the HTSE unit. The remaining heat produced by nuclear reactor #1 and all of the heat produced by nuclear reactor #2 is transferred to the PCU to produce the electricity necessary to drive electrolysis in the HTSE unit.

The focus of this preliminary study will be on the behavior of nuclear reactor #1 and the heat transfer loop during accidents. The safety of nuclear reactors coupled

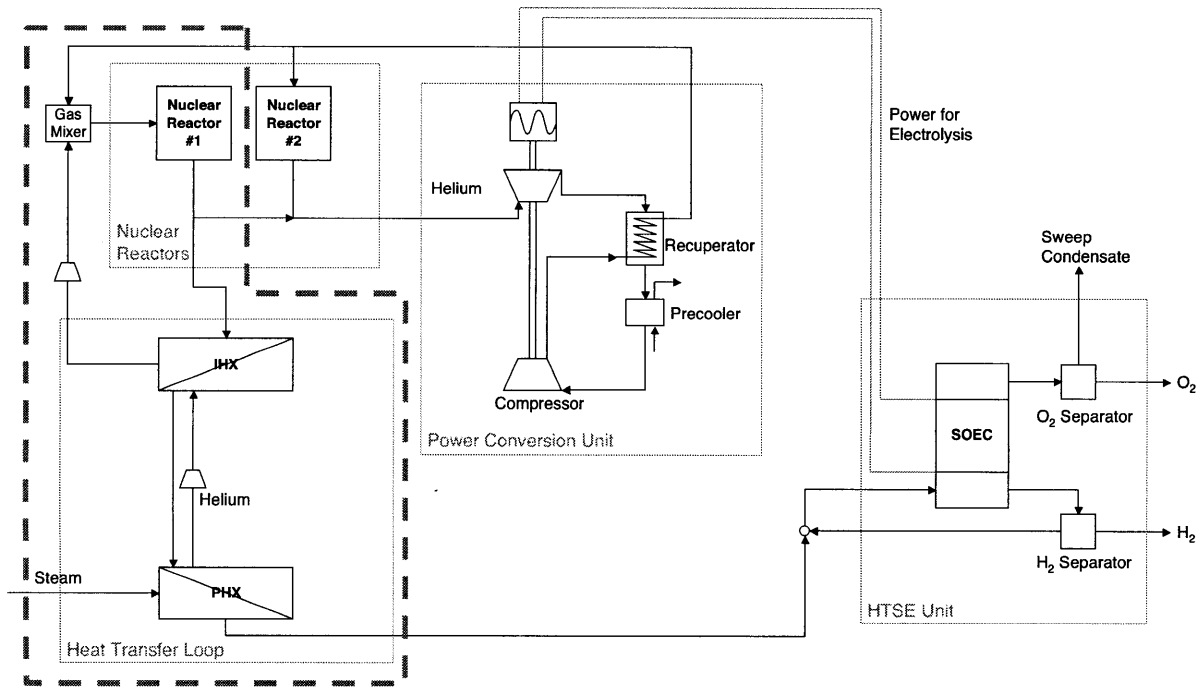


Figure 4-1: Nuclear hydrogen production system studied; the units surrounded by the dashed line will be simulated in this study.

to PCUs has been studied extensively in the past and we do not need to re-study their interaction. In this new system then, it is necessary to understand how the new parts, the heat transfer loop and the HTSE unit, affect safety. Three accident scenarios with potential severe impact on the nuclear reactor were studied: (1) a loss of heat sink accident, (2) a loss of flow in the heat transfer loop, and (3) a leak in the heat transfer loop. The study of these transients requires a detailed simulation of nuclear reactor #1 coupled with the heat transfer loop; the HTSE unit can be reduced to a heat sink at the cold side of the PHX (the steam superheater) (Fig. 4-1).

Nuclear reactor

The nuclear reactor used in the system is a bundle of two pebble bed modular reactors (PBMR). PBMRs are an ideal choice for the nuclear hydrogen production system because they can produce the high temperatures needed [37]. At the same time, they are safe, modular and present good economics [22, 65]. The specifications for the

reactors are based on the PBMR designed at MIT [23, 60] and each of these reactors can produce 250 MWth [22]. Their cores consist of a combination of fuel pebble balls and pure graphite pebble balls that allow online refueling (Fig. 4-2). Helium is used as the heat transfer fluid to bring the heat to the IHX and PCU. The cold helium enters in the lower part of the reactor, rises through channels in the side reflector, then is heated in the core, and then leaves the reactor at the bottom. A similar bundle of reactors has been proven to be technically and economically more convenient than the construction of a single nuclear reactor with the same power output [65].

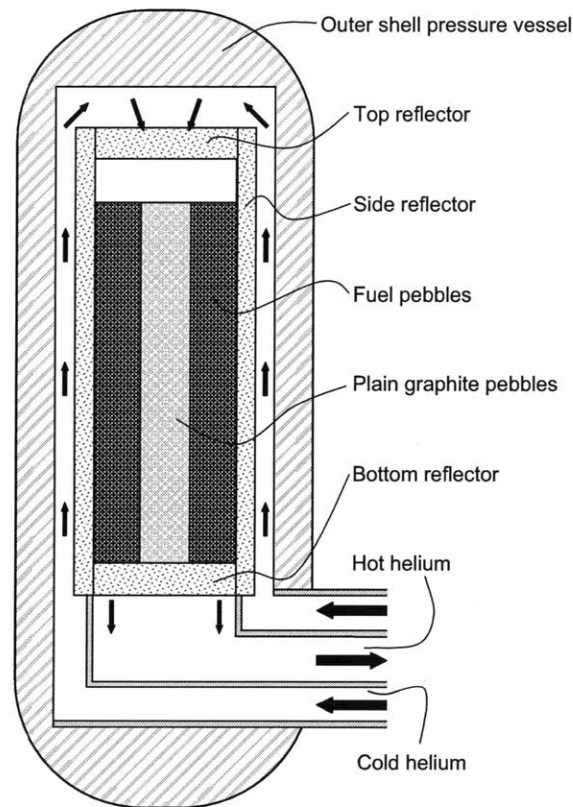


Figure 4-2: The PBMR is safe, modular, and economical, and it can produce the high-temperature heat needed to run hydrogen production plants.

Heat transfer loop

The heat transfer loop in this system is based on the heat transfer loop engineered at the INL [8], because of its detailed design. This heat transfer loop consists of an

intermediate heat exchanger (IHX), a process heat exchanger (PHX), a hot leg, a cold leg, and a compressor (Fig. 4-1). It transfers 50 MWth from the nuclear reactor to the chemical plant, and it has to withstand very high temperatures (up to 900°C) and high pressures (up to 7 MPa) [8]. These challenging conditions require a design created from scratch using new materials and new pieces of equipment.

Researchers at INL determined the following equipment characteristics for the heat transfer loop [8]:

1. The IHX is a compact heat exchanger made of Alloy 617 with 786,560 semi-circular channels 1.5 mm in diameter. The length of the IHX was 0.99 m and its width was 1.44 m.
2. The PHX is a tube-in-shell heat exchanger with 3,500 circular tubes; each tube has an internal diameter of 10 mm. High-temperature helium flows on the inside of the tubes and the steam flows on the outside. The length of the exchanger is 8.66 m and its material is Alloy 800.
3. The hot leg and cold leg are pipes of 90 m in length with internal diameters of 0.44 m and 0.41 m, thickness-to-diameter ratio of 0.117 and 0.114, and insulation thickness 59 mm and 58 mm, respectively. Both legs are made of Alloy 800.
4. The compressor should be able to produce a pressure differential of at least 0.4 MPa.

These specifications were used to build the dynamic models for the loop in JACOBIAN—one of the best equation-based simulators available [35].

4.3 Dynamic model of a nuclear hydrogen production system

As mentioned before, legacy codes normally used to study safety in nuclear reactors cannot be easily used to study nuclear hydrogen production systems. The reason for

this is that these codes cannot simulate all the phenomena involved in nuclear hydrogen production systems. In particular, they cannot incorporate chemical reactions. Equation-based simulators, on the other hand, are flexible and extensible platforms for system simulation that do not present these problems; we decided to use them instead to model our system. This section explains what equation-based simulators are, their strengths, and the models created for each part of the system considered.

4.3.1 Equation-based simulators as a simulation platform

Equation-based simulators are simulation tools created by the chemical engineering discipline to model the vast range of processes the chemical industry handles. They have been developed for more than 30 years to have flexibility, speed and accuracy. Their flexibility comes from supporting a declarative and hierarchical equation-based simulation language, which allows them to accommodate new models and different processes easily. Their speed and accuracy comes from having powerful numerical algorithms. These characteristics make them a good alternative for the simulation of new nuclear applications, which require the simulation of new phenomena and system-wide simulation of several interacting processes. We decided to use JACOBIAN [35], one of the best equation-based languages available.

A declarative equation-based language such as the one supported by JACOBIAN lets the user represent any physical or chemical system as a set of differential-algebraic equations (DAEs) [3]:

$$\begin{aligned}\mathbf{f}(\mathbf{x}(t), \dot{\mathbf{x}}(t), \mathbf{y}(t), t) &= \mathbf{0} \\ \mathbf{g}(\mathbf{x}(t), \mathbf{y}(t), t) &= \mathbf{0}\end{aligned}$$

where $\mathbf{x}(t) \in \mathbb{R}^{n_x}$ and $\dot{\mathbf{x}}(t) \in \mathbb{R}^{n_x}$ represent the differential variables (those whose time derivatives appear explicitly in the model) and the time derivatives of these variables, respectively. $\mathbf{y}(t) \in \mathbb{R}^{n_y}$ corresponds to the algebraic variables. $\mathbf{f} : \mathbb{R}^{n_x} \times \mathbb{R}^{n_x} \times \mathbb{R}^{n_y} \times \mathbb{R} \rightarrow \mathbb{R}^{n_x}$ are the differential equations, and $\mathbf{g} : \mathbb{R}^{n_x} \times \mathbb{R}^{n_y} \times \mathbb{R} \rightarrow \mathbb{R}^{n_y}$ are the algebraic equations. The philosophy of an equation-based simulator is that the

process model so defined is completely decoupled from the numerical methods used to solve it, which lets the user focus solely on the model formulation. This gives the user complete control over the model and he can create models from scratch, modify existing models accordingly and reuse other models.

Furthermore, declarative simulation languages support hierarchical model decomposition, which greatly simplifies the coding of large models [5]. It allows building models in levels in the same way one would conceptualize a real plant. For example, a first level of simple models can represent basic units (e.g., pipes, heat exchangers, chemical reactors). A second level uses models from the first to represent subsystems (e.g., heat transfer loop). Finally, a third level could incorporate all the subsystems to assemble a plant-wide model. With this approach, lower-level models can be easily tested and corrected, avoiding hard-to-find errors in higher-level models.

Equally important, equation-based simulators find solutions to simulations quickly and accurately. They assemble all the models' equations in one single equation system, which is solved simultaneously by general-purpose codes for root finding and implicit numerical integration. They also exploit the characteristics of the equation system (e.g., sparsity, block decomposition) to accelerate the solutions and solve 100,000s of equations in minutes. They are accurate too, because their error control is based on theoretical guarantees for consistency and stability, and the error can be controlled automatically.

4.3.2 Nuclear reactor model

The flexibility of JACOBIAN enables formulation of all the models required for simulation of the nuclear hydrogen production plant. As stated previously, only the nuclear reactor and the heat transfer loop need to be simulated to understand the system's behavior during the selected accidents. In this section, the model for the nuclear reactor is explained.

The nuclear reactor model is adapted from the model developed at MIT [60], which has the adequate level of detail for this study. This model only represents the pebble bed region in the core and the reflectors (Fig. 4-2), and it assumes the heat loss

from the reactor vessel is negligible. The pebble bed region in the core is cylindrical, its height is 8.5 m, the diameter of its passive region (plain graphite pebbles) is 1.75 m, and the total diameter of its active region (fuel pebbles) is 3.5 m (Fig. 4-2). The thickness of all reflectors is 1.15 m.

The model has to represent the conduction, convection and radiation of heat occurring among the different elements (pebbles, reflectors, helium), and the fission reactions in the core. To represent these phenomena, the core and reflectors are discretized using cylindrical coordinates. The axial discretization consists of 12 intervals; the top one and the bottom one represent the top and bottom reflectors, and 10 intervals in the center represent the core. The radial discretization consists of eight intervals; the center one represents the passive region, the next five represent the active region, and the final two represent the side reflectors. At each of the intervals, it is necessary to determine the temperature of the solid phases (pebbles and reflectors), and the temperature and pressure of the helium. The equations to determine these values are explained in the next section.

Temperature model for solid phases in the reactor

The behavior of the temperature of solid phases in the reactor (pebbles or reflectors) can be represented by the following general formula:

$$\rho C_P \frac{\partial T_{Solid}}{\partial t} = q_{Conduction} + q_{Radiation} + q_{Fission} + q_{Convection} \quad (4.1)$$

where T_{Solid} is the temperature of the solid phase (K), ρ is the density of the solid phase (kg/m^3) and C_P is heat capacity ($\text{J}/(\text{kg}\cdot\text{K})$). $q_{Conduction}$ corresponds to the heat conducted through the pebbles and the reflectors, and $q_{Radiation}$ is the heat radiated through the voids between the pebbles. $q_{Fission}$ represents the heat generated from fission in the pebbles, and $q_{Convection}$ is the heat transferred to the helium by convection. The definition of each of these terms in the equation is as follows.

1. Calculation of ρC_P . The heat capacity of the pebble bed can be calculated by

using the following equation [46]:

$$\rho C_P = 1.75 \cdot 10^6 (1 - \varepsilon) \left[0.645 + 3.14 \left(\frac{T_{Solid} - T_0}{1000} \right) - 2.809 \left(\frac{T_{Solid} - T_0}{1000} \right)^2 + 0.959 \left(\frac{T_{Solid} - T_0}{1000} \right)^3 \right]. \quad (4.2)$$

In this equation, ε corresponds to the void fraction in the pebble bed, and T_0 is the reference temperature (273.15 K).

For the reflectors, ρ can be treated as a constant, with the value 1394.8 kg/m³ [45]; C_P can be expressed as:

$$C_P = \frac{0.42 \cdot T_{Solid}}{1500}. \quad (4.3)$$

2. Calculation of $q_{Conduction}$ and $q_{Radiation}$. For the pebbles, $q_{Conduction}$ and $q_{Radiation}$ can be calculated as a single term by using

$$q_{Conduction} + q_{Radiation} = \frac{1}{r} \frac{\partial}{\partial r} \left(kr \frac{\partial T_{Solid}}{\partial r} \right) + \frac{\partial}{\partial z} \left(kr \frac{\partial T_{Solid}}{\partial z} \right), \quad (4.4)$$

and by using a conductivity constant that incorporates the radiation effect [45]:

$$k = 1.1536 \cdot 10^{-4} (T_{Solid} - 173.16)^{1.6622}. \quad (4.5)$$

The same equation is used for the reflectors, but in this case there is no radiation effect and the conductivity in this case is roughly constant at 40 W/(m·K) [46].

3. Calculation of $q_{Fission}$. To calculate $q_{Fission}$, it is assumed that the power distribution in the pebble bed region is constant over time. Then $q_{Fission}$ for the control volume in the axial interval i (starting at the top of the core) and in the radial interval j (starting at the center of the core) can be calculated by using

the following equation:

$$q_{Fission,i,j} = \alpha_i \alpha_j Q_T \quad (4.6)$$

where Q_T is the total reactor power, and α_i and α_j are the normalized fission power factors in the axial and radial directions, respectively. The α_i factors correspond to the eight axial core intervals and their values are (from top to bottom): 0.025, 0.034, 0.053, 0.071, 0.091, 0.121, 0.148, 0.171, 0.162, 0.124 [60]. The radial α_j factors correspond to the six radial core intervals and their values are (from center to outer): 0.0 (passive section), 0.218, 0.207, 0.195, 0.19, 0.19 [60].

The nuclear reactor power can be calculated as a function of the neutronics of the reactor using the point kinetics equations. These equations use the mean values of the different variables in the reactor to calculate the total reactor power (Q_T) [21]. In this study, we use a simplified version:

$$Q_T = \omega_f V \Sigma_f \phi, \quad (4.7)$$

$$\frac{d\phi}{dt} = \frac{\rho - \beta}{\Lambda} \phi + \nu \lambda C_L, \quad (4.8)$$

$$\frac{dC_L}{dt} = \frac{\beta}{\Lambda} \phi - \lambda C_L. \quad (4.9)$$

In these equations Q_T , ϕ , C_L and ρ are variables. Eq. (4.7) calculates the total reactor power Q_T in terms of the average neutron flux density ϕ . The value of the neutron density ϕ is calculated using Eq. (4.8), and it depends on its own value, the reactivity ρ and the lumped delayed precursor concentration C_L . Eq. (4.8) does not consider a term to represent the control rods, because the accidents considered are unprotected. C_L lumps the six precursor groups used traditionally in the point kinetics equations, so only one equation, Eq. (4.9), is needed to represent them.

ω_f , V , Σ_f , λ , β and Λ are parameters. ω_f is the usable energy released per fission event (200 MeV), V is the active core volume, Σ_f is the macroscopic fission cross section (0.133 m²), λ is the decay constant of the delayed precursor

(0.0584), and β is the total effective delayed-neutron fraction (0.005), and Λ is the prompt-neutron life time (4.0×10^{-4} s).

The reactivity ρ , the remaining variable to calculate, can be calculated from

$$\rho = \Delta\rho_X + \Delta\rho_T \quad (4.10)$$

where $\Delta\rho_X$ is the reactivity contribution from the fission product poisoning by Xenon (Xe^{135}) and $\Delta\rho_T$ is the reactivity contribution from the core temperature feedback. $\Delta\rho_X$ can be eliminated in this study, because its effects are very slow [60] in relation to the timeframe of interest (1 min to 1 hr). $\Delta\rho_T$ is calculated using

$$\Delta\rho_T = \alpha_T(T_{Core} - T_{Core,ref}). \quad (4.11)$$

T_{Core} is the average temperature in the core and a variable; it is calculated using $T_{Solid,i,j}$ with i and j corresponding to the core axial and radial intervals. α_T and $T_{Core,ref}$ are parameters. α_T is the temperature coefficient of reactivity (-3.5×10^{-5}) and $T_{Core,ref}$ is the reference temperature (999.075 K) [60].

4. Calculation of $q_{Convection}$. $q_{Convection}$ is the heat transferred to the helium gas by the pebbles. Given the high flow rates, it is assumed that radial flow can be ignored and only axial flow takes place in each node. Then the convected heat in each node (i,j) can be calculated by:

$$q_{Convection,i,j} = F_{i,j}C_{pg,i,j}(T_{g,out,i,j} - T_{g,in,i,j}) \quad (4.12)$$

where $F_{i,j}$ is the helium mass flowrate, and $T_{g,in,i,j}$ and $T_{g,out,i,j}$ are the temperature of the helium gas entering and exiting the node, respectively. These variables are calculated using the equations in the following section that explains the models for the flow of helium inside the core. $C_{pg,i,j}$ is the helium heat capacity parameter.

Now each of the terms in Eq. (4.1) is defined and they can be discretized using finite differences to find an expression for the temperature $T_{Solid,i,j}$ in each control volume in the core.

Temperature and pressure models for the helium flow in the reactor

This section explains how the temperature and pressure of the helium flowing through the core are calculated at each node. The flow of helium in the core, F_{Total} is an input variable, and the flow of helium at each node $F_{i,j}$ is calculated as a fraction of the total flowrate inside the core. The temperature of the gas in the core is calculated using an analytical expression for the heat equilibrium at each node:

$$T_{g,out,i,j} = T_{g,in,i,j} + (T_{Solid,i,j} - T_{g,in,i,j}) \left[1 - \exp\left(-\frac{hA_c}{F_{i,j}C_{pg,i,j}}\right) \right] \quad (4.13)$$

where $T_{g,out,i,j}$, $T_{g,in,i,j}$, $T_{Solid,i,j}$, $F_{i,j}$, and $C_{pg,i,j}$ are the same variables and parameters as defined before. h is the convective heat transfer coefficient calculated according to Wang [60] and A_c is the total heat transfer area in a node. To calculate the pressure drop in the core we use

$$\frac{R_{\Delta P}}{F_{Total}^2} = \frac{R_{\Delta P,ref}}{F_{Total,ref}^2} \quad (4.14)$$

with

$$R_{\Delta P} = \frac{P_{in} - P_{out}}{P_{in}} \quad (4.15)$$

P_{in} and P_{out} are the pressure values at the reactor's inlet and outlet, respectively. $R_{\Delta P}$ is the pressure drop ratio for the core and F_{Total} is the total helium mass flowrate inside the core as defined before. $R_{\Delta P,ref}$ and $F_{Total,ref}$ are the values of $R_{\Delta P}$ and F_{Total} at the designed operating point.

4.3.3 Heat Transfer Loop Model

The heat transfer loop is the other part of system that needs to be modeled in detail for this study. The model for the heat transfer loop is similar to the one explained in the previous chapter, and it is based on the design from INL specified in the

previous subsection [8]. The heat transfer model needs to represent two main type of phenomena: the gas dynamics of helium in the pipes, and the heat exchange with the nuclear reactor loop and the chemical plant.

The models used to represent the behavior of pipes, compressor and heat exchanger are the same ones developed in Chapter 3. In particular, to represent the gas dynamics in the loop the *QSS Approximation* model was used in combination with the correct coupling conditions.

4.4 Transient simulations

The model of the nuclear hydrogen plant developed in the previous section was tested against several different accident scenarios. Nuclear reactors and their behavior in response to accidents have been extensively studied in the past, because this is fundamental to obtain regulatory approval. However, their coupling to a chemical plant adds complexity and the transient behavior of this new system is not immediately obvious. To show that this new system is safe, this study focused on understanding how sudden changes in the chemical plant and heat transfer loop affect the nuclear reactor. We simulated three scenarios that can easily occur and might have an impact on the nuclear reactor:

1. a loss of heat sink,
2. a loss of flow in the heat transfer loop, and
3. a helium leak.

We focused on the effect of the different scenarios on the temperature in the nuclear reactor core, in terms of magnitude and time scale. We also explored other interesting variables depending on the scenario. The following sections explain how each of this scenarios were implemented and how the system responded.

4.4.1 Loss of heat sink accident

The loss of heat sink accident occurs when the chemical plant side loses its capacity to remove heat from the system at the PHX. This failure can be triggered by problems with valves, pumps or membranes at the electrolysis unit, or problems with the supply of steam. To model it, the steam flowrate was ramped down by 99% over 15 s. The system's response to this accident was studied by tracking the temperature and other relevant variables in the heat transfer loop and in the nuclear reactor. The accident causes minor effects on the nuclear reactor because of the reactor's inherent safety, but it has the potential to cause structural damage to the heat transfer loop.

1. *Heat transfer loop Response.* After the steam flowrate reduction at the PHX, the helium temperature stays within specifications at the IHX, hot leg and PHX. To understand the helium temperature's behavior against specifications along the IHX, hot leg and PHX, it suffices to study the maximum helium temperature in each section. These maximum temperatures are close to each other in a range of 10°C, so a good proxy for them is the helium temperature at the end of the IHX. This is the maximum helium temperature reached in the loop, and it increases slightly shortly after the steam reduction event (first 100 s). Then it drops to reach 851°C, which is 27°C colder than before the event is introduced (Fig. 4-3). This behavior is explained by the safe response of the nuclear reactor, which is explained in the next subsection.

In contrast, the maximum helium temperature along the cold leg increases more than 330°C over the design point, reaching 908°C. The reduction of the cold stream at the PHX decreases the PHX's heat removal capacity, which leads to an increased temperature at the PHX's outlet (Fig. 4-3). Thus, the temperature increase at the PHX's outlet is over 310°C. This increase in temperature is amplified by the compressor, and the cold leg receives gas that is 330°C hotter than during normal operation.

The high temperature reached in the cold leg decreases the stress resistance of the pipe's alloy below safety levels. The pressure difference between the inside

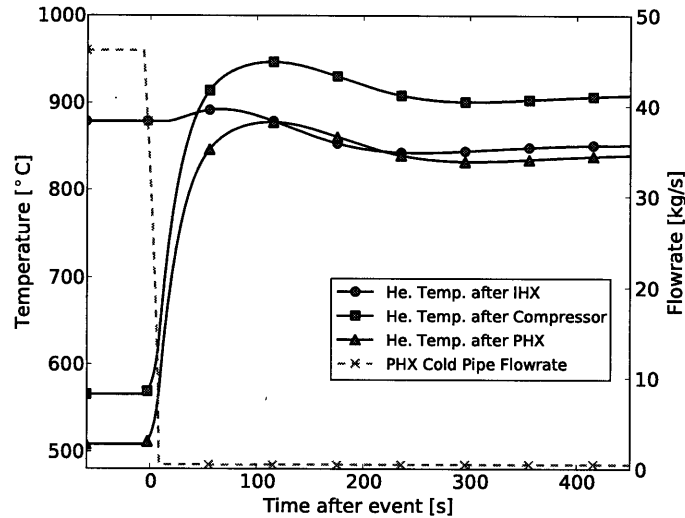


Figure 4-3: After a loss of heat sink accident, the temperature in the cold leg of the heat transfer loop increases more than 330°C.

of the pipe (2 MPa) and the outside (0.1 MPa) results in a stress on the pipe walls of 120 MPa [8]. The pipe design can easily tolerate this stress at the operating temperature (approx. 560°C) because it is made of Alloy 800 [33]. This alloy has a creep rupture strength in those conditions of 240 MPa for 10⁵ hrs. However, when the temperature in the pipe reaches over 870°C, the creep rupture strength decreases dramatically. In these conditions, the pipe can only sustain 120 MPa for less than 1 hr (Fig. 4-4).

The lower stress resistance in the cold pipe could cause the pipe to rupture with serious consequences for the heat transfer loop but not for the reactor. The rupture of the cold pipe would not only damage the cold pipe, but also the surrounding hot pipe, compressor, PHX and IHX. This will render the whole system unusable and the heat sink capacity will be completely lost. Yet, the accident will not damage the reactor because the reactor's safety features can endure these changes without affecting the core. This is explained in the next section.

This accident can be prevented by using the hot pipe's material specifications to build the cold pipe, because the hot pipe is designed to withstand similar pressures at 900°C.

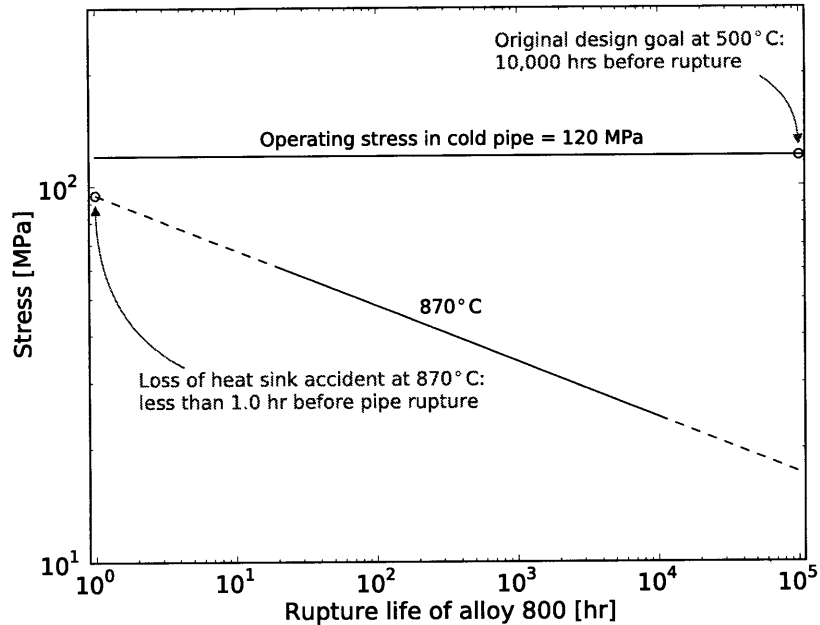


Figure 4-4: Increased temperature in cold pipe after loss of heat sink accident decreases pipe's stress resistance from over 10^5 hrs to less than 1 hr.

2. *Nuclear reactor response.* The temperature increase in the heat transfer loop's cold leg is propagated to the nuclear reactor's coolant loop, increasing the temperature of the coolant entering the core. The coolant temperature rises 260°C at the end of the IHX (Fig. 4-5) because of the loss of the heat sink at the heat transfer loop. This hotter coolant is mixed with the coolant coming at 540°C from the PCU, so the temperature of the coolant entering the core rises in only 65°C . The temperature of the coolant exiting the core actually drops because of the core response; this is explained in the next paragraph.

The nuclear reactor core responds to the increased coolant temperature by decreasing its power. The increase in the coolant temperature entering the core slightly raises the average temperature of the fuel in the reactor core (Fig. 4-6). This temperature rise of the fuel introduces negative reactivity by increasing the fuel non-fission absorption for neutrons, which reduces the power produced and stabilizes the average temperature in the core (Fig. 4-6). Even though the average temperature in the core is the same, the lower power in the core changes the core temperature profile. The temperature at the coldest point in the core

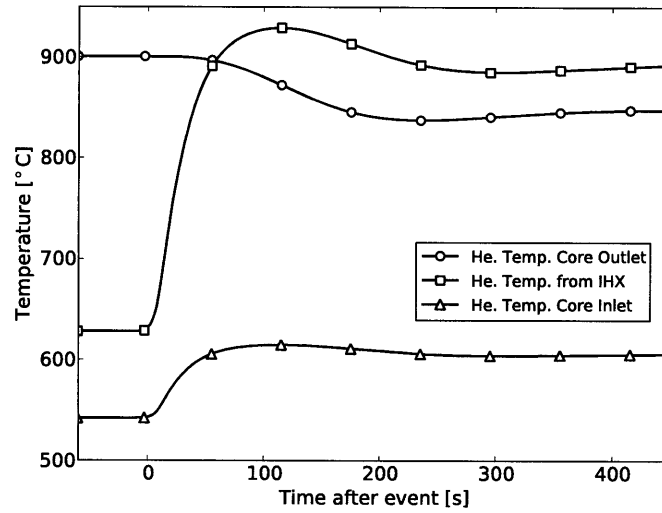


Figure 4-5: After a loss of heat sink accident, the helium entering the core is hotter, but its temperature is lower at the outlet.

(inlet) increases 60°C, and the temperature at the hottest point in the core (outlet) decreases 80°C. The lower core power explains the temperatures drop of the coolant at the core outlet and of the helium at the IHX outlet in the heat transfer loop.

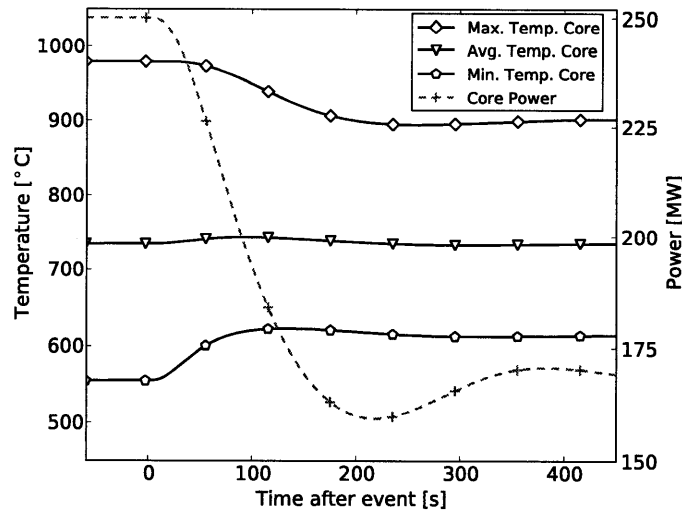


Figure 4-6: After a loss of heat sink accident, the average temperature in the fuel slightly increases, which leads to a reduction in the reactor power.

4.4.2 Loss of flow in the heat transfer loop

The loss of flow accident in the heat transfer loop happens when the compressor circulating helium inside the heat transfer loop stops. The lack of forced convection in the heat transfer loop halts the heat removal from the nuclear reactor's coolant loop. This failure can happen when the compressor surges or malfunctions. A similar accident is normally used to test the nuclear reactor's coolant loop. To represent this accident, the compressor flowrate was reduced to 1% of the operating flowrate over 5 s. The heat transfer loop and the reactor react safely in this scenario.

1. *Heat transfer loop response.* The lack of forced convection affects the helium temperature profile along the heat transfer loop, but this profile remains within design limits. The low helium flowrate along the PHX provides enough time to remove all the possible heat from it. As a result, the helium temperature at the end of the PHX drops from 510°C to 341°C (Fig. 4-7). On the other side of the loop, the helium temperature at the end of the IHX quickly increases 22°C and then drops below its normal operating temperature. This increase is induced again by the lower helium flowrate, which allows for a better heat exchange with the reactor coolant. The drop is a consequence of the reactor's power response, which is explained in the following paragraphs.
2. *Nuclear reactor response.* The low flowrate in the heat transfer loop stops the heat removal from the reactor coolant. The lack of heat removal at the IHX causes the coolant temperature at the IHX's outlet to rise initially from 628°C to 894°C (after 40 s) (Fig. 4-8). Afterwards, the coolant then reaches 850°C (after 400 s). This hotter coolant is mixed with the coolant coming from the PCU at 540°C. As a consequence, the temperature of the coolant entering the core rises 64° (after 40 s). This temperature rise produces a power response in the core, which results in a lower coolant temperature at the outlet of the core. The characteristics of this response are explained next.

Again, the nuclear reactor core decreases its power in response to the higher coolant temperature at its inlet. The response of the core in this case is similar

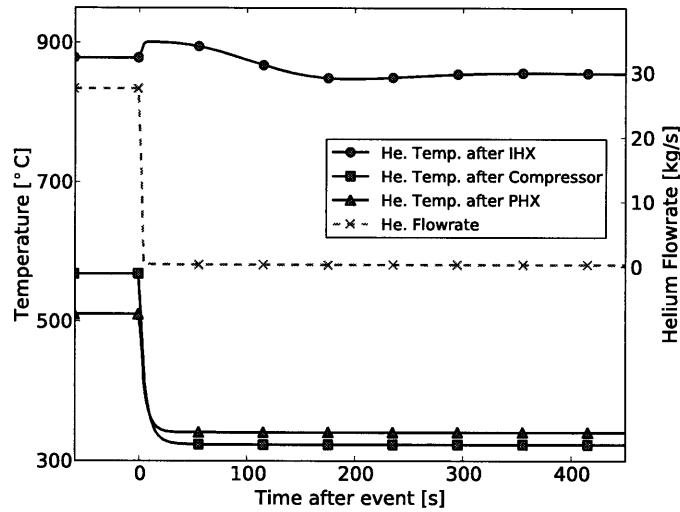


Figure 4-7: After a loss of flow in the heat transfer loop, the helium temperature around the loop stays within specifications.

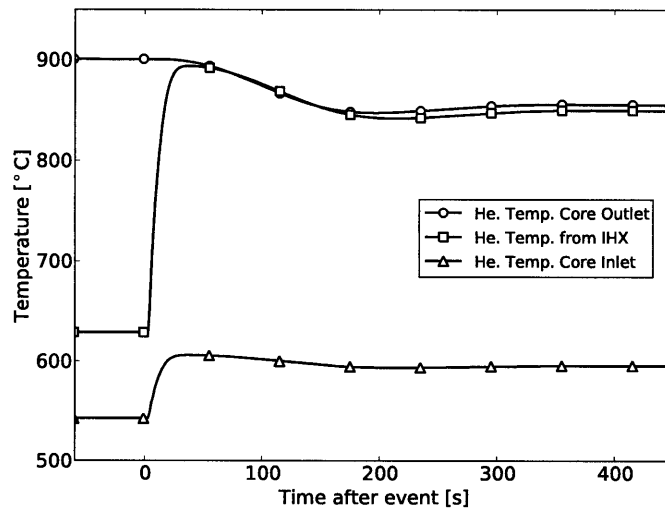


Figure 4-8: After a loss of flow in the heat transfer loop, the temperature of helium at the core inlet increases. The core response reduces the temperature at the core outlet.

to the response in the loss of heat sink accident. The higher coolant temperature increases slightly the average temperature of the core. As a response, the fuel's negative reactivity rises, which decreases the power produced in the core to 175 MWth (Fig. 4-9). Consequently, the temperature of the coolant at the core outlet is lower. So is the helium temperature at the outlet of the IHX's cold stream.

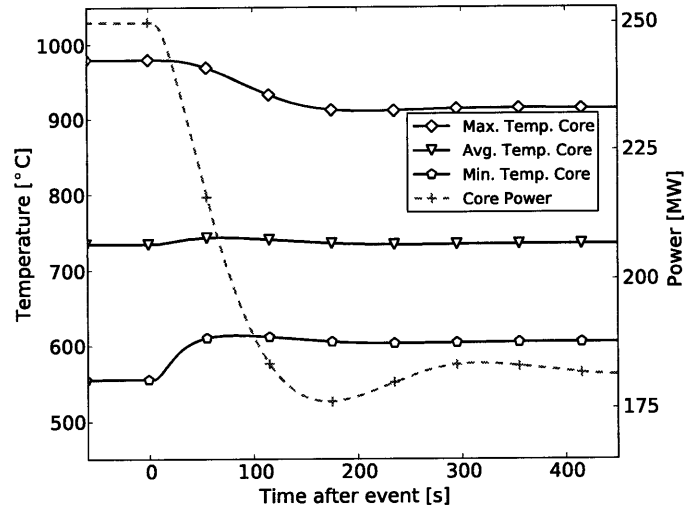


Figure 4-9: After a loss of flow in the heat transfer loop, the core reacts safely by reducing the fission power.

4.4.3 Leak in the heat transfer loop

Another potential accident that can affect the system is the loss of helium in the heat transfer loop. This failure can occur when a pipe leaks or a valve malfunctions. It results in less helium mass in the loop, which makes the loop less capable to remove heat from the nuclear reactor. To represent this accident, the total mass in the loop was linearly decreased by 50% over 1 min.

1. *Heat transfer loop response.* After introducing the leak, the heat transfer loop's response is similar, but milder, to the response to the loss of flow accident. These responses are similar because the loss of compressor power and the loss of helium mass have the same effect: a lower helium flowrate in the loop. The lower flowrate in this accident causes the helium temperature at the end of the PHX to drop from 508°C to 353°C in 400 s. On the other side of the loop, the temperature of helium at the end of the IHX rises from 878°C to 898°C in the first 70 s. The response in this case is milder compared to the response in the previous accident because the loop still has 50% of the original flowrate and can still remove a significant amount of heat from the nuclear reactor coolant. Then this temperature drops to 890°C after 400 s from the event introduction;

this drop is explained by the nuclear reactor response.

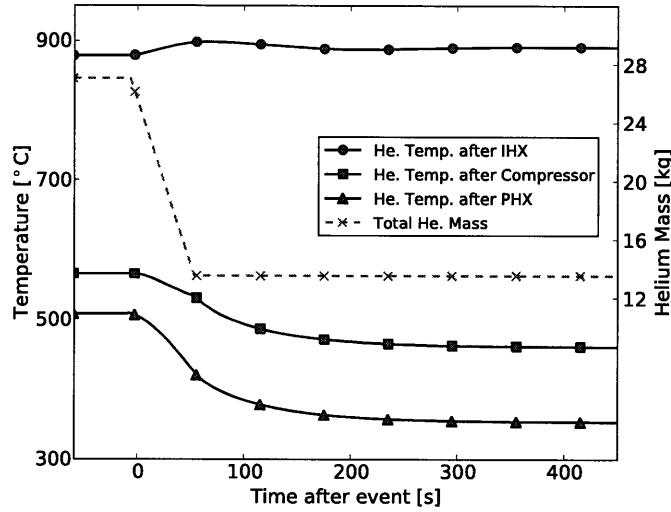


Figure 4-10: After a leak accident in the heat transfer loop, the temperature of helium along the loop stays within specifications.

The lower pressure inside the loop caused by the loss of helium increases the stress on the IHX, but the design specifications are enough to resist this stress. The IHX's walls experience a large pressure differential because the coolant from the nuclear reactor has a pressure of 7 MPa and the helium in the heat transfer loop has a pressure of 2 MPa. To withstand this pressure differential, the IHX's walls are designed using a pitch to channel diameter ratio of 1.5. This ratio is calculated as

$$\frac{p}{d} = 1 + \frac{\Delta P}{\sigma_D} \quad (4.16)$$

where ΔP is the pressure differential inside the IHX (5 MPa) and σ_D corresponds to the allowable stress over the internal walls of the IHX. σ_D is set as 10 MPa, which corresponds to half of the creep rupture stress of Alloy 800 at 900°C for 10⁵ hrs [33]. ΔP increases to 6.1 MPa after the leak, because the pressure on the cold side of the IHX drops to 0.9 MPa. Under this new pressure difference, the allowable stress in the IHX's walls rises to 12.2 MPa, which is still below the creep rupture strength. Thus, this accident does not pose risks to the heat transfer loop.

2. *Nuclear reactor response.* The lower heat removal capacity in the heat transfer loop increases the temperature of the coolant entering the core. The temperature of the coolant at the end of the IHX rises from 628°C to 673°C after 400 s. This temperature change is propagated to the coolant at the core inlet, whose temperature rises from 542°C to 553°C. At the core outlet, the coolant temperature drops from 900°C to 891°C because the reactor power reduction in response to the higher coolant temperature at the core inlet.

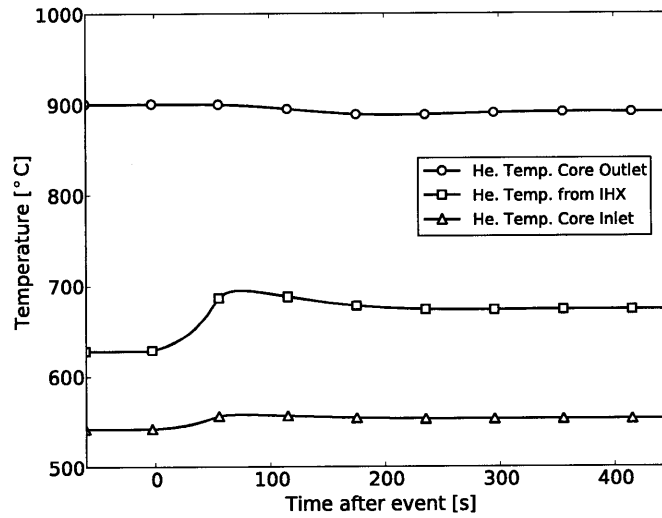


Figure 4-11: After a leak accident in the heat transfer loop, the temperature at the core inlet slightly increases, which results in a minor temperature decrease at the core outlet.

The core power reduction in this case is lower than in the previous accidents. The slightly hotter coolant at the inlet of the core increases the average temperature and the negative reactivity in the core (Fig. 4-12). This reduces the power in the reactor in 24 MWth. The lower power reduction compared to the previous accident is explained by the higher heat removal capacity remaining in the heat transfer loop.

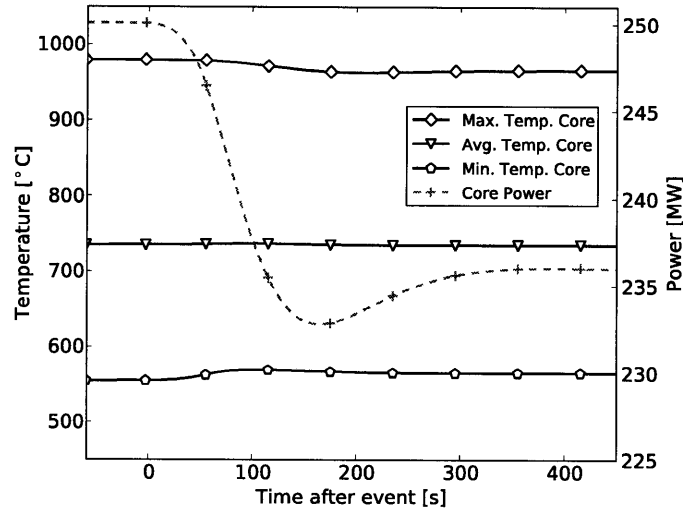


Figure 4-12: After a leak accident in the heat transfer loop, the heat transfer loop still can remove a significant amount of heat from the nuclear reactor coolant. This results in a power reduction of 24 MWth.

4.5 Conclusion

The nuclear hydrogen production plant studied is proven to have good safety features in the scenarios tested, but changes to the design might be needed. All the scenarios tested—directly or indirectly—lead to a loss of heat sink capacity at the nuclear reactor. This resulted in an increase of the nuclear reactor core temperature, which was quickly stopped by the fission power reduction at the fuel pebbles and by the safe design of the PBMR. As a result, the maximum temperature reached in the core was always less than 1000°C, which is below the melting point of the fuel pebbles (2000°C). Thus, the nuclear reactor was always safe. At the heat transfer loop, pressure and temperature remained within specified limits in two of the scenarios tested. However, in the *loss of heat sink* scenario the temperature in the cold leg increased by more than 330°C, which could result in the rupture of this pipe. This could be prevented by replacing the design specifications of the cold leg with those of the hot leg.

Adding more details to the studied nuclear hydrogen plant model would help to understand its behavior further. This study's purpose was representing the response to accidents of a nuclear hydrogen plant, and in particular, it focused on the nuclear reactor and heat transfer loop. Consequently, these two units were modeled in detail.

In contrast, the PCU was assumed as a set of external conditions that remained constant, and the interaction with the HTSE unit was represented by the steam flowing through the PHX. Including a model of the PCU would help to verify the simplifying assumption, or show potential disruptions in its operation during accidents. At the same time, including a model of the HTSE unit would help to study the behavior of the plant during normal operational transients (e.g., start-up, shutdown, and restart). The SOECs in the HTSE unit are very sensitive to thermal gradients and it will be particularly important to include this behavior in operational transients.

Finally, the analysis of the nuclear hydrogen plant behavior in this chapter has shown that equation-based simulators can successfully simulate transients of new nuclear applications. Equation-based simulators are a good platform to simulate this kind of process because they are flexible, extendable, fast and accurate. Also, they can be easily audited by regulators, because they are open and declarative modeling environments. Future safety studies should use them and focus on adding more details to the plant model and on representing the plant's normal operation. These efforts could demonstrate the safety of nuclear hydrogen production using HTSE, and help develop a cleaner way to produce liquid fuels based on alternative feedstocks.

Chapter 5

Conclusions

This thesis has shown that nuclear hydrogen production can be safe, and that equation-based simulators are a good platform to test the safety of this kind of facility. Nuclear hydrogen production is one of the new nuclear applications that could have a large impact in the production liquid fuels, but its safety needs to be demonstrated using computational simulations. For that, a nuclear hydrogen production plant was represented using equation-based simulators, and models for all its units were created. The models were tested in different accident scenarios showing that the system was safe. Here, these results are summarized and potential future work is proposed.

The second chapter of this thesis explained the rationale for new nuclear applications supporting liquid fuel production, and the need for equation-based simulators to demonstrate their safety. Using more local and affordable feedstocks—such as oil sands, coal or biomass—to produce liquid fuels requires large amounts of energy and generates significant CO₂ emissions. These issues can be resolved by using nuclear hydrogen production and nuclear heat integration with production facilities. It is nuclear hydrogen production, however, that offers the most possibilities, as it is the most versatile to use. Thus, this technology was selected to study the safety in new nuclear applications. Unfortunately, the study of the safety of these new applications cannot be done with legacy codes used for the analysis of nuclear power plants. The reason for this is that legacy codes lack the required flexibility, computational speed and accuracy to represent the different chemical and physical phenomena. Instead,

equation-based simulators are the appropriate simulation platform, because they have been designed to represent complex and transient processes such as nuclear hydrogen production.

Chapter 3 proposed a set of equation-based models to simulate the heat transfer loop in a nuclear hydrogen plant and found that the models based on the *Zero Mach Number Limit* model and the *QSS Approximation* model for gas dynamics were suitable to model the interesting transients. The heat transfer loop uses helium as the heat transfer fluid, and this makes simulating its behavior difficult. To resolve this, three models for gas dynamics and two set of coupling conditions for boundary variables were tested in JACOBIAN, an equation-based simulator. The *Zero Mach Number Limit* model and the *QSS Approximation* model in combination with a new approach to set coupling conditions for boundary variables were able to represent the interesting time scales accurately in transient scenarios. These simulations were confirmed with a reference model written in the legacy code RELAP. Additionally, the computation of these simulations in JACOBIAN was faster and more accurate than the computation of the simulations in RELAP.

Chapter 4 used equation-based models to show the safety of a nuclear hydrogen production plant during accidents. The analysis of the hydrogen production plant focused on the nuclear reactor and heat transfer loop, and detailed dynamic models for these units were created. This plant model was then subjected to three accident scenarios: a loss of heat sink at the HTSE, a loss of flow in the heat transfer loop, and a leak in the heat transfer loop. All the scenarios—directly or indirectly—lead to a loss of heat sink capacity at the nuclear reactor. This resulted in an increase of the nuclear reactor core temperature, which was quickly moderated by the fission power reduction in the fuel pebbles and by the safe design of the PBMR. As a result, the maximum temperature reached in the core was always less than 1000°C, which is below the melting point of the fuel pebbles (2000°C). Thus, the nuclear reactor was always safe. At the heat transfer loop, pressure and temperature remained within specified limits in two of the scenarios tested. However, in the *loss of heat sink* scenario the temperature in the cold leg increased by more than 330°C, which could

result in the rupture of this pipe. This could be prevented by replacing the design specifications of the cold leg with those of the hot leg.

Future work in this area involves testing other scenarios and expanding the models used. This preliminary study of the safety in a nuclear hydrogen production plant was focused on the behavior of the plant during selected accidents. In particular, emphasis was on the behavior of the nuclear reactor and the heat transfer loop. However, to show a complete picture of the safety of the plant, accidents involving the operation of the PCU and HTSE unit should be included. To do this, the dynamic model of the plant will need to incorporate models representing the different parts in the PCU (e.g., turbine, compressor, generator) and in the HTSE unit (e.g., SOEC, separators). Additionally, the behavior of the system during normal operational transients should also be tested (e.g., start-up, shut-down, and re-start) to guarantee safety and operability. Indeed, the SOECs in the HTSE unit are very sensitive to thermal gradients and it will be particularly important to include this behavior in operational transients. Expanding and modifying the nuclear hydrogen plant model created in this thesis could be easily done, for these models have been created in equation-based simulators with flexibility and extendability features.

This thesis' results show that nuclear hydrogen production plants could be safe, and simultaneously, that equation-based simulators are good platforms to prove the safety of this plants. Developing these models and tests further will help to guarantee the safety of the plant and obtain regulatory and public approval. In the end, this will help to transition from the current liquid fuel supply chain based on foreign oil, which is polluting, expensive and risky, to a liquid fuel supply chain based on more affordable, local and secure feedstocks. In particular, using biomass as a feedstock in combination with nuclear hydrogen production and nuclear heat integration could achieve liquid fuel supply chain that will be clean, sustainable, efficient and local.

Appendix A

Discretization of Gas Dynamic Equations

The partial differential algebraic equations used to describe gas dynamics in the loop were the following:

$$\text{Continuity} \quad \frac{\partial \rho}{\partial t} = -\frac{\partial \phi}{\partial x}, \quad (\text{A.1})$$

$$\text{Momentum} \quad \frac{\partial \phi}{\partial t} = -\frac{\partial P}{\partial x} - \frac{\partial}{\partial x} \frac{\phi^2}{\rho} - \frac{2f|\phi|\phi}{D\rho}, \quad (\text{A.2})$$

$$\text{Energy} \quad \frac{\partial \psi}{\partial t} = -\frac{\partial}{\partial x} \phi h - \frac{4U(T - T_{Ext})}{D}, \quad (\text{A.3})$$

$$\text{Physical Properties} \quad \psi = \rho h - P, \quad (\text{A.4})$$

$$h = h_{form} + \frac{C_P}{M} (T - T_{stand}), \quad (\text{A.5})$$

$$P = \frac{R_C \rho T}{M}. \quad (\text{A.6})$$

To simplify the writing of these equations, ϕ was replaced by $\frac{F}{A}$; then the equations are the following:

$$\text{Continuity} \quad \frac{\partial \rho}{\partial t} = - \frac{\partial F}{\partial x A}, \quad (\text{A.7})$$

$$\text{Momentum} \quad \frac{\partial F}{\partial t A} = - \frac{\partial P}{\partial x} - \frac{\partial F^2}{\partial x \rho A^2} - \frac{2f|F|F}{D\rho A^2}, \quad (\text{A.8})$$

$$\text{Energy} \quad \frac{\partial \psi}{\partial t} = - \frac{\partial Fh}{\partial x A} - \frac{4U(T - T_{Ext})}{D}, \quad (\text{A.9})$$

$$\text{Physical Properties} \quad \psi = \rho h - P, \quad (\text{A.10})$$

$$h = h_{form} + \frac{C_P}{M} (T - T_{stand}), \quad (\text{A.11})$$

$$P = \frac{R_C \rho T}{M}. \quad (\text{A.12})$$

These equations were discretized using a combination of a standard and a staggered grid (Fig. A-1).

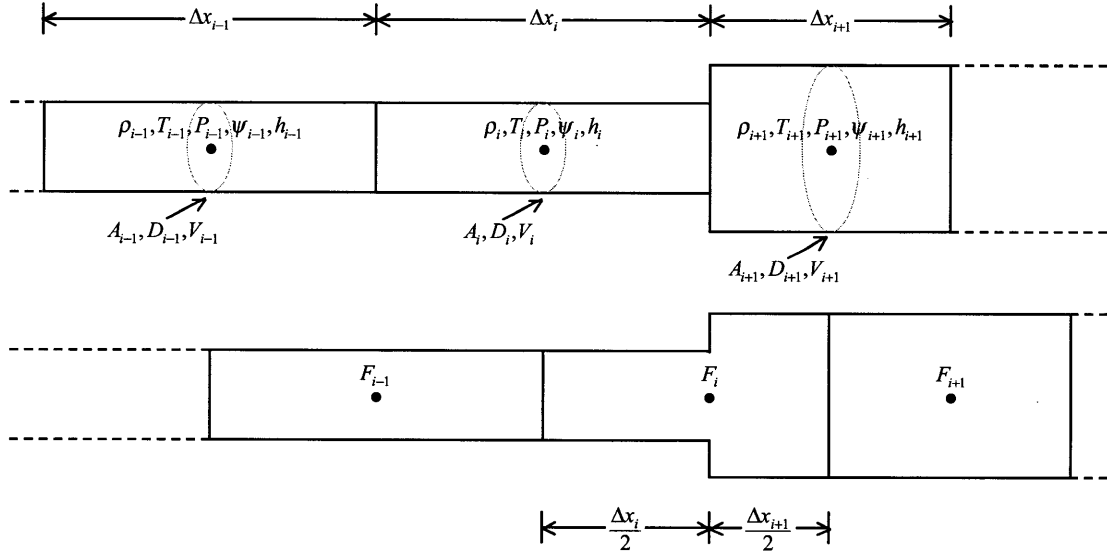


Figure A-1: A combination of standard grid and a staggered grid is used to discretize the gas dynamics equations.

In this grid, the values of the discretized differential variables ρ_i and ψ_i were assumed to be the average value of ρ and ψ over the control volume i in the standard

grid. Then these variables can be represented as

$$\rho_i = \frac{1}{V_i} \int_{V_i} \rho dV, \quad (\text{A.13})$$

$$\psi_i = \frac{1}{V_i} \int_{V_i} \psi dV. \quad (\text{A.14})$$

Similarly, the value of F_i is defined as the average value of F over the control volume i in the staggered grid,

$$F_i = \frac{1}{\frac{\Delta x_i}{2} + \frac{\Delta x_{i+1}}{2}} \int_{\frac{\Delta x_i}{2} + \frac{\Delta x_{i+1}}{2}} F dx. \quad (\text{A.15})$$

The values of the algebraic variables calculated using the algebraic equations definitions:

$$\psi_i = \rho_i h_i - P_i, \quad (\text{A.16})$$

$$h_i = h_{form} + \frac{C_P}{M} (T_i - T_{stand}), \quad (\text{A.17})$$

$$P_i = \frac{R_C \rho_i T_i}{M}. \quad (\text{A.18})$$

The following explains how Eq. (A.7)-(A.9) were discretized.

A.1 Discretization of the continuity equation

The continuity equation,

$$\frac{\partial \rho}{\partial t} dV = - \frac{\partial F}{\partial x} \frac{dV}{A}, \quad (\text{A.19})$$

was integrated over each control volume in the standard grid. The i^{th} control volume is used to explain the discretization.

Integrating this equation over the volume of the i^{th} control volume produces the

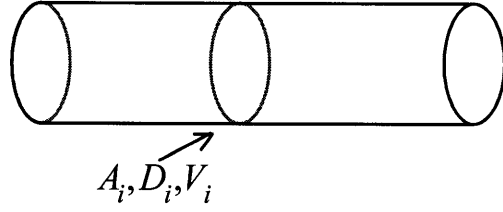


Figure A-2: i^{th} control volume in the standard grid.

equation

$$\underbrace{\int_{V_i} \frac{\partial \rho}{\partial t} dV}_{\text{Term (1)}} = - \underbrace{\int_{V_i} \frac{\partial}{\partial x} \frac{F}{A} dV}_{\text{Term (2)}}. \quad (\text{A.20})$$

Term (1) can be simplified by using the fact that V_i is constant over time,

$$\int_{V_i} \frac{\partial \rho}{\partial t} dV = \frac{\partial}{\partial t} \int_{V_i} \rho dV. \quad (\text{A.21})$$

Then, we can use the definition of ρ_i to get the discretized approximation of Term (1):

$$\frac{\partial}{\partial t} \int_{V_i} \rho dV = \frac{\partial \rho_i}{\partial t} V_i. \quad (\text{A.22})$$

Term (2) can be calculated by using the divergence theorem:

$$\int_{V_i} \frac{\partial}{\partial x} \frac{F}{A} dV = \int_{S_i} \frac{F}{A} (\mathbf{n} \cdot \mathbf{e}_x) dS. \quad (\text{A.23})$$

In this case, S_i corresponds to the sum of the surfaces surrounding the i^{th} control volume [$S_i = S_1 + S_2 + S_3$ (Fig. A-3)].

The right hand side of Eq. (A.23) can be separated into the integrals over each surface surrounding the i^{th} control volume and the resulting expression can be sim-

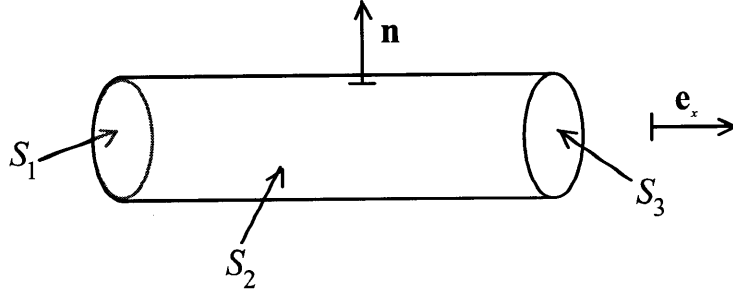


Figure A-3: i^{th} control volume in the standard grid.

simplified:

$$\begin{aligned}
 \int_{S_i} \frac{F}{A} (\mathbf{n} \cdot \mathbf{e}_x) dS &= \int_{S_1} \frac{F}{A} \underbrace{(\mathbf{n} \cdot \mathbf{e}_x)}_{-1} dS + \int_{S_2} \frac{F}{A} \underbrace{(\mathbf{n} \cdot \mathbf{e}_x)}_0 dS + \int_{S_3} \frac{F}{A} \underbrace{(\mathbf{n} \cdot \mathbf{e}_x)}_1 dS \\
 &= - \int_{S_1} \frac{F}{A} dS + \int_{S_3} \frac{F}{A} dS.
 \end{aligned} \tag{A.24}$$

Approximating F at S_1 by F_{i-1} and F at S_3 we obtain

$$\int_{S_i} \frac{F}{A} (\mathbf{n} \cdot \mathbf{e}_x) dS = -F_{i-1} + F_i. \tag{A.25}$$

Finally, we can write the discretized continuity equation as

$$\frac{d\rho_i}{dt} V_i = F_{i-1} - F_i. \tag{A.26}$$

A.2 Discretization of the momentum equation

The momentum equation,

$$\frac{\partial F}{\partial t A} = -\frac{\partial P}{\partial x} - \frac{\partial F^2}{\partial x \rho A^2} - \frac{2f|F|F}{D\rho A^2}, \tag{A.27}$$

is discretized using the staggered grid. The most general case corresponds to a staggered control volume that includes a change in section (Fig. A-4).

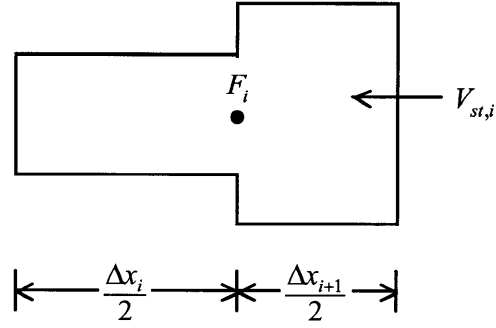


Figure A-4: i^{th} control volume in the staggered grid.

Integrating Eq. (A.27) over $V_{st,i}$ produces

$$\underbrace{\int_{V_{st,i}} \frac{\partial F}{\partial t} \frac{dV}{A}}_{\text{Term (1)}} = - \underbrace{\int_{V_{st,i}} \frac{\partial P}{\partial x} dV}_{\text{Term (2)}} - \underbrace{\int_{V_{st,i}} \frac{\partial}{\partial x} \frac{F^2}{\rho A^2} dV}_{\text{Term (3)}} - \underbrace{\int_{V_{st,i}} \frac{2f|F|F}{D\rho A^2} dV}_{\text{Term (4)}} \quad (\text{A.28})$$

Term (1) can be simplified by considering that $V_{st,i}$ is constant over time, and by dividing the control volume into two control volumes with different section (Fig. A-8).

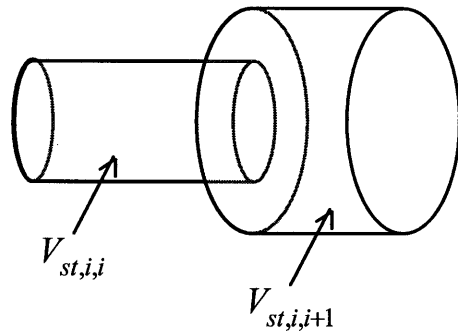


Figure A-5: i^{th} control volume in the staggered grid.

$$\int_{V_{st,i}} \frac{\partial F}{\partial t} \frac{F}{A} dV = \frac{\partial}{\partial t} \int_{V_{st,i}} \frac{F}{A} dV \quad (\text{A.29})$$

$$= \frac{\partial}{\partial t} \left(\int_{V_{st,i,i}} \frac{F}{A} dV + \int_{V_{st,i,i+1}} \frac{F}{A} dV \right) \quad (\text{A.30})$$

$$= \frac{\partial}{\partial t} \left(\int_{\frac{\Delta x_i}{2}} \frac{F}{A_i} A_i dx + \int_{\frac{\Delta x_{i+1}}{2}} \frac{F}{A_{i+1}} A_{i+1} dx \right) \quad (\text{A.31})$$

$$= \frac{\partial}{\partial t} \int_{\frac{\Delta x_i}{2} + \frac{\Delta x_{i+1}}{2}} F dx \quad (\text{A.32})$$

$$= \frac{\partial}{\partial t} \left[\left(\frac{\Delta x_i}{2} + \frac{\Delta x_{i+1}}{2} \right) F_i \right] \quad (\text{A.33})$$

$$= \left(\frac{\Delta x_i}{2} + \frac{\Delta x_{i+1}}{2} \right) \frac{\partial F_i}{\partial t} \quad (\text{A.34})$$

Term (2) can be approximated by using the divergence theorem and by decomposing the surface surrounding the i^{th} control volume in the staggered grid (Fig. A-6).

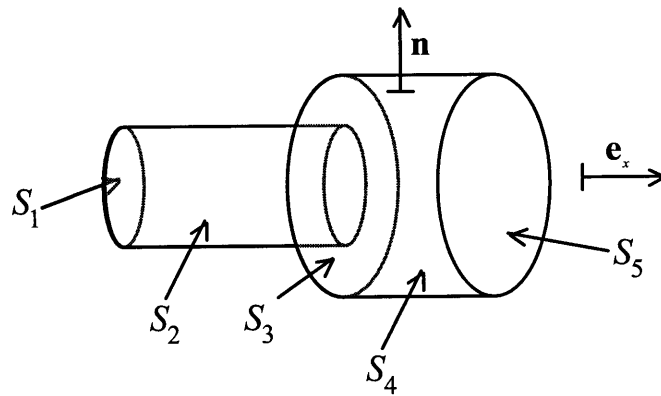


Figure A-6: i^{th} control volume in the staggered grid with a change in section.

$$\int_{V_{st,i}} \frac{\partial P}{\partial x} dV = \int_{S_{st,i}} P \mathbf{n} \cdot \mathbf{e}_x dS \quad (\text{A.35})$$

Considering that $S_{st,i}$ can be decomposed in five surfaces [$S_{st,i} = S_1 + S_2 + S_3 + S_4 + S_5$ (Fig. A-6)], then the previous equation can be written and simplified as

$$\begin{aligned} \int_{V_{st,i}} \frac{\partial P}{\partial x} dV &= \int_{S_1} P \underbrace{\mathbf{n} \cdot \mathbf{e}_x}_{-1} dS + \int_{S_2} P \underbrace{\mathbf{n} \cdot \mathbf{e}_x}_0 dS + \int_{S_3} P \underbrace{\mathbf{n} \cdot \mathbf{e}_x}_{-1} dS + \int_{S_4} P \underbrace{\mathbf{n} \cdot \mathbf{e}_x}_0 dS \\ &\quad + \int_{S_5} P \underbrace{\mathbf{n} \cdot \mathbf{e}_x}_1 dS, \end{aligned} \quad (\text{A.36})$$

$$\int_{V_{st,i}} \frac{\partial P}{\partial x} dV = - \int_{S_1} P dS - \int_{S_3} P dS + \int_{S_5} P dS. \quad (\text{A.37})$$

The three terms in the right hand side of Eq. (A.37) represent the forces exerted over the gas in the staggered control volume at the different vertical faces. In particular, the force at S_3 represents the force exerted by the wall over the gas as a reaction to the force exerted by the gas over the wall. This force is significant and it needs to be included to correctly model the behavior of the gas.

P at S_1 can be approximated by P_i and P at S_5 can be approximated by using P_{i+1} . P at S_3 can be approximated by $\bar{P}_{(i,i+1)}$, a linear interpolation between P_i and P_{i+1} :

$$\bar{P}_{(i,i+1)} = \frac{P_i \frac{\Delta x_{i+1}}{2} + P_{i+1} \frac{\Delta x_i}{2}}{\frac{\Delta x_i}{2} + \frac{\Delta x_{i+1}}{2}}. \quad (\text{A.38})$$

Then Eq. (A.37) can be written as

$$\int_{V_{st,i}} \frac{\partial P}{\partial x} dV = - P_i A_i - \bar{P}_{(i,i+1)} (A_{i+1} - A_i) + P_{i+1} A_{i+1}. \quad (\text{A.39})$$

Finally,

$$\int_{V_{st,i}} \frac{\partial P}{\partial x} dV = -P_i A_i - \frac{P_i \frac{\Delta x_{i+1}}{2} + P_{i+1} \frac{\Delta x_i}{2}}{\frac{\Delta x_i}{2} + \frac{\Delta x_{i+1}}{2}} (A_{i+1} - A_i) + P_{i+1} A_{i+1}. \quad (\text{A.40})$$

Term (3) can be approximated using a similar approach:

$$\int_{V_{st,i}} \frac{\partial}{\partial x} \frac{F^2}{\rho A^2} dV = \int_{S_{st,i}} \frac{F^2}{\rho A^2} \mathbf{n} \cdot \mathbf{e}_x dS \quad (\text{A.41})$$

$$= \int_{S_1} \frac{F^2}{\rho A^2} \underbrace{\mathbf{n} \cdot \mathbf{e}_x}_{-1} dS + \int_{S_2} \frac{F^2}{\rho A^2} \underbrace{\mathbf{n} \cdot \mathbf{e}_x}_0 dS + \int_{S_3} \overbrace{\frac{F^2}{\rho A^2}}^0 \underbrace{\mathbf{n} \cdot \mathbf{e}_x}_{-1} dS \quad (\text{A.42})$$

$$+ \int_{S_4} \frac{F^2}{\rho A^2} \underbrace{\mathbf{n} \cdot \mathbf{e}_x}_0 dS + \int_{S_5} \frac{F^2}{\rho A^2} \underbrace{\mathbf{n} \cdot \mathbf{e}_x}_1 dS. \quad (\text{A.43})$$

The resulting equation is

$$\int_{V_{st,i}} \frac{\partial}{\partial x} \frac{F^2}{\rho A^2} dV = - \int_{S_1} \frac{F^2}{\rho A^2} dS + \int_{S_5} \frac{F^2}{\rho A^2} dS. \quad (\text{A.44})$$

In this case, the term at S_3 is discarded because there is no flow through that wall.

F at S_1 can be approximated by using a linear interpolation between F_{i-1} and F_i :

$$\overline{F}_{(i-1,i)} = \frac{F_{i-1} \frac{\Delta x_i}{2} + F_i \frac{\Delta x_{i-1}}{2}}{\frac{\Delta x_i}{2} + \frac{\Delta x_{i-1}}{2}} = \frac{F_{i-1} + F_i}{2}. \quad (\text{A.45})$$

Similarly, the linear approximation of F at S_5 is

$$\overline{F}_{(i,i+1)} = \frac{F_i \frac{\Delta x_{i+1}}{2} + F_{i+1} \frac{\Delta x_i}{2}}{\frac{\Delta x_{i+1}}{2} + \frac{\Delta x_i}{2}} = \frac{F_i + F_{i+1}}{2}. \quad (\text{A.46})$$

Considering that $S_1 = A_i$ and $S_5 = A_{i+1}$, and that ρ at S_1 and S_5 can be approx-

imated by ρ_i and ρ_{i+1} respectively then Eq. (A.44) can be written as

$$\int_{V_{st,i}} \frac{\partial}{\partial x} \frac{F^2}{\rho A^2} dV = - \int_{S_1} \frac{\bar{F}_{(i-1,i)}^2}{\rho_i A_i^2} dS + \int_{S_5} \frac{\bar{F}_{(i,i+1)}^2}{\rho_{i+1} A_{i+1}^2} dS \quad (\text{A.47})$$

$$= - \frac{\bar{F}_{(i-1,i)}^2}{\rho_i A_i} + \frac{\bar{F}_{(i,i+1)}^2}{\rho_{i+1} A_{i+1}}. \quad (\text{A.48})$$

Finally, Term (3) can be written as

$$\int_{V_{st,i}} \frac{\partial}{\partial x} \frac{F^2}{\rho A^2} dV = - \left(\frac{F_{i-1} + F_i}{2} \right)^2 \frac{1}{\rho_i A_i} + \left(\frac{F_i + F_{i+1}}{2} \right)^2 \frac{1}{\rho_{i+1} A_{i+1}}. \quad (\text{A.49})$$

Term (4) can be calculated by using the i^{th} control volume in the staggered grid. For this calculation, the control volume is separated into two subcontrol volumes with different section (Fig. A-7).

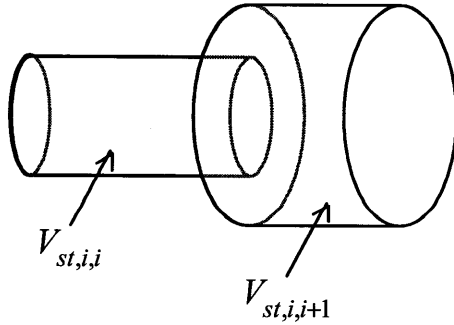


Figure A-7: i^{th} control volume in the staggered grid.

$$\int_{V_{st,i}} \frac{2f|F|F}{D\rho A^2} dV = \int_{V_{st,i,i}} \frac{2f|F|F}{D\rho A^2} dV + \int_{V_{st,i,i+1}} \frac{2f|F|F}{D\rho A^2} dV \quad (\text{A.50})$$

It is assumed that the prevailing value for ρ in each of the subcontrol volumes is the value of ρ in the corresponding control volume in the standard grid. Then

Eq. (A.50) can be written as

$$\int_{V_{st,i}} \frac{2f|F|F}{D\rho A^2} dV = \frac{2f_i}{D_i\rho_i A_i^2} \int_{V_{st,i,i}} |F| F dV + \frac{2f_{i+1}}{D_{i+1}\rho_{i+1} A_{i+1}} \int_{V_{st,i,i+1}} |F| F dV \quad (\text{A.51})$$

$\int_{V_{st,i,i}} |F| F dV$ and $\int_{V_{st,i,i+1}} |F| F dV$ can be approximated by $|F_i| F_i A_i \frac{\Delta x_i}{2}$ and $|F_i| F_i A_{i+1} \frac{\Delta x_{i+1}}{2}$, respectively. Then Eq. (A.51) can be written as

$$\int_{V_{st,i}} \frac{2f|F|F}{D\rho A^2} dV = \frac{2f_i}{D_i\rho_i A_i^2} |F_i| F_i A_i \frac{\Delta x_i}{2} + \frac{2f_{i+1}}{D_{i+1}\rho_{i+1} A_{i+1}^2} |F_i| F_i A_{i+1} \frac{\Delta x_{i+1}}{2} \quad (\text{A.52})$$

$$= \frac{2f_i |F_i| F_i \Delta x_i}{D_i \rho_i A_i} + \frac{2f_{i+1} |F_i| F_i \Delta x_{i+1}}{D_{i+1} \rho_{i+1} A_{i+1}} \quad (\text{A.53})$$

Having calculated all the terms for the momentum equation (Eq. (A.28)), the discretized momentum equation can be written as

$$\left(\frac{\Delta x_i}{2} + \frac{\Delta x_{i+1}}{2} \right) \frac{dF_i}{dt} = + P_i A_i + \frac{P_i \frac{\Delta x_{i+1}}{2} + P_{i+1} \frac{\Delta x_i}{2}}{\frac{\Delta x_i}{2} + \frac{\Delta x_{i+1}}{2}} (A_{i+1} - A_i) - P_{i+1} A_{i+1} \quad (\text{A.54})$$

$$+ \left(\frac{F_{i-1} + F_i}{2} \right)^2 \frac{1}{\rho_i A_i} - \left(\frac{F_i + F_{i+1}}{2} \right)^2 \frac{1}{\rho_{i+1} A_{i+1}} \quad (\text{A.55})$$

$$- \frac{2f_i |F_i| F_i \Delta x_i}{D_i \rho_i A_i} - \frac{2f_{i+1} |F_i| F_i \Delta x_{i+1}}{D_{i+1} \rho_{i+1} A_{i+1}} \quad (\text{A.56})$$

A.3 Discretization of the energy equation

The energy equation,

$$\frac{\partial \psi}{\partial t} = - \frac{\partial Fh}{\partial x} \frac{1}{A} - \frac{4U(T - T_{Ext})}{D}, \quad (\text{A.57})$$

is discretized using the standard grid and the i^{th} control volume. Integrating Eq. (A.57) over this volume produces the following equation:

$$\underbrace{\int_{V_i} \frac{\partial \psi}{\partial t} dV}_{\text{Term (1)}} = - \underbrace{\int_{V_i} \frac{\partial}{\partial x} \frac{Fh}{A} dV}_{\text{Term (2)}} - \underbrace{\int_{V_i} \frac{4U}{D} (T - T_{ext}) dV}_{\text{Term (3)}}. \quad (\text{A.58})$$

Term (1) can be simplified by using the fact that V_i is constant over time and by using the definition of ψ_i (Eq. (A.14)):

$$\int_{V_i} \frac{\partial \psi}{\partial t} dV = \frac{\partial}{\partial t} \int_{V_i} \psi dV = \frac{\partial \psi_i}{\partial t} V_i. \quad (\text{A.59})$$

Term (2) can be calculated using the divergence theorem:

$$\int_{V_i} \frac{\partial}{\partial x} \frac{Fh}{A} dV = \int_{S_i} \frac{Fh}{A} \mathbf{n} \cdot \mathbf{e}_x dS. \quad (\text{A.60})$$

Again, S_i corresponds to the sum of the surfaces surrounding the i^{th} control volume [$S_i = S_1 + S_2 + S_3$ (Fig. A-8)].

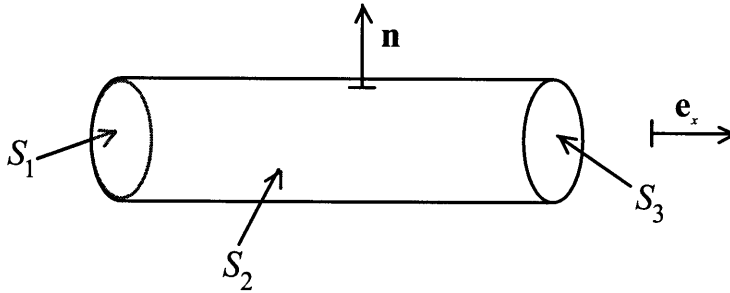


Figure A-8: i^{th} control volume in the standard grid.

Then, the right hand side of Eq. (A.60) can be separated into the integrals over each surface surrounding the i^{th} control volume and the resulting expression can be

simplified:

$$\int_{V_i} \frac{\partial}{\partial x} \frac{Fh}{A} dV = \int_{S_1} \frac{Fh}{A} \underbrace{\mathbf{n} \cdot \mathbf{e}_x}_{-1} dS + \int_{S_2} \frac{Fh}{A} \underbrace{\mathbf{n} \cdot \mathbf{e}_x}_0 dS + \int_{S_3} \frac{Fh}{A} \underbrace{\mathbf{n} \cdot \mathbf{e}_x}_1 dS \quad (\text{A.61})$$

$$= - \int_{S_1} \frac{Fh}{A} dS + \int_{S_3} \frac{Fh}{A} dS. \quad (\text{A.62})$$

At S_1 , A corresponds to A_{i-1} , F corresponds to F_{i-1} , and h corresponds to h_{i-1} (upwind differencing scheme [27]). At S_3 , A corresponds to A_i , F corresponds to F_i , and h corresponds to h_i . Then Eq. (A.62) can be written as

$$\int_{V_i} \frac{\partial}{\partial x} \frac{Fh}{A} dV = - \frac{F_{i-1}h_{i-1}}{A_{i-1}} \underbrace{\int_{S_1} dS}_{A_{i-1}} + \frac{F_i h_i}{A_i} \underbrace{\int_{S_3} dS}_{A_i} \quad (\text{A.63})$$

$$= - h_{i-1}F_{i-1} + h_iF_i. \quad (\text{A.64})$$

Solving for Term (3). At the i^{th} control volume U, D, T and T_{ext} can be approximated by using U_i, D_i, T_i and $T_{ext,i}$, respectively. Then Term (3) can be written as

$$\int_{V_i} \frac{4U}{D} (T - T_{ext}) dV = \frac{4U_i}{D_i} (T_i - T_{ext,i}) V_i. \quad (\text{A.65})$$

Finally, the discretized energy equation is:

$$V_i \frac{d\psi_i}{dt} = h_{i-1}F_{i-1} - h_iF_i - \frac{4U_i}{D_i} (T_i - T_{ext,i}) V_i. \quad (\text{A.66})$$

Appendix B

JACOBIAN code

MODELS_PHYSICALPROPERTIES.JAC

```
1 *****
2 DECLARE
3 *****
4 TYPE #Default Min Max Units
5 Area = 1 : -1e10 : 1e2 UNIT = "m2"
6 ConcPrecursors = 0: -1.0e-7 : 1.0e10 unit = ""
7 DeltaTemperature = 0 : -13 : 13 UNIT = "K"
8 Density = 0.755 : -1e-10 : 1e5 UNIT = "kg/m3"
9 DynViscosity = 0.1 : -1.0e-12 : 1.0e10 unit = "N*s/m^2"
10 Energy = 0 : -1e10 : 1e10 UNIT = "J/m3"
11 Flowrate = 0.001: -1.0e5 : 1.0e5 unit = "Kg/s"
12 Heat = 1: -1e10 : 1e10 UNIT = "W"
13 HTCoeff = 0.1 : -1.0e-12:1.0E5 unit = "W/(m^2*K)" # heat transfer coefficient
14 IConcentration = 0: -1.0e-7 : 1.0e25 unit = ""
15 KinViscosity = 0.1 : -1.0e-12 : 1.0e10 unit = "m^2/s"
16 Length = 0.01 : -1.0e-10:1.0e3 unit = "m" # length
17 MassFlowRate = 0 : -1.0e6 : 1.0e6 unit = "kg/s"
18 MassFlux = 218.0 : 0 : 1e8 UNIT = "Kg/(m2*s)"
19 MassVelocity = 1 : -1e-7 : 1e4 UNIT = "kg/m^2/s"
20 Momentum = 218.0 : 0 : 1e8 UNIT = "Kg/(m2*s)"
21 Nondimensional = 0.01 : -1.0e-10 : 1.0e12 unit = "dimensionless" # for the nondimensional numbers
22 PhiConcentration = 0: -1.0e-7 : 1.0e25 unit = "neutrons/(m2*s)"
23 Power = 0: -1.0e-7 : 1.0e10 unit = ""
24 Pressure = 1.8e6 : 0 : 2e8 UNIT = "Pa"
25 Reactivity = 0: -1.0e6 : 1.0e6 unit = ""
26 RealVar = 0: -1.0e10 : 1.0e10 unit = ""
27 SpecificEnergy = 0 : -1e10 : 1e10 UNIT = "J/Kg"
28 SpHeatCapacity = 0 : -1.0e-7 : 1.0e6 unit = "J/(kg*K)"
29 SpHeatCapacityV = 0: -1.0e-7 : 1.0e10 unit = "J/(m3*K)"
30 Temperature = 0: 0 : 1e10 UNIT = "K"
31 ThConduct = 0.01 : -1.0e-10 : 1.0e5 unit = "W/(m*K)" #thermal conductivity
32 Velocity = 2 : -1.0e-7 : 1.0e5 unit = "m/s"
33 XeConcentration = 0: -1.0e-7 : 1.0e25 unit = ""
34 END # declare
35 *****
36
37
38
39 *****
40 MODEL HTCoeffGasPipeInsAir
41 *****
42 PARAMETER
43 #SET
44 dynViscHe AS REAL # dynamic viscosity of Helium inside the pipe unit = "Pa*s" : set
45 CpHe AS REAL # heat capacity unit= "J/(K*kg)" : set
46 k1 AS REAL # ThConduct # thermal conductivity of Alloy 617 unit = "W/(m*K)" : set
47 k2 AS REAL # ThConduct # thermal conductivity of insulation unit = "W/(m*K)" : set
48 kHe AS REAL # thermal conductivity of Helium inside pipe unit = "W/(m*K)" : set
49 #EXTERNAL
50 r0 AS REAL # pipe internal radius unit="m" : external
51 r1 AS REAL # pipe internal radius + metal thickness unit = "m": external
52 r2 AS REAL # pipe internal radius + metal thickness + insulations thickness unit = "m": external
53 VARIABLE
54 h2 AS HTCoeff # heat transfer coefficient of Air outside pipe, I will set it as a constant for now : set
```

```

55
56 rhoPipeHe AS Density # average density of Helium inside the pipe : external
57 vPipe AS Velocity # velocity inside the pipe : external
58
59 h0 AS HTCoeff # heat transfer coefficient of Helium inside pipe, depends on v and rho : calculated
60 U AS HTCoeff # overall heat transfer coefficient : calculated
61 SET
62 dynViscHe := 3.963e-5; # INL calculations # 34.9e-6; # from NIST
63 CpHe := 5.192e3; # from NIST at 400 C , 1-2 MPa
64 k1 := 26.0; # from INL calculations #19.3; # thermal conductivity of Alloy 617 at 400C from material sheet
    information
65 k2 := 0.1; # thermal conductivity of insulation from INL OK
66 kHe := 0.31102; # from INL calculations # 0.274; # thermal conductivity Helium at 400C , 1-2 MPa
67 INTERMEDIATE
68 kinViscHe := dynViscHe/rhoPipeHe; # kinViscHe AS KinViscosity # kinematic viscosity of Helium inside the pipe
    : calculated
69 ReHe := vPipe * 2*r0/ kinViscHe; # ReHe AS Nondimensional # reynolds number : calculated
70 PrHe := dynViscHe * CpHe/kHe; # PrHe AS Nondimensional # Prandtl number : calculated
71 Nu01 := 4.364;
72 Nu03 := 0.021*ReHe^0.8*PrHe^0.4;
73 Nu03ReHe5000 := 0.021*5000^0.8*PrHe^0.4; # Nu03 at ReHe = 5000
74 Nu02 := Nu01 + (Nu03ReHe5000 - Nu01)/(5000-2300)*(ReHe -2300); # linearized Nu0 between
75 EQUATION
76 IF ReHe <= 2300 THEN
77 h0*2*r0 = kHe*Nu01; # linear model Oh paper June 2007 ANS
78 ELSE
79 IF ReHe <=5000 THEN
80 h0*2*r0 = kHe*Nu02;
81 ELSE
82 h0*2*r0 = kHe*Nu03; #Dittus-Boelter equation [Kays and Crawford, 1980]
83 END #if
84 END # if
85 h2 = 17.344; # INL calculations # 0.0515;#engineeringtoolbox.com
86 U = 1/(r0* ( 1/(r0*h0) + log(r1/r0)/k1 + log(r2/r1)/k2 + 1/(r2*h2) ) ); # overall heat transfer coefficient,
    [Bird et al]
87 END # HTCoeffPipeAir
88 #####
89
90
91 #####
92 MODEL HTCoeffGasMetalHX
93 #####
94 PARAMETER
95 #SET
96 dynViscHe AS REAL # dynamic viscosity of Helium inside the pipe unit = "Pa*s" : set
97 CpHe AS REAL # heat capacity unit= "J/(K*kg)" : set
98 k1 AS REAL # ThConduct # thermal conductivity of Alloy 617 unit = "W/(m*K)" : set
99 Pi AS REAL
100 #EXTERNAL
101 kHe AS REAL # thermal conductivity of Helium inside pipe unit = "W/(m*K)" : set
102 r0 AS REAL # pipe internal radius unit= "m" : external
103 t AS REAL # plate thickness = "m": external
104 #CALCULATED
105 r0eq AS REAL # pipe internal radius unit = "m": calculated
106 VARIABLE
107 #EXTERNAL
108 rhoPipeHe AS Density # average density of Helium inside the pipe : external
109 vPipe AS Velocity # velocity inside the pipe : external
110 #CALCULATED
111 h0 AS HTCoeff # heat transfer coefficient of Helium inside pipe, depends on v and rho : calculated
112 U AS HTCoeff # overall heat transfer coefficient : calculated
113 SET
114 #SET
115 dynViscHe := 34.9e-6; # from NIST
116 CpHe := 5.191e3; # from NIST at 400 C , 1-2 MPa
117 k1 := 22.0; # from INL calculations # 19.3; # thermal conductivity of Alloy 617 at 400C from material sheet
    information
118 Pi := 4*ATAN(1);
119 #CALCULATED
120 r0eq:= Pi*r0^2/(2*(Pi*r0/2 + r0));
121 INTERMEDIATE
122 kinViscHe := dynViscHe/rhoPipeHe; # kinViscHe AS KinViscosity # kinematic viscosity of Helium inside the pipe
    : calculated
123 ReHe := vPipe * 2*r0/ kinViscHe; # ReHe AS Nondimensional # reynolds number : calculated
124 PrHe := dynViscHe * CpHe/kHe; # PrHe AS Nondimensional # Prandtl number : calculated
125 Nu01 := 4.364;
126 Nu03 := 0.021*ReHe^0.8*PrHe^0.4;
127 Nu03ReHe5000 := 0.021*5000^0.8*PrHe^0.4; # Nu03 at ReHe = 5000
128 Nu02 := Nu01 + (Nu03ReHe5000 - Nu01)/(5000-2300)*(ReHe -2300); # linearized Nu0 between
129 EQUATION
130 IF ReHe <= 1e8 THEN
131 h0*2*r0 = kHe*Nu01; # linear model Oh paper June 2007 ANS
132 ELSE
133 IF ReHe <=5000 THEN
134 h0*2*r0 = kHe*Nu02;
135 ELSE
136 h0*2*r0 = kHe*Nu03; #Dittus-Boelter equation [Kays and Crawford, 1980]
137 END #if
138 END # if
139 U = 1/ (1/h0 + (t/2)/k1);
140 END # HTCoeffGasMetalHX
141 #####

```



```

142
143
144 *****
145 MODEL HTCoeffGasMetalHXDummyInner
146 *****
147 PARAMETER
148 # SET
149 k1 AS REAL # ThConduct # thermal conductivity of Alloy 617 unit = "W/(m*K)" : set
150 rOuter AS REAL # pipe external radius unit= "m" : set
151 rInner AS REAL # pipe internal radius unit= "m" : set
152 hInner AS REAL # heat transfer coefficient inside the pipe= "W/(m^2*K)"
153 # CALCULATED
154 rM AS REAL # pipe intermediate radius unit = "m" : calculated
155 VARIABLE
156 #EXTERNAL
157 rhoPipeHe AS Density # average density of Helium inside the pipe : external
158 vPipe AS Velocity # velocity inside the pipe : external
159 #CALCULATED
160 U AS HTCoeff # overall heat transfer coefficient : calculated
161 SET
162 #SET
163 k1 := 22.0; # from INL calculations # 19.3; # thermal conductivity of Alloy 617 at 400C from material sheet
164 information
165 rInner:= 0.01/2; rOuter:= 0.013/2; hInner := 2000;
166 # CALCULATED
167 rM:= (rInner + rOuter)/2;
168 INTERMEDIATE
169 EQUATION
170 U = 1/(1/hInner + rInner*log(rM/rInner)/k1); # this one is calculated with respect to AInner
171 END # HTCoeffGasMetalHX
172 *****
173 *****
174 MODEL HTCoeffGasMetalHXDummyOuter
175 *****
176 PARAMETER
177 # SET
178 k1 AS REAL # ThConduct # thermal conductivity of Alloy 617 unit = "W/(m*K)" : set
179 rOuter AS REAL # pipe external radius unit= "m" : set
180 rInner AS REAL # pipe internal radius unit= "m" : set
181 hOuter AS REAL # heat transfer coefficient inside the pipe= "W/(m^2*K)"
182
183 # CALCULATED
184 rM AS REAL # pipe intermediate radius unit = "m" : calculated
185 VARIABLE
186 #EXTERNAL
187 rhoPipeHe AS Density # average density of Helium inside the pipe : external
188 vPipe AS Velocity # velocity inside the pipe : external
189 #CALCULATED
190 U AS HTCoeff # overall heat transfer coefficient : calculated
191 SET
192 #SET
193 k1 := 22.0; # from INL calculations # 19.3; # thermal conductivity of Alloy 617 at 400C from material sheet
194 information
195 rInner:= 0.01/2; rOuter:= 0.013/2; hOuter:= 1364; # INL report
196 # CALCULATED
197 rM:= (rInner + rOuter)/2;
198 INTERMEDIATE
199 EQUATION
200 U = 1/(rOuter*log(rOuter/rM)/k1 + 1/hOuter); # this one is calculated with respect to AOuter
201 END # HTCoeffGasMetalHX
202 *****
203 *****
204 *****
205 MODEL HEEFM # heat transfer coefficient solid to helium in nuclear reactor core
206 *****
207 PARAMETER
208 # SET here
209 d AS REAL
210 # EXTERNAL
211 VoidF AS REAL # VoidFraction
212 Area AS REAL
213 VARIABLE
214 # OUTPUT
215 HTCoeffR AS HTCoeff
216 # EXTERNAL
217 Temp AS Temperature
218 W AS MassFlowRate
219 SET
220 d:= 0.06; # dPebble= 60 mm, L 533
221 INTERMEDIATE
222 Ac:= Area*VoidF;
223 HeVis:= 1e-7*3.953*Temp^0.687; # temp in K, L37
224 Renold:= W*d/(Ac*HeVis);
225 HePr:= 0.740*Temp^(-0.014);
226 Nu:=1.27*HePr^0.333*Renold^0.36/VoidF^1.18+ 0.033*HePr^0.5*Renold^0.86/VoidF^1.07;
227 KGas:= 2.774*Temp^0.701*0.001;
228 EQUATION
229 HTCoeffR=KGas*Nu/d;
230 END # HEEFM
231 *****

```

```

232
233
234 *****
235 MODEL HEFPM2 # heat transfer coefficient solid to helium in nuclear reactor core
236 *****
237 PARAMETER
238 # SET here
239 d AS REAL
240 # EXTERNAL
241 VoidF AS REAL # VoidFraction
242 Area AS REAL
243 VARIABLE
244 # OUTPUT
245 HTCoeffR AS HTCoeff
246 # EXTERNAL
247 Temp AS Temperature
248 W AS MassFlowRate
249 SET
250 d:= 0.06; # dPebble= 60 mm, L 533
251 INTERMEDIATE
252 Ac:= Area*VoidF;
253 HeVis:= 1e-7*3.953*Temp^0.687; # temp in K, L37
254 Renold:= W*d/(Ac*HeVis);
255 HePr:= 0.740*Temp^(-0.014);
256 Nu:=1.27*HePr^0.333*Renold^0.36/VoidF^1.18+ 0.033*HePr^0.5*Renold^0.86/VoidF^1.07;
257 KGas:= 2.774*Temp^0.701*0.001;
258 EQUATION
259 HTCoeffR=KGas*Nu/d;
260 END # HEFPM
261 *****
262
263 *****
264 MODEL CPRF # reflector heat capacity
265 *****
266 PARAMETER
267 # SET here
268 # EXTERNAL
269 VARIABLE
270 # OUTPUT
271 Cp AS SpHeatCapacity
272 # EXTERNAL
273 Temp AS Temperature
274 SET
275 INTERMEDIATE
276 TF:= (Temp - 273.16)*9/5 + 32; # transformation from K to F
277 CPi:= 0.127+0.374*(1.0-EXP(-TF/960.0));
278 EQUATION
279 CP=CPi*4.1868*1000;
280 END # CPRF
281 *****
282
283 *****
284 MODEL CPFuel # fuel heat capacity
285 *****
286 PARAMETER
287 # SET here
288 # EXTERNAL
289 VoidF AS REAL
290 TO AS REAL #reference temperature, freezing point in K
291 VARIABLE
292 # OUTPUT
293 Cp AS SpHeatCapacityV
294 # EXTERNAL
295 Temp AS Temperature
296 SET
297 TO:= 273.16;
298 INTERMEDIATE
299 CPF:=1.75*(1-VoidF);
300 F1:=0.645+3.14*(Temp-TO)/1000-2.809*((Temp-TO)/1000)^2+0.959*((Temp-TO)/1000)^3;
301 EQUATION
302 CP=CPF*F1*(100^3);
303 END # CPFuel
304 *****
305
306 *****

```

MODELS_PIPEMODELS.JAC

```

1 *****
2 MODEL LoopFullDyn
3 *****
4 PARAMETER
5 Pi AS REAL

```

```

6     N_Pipes AS INTEGER # number of sections with different properties
7     R_c AS REAL #Rc constant "J/(mol*K)"
8     Mw AS REAL #Molecular weight "Kg/mol"
9     T_stand AS REAL #Standard Temp "K"
10    Cp AS REAL #specific heat at constant pressure "J/Kg/K"
11    h_form AS REAL #specific enthalpy of formation "J/Kg"
12    gamma AS REAL #gamma helium "no units"
13    InitT AS REAL #Temperature "K"
14    InitP AS REAL #initial pressure "Pa"
15    NG AS INTEGER #number of control volumes in the grid : external
16    SectionL AS ARRAY(N_Pipes) OF REAL # length of each section "m"
17    r0 AS ARRAY(N_Pipes) OF REAL # radius of each section "m"
18    muVisc AS ARRAY(N_Pipes) OF REAL # average viscosity in pipe
19    Tw AS REAL # In Plant Model
20    InitDeltaP AS REAL # In Simulation
21    MaxDeltaP AS REAL # In Simulation
22    A AS ARRAY(NG) OF REAL #area of each section 'm^2'
23    A_In AS REAL
24    A_Out AS REAL
25    SectionEnd AS ARRAY(N_Pipes) OF INTEGER # end point sections
26    SectionSpan AS ARRAY(N_Pipes) OF INTEGER # length section
27    SectionDelta_x AS ARRAY(N_Pipes) OF REAL # length of control volume "m"
28    Delta_x AS ARRAY(NG) OF REAL # length of control volume for each point "m"
29    Delta_xShift AS ARRAY(NG) OF REAL # length of control volume for each point in the shifted grid (non v) "m"
30    Delta_xExtra AS REAL
31    Vol AS ARRAY(NG) OF REAL
32  UNIT
33    HT1 AS HTCoeffGasPipeInsAir # section 1-10
34    HT2 AS HTCoeffGasMetalHX # section 11-30
35    HT3 AS HTCoeffGasPipeInsAir # section 31-50
36    HT4 AS HTCoeffGasMetalHXDummyOuter # section 51-70 # this is not necessary, the number is defined directly
37    INL report p 12
38  VARIABLE
39    AdaptFactor1 AS Nondimensional
40    AdaptFactor2 AS Nondimensional
41    rho AS ARRAY(NG) OF Density
42    P AS ARRAY(NG) OF Pressure
43    P_Out AS Pressure
44    h AS ARRAY(NG) OF SpecificEnergy
45    h0 AS SpecificEnergy
46    T AS ARRAY(NG) OF Temperature
47    TO AS Temperature
48    TExtrnl AS ARRAY(NG) OF Temperature
49    DeltaP AS Pressure
50    psi AS ARRAY(NG) OF Energy # 2 to NG Differential
51    F AS ARRAY(NG) OF Flowrate
52    F_In AS Flowrate
53    rho_avg AS Density
54    totalMass AS Nondimensional
55    ModifyFlow AS Nondimensional
56    comp_leak AS Nondimensional
57    #Extra Variables For Section Change at Compressor
58    rhoExtra AS ARRAY(2) OF Density
59    PExtra AS ARRAY(2) OF Pressure
60    hExtra AS ARRAY(2) OF SpecificEnergy
61    TExtra AS ARRAY(2) OF Temperature
62    psiExtra AS ARRAY(2) OF Energy
63    FExtra AS ARRAY(2) OF Flowrate
64  SET
65    Pi:= 4*ATAN(1);
66    R_c := 8.314; Mw := 4.0E-3;
67    T_stand := 298; Cp := 20.78; h_form := 0; gamma := 1.667;
68    InitT:=291.15; InitP:= 2.0e6; NG:=100; N_Pipes := 4;
69    A((SectionEnd(1)+1):SectionEnd(2)):= 0.3475; #:= achan*nhot = PI*d^2/8*nhot # A(2)
70    A((SectionEnd(3)+1):SectionEnd(4)):= 0.4012; # from filewith LMtD # A(4)
71    HT2.kHe:= 0.34981; # from INL calculations, file with LMtD
72    SectionEnd(1) := 10;
73    SectionEnd(2) := SectionEnd(1) + 40;
74    SectionEnd(3) := SectionEnd(2) + 10;
75    SectionEnd(N_Pipes):= NG;
76    SectionL(1) := 90; SectionL(2) := 0.98807; SectionL(3) := 90;
77    SectionL(4) :=8.656;
78    r0(1) := 0.413/2; r0(2) := (9.1652e-4)/2; # dhyd in the PCHE, this is needed to calculate Re
79    r0(3) := 0.444/2; r0(4):= 0.01123/2; # dhyd in the PHX
80    A(1:SectionEnd(1)):=Pi*r0(1)^2; # A(1) # 0.133964579
81    A_In:= A(1);
82    A_Out := A(NG);
83    A((SectionEnd(2)+1):SectionEnd(3)):=Pi*r0(3)^2; # A(3) # 0.154830252
84    HT1.r0 := r0(1);
85    HT1.r1 := HT1.r0*(2*0.01 + 1); # r1 depends on the t/d ratio, t/d = 0.01 for cold leg with P = 2MPa, INL
86    report p16 OK
87    HT1.r2 := HT1.r1 + 0.0058; # INL report p34
88    HT2.r0 := r0(2);
89    HT2.t := (HT2.r0*2*0.78*2 - HT2.r0)/3; # according to INL, an average of 2*tmax + 1*tmin
90    HT3.r0 := r0(3);
91    HT3.r1 := HT3.r0*(2*0.11 + 1); # r1 depends on the t/d ratio, t/d = 0.11 for hot leg with P = 2MPa, INL
92    report p16
93    HT3.r2 := HT3.r1 + 0.0059; # INL report p34
94    SectionSpan(1) := SectionEnd(1);
95    FOR I:=2 TO N_Pipes DO
96      SectionSpan(I) := SectionEnd(I) - SectionEnd(I-1);
97    END # for

```

```

95 SectionDelta_x(1) := SectionL(1)/(SectionSpan(1));
96 SectionDelta_x(2) := SectionL(2)/SectionSpan(2);
97 SectionDelta_x(3) := SectionL(3)/SectionSpan(3);
98 SectionDelta_x(4) := SectionL(4)/SectionSpan(4);
99 Delta_x(1:SectionEnd(1)) := SectionDelta_x(1);
100 Delta_xExtra := 0.01;
101 FOR I:=1 TO N_Pipes-1 DO
102   Delta_x((SectionEnd(I)+1):SectionEnd(I+1)) := SectionDelta_x(I+1);
103 END # for I # 20071112 changed
104 Delta_xShift(1:SectionEnd(1)) := SectionDelta_x(1);
105 FOR I := 1 TO N_Pipes-1 DO
106   Delta_xShift(SectionEnd(I)+1) := (SectionDelta_x(I)+SectionDelta_x(I+1))/2;
107   Delta_xShift(SectionEnd(I)+2:SectionEnd(I+1)) := SectionDelta_x(I+1);
108 END # for
109 Vol(1) := A(1)*SectionDelta_x(1);
110 Vol(2:SectionEnd(1)) := A(2:SectionEnd(1))*SectionDelta_x(1);
111 FOR I:= 1 TO (N_Pipes-1) DO
112   Vol(SectionEnd(I)+1:SectionEnd(I+1)) := A(SectionEnd(I)+1:SectionEnd(I+1))*SectionDelta_x(I+1);
113 END # for
114 INTERMEDIATE
115 Dimension i_U(NG), i_r0(NG), fr(NG)
116 Dimension i_mdot(NG) # mdot at each grid point, all the values should be equal
117 DIMENSION intRe(NG), intfArray(NG), intEps(N_Pipes)
118 i_U(1:SectionEnd(1)) := HT1.U ;
119 i_U((SectionEnd(1)+1):SectionEnd(2)) := HT2.U ;
120 i_U((SectionEnd(2)+1):SectionEnd(3)) := HT3.U ;
121 i_U((SectionEnd(3)+1):SectionEnd(4)) := HT4.U ;
122 i_r0(1:SectionEnd(1)) := r0(1) ;
123 i_r0((SectionEnd(1)+1):SectionEnd(2)) := r0(2) ;
124 i_r0((SectionEnd(2)+1):SectionEnd(3)) := r0(3) ;
125 i_r0((SectionEnd(3)+1):SectionEnd(4)) := r0(4) ;
126 i_rhoPipeHe1 := sigma(rho(1:SectionEnd(1)))/SectionSpan(1) ;
127 i_vPipe1 := sigma(F(1:SectionEnd(1)))/A(1:SectionEnd(1))/rho(1:SectionEnd(1))/SectionSpan(1) ;
128 i_rhoPipeHe2 := sigma(rho(SectionEnd(1)+1:SectionEnd(2)))/SectionSpan(2) ;
129 i_vPipe2 := sigma(F(SectionEnd(1)+1:SectionEnd(2)))/A(SectionEnd(1)+1:SectionEnd(2))/rho(SectionEnd(1)+1:
   SectionEnd(2))/SectionSpan(2) ;
130 i_rhoPipeHe3 := sigma(rho(SectionEnd(2)+1:SectionEnd(3)))/SectionSpan(3) ;
131 i_vPipe3 := sigma(F(SectionEnd(2)+1:SectionEnd(3)))/A(SectionEnd(2)+1:SectionEnd(3))/rho(SectionEnd(2)+1:
   SectionEnd(3))/SectionSpan(3) ;
132 i_rhoPipeHe4 := sigma(rho(SectionEnd(3)+1:SectionEnd(4)))/SectionSpan(4) ; #20080311
133 i_vPipe4 := sigma(F(SectionEnd(3)+1:SectionEnd(4)))/A(SectionEnd(3)+1:SectionEnd(4))/rho(SectionEnd(3)+1:
   SectionEnd(4))/SectionSpan(4) ;
134 intEps(1) := 4.57e-5;
135 intEps(2) := r0(2)*1e-9;
136 intEps(3) := 4.57e-5;
137 intEps(4) := r0(4)*1e-9;
138 intRe(1) := (F_In/A_In + F(1)/A(1))/2*r0(1)*2/muVisc(1);
139 intRe(2:SectionEnd(1)) := (F(1:SectionEnd(1)-1)/A(1:SectionEnd(1)-1)+F(2:SectionEnd(1))/A(2:SectionEnd(1)))/2*
   r0(1)*2/muVisc(1);
140 intRe(SectionEnd(1)+1) := (F(SectionEnd(1))/A(SectionEnd(1))+F(SectionEnd(1)+1)/A(SectionEnd(1)+1))/2*r0(2)*2/
   muVisc(2);
141 intRe(SectionEnd(1)+2:SectionEnd(2)) := (F(SectionEnd(1)+1:SectionEnd(2)-1)/A(SectionEnd(1)+
   1:SectionEnd(2)-1)+F(SectionEnd(1)+2:SectionEnd(2))/A(SectionEnd(1)+2:SectionEnd(2)))/2*r0(2)*2/muVisc(2);
142 intRe(SectionEnd(2)+1) := (F(SectionEnd(2))/A(SectionEnd(2))+F(SectionEnd(2)+1)/A(SectionEnd(2)+1))/2*r0(3)*2/
   muVisc(3);
143 intRe(SectionEnd(2)+2:SectionEnd(3)) := (F(SectionEnd(2)+1:SectionEnd(3)-1)/A(SectionEnd(2)+
   1:SectionEnd(3)-1)+F(SectionEnd(2)+2:SectionEnd(3))/A(SectionEnd(2)+2:SectionEnd(3)))/2*r0(3)*2/muVisc(3);
144 intRe(SectionEnd(3)+1) := (F(SectionEnd(3))/A(SectionEnd(3))+F(SectionEnd(3)+1)/A(SectionEnd(3)+1))/2*r0(4)*2/
   muVisc(4);
145 intRe(SectionEnd(3)+2:SectionEnd(4)) := (F(SectionEnd(3)+1:SectionEnd(4)-1)/A(SectionEnd(3)+
   1:SectionEnd(4)-1)+F(SectionEnd(3)+2:SectionEnd(4))/A(SectionEnd(3)+2:SectionEnd(4)))/2*r0(4)*2/muVisc(4);
146 intfArray(1:SectionEnd(1)) := 1/((-2*LOG10(intEps(1)/(3.7*r0(1)) + 2.51/intRe(1:SectionEnd(1))))^2/4;
   *(1.14 -2*LOG10(intEps(1)/r0(1) + 21.25/(intRe(1:SectionEnd(1))^0.9))))^2/4;
147 intfArray(SectionEnd(1)+1:SectionEnd(2)) := 1/((-2*LOG10(intEps(2)/(3.7*r0(2))
   + 2.51/intRe(SectionEnd(1)+1:SectionEnd(2))))^2/4;
   *(1.14 -2*LOG10(intEps(2)/r0(2) + 21.25/(intRe(SectionEnd(1)+1:SectionEnd(2))^0.9))))^2/4;
148 intfArray(SectionEnd(2)+1:SectionEnd(3)) := 1/((-2*LOG10(intEps(3)/(3.7*r0(3))
   + 2.51/intRe(SectionEnd(2)+1:SectionEnd(3))))^2/4;
   *(1.14 -2*LOG10(intEps(3)/r0(3) + 21.25/(intRe(SectionEnd(2)+1:SectionEnd(3))^0.9))))^2/4;
149 intfArray(SectionEnd(3)+1:SectionEnd(4)) := 1/((-2*LOG10(intEps(4)/(3.7*r0(4))
   + 2.51/intRe(SectionEnd(3)+1:SectionEnd(4))))^2/4;
   *(1.14 -2*LOG10(intEps(4)/r0(4) + 21.25/(intRe(SectionEnd(3)+1:SectionEnd(4))^0.9))))^2/4;
150 fr(1:SectionEnd(1)) := intfArray(1:SectionEnd(1)); #0.01294/4; # OK
151 fr((SectionEnd(1)+1):SectionEnd(2)) := intfArray(SectionEnd(1)+1:SectionEnd(2)); #4.009E-02/4; # OK
152 fr((SectionEnd(2)+1):SectionEnd(3)) := intfArray(SectionEnd(2)+1:SectionEnd(3)); #0.01348/4; # OK
153 fr((SectionEnd(3)+1):SectionEnd(4)) := intfArray(SectionEnd(3)+1:SectionEnd(4)); #2.758E-02/4; # OK
154 EQUATION
155 # Mass Balance
156 Delta_xExtra*A(1)*rhoExtra(1) = (F_In - FExtra(1));
157 Delta_xExtra*A(1)*rhoExtra(2) = (FExtra(1) - FExtra(2));
158 Delta_x(1)*A(1)*rho(1) = (FExtra(2) - F(1));
159 FOR I:= 2 TO NG DO
160   Delta_x(I)*A(I)*rho(I) = (F(I-1) - F(I));
161 END # for
162 # Momentum Balance
163 (Delta_xExtra + Delta_xExtra/2)*FExtra(1) =
164   -(PEXtra(2)*A(NG) - PEXtra(1)*A(NG))
165   + ( F_In )^2 / ( rhoExtra(1)*A(NG) )
166   - ( ( FExtra(1) + FExtra(2) )/2 )^2 / ( rhoExtra(2)*A(NG) );
167 (Delta_xExtra/2 + Delta_x(1)/2)*FExtra(2) =
168   - ( P(1)*A(1) - ( PEXtra(2)*Delta_x(1)/2 + P(1)*Delta_xExtra/2 ) / ( Delta_x(1)/2 +
   Delta_xExtra/2 ) * ( A(1) - A(NG) ) - PEXtra(2)*A(NG) )
169   + ( ( FExtra(1) + FExtra(2) )/2 )^2 / ( rhoExtra(2)*A(NG) )
170   - ( ( F(1) + FExtra(2) )/2 )^2 / ( rho(1)*A(1) )

```

```

179 - 2*fr(1)/( 2*i_r0(1) ) * ( ABS(FExtra(2))*FExtra(2) )/ ( rho(1)*A(1) ) * Delta_x(1)/2;
180 (Delta_x(1)/2 + Delta_x(2)/2) * $F(1) =
181 - ( P(2)*A(2) - ( P(1)*Delta_x(2)/2 + P(2)*Delta_x(1)/2 ) / ( Delta_x(1)/2+Delta_x(2)/2 )
    * ( A(2) - A(1) ) - P(1)*A(1) )
182 + ( ( FExtra(2) + F(1) )/2 )^2 / ( rho(1)*A(1) )
183 - ( ( F(2) + F(1) )/2 )^2 / ( rho(2)*A(2) )
184 - 2*fr(1)/( 2*i_r0(1) ) * ( ABS(F(1))*F(1) )/ ( rho(1)*A(1) ) * Delta_x(1)/2
185 - 2*fr(2)/( 2*i_r0(2) ) * ( ABS(F(1))*F(1) )/ ( rho(2)*A(2) ) * Delta_x(2)/2;
186 FOR I:=2 TO SectionEnd(4)-1 DO
187   ( Delta_x(I)/2 + Delta_x(I+1)/2 ) * $F(I) =
188   - ( P(I+1)*A(I+1) - ( P(I)*Delta_x(I+1)/2 + P(I+1)*Delta_x(I)/2 ) / ( Delta_x(I)/2+
    Delta_x(I+1)/2 ) * ( A(I+1) - A(I) ) - P(I)*A(I) )
189 + ( ( F(I-1) + F(I) )/2 )^2 / ( rho(I)*A(I) )
190 - ( ( F(I+1) + F(I) )/2 )^2 / ( rho(I+1)*A(I+1) )
191 - 2*fr(I)/( 2*i_r0(I) ) * ( ABS(F(I))*F(I) )/ ( rho(I)*A(I) ) * Delta_x(I)/2
192 - 2*fr(I+1)/( 2*i_r0(I+1) ) * ( ABS(F(I))*F(I) )/ ( rho(I+1)*A(I+1) ) * Delta_x(I+1)/2;
193 END
194 Delta_x(NG)/2 * $F(NG) =
195 - ( P_Out*A_Out - P(NG)*A(NG) )
196 + ( ( F(NG-1) + F(NG) )/2 )^2 / ( rho(NG)*A(NG) )
197 - ( F(NG) )^2 / ( rho(NG)*A(NG) )
198 - 2*fr(NG)/( 2*i_r0(NG) ) * ( ABS(F(NG))*F(NG) ) / ( rho(NG)*A(NG) ) * Delta_x(NG)/2;
199
200 # Energy Balance
201 Delta_xExtra*A(NG)*$psiExtra(1) = (F_In*h0 - FExtra(1)*hExtra(1));
202 Delta_xExtra*A(NG)*$psiExtra(2) = (FExtra(1)*hExtra(1) - FExtra(2)*hExtra(2));
203 Vol(1)*$psi(1) = (FExtra(2)*hExtra(2) - F(1)*h(1)
204 + 4*i_U(1)/(2*i_r0(1))*(TEextrnl(1)-T(1))*Vol(1));
205 FOR I:=2 TO NG DO
206   Vol(I)*$psi(I) = (F(I-1)*h(I-1) - F(I)*h(I)
207 + 4*i_U(I)/(2*i_r0(I))*(TEextrnl(I)-T(I))*Vol(I));
208 END # for
209
210 # Algebraic Equations
211 0 = (psiExtra(1) - (rhoExtra(1)*hExtra(1) - PExtra(1)));
212 0 = (psiExtra(2) - (rhoExtra(2)*hExtra(2) - PExtra(2)));
213 FOR I:=1 TO NG DO
214   0 = (psi(I) - (rho(I)*h(I) - P(I)));
215 END # for
216
217 # 2- Thermodynamical Part
218 0 = 1e-7*(hExtra(1) - (h_form + Cp/Mw*(TEExtra(1)-T_stand)));
219 0 = 1e-7*(hExtra(2) - (h_form + Cp/Mw*(TEExtra(2)-T_stand)));
220 FOR I:= 1 TO NG DO
221   0 = 1e-7*(h(I) - (h_form + Cp/Mw*(T(I)-T_stand)));
222 END # for
223 0 = (h0 - (h_form + Cp/Mw*(T0 - T_stand)));
224
225 # Equation of State
226 0 = (PExtra(1)*Mw - rhoExtra(1)*R_c*TEExtra(1));
227 0 = (PExtra(2)*Mw - rhoExtra(2)*R_c*TEExtra(2));
228 FOR I:=1 TO NG DO
229   0 = (P(I)*Mw - rho(I)*R_c*T(I));
230 END # for
231
232 # 3 - Forced Continuity
233 # Equation to set the amount of Gas <=> average density
234 rho_avg = (SIGMA(rho*Vol) + (rhoExtra(1) + rhoExtra(2))*Delta_xExtra*A(NG) ) / (SIGMA(Vol) + 2*Delta_xExtra*A(NG)
    ) );
235 totalMass = SIGMA(rho*Vol) + (rhoExtra(1) + rhoExtra(2))*Delta_xExtra*A(NG);
236 F_In = F(NG)*(1-comp_leak) + ModifyFlow;
237
238 # Compressor Equations
239 # deltaP
240 0 = (DeltaP - (PExtra(1) - P_Out));
241
242 # energy 1
243 0 = P_Out^(gamma-1)*T0^gamma - PExtra(1)^(gamma-1)*T(NG)^gamma;
244
245 #HT1 equations
246 HT1.rhoPipeHe = i_rhoPipeHe1;
247 HT1.vPipe = i_vPipe1;
248 HT2.rhoPipeHe = i_rhoPipeHe2;
249 HT2.vPipe = i_vPipe2;
250 HT3.rhoPipeHe = i_rhoPipeHe3;
251 HT3.vPipe = i_vPipe3;
252 HT4.rhoPipeHe = i_rhoPipeHe4;
253 HT4.vPipe = i_vPipe4;
254 END
255 #####
256
257
258 #####
259 MODEL Loop0Mach
260 #####
261 PARAMETER
262 Pi AS REAL
263 N_Pipes AS INTEGER # number of sections with different properties
264 R_c AS REAL #Rc constant "J/(mol*K)"
265 Mw AS REAL #Molecular weight "Kg/mol"
266 T_stand AS REAL #Standard Temp "K"
267 Cp AS REAL #specific heat at constant pressure "J/Kg/K"

```

```

268 h_form AS REAL #specific enthalpy of formation "J/Kg"
269 gamma AS REAL #gamma helium "no units"
270 InitT AS REAL #Temperature "K"
271 InitP AS REAL #initial pressure "Pa"
272 NG AS INTEGER #number of control volumes in the grid : external
273 SectionL AS ARRAY(N_Pipes) OF REAL # length of each section "m"
274 r0 AS ARRAY(N_Pipes) OF REAL # radus of each section "m"
275 muVisc AS ARRAY(N_Pipes) OF REAL # average viscosity in pipe
276 Tw AS REAL # In Plant Model
277 InitDeltaP AS REAL # In Simulation
278 MaxDeltaP AS REAL # In Simulation
279 A AS ARRAY(NG) OF REAL #area of each section 'm^2'
280 A_In AS REAL
281 A_Out AS REAL
282 SectionEnd AS ARRAY(N_Pipes) OF INTEGER # end point sections
283 SectionSpan AS ARRAY(N_Pipes) OF INTEGER # length section
284 SectionDelta_x AS ARRAY(N_Pipes) OF REAL # length of control volume "m"
285 Delta_x AS ARRAY(NG) OF REAL # length of control volume for each point "m"
286 Delta_xShift AS ARRAY(NG) OF REAL # length of control volume for each point in the shifted grid (non v) "m"
287 Delta_xExtra AS REAL
288 Vol AS ARRAY(NG) OF REAL
289 UNIT
290 HT1 AS HTCoeffGasPipeInsAir # section 1-10
291 HT2 AS HTCoeffGasMetalHX # section 11-30
292 HT3 AS HTCoeffGasPipeInsAir # section 31-50
293 HT4 AS HTCoeffGasMetalHXDummyOuter # section 51-70 # this is not necessary, the number is defined directly
INL report p 12
294 VARIABLE
295 AdaptFactor1 AS Nondimensional
296 AdaptFactor2 AS Nondimensional
297 rho AS ARRAY(NG) OF Density
298 P AS ARRAY(NG) OF Pressure
299 P_Out AS Pressure
300 h AS ARRAY(NG) OF SpecificEnergy
301 h0 AS SpecificEnergy
302 T AS ARRAY(NG) OF Temperature
303 TO AS Temperature
304 TExtrnl AS ARRAY(NG) OF Temperature
305 DeltaP AS Pressure
306 psi AS ARRAY(NG) OF Energy # 2 to NG Differential
307 F AS ARRAY(NG) OF Flowrate
308 F_In AS Flowrate
309 rho_avg AS Density
310 totalMass AS Nondimensional
311 ModifyFlow AS Nondimensional
312 comp_leak AS Nondimensional
313 #Extra Variables For Section Change at Compressor
314 rhoExtra AS ARRAY(2) OF Density
315 PExtra AS ARRAY(2) OF Pressure
316 hExtra AS ARRAY(2) OF SpecificEnergy
317 TExtra AS ARRAY(2) OF Temperature
318 psiExtra AS ARRAY(2) OF Energy
319 FExtra AS ARRAY(2) OF Flowrate
320 SET
321 Pi:= 4*ATAN(1);
322 R_c := 8.314; Mw := 4.0E-3;
323 T_stand := 298; Cp := 20.78; h_form := 0; gamma := 1.667;
324 InitT:=291.15; InitP:= 2.0e6; NG:=100; N_Pipes := 4;
325 A((SectionEnd(1)+1):SectionEnd(2)):= 0.3475; #:= achan*nhot = PI*d^2/8*nhot # A(2)
326 A((SectionEnd(3)+1):SectionEnd(4)):= 0.4012; # from filewith LMTD # A(4)
327 HT2.kHe:= 0.34981; # from INL calculations, file with LMTD
328 SectionEnd(1) := 10;
329 SectionEnd(2) := SectionEnd(1) + 40;
330 SectionEnd(3) := SectionEnd(2) + 10;
331 SectionEnd(N_Pipes):= NG;
332 SectionL(1) := 90; SectionL(2) := 0.98807; SectionL(3) := 90;
333 SectionL(4) :=8.656;
334 r0(1) := 0.413/2; r0(2) := (9.1652e-4)/2; # dhyd in the PCHE, this is needed to calculate Re
335 r0(3) := 0.444/2; r0(4):= 0.01123/2; # dhyd in the PHX
336 A(1:SectionEnd(1)):=Pi*r0(1)^2; # A(1) # 0.133964579
337 A_In:= A(1);
338 A_Out := A(NG);
339 A((SectionEnd(2)+1):SectionEnd(3)):=Pi*r0(3)^2; # A(3) # 0.154830252
340 HT1.r0 := r0(1);
341 HT1.r1 := HT1.r0*(2*0.01 + 1); # r1 depends on the t/d ratio, t/d = 0.01 for cold leg with P = 2MPa, INL
report p16 OK
342 HT1.r2 := HT1.r1 + 0.0058; # INL report p34
343 HT2.r0 := r0(2);
344 HT2.t := (HT2.r0*2*0.78*2 - HT2.r0)/3; # according to INL, an average of 2*tmax + 1*tmin
345 HT3.r0 := r0(3);
346 HT3.r1 := HT3.r0*(2*0.11 + 1); # r1 depends on the t/d ratio, t/d = 0.11 for hot leg with P = 2MPa, INL
report p16
347 HT3.r2 := HT3.r1 + 0.0059; # INL report p34
348 SectionSpan(1) := SectionEnd(1);
349 FOR I:=2 TO N_Pipes DO
350 SectionSpan(I) := SectionEnd(I) - SectionEnd(I-1);
351 END # for
352 SectionDelta_x(1) := SectionL(1)/(SectionSpan(1));
353 SectionDelta_x(2):= SectionL(2)/SectionSpan(2);
354 SectionDelta_x(3):=SectionL(3)/SectionSpan(3);
355 SectionDelta_x(4):=SectionL(4)/SectionSpan(4);
356 Delta_xExtra:= 0.01;

```

```

357 Delta_x(1:SectionEnd(1)):= SectionDelta_x(1);
358 FOR I:=1 TO N_Pipes-1 DO
359   Delta_x((SectionEnd(I)+1):SectionEnd(I+1)):= SectionDelta_x(I+1);
360 END # for I # 20071112 changed
361 Delta_xShift(1:SectionEnd(1)):= SectionDelta_x(1);
362 FOR I := 1 TO N_Pipes-1 DO
363   Delta_xShift(SectionEnd(I)+1):=(SectionDelta_x(I)+SectionDelta_x(I+1))/2;
364   Delta_xShift(SectionEnd(I)+2:SectionEnd(I+1)):= SectionDelta_x(I+1);
365 END # for
366 Vol(1) := A(1)*SectionDelta_x(1);
367 Vol(2:SectionEnd(1)):= A(2:SectionEnd(1))*SectionDelta_x(1);
368 FOR I:= 1 TO (N_Pipes-1) DO
369   Vol(SectionEnd(I)+1:SectionEnd(I+1)):= A(SectionEnd(I)+1:SectionEnd(I+1))*SectionDelta_x(I+1);
370 END # for
371 INTERMEDIATE
372 Dimension i_U(NG), i_r0(NG), fr(NG)
373 Dimension i_mdot(NG) # mdot at each grid point, all the values should be equal
374 DIMENSION intRe(NG), intfArray(NG),intEps(N_Pipes)
375 i_U(1:SectionEnd(1)):=HT1.U ;
376 i_U((SectionEnd(1)+1):SectionEnd(2)):=HT2.U;
377 i_U((SectionEnd(2)+1):SectionEnd(3)):=HT3.U;
378 i_U((SectionEnd(3)+1):SectionEnd(4)):=HT4.U;
379 i_r0(1:SectionEnd(1)):=r0(1) ;
380 i_r0((SectionEnd(1)+1):SectionEnd(2)):=r0(2);
381 i_r0((SectionEnd(2)+1):SectionEnd(3)):=r0(3);
382 i_r0((SectionEnd(3)+1):SectionEnd(4)):=r0(4);
383 i_rhoPipeHe1:= sigma(rho(1:SectionEnd(1)))/SectionSpan(1);
384 i_vPipe1:=sigma(F(1:SectionEnd(1))/A(1:SectionEnd(1))/rho(1:SectionEnd(1)))/SectionSpan(1);
385 i_rhoPipeHe2:= sigma(rho(SectionEnd(1)+1:SectionEnd(2)))/SectionSpan(2);
386 i_vPipe2:=sigma(F(SectionEnd(1)+1:SectionEnd(2))/A(SectionEnd(1)+1:SectionEnd(2))/rho(SectionEnd(1)+1:
SectionEnd(2)))/SectionSpan(2);
387 i_rhoPipeHe3:= sigma(rho(SectionEnd(2)+1:SectionEnd(3)))/SectionSpan(3);
388 i_vPipe3:=sigma(F(SectionEnd(2)+1:SectionEnd(3))/A(SectionEnd(2)+1:SectionEnd(3))/rho(SectionEnd(2)+1:
SectionEnd(3)))/SectionSpan(3);
389 i_rhoPipeHe4:= sigma(rho(SectionEnd(3)+1:SectionEnd(4)))/SectionSpan(4); #20080311
390 i_vPipe4:= sigma(F(SectionEnd(3)+1:SectionEnd(4))/A(SectionEnd(3)+1:SectionEnd(4))/rho(SectionEnd(3)+1:
SectionEnd(4)))/SectionSpan(4);
391 intEps(1)=4.57e-5;
392 intEps(2)=r0(2)*1e-9;
393 intEps(3)=4.57e-5;
394 intEps(4)=r0(4)*1e-9;
395 intRe(1):= (F_In/A_In + F(1)/A(1))/2*r0(1)*2/muVisc(1);
396 intRe(2:SectionEnd(1)):= (F(1:SectionEnd(1)-1)/A(1:SectionEnd(1)-1)+F(2:SectionEnd(1))/A(2:SectionEnd(1)))/2*
r0(1)*2/muVisc(1);
397 intRe(SectionEnd(1)+1):= (F(SectionEnd(1))/A(SectionEnd(1))+F(SectionEnd(1)+1)/A(SectionEnd(1)+1))/2*r0(2)*2/
muVisc(2);
398 intRe(SectionEnd(1)+2:SectionEnd(2)):=F(SectionEnd(1)+1:SectionEnd(2)-1)/A(SectionEnd(1)+
1:SectionEnd(2)-1)+F(SectionEnd(1)+2:SectionEnd(2))/A(SectionEnd(1)+2:SectionEnd(2))/2*r0(2)*2/muVisc(2);
399 intRe(SectionEnd(2)+1):= (F(SectionEnd(2))/A(SectionEnd(2))+F(SectionEnd(2)+1)/A(SectionEnd(2)+1))/2*r0(3)*2/
muVisc(3);
400 intRe(SectionEnd(2)+2:SectionEnd(3)):=F(SectionEnd(2)+1:SectionEnd(3)-1)/A(SectionEnd(2)+
1:SectionEnd(3)-1)+F(SectionEnd(2)+2:SectionEnd(3))/A(SectionEnd(2)+2:SectionEnd(3))/2*r0(3)*2/muVisc(3);
401 intRe(SectionEnd(3)+1):= (F(SectionEnd(3))/A(SectionEnd(3))+F(SectionEnd(3)+1)/A(SectionEnd(3)+1))/2*r0(4)*2/
muVisc(4);
402 intRe(SectionEnd(3)+2:SectionEnd(4)):=F(SectionEnd(3)+1:SectionEnd(4)-1)/A(SectionEnd(3)+
1:SectionEnd(4)-1)+F(SectionEnd(3)+2:SectionEnd(4))/A(SectionEnd(3)+2:SectionEnd(4))/2*r0(4)*2/muVisc(4);
403 intArray(1:SectionEnd(1)):=1/(-2*LOG10(intEps(1)/(3.7*r0(1)) + 2.51/intRe(1:SectionEnd(1))
*(1.14 -2*LOG10(intEps(1)/r0(1) + 21.25/(intRe(1:SectionEnd(1))^0.9))))^2/4;
404 intArray(SectionEnd(1)+1:SectionEnd(2)):=64/intRe(SectionEnd(1)+1:SectionEnd(2))/4;
405 intArray(SectionEnd(2)+1:SectionEnd(3)):=1/(-2*LOG10(intEps(3)/(3.7*r0(3))
+ 2.51/intRe(SectionEnd(2)+1:SectionEnd(3))
*(1.14 -2*LOG10(intEps(3)/r0(3) + 21.25/(intRe(SectionEnd(2)+1:SectionEnd(3))^0.9))))^2/4;
406 intArray(SectionEnd(3)+1:SectionEnd(4)):=1/(-2*LOG10(intEps(4)/(3.7*r0(4))
+ 2.51/intRe(SectionEnd(3)+1:SectionEnd(4))
*(1.14 -2*LOG10(intEps(4)/r0(4) + 21.25/(intRe(SectionEnd(3)+1:SectionEnd(4))^0.9))))^2/4;
407 fr(1:SectionEnd(1)) := intfArray(1:SectionEnd(1));#0.01294/4; # OK
408 fr((SectionEnd(1)+1):SectionEnd(2)) := intfArray(SectionEnd(1)+1:SectionEnd(2));#4.009E-02/4; # OK
409 fr((SectionEnd(2)+1):SectionEnd(3)) := intfArray(SectionEnd(2)+1:SectionEnd(3));#0.01348/4; # OK
410 fr((SectionEnd(3)+1):SectionEnd(4)) := intfArray(SectionEnd(3)+1:SectionEnd(4));#2.758E-02/4; # OK
411 EQUATION
412 # Mass Balance
413 Delta_xExtra*A(1)*$rhoExtra(1) = (F_In - FExtra(1));
414 Delta_xExtra*A(1)*$rhoExtra(2) = (FExtra(1) - FExtra(2));
415 Delta_x(1)*A(1)*$rho(1) = (FExtra(2) - F(1));
416 FOR I:= 2 TO NG DO
417   Delta_x(I)*A(I)*$rho(I) = (F(I-1) - F(I));
418 END # for
419 # Momentum Balance
420 0 =
421 -(PExtra(2)*A(NG) - PExtra(1)*A(NG))
422 +( F_In )^2/ (rhoExtra(1)*A(NG))
423 -( ( FExtra(1) + FExtra(2) )/2 )^2 / (rhoExtra(2)*A(NG));
424 0 =
425 -( P(1)*A(1) - ( PExtra(2)*Delta_x(1)/2 + P(1)*Delta_xExtra/2 ) / ( Delta_x(1)/2 +
Delta_xExtra/2 ) * ( A(1) - A(NG) ) - PExtra(2)*A(NG) )
426 +( ( FExtra(1) + FExtra(2) )/2 )^2 / ( rhoExtra(2)*A(NG) )
427 -( ( F(1) + FExtra(2) )/2 )^2 / ( rho(1)*A(1) )
428 - 2*fr(1)/( 2*i_r0(1) ) * ( ABS(FExtra(2))*FExtra(2) )/ ( rho(1)*A(1) ) * Delta_x(1)/2;
429 0 =
430 -( P(2)*A(2) - ( P(1)*Delta_x(2)/2 + P(2)*Delta_x(1)/2 ) / ( Delta_x(1)/2+Delta_x(2)/2 )
* ( A(2) - A(1) ) - P(1)*A(1) )
431 +( ( FExtra(2) + F(1) )/2 )^2 / ( rho(1)*A(1) )

```

```

440      -( ( F(2) + F(1) )/2 )^2 / ( rho(2)*A(2) )
441      - 2*fr(1)/( 2*i_r0(1) ) * ( ABS(F(1))*F(1) )/ ( rho(1)*A(1) ) * Delta_x(1)/2
442      - 2*fr(2)/( 2*i_r0(2) ) * ( ABS(F(1))*F(1) )/ ( rho(2)*A(2) ) * Delta_x(2)/2;
443  FOR I:=2 TO SectionEnd(4)-1 DO
444      0 =
445      -( P(I+1)*A(I+1) - ( P(I)*Delta_x(I+1)/2 + P(I+1)*Delta_x(I)/2 ) / ( Delta_x(I)/2+
446      Delta_x(I+1)/2 ) * ( A(I+1) - A(I) ) - P(I)*A(I) )
447      +( ( F(I-1) + F(I) )/2 )^2 / ( rho(I)*A(I) )
448      -( ( F(I+1) + F(I) )/2 )^2 / ( rho(I+1)*A(I+1) )
449      - 2*fr(I)/( 2*i_r0(I) ) * ( ABS(F(I))*F(I) )/ ( rho(I)*A(I) ) * Delta_x(I)/2
450      - 2*fr(I+1)/( 2*i_r0(I+1) ) * ( ABS(F(I))*F(I) )/ ( rho(I+1)*A(I+1) ) * Delta_x(I+1)/2;
451  END
452  0 =
453  -( P_Out*A_Out - P(NG)*A(NG) )
454  +( ( F(NG-1) + F(NG) )/2 )^2 / ( rho(NG)*A(NG) )
455  -( F(NG) )^2 / ( rho(NG)*A(NG) )
456  - 2*fr(NG)/( 2*i_r0(NG) ) * ( ABS(F(NG))*F(NG) ) / ( rho(NG)*A(NG) ) * Delta_x(NG)/2;
457  # Energy Balance
458  Delta_xExtra*A(NG)*$psiExtra(1) = (F_In*h0 - FExtra(1)*hExtra(1));
459  Delta_xExtra*A(NG)*$psiExtra(2) = (FExtra(1)*hExtra(1) - FExtra(2)*hExtra(2));
460  Vol(1)*$psi(1) = (FExtra(2)*hExtra(2) - F(1)*h(1)
461  +4*i_U(1)/(2*i_r0(1))*(TEextrnl(1)-T(1))*Vol(1));
462  FOR I:=2 TO NG DO
463  Vol(I)*$psi(I) = (F(I-1)*h(I-1) - F(I)*h(I)
464  +4*i_U(I)/(2*i_r0(I))*(TEextrnl(I)-T(I))*Vol(I));
465  END # for
466
467  # Algebraic Equations
468  0 = (psiExtra(1) - (rhoExtra(1)*hExtra(1) - PExtra(1)));
469  0 = (psiExtra(2) - (rhoExtra(2)*hExtra(2) - PExtra(2)));
470  FOR I:=1 TO NG DO
471  0 = (psi(I) - (rho(I)*h(I) - P(I)));
472  END # for
473
474  # 2- Thermodynamical Part
475  0 = 1e-7*(hExtra(1) - (h_form + Cp/Mw*(TEExtra(1)-T_stand)));
476  0 = 1e-7*(hExtra(2) - (h_form + Cp/Mw*(TEExtra(2)-T_stand)));
477  FOR I:= 1 TO NG DO
478  0 = 1e-7*(h(I) - (h_form + Cp/Mw*(T(I)-T_stand)));
479  END # for
480  0 = (h0 - (h_form + Cp/Mw*(T0 - T_stand)));
481
482  # Equation of State
483  0 = (PExtra(1)*Mw - rhoExtra(1)*R_c*TEExtra(1));
484  0 = (PExtra(2)*Mw - rhoExtra(2)*R_c*TEExtra(2));
485  FOR I:=1 TO NG DO
486  0 = (P(I)*Mw - rho(I)*R_c*T(I));
487  END # for
488
489  # 3 - Forced Continuity
490  # Equation to set the amount of Gas <=> average density
491  rho_avg = (SIGMA(rho*Vol) + (rhoExtra(1) + rhoExtra(2))*Delta_xExtra*A(NG) ) / (SIGMA(Vol) + 2*Delta_xExtra*A(NG)
492  );
493  totalMass = SIGMA(rho*Vol) + (rhoExtra(1) + rhoExtra(2))*Delta_xExtra*A(NG);
494  F_In = F(NG)*(1-comp_leak) + ModifyFlow;
495
496  # Compressor Equations
497  # deltaP
498  0 = (DeltaP - (PExtra(1) - P_Out));
499
500  # energy 1
501  0 = P_Out^(gamma-1)*T0^gamma - PExtra(1)^(gamma-1)*T(NG)^gamma;
502
503  #HT1 equations
504  HT1.rhoPipeHe = i_rhoPipeHe1;
505  HT1.vPipe = i_vPipe1;
506  HT2.rhoPipeHe = i_rhoPipeHe2;
507  HT2.vPipe = i_vPipe2;
508  HT3.rhoPipeHe = i_rhoPipeHe3;
509  HT3.vPipe = i_vPipe3;
510  HT4.rhoPipeHe = i_rhoPipeHe4;
511  HT4.vPipe = i_vPipe4;
512  END
513  #####
514
515  #####
516  MODEL LoopQSS
517  #####
518  PARAMETER
519  Pi AS REAL
520  N_Pipes AS INTEGER # number of sections with different properties
521  R_c AS REAL #Rc constant "J/(mol*K)"
522  Mw AS REAL #Molecular weight "Kg/mol"
523  T_stand AS REAL #Standard Temp "K"
524  Cp AS REAL #specific heat at constant pressure "J/Kg/K"
525  h_form AS REAL #specific enthalpy of formation "J/Kg"
526  gamma AS REAL #gamma helium "no units"
527  InitT AS REAL #Temperature "K"
528  InitP AS REAL #initial pressure "Pa"
529  NG AS INTEGER #number of control volumes in the grid : external

```



```

530 SectionL AS ARRAY(N_Pipes) OF REAL # length of each section "m"
531 r0 AS ARRAY(N_Pipes) OF REAL # radius of each section "m"
532 muVisc AS ARRAY(N_Pipes) OF REAL # average viscosity in pipe
533 Tv AS REAL # In Plant Model
534 InitDeltaP AS REAL # In Simulation
535 MaxDeltaP AS REAL # In Simulation
536 A AS ARRAY(NG) OF REAL #area of each section 'm^2'
537 A_In AS REAL
538 A_Out AS REAL
539 SectionEnd AS ARRAY(N_Pipes) OF INTEGER # end point sections
540 SectionSpan AS ARRAY(N_Pipes) OF INTEGER # length section
541 SectionDelta_x AS ARRAY(N_Pipes) OF REAL # length of control volume "m"
542 Delta_x AS ARRAY(NG) OF REAL # length of control volume for each point "m"
543 Delta_xShift AS ARRAY(NG) OF REAL # length of control volume for each point in the shifted grid (non v) "m"
544 Delta_xExtra AS REAL
545 Vol AS ARRAY(NG) OF REAL
546 UNIT
547 HT1 AS HTCoeffGasPipeInsAir # section 1-10
548 HT2 AS HTCoeffGasMetalHX # section 11-30
549 HT3 AS HTCoeffGasPipeInsAir # section 31-50
550 HT4 AS HTCoeffGasMetalHXDummyOuter # section 51-70 # this is not necessary, the number is defined directly
    INL report p 12
551 VARIABLE
552 AdaptFactor1 AS Nondimensional
553 AdaptFactor2 AS Nondimensional
554 rho AS ARRAY(NG) OF Density
555 P AS ARRAY(NG) OF Pressure
556 P_Out AS Pressure
557 h AS ARRAY(NG) OF SpecificEnergy
558 h0 AS SpecificEnergy
559 T AS ARRAY(NG) OF Temperature
560 TO AS Temperature
561 TExtrnl AS ARRAY(NG) OF Temperature
562 DeltaP AS Pressure
563 psi AS ARRAY(NG) OF Energy # 2 to NG Differential
564 F AS ARRAY(NG) OF Flowrate
565 F_In AS Flowrate
566 rho_avg AS Density
567 totalMass AS Nondimensional
568 ModifyFlow AS Nondimensional
569 #Extra Variables For Section Change at Compressor
570 rhoExtra AS ARRAY(2) OF Density
571 PExtra AS ARRAY(2) OF Pressure
572 hExtra AS ARRAY(2) OF SpecificEnergy
573 TExtra AS ARRAY(2) OF Temperature
574 psiExtra AS ARRAY(2) OF Energy
575 FExtra AS ARRAY(2) OF Flowrate
576 SET
577 Pi := 4*ATAN(1);
578 R_c := 8.314;      Mw := 4.0E-3;
579 T_stand := 298;   Cp := 20.78;      h_form := 0;      gamma := 1.667;
580 InitT:=291.15;   InitP:= 2.0e6;      NG:=100;      N_Pipes := 4;
581 A((SectionEnd(1)+1):SectionEnd(2)):= 0.3475; #:= achan*nhot = PI*d^2/8*nhot # A(2)
582 A((SectionEnd(3)+1):SectionEnd(4)):= 0.4012; # from filewith LMTD # A(4)
583 HT2.kHe:= 0.34981; # from INL calculations, file with LMTD
584 SectionEnd(1) := 10;
585 SectionEnd(2) := SectionEnd(1) + 40;
586 SectionEnd(3) := SectionEnd(2) + 10;
587 SectionEnd(N_Pipes):= NG;
588 SectionL(1) := 90;      SectionL(2) := 0.98807; SectionL(3) := 90;
589 SectionL(4) :=8.656;
590 r0(1) := 0.413/2;      r0(2) := (9.1652e-4)/2; # dhyd in the PCHE, this is needed to calculate Re
591 r0(3) := 0.444/2;      r0(4):= 0.01123/2; # dhyd in the PHX
592 A(1:SectionEnd(1)):=Pi*r0(1)^2; # A(1) # 0.133964579
593 A_In:= A(1);
594 A_Out := A(NG);
595 A((SectionEnd(2)+1):SectionEnd(3)):=Pi*r0(3)^2; # A(3) # 0.154830252
596 HT1.r0 := r0(1);
597 HT1.r1 := HT1.r0*(2*0.01 + 1); # r1 depends on the t/d ratio, t/d = 0.01 for cold leg with P = 2MPa, INL
    report p16 OK
598 HT1.r2 := HT1.r1 + 0.0058; # INL report p34
599 HT2.r0 := r0(2);
600 HT2.t := (HT2.r0*2*0.78*2 - HT2.r0)/3; # according to INL, an average of 2*tmax + 1*tmin
601 HT3.r0 := r0(3);
602 HT3.r1 := HT3.r0*(2*0.11 + 1); # r1 depends on the t/d ratio, t/d = 0.11 for hot leg with P = 2MPa, INL
    report p16
603 HT3.r2 := HT3.r1 + 0.0059; # INL report p34
604 SectionSpan(1) := SectionEnd(1);
605 FOR I:=2 TO N_Pipes DO
606     SectionSpan(I) := SectionEnd(I) - SectionEnd(I-1);
607 END # for
608 SectionDelta_x(1) := SectionL(1)/(SectionSpan(1));
609 SectionDelta_x(2):= SectionL(2)/SectionSpan(2);
610 SectionDelta_x(3):=SectionL(3)/SectionSpan(3);
611 SectionDelta_x(4):=SectionL(4)/SectionSpan(4);
612 Delta_x(1:SectionEnd(1)):= SectionDelta_x(1);
613 Delta_xExtra:= 0.01;
614 FOR I:=1 TO N_Pipes-1 DO
615     Delta_x((SectionEnd(I)+1):SectionEnd(I+1)):= SectionDelta_x(I+1);
616 END # for I # 20071112 changed
617 Delta_xShift(1:SectionEnd(1)):= SectionDelta_x(1);
618 FOR I := 1 TO N_Pipes-1 DO

```

```

619     Delta_xShift(SectionEnd(I)+1):= (SectionDelta_x(I)+SectionDelta_x(I+1))/2;
620     Delta_xShift(SectionEnd(I)+2:SectionEnd(I+1)):= SectionDelta_x(I+1);
621 END # for
622 Vol(1) := A(1)*SectionDelta_x(1);
623 Vol(2:SectionEnd(1)):= A(2:SectionEnd(1))*SectionDelta_x(1);
624 FOR I:= 1 TO (N_Pipes-1) DO
625     Vol(SectionEnd(I)+1:SectionEnd(I+1)):= A(SectionEnd(I)+1:SectionEnd(I+1))*SectionDelta_x(I+1);
626 END # for
627 INTERMEDIATE
628 Dimension i_U(NG), i_r0(NG), fr(NG)
629 Dimension i_mdots(NG) # mdot at each grid point, all the values should be equal
630 DIMENSION intRe(NG), intfArray(NG),intEps(N_Pipes)
631 i_U(1:SectionEnd(1)):=HT1.U;
632 i_U((SectionEnd(1)+1):SectionEnd(2)):=HT2.U;
633 i_U((SectionEnd(2)+1):SectionEnd(3)):=HT3.U;
634 i_U((SectionEnd(3)+1):SectionEnd(4)):=HT4.U;
635 i_r0(1:SectionEnd(1)):=r0(1);
636 i_r0((SectionEnd(1)+1):SectionEnd(2)):=r0(2);
637 i_r0((SectionEnd(2)+1):SectionEnd(3)):=r0(3);
638 i_r0((SectionEnd(3)+1):SectionEnd(4)):=r0(4);
639 i_rhoPipeHe1:= sigma(rho(1:SectionEnd(1))/SectionSpan(1);
640 i_vPipe1:=sigma(F(1:SectionEnd(1))/A(1:SectionEnd(1))/rho(1:SectionEnd(1))/SectionSpan(1);
641 i_rhoPipeHe2:= sigma(rho(SectionEnd(1)+1:SectionEnd(2))/SectionSpan(2);
642 i_vPipe2:=sigma(F(SectionEnd(1)+1:SectionEnd(2))/A(SectionEnd(1)+1:SectionEnd(2))/rho(SectionEnd(1)+1:
        SectionEnd(2))/SectionSpan(2);
643 i_rhoPipeHe3:= sigma(rho(SectionEnd(2)+1:SectionEnd(3))/SectionSpan(3);
644 i_vPipe3:=sigma(F(SectionEnd(2)+1:SectionEnd(3))/A(SectionEnd(2)+1:SectionEnd(3))/rho(SectionEnd(2)+1:
        SectionEnd(3))/SectionSpan(3);
645 i_rhoPipeHe4:= sigma(rho(SectionEnd(3)+1:SectionEnd(4))/SectionSpan(4); #20080311
646 i_vPipe4:= sigma(F(SectionEnd(3)+1:SectionEnd(4))/A(SectionEnd(3)+1:SectionEnd(4))/rho(SectionEnd(3)+1:
        SectionEnd(4))/SectionSpan(4);
647 intEps(1):=4.57e-5;
648 intEps(2):=r0(2)*1e-9;
649 intEps(3):=4.57e-5;
650 intEps(4):=r0(4)*1e-9;
651 intRe(1):= (F_In/A_In + F(1)/A(1))/2*r0(1)*2/muVisc(1);
652 intRe(2:SectionEnd(1)):= (F(1:SectionEnd(1)-1)/A(1:SectionEnd(1)-1)+F(2:SectionEnd(1))/A(2:SectionEnd(1)))/2*
        r0(1)*2/muVisc(1);
653 intRe(SectionEnd(1)+1):= (F(SectionEnd(1))/A(SectionEnd(1))+F(SectionEnd(1)+1)/A(SectionEnd(1)+1))/2*r0(2)*2/
        muVisc(2);
654 intRe(SectionEnd(1)+2:SectionEnd(2)):= (F(SectionEnd(1)+1:SectionEnd(2)-1)/A(SectionEnd(1)+
        1:SectionEnd(2)-1)+F(SectionEnd(1)+2:SectionEnd(2))/A(SectionEnd(1)+2:SectionEnd(2)))/2*r0(2)*2/muVisc(2);
655 intRe(SectionEnd(2)+1):= (F(SectionEnd(2))/A(SectionEnd(2))+F(SectionEnd(2)+1)/A(SectionEnd(2)+1))/2*r0(3)*2/
        muVisc(3);
656 intRe(SectionEnd(2)+2:SectionEnd(3)):= (F(SectionEnd(2)+1:SectionEnd(3)-1)/A(SectionEnd(2)+
        1:SectionEnd(3)-1)+F(SectionEnd(2)+2:SectionEnd(3))/A(SectionEnd(2)+2:SectionEnd(3)))/2*r0(3)*2/muVisc(3);
657 intRe(SectionEnd(3)+1):= (F(SectionEnd(3))/A(SectionEnd(3))+F(SectionEnd(3)+1)/A(SectionEnd(3)+1))/2*r0(4)*2/
        muVisc(4);
658 intRe(SectionEnd(3)+2:SectionEnd(4)):= (F(SectionEnd(3)+1:SectionEnd(4)-1)/A(SectionEnd(3)+
        1:SectionEnd(4)-1)+F(SectionEnd(3)+2:SectionEnd(4))/A(SectionEnd(3)+2:SectionEnd(4)))/2*r0(4)*2/muVisc(4);
659 intfArray(1:SectionEnd(1)):=1/(-2*LOG10(intEps(1)/(3.7*r0(1)) + 2.51/intRe(1:SectionEnd(1))
        *(1.14 -2*LOG10(intEps(1)/r0(1) + 21.25/(intRe(1:SectionEnd(1))^0.9))))^2/4;
660 intfArray(SectionEnd(1)+1:SectionEnd(2)):=64/intRe(SectionEnd(1)+1:SectionEnd(2))/4;
661 intfArray(SectionEnd(2)+1:SectionEnd(3)):=1/(-2*LOG10(intEps(3)/(3.7*r0(3))
        + 2.51/intRe(SectionEnd(2)+1:SectionEnd(3))
        *(1.14 -2*LOG10(intEps(3)/r0(3) + 21.25/(intRe(SectionEnd(2)+1:SectionEnd(3))^0.9))))^2/4;
662 intfArray(SectionEnd(3)+1:SectionEnd(4)):=1/(-2*LOG10(intEps(4)/(3.7*r0(4))
        + 2.51/intRe(SectionEnd(3)+1:SectionEnd(4))
        *(1.14 -2*LOG10(intEps(4)/r0(4) + 21.25/(intRe(SectionEnd(3)+1:SectionEnd(4))^0.9))))^2/4;
663 fr(1:SectionEnd(1)) := intfArray(1:SectionEnd(1));#0.01294/4; # OK
664 fr((SectionEnd(1)+1):SectionEnd(2)) := intfArray(SectionEnd(1)+1:SectionEnd(2));#4.009E-02/4; # OK
665 fr((SectionEnd(2)+1):SectionEnd(3)) := intfArray(SectionEnd(2)+1:SectionEnd(3));#0.01348/4; # OK
666 fr((SectionEnd(3)+1):SectionEnd(4)) := intfArray(SectionEnd(3)+1:SectionEnd(4));#2.758E-02/4; # OK
667 EQUATION
668 # Mass Balance
669 0 = (F_In - FExtra(1));
670 0 = (FExtra(1) - FExtra(2));
671 0 = (FExtra(2) - F(1));
672 FOR I:= 2 TO NG-1 DO
673     0 = (F(I-1) - F(I));
674 END # for
675 # Momentum Balance
676 0 =
677     -(PExtra(2)*A(NG) - PExtra(1)*A(NG))
678     + ( F_In )^2 / ( rhoExtra(1)*A(NG) )
679     - ( ( FExtra(1) + FExtra(2) )/2 )^2 / ( rhoExtra(2)*A(NG) );
680 0 =
681     - ( P(1)*A(1) - ( PExtra(2)*Delta_x(1)/2 + P(1)*Delta_xExtra/2 ) / ( Delta_x(1)/2 +
        Delta_xExtra/2 ) * ( A(1) - A(NG) ) - PExtra(2)*A(NG) )
682     + ( ( FExtra(1) + FExtra(2) )/2 )^2 / ( rhoExtra(2)*A(NG) )
683     - ( ( F(1) + FExtra(2) )/2 )^2 / ( rho(1)*A(1) )
684     - 2*fr(1)/( 2*i_r0(1) ) * ( ABS(FExtra(2))*FExtra(2) ) / ( rho(1)*A(1) ) * Delta_x(1)/2;
685 0 =
686     - ( P(2)*A(2) - ( P(1)*Delta_x(2)/2 + P(2)*Delta_x(1)/2 ) / ( Delta_x(1)/2+Delta_x(2)/2 )
        * ( A(2) - A(1) ) - P(1)*A(1) )
687     + ( ( FExtra(2) + F(1) )/2 )^2 / ( rho(1)*A(1) )
688     - ( ( F(2) + F(1) )/2 )^2 / ( rho(2)*A(2) )
689     - 2*fr(1)/( 2*i_r0(1) ) * ( ABS(F(1))*F(1) ) / ( rho(1)*A(1) ) * Delta_x(1)/2
690     - 2*fr(2)/( 2*i_r0(2) ) * ( ABS(F(1))*F(1) ) / ( rho(2)*A(2) ) * Delta_x(2)/2;
691 FOR I:=2 TO SectionEnd(4)-1 DO
692     0 =

```

```

701      -( P(I+1)*A(I+1) - ( P(I)*Delta_x(I+1)/2 + P(I+1)*Delta_x(I)/2 ) / ( Delta_x(I)/2+
          Delta_x(I+1)/2 ) * ( A(I+1) - A(I) ) - P(I)*A(I) )
702      +( ( F(I-1) + F(I) )/2 )^2 / ( rho(I)*A(I) )
703      -( ( F(I+1) + F(I) )/2 )^2 / ( rho(I+1)*A(I+1) )
704      - 2*fr(I)/( 2*i_r0(I) ) * ( ABS(F(I))*F(I) )/ ( rho(I)*A(I) ) * Delta_x(I)/2
705      - 2*fr(I+1)/( 2*i_r0(I+1) ) * ( ABS(F(I))*F(I) )/ ( rho(I+1)*A(I+1) ) * Delta_x(I+1)/2;
706  END
707  0 =
708      -( P_Out*A_Out - P(NG)*A(NG) )
709      +( ( F(NG-1) + F(NG) )/2 )^2 / ( rho(NG)*A(NG) )
710      -( F(NG) )^2 / ( rho(NG)*A(NG) )
711      - 2*fr(NG)/( 2*i_r0(NG) ) * ( ABS(F(NG))*F(NG) ) / ( rho(NG)*A(NG) ) * Delta_x(NG)/2;
712
713  # Energy Balance
714  Delta_xExtra*A(NG)*$psiExtra(1) = (F_In*h0 - FExtra(1)*hExtra(1));
715  Delta_xExtra*A(NG)*$psiExtra(2) = (FExtra(1)*hExtra(1) - FExtra(2)*hExtra(2));
716  Vol(1)*$psi(1) = (FExtra(2)*hExtra(2) - F(1)*h(1)
717      +4*i_U(1)/(2*i_r0(1))*(TEextrnl(1)-T(1))*Vol(1));
718  FOR I:=2 TO NG DO
719      Vol(I)*$psi(I) = (F(I-1)*h(I-1) - F(I)*h(I)
720      +4*i_U(I)/(2*i_r0(I))*(TEextrnl(I)-T(I))*Vol(I));
721  END # for
722
723  # Algebraic Equations
724  0 = (psiExtra(1) - (rhoExtra(1)*hExtra(1) - PExtra(1)));
725  0 = (psiExtra(2) - (rhoExtra(2)*hExtra(2) - PExtra(2)));
726  FOR I:=1 TO NG DO
727      0 = (psi(I) - (rho(I)*h(I) - P(I)));
728  END # for
729
730  # 2- Thermodynamical Part
731  0 = 1e-7*(hExtra(1) - (h_form + Cp/Mw*(TEextra(1)-T_stand)));
732  0 = 1e-7*(hExtra(2) - (h_form + Cp/Mw*(TEextra(2)-T_stand)));
733  FOR I:= 1 TO NG DO
734      0 = 1e-7*(h(I) - (h_form + Cp/Mw*(T(I)-T_stand)));
735  END # for
736  0 = (h0 - (h_form + Cp/Mw*(T0 - T_stand)));
737
738  # Equation of State
739  FOR I:=1 TO NG DO
740      0 = (P(I)*Mw - rho(I)*R_c*T(I));
741  END # for
742  0 = (PExtra(1)*Mw - rhoExtra(1)*R_c*TEextra(1));
743  0 = (PExtra(2)*Mw - rhoExtra(2)*R_c*TEextra(2));
744
745  # 3 - Forced Continuity
746  # Equation to set the amount of Gas <=> average density
747  rho_avg = (SIGMA(rho*Vol) + (rhoExtra(1) + rhoExtra(2))*Delta_xExtra*A(NG) ) / (SIGMA(Vol) + 2*Delta_xExtra*A(NG)
          );
748  totalMass = SIGMA(rho*Vol) + (rhoExtra(1) + rhoExtra(2))*Delta_xExtra*A(NG);
749  F_In = F(NG) + ModifyFlow;
750
751  # Compressor Equations
752  # deltaP
753  0 = (DeltaP - (PExtra(1) - P_Out));
754  # energy 1
755  0 = P_Out^(gamma-1)*T0^gamma - PExtra(1)^(gamma-1)*T(NG)^gamma;
756
757  #HT1 equations
758  HT1.rhoPipeHe = i_rhoPipeHe1;
759  HT1.vPipe = i_vPipe1;
760  HT2.rhoPipeHe = i_rhoPipeHe2;
761  HT2.vPipe = i_vPipe2;
762  HT3.rhoPipeHe = i_rhoPipeHe3;
763  HT3.vPipe = i_vPipe3;
764  HT4.rhoPipeHe = i_rhoPipeHe4;
765  HT4.vPipe = i_vPipe4;
766  END
767  #####
768
769
770  #####
771  MODEL PipeQSS
772  #####
773  PARAMETER
774      #SET here
775      Pi AS REAL
776      R_c AS REAL      #Rc constant "J/(mol*K)"
777      Mw AS REAL      #Molecular weight "Kg/mol"
778      T_stand AS REAL  #Standard Temp "K"
779      Cp AS REAL      #specific heat at constant pressure "J/Kg/K"
780      h_form AS REAL   #specific enthalpy of formation "J/Kg"
781      A AS REAL
782      r0 AS REAL      #diameter of pipe "m"
783      muVisc as REAL  # average viscosity in pipe
784
785  #EXTERNALLY set
786  SectionL AS REAL      #length of pipe "m"
787  NG AS INTEGER         #number of control volumes in the grid
788  Temp AS REAL         #Temperature "K"
789  InitP AS REAL
790  InitT AS REAL

```

```

791
792 #CALCULATED
793 InitRho AS REAL      InitH AS REAL
794 InitRho_e AS REAL   Delta_x AS REAL      #length of control volume "m"
795 Vol AS REAL
796 UNIT
797 HT AS HTCoeffGasMetalHX
798 VARIABLE
799 rho AS ARRAY(NG) OF Density
800 P AS ARRAY(NG) OF Pressure
801 P_In AS Pressure
802 P_Out AS Pressure
803 h AS ARRAY(NG) OF SpecificEnergy
804 h0 AS SpecificEnergy
805 T AS ARRAY(NG) OF Temperature
806 TExtrnl AS ARRAY(NG) OF Temperature
807 TO AS Temperature
808 #DIFFERENTIAL
809 F AS ARRAY(NG) OF Flowrate
810 F_In AS Flowrate
811 psi AS ARRAY(NG) OF Energy
812 SET
813 #SET
814 Pi:=4*ATAN(1);
815 R_c := 8.314;      Mw := 4.0E-3;
816 T_stand := 298;   Cp := 20.78;      h_form := 0;
817 r0 := 9.1652e-4/2 ; # dhyd in the PCHE, this is needed to calculate Re
818 A:=0.3475;
819 #CALCULATED
820 Delta_x := SectionL/(NG-1);
821 InitRho := InitP*Mw/(R_c*Temp);
822 InitH := h_form + Cp/Mw*(Temp-T_stand);
823 InitRho_e := InitRho*InitH - InitP;
824 HT.r0:=r0;      HT.t:= (HT.r0*2*0.78*2 - HT.r0)/3; # according to INL, an average of 2*tmax +1*tmin
825 Vol := A*Delta_x;
826 INTERMEDIATE
827 DIMENSION intRe(NG)
828 DIMENSION intfArray(NG)
829 U:= HT.U;
830 intRe:= F*r0*2/muVisc/A;
831 intfArray:=64/intRe/4;
832 EQUATION
833 # Mass Balance
834 0 = F_In - F(1);
835 FOR I:= 2 TO NG DO
836   0 = (F(I-1) - F(I));
837 END # for
838 # Momentum Balance
839 0 = -(P(1)*A - P_In*A)
840   + ( ( F_In )^2 / (rho(1)*A)
841   - ( ( F_In + F(1) )/2 )^2 / (rho(1)*A)
842   - (2*intfArray(1)/(2*r0)) * ( ABS(F_In)*F_In ) / (rho(1)*A) * (Delta_x)/2;
843
844 0 = -( P(2)*A - P(1)*A )
845   + ( ( F_In + F(1) )/2 )^2 / (rho(1)*A)
846   - ( ( F(2) + F(1) )/2 )^2 / (rho(2)*A)
847   - 2*intfArray(1)/(2*r0) * ( ABS(F(1))*F(1) )/ (rho(1)*A) * Delta_x/2
848   - 2*intfArray(2)/(2*r0) * ( ABS(F(1))*F(1) )/ (rho(2)*A) * Delta_x/2;
849 FOR I:=2 TO NG-1 DO
850   0 =
851   -( P(I+1)*A - P(I)*A )
852   + ( ( F(I-1) + F(I) )/2 )^2 / (rho(I)*A)
853   - ( ( F(I+1) + F(I) )/2 )^2 / (rho(I+1)*A)
854   - 2*intfArray(I)/(2*r0) * ( ABS(F(I))*F(I) )/ (rho(I)*A) * Delta_x/2
855   - 2*intfArray(I+1)/(2*r0) * ( ABS(F(I))*F(I) )/ (rho(I+1)*A) * Delta_x/2;
856 END # for
857 0 =
858 -( P_Out*A - P(NG)*A )
859 + ( ( F(NG-1) + F(NG) )/2 )^2 / (rho(NG)*A)
860 - ( F(NG) )^2 / (rho(NG)*A)
861 - 2*intfArray(NG)/(2*r0) * ( ABS(F(NG))*F(NG) ) / (rho(NG)*A) * Delta_x/2;
862 # Energy Balance
863 1e-7*$psi(1)*Vol = 1e-7*(F_In*h0 - F(1)*h(1)
864 +4*U/(2*r0)*(TExtrnl(1)-T(1))*Vol);
865 FOR I:=(2) TO (NG) DO
866   1e-7*$psi(I)*Vol = 1e-7*(F(I-1)*h(I-1) - F(I)*h(I)
867 +4*U/(2*r0)*(TExtrnl(I)-T(I))*Vol);
868 END # for
869
870 # Algebraic Equations
871 FOR I:=1 TO NG DO
872   0 = 1e-7*(psi(I) - (rho(I)*h(I) - P(I)));
873 END # for
874
875 # 2- Thermodynamical Part
876 FOR I:= 1 TO NG DO
877   0 = 1e-7*(h(I) - (h_form + Cp/Mw*(T(I)-T_stand)));
878 END # for
879 0 = (h0 - (h_form + Cp/Mw*(TO - T_stand)));
880
881 # Equation of State
882 FOR I:=1 TO NG DO

```

```

883      0=1e-3*(P(I)*Mw - rho(I)*R_c*T(I));
884      END # for
885
886      #Equations to assign variables for heat transfer coefficients
887      HT.rhoPipeHe = sigma(rho(2:NG))/NG;
888      HT.vPipe = sigma(F(2:NG)/rho(2:NG)/A)/NG;
889      END
890      #####
891
892
893      #####
894      MODEL Pipe0Mach
895      #####
896      PARAMETER
897      #SET here
898      Pi AS REAL
899      R_c AS REAL      #Rc constant "J/(mol*K)
900      Mw AS REAL      #Molecular weight "Kg/mol"
901      T_stand AS REAL #Standard Temp "K"
902      Cp AS REAL      #specific heat at constant pressure "J/Kg/K"
903      h_form AS REAL  #specific enthalpy of formation "J/Kg"
904      A AS REAL
905      r0 AS REAL      #diameter of pipe "m"
906      muVisc as REAL # average viscosity in pipe
907
908      #EXTERNALLY set
909      SectionL AS REAL      #length of pipe "m"
910      NG AS INTEGER        #number of control volumes in the grid
911      Temp AS REAL         #Temperature "K"
912      InitP AS REAL
913      InitT AS REAL
914
915      #CALCULATED
916      InitRho AS REAL      InitH AS REAL
917      InitRho_e AS REAL    Delta_x AS REAL      #length of control volume "m"
918      Vol AS REAL
919      UNIT
920      HT AS HTCoeffGasMetalHX
921      VARIABLE
922      rho AS ARRAY(NG) OF Density
923      P AS ARRAY(NG) OF Pressure
924      P_In AS Pressure
925      P_Out AS Pressure
926      h AS ARRAY(NG) OF SpecificEnergy
927      h0 AS SpecificEnergy
928      T AS ARRAY(NG) OF Temperature
929      TExtrnl AS ARRAY(NG) OF Temperature
930      T0 AS Temperature
931      #DIFFERENTIAL
932      F AS ARRAY(NG) OF Flowrate
933      F_In AS Flowrate
934      psi AS ARRAY(NG) OF Energy
935      SET
936      #SET
937      Pi:=4*ATAN(1);
938      R_c := 8.314;      Mw := 4.0E-3;
939      T_stand := 298;    Cp := 20.78;      h_form := 0;
940      r0 := 9.1652e-4/2; # dhyd in the PCHE, this is needed to calculate Re
941      A:=0.3475;
942      #CALCULATED
943      Delta_x := SectionL/(NG-1);
944      InitRho := InitP*Mw/(R_c*Temp);
945      InitH := h_form + Cp/Mw*(Temp-T_stand);
946      InitRho_e := InitRho*InitH - InitP;
947      HT.r0:=r0;      HT.t:= (HT.r0*2*0.78*2 - HT.r0)/3; # according to INL, an average of 2*tmax +1*tmin
948      Vol := A*Delta_x;
949      INTERMEDIATE
950      DIMENSION intRe(NG)
951      DIMENSION intfArray(NG)
952      U:= HT.U;
953      intRe:= F*r0*2/muVisc/A;
954      intfArray:=64/intRe/4;
955      EQUATION
956      # Mass Balance
957      Delta_x*A*$rho(1) = F_In - F(1);
958      FOR I:= 2 TO NG DO
959        Delta_x*A*$rho(I) = (F(I-1) - F(I));
960      END # for
961      # Momentum Balance
962      0 = -(P(1)*A -P_In*A)
963        +( F_In )^2 / (rho(1)*A)
964        - ( ( F_In + F(1) )/2 )^2 / (rho(1)*A)
965        - (2*intfArray(1)/(2*r0)) * ( ABS(F_In)*F_In ) / (rho(1)*A) * (Delta_x)/2;
966
967      0 =
968        -( P(2)*A - P(1)*A )
969        +( ( F_In + F(1) )/2 )^2 / ( rho(1)*A )
970        - ( ( F(2) + F(1) )/2 )^2 / ( rho(2)*A )
971        - 2*intfArray(1)/( 2*r0 ) * ( ABS(F(1))*F(1) ) / ( rho(1)*A ) * Delta_x/2
972        - 2*intfArray(2)/( 2*r0 ) * ( ABS(F(1))*F(1) ) / ( rho(2)*A ) * Delta_x/2;
973      FOR I:=2 TO NG-1 DO
974      0 =
975        -( P(I+1)*A - P(I)*A )

```

```

975      +( ( F(I-1) + F(I) )/2 )^2 / ( rho(I)*A )
976      -( ( F(I+1) + F(I) )/2 )^2 / ( rho(I+1)*A )
977      - 2*intfArray(I)/( 2*r0 ) * ( ABS(F(I))*F(I) )/ ( rho(I)*A ) * Delta_x/2
978      - 2*intfArray(I+1)/( 2*r0 ) * ( ABS(F(I))*F(I) )/ ( rho(I+1)*A ) * Delta_x/2;
979  END # for
980  0 =
981      -( P_Out*A - P(NG)*A )
982      +( ( F(NG-1) + F(NG) )/2 )^2 / ( rho(NG)*A )
983      -( F(NG) )^2 / ( rho(NG)*A )
984      - 2*intfArray(NG)/( 2*r0 ) * ( ABS(F(NG))*F(NG) ) / ( rho(NG)*A ) * Delta_x/2;
985  # Energy Balance
986      1e-7*$psi(1)*Vol = 1e-7*(F_In*h0 - F(1)*h(1)
987      +4*U/(2*r0)*(TEextrnl(1)-T(1))*Vol);
988  FOR I:=(2) TO (NG) DO
989      1e-7*$psi(I)*Vol = 1e-7*(F(I-1)*h(I-1) - F(I)*h(I)
990      +4*U/(2*r0)*(TEextrnl(I)-T(I))*Vol);
991  END # for
992
993  # Algebraic Equations
994  FOR I:=1 TO NG DO
995      0 = 1e-7*(psi(I) - (rho(I)*h(I) - P(I)));
996  END # for
997
998  # 2- Thermodynamical Part
999  FOR I:= 1 TO NG DO
1000      0 = 1e-7*(h(I) - (h_form + Cp/Mw*(T(I)-T_stand)));
1001  END # for
1002  0 = (h0 - (h_form + Cp/Mw*(T0 - T_stand)));
1003
1004  # Equation of State
1005  FOR I:=1 TO NG DO
1006      0=1e-3*(P(I)*Mw - rho(I)*R_c*T(I));
1007  END # for
1008
1009  #Equations to assign variables for heat transfer coefficients
1010  HT.rhoPipeHe = sigma(rho(2:NG))/NG;
1011  HT.vPipe = sigma(F(2:NG)/rho(2:NG)/A)/NG;
1012  END
1013  #####
1014
1015  #####
1016  #####
1017  MODEL PipeFullDyn
1018  #####
1019  PARAMETER
1020      #SET here
1021      Pi AS REAL
1022      R_c AS REAL #Rc constant "J/(mol*K)"
1023      Mw AS REAL #Molecular weight "Kg/mol"
1024      T_stand AS REAL #Standard Temp "K"
1025      Cp AS REAL #specific heat at constant pressure "J/Kg/K"
1026      h_form AS REAL #specific enthalpy of formation "J/Kg"
1027      A AS REAL
1028      r0 AS REAL #diameter of pipe "m"
1029      muVisc AS REAL # average viscosity in pipe
1030
1031  #EXTERNALLY set
1032      SectionL AS REAL #length of pipe "m"
1033      NG AS INTEGER #number of control volumes in the grid
1034      Temp AS REAL #Temperature "K"
1035      InitP AS REAL
1036      InitT AS REAL
1037
1038  #CALCULATED
1039      InitRho AS REAL InitH AS REAL
1040      InitRho_e AS REAL Delta_x AS REAL #length of control volume "m"
1041      Vol AS REAL
1042  UNIT
1043      HT AS HTCcoeffGasMetalHX
1044  VARIABLE
1045      rho AS ARRAY(NG) OF Density
1046      P AS ARRAY(NG) OF Pressure
1047      P_In AS Pressure
1048      P_Out AS Pressure
1049      h AS ARRAY(NG) OF SpecificEnergy
1050      h0 AS SpecificEnergy
1051      T AS ARRAY(NG) OF Temperature
1052      TExtrnl AS ARRAY(NG) OF Temperature
1053      T0 AS Temperature
1054      F AS ARRAY(NG) OF Flowrate
1055      F_In AS Flowrate
1056      psi AS ARRAY(NG) OF Energy
1057  SET
1058      #SET
1059      Pi:=4*ATAN(1);
1060      R_c := 8.314; Mw := 4.0E-3;
1061      T_stand := 298; Cp := 20.78; h_form := 0;
1062      r0 := 9.1652e-4/2 ; # dhyd in the PCHE, this is needed to calculate Re
1063      A:=0.3475;
1064      #CALCULATED
1065      Delta_x := SectionL/(NG-1);
1066      InitRho := InitP*Mw/(R_c*Temp);

```

```

1067      InitH := h_form + Cp/Mw*(Temp-T_stand);
1068      InitRho_e := InitRho*InitH - InitP;
1069      HT.r0:=r0;      HT.t:= (HT.r0*2*0.78*2 - HT.r0)/3; # according to INL, an average of 2*tmax +1*tmin
1070      Vol := A*Delta_x;
1071      INTERMEDIATE
1072      DIMENSION intRe(NG)
1073      DIMENSION intfArray(NG)
1074      U:= HT.U;
1075      intRe:= F*r0*2/muVisc/A;
1076      intfArray:=64/intRe/4;
1077      EQUATION
1078      # Mass Balance
1079      Delta_x*A*$rho(1) = F_In - F(1);
1080      FOR I:= 2 TO NG DO
1081        Delta_x*A*$rho(I) = (F(I-1) - F(I));
1082      END # for
1083      # Momentum Balance
1084      Delta_x/2*$F_In = -(P(1)*A -P_In*A)
1085      +( F_In )^2 / (rho(1)*A)
1086      -( ( F_In + F(1) )/2 )^2 / (rho(1)*A)
1087      - (2*intfArray(1)/(2*r0) ) * (ABS(F_In)*F_In ) / (rho(1)*A ) * (Delta_x)/2;
1088      Delta_x * $F(1) = -
1089      -( P(2)*A - P(1)*A )
1090      +( ( F_In + F(1) )/2 )^2 / ( rho(1)*A )
1091      -( ( F(2) + F(1) )/2 )^2 / ( rho(2)*A )
1092      - 2*intfArray(1)/( 2*r0 ) * ( ABS(F(1))*F(1) )/ ( rho(1)*A ) * Delta_x/2
1093      - 2*intfArray(2)/( 2*r0 ) * ( ABS(F(1))*F(1) )/ ( rho(2)*A ) * Delta_x/2;
1094      FOR I:=2 TO NG-1 DO
1095        Delta_x * $F(I) = -
1096        -( P(I+1)*A - P(I)*A )
1097        +( ( F(I-1) + F(I) )/2 )^2 / ( rho(I)*A )
1098        -( ( F(I) + F(I+1) )/2 )^2 / ( rho(I+1)*A )
1099        - 2*intfArray(I)/( 2*r0 ) * ( ABS(F(I))*F(I) )/ ( rho(I)*A ) * Delta_x/2
1100        - 2*intfArray(I+1)/( 2*r0 ) * ( ABS(F(I))*F(I) )/ ( rho(I+1)*A ) * Delta_x/2;
1101      END # for
1102      Delta_x /2 * $F(NG) = -
1103      -( P_Out*A - P(NG)*A )
1104      +( ( F(NG-1) + F(NG) )/2 )^2 / ( rho(NG)*A )
1105      -( F(NG) )^2 / ( rho(NG)*A )
1106      - 2*intfArray(NG)/( 2*r0 ) * ( ABS(F(NG))*F(NG) ) / ( rho(NG)*A ) * Delta_x/2;
1107      # Energy Balance
1108      1e-7*$psi(1)*Vol = 1e-7*(F_In*h0 - F(1)*h(1)
1109      +4*U/(2*r0)*(TExtrnl(1)-T(1))*Vol);
1110      FOR I:=(2) TO (NG) DO
1111        1e-7*$psi(I)*Vol = 1e-7*(F(I-1)*h(I-1) - F(I)*h(I)
1112        +4*U/(2*r0)*(TExtrnl(I)-T(I))*Vol);
1113      END # for
1114
1115      # Algebraic Equations
1116      FOR I:=1 TO NG DO
1117        0 = 1e-7*(psi(I) - (rho(I)*h(I) - P(I)));
1118      END # for
1119
1120      # 2- Thermodynamical Part
1121      FOR I:= 1 TO NG DO
1122        0 = 1e-7*(h(I) - (h_form + Cp/Mw*(T(I)-T_stand)));
1123      END # for
1124      0 = (h0 - (h_form + Cp/Mw*(T0 - T_stand)));
1125
1126      # Equation of State
1127      FOR I:=1 TO NG DO
1128        0=1e-3*(P(I)*Mw - rho(I)*R_c*T(I));
1129      END # for
1130
1131      #Equations to assign variables for heat transfer coefficients
1132      HT.rhoPipeHe = sigma(rho(2:NG))/NG;
1133      HT.vPipe = sigma(F(2:NG)/rho(2:NG)/A)/NG;
1134      END
1135      *****
1136
1137
1138      *****
1139      MODEL PipeInnerQSS
1140      *****
1141      PARAMETER
1142      Pi AS REAL
1143      R_c AS REAL #Rc constant "J/(mol*K)"
1144      Mw AS REAL #Molecular weight "Kg/mol"
1145      T_stand AS REAL #Standard Temp "K"
1146      Cp AS REAL #specific heat at constant pressure "J/Kg/K"
1147      h_form AS REAL #specific enthalpy of formation "J/Kg"
1148      A AS REAL
1149      r0 AS REAL #diameter of pipe "m"
1150      muVisc AS REAL # average viscosity in
1151      SectionL AS REAL #length of pipe "m"
1152      NG AS INTEGER #number of control volumes in the grid
1153      Temp AS REAL #Temperature "K"
1154      InitP AS REAL
1155      InitRho AS REAL InitH AS REAL
1156      InitRho_e AS REAL Delta_x AS REAL #length of control volume "m"
1157      Vol AS REAL
1158      UNIT

```

```

1159 HT AS HTCoeffGasMetalHXDummyInner
1160 VARIABLE
1161 rho AS ARRAY(NG) OF Density
1162 P AS ARRAY(NG) OF Pressure
1163 P_In AS Pressure
1164 P_Out AS Pressure
1165 h AS ARRAY(NG) OF SpecificEnergy
1166 h0 AS SpecificEnergy
1167 T AS ARRAY(NG) OF Temperature
1168 T0 AS Temperature
1169 TExtrnl AS ARRAY(NG) OF Temperature
1170 F AS ARRAY(NG) OF Flowrate
1171 F_In AS Flowrate
1172 psi AS ARRAY(NG) OF Energy
1173 SET
1174 #SET
1175 Pi:=4*ATAN(1);
1176 R_c := 8.314; Mw := 18.02E-3; #steam # 4.0E-3; # helium
1177 T_stand := 298; Cp := 40.65; #steam #20.78; #helium
1178 h_form := 0.0; # -57.8; #enthalpy of formation from perry's water gas
1179 r0 :=0.01/2; # Hyd radious based on PCHE INL report,
1180 A:=0.2750;
1181 #CALCULATED
1182 Delta_x := SectionL/(NG-1);
1183 InitRho := InitP*Mw/(R_c*Temp);
1184 InitH := h_form + Cp/Mw*(Temp-T_stand);
1185 InitRho_e := InitRho*InitH - InitP;
1186 Vol := A*Delta_x;
1187 INTERMEDIATE
1188 DIMENSION intRe(NG)
1189 DIMENSION intfArray(NG)
1190 U:= HT.U;
1191 intEps:= r0*1e-9;
1192 intRe:=F*r0*2/A/muVisc;
1193 intfArray:=1/((-2*LOG10(intEps/(3.7*r0) + 2.51/intRe*(1.14 -2*LOG10(intEps/r0 + 21.25/(intRe^0.9))))))^2/4;
1194 EQUATION
1195 # Mass Balance
1196 0 = F_In - F(1);
1197 FOR I:= 2 TO NG DO
1198 0 = (F(I-1) - F(I));
1199 END # for
1200 # Momentum Balance
1201 0 = -(P(1)*A -P_In*A)
1202 + ( F_In )^2 / (rho(1)*A)
1203 - ( ( F_In + F(1) )/2 )^2 / (rho(1)*A)
1204 - (2*intfArray(1)/(2*r0)) * (ABS(F_In)*F_In) / (rho(1)*A) * (Delta_x)/2;
1205 0 =
1206 - ( P(2)*A - P(1)*A )
1207 + ( ( F_In + F(1) )/2 )^2 / ( rho(1)*A )
1208 - ( ( F(2) + F(1) )/2 )^2 / ( rho(2)*A )
1209 - 2*intfArray(1)/(2*r0) * ( ABS(F(1))*F(1) ) / ( rho(1)*A ) * Delta_x/2
1210 - 2*intfArray(2)/(2*r0) * ( ABS(F(1))*F(1) ) / ( rho(2)*A ) * Delta_x/2;
1211 FOR I:=2 TO NG-1 DO
1212 0 =
1213 - ( P(I+1)*A - P(I)*A )
1214 + ( ( F(I-1) + F(I) )/2 )^2 / ( rho(I)*A )
1215 - ( ( F(I+1) + F(I) )/2 )^2 / ( rho(I+1)*A )
1216 - 2*intfArray(I)/(2*r0) * ( ABS(F(I))*F(I) ) / ( rho(I)*A ) * Delta_x/2
1217 - 2*intfArray(I+1)/(2*r0) * ( ABS(F(I))*F(I) ) / ( rho(I+1)*A ) * Delta_x/2;
1218 END # for
1219 0 =
1220 - ( P_Out*A - P(NG)*A )
1221 + ( ( F(NG-1) + F(NG) )/2 )^2 / ( rho(NG)*A )
1222 - ( F(NG) )^2 / ( rho(NG)*A )
1223 - 2*intfArray(NG)/(2*r0) * ( ABS(F(NG))*F(NG) ) / ( rho(NG)*A ) * Delta_x/2;
1224 # Energy Balance
1225 1e-7*$psi(1)*Vol = 1e-7*(F_In*h0 - F(1)*h(1)
1226 +4*U/(2*r0)*(TExtrnl(1)-T(1))*Vol);
1227 FOR I:=(2) TO (NG) DO
1228 1e-7*$psi(I)*Vol = 1e-7*(F(I-1)*h(I-1) - F(I)*h(I)
1229 +4*U/(2*r0)*(TExtrnl(I)-T(I))*Vol); # the last term comes from heat in/volume to heat in Work: Pipe
Simulation
1230 END # for
1231
1232 # Algebraic Equations
1233 FOR I:=1 TO NG DO
1234 0 = 1e-7*(psi(I) - (rho(I)*h(I) - P(I)));
1235 END # for
1236
1237 # 2- Thermodynamical Part
1238 FOR I:= 1 TO NG DO
1239 0 = 1e-7*(h(I) - (h_form + Cp/Mw*(T(I)-T_stand)));
1240 END # for
1241 0 = (h0 - (h_form + Cp/Mw*(T0 - T_stand)));
1242 # Equation of State
1243 FOR I:=1 TO NG DO
1244 0=1e-3*(P(I)*Mw - rho(I)*R_c*T(I));
1245 END # for
1246
1247 #Equations to assign variables for heat transfer coefficients
1248 HT.rhoPipeHe = sigma(rho(2:NG))/NG;
1249 HT.vPipe = sigma(F(2:NG)/rho(2:NG)/A)/NG;

```



```

1250 END
1251 #####
1252
1253
1254 #####
1255 MODEL PipeInnerOMach
1256 #####
1257 PARAMETER
1258   Pi AS REAL
1259   R_c AS REAL      #Rc constant "J/(mol*K)"
1260   Mw AS REAL      #Molecular weight "Kg/mol"
1261   T_stand AS REAL  #Standard Temp "K"
1262   Cp AS REAL      #specific heat at constant pressure "J/Kg/K"
1263   h_form AS REAL  #specific enthalpy of formation "J/Kg"
1264   A AS REAL
1265   r0 AS REAL      #diameter of pipe "m"
1266   muVisc AS REAL  # average viscosity in
1267   SectionL AS REAL #length of pipe "m"
1268   NG AS INTEGER   #number of control volumes in the grid
1269   Temp AS REAL    #Temperature "K"
1270   InitP AS REAL
1271   InitRho AS REAL  InitH AS REAL
1272   InitRho_e AS REAL  Delta_x AS REAL  #length of control volume "m"
1273   Vol AS REAL
1274 UNIT
1275   HT AS HTCoeffGasMetalHXDummyInner
1276 VARIABLE
1277   rho AS ARRAY(NG) OF Density
1278   P AS ARRAY(NG) OF Pressure
1279   P_In AS Pressure
1280   P_Out AS Pressure
1281   h AS ARRAY(NG) OF SpecificEnergy
1282   h0 AS SpecificEnergy
1283   T AS ARRAY(NG) OF Temperature
1284   TO AS Temperature
1285   TExtrnl AS ARRAY(NG) OF Temperature
1286   F AS ARRAY(NG) OF Flowrate
1287   F_In AS Flowrate
1288   psi AS ARRAY(NG) OF Energy
1289 SET
1290 #SET
1291   Pi:=4*ATAN(1);
1292   R_c := 8.314;      Mw := 18.02E-3; #steam # 4.0E-3; # helium
1293   T_stand := 298;   Cp := 40.65; #steam #20.78; #helium
1294   h_form := 0.0; # -57.8; #enthalpy of formation from perry's water gas
1295   r0 :=0.01/2 ; # Hyd radius based on PCHE INL report,
1296   A:=0.2750;
1297 #CALCULATED
1298   Delta_x := SectionL/(NG-1);
1299   InitRho := InitP*Mw/(R_c*Temp);
1300   InitH := h_form + Cp/Mw*(Temp-T_stand);
1301   InitRho_e := InitRho*InitH - InitP;
1302   Vol := A*Delta_x;
1303 INTERMEDIATE
1304 DIMENSION intRe(NG)
1305 DIMENSION intfArray(NG)
1306 U:= HT.U;
1307 intEps:= r0*1e-9;
1308 intRe:=F*r0*2/A/muVisc;
1309 intfArray:=1/((-2*LOG10(intEps/(3.7*r0) + 2.51/intRe*(1.14 -2*LOG10(intEps/r0 + 21.25/(intRe^0.9))))))^2/4;
1310 EQUATION
1311 # Mass Balance
1312 Delta_x*A*$rho(1) = F_In - F(1);
1313 FOR I:= 2 TO NG DO
1314   Delta_x*A*$rho(I) = (F(I-1) - F(I));
1315 END # for
1316 # Momentum Balance
1317 0 = 1e-4*( -(P(1)*A -P_In*A)
1318   +( F_In )^2 / (rho(1)*A)
1319   -( ( F_In + F(1) )/2 )^2 / (rho(1)*A)
1320   - (2*intfArray(1)/(2*r0)) * ( ABS(F_In)*F_In ) / (rho(1)*A ) * (Delta_x)/2 );
1321 0 =
1322 1e-4*( -( P(2)*A - P(1)*A )
1323   +( ( F_In + F(1) )/2 )^2 / ( rho(1)*A )
1324   -( ( F(2) + F(1) )/2 )^2 / ( rho(2)*A )
1325   - 2*intfArray(1)/( 2*r0 ) * ( ABS(F(1))*F(1) )/ ( rho(1)*A ) * Delta_x/2
1326   - 2*intfArray(2)/( 2*r0 ) * ( ABS(F(1))*F(1) )/ ( rho(2)*A ) * Delta_x/2 );
1327 FOR I:=2 TO NG-1 DO
1328 0 =
1329 1e-4*( -( P(I+1)*A - P(I)*A )
1330   +( ( F(I-1) + F(I) )/2 )^2 / ( rho(I)*A )
1331   -( ( F(I+1) + F(I) )/2 )^2 / ( rho(I+1)*A )
1332   - 2*intfArray(I)/( 2*r0 ) * ( ABS(F(I))*F(I) )/ ( rho(I)*A ) * Delta_x/2
1333   - 2*intfArray(I+1)/( 2*r0 ) * ( ABS(F(I))*F(I) )/ ( rho(I+1)*A ) * Delta_x/2 );
1334 END # for
1335 0 =
1336 1e-4*( -( P_Out*A - P(NG)*A )
1337   +( ( F(NG-1) + F(NG) )/2 )^2 / ( rho(NG)*A )
1338   -( F(NG) )^2 / ( rho(NG)*A )
1339   - 2*intfArray(NG)/( 2*r0 ) * ( ABS(F(NG))*F(NG) ) / ( rho(NG)*A ) * Delta_x/2 );
1340 # Energy Balance
1341 1e-7*$psi(1)*Vol = 1e-7*(F_In*h0 - F(1)*h(1)

```

```

1342      +4*U/(2*r0)*(TEextrnl(1)-T(1))*Vol);
1343  FOR I:=(2) TO (NG) DO
1344      1e-7*$psi(I)*Vol = 1e-7*(F(I-1)*h(I-1) - F(I)*h(I)
1345      +4*U/(2*r0)*(TEextrnl(I)-T(I))*Vol); # the last term comes from heat in/volume to heat in Work: Pipe
Simulation
1346  END # for
1347
1348  # Algebraic Equations
1349  FOR I:=1 TO NG DO
1350      0 = 1e-7*(psi(I) - (rho(I)*h(I) - P(I)));
1351  END # for
1352
1353  # 2- Thermodynamical Part
1354  FOR I:= 1 TO NG DO
1355      0 = 1e-7*(h(I) - (h_form + Cp/Mw*(T(I)-T_stand)));
1356  END # for
1357  0 = (h0 - (h_form + Cp/Mw*(T0 - T_stand)));
1358  # Equation of State
1359  FOR I:=1 TO NG DO
1360      0=1e-3*(P(I)*Mw - rho(I)*R_c*T(I));
1361  END # for
1362
1363  #Equations to assign variables for heat transfer coefficients
1364  HT.rhoPipeHe = sigma(rho(2:NG))/NG;
1365  HT.vPipe = sigma(P(2:NG)/rho(2:NG)/A)/NG;
1366  END
1367  #####
1368
1369
1370  #####
1371  MODEL PipeInnerFullDyn
1372  #####
1373  PARAMETER
1374      Pi AS REAL
1375      R_c AS REAL      #Rc constant "J/(mol*K)"
1376      Mw AS REAL      #Molecular weight "Kg/mol"
1377      T_stand AS REAL #Standard Temp "K"
1378      Cp AS REAL      #specific heat at constant pressure "J/Kg/K"
1379      h_form AS REAL  #specific enthalpy of formation "J/Kg"
1380      A AS REAL
1381      r0 AS REAL      #diameter of pipe "m"
1382      muVisc AS REAL # average viscosity in
1383      SectionL AS REAL #length of pipe "m"
1384      NG AS INTEGER  #number of control volumes in the grid
1385      Temp AS REAL   #Temperature "K"
1386      InitP AS REAL
1387      InitRho AS REAL  InitH AS REAL
1388      InitRho_e AS REAL Delta_x AS REAL #length of control volume "m"
1389      Vol AS REAL
1390  UNIT
1391      HT AS HTCoeffGasMetalHXDummyInner
1392  VARIABLE
1393      rho AS ARRAY(NG) OF Density
1394      P AS ARRAY(NG) OF Pressure
1395      P_In AS Pressure
1396      P_Out AS Pressure
1397      h as ARRAY(NG) OF SpecificEnergy
1398      h0 AS SpecificEnergy
1399      T as ARRAY(NG) OF Temperature
1400      T0 AS Temperature
1401      TExtrnl AS ARRAY(NG) OF Temperature
1402      F AS ARRAY(NG) OF Flowrate
1403      F_In AS Flowrate
1404      psi AS ARRAY(NG) OF Energy
1405  SET
1406      #SET
1407      Pi:=4*ATAN(1);
1408      R_c := 8.314; Mw := 18.02E-3; #steam # 4.0E-3; # helium
1409      T_stand := 298; Cp := 40.65; #steam #20.78; #helium
1410      h_form := 0.0; # -57.8; #enthalpy of formation from perry's water gas
1411      r0 :=0.01/2 ; # Hyd radious based on PCHE INL report,
1412      A:=0.2750;
1413      #CALCULATED
1414      Delta_x := SectionL/(NG-1);
1415      InitRho := InitP*Mw/(R_c*Temp);
1416      InitH := h_form + Cp/Mw*(Temp-T_stand);
1417      InitRho_e := InitRho*InitH - InitP;
1418      Vol := A*Delta_x;
1419  INTERMEDIATE
1420      DIMENSION intRe(NG)
1421      DIMENSION intfArray(NG)
1422      U:= HT.U;
1423      intEps:= r0*1e-9;
1424      intRe:=F*r0*2/A/muVisc;
1425      intfArray:=1/((-2*LOG10(intEps/(3.7*r0) + 2.51/intRe*(1.14 -2*LOG10(intEps/r0 + 21.25/(intRe^0.9))))))^2/4;
1426  EQUATION
1427      # Mass Balance
1428      Delta_x*A*$rho(1) = F_In - F(1);
1429      FOR I:= 2 TO NG DO
1430          Delta_x*A*$rho(I) = (F(I-1) - F(I));
1431      END # for
1432      # Momentum Balance

```

```

1433 Delta_x/2*$F_In = -(P(1)*A -P_In*A)
1434 +( F_In )^2 / (rho(1)*A)
1435 -( ( F_In + F(1) )/2 )^2 / (rho(1)*A)
1436 - (2*intfArray(1)/(2*r0)) * ( ABS(F_In)*F_In ) / (rho(1)*A) * (Delta_x)/2;
1437 Delta_x
1438 * $F(1) =
1439 -( P(2)*A - P(1)*A )
1440 +( ( F_In + F(1) )/2 )^2 / ( rho(1)*A )
1441 -( ( F(2) + F(1) )/2 )^2 / ( rho(2)*A )
1442 - 2*intfArray(1)/( 2*r0 ) * ( ABS(F(1))*F(1) )/ ( rho(1)*A ) * Delta_x/2
1443 - 2*intfArray(2)/( 2*r0 ) * ( ABS(F(1))*F(1) )/ ( rho(2)*A ) * Delta_x/2;
1444 FOR I:=2 TO NG-1 DO
1445 Delta_x * $F(I) =
1446 -( P(I+1)*A - P(I)*A )
1447 +( ( F(I-1) + F(I) )/2 )^2 / ( rho(I)*A )
1448 -( ( F(I+1) + F(I) )/2 )^2 / ( rho(I+1)*A )
1449 - 2*intfArray(I)/( 2*r0 ) * ( ABS(F(I))*F(I) )/ ( rho(I)*A ) * Delta_x/2
1450 - 2*intfArray(I+1)/( 2*r0 ) * ( ABS(F(I))*F(I) )/ ( rho(I+1)*A ) * Delta_x/2;
1451 END # for
1452 Delta_x /2 * $F(NG) =
1453 -( P_Out*A - P(NG)*A )
1454 +( ( F(NG-1) + F(NG) )/2 )^2 / ( rho(NG)*A )
1455 -( F(NG) )^2 / ( rho(NG)*A )
1456 - 2*intfArray(NG)/( 2*r0 ) * ( ABS(F(NG))*F(NG) ) / ( rho(NG)*A ) * Delta_x/2;
1457 # Energy Balance
1458 1e-7*$psi(1)*Vol = 1e-7*(F_In*h0 - F(1)*h(1)
1459 +4*U/(2*r0)*(TExtrnl(1)-T(1))*Vol);
1460 FOR I:=(2) TO (NG) DO
1461 1e-7*$psi(I)*Vol = 1e-7*(F(I-1)*h(I-1) - F(I)*h(I)
1462 +4*U/(2*r0)*(TExtrnl(I)-T(I))*Vol); # the last term comes from heat in/volume to heat in Work: Pipe
1463 Simulation
1464 END # for
1465 # Algebraic Equations
1466 FOR I:=1 TO NG DO
1467 0 = 1e-7*(psi(I) - (rho(I)*h(I) - P(I)));
1468 END # for
1469 # 2- Thermodynamical Part
1470 FOR I:= 1 TO NG DO
1471 0 = 1e-7*(h(I) - (h_form + Cp/Mw*(T(I)-T_stand)));
1472 END # for
1473 0 = (h0 - (h_form + Cp/Mw*(TO - T_stand)));
1474 # Equation of State
1475 FOR I:=1 TO NG DO
1476 0=1e-3*(P(I)*Mw - rho(I)*R_c*T(I));
1477 END # for
1478
1479 #Equations to assign variables for heat transfer coefficients
1480 HT.rhoPipeHe = sigma(rho(2:NG))/NG;
1481 HT.vPipe = sigma(F(2:NG)/rho(2:NG)/A)/NG;
1482 END
1483 *****

```

MODELS_NUCLEARREACTORPROPERTIES.JAC

```

1 *****
2 MODEL ThermalHyd3
3 *****
4 PARAMETER
5 # SET here
6 P1 AS REAL
7 NGHOr AS INTEGER
8 NGVer AS INTEGER # Number of grid points in the vertical direction
9 Cp AS REAL
10 VoidF AS REAL
11 DenGraphite AS REAL
12 PDropCore0 AS REAL #
13 LNode AS ARRAY(NGVer) OF REAL # |
14 R AS ARRAY(NGHor) OF REAL
15 RPF AS ARRAY(NGHor) OF REAL # radial peaking factors
16 APF AS ARRAY(NGVer-2) OF REAL # axial peaking factors
17 WF AS ARRAY(NGHor) OF REAL
18 # CALCULATED
19 LVer AS ARRAY(NGVer-1) OF REAL # | delta Z
20 LHor AS ARRAY(NGHor-1) OF REAL # - delta R
21 AVer AS ARRAY(NGHor) OF REAL # -
22 AHor AS ARRAY(NGVer,NGHor-1) OF REAL# |
23 # EXTERNAL
24 WPrim0 AS REAL
25 UNIT
26 HTCORE AS ARRAY(NGVer-2,NGHor-2) OF HEEFM2
27 CPRflTop AS ARRAY(1,NGHor) OF CPRF
28 CPRflSide AS ARRAY(NGVer-2, 2) OF CPRF

```

```

29   CPRef1Down AS ARRAY(1,NGHor) OF CPRF
30   CPFuel AS ARRAY(NGVer-2,NGHor-2) OF CPFuel
31   VARIABLE
32   # CALCULATED
33   T_FuelAvg AS Temperature
34   TCoreOut AS Temperature # temperature of gas
35   PCoreOut AS Pressure ### check units
36   PDropRCore AS RealVar
37   TSolid AS ARRAY(NGVer,NGHor) OF Density
38   TGas AS ARRAY(NGVer-1,NGHor-2) OF Temperature
39   # EXTERNAL
40   WPrim AS MassFlowRate
41   QFission AS Power #
42   TCoreIn AS Temperature
43   PCoreIn AS Pressure
44   SET
45   # SET
46   Pi:= 4*ATAN(1);
47   NGHor:= 8; NGVer:= 12;
48   Cp:=5193.0; #L1095
49   VoidF:= 0.39; #L1102
50   DenGraphite:=1394.8; #kg/m^3
51   PDropRCore0:= 0.02; # L1171
52   LNode(1):= 1.15; # LUpperRef1 L1124
53   LNode(2:NGVer-1):= 0.79309; #LCoreNode L1126
54   LNode(NGVer):= 1.15; #LLowerRef1 L1124
55   R:=[0.8239,1.0726,1.2735,1.4469,1.6014,1.7425,2.3878,2.8926];
56   RPF:=[0.0,0.218,0.207,0.195,0.19,0.19,0.0,0.0]; # radial peaking factors, 5 nodes
57   APF:=[0.025,0.034,0.053,0.071,0.091,0.121,0.148,0.171,0.162,0.124]; # axial peaking factors, 10 nodes
      excluding top and bottom reflectors
58   WF:=[0.22,0.156,0.156,0.156,0.156,0.156,0.0,0.0]; # mass flow fraction
59   # CALCULATED
60   LVer(1):= (LNode(1)+LNode(2))/2;
61   LVer(2:(NGVer-2)):= LNode(2:(NGVer-2));
62   LVer(NGVer-1):=(LNode(NGVer-1)+LNode(NGVer))/2;
63   FOR J:=1 TO NGHor-1 DO
64     LHor(J):= (R(J+1)-R(J))/2;
65   END # for J
66   AVer(1):= Pi*R(1)^2;
67   FOR J:=2 TO NGHor DO
68     AVer(J):= Pi*(R(J)^2-R(J-1)^2);
69   END # for
70   FOR I:=1 TO NGVer DO
71     AHor(I):= 2*Pi*R(1:NGHor-1)*LNode(I); # A1_Right_C or A1_Left_C
72   END # for I
73   # CALCULATED UNITS
74   HTCore.VoidF:= VoidF; # Gas heat transfer parameters
75   FOR I:= 1 TO NGVer-2 DO
76     FOR J:= 1 TO NGHor-2 DO
77       HTCore(I,J).Area:= AVer(J);
78     END # for J
79   END # for I
80   CPFuel.VoidF:= VoidF; # VoidF in CPFuel
81   INTERMEDIATE
82   DIMENSION QCond(NGVer,NGHor), QFissionRing(NGVer,NGHor), QC(NGVer,NGHor)
83   DIMENSION K(NGVer,NGHor), KVer(NGVer-1,NGHor), KHor(NGVer,NGHor-1)
84   DIMENSION WCore(NGHor), EXPP(NGVer-2,NGHor-2), HeatCap(NGVer,NGHor)
85   DIMENSION T_FuelAvgSlice(NGVer-2)
86   DIMENSION QSlice(NGVer-2)
87   QSlice:= QFission*APF;
88   # K, thermal conductivity for each node
89   # reflectors, from FORTRAN function KRT(T)
90   # (1,1) - (1,8), (12,1)-(12,8)
91   FOR J:= 1 TO NGHor DO
92     K(1,J):= -0.0092*(TSolid(1,J)/200)^5+0.267*(TSolid(1,J)/200)^4 -2.9746*(TSolid(1,J)/200)^3+16.8883*(
      TSolid(1,J)/200)^2
93     -59.4691*(TSolid(1,J)/200)+170.884;
94     K(12,J):= -0.0092*(TSolid(12,J)/200)^5+0.267*(TSolid(12,J)/200)^4-2.9746*(TSolid(12,J)/200)^3+16.8883*(
      TSolid(12,J)/200)^2
95     -59.4691*(TSolid(12,J)/200)+170.884;
96   END # for
97   # (2,7)-(11,8)
98   FOR I:= 2 TO NGVer-1 DO
99     FOR J:= 7 TO NGHor DO
100      K(I,J):= -0.0092*(TSolid(I,J)/200)^5+0.267*(TSolid(I,J)/200)^4-2.9746*(TSolid(I,J)/200)^3+16.8883*(
      TSolid(I,J)/200)^2
101      -59.4691*(TSolid(I,J)/200)+170.884;
102   END # for
103   END # for
104   # (2,1)-(11,6) pebbles
105   FOR I:= 2 TO NGVer-1 DO
106     FOR J:= 1 TO 6 DO
107       K(I,J):=0.00011536*(TSolid(I,J)-173.16)^1.6622;
108     END # for J
109   END # for I
110   # KVer, Interface conductivity for intermediate nodes in the vertical direction
111   FOR I:= 1 TO NGVer-1 DO
112     FOR J:= 1 TO NGHor DO
113       KVer(I,J):= (K(I,J)+K(I+1,J))/2;
114     END # for J
115   END # for I
116   # KHor, Interface conductivity for intermediate nodes in the horizontal direction

```

```

117     FOR I:= 1 TO NGVer DO
118         FOR J:= 1 TO NGHOr -1 DO
119             KHor(I,J):= (K(I,J)+K(I,J+1))/2;
120         END # for J
121     END # for I
122 # QCond: Heat by conduction
123 # top reflector (1,1) - (1,8)
124 # first ring (1,1)
125 QCond(1,1):= kHor(1,1)*(TSolid(1,2)-TSolid(1,1))*AHor(1,1)/LHor(1)
126           + kVer(1,1)*(TSolid(2,1)-TSolid(1,1))*AVer(1)/LVer(1);
127 # middle rings (1,2) - (1,7)
128 FOR J:= 2 TO NGHOr-1 DO
129     QCond(1,J):= kHor(1,J-1)*(TSolid(1,J-1)-TSolid(1,J))*AHor(1,J-1)/LHor(J-1)
130               + kHor(1,J)*(TSolid(1,J+1)-TSolid(1,J))*AHor(1,J)/LHor(J)
131               + kVer(1,J)*(TSolid(2,J)-TSolid(1,J))*AVer(J)/LVer(1);
132 END # for J
133 # last ring (1,8)
134 QCond(1,8):= kHor(1,7)*(TSolid(1,7)-TSolid(1,8))*AHor(1,7)/LHor(7)
135           + kVer(1,8)*(TSolid(2,8)-TSolid(1,8))*AVer(8)/LVer(1);
136 # lower reflector (12,1) - (12,8)
137 # first ring (12,1)
138 QCond(12,1):=kHor(12,1)*(TSolid(12,2)-TSolid(12,1))*AHor(12,1)/LHor(1)
139           + kVer(11,1)*(TSolid(11,1)-TSolid(12,1))*AVer(1)/LVer(11);
140 # middle rings (12,2) - (12,7)
141 FOR J:= 2 TO NGHOr-1 DO
142     QCond(12,J):= kHor(12,J-1)*(TSolid(12,J-1)-TSolid(12,J))*AHor(12,J-1)/LHor(J-1)
143               + kHor(12,J)*(TSolid(12,J+1)-TSolid(12,J))*AHor(12,J)/LHor(J)
144               + kVer(11,J)*(TSolid(11,J)-TSolid(12,J))*AVer(J)/LVer(11);
145 END # for J
146 # last ring (12,8)
147 QCond(12,8):=kHor(12,7)*(TSolid(12,7)-TSolid(12,8))*AHor(12,7)/LHor(7)
148           + kVer(11,8)*(TSolid(11,8)-TSolid(12,8))*AVer(8)/LVer(11);
149 # center of core (2,2) - (11,7)
150 FOR I := 2 TO NGVer-1 DO
151     FOR J:= 2 TO NGHOr - 1 DO
152         QCond(I,J):= kHor(I,J-1)*(TSolid(I,J-1)-TSolid(I,J))*AHor(I,J-1)/LHor(J-1)
153               + kHor(I,J)*(TSolid(I,J+1)-TSolid(I,J))*AHor(I,J)/LHor(J)
154               + kVer(I-1,J)*(TSolid(I-1,J)-TSolid(I,J))*AVer(J)/LVer(I-1)
155               + kVer(I,J)*(TSolid(I+1,J)-TSolid(I,J))*AVer(J)/LVer(I);
156     END # for J
157 END # for I
158 # left core column or first ring J = 1, (2,1) - (11,1)
159 FOR I:= 2 TO NGVer-1 DO
160     QCond(I,1):= kHor(I,1)*(TSolid(I,2)-TSolid(I,1))*AHor(I,1)/LHor(1)
161           + kVer(I-1,1)*(TSolid(I-1,1)-TSolid(I,1))*AVer(1)/LVer(I-1)
162           + kVer(I,1)*(TSolid(I+1,1)-TSolid(I,1))*AVer(1)/LVer(I);
163 END # for I
164 # right reflector J = 8, (2,8) - (11,8)
165 FOR I:= 2 TO NGVer-1 DO
166     QCond(I,8):= kHor(I,7)*(TSolid(I,7)-TSolid(I,8))*AHor(I,7)/LHor(7)
167           + kVer(I-1,8)*(TSolid(I-1,8)-TSolid(I,8))*AVer(8)/LVer(I-1)
168           + kVer(I,8)*(TSolid(I+1,8)-TSolid(I,8))*AVer(8)/LVer(I);
169 END
170 # lower reflector
171 # QFissionRing: Heat by fission
172 # the nodes with a real effect
173 FOR I:= 2 TO NGVer-1 DO
174     FOR J:= 2 TO 6 DO
175         QFissionRing(I,J) := QSlice(I-1)*RPF(J);
176     END # for J
177 END # for I
178 # nodes without effect
179 QFissionRing(1,1:8) := 0; # top reflector (1,1) - (1,8)
180 QFissionRing(2:11,1) := 0; # inner graphite pebble (2,1) - (11,1)
181 QFissionRing(2:11,7:8) := 0; # side reflectors (2,7) - (11,8)
182 QFissionRing(12,1:8) := 0; # bottom reflector (12,1) - (12,8)
183 # WCore
184 WCore:= WPrim*WF; # this is a vector
185 # Calculation of the intermediate parameters for Convection calculation, L791
186 FOR I:= 1 TO NGVer-2 DO
187     FOR J:= 1 TO NGHOr-2 DO
188         EXPP(I,J) := HTCoeffR*AVer(J)*74.048*LNode(I+1)/(WCore(J)*Cp);
189     END # for J
190 END # for I
191 # QC: Q by convection with gas
192 FOR I:=2 TO NGVer-1 DO # excluding top and bottom reflector
193     FOR J:=1 TO NGHOr-2 DO # excluding 2 side reflectors
194         QC(I,J):= (TGas(I,J)-TGas(I-1,J))*WCore(J)*Cp;
195     END # for J
196 END # for I
197 QC(1,1:8) := 0; # top reflector (1,1) - (1,8)
198 QC(2:11,7:8) := 0; # side reflectors (2,7) - (11,8)
199 QC(12,1:8) := 0; # bottom reflector (12,1) - (12,8)
200 # Calculate HeatCapacity
201 FOR J:= 1 TO NGHOr DO
202     HeatCap(1,J) := DenGraphite*LNode(1)*AVer(J)*CPrflTop(1,J).Cp; # top refl
203     HeatCap(12,J) := DenGraphite*LNode(12)*AVer(J)*CPrflDown(1,J).Cp; # lower refl
204 END # for J
205 FOR I:= 2 TO NGVer-1 DO
206     HeatCap(I,7) := DenGraphite*LNode(I)*AVer(7)*CPrflSide(I-1,1).Cp; # side refl
207     HeatCap(I,8) := DenGraphite*LNode(I)*AVer(8)*CPrflSide(I-1,2).Cp; # side refl
208     FOR J:= 1 TO NGHOr-2 DO

```

```

209      HeatCap(I,J):= LNode(I)*Aver(J)*CPFuel(I-1,J).Cp; # fuel
210      END # for J
211      END # for I
212      # Calculate Average Fuel Temperature per Slice
213      FOR I:= 2 TO 11 DO
214          T_FuelAvgSlice(I-1):= sigma(AVer(2:NGHor-2)*TSolid(I,2:NGHor-2))/sigma(AVer(2:NGHor-2));
215      END # for I
216      EQUATION
217      T_FuelAvg = sigma(T_FuelAvgSlice)/(NGVer-2);
218      # Temperature of Core and reflectors
219      $TSolid*HeatCap = QCond + QFissionRing - QC; # array equation
220      TGas(1,1:NGHor-2) = TCoreIn;
221      FOR I:= 2 TO NGVer-1 DO
222          FOR J:= 1 TO NGHor -2 DO
223              # Calculate temperature of gas due to convection
224              TGas(I,J)= TGas(I-1,J)+(TSolid(I,J)-TGas(I-1,J))*(1-EXP(-EXPP(I-1,J)));
225          END # for J
226      END # for I
227      # output
228      TCoreOut = sigma(TGas(NGVer-1,)*WF(1:NGHor-2)); ### check multiplication is right
229      PCoreOut = (1-PDropRCore)*PCoreIn;
230      PDropRCore*WPrim0^2 = PDropRCore0*WPrim^2;
231      # Assign the variables for the gas heat transfer coeff calculations
232      FOR I:= 2 TO NGVer-1 DO
233          FOR J:= 1 TO NGHor -2 DO
234              HTCore(I-1,J).Temp=TSolid(I,J);
235              HTCore(I-1,J).W=WCore(J);
236          END # for J
237      END # for I
238      # assign temperature for the CP units
239      # top and lower reflectors
240      CPReflTop(1,1:NGHor).Temp = TSolid(1,1:NGHor);
241      CPReflDown(1,1:NGHor).Temp = TSolid(12,1:NGHor);
242      # side reflectors
243      CPReflSide(1:NGVer-2,1:2).Temp = TSolid(2:NGVer-1,7:8);
244      # cp fuel
245      CPFuel(1:NGVer-2,1:NGHor-2).Temp = TSolid(2:NGVer-1,1:NGHor-2);
246      END # Model
247      #####
248
249
250      #####
251      MODEL ReactivityTempSimple
252      #####
253      PARAMETER
254          alpha AS REAL
255          T_FuelAvg0 AS REAL
256      UNIT
257      VARIABLE
258          T_FuelAvg AS Temperature
259          pho_temp AS Reactivity
260      SET
261          alpha:= -3.5e-5;
262          T_FuelAvg0 := 725.925 + 273.16;
263      INTERMEDIATE
264      EQUATION
265          pho_temp = alpha*(T_FuelAvg - T_FuelAvg0);
266          # the original equation is
267          # pho_temp = -3.5e-5*(TFuelAvg-T_FuelAvg0), with T_FuelAvg = 725.925
268      END
269      #####
270
271
272      #####
273      MODEL ReactivityPoison
274      #####
275      PARAMETER
276          # SET
277          gamma_I AS REAL
278          lambda_I AS REAL
279          gamma_Xe AS REAL
280          lambda_Xe AS REAL
281          sigma_total AS REAL
282          sigma_absorb AS REAL
283          sigma_Xe AS REAL
284          # EXTERNAL
285          phi0 AS REAL
286      UNIT
287      VARIABLE
288          # CALCULATED
289          phi AS PhiConcentration
290          IConc AS IConcentration # fix this
291          Xe AS XeConcentration# fix this
292          pho_poison AS Reactivity
293          # EXTERNAL
294          Q AS Power ### fix this
295      SET
296          gamma_I:=0.06386; # Wang Thesis p. 102
297          lambda_I:=2.87e-5;
298          gamma_Xe:=0.00288;
299          lambda_Xe:=2.09e-5;
300          sigma_total:=0.133; # total fission cross section, macroscopic fission section

```

```

301     sigma_Absorb:=0.1487; # total absorbtion cross section
302     sigma_Xe:=3e-22; #micro Xe absorbtion cross section
303 INTERMEDIATE
304 EQUATION
305     0= 1e-13*(phi-Q/(250e6)*phi0); # neutron flux
306     $IConc = gamma_I*sigma_total*phi-lambda_I*IConc;
307     $Xe = gamma_xe*sigma_total*phi+lambda_I*IConc - (lambda_Xe + sigma_Xe*phi)*Xe;
308     pho_poison=-sigma_xe*Xe/sigma_Absorb;
309 END
310 #####
311
312
313 #####
314 MODEL Kinetics
315 #####
316 PARAMETER
317     #EXTERNAL
318     # SET here
319     beta AS REAL # total effective delayed-neutron fraction
320     Lambda AS REAL # decay constant
321     TimeLen AS REAL # prompt-neutron lifetime
322 UNIT
323 VARIABLE
324     #EXTERNAL
325     Pho AS Reactivity
326     # CALCULATED
327     QFission_K AS RealVar # fission power # this Q = QFull/1e8
328     C AS ConcPrecursors # concentration of delayed precursors
329 SET
330     Beta:=5*1e-3; #0.001
331     Lambda:=0.0584e0;
332     TimeLen:=4.0*1e-4; # 0.0001
333 INTERMEDIATE
334 EQUATION
335     $QFission_K = (Pho-beta)*QFission_K/timeLen+Lambda*C;
336     $C = beta*QFission_K/timeLen -Lambda*C;
337 END
338 #####

```

MODELS_HEATEXCHANGERS.JAC

```

1 #####
2 MODEL HX2
3 #####
4 PARAMETER
5     # SET here
6     Pi AS REAL
7     CpHX AS REAL # J/(Kg*K)
8     rhoHX AS REAL
9     k AS REAL # W/(m*K)
10    dch AS REAL # diameter gas channels in heat exchanger
11    pc AS REAL # horizontal distance between gas channels
12
13    # EXTERNALLY set
14    Length AS REAL # actual length of HX 'm'
15    NGHX AS INTEGER
16
17    # CALCULATED
18    tp AS REAL # vertical distance between gas channels
19    delta_x AS REAL
20    ASection AS REAL # vertical section of the control V of metal in the PCHE
21    AEnvelope AS REAL # horizontal area of the channels in the PCHE
22    VMetal AS REAL # Volume of the section of metal in the PCHE containing 1 hot and 1 cold channel
23
24 VARIABLE
25    TGasHot AS ARRAY(NGHX) OF Temperature
26    TGasCold AS ARRAY(NGHX) OF Temperature
27    UHot AS HTCoeff # overall heat transfer coefficient in the hot side
28    UCold AS HTCoeff # overall heat transfer coefficient in the cold side
29    #Differential
30    THX AS ARRAY(NGHX) OF Temperature
31 SET
32 # SET
33 Pi := 4*ATAN(1);    CpHX:=500;    rhoHX:=8.03e3;
34 k:=22.0;    dch:=1.5e-3;    pc:=2.25e-3;
35
36 #CALCULATED
37 tp:= dch * 0.78;
38 delta_x:= Length/NGHX;
39 ASection:= 2*tp*pc - 2*(dch/2)^2*Pi; # A of metal surrounding 2 channels, 1 hot and 1 cold
40 AEnvelope:= (Pi*dch/2+dch)*delta_x; # Contact Area of 1 channel in Control Volume
41 VMetal:= ASection*delta_x;
42 EQUATION

```

```

43 # zero heat flux out of HX
44 VMetal*CpHX*rhoHX*$THX(1)=k*(THX(2)-1*THX(1))/delta_x*ASection
45 +UHot*(TGasHot(1)-THX(1))*AEnvelope
46 +UCold*(TGasCold(1)-THX(1))*AEnvelope;
47 FOR I:=2 TO NGHX-1 DO
48 VMetal*CpHX*rhoHX*$THX(I)=k*(THX(I+1)-2*THX(I)+THX(I-1))/delta_x*ASection
49 +UHot*(TGasHot(I)-THX(I))*AEnvelope
50 +UCold*(TGasCold(I)-THX(I))*AEnvelope;
51 END # for
52 # zero heat flux out of HX
53 VMetal*CpHX*rhoHX*$THX(NGHX)=k*(-1*THX(NGHX)+THX(NGHX-1))/delta_x*ASection
54 +UHot*(TGasHot(NGHX)-THX(NGHX))*AEnvelope
55 +UCold*(TGasCold(NGHX)-THX(NGHX))*AEnvelope;
56 END # model HeatExchanger
57 #####
58
59
60 #####
61 MODEL PHX
62 #####
63 PARAMETER
64 # SET here
65 Pi AS REAL
66 CpHX AS REAL # J/(Kg*K)
67 rhoHX AS REAL
68 k AS REAL # W/(m*K)
69 dinner AS REAL # inner diameter of tubes 'm'
70 douter AS REAL # outer diameter of tubes 's'
71
72 # EXTERNALLY set
73 Length AS REAL # actual length of HX 'm'
74 NGHX AS INTEGER
75
76 # CALCULATED
77 delta_x AS REAL
78 ASection AS REAL # vertical section of the control V of metal in the PHX
79 AEnvelopeInner AS REAL # internal horizontal area of the pipe
80 AEnvelopeOuter AS REAL # external horizontal area of the pipe
81 VMetal AS REAL # Volume of the section of metal in a triangular unit, it corresponds to half a pipe
82
83 VARIABLE
84 TGasHot AS ARRAY(NGHX) OF Temperature
85 TGasCold AS ARRAY(NGHX) OF Temperature
86 UHot AS HTCoeff # overall heat transfer coefficient in the hot side
87 UCold AS HTCoeff # overall heat transfer coefficient in the cold side
88 #Differential
89 THX AS ARRAY(NGHX) OF Temperature
90 SET
91 # SET
92 Pi := 4*ATAN(1); CpHX:=500; rhoHX:=8.03e3;
93 k:=22; dinner:= 0.01; douter:= 0.013;
94
95 #CALCULATED
96 delta_x:= Length/NGHX;
97 ASection:= Pi*((douter/2)^2-(dinner/2)^2)/2; # it is divided by 2 because the unit of calculation only
98 involves half a pipe
99 AEnvelopeInner:=Pi*dinner/2*delta_x ;
100 AEnvelopeOuter:= Pi*douter/2*delta_x;
101 VMetal:= ASection*delta_x;
102 EQUATION
103 # zero heat flux out of HX
104 VMetal*CpHX*rhoHX*$THX(1)=k*(THX(2)-1*THX(1))/delta_x*ASection
105 +UHot*(TGasHot(1)-THX(1))*AEnvelopeOuter
106 +UCold*(TGasCold(1)-THX(1))*AEnvelopeInner;
107 FOR I:=2 TO NGHX-1 DO
108 VMetal*CpHX*rhoHX*$THX(I)=k*(THX(I+1)-2*THX(I)+THX(I-1))/delta_x*ASection
109 +UHot*(TGasHot(I)-THX(I))*AEnvelopeOuter
110 +UCold*(TGasCold(I)-THX(I))*AEnvelopeInner;
111 END # for
112 # zero heat flux out of HX
113 VMetal*CpHX*rhoHX*$THX(NGHX)=k*(-1*THX(NGHX)+THX(NGHX-1))/delta_x*ASection
114 +UHot*(TGasHot(NGHX)-THX(NGHX))*AEnvelopeOuter
115 +UCold*(TGasCold(NGHX)-THX(NGHX))*AEnvelopeInner;
116 END # model HeatExchanger
117 #####

```

MODELS_HEATTRANSFERLOOP.JAC

```

1 #####
2 MODEL HeatTransferLoopFullDynPipesFullDyn
3 #####
4 PARAMETER
5 Tw AS REAL

```



```

6      Pi AS REAL
7      InitT AS REAL
8  UNIT
9      HX AS HX2
10     Loop1 AS LoopFullDyn
11     PipeH AS PipeFullDyn
12     HX2 AS PHX
13     PipeC2 AS PipeInnerFullDyn
14  SET
15     # SET here
16     # Plant parameters
17     Pi := 4*ATAN(1);
18     Tw:= 291.15; # setting Loop.Tw and Plant.Tw 2 x
19     PipeH.HT.kHe:= 0.36983;
20     PipeH.muVisc:=4.445E-05;
21     Loop1.muVisc(1):=3.963E-05; #from excel
22     Loop1.muVisc(2):=4.319E-05; # avg from relap
23     Loop1.muVisc(3):=5.094E-05; #from excel
24     Loop1.muVisc(4):=4.291E-05; # avg from relap
25     #CALCULATED
26     Loop1.Tw:=Tw;
27     # HX parameters
28     HX.NGHX := Loop1.SectionSpan(2); # this was set in the simulation before
29     HX.Length := Loop1.SectionL(2);
30     # PipeH
31     PipeH.NG := HX.NGHX;
32     PipeH.SectionL:= HX.Length;
33     PipeH.Temp:= Tw;
34     # HX2
35     HX2.NGHX:= Loop1.SectionSpan(4);
36     HX2.Length:= Loop1.SectionL(4);
37     # PipeC, PHX
38     PipeC2.NG:= HX.NGHX;      PipeC2.SectionL:=HX2.Length;
39     PipeC2.Temp:=InitT;
40     PipeC2.muVisc:=4.135E-05;
41  EQUATION
42     #Loop1
43     FOR I:=1 TO Loop1.SectionEnd(1) DO # 1-SectionEnd(1)
44         Loop1.TExtrnl(I)=Loop1.Tw;
45     END # for
46     FOR I:=1 TO HX.NGHX DO # SectionEnd(1)+1 - SectionEnd(2)
47         HX.TGasCold(I)=Loop1.T(I+ Loop1.SectionEnd(1));
48         HX.THX(I)=Loop1.TExtrnl(I+Loop1.SectionEnd(1));
49     END # for
50     FOR I:=Loop1.SectionEnd(2) + 1 TO Loop1.SectionEnd(3) DO # SectionEnd(2)+1 - SectionEnd(3)
51         Loop1.TExtrnl(I)=Loop1.Tw;
52     END # for
53     # this section corresponds to the PHX and it is reset in the simulation file # SectionEnd(3)+1 - SectionEnd
54     (4)
55     FOR I:=1 TO HX2.NGHX DO # SectionEnd(3) + 1 - SectionEnd(4)
56         HX2.TGasHot(I) = Loop1.T(Loop1.SectionEnd(3) + I);
57         HX2.THX(I) = Loop1.TExtrnl(I + Loop1.SectionEnd(3));
58     END # for
59     #HX
60     FOR I:= 1 TO HX.NGHX DO
61         HX.TGasHot(I) = PipeH.T(PipeH.NG + 1 - I);
62     END #for
63     HX.UHot = PipeH.HT.U;
64     HX.UCold = Loop1.HT2.U;
65     #HX2
66     FOR I:=1 TO HX2.NGHX DO
67         HX2.TGasCold(I) = PipeC2.T(PipeC2.NG + 1 -I);
68     END # for
69     HX2.UHot = Loop1.HT4.U; #20070311
70     HX2.UCold = PipeC2.HT.U;
71     #PipeH
72     FOR I:=1 TO PipeH.NG DO
73         PipeH.TExtrnl(PipeH.NG+1-I) = HX.THX(I); #PipeH.Temp; #
74     END # for
75     #PipeC PHX
76     FOR I:= 1 TO PipeC2.NG DO
77         PipeC2.TExtrnl(PipeC2.NG+1-I)=HX2.THX(I);
78     END
79  END # Model
80  *****
81
82  *****
83  MODEL HeatTransferLoop0MachPipesFullDyn
84  *****
85  PARAMETER
86     Tw AS REAL
87     Pi AS REAL
88     InitT AS REAL
89  UNIT
90     HX AS HX2
91     Loop1 AS Loop0Mach
92     PipeH AS PipeFullDyn
93     HX2 AS PHX
94     PipeC2 AS PipeInnerFullDyn
95  SET
96     # SET here

```

```

97 # Plant parameters
98 Pi := 4*ATAN(1);
99 Tw:= 291.15; # setting Loop.Tw and Plant.Tw 2 x
100 PipeH.HT.kHe:= 0.36983;
101 PipeH.muVisc:=4.445E-05;
102 Loop1.muVisc(1):=3.963E-05; #from excel
103 Loop1.muVisc(2):=4.319E-05; # avg from relap
104 Loop1.muVisc(3):=5.094E-05; #from excel
105 Loop1.muVisc(4):=4.291E-05; # avg from relap
106 #CALCULATED
107 Loop1.Tw:=Tw;
108 # HX parameters
109 HX.NGHX := Loop1.SectionSpan(2); # this was set in the simulation before
110 HX.Length := Loop1.SectionL(2);
111 # PipeH
112 PipeH.NG := HX.NGHX;
113 PipeH.SectionL:= HX.Length;
114 PipeH.Temp:= Tw;
115 # HX2
116 HX2.NGHX:= Loop1.SectionSpan(4);
117 HX2.Length:= Loop1.SectionL(4);
118 # PipeC, PHX
119 PipeC2.NG:= HX.NGHX; PipeC2.SectionL:=HX2.Length;
120 PipeC2.Temp:=InitT;
121 PipeC2.muVisc:=4.135E-05;
122 EQUATION
123 #Loop1
124 FOR I:=1 TO Loop1.SectionEnd(1) DO # 1-SectionEnd(1)
125   Loop1.TExtrnl(I)=Loop1.Tw;
126 END # for
127 FOR I:=1 TO HX.NGHX DO # SectionEnd(1)+1 - SectionEnd(2)
128   HX.TGasCold(I)=Loop1.T(I+ Loop1.SectionEnd(1));
129   HX.THX(I)=Loop1.TExtrnl(I+Loop1.SectionEnd(1));
130 END # for
131 FOR I:=Loop1.SectionEnd(2) + 1 TO Loop1.SectionEnd(3) DO # SectionEnd(2)+1 - SectionEnd(3)
132   Loop1.TExtrnl(I)=Loop1.Tw;
133 END # for
134 # this section corresponds to the PHX and it is reset in the simulation file # SectionEnd(3)+1 - SectionEnd
135 (4)
136 FOR I:=1 TO HX2.NGHX DO # SectionEnd(3) + 1 - SectionEnd(4)
137   HX2.TGasHot(I) = Loop1.T(Loop1.SectionEnd(3) + I);
138   HX2.THX(I) = Loop1.TExtrnl(I + Loop1.SectionEnd(3));
139 END # for
140 #HX
141 FOR I:= 1 TO HX.NGHX DO
142   HX.TGasHot(I) = PipeH.T(PipeH.NG + 1 - I);
143 END #for
144 HX.UHot = PipeH.HT.U;
145 HX.UCold = Loop1.HT2.U;
146 #HX2
147 FOR I:=1 TO HX2.NGHX DO
148   HX2.TGasCold(I) = PipeC2.T(PipeC2.NG + 1 -I);
149 END # for
150 HX2.UHot = Loop1.HT4.U; #20070311
151 HX2.UCold = PipeC2.HT.U;
152 #PipeH
153 FOR I:=1 TO PipeH.NG DO
154   PipeH.TExtrnl(PipeH.NG+1-I) = HX.THX(I); #PipeH.Temp; #
155 END # for
156 #PipeC PHX
157 FOR I:= 1 TO PipeC2.NG DO
158   PipeC2.TExtrnl(PipeC2.NG+1-I)=HX2.THX(I);
159 END
160 END # Model
161 *****
162 *****
163 *****
164 MODEL HeatTransferLoopQSSPipesFullDyn
165 *****
166 PARAMETER
167   Tw AS REAL
168   Pi AS REAL
169   InitT AS REAL
170 UNIT
171   HX AS HX2
172   Loop1 AS LoopQSS
173   PipeH AS PipeFullDyn
174   HX2 AS PHX
175   PipeC2 AS PipeInnerFullDyn
176 SET
177 # SET here
178 # Plant parameters
179 Pi := 4*ATAN(1);
180 Tw:= 291.15; # setting Loop.Tw and Plant.Tw 2 x
181 PipeH.HT.kHe:= 0.36983;
182 PipeH.muVisc:=4.445E-05;
183 Loop1.muVisc(1):=3.963E-05; #from excel
184 Loop1.muVisc(2):=4.319E-05; # avg from relap
185 Loop1.muVisc(3):=5.094E-05; #from excel
186 Loop1.muVisc(4):=4.291E-05; # avg from relap
187 #CALCULATED

```

```

188     Loop1.Tw:=Tw;
189     # HX parameters
190     HX.NGHX := Loop1.SectionSpan(2); # this was set in the simulation before
191     HX.Length := Loop1.SectionL(2);
192     # PipeH
193     PipeH.NG := HX.NGHX;
194     PipeH.SectionL:= HX.Length;
195     PipeH.Temp:= Tw;
196     # HX2
197     HX2.NGHX:= Loop1.SectionSpan(4);
198     HX2.Length:= Loop1.SectionL(4);
199     # PipeC, PHX
200     PipeC2.NG:= HX.NGHX;      PipeC2.SectionL:=HX2.Length;
201     PipeC2.Temp:=InitT;
202     PipeC2.muVisc:=4.135E-05;
203 EQUATION
204 #Loop1
205 FOR I:=1 TO Loop1.SectionEnd(1) DO # 1-SectionEnd(1)
206     Loop1.TExtrnl(I)=Loop1.Tw;
207 END # for
208 FOR I:=1 TO HX.NGHX DO # SectionEnd(1)+1 - SectionEnd(2)
209     HX.TGasCold(I)=Loop1.T(I+ Loop1.SectionEnd(1));
210     HX.THX(I)=Loop1.TExtrnl(I+Loop1.SectionEnd(1));
211 END # for
212 FOR I:=Loop1.SectionEnd(2) + 1 TO Loop1.SectionEnd(3) DO # SectionEnd(2)+1 - SectionEnd(3)
213     Loop1.TExtrnl(I)=Loop1.Tw;
214 END # for
215 # this section corresponds to the PHX and it is reset in the simulation file # SectionEnd(3)+1 - SectionEnd
    (4)
216 FOR I:=1 TO HX2.NGHX DO # SectionEnd(3) + 1 - SectionEnd(4)
217     HX2.TGasHot(I) = Loop1.T(Loop1.SectionEnd(3) + I);
218     HX2.THX(I) = Loop1.TExtrnl(I + Loop1.SectionEnd(3));
219 END # for
220 #HX
221 FOR I:= 1 TO HX.NGHX DO
222     HX.TGasHot(I) = PipeH.T(PipeH.NG + 1 - I);
223 END #for
224 HX.UHot = PipeH.HT.U;
225 HX.UCold = Loop1.HT2.U;
226 #HX2
227 FOR I:=1 TO HX2.NGHX DO
228     HX2.TGasCold(I) = PipeC2.T(PipeC2.NG + 1 -I);
229 END # for
230 HX2.UHot = Loop1.HT4.U; #20070311
231 HX2.UCold = PipeC2.HT.U;
232 #PipeH
233 FOR I:=1 TO PipeH.NG DO
234     PipeH.TExtrnl(PipeH.NG+1-I) = HX.THX(I); #PipeH.Temp; #
235 END # for
236 #PipeC PHX
237 FOR I:= 1 TO PipeC2.NG DO
238     PipeC2.TExtrnl(PipeC2.NG+1-I)=HX2.THX(I);
239 END
240 END # Model
241 #####
242
243
244 #####
245 MODEL HeatTransferLoopQSSPipesQSS
246 #####
247 PARAMETER
248     Tw AS REAL
249     Pi AS REAL
250     InitT AS REAL
251 UNIT
252     HX AS HX2
253     Loop1 AS LoopQSS
254     PipeH AS PipeQSS
255     HX2 AS PHX
256     PipeC2 AS PipeInnerQSS
257 SET
258 # SET here
259 # Plant parameters
260     Pi := 4*ATAN(1);
261     Tw:= 291.15; # setting Loop.Tw and Plant.Tw 2 x
262     PipeH.HT.kHe:= 0.36983;
263     PipeH.muVisc:=4.445E-05;
264     Loop1.muVisc(1):=3.963E-05; #from excel
265     Loop1.muVisc(2):=4.319E-05; # avg from relap
266     Loop1.muVisc(3):=5.094E-05; #from excel
267     Loop1.muVisc(4):=4.291E-05; # avg from relap
268 #CALCULATED
269     Loop1.Tw:=Tw;
270 # HX parameters
271     HX.NGHX := Loop1.SectionSpan(2); # this was set in the simulation before
272     HX.Length := Loop1.SectionL(2);
273     # PipeH
274     PipeH.NG := HX.NGHX;
275     PipeH.SectionL:= HX.Length;
276     PipeH.Temp:= Tw;
277     # HX2
278     HX2.NGHX:= Loop1.SectionSpan(4);

```

```

279 HX2.Length:= Loop1.SectionL(4);
280 # PipeC, PHX
281 PipeC2.NG:= HX.NGHX; PipeC2.SectionL:=HX2.Length;
282 PipeC2.Temp:=InitT;
283 PipeC2.muVisc:=4.135E-05;
284 EQUATION
285 #Loop1
286 FOR I:=1 TO Loop1.SectionEnd(1) DO # 1-SectionEnd(1)
287 Loop1.TExtrnl(I)=Loop1.Tw;
288 END # for
289 FOR I:=1 TO HX.NGHX DO # SectionEnd(1)+1 - SectionEnd(2)
290 HX.TGasCold(I)=Loop1.T(I+ Loop1.SectionEnd(1));
291 HX.THX(I)=Loop1.TExtrnl(I+Loop1.SectionEnd(1));
292 END # for
293 FOR I:=Loop1.SectionEnd(2) + 1 TO Loop1.SectionEnd(3) DO # SectionEnd(2)+1 - SectionEnd(3)
294 Loop1.TExtrnl(I)=Loop1.Tw;
295 END # for
296 # this section corresponds to the PHX and it is reset in the simulation file # SectionEnd(3)+1 - SectionEnd(4)
297 FOR I:=1 TO HX2.NGHX DO # SectionEnd(3) + 1 - SectionEnd(4)
298 HX2.TGasHot(I) = Loop1.T(Loop1.SectionEnd(3) + I);
299 HX2.THX(I) = Loop1.TExtrnl(I + Loop1.SectionEnd(3));
300 END # for
301 #HX
302 FOR I:= 1 TO HX.NGHX DO
303 HX.TGasHot(I) = PipeH.T(PipeH.NG + 1 - I);
304 END #for
305 HX.UHot = PipeH.HT.U;
306 HX.UCold = Loop1.HT2.U;
307 #HX2
308 FOR I:=1 TO HX2.NGHX DO
309 HX2.TGasCold(I) = PipeC2.T(PipeC2.NG + 1 -I);
310 END # for
311 HX2.UHot = Loop1.HT4.U; #20070311
312 HX2.UCold = PipeC2.HT.U;
313 #PipeH
314 FOR I:=1 TO PipeH.NG DO
315 PipeH.TExtrnl(PipeH.NG+1-I) = HX.THX(I); #PipeH.Temp; #
316 END # for
317 #PipeC PHX
318 FOR I:= 1 TO PipeC2.NG DO
319 PipeC2.TExtrnl(PipeC2.NG+1-I)=HX2.THX(I);
320 END
321 END # Model
322 #####
323
324 #####
325 #####
326 MODEL HeatTransferLoopFullDynNoPipeH
327 #####
328 PARAMETER
329 Tw AS REAL
330 Pi AS REAL
331 InitT AS REAL
332 UNIT
333 HX AS HX2
334 Loop1 AS LoopFullDyn
335 HX2 AS PHX
336 PipeC2 AS PipeInnerFullDyn
337 SET
338 # SET here
339 # Plant parameters
340 Pi := 4*ATAN(1);
341 Tw:= 291.15; # setting Loop.Tw and Plant.Tw 2 x
342 Loop1.muVisc(1):=3.963E-05; #from excel
343 Loop1.muVisc(2):=4.319E-05; # avg from relap
344 Loop1.muVisc(3):=5.094E-05; #from excel
345 Loop1.muVisc(4):=4.291E-05; # avg from relap
346 #CALCULATED
347 Loop1.Tw:=Tw;
348 # HX parameters
349 HX.NGHX := Loop1.SectionSpan(2); # this was set in the simulation before
350 HX.Length := Loop1.SectionL(2);
351 # HX2
352 HX2.NGHX:= Loop1.SectionSpan(4);
353 HX2.Length:= Loop1.SectionL(4);
354 # PipeC, PHX
355 PipeC2.NG:= HX.NGHX; PipeC2.SectionL:=HX2.Length;
356 PipeC2.Temp:=InitT;
357 PipeC2.muVisc:=4.135E-05;
358 EQUATION
359 #Loop1
360 FOR I:=1 TO Loop1.SectionEnd(1) DO # 1-SectionEnd(1)
361 Loop1.TExtrnl(I)=Loop1.Tw;
362 END # for
363 FOR I:=1 TO HX.NGHX DO # SectionEnd(1)+1 - SectionEnd(2)
364 HX.TGasCold(I)=Loop1.T(I+ Loop1.SectionEnd(1));
365 HX.THX(I)=Loop1.TExtrnl(I+Loop1.SectionEnd(1));
366 END # for
367 FOR I:=Loop1.SectionEnd(2) + 1 TO Loop1.SectionEnd(3) DO # SectionEnd(2)+1 - SectionEnd(3)
368 Loop1.TExtrnl(I)=Loop1.Tw;
369 END # for

```

```

370 # this section corresponds to the PHX and it is reset in the simulation file # SectionEnd(3)+1 - SectionEnd
      (4)
371 FOR I:=1 TO HX2.NGHX DO # SectionEnd(3) + 1 - SectionEnd(4)
372   HX2.TGasHot(I) = Loop1.T(Loop1.SectionEnd(3) + I);
373   HX2.THX(I) = Loop1.TExtrnl(I + Loop1.SectionEnd(3));
374 END # for
375 #HX
376 HX.UCold = Loop1.HT2.U;
377 #HX2
378 FOR I:=1 TO HX2.NGHX DO
379   HX2.TGasCold(I) = PipeC2.T(PipeC2.NG + 1 -I);
380 END # for
381 HX2.UHot = Loop1.HT4.U; #20070311
382 HX2.UCold = PipeC2.HT.U;
383 #PipeC PHX
384 FOR I:= 1 TO PipeC2.NG DO
385   PipeC2.TExtrnl(PipeC2.NG+1-I)=HX2.THX(I);
386 END
387 END # Model
388 #####
389
390
391 #####
392 MODEL HeatTransferLoop0MachNoPipeH
393 #####
394 PARAMETER
395   Tw AS REAL
396   Pi AS REAL
397   InitT AS REAL
398 UNIT
399   HX AS HX2
400   Loop1 AS Loop0Mach
401   HX2 AS PHX
402   PipeC2 AS PipeInner0Mach
403 SET
404 # SET here
405 # Plant parameters
406 Pi := 4*ATAN(1);
407 Tw:= 291.15; # setting Loop.Tw and Plant.Tw 2 x
408 Loop1.muVisc(1):=3.963E-05; #from excel
409 Loop1.muVisc(2):=4.319E-05; # avg from relap
410 Loop1.muVisc(3):=5.094E-05; #from excel
411 Loop1.muVisc(4):=4.291E-05; # avg from relap
412 #CALCULATED
413 Loop1.Tw:=Tw;
414 # HX parameters
415 HX.NGHX := Loop1.SectionSpan(2); # this was set in the simulation before
416 HX.Length := Loop1.SectionL(2);
417 # HX2
418 HX2.NGHX:= Loop1.SectionSpan(4);
419 HX2.Length:= Loop1.SectionL(4);
420 # PipeC, PHX
421 PipeC2.NG:= HX.NGHX; PipeC2.SectionL:=HX2.Length;
422 PipeC2.Temp:=InitT;
423 PipeC2.muVisc:=4.135E-05;
424 EQUATION
425 #Loop1
426 FOR I:=1 TO Loop1.SectionEnd(1) DO # 1-SectionEnd(1)
427   Loop1.TExtrnl(I)=Loop1.Tw;
428 END # for
429 FOR I:=1 TO HX.NGHX DO # SectionEnd(1)+1 - SectionEnd(2)
430   HX.TGasCold(I)=Loop1.T(I+ Loop1.SectionEnd(1));
431   HX.THX(I)=Loop1.TExtrnl(I+Loop1.SectionEnd(1));
432 END # for
433 FOR I:=Loop1.SectionEnd(2) + 1 TO Loop1.SectionEnd(3) DO # SectionEnd(2)+1 - SectionEnd(3)
434   Loop1.TExtrnl(I)=Loop1.Tw;
435 END # for
436 # this section corresponds to the PHX and it is reset in the simulation file # SectionEnd(3)+1 - SectionEnd
      (4)
437 FOR I:=1 TO HX2.NGHX DO # SectionEnd(3) + 1 - SectionEnd(4)
438   HX2.TGasHot(I) = Loop1.T(Loop1.SectionEnd(3) + I);
439   HX2.THX(I) = Loop1.TExtrnl(I + Loop1.SectionEnd(3));
440 END # for
441 #HX
442 HX.UCold = Loop1.HT2.U;
443 #HX2
444 FOR I:=1 TO HX2.NGHX DO
445   HX2.TGasCold(I) = PipeC2.T(PipeC2.NG + 1 -I);
446 END # for
447 HX2.UHot = Loop1.HT4.U; #20070311
448 HX2.UCold = PipeC2.HT.U;
449 #PipeC PHX
450 FOR I:= 1 TO PipeC2.NG DO
451   PipeC2.TExtrnl(PipeC2.NG+1-I)=HX2.THX(I);
452 END
453 END # Model
454 #####
455
456
457 #####
458 MODEL HeatTransferLoopQSSNoPipeH
459 #####

```

```

460 PARAMETER
461 Tw AS REAL
462 Pi AS REAL
463 InitT AS REAL
464 UNIT
465 HX AS HX2
466 Loop1 AS LoopQSS
467 HX2 AS PHX
468 PipeC2 AS PipeInnerQSS
469 SET
470 # SET here
471 # Plant parameters
472 Pi := 4*ATAN(1);
473 Tw:= 291.15; # setting Loop.Tw and Plant.Tw 2 x
474 Loop1.muVisc(1):=3.963E-05; #from excel
475 Loop1.muVisc(2):=4.319E-05; # avg from relap
476 Loop1.muVisc(3):=5.094E-05; #from excel
477 Loop1.muVisc(4):=4.291E-05; # avg from relap
478 #CALCULATED
479 Loop1.Tw:=Tw;
480 # HX parameters
481 HX.NGHX := Loop1.SectionSpan(2); # this was set in the simulation before
482 HX.Length := Loop1.SectionL(2);
483 # HX2
484 HX2.NGHX:= Loop1.SectionSpan(4);
485 HX2.Length:= Loop1.SectionL(4);
486 # PipeC, PHX
487 PipeC2.NG:= HX.NGHX; PipeC2.SectionL:=HX2.Length;
488 PipeC2.Temp:=InitT;
489 PipeC2.muVisc:=4.135E-05;
490 EQUATION
491 #Loop1
492 FOR I:=1 TO Loop1.SectionEnd(1) DO # 1-SectionEnd(1)
493 Loop1.TExtrnl(I)=Loop1.Tw;
494 END # for
495 FOR I:=1 TO HX.NGHX DO # SectionEnd(1)+1 - SectionEnd(2)
496 HX.TGasCold(I)=Loop1.T(I+ Loop1.SectionEnd(1));
497 HX.THX(I)=Loop1.TExtrnl(I+Loop1.SectionEnd(1));
498 END # for
499 FOR I:=Loop1.SectionEnd(2) + 1 TO Loop1.SectionEnd(3) DO # SectionEnd(2)+1 - SectionEnd(3)
500 Loop1.TExtrnl(I)=Loop1.Tw;
501 END # for
502 # this section corresponds to the PHX and it is reset in the simulation file # SectionEnd(3)+1 - SectionEnd
(4)
503 FOR I:=1 TO HX2.NGHX DO # SectionEnd(3) + 1 - SectionEnd(4)
504 HX2.TGasHot(I) = Loop1.T(Loop1.SectionEnd(3) + I);
505 HX2.THX(I) = Loop1.TExtrnl(I + Loop1.SectionEnd(3));
506 END # for
507 #HX
508 HX.UCold = Loop1.HT2.U;
509 #HX2
510 FOR I:=1 TO HX2.NGHX DO
511 HX2.TGasCold(I) = PipeC2.T(PipeC2.NG + 1 -I);
512 END # for
513 HX2.UHot = Loop1.HT4.U; #20070311
514 HX2.UCold = PipeC2.HT.U;
515 #PipeC PHX
516 FOR I:= 1 TO PipeC2.NG DO
517 PipeC2.TExtrnl(PipeC2.NG+1-I)=HX2.THX(I);
518 END
519 END # Model
520 *****

```

MODELS_NUCLEARREACTORANDAUXS.JAC

```

1 *****
2 MODEL PipeRhoConst # oneboundary_tube2
3 *****
4 PARAMETER
5 #SET here
6 Pi AS REAL
7 R_c AS REAL #Rc constant "J/(mol*K)"
8 Mw AS REAL #Molecular weight "Kg/mol"
9 f AS REAL #Friction Coefficient
10 T_stand AS REAL #Standard Temp "K"
11 Cp AS REAL #specific heat at constant pressure "J/Kg/K"
12 h_form AS REAL #specific enthalpy of formation "J/Kg"
13 A AS REAL
14 r0 AS REAL #diameter of pipe "m"
15 SectionL AS REAL #length of pipe "m"
16
17 #EXTERNALLY set
18 NG AS INTEGER #number of control volumes in the grid

```

```

19     Temp AS REAL           #Temperature "K"
20     InitP AS REAL
21     rho AS ARRAY(NG) OF REAL # I am setting rho as an array of parameters to avoid big
22
23     #CALCULATED
24     InitRho AS REAL       InitH AS REAL
25     InitRho_e AS REAL    Delta_x AS REAL      #length of control volume "m"
26     Vol AS REAL
27     UNIT
28     HT AS HTCoeffGasMetalHX
29     VARIABLE
30     v AS ARRAY(NG) OF Velocity
31     P AS ARRAY(NG+1) OF Pressure
32     h AS ARRAY(NG) OF SpecificEnergy
33     T AS ARRAY(NG) OF Temperature
34     TExtrnl AS ARRAY(NG) OF Temperature
35     #DIFFERENTIAL
36     rho_e AS ARRAY(NG) OF Energy
37     SET
38     #SET
39     Pi:=4*ATAN(1);
40     R_c := 8.314;      Mw := 4.0E-3;
41     T_stand := 298;   Cp := 20.78;      h_form := 0;
42     r0 := 9.1652e-4/2 ; # Hyd radius based on PCHE INL report pi8 #14
43     A:=0.34749156;
44     #CALCULATED
45     Delta_x := SectionL/(NG-1);
46     InitRho := InitP*Mw/(R_c*Temp);
47     InitH := h_form + Cp/Mw*(Temp-T_stand);
48     InitRho_e := InitRho*InitH - InitP;
49     HT.r0:=r0;      HT.t:= (HT.r0*2*0.78*3 - HT.r0)/3; # according to INL, an average of 2*tmax +1*tmin
50     Vol := A*Delta_x;
51     INTERMEDIATE
52     U:= HT.U;
53     EQUATION
54     # Mass Balance
55     FOR I:= 2 TO NG DO
56       0 = 1e-7*(rho(I-1)*v(I-1)*A - rho(I)*v(I)*A);
57     END # for
58     # Momentum Balance
59     0 = -(P(2)-P(1))
60       - ((2*f/(2*r0))*rho(1)*v(1)^2)*(Delta_x);
61     FOR I:=2 TO NG-1 DO
62       0 = -(P(I+1)-P(I))
63         - ((2*f/(2*r0))*(rho(I)+rho(I+1))/2*v(I)^2)*Delta_x;
64     END # for
65     0 = -(P(NG+1)-P(NG))
66       - ((2*f/(2*r0))*rho(NG)*v(NG)^2)*(Delta_x);
67     # Energy Balance
68     FOR I:=(2) TO (NG) DO
69       1e-7*$rho_E(I)*Vol = 1e-7*(rho(I-1)*h(I-1)*v(I-1)*A - rho(I)*h(I)*v(I)*A
70         +4*U/(2*r0)*(TExtrnl(I)-T(I))*Vol);
71     END # for
72
73     # Algebraic Equations
74     FOR I:=1 TO NG DO
75       0 = 1e-7*(rho_e(I) - (rho(I)*h(I) - P(I)));
76     END # for
77
78     # 2- Thermodynamical Part
79     FOR I:= 1 TO NG DO
80       0 = 1e-7*(h(I) - (h_form + Cp/Mw*(T(I)-T_stand)));
81     END # for
82
83     #Equations to assign variables for heat transfer coefficients
84     HT.rhoPipeHe = sigma(rho(2:NG))/NG;
85     HT.vPipe = sigma(v(2:NG))/NG;
86     END
87     #####
88
89
90     #####
91     MODEL Comp
92     #####
93     PARAMETER
94     # EXTERNAL
95     Eff AS REAL # isentropic efficiency
96     # EffCir=0.9
97     Gamma AS REAL
98     # Gamma=1.6667;
99     Cp AS REAL
100    # Cp=5193.0d0
101    UNIT
102    VARIABLE
103    # CALCULATED
104    T2 AS Temperature # outlet temperature
105    P2 AS Pressure # outlet pressure
106    PWR AS Power # compressor power
107    # EXTERNAL
108    PR AS RealVar # pressure ratio # PRCir = 1.038794831;
109    P1 AS Pressure # pressure in
110    T1 AS Temperature # temperature in

```

```

111     W AS MassFlowRate # mass flowrate
112     SET
113     INTERMEDIATE
114     Rgas:=2077.22;
115     C1:=(Gamma-1)/Gamma;
116     C2:=PR^C1-1;
117     C3:=1+C2/Eff;
118     EQUATION
119     T2=(T1)*C3;
120     P2=P1*PR;
121     PWR=W*Cp*(T2-T1);
122     END
123     #####
124
125
126     #####
127     MODEL NReactor
128     #####
129     PARAMETER
130     # EXTERNAL
131     WPrim0 AS REAL
132     UNIT
133     THyd AS ThermalHyd3
134     Kinetics AS Kinetics
135     Poison AS ReactivityPoison
136     React AS ReactivityTempSimple
137     VARIABLE
138     TCoreIn AS Temperature # temperature of gas going in the core
139     PCoreIn AS Pressure
140     # CALCULATED
141     PhoTotal AS Reactivity #
142     PhoPoison AS Reactivity #
143     PhoTemp AS Reactivity #
144     PhoControl AS Reactivity
145     PhoExtra1 AS Reactivity
146     wPhoExtra1 AS Nondimensional
147     PhoExtra2 AS Reactivity
148     # INPUTS
149     SET
150     THyd.WPrim0 := WPrim0;
151     EQUATION
152     # Calculating units variables
153     THyd.QFission = Kinetics.QFission_K*1e+8; # L 1696
154     Poison.Q = THyd.QFission;
155     PhoPoison = 0;
156     React.T_FuelAvg = THyd.T_FuelAvg;
157     PhoTemp = React.pho_temp;
158     PhoTotal = PhoTemp + PhoControl + wPhoExtra1*PhoExtra1 + PhoExtra2; #PhoPoison + PhoTemp + PhoControl;
159     Kinetics.Pho = PhoTotal;
160     THyd.TCoreIn = TCoreIn;
161     THyd.PCoreIn = PCoreIn;
162     PhoTemp = -PhoExtra1;
163     END # model
164     #####

```

MODELS_NUCLEARREACTORLOOP.JAC

```

1     #####
2     MODEL PlantNR
3     #####
4     PARAMETER
5     NG AS INTEGER
6     L AS REAL
7     InitT AS REAL
8     InitDeltaP AS REAL
9     MaxDeltaP AS REAL
10
11     T_stand AS REAL
12     Cp AS REAL
13     Mw AS REAL
14     rhomix AS REAL
15     R_c AS REAL
16     Tpcu AS REAL
17     Ppcu AS REAL
18     h_form AS REAL
19     WpcupipeRatio AS REAL
20     UNIT
21     NR AS NReactor
22     PipeH AS PipeRhoConst
23     Comp AS Comp
24     VARIABLE
25     DeltaP AS Pressure
26     Tpipe AS Temperature

```



```

27      Tmix AS Temperature
28      Wpipe AS MassFlowRate
29      Wpcu AS MassFlowRate
30      Wmix AS MassFlowRate
31      hpcu AS SpecificEnergy
32      hpipe AS SpecificEnergy
33      hmix AS SpecificEnergy
34      Pmix AS Pressure
35      Ppipe AS Pressure
36  SET
37      # SET
38      NG:= 40;           L:= 0.98807;
39      PipeH.f := 3.546e-2/4;
40      PipeH.HT.kHe:= 0.36983;
41      Comp.Eff:= 0.9;
42      Comp.Gamma:=1.6667;
43      Comp.Cp:=5193.0e0;
44      NR.WPrim0 := 126.7;
45      NR.Poison.phi0 := 1e18;
46
47      #CALCULATED
48      PipeH.NG:= NG;
49      PipeH.SectionL:=L;
50      PipeH.Temp:= InitT;
51
52      T_stand:= 298;
53      Cp:= 20.78;
54      Mw:= 4.0e-3;
55      R_c := 8.314;
56      rhomix := 3.93;#4.7; # from page 186 in Wang's thesis; calculated using P and T at the outlet of the IHX.
57      Tpcu := 512.0 +273.15;
58      Ppcu := 7.00e6;
59      h_form:= 5557;
60  EQUATION
61      PipeH.T(1) = NR.THyd.TCoreOut;
62      PipeH.P(1) = NR.THyd.PCoreOut;
63      0 = 1e-7*(DeltaP - (Comp.P2 - Comp.P1));
64
65      Tpipe = PipeH.T(PipeH.NG);
66      Ppipe = PipeH.P(PipeH.NG +1);
67      Wpipe = PipeH.A*PipeH.v(PipeH.NG)*PipeH.rho(PipeH.NG);
68      Wpcu = Wpipe*WpcupipeRatio;
69      Wmix = Wpipe + Wpcu;
70      hpcu = h_form + Cp/Mw*(Tpcu - T_stand);
71      hpipe = h_form + Cp/Mw*(Tpipe - T_stand);
72      Wmix*hmix = Wpcu*hpcu + Wpipe*hpipe; # Wpcu*hpcu + Wpipe*hpipe;
73      Wmix*Pmix = Wpcu*Ppcu + Wpipe*Ppipe;
74      hmix = h_form + Cp/Mw*(Tmix - T_stand);
75
76      Comp.T1 = Tmix; #PipeH.T(PipeH.NG);
77      Comp.P1 = Ppipe*1/(WpcupipeRatio + 1) + Ppcu*WpcupipeRatio/(WpcupipeRatio + 1); #PipeH.P(PipeH.NG+1);
78      Comp.W = PipeH.A*PipeH.v(PipeH.NG)*PipeH.rho(PipeH.NG)*(WpcupipeRatio + 1);
79
80      NR.TCoreIn = Comp.T2;
81      NR.PCoreIn = Comp.P2;
82      NR.THyd.WPrim = Comp.W;
83  END # model
84  #####

```

HTLFDULLDYN_SS_INI.INITIAL

```

1  # Values for differential variables in computation HTLFDULLDYN_SS
2  # Saved at time 1000
3  PLANT.HX.TH(1) = 879.893 ; # 1
4  PLANT.HX.TH(2) = 892.184 ; # 2
5  PLANT.HX.TH(3) = 904.161 ; # 3
6  PLANT.HX.TH(4) = 915.766 ; # 4
7  PLANT.HX.TH(5) = 927.009 ; # 5
8  PLANT.HX.TH(6) = 937.904 ; # 6
9  PLANT.HX.TH(7) = 948.459 ; # 7
10 PLANT.HX.TH(8) = 958.687 ; # 8
11 PLANT.HX.TH(9) = 968.596 ; # 9
12 PLANT.HX.TH(10) = 978.197 ; # 10
13 PLANT.HX.TH(11) = 987.5 ; # 11
14 PLANT.HX.TH(12) = 996.513 ; # 12
15 PLANT.HX.TH(13) = 1005.25 ; # 13
16 PLANT.HX.TH(14) = 1013.71 ; # 14
17 PLANT.HX.TH(15) = 1021.91 ; # 15
18 PLANT.HX.TH(16) = 1029.85 ; # 16
19 PLANT.HX.TH(17) = 1037.55 ; # 17
20 PLANT.HX.TH(18) = 1045 ; # 18
21 PLANT.HX.TH(19) = 1052.23 ; # 19
22 PLANT.HX.TH(20) = 1059.23 ; # 20

```

23 PLANT.HX.THX(21) = 1066.01 ; # 21
24 PLANT.HX.THX(22) = 1072.58 ; # 22
25 PLANT.HX.THX(23) = 1078.95 ; # 23
26 PLANT.HX.THX(24) = 1085.12 ; # 24
27 PLANT.HX.THX(25) = 1091.1 ; # 25
28 PLANT.HX.THX(26) = 1096.89 ; # 26
29 PLANT.HX.THX(27) = 1102.5 ; # 27
30 PLANT.HX.THX(28) = 1107.94 ; # 28
31 PLANT.HX.THX(29) = 1113.21 ; # 29
32 PLANT.HX.THX(30) = 1118.31 ; # 30
33 PLANT.HX.THX(31) = 1123.26 ; # 31
34 PLANT.HX.THX(32) = 1128.05 ; # 32
35 PLANT.HX.THX(33) = 1132.69 ; # 33
36 PLANT.HX.THX(34) = 1137.19 ; # 34
37 PLANT.HX.THX(35) = 1141.55 ; # 35
38 PLANT.HX.THX(36) = 1145.77 ; # 36
39 PLANT.HX.THX(37) = 1149.86 ; # 37
40 PLANT.HX.THX(38) = 1153.83 ; # 38
41 PLANT.HX.THX(39) = 1157.67 ; # 39
42 PLANT.HX.THX(40) = 1161.37 ; # 40
43 PLANT.LOOP1.RHO(1) = 1.15317 ; # 41
44 PLANT.LOOP1.RHO(2) = 1.15067 ; # 42
45 PLANT.LOOP1.RHO(3) = 1.14817 ; # 43
46 PLANT.LOOP1.RHO(4) = 1.14565 ; # 44
47 PLANT.LOOP1.RHO(5) = 1.14313 ; # 45
48 PLANT.LOOP1.RHO(6) = 1.14059 ; # 46
49 PLANT.LOOP1.RHO(7) = 1.13804 ; # 47
50 PLANT.LOOP1.RHO(8) = 1.13549 ; # 48
51 PLANT.LOOP1.RHO(9) = 1.13292 ; # 49
52 PLANT.LOOP1.RHO(10) = 1.13034 ; # 50
53 PLANT.LOOP1.RHO(11) = 1.12115 ; # 51
54 PLANT.LOOP1.RHO(12) = 1.1026 ; # 52
55 PLANT.LOOP1.RHO(13) = 1.08477 ; # 53
56 PLANT.LOOP1.RHO(14) = 1.06791 ; # 54
57 PLANT.LOOP1.RHO(15) = 1.05196 ; # 55
58 PLANT.LOOP1.RHO(16) = 1.03683 ; # 56
59 PLANT.LOOP1.RHO(17) = 1.02247 ; # 57
60 PLANT.LOOP1.RHO(18) = 1.00882 ; # 58
61 PLANT.LOOP1.RHO(19) = 0.99583 ; # 59
62 PLANT.LOOP1.RHO(20) = 0.983453 ; # 60
63 PLANT.LOOP1.RHO(21) = 0.971645 ; # 61
64 PLANT.LOOP1.RHO(22) = 0.960369 ; # 62
65 PLANT.LOOP1.RHO(23) = 0.949588 ; # 63
66 PLANT.LOOP1.RHO(24) = 0.939271 ; # 64
67 PLANT.LOOP1.RHO(25) = 0.929389 ; # 65
68 PLANT.LOOP1.RHO(26) = 0.919912 ; # 66
69 PLANT.LOOP1.RHO(27) = 0.910817 ; # 67
70 PLANT.LOOP1.RHO(28) = 0.90208 ; # 68
71 PLANT.LOOP1.RHO(29) = 0.893679 ; # 69
72 PLANT.LOOP1.RHO(30) = 0.885595 ; # 70
73 PLANT.LOOP1.RHO(31) = 0.87781 ; # 71
74 PLANT.LOOP1.RHO(32) = 0.870305 ; # 72
75 PLANT.LOOP1.RHO(33) = 0.863066 ; # 73
76 PLANT.LOOP1.RHO(34) = 0.856077 ; # 74
77 PLANT.LOOP1.RHO(35) = 0.849325 ; # 75
78 PLANT.LOOP1.RHO(36) = 0.842796 ; # 76
79 PLANT.LOOP1.RHO(37) = 0.83648 ; # 77
80 PLANT.LOOP1.RHO(38) = 0.830363 ; # 78
81 PLANT.LOOP1.RHO(39) = 0.824437 ; # 79
82 PLANT.LOOP1.RHO(40) = 0.818691 ; # 80
83 PLANT.LOOP1.RHO(41) = 0.813116 ; # 81
84 PLANT.LOOP1.RHO(42) = 0.807703 ; # 82
85 PLANT.LOOP1.RHO(43) = 0.802444 ; # 83
86 PLANT.LOOP1.RHO(44) = 0.797332 ; # 84
87 PLANT.LOOP1.RHO(45) = 0.792358 ; # 85
88 PLANT.LOOP1.RHO(46) = 0.787518 ; # 86
89 PLANT.LOOP1.RHO(47) = 0.782803 ; # 87
90 PLANT.LOOP1.RHO(48) = 0.778207 ; # 88
91 PLANT.LOOP1.RHO(49) = 0.773726 ; # 89
92 PLANT.LOOP1.RHO(50) = 0.769358 ; # 90
93 PLANT.LOOP1.RHO(51) = 0.757959 ; # 91
94 PLANT.LOOP1.RHO(52) = 0.756103 ; # 92
95 PLANT.LOOP1.RHO(53) = 0.754256 ; # 93
96 PLANT.LOOP1.RHO(54) = 0.752399 ; # 94
97 PLANT.LOOP1.RHO(55) = 0.750533 ; # 95
98 PLANT.LOOP1.RHO(56) = 0.748658 ; # 96
99 PLANT.LOOP1.RHO(57) = 0.746773 ; # 97
100 PLANT.LOOP1.RHO(58) = 0.744879 ; # 98
101 PLANT.LOOP1.RHO(59) = 0.742974 ; # 99
102 PLANT.LOOP1.RHO(60) = 0.74106 ; # 100
103 PLANT.LOOP1.RHO(61) = 0.750585 ; # 101
104 PLANT.LOOP1.RHO(62) = 0.751689 ; # 102
105 PLANT.LOOP1.RHO(63) = 0.752856 ; # 103
106 PLANT.LOOP1.RHO(64) = 0.754135 ; # 104
107 PLANT.LOOP1.RHO(65) = 0.755533 ; # 105
108 PLANT.LOOP1.RHO(66) = 0.757058 ; # 106
109 PLANT.LOOP1.RHO(67) = 0.75872 ; # 107
110 PLANT.LOOP1.RHO(68) = 0.760528 ; # 108
111 PLANT.LOOP1.RHO(69) = 0.762492 ; # 109
112 PLANT.LOOP1.RHO(70) = 0.764623 ; # 110
113 PLANT.LOOP1.RHO(71) = 0.766934 ; # 111
114 PLANT.LOOP1.RHO(72) = 0.769438 ; # 112

115 PLANT.LOOP1.RHO(73) = 0.772149 ; # 113
116 PLANT.LOOP1.RHO(74) = 0.775082 ; # 114
117 PLANT.LOOP1.RHO(75) = 0.778256 ; # 115
118 PLANT.LOOP1.RHO(76) = 0.781688 ; # 116
119 PLANT.LOOP1.RHO(77) = 0.785399 ; # 117
120 PLANT.LOOP1.RHO(78) = 0.789411 ; # 118
121 PLANT.LOOP1.RHO(79) = 0.793749 ; # 119
122 PLANT.LOOP1.RHO(80) = 0.79844 ; # 120
123 PLANT.LOOP1.RHO(81) = 0.803515 ; # 121
124 PLANT.LOOP1.RHO(82) = 0.809005 ; # 122
125 PLANT.LOOP1.RHO(83) = 0.814949 ; # 123
126 PLANT.LOOP1.RHO(84) = 0.821387 ; # 124
127 PLANT.LOOP1.RHO(85) = 0.828364 ; # 125
128 PLANT.LOOP1.RHO(86) = 0.835933 ; # 126
129 PLANT.LOOP1.RHO(87) = 0.844151 ; # 127
130 PLANT.LOOP1.RHO(88) = 0.853082 ; # 128
131 PLANT.LOOP1.RHO(89) = 0.8628 ; # 129
132 PLANT.LOOP1.RHO(90) = 0.873389 ; # 130
133 PLANT.LOOP1.RHO(91) = 0.884944 ; # 131
134 PLANT.LOOP1.RHO(92) = 0.897573 ; # 132
135 PLANT.LOOP1.RHO(93) = 0.911403 ; # 133
136 PLANT.LOOP1.RHO(94) = 0.926579 ; # 134
137 PLANT.LOOP1.RHO(95) = 0.94327 ; # 135
138 PLANT.LOOP1.RHO(96) = 0.961674 ; # 136
139 PLANT.LOOP1.RHO(97) = 0.982026 ; # 137
140 PLANT.LOOP1.RHO(98) = 1.0046 ; # 138
141 PLANT.LOOP1.RHO(99) = 1.02974 ; # 139
142 PLANT.LOOP1.RHO(100) = 1.05783 ; # 140
143 PLANT.LOOP1.PSI(1) = 1.23127e+006 ; # 141
144 PLANT.LOOP1.PSI(2) = 1.22711e+006 ; # 142
145 PLANT.LOOP1.PSI(3) = 1.22294e+006 ; # 143
146 PLANT.LOOP1.PSI(4) = 1.21877e+006 ; # 144
147 PLANT.LOOP1.PSI(5) = 1.2146e+006 ; # 145
148 PLANT.LOOP1.PSI(6) = 1.21042e+006 ; # 146
149 PLANT.LOOP1.PSI(7) = 1.20624e+006 ; # 147
150 PLANT.LOOP1.PSI(8) = 1.20206e+006 ; # 148
151 PLANT.LOOP1.PSI(9) = 1.19787e+006 ; # 149
152 PLANT.LOOP1.PSI(10) = 1.19368e+006 ; # 150
153 PLANT.LOOP1.PSI(11) = 1.23208e+006 ; # 151
154 PLANT.LOOP1.PSI(12) = 1.25743e+006 ; # 152
155 PLANT.LOOP1.PSI(13) = 1.28069e+006 ; # 153
156 PLANT.LOOP1.PSI(14) = 1.30237e+006 ; # 154
157 PLANT.LOOP1.PSI(15) = 1.32259e+006 ; # 155
158 PLANT.LOOP1.PSI(16) = 1.34148e+006 ; # 156
159 PLANT.LOOP1.PSI(17) = 1.35911e+006 ; # 157
160 PLANT.LOOP1.PSI(18) = 1.37558e+006 ; # 158
161 PLANT.LOOP1.PSI(19) = 1.39098e+006 ; # 159
162 PLANT.LOOP1.PSI(20) = 1.40537e+006 ; # 160
163 PLANT.LOOP1.PSI(21) = 1.41883e+006 ; # 161
164 PLANT.LOOP1.PSI(22) = 1.4314e+006 ; # 162
165 PLANT.LOOP1.PSI(23) = 1.44316e+006 ; # 163
166 PLANT.LOOP1.PSI(24) = 1.45415e+006 ; # 164
167 PLANT.LOOP1.PSI(25) = 1.46441e+006 ; # 165
168 PLANT.LOOP1.PSI(26) = 1.474e+006 ; # 166
169 PLANT.LOOP1.PSI(27) = 1.48294e+006 ; # 167
170 PLANT.LOOP1.PSI(28) = 1.49129e+006 ; # 168
171 PLANT.LOOP1.PSI(29) = 1.49907e+006 ; # 169
172 PLANT.LOOP1.PSI(30) = 1.50631e+006 ; # 170
173 PLANT.LOOP1.PSI(31) = 1.51304e+006 ; # 171
174 PLANT.LOOP1.PSI(32) = 1.5193e+006 ; # 172
175 PLANT.LOOP1.PSI(33) = 1.5251e+006 ; # 173
176 PLANT.LOOP1.PSI(34) = 1.53047e+006 ; # 174
177 PLANT.LOOP1.PSI(35) = 1.53543e+006 ; # 175
178 PLANT.LOOP1.PSI(36) = 1.54001e+006 ; # 176
179 PLANT.LOOP1.PSI(37) = 1.54421e+006 ; # 177
180 PLANT.LOOP1.PSI(38) = 1.54807e+006 ; # 178
181 PLANT.LOOP1.PSI(39) = 1.5516e+006 ; # 179
182 PLANT.LOOP1.PSI(40) = 1.5548e+006 ; # 180
183 PLANT.LOOP1.PSI(41) = 1.55771e+006 ; # 181
184 PLANT.LOOP1.PSI(42) = 1.56032e+006 ; # 182
185 PLANT.LOOP1.PSI(43) = 1.56266e+006 ; # 183
186 PLANT.LOOP1.PSI(44) = 1.56474e+006 ; # 184
187 PLANT.LOOP1.PSI(45) = 1.56657e+006 ; # 185
188 PLANT.LOOP1.PSI(46) = 1.56816e+006 ; # 186
189 PLANT.LOOP1.PSI(47) = 1.56951e+006 ; # 187
190 PLANT.LOOP1.PSI(48) = 1.57065e+006 ; # 188
191 PLANT.LOOP1.PSI(49) = 1.57158e+006 ; # 189
192 PLANT.LOOP1.PSI(50) = 1.5723e+006 ; # 190
193 PLANT.LOOP1.PSI(51) = 1.54707e+006 ; # 191
194 PLANT.LOOP1.PSI(52) = 1.54135e+006 ; # 192
195 PLANT.LOOP1.PSI(53) = 1.53567e+006 ; # 193
196 PLANT.LOOP1.PSI(54) = 1.52997e+006 ; # 194
197 PLANT.LOOP1.PSI(55) = 1.52427e+006 ; # 195
198 PLANT.LOOP1.PSI(56) = 1.51856e+006 ; # 196
199 PLANT.LOOP1.PSI(57) = 1.51284e+006 ; # 197
200 PLANT.LOOP1.PSI(58) = 1.50712e+006 ; # 198
201 PLANT.LOOP1.PSI(59) = 1.50138e+006 ; # 199
202 PLANT.LOOP1.PSI(60) = 1.49564e+006 ; # 200
203 PLANT.LOOP1.PSI(61) = 1.50921e+006 ; # 201
204 PLANT.LOOP1.PSI(62) = 1.50544e+006 ; # 202
205 PLANT.LOOP1.PSI(63) = 1.50142e+006 ; # 203
206 PLANT.LOOP1.PSI(64) = 1.49724e+006 ; # 204

207 PLANT.LOOP1.PSI(65) = 1.49288e+006 ; # 205
 208 PLANT.LOOP1.PSI(66) = 1.48832e+006 ; # 206
 209 PLANT.LOOP1.PSI(67) = 1.48357e+006 ; # 207
 210 PLANT.LOOP1.PSI(68) = 1.47859e+006 ; # 208
 211 PLANT.LOOP1.PSI(69) = 1.47338e+006 ; # 209
 212 PLANT.LOOP1.PSI(70) = 1.46791e+006 ; # 210
 213 PLANT.LOOP1.PSI(71) = 1.46218e+006 ; # 211
 214 PLANT.LOOP1.PSI(72) = 1.45616e+006 ; # 212
 215 PLANT.LOOP1.PSI(73) = 1.44982e+006 ; # 213
 216 PLANT.LOOP1.PSI(74) = 1.44315e+006 ; # 214
 217 PLANT.LOOP1.PSI(75) = 1.43612e+006 ; # 215
 218 PLANT.LOOP1.PSI(76) = 1.4287e+006 ; # 216
 219 PLANT.LOOP1.PSI(77) = 1.42087e+006 ; # 217
 220 PLANT.LOOP1.PSI(78) = 1.41258e+006 ; # 218
 221 PLANT.LOOP1.PSI(79) = 1.40379e+006 ; # 219
 222 PLANT.LOOP1.PSI(80) = 1.39448e+006 ; # 220
 223 PLANT.LOOP1.PSI(81) = 1.38459e+006 ; # 221
 224 PLANT.LOOP1.PSI(82) = 1.37407e+006 ; # 222
 225 PLANT.LOOP1.PSI(83) = 1.36287e+006 ; # 223
 226 PLANT.LOOP1.PSI(84) = 1.35093e+006 ; # 224
 227 PLANT.LOOP1.PSI(85) = 1.33817e+006 ; # 225
 228 PLANT.LOOP1.PSI(86) = 1.32451e+006 ; # 226
 229 PLANT.LOOP1.PSI(87) = 1.30988e+006 ; # 227
 230 PLANT.LOOP1.PSI(88) = 1.29416e+006 ; # 228
 231 PLANT.LOOP1.PSI(89) = 1.27725e+006 ; # 229
 232 PLANT.LOOP1.PSI(90) = 1.25903e+006 ; # 230
 233 PLANT.LOOP1.PSI(91) = 1.23934e+006 ; # 231
 234 PLANT.LOOP1.PSI(92) = 1.21801e+006 ; # 232
 235 PLANT.LOOP1.PSI(93) = 1.19486e+006 ; # 233
 236 PLANT.LOOP1.PSI(94) = 1.16967e+006 ; # 234
 237 PLANT.LOOP1.PSI(95) = 1.14217e+006 ; # 235
 238 PLANT.LOOP1.PSI(96) = 1.11205e+006 ; # 236
 239 PLANT.LOOP1.PSI(97) = 1.07896e+006 ; # 237
 240 PLANT.LOOP1.PSI(98) = 1.04248e+006 ; # 238
 241 PLANT.LOOP1.PSI(99) = 1.00208e+006 ; # 239
 242 PLANT.LOOP1.PSI(100) = 957155 ; # 240
 243 PLANT.LOOP1.F(1) = 26.308 ; # 241
 244 PLANT.LOOP1.F(2) = 26.308 ; # 242
 245 PLANT.LOOP1.F(3) = 26.308 ; # 243
 246 PLANT.LOOP1.F(4) = 26.308 ; # 244
 247 PLANT.LOOP1.F(5) = 26.308 ; # 245
 248 PLANT.LOOP1.F(6) = 26.308 ; # 246
 249 PLANT.LOOP1.F(7) = 26.308 ; # 247
 250 PLANT.LOOP1.F(8) = 26.308 ; # 248
 251 PLANT.LOOP1.F(9) = 26.308 ; # 249
 252 PLANT.LOOP1.F(10) = 26.308 ; # 250
 253 PLANT.LOOP1.F(11) = 26.308 ; # 251
 254 PLANT.LOOP1.F(12) = 26.308 ; # 252
 255 PLANT.LOOP1.F(13) = 26.308 ; # 253
 256 PLANT.LOOP1.F(14) = 26.308 ; # 254
 257 PLANT.LOOP1.F(15) = 26.308 ; # 255
 258 PLANT.LOOP1.F(16) = 26.308 ; # 256
 259 PLANT.LOOP1.F(17) = 26.308 ; # 257
 260 PLANT.LOOP1.F(18) = 26.308 ; # 258
 261 PLANT.LOOP1.F(19) = 26.308 ; # 259
 262 PLANT.LOOP1.F(20) = 26.308 ; # 260
 263 PLANT.LOOP1.F(21) = 26.308 ; # 261
 264 PLANT.LOOP1.F(22) = 26.308 ; # 262
 265 PLANT.LOOP1.F(23) = 26.308 ; # 263
 266 PLANT.LOOP1.F(24) = 26.308 ; # 264
 267 PLANT.LOOP1.F(25) = 26.308 ; # 265
 268 PLANT.LOOP1.F(26) = 26.308 ; # 266
 269 PLANT.LOOP1.F(27) = 26.308 ; # 267
 270 PLANT.LOOP1.F(28) = 26.308 ; # 268
 271 PLANT.LOOP1.F(29) = 26.308 ; # 269
 272 PLANT.LOOP1.F(30) = 26.308 ; # 270
 273 PLANT.LOOP1.F(31) = 26.308 ; # 271
 274 PLANT.LOOP1.F(32) = 26.308 ; # 272
 275 PLANT.LOOP1.F(33) = 26.308 ; # 273
 276 PLANT.LOOP1.F(34) = 26.308 ; # 274
 277 PLANT.LOOP1.F(35) = 26.308 ; # 275
 278 PLANT.LOOP1.F(36) = 26.308 ; # 276
 279 PLANT.LOOP1.F(37) = 26.308 ; # 277
 280 PLANT.LOOP1.F(38) = 26.308 ; # 278
 281 PLANT.LOOP1.F(39) = 26.308 ; # 279
 282 PLANT.LOOP1.F(40) = 26.308 ; # 280
 283 PLANT.LOOP1.F(41) = 26.308 ; # 281
 284 PLANT.LOOP1.F(42) = 26.308 ; # 282
 285 PLANT.LOOP1.F(43) = 26.308 ; # 283
 286 PLANT.LOOP1.F(44) = 26.308 ; # 284
 287 PLANT.LOOP1.F(45) = 26.308 ; # 285
 288 PLANT.LOOP1.F(46) = 26.308 ; # 286
 289 PLANT.LOOP1.F(47) = 26.308 ; # 287
 290 PLANT.LOOP1.F(48) = 26.308 ; # 288
 291 PLANT.LOOP1.F(49) = 26.308 ; # 289
 292 PLANT.LOOP1.F(50) = 26.308 ; # 290
 293 PLANT.LOOP1.F(51) = 26.308 ; # 291
 294 PLANT.LOOP1.F(52) = 26.308 ; # 292
 295 PLANT.LOOP1.F(53) = 26.308 ; # 293
 296 PLANT.LOOP1.F(54) = 26.308 ; # 294
 297 PLANT.LOOP1.F(55) = 26.308 ; # 295
 298 PLANT.LOOP1.F(56) = 26.308 ; # 296

299 PLANT.LOOP1.F(57) = 26.308 ; # 297
300 PLANT.LOOP1.F(58) = 26.308 ; # 298
301 PLANT.LOOP1.F(59) = 26.308 ; # 299
302 PLANT.LOOP1.F(60) = 26.308 ; # 300
303 PLANT.LOOP1.F(61) = 26.308 ; # 301
304 PLANT.LOOP1.F(62) = 26.308 ; # 302
305 PLANT.LOOP1.F(63) = 26.308 ; # 303
306 PLANT.LOOP1.F(64) = 26.308 ; # 304
307 PLANT.LOOP1.F(65) = 26.308 ; # 305
308 PLANT.LOOP1.F(66) = 26.308 ; # 306
309 PLANT.LOOP1.F(67) = 26.308 ; # 307
310 PLANT.LOOP1.F(68) = 26.308 ; # 308
311 PLANT.LOOP1.F(69) = 26.308 ; # 309
312 PLANT.LOOP1.F(70) = 26.308 ; # 310
313 PLANT.LOOP1.F(71) = 26.308 ; # 311
314 PLANT.LOOP1.F(72) = 26.308 ; # 312
315 PLANT.LOOP1.F(73) = 26.308 ; # 313
316 PLANT.LOOP1.F(74) = 26.308 ; # 314
317 PLANT.LOOP1.F(75) = 26.308 ; # 315
318 PLANT.LOOP1.F(76) = 26.308 ; # 316
319 PLANT.LOOP1.F(77) = 26.308 ; # 317
320 PLANT.LOOP1.F(78) = 26.308 ; # 318
321 PLANT.LOOP1.F(79) = 26.308 ; # 319
322 PLANT.LOOP1.F(80) = 26.308 ; # 320
323 PLANT.LOOP1.F(81) = 26.308 ; # 321
324 PLANT.LOOP1.F(82) = 26.308 ; # 322
325 PLANT.LOOP1.F(83) = 26.308 ; # 323
326 PLANT.LOOP1.F(84) = 26.308 ; # 324
327 PLANT.LOOP1.F(85) = 26.308 ; # 325
328 PLANT.LOOP1.F(86) = 26.308 ; # 326
329 PLANT.LOOP1.F(87) = 26.308 ; # 327
330 PLANT.LOOP1.F(88) = 26.308 ; # 328
331 PLANT.LOOP1.F(89) = 26.308 ; # 329
332 PLANT.LOOP1.F(90) = 26.308 ; # 330
333 PLANT.LOOP1.F(91) = 26.308 ; # 331
334 PLANT.LOOP1.F(92) = 26.308 ; # 332
335 PLANT.LOOP1.F(93) = 26.308 ; # 333
336 PLANT.LOOP1.F(94) = 26.308 ; # 334
337 PLANT.LOOP1.F(95) = 26.308 ; # 335
338 PLANT.LOOP1.F(96) = 26.308 ; # 336
339 PLANT.LOOP1.F(97) = 26.308 ; # 337
340 PLANT.LOOP1.F(98) = 26.308 ; # 338
341 PLANT.LOOP1.F(99) = 26.308 ; # 339
342 PLANT.LOOP1.F(100) = 26.308 ; # 340
343 PLANT.LOOP1.RHOEXTRA(1) = 1.1654 ; # 341
344 PLANT.LOOP1.RHOEXTRA(2) = 1.1654 ; # 342
345 PLANT.LOOP1.PSIEXTRA(1) = 1.24585e+006 ; # 343
346 PLANT.LOOP1.PSIEXTRA(2) = 1.24585e+006 ; # 344
347 PLANT.LOOP1.FEXTRA(1) = 26.308 ; # 345
348 PLANT.LOOP1.FEXTRA(2) = 26.308 ; # 346
349 PLANT.PIPEH.RHO(1) = 2.87869 ; # 347
350 PLANT.PIPEH.RHO(2) = 2.88664 ; # 348
351 PLANT.PIPEH.RHO(3) = 2.89491 ; # 349
352 PLANT.PIPEH.RHO(4) = 2.90353 ; # 350
353 PLANT.PIPEH.RHO(5) = 2.9125 ; # 351
354 PLANT.PIPEH.RHO(6) = 2.92184 ; # 352
355 PLANT.PIPEH.RHO(7) = 2.93156 ; # 353
356 PLANT.PIPEH.RHO(8) = 2.9417 ; # 354
357 PLANT.PIPEH.RHO(9) = 2.95225 ; # 355
358 PLANT.PIPEH.RHO(10) = 2.96325 ; # 356
359 PLANT.PIPEH.RHO(11) = 2.97471 ; # 357
360 PLANT.PIPEH.RHO(12) = 2.98666 ; # 358
361 PLANT.PIPEH.RHO(13) = 2.99912 ; # 359
362 PLANT.PIPEH.RHO(14) = 3.01211 ; # 360
363 PLANT.PIPEH.RHO(15) = 3.02567 ; # 361
364 PLANT.PIPEH.RHO(16) = 3.03982 ; # 362
365 PLANT.PIPEH.RHO(17) = 3.05458 ; # 363
366 PLANT.PIPEH.RHO(18) = 3.07 ; # 364
367 PLANT.PIPEH.RHO(19) = 3.08611 ; # 365
368 PLANT.PIPEH.RHO(20) = 3.10294 ; # 366
369 PLANT.PIPEH.RHO(21) = 3.12053 ; # 367
370 PLANT.PIPEH.RHO(22) = 3.13892 ; # 368
371 PLANT.PIPEH.RHO(23) = 3.15816 ; # 369
372 PLANT.PIPEH.RHO(24) = 3.1783 ; # 370
373 PLANT.PIPEH.RHO(25) = 3.19939 ; # 371
374 PLANT.PIPEH.RHO(26) = 3.22148 ; # 372
375 PLANT.PIPEH.RHO(27) = 3.24463 ; # 373
376 PLANT.PIPEH.RHO(28) = 3.2689 ; # 374
377 PLANT.PIPEH.RHO(29) = 3.29437 ; # 375
378 PLANT.PIPEH.RHO(30) = 3.32112 ; # 376
379 PLANT.PIPEH.RHO(31) = 3.34921 ; # 377
380 PLANT.PIPEH.RHO(32) = 3.37874 ; # 378
381 PLANT.PIPEH.RHO(33) = 3.4098 ; # 379
382 PLANT.PIPEH.RHO(34) = 3.4425 ; # 380
383 PLANT.PIPEH.RHO(35) = 3.47695 ; # 381
384 PLANT.PIPEH.RHO(36) = 3.51328 ; # 382
385 PLANT.PIPEH.RHO(37) = 3.55161 ; # 383
386 PLANT.PIPEH.RHO(38) = 3.59209 ; # 384
387 PLANT.PIPEH.RHO(39) = 3.6349 ; # 385
388 PLANT.PIPEH.RHO(40) = 3.68012 ; # 386
389 PLANT.PIPEH.F(1) = 32.3305 ; # 387
390 PLANT.PIPEH.F(2) = 32.3305 ; # 388

391 PLANT.PIPEH.F(3) = 32.3305 ; # 389
392 PLANT.PIPEH.F(4) = 32.3305 ; # 390
393 PLANT.PIPEH.F(5) = 32.3305 ; # 391
394 PLANT.PIPEH.F(6) = 32.3305 ; # 392
395 PLANT.PIPEH.F(7) = 32.3305 ; # 393
396 PLANT.PIPEH.F(8) = 32.3305 ; # 394
397 PLANT.PIPEH.F(9) = 32.3305 ; # 395
398 PLANT.PIPEH.F(10) = 32.3305 ; # 396
399 PLANT.PIPEH.F(11) = 32.3305 ; # 397
400 PLANT.PIPEH.F(12) = 32.3305 ; # 398
401 PLANT.PIPEH.F(13) = 32.3305 ; # 399
402 PLANT.PIPEH.F(14) = 32.3305 ; # 400
403 PLANT.PIPEH.F(15) = 32.3305 ; # 401
404 PLANT.PIPEH.F(16) = 32.3305 ; # 402
405 PLANT.PIPEH.F(17) = 32.3305 ; # 403
406 PLANT.PIPEH.F(18) = 32.3305 ; # 404
407 PLANT.PIPEH.F(19) = 32.3305 ; # 405
408 PLANT.PIPEH.F(20) = 32.3305 ; # 406
409 PLANT.PIPEH.F(21) = 32.3305 ; # 407
410 PLANT.PIPEH.F(22) = 32.3305 ; # 408
411 PLANT.PIPEH.F(23) = 32.3305 ; # 409
412 PLANT.PIPEH.F(24) = 32.3305 ; # 410
413 PLANT.PIPEH.F(25) = 32.3305 ; # 411
414 PLANT.PIPEH.F(26) = 32.3305 ; # 412
415 PLANT.PIPEH.F(27) = 32.3305 ; # 413
416 PLANT.PIPEH.F(28) = 32.3305 ; # 414
417 PLANT.PIPEH.F(29) = 32.3305 ; # 415
418 PLANT.PIPEH.F(30) = 32.3305 ; # 416
419 PLANT.PIPEH.F(31) = 32.3305 ; # 417
420 PLANT.PIPEH.F(32) = 32.3305 ; # 418
421 PLANT.PIPEH.F(33) = 32.3305 ; # 419
422 PLANT.PIPEH.F(34) = 32.3305 ; # 420
423 PLANT.PIPEH.F(35) = 32.3305 ; # 421
424 PLANT.PIPEH.F(36) = 32.3305 ; # 422
425 PLANT.PIPEH.F(37) = 32.3305 ; # 423
426 PLANT.PIPEH.F(38) = 32.3305 ; # 424
427 PLANT.PIPEH.F(39) = 32.3305 ; # 425
428 PLANT.PIPEH.F(40) = 32.3305 ; # 426
429 PLANT.PIPEH.F_IN = 32.3305 ; # 427
430 PLANT.PIPEH.PSI(1) = 6.03823e+006 ; # 428
431 PLANT.PIPEH.PSI(2) = 6.02385e+006 ; # 429
432 PLANT.PIPEH.PSI(3) = 6.00898e+006 ; # 430
433 PLANT.PIPEH.PSI(4) = 5.9936e+006 ; # 431
434 PLANT.PIPEH.PSI(5) = 5.97767e+006 ; # 432
435 PLANT.PIPEH.PSI(6) = 5.96117e+006 ; # 433
436 PLANT.PIPEH.PSI(7) = 5.94408e+006 ; # 434
437 PLANT.PIPEH.PSI(8) = 5.92638e+006 ; # 435
438 PLANT.PIPEH.PSI(9) = 5.90802e+006 ; # 436
439 PLANT.PIPEH.PSI(10) = 5.88899e+006 ; # 437
440 PLANT.PIPEH.PSI(11) = 5.86924e+006 ; # 438
441 PLANT.PIPEH.PSI(12) = 5.84876e+006 ; # 439
442 PLANT.PIPEH.PSI(13) = 5.82749e+006 ; # 440
443 PLANT.PIPEH.PSI(14) = 5.8054e+006 ; # 441
444 PLANT.PIPEH.PSI(15) = 5.78245e+006 ; # 442
445 PLANT.PIPEH.PSI(16) = 5.75859e+006 ; # 443
446 PLANT.PIPEH.PSI(17) = 5.73379e+006 ; # 444
447 PLANT.PIPEH.PSI(18) = 5.70799e+006 ; # 445
448 PLANT.PIPEH.PSI(19) = 5.68113e+006 ; # 446
449 PLANT.PIPEH.PSI(20) = 5.65317e+006 ; # 447
450 PLANT.PIPEH.PSI(21) = 5.62404e+006 ; # 448
451 PLANT.PIPEH.PSI(22) = 5.59367e+006 ; # 449
452 PLANT.PIPEH.PSI(23) = 5.56201e+006 ; # 450
453 PLANT.PIPEH.PSI(24) = 5.52897e+006 ; # 451
454 PLANT.PIPEH.PSI(25) = 5.49447e+006 ; # 452
455 PLANT.PIPEH.PSI(26) = 5.45844e+006 ; # 453
456 PLANT.PIPEH.PSI(27) = 5.42078e+006 ; # 454
457 PLANT.PIPEH.PSI(28) = 5.38139e+006 ; # 455
458 PLANT.PIPEH.PSI(29) = 5.34016e+006 ; # 456
459 PLANT.PIPEH.PSI(30) = 5.29699e+006 ; # 457
460 PLANT.PIPEH.PSI(31) = 5.25174e+006 ; # 458
461 PLANT.PIPEH.PSI(32) = 5.20427e+006 ; # 459
462 PLANT.PIPEH.PSI(33) = 5.15446e+006 ; # 460
463 PLANT.PIPEH.PSI(34) = 5.10212e+006 ; # 461
464 PLANT.PIPEH.PSI(35) = 5.0471e+006 ; # 462
465 PLANT.PIPEH.PSI(36) = 4.98919e+006 ; # 463
466 PLANT.PIPEH.PSI(37) = 4.92819e+006 ; # 464
467 PLANT.PIPEH.PSI(38) = 4.86388e+006 ; # 465
468 PLANT.PIPEH.PSI(39) = 4.796e+006 ; # 466
469 PLANT.PIPEH.PSI(40) = 4.7244e+006 ; # 467
470 PLANT.HX2.TH(1) = 1133.71 ; # 468
471 PLANT.HX2.TH(2) = 1130.67 ; # 469
472 PLANT.HX2.TH(3) = 1127.46 ; # 470
473 PLANT.HX2.TH(4) = 1124.06 ; # 471
474 PLANT.HX2.TH(5) = 1120.46 ; # 472
475 PLANT.HX2.TH(6) = 1116.65 ; # 473
476 PLANT.HX2.TH(7) = 1112.63 ; # 474
477 PLANT.HX2.TH(8) = 1108.36 ; # 475
478 PLANT.HX2.TH(9) = 1103.85 ; # 476
479 PLANT.HX2.TH(10) = 1099.08 ; # 477
480 PLANT.HX2.TH(11) = 1094.03 ; # 478
481 PLANT.HX2.TH(12) = 1088.69 ; # 479
482 PLANT.HX2.TH(13) = 1083.03 ; # 480

483 PLANT.HX2.THX(14) = 1077.05 ; # 481
484 PLANT.HX2.THX(15) = 1070.72 ; # 482
485 PLANT.HX2.THX(16) = 1064.02 ; # 483
486 PLANT.HX2.THX(17) = 1056.93 ; # 484
487 PLANT.HX2.THX(18) = 1049.43 ; # 485
488 PLANT.HX2.THX(19) = 1041.49 ; # 486
489 PLANT.HX2.THX(20) = 1033.09 ; # 487
490 PLANT.HX2.THX(21) = 1024.2 ; # 488
491 PLANT.HX2.THX(22) = 1014.8 ; # 489
492 PLANT.HX2.THX(23) = 1004.84 ; # 490
493 PLANT.HX2.THX(24) = 994.314 ; # 491
494 PLANT.HX2.THX(25) = 983.171 ; # 492
495 PLANT.HX2.THX(26) = 971.38 ; # 493
496 PLANT.HX2.THX(27) = 958.903 ; # 494
497 PLANT.HX2.THX(28) = 945.701 ; # 495
498 PLANT.HX2.THX(29) = 931.731 ; # 496
499 PLANT.HX2.THX(30) = 916.948 ; # 497
500 PLANT.HX2.THX(31) = 901.306 ; # 498
501 PLANT.HX2.THX(32) = 884.754 ; # 499
502 PLANT.HX2.THX(33) = 867.239 ; # 500
503 PLANT.HX2.THX(34) = 848.706 ; # 501
504 PLANT.HX2.THX(35) = 829.095 ; # 502
505 PLANT.HX2.THX(36) = 808.344 ; # 503
506 PLANT.HX2.THX(37) = 786.385 ; # 504
507 PLANT.HX2.THX(38) = 763.15 ; # 505
508 PLANT.HX2.THX(39) = 738.563 ; # 506
509 PLANT.HX2.THX(40) = 712.554 ; # 507
510 PLANT.PIPEC2.RHO(1) = 3.72389 ; # 508
511 PLANT.PIPEC2.RHO(2) = 3.55368 ; # 509
512 PLANT.PIPEC2.RHO(3) = 3.4055 ; # 510
513 PLANT.PIPEC2.RHO(4) = 3.27543 ; # 511
514 PLANT.PIPEC2.RHO(5) = 3.16041 ; # 512
515 PLANT.PIPEC2.RHO(6) = 3.05803 ; # 513
516 PLANT.PIPEC2.RHO(7) = 2.96638 ; # 514
517 PLANT.PIPEC2.RHO(8) = 2.88388 ; # 515
518 PLANT.PIPEC2.RHO(9) = 2.80928 ; # 516
519 PLANT.PIPEC2.RHO(10) = 2.74152 ; # 517
520 PLANT.PIPEC2.RHO(11) = 2.67973 ; # 518
521 PLANT.PIPEC2.RHO(12) = 2.62316 ; # 519
522 PLANT.PIPEC2.RHO(13) = 2.57121 ; # 520
523 PLANT.PIPEC2.RHO(14) = 2.52333 ; # 521
524 PLANT.PIPEC2.RHO(15) = 2.47909 ; # 522
525 PLANT.PIPEC2.RHO(16) = 2.43808 ; # 523
526 PLANT.PIPEC2.RHO(17) = 2.39997 ; # 524
527 PLANT.PIPEC2.RHO(18) = 2.36446 ; # 525
528 PLANT.PIPEC2.RHO(19) = 2.3313 ; # 526
529 PLANT.PIPEC2.RHO(20) = 2.30026 ; # 527
530 PLANT.PIPEC2.RHO(21) = 2.27113 ; # 528
531 PLANT.PIPEC2.RHO(22) = 2.24375 ; # 529
532 PLANT.PIPEC2.RHO(23) = 2.21796 ; # 530
533 PLANT.PIPEC2.RHO(24) = 2.19361 ; # 531
534 PLANT.PIPEC2.RHO(25) = 2.17058 ; # 532
535 PLANT.PIPEC2.RHO(26) = 2.14875 ; # 533
536 PLANT.PIPEC2.RHO(27) = 2.12804 ; # 534
537 PLANT.PIPEC2.RHO(28) = 2.10834 ; # 535
538 PLANT.PIPEC2.RHO(29) = 2.08957 ; # 536
539 PLANT.PIPEC2.RHO(30) = 2.07166 ; # 537
540 PLANT.PIPEC2.RHO(31) = 2.05454 ; # 538
541 PLANT.PIPEC2.RHO(32) = 2.03814 ; # 539
542 PLANT.PIPEC2.RHO(33) = 2.02242 ; # 540
543 PLANT.PIPEC2.RHO(34) = 2.00733 ; # 541
544 PLANT.PIPEC2.RHO(35) = 1.9928 ; # 542
545 PLANT.PIPEC2.RHO(36) = 1.97881 ; # 543
546 PLANT.PIPEC2.RHO(37) = 1.96531 ; # 544
547 PLANT.PIPEC2.RHO(38) = 1.95226 ; # 545
548 PLANT.PIPEC2.RHO(39) = 1.93964 ; # 546
549 PLANT.PIPEC2.RHO(40) = 1.92741 ; # 547
550 PLANT.PIPEC2.F(1) = 43.3743 ; # 548
551 PLANT.PIPEC2.F(2) = 43.3743 ; # 549
552 PLANT.PIPEC2.F(3) = 43.3743 ; # 550
553 PLANT.PIPEC2.F(4) = 43.3743 ; # 551
554 PLANT.PIPEC2.F(5) = 43.3743 ; # 552
555 PLANT.PIPEC2.F(6) = 43.3743 ; # 553
556 PLANT.PIPEC2.F(7) = 43.3743 ; # 554
557 PLANT.PIPEC2.F(8) = 43.3743 ; # 555
558 PLANT.PIPEC2.F(9) = 43.3743 ; # 556
559 PLANT.PIPEC2.F(10) = 43.3743 ; # 557
560 PLANT.PIPEC2.F(11) = 43.3743 ; # 558
561 PLANT.PIPEC2.F(12) = 43.3743 ; # 559
562 PLANT.PIPEC2.F(13) = 43.3743 ; # 560
563 PLANT.PIPEC2.F(14) = 43.3743 ; # 561
564 PLANT.PIPEC2.F(15) = 43.3743 ; # 562
565 PLANT.PIPEC2.F(16) = 43.3743 ; # 563
566 PLANT.PIPEC2.F(17) = 43.3743 ; # 564
567 PLANT.PIPEC2.F(18) = 43.3743 ; # 565
568 PLANT.PIPEC2.F(19) = 43.3743 ; # 566
569 PLANT.PIPEC2.F(20) = 43.3743 ; # 567
570 PLANT.PIPEC2.F(21) = 43.3743 ; # 568
571 PLANT.PIPEC2.F(22) = 43.3743 ; # 569
572 PLANT.PIPEC2.F(23) = 43.3743 ; # 570
573 PLANT.PIPEC2.F(24) = 43.3743 ; # 571
574 PLANT.PIPEC2.F(25) = 43.3743 ; # 572

```

575 PLANT.PIPEC2.F(26) = 43.3743 ; # 573
576 PLANT.PIPEC2.F(27) = 43.3743 ; # 574
577 PLANT.PIPEC2.F(28) = 43.3743 ; # 575
578 PLANT.PIPEC2.F(29) = 43.3743 ; # 576
579 PLANT.PIPEC2.F(30) = 43.3743 ; # 577
580 PLANT.PIPEC2.F(31) = 43.3743 ; # 578
581 PLANT.PIPEC2.F(32) = 43.3743 ; # 579
582 PLANT.PIPEC2.F(33) = 43.3743 ; # 580
583 PLANT.PIPEC2.F(34) = 43.3743 ; # 581
584 PLANT.PIPEC2.F(35) = 43.3743 ; # 582
585 PLANT.PIPEC2.F(36) = 43.3743 ; # 583
586 PLANT.PIPEC2.F(37) = 43.3743 ; # 584
587 PLANT.PIPEC2.F(38) = 43.3743 ; # 585
588 PLANT.PIPEC2.F(39) = 43.3743 ; # 586
589 PLANT.PIPEC2.F(40) = 43.3743 ; # 587
590 PLANT.PIPEC2.F_IN = 43.3743 ; # 588
591 PLANT.PIPEC2.PSI(1) = 1.81063e+006 ; # 589
592 PLANT.PIPEC2.PSI(2) = 1.91725e+006 ; # 590
593 PLANT.PIPEC2.PSI(3) = 2.00881e+006 ; # 591
594 PLANT.PIPEC2.PSI(4) = 2.08797e+006 ; # 592
595 PLANT.PIPEC2.PSI(5) = 2.15688e+006 ; # 593
596 PLANT.PIPEC2.PSI(6) = 2.21692e+006 ; # 594
597 PLANT.PIPEC2.PSI(7) = 2.26963e+006 ; # 595
598 PLANT.PIPEC2.PSI(8) = 2.31599e+006 ; # 596
599 PLANT.PIPEC2.PSI(9) = 2.35686e+006 ; # 597
600 PLANT.PIPEC2.PSI(10) = 2.39296e+006 ; # 598
601 PLANT.PIPEC2.PSI(11) = 2.42488e+006 ; # 599
602 PLANT.PIPEC2.PSI(12) = 2.45312e+006 ; # 600
603 PLANT.PIPEC2.PSI(13) = 2.47811e+006 ; # 601
604 PLANT.PIPEC2.PSI(14) = 2.50021e+006 ; # 602
605 PLANT.PIPEC2.PSI(15) = 2.51973e+006 ; # 603
606 PLANT.PIPEC2.PSI(16) = 2.53693e+006 ; # 604
607 PLANT.PIPEC2.PSI(17) = 2.55205e+006 ; # 605
608 PLANT.PIPEC2.PSI(18) = 2.56553e+006 ; # 606
609 PLANT.PIPEC2.PSI(19) = 2.57684e+006 ; # 607
610 PLANT.PIPEC2.PSI(20) = 2.58684e+006 ; # 608
611 PLANT.PIPEC2.PSI(21) = 2.59544e+006 ; # 609
612 PLANT.PIPEC2.PSI(22) = 2.60275e+006 ; # 610
613 PLANT.PIPEC2.PSI(23) = 2.60889e+006 ; # 611
614 PLANT.PIPEC2.PSI(24) = 2.61395e+006 ; # 612
615 PLANT.PIPEC2.PSI(25) = 2.61803e+006 ; # 613
616 PLANT.PIPEC2.PSI(26) = 2.62119e+006 ; # 614
617 PLANT.PIPEC2.PSI(27) = 2.62352e+006 ; # 615
618 PLANT.PIPEC2.PSI(28) = 2.62507e+006 ; # 616
619 PLANT.PIPEC2.PSI(29) = 2.62591e+006 ; # 617
620 PLANT.PIPEC2.PSI(30) = 2.62607e+006 ; # 618
621 PLANT.PIPEC2.PSI(31) = 2.62562e+006 ; # 619
622 PLANT.PIPEC2.PSI(32) = 2.6246e+006 ; # 620
623 PLANT.PIPEC2.PSI(33) = 2.62304e+006 ; # 621
624 PLANT.PIPEC2.PSI(34) = 2.62099e+006 ; # 622
625 PLANT.PIPEC2.PSI(35) = 2.61847e+006 ; # 623
626 PLANT.PIPEC2.PSI(36) = 2.61551e+006 ; # 624
627 PLANT.PIPEC2.PSI(37) = 2.61215e+006 ; # 625
628 PLANT.PIPEC2.PSI(38) = 2.6084e+006 ; # 626
629 PLANT.PIPEC2.PSI(39) = 2.6043e+006 ; # 627
630 PLANT.PIPEC2.PSI(40) = 2.59986e+006 ; # 628

```

HTLFULLDYN_SS_IN_PRE.PRESETS

```

1 # Values for computation HTLFULLDYN_SS
2 # Saved at time 1000
3 PLANT.HX.TGASHOT(1) := 908.671 ; # 1
4 PLANT.HX.TGASHOT(2) := 920.116 ; # 2
5 PLANT.HX.TGASHOT(3) := 931.225 ; # 3
6 PLANT.HX.TGASHOT(4) := 941.988 ; # 4
7 PLANT.HX.TGASHOT(5) := 952.416 ; # 5
8 PLANT.HX.TGASHOT(6) := 962.521 ; # 6
9 PLANT.HX.TGASHOT(7) := 972.311 ; # 7
10 PLANT.HX.TGASHOT(8) := 981.796 ; # 8
11 PLANT.HX.TGASHOT(9) := 990.987 ; # 9
12 PLANT.HX.TGASHOT(10) := 999.892 ; # 10
13 PLANT.HX.TGASHOT(11) := 1008.52 ; # 11
14 PLANT.HX.TGASHOT(12) := 1016.88 ; # 12
15 PLANT.HX.TGASHOT(13) := 1024.98 ; # 13
16 PLANT.HX.TGASHOT(14) := 1032.83 ; # 14
17 PLANT.HX.TGASHOT(15) := 1040.43 ; # 15
18 PLANT.HX.TGASHOT(16) := 1047.8 ; # 16
19 PLANT.HX.TGASHOT(17) := 1054.94 ; # 17
20 PLANT.HX.TGASHOT(18) := 1061.85 ; # 18
21 PLANT.HX.TGASHOT(19) := 1068.55 ; # 19
22 PLANT.HX.TGASHOT(20) := 1075.05 ; # 20
23 PLANT.HX.TGASHOT(21) := 1081.34 ; # 21
24 PLANT.HX.TGASHOT(22) := 1087.43 ; # 22

```


25 PLANT.HX.TGASHOT(23) := 1093.34 ; # 23
26 PLANT.HX.TGASHOT(24) := 1099.06 ; # 24
27 PLANT.HX.TGASHOT(25) := 1104.6 ; # 25
28 PLANT.HX.TGASHOT(26) := 1109.98 ; # 26
29 PLANT.HX.TGASHOT(27) := 1115.18 ; # 27
30 PLANT.HX.TGASHOT(28) := 1120.22 ; # 28
31 PLANT.HX.TGASHOT(29) := 1125.11 ; # 29
32 PLANT.HX.TGASHOT(30) := 1129.84 ; # 30
33 PLANT.HX.TGASHOT(31) := 1134.43 ; # 31
34 PLANT.HX.TGASHOT(32) := 1138.87 ; # 32
35 PLANT.HX.TGASHOT(33) := 1143.18 ; # 33
36 PLANT.HX.TGASHOT(34) := 1147.35 ; # 34
37 PLANT.HX.TGASHOT(35) := 1151.39 ; # 35
38 PLANT.HX.TGASHOT(36) := 1155.31 ; # 36
39 PLANT.HX.TGASHOT(37) := 1159.11 ; # 37
40 PLANT.HX.TGASHOT(38) := 1162.78 ; # 38
41 PLANT.HX.TGASHOT(39) := 1166.35 ; # 39
42 PLANT.HX.TGASHOT(40) := 1169.8 ; # 40
43 PLANT.HX.TGASCOLD(1) := 849.368 ; # 41
44 PLANT.HX.TGASCOLD(2) := 862.676 ; # 42
45 PLANT.HX.TGASCOLD(3) := 875.571 ; # 43
46 PLANT.HX.TGASCOLD(4) := 888.065 ; # 44
47 PLANT.HX.TGASCOLD(5) := 900.17 ; # 45
48 PLANT.HX.TGASCOLD(6) := 911.899 ; # 46
49 PLANT.HX.TGASCOLD(7) := 923.264 ; # 47
50 PLANT.HX.TGASCOLD(8) := 934.274 ; # 48
51 PLANT.HX.TGASCOLD(9) := 944.943 ; # 49
52 PLANT.HX.TGASCOLD(10) := 955.279 ; # 50
53 PLANT.HX.TGASCOLD(11) := 965.295 ; # 51
54 PLANT.HX.TGASCOLD(12) := 974.998 ; # 52
55 PLANT.HX.TGASCOLD(13) := 984.4 ; # 53
56 PLANT.HX.TGASCOLD(14) := 993.51 ; # 54
57 PLANT.HX.TGASCOLD(15) := 1002.34 ; # 55
58 PLANT.HX.TGASCOLD(16) := 1010.89 ; # 56
59 PLANT.HX.TGASCOLD(17) := 1019.17 ; # 57
60 PLANT.HX.TGASCOLD(18) := 1027.2 ; # 58
61 PLANT.HX.TGASCOLD(19) := 1034.98 ; # 59
62 PLANT.HX.TGASCOLD(20) := 1042.52 ; # 60
63 PLANT.HX.TGASCOLD(21) := 1049.82 ; # 61
64 PLANT.HX.TGASCOLD(22) := 1056.9 ; # 62
65 PLANT.HX.TGASCOLD(23) := 1063.75 ; # 63
66 PLANT.HX.TGASCOLD(24) := 1070.39 ; # 64
67 PLANT.HX.TGASCOLD(25) := 1076.83 ; # 65
68 PLANT.HX.TGASCOLD(26) := 1083.06 ; # 66
69 PLANT.HX.TGASCOLD(27) := 1089.11 ; # 67
70 PLANT.HX.TGASCOLD(28) := 1094.96 ; # 68
71 PLANT.HX.TGASCOLD(29) := 1100.63 ; # 69
72 PLANT.HX.TGASCOLD(30) := 1106.13 ; # 70
73 PLANT.HX.TGASCOLD(31) := 1111.45 ; # 71
74 PLANT.HX.TGASCOLD(32) := 1116.61 ; # 72
75 PLANT.HX.TGASCOLD(33) := 1121.61 ; # 73
76 PLANT.HX.TGASCOLD(34) := 1126.45 ; # 74
77 PLANT.HX.TGASCOLD(35) := 1131.14 ; # 75
78 PLANT.HX.TGASCOLD(36) := 1135.69 ; # 76
79 PLANT.HX.TGASCOLD(37) := 1140.09 ; # 77
80 PLANT.HX.TGASCOLD(38) := 1144.36 ; # 78
81 PLANT.HX.TGASCOLD(39) := 1148.5 ; # 79
82 PLANT.HX.TGASCOLD(40) := 1152.5 ; # 80
83 PLANT.HX.UHOT := 1738.41 ; # 81
84 PLANT.HX.UCOLD := 1646.45 ; # 82
85 PLANT.HX.TH(1) := 879.893 ; # 83
86 PLANT.HX.TH(2) := 892.184 ; # 84
87 PLANT.HX.TH(3) := 904.161 ; # 85
88 PLANT.HX.TH(4) := 915.766 ; # 86
89 PLANT.HX.TH(5) := 927.009 ; # 87
90 PLANT.HX.TH(6) := 937.904 ; # 88
91 PLANT.HX.TH(7) := 948.459 ; # 89
92 PLANT.HX.TH(8) := 958.687 ; # 90
93 PLANT.HX.TH(9) := 968.596 ; # 91
94 PLANT.HX.TH(10) := 978.197 ; # 92
95 PLANT.HX.TH(11) := 987.5 ; # 93
96 PLANT.HX.TH(12) := 996.513 ; # 94
97 PLANT.HX.TH(13) := 1005.25 ; # 95
98 PLANT.HX.TH(14) := 1013.71 ; # 96
99 PLANT.HX.TH(15) := 1021.91 ; # 97
100 PLANT.HX.TH(16) := 1029.85 ; # 98
101 PLANT.HX.TH(17) := 1037.55 ; # 99
102 PLANT.HX.TH(18) := 1045 ; # 100
103 PLANT.HX.TH(19) := 1052.23 ; # 101
104 PLANT.HX.TH(20) := 1059.23 ; # 102
105 PLANT.HX.TH(21) := 1066.01 ; # 103
106 PLANT.HX.TH(22) := 1072.58 ; # 104
107 PLANT.HX.TH(23) := 1078.95 ; # 105
108 PLANT.HX.TH(24) := 1085.12 ; # 106
109 PLANT.HX.TH(25) := 1091.1 ; # 107
110 PLANT.HX.TH(26) := 1096.89 ; # 108
111 PLANT.HX.TH(27) := 1102.5 ; # 109
112 PLANT.HX.TH(28) := 1107.94 ; # 110
113 PLANT.HX.TH(29) := 1113.21 ; # 111
114 PLANT.HX.TH(30) := 1118.31 ; # 112
115 PLANT.HX.TH(31) := 1123.26 ; # 113
116 PLANT.HX.TH(32) := 1128.05 ; # 114

```

117 PLANT.HX.THX(33) := 1132.69 ; # 115
118 PLANT.HX.THX(34) := 1137.19 ; # 116
119 PLANT.HX.THX(35) := 1141.55 ; # 117
120 PLANT.HX.THX(36) := 1145.77 ; # 118
121 PLANT.HX.THX(37) := 1149.86 ; # 119
122 PLANT.HX.THX(38) := 1153.83 ; # 120
123 PLANT.HX.THX(39) := 1157.67 ; # 121
124 PLANT.HX.THX(40) := 1161.37 ; # 122
125 PLANT.LOOP1.RHO(1) := 1.15317 ; # 123
126 PLANT.LOOP1.RHO(2) := 1.15067 ; # 124
127 PLANT.LOOP1.RHO(3) := 1.14817 ; # 125
128 PLANT.LOOP1.RHO(4) := 1.14565 ; # 126
129 PLANT.LOOP1.RHO(5) := 1.14313 ; # 127
130 PLANT.LOOP1.RHO(6) := 1.14059 ; # 128
131 PLANT.LOOP1.RHO(7) := 1.13804 ; # 129
132 PLANT.LOOP1.RHO(8) := 1.13549 ; # 130
133 PLANT.LOOP1.RHO(9) := 1.13292 ; # 131
134 PLANT.LOOP1.RHO(10) := 1.13034 ; # 132
135 PLANT.LOOP1.RHO(11) := 1.12115 ; # 133
136 PLANT.LOOP1.RHO(12) := 1.1026 ; # 134
137 PLANT.LOOP1.RHO(13) := 1.08477 ; # 135
138 PLANT.LOOP1.RHO(14) := 1.06791 ; # 136
139 PLANT.LOOP1.RHO(15) := 1.05196 ; # 137
140 PLANT.LOOP1.RHO(16) := 1.03683 ; # 138
141 PLANT.LOOP1.RHO(17) := 1.02247 ; # 139
142 PLANT.LOOP1.RHO(18) := 1.00882 ; # 140
143 PLANT.LOOP1.RHO(19) := 0.99583 ; # 141
144 PLANT.LOOP1.RHO(20) := 0.983453 ; # 142
145 PLANT.LOOP1.RHO(21) := 0.971645 ; # 143
146 PLANT.LOOP1.RHO(22) := 0.960369 ; # 144
147 PLANT.LOOP1.RHO(23) := 0.949588 ; # 145
148 PLANT.LOOP1.RHO(24) := 0.939271 ; # 146
149 PLANT.LOOP1.RHO(25) := 0.929389 ; # 147
150 PLANT.LOOP1.RHO(26) := 0.919912 ; # 148
151 PLANT.LOOP1.RHO(27) := 0.910817 ; # 149
152 PLANT.LOOP1.RHO(28) := 0.90208 ; # 150
153 PLANT.LOOP1.RHO(29) := 0.893679 ; # 151
154 PLANT.LOOP1.RHO(30) := 0.885595 ; # 152
155 PLANT.LOOP1.RHO(31) := 0.87781 ; # 153
156 PLANT.LOOP1.RHO(32) := 0.870305 ; # 154
157 PLANT.LOOP1.RHO(33) := 0.863066 ; # 155
158 PLANT.LOOP1.RHO(34) := 0.856077 ; # 156
159 PLANT.LOOP1.RHO(35) := 0.849325 ; # 157
160 PLANT.LOOP1.RHO(36) := 0.842796 ; # 158
161 PLANT.LOOP1.RHO(37) := 0.83648 ; # 159
162 PLANT.LOOP1.RHO(38) := 0.830363 ; # 160
163 PLANT.LOOP1.RHO(39) := 0.824437 ; # 161
164 PLANT.LOOP1.RHO(40) := 0.818691 ; # 162
165 PLANT.LOOP1.RHO(41) := 0.813116 ; # 163
166 PLANT.LOOP1.RHO(42) := 0.807703 ; # 164
167 PLANT.LOOP1.RHO(43) := 0.802444 ; # 165
168 PLANT.LOOP1.RHO(44) := 0.797332 ; # 166
169 PLANT.LOOP1.RHO(45) := 0.792358 ; # 167
170 PLANT.LOOP1.RHO(46) := 0.787518 ; # 168
171 PLANT.LOOP1.RHO(47) := 0.782803 ; # 169
172 PLANT.LOOP1.RHO(48) := 0.778207 ; # 170
173 PLANT.LOOP1.RHO(49) := 0.773726 ; # 171
174 PLANT.LOOP1.RHO(50) := 0.769358 ; # 172
175 PLANT.LOOP1.RHO(51) := 0.765082 ; # 173
176 PLANT.LOOP1.RHO(52) := 0.760903 ; # 174
177 PLANT.LOOP1.RHO(53) := 0.756826 ; # 175
178 PLANT.LOOP1.RHO(54) := 0.752856 ; # 176
179 PLANT.LOOP1.RHO(55) := 0.750533 ; # 177
180 PLANT.LOOP1.RHO(56) := 0.748658 ; # 178
181 PLANT.LOOP1.RHO(57) := 0.746773 ; # 179
182 PLANT.LOOP1.RHO(58) := 0.744879 ; # 180
183 PLANT.LOOP1.RHO(59) := 0.742974 ; # 181
184 PLANT.LOOP1.RHO(60) := 0.741106 ; # 182
185 PLANT.LOOP1.RHO(61) := 0.750585 ; # 183
186 PLANT.LOOP1.RHO(62) := 0.751689 ; # 184
187 PLANT.LOOP1.RHO(63) := 0.752856 ; # 185
188 PLANT.LOOP1.RHO(64) := 0.754135 ; # 186
189 PLANT.LOOP1.RHO(65) := 0.755533 ; # 187
190 PLANT.LOOP1.RHO(66) := 0.757058 ; # 188
191 PLANT.LOOP1.RHO(67) := 0.75872 ; # 189
192 PLANT.LOOP1.RHO(68) := 0.760528 ; # 190
193 PLANT.LOOP1.RHO(69) := 0.762492 ; # 191
194 PLANT.LOOP1.RHO(70) := 0.764623 ; # 192
195 PLANT.LOOP1.RHO(71) := 0.766934 ; # 193
196 PLANT.LOOP1.RHO(72) := 0.769438 ; # 194
197 PLANT.LOOP1.RHO(73) := 0.772149 ; # 195
198 PLANT.LOOP1.RHO(74) := 0.775082 ; # 196
199 PLANT.LOOP1.RHO(75) := 0.778256 ; # 197
200 PLANT.LOOP1.RHO(76) := 0.781688 ; # 198
201 PLANT.LOOP1.RHO(77) := 0.785399 ; # 199
202 PLANT.LOOP1.RHO(78) := 0.789411 ; # 200
203 PLANT.LOOP1.RHO(79) := 0.793749 ; # 201
204 PLANT.LOOP1.RHO(80) := 0.79844 ; # 202
205 PLANT.LOOP1.RHO(81) := 0.803515 ; # 203
206 PLANT.LOOP1.RHO(82) := 0.809005 ; # 204
207 PLANT.LOOP1.RHO(83) := 0.814949 ; # 205
208 PLANT.LOOP1.RHO(84) := 0.821387 ; # 206

```

209 PLANT.LOOP1.RHO(85) := 0.828364 ; # 207
210 PLANT.LOOP1.RHO(86) := 0.835933 ; # 208
211 PLANT.LOOP1.RHO(87) := 0.844151 ; # 209
212 PLANT.LOOP1.RHO(88) := 0.853082 ; # 210
213 PLANT.LOOP1.RHO(89) := 0.8628 ; # 211
214 PLANT.LOOP1.RHO(90) := 0.873389 ; # 212
215 PLANT.LOOP1.RHO(91) := 0.884944 ; # 213
216 PLANT.LOOP1.RHO(92) := 0.897573 ; # 214
217 PLANT.LOOP1.RHO(93) := 0.911403 ; # 215
218 PLANT.LOOP1.RHO(94) := 0.926579 ; # 216
219 PLANT.LOOP1.RHO(95) := 0.94327 ; # 217
220 PLANT.LOOP1.RHO(96) := 0.961674 ; # 218
221 PLANT.LOOP1.RHO(97) := 0.982026 ; # 219
222 PLANT.LOOP1.RHO(98) := 1.0046 ; # 220
223 PLANT.LOOP1.RHO(99) := 1.02974 ; # 221
224 PLANT.LOOP1.RHO(100) := 1.05783 ; # 222
225 PLANT.LOOP1.P(1) := 2.01181e+006 ; # 223
226 PLANT.LOOP1.P(2) := 2.00646e+006 ; # 224
227 PLANT.LOOP1.P(3) := 2.00109e+006 ; # 225
228 PLANT.LOOP1.P(4) := 1.99571e+006 ; # 226
229 PLANT.LOOP1.P(5) := 1.99032e+006 ; # 227
230 PLANT.LOOP1.P(6) := 1.98491e+006 ; # 228
231 PLANT.LOOP1.P(7) := 1.9795e+006 ; # 229
232 PLANT.LOOP1.P(8) := 1.97407e+006 ; # 230
233 PLANT.LOOP1.P(9) := 1.96863e+006 ; # 231
234 PLANT.LOOP1.P(10) := 1.96317e+006 ; # 232
235 PLANT.LOOP1.P(11) := 1.97929e+006 ; # 233
236 PLANT.LOOP1.P(12) := 1.97704e+006 ; # 234
237 PLANT.LOOP1.P(13) := 1.97414e+006 ; # 235
238 PLANT.LOOP1.P(14) := 1.9712e+006 ; # 236
239 PLANT.LOOP1.P(15) := 1.96822e+006 ; # 237
240 PLANT.LOOP1.P(16) := 1.96519e+006 ; # 238
241 PLANT.LOOP1.P(17) := 1.96212e+006 ; # 239
242 PLANT.LOOP1.P(18) := 1.95902e+006 ; # 240
243 PLANT.LOOP1.P(19) := 1.95587e+006 ; # 241
244 PLANT.LOOP1.P(20) := 1.95269e+006 ; # 242
245 PLANT.LOOP1.P(21) := 1.94947e+006 ; # 243
246 PLANT.LOOP1.P(22) := 1.94622e+006 ; # 244
247 PLANT.LOOP1.P(23) := 1.94293e+006 ; # 245
248 PLANT.LOOP1.P(24) := 1.93961e+006 ; # 246
249 PLANT.LOOP1.P(25) := 1.93625e+006 ; # 247
250 PLANT.LOOP1.P(26) := 1.93286e+006 ; # 248
251 PLANT.LOOP1.P(27) := 1.92943e+006 ; # 249
252 PLANT.LOOP1.P(28) := 1.92598e+006 ; # 250
253 PLANT.LOOP1.P(29) := 1.92249e+006 ; # 251
254 PLANT.LOOP1.P(30) := 1.91897e+006 ; # 252
255 PLANT.LOOP1.P(31) := 1.91543e+006 ; # 253
256 PLANT.LOOP1.P(32) := 1.91185e+006 ; # 254
257 PLANT.LOOP1.P(33) := 1.90824e+006 ; # 255
258 PLANT.LOOP1.P(34) := 1.90461e+006 ; # 256
259 PLANT.LOOP1.P(35) := 1.90095e+006 ; # 257
260 PLANT.LOOP1.P(36) := 1.89726e+006 ; # 258
261 PLANT.LOOP1.P(37) := 1.89354e+006 ; # 259
262 PLANT.LOOP1.P(38) := 1.8898e+006 ; # 260
263 PLANT.LOOP1.P(39) := 1.88603e+006 ; # 261
264 PLANT.LOOP1.P(40) := 1.88224e+006 ; # 262
265 PLANT.LOOP1.P(41) := 1.87842e+006 ; # 263
266 PLANT.LOOP1.P(42) := 1.87458e+006 ; # 264
267 PLANT.LOOP1.P(43) := 1.87071e+006 ; # 265
268 PLANT.LOOP1.P(44) := 1.86681e+006 ; # 266
269 PLANT.LOOP1.P(45) := 1.8629e+006 ; # 267
270 PLANT.LOOP1.P(46) := 1.85896e+006 ; # 268
271 PLANT.LOOP1.P(47) := 1.855e+006 ; # 269
272 PLANT.LOOP1.P(48) := 1.85101e+006 ; # 270
273 PLANT.LOOP1.P(49) := 1.847e+006 ; # 271
274 PLANT.LOOP1.P(50) := 1.84297e+006 ; # 272
275 PLANT.LOOP1.P(51) := 1.81438e+006 ; # 273
276 PLANT.LOOP1.P(52) := 1.80865e+006 ; # 274
277 PLANT.LOOP1.P(53) := 1.80295e+006 ; # 275
278 PLANT.LOOP1.P(54) := 1.79723e+006 ; # 276
279 PLANT.LOOP1.P(55) := 1.7915e+006 ; # 277
280 PLANT.LOOP1.P(56) := 1.78576e+006 ; # 278
281 PLANT.LOOP1.P(57) := 1.78e+006 ; # 279
282 PLANT.LOOP1.P(58) := 1.77423e+006 ; # 280
283 PLANT.LOOP1.P(59) := 1.76844e+006 ; # 281
284 PLANT.LOOP1.P(60) := 1.76263e+006 ; # 282
285 PLANT.LOOP1.P(61) := 1.78151e+006 ; # 283
286 PLANT.LOOP1.P(62) := 1.78014e+006 ; # 284
287 PLANT.LOOP1.P(63) := 1.77866e+006 ; # 285
288 PLANT.LOOP1.P(64) := 1.77719e+006 ; # 286
289 PLANT.LOOP1.P(65) := 1.77573e+006 ; # 287
290 PLANT.LOOP1.P(66) := 1.77427e+006 ; # 288
291 PLANT.LOOP1.P(67) := 1.77281e+006 ; # 289
292 PLANT.LOOP1.P(68) := 1.77136e+006 ; # 290
293 PLANT.LOOP1.P(69) := 1.76991e+006 ; # 291
294 PLANT.LOOP1.P(70) := 1.76847e+006 ; # 292
295 PLANT.LOOP1.P(71) := 1.76703e+006 ; # 293
296 PLANT.LOOP1.P(72) := 1.7656e+006 ; # 294
297 PLANT.LOOP1.P(73) := 1.76417e+006 ; # 295
298 PLANT.LOOP1.P(74) := 1.76275e+006 ; # 296
299 PLANT.LOOP1.P(75) := 1.76134e+006 ; # 297
300 PLANT.LOOP1.P(76) := 1.75993e+006 ; # 298

```

301 PLANT.LOOP1.P(77) := 1.75854e+006 ; # 299
302 PLANT.LOOP1.P(78) := 1.75715e+006 ; # 300
303 PLANT.LOOP1.P(79) := 1.75577e+006 ; # 301
304 PLANT.LOOP1.P(80) := 1.75441e+006 ; # 302
305 PLANT.LOOP1.P(81) := 1.75305e+006 ; # 303
306 PLANT.LOOP1.P(82) := 1.7517e+006 ; # 304
307 PLANT.LOOP1.P(83) := 1.75037e+006 ; # 305
308 PLANT.LOOP1.P(84) := 1.74905e+006 ; # 306
309 PLANT.LOOP1.P(85) := 1.74774e+006 ; # 307
310 PLANT.LOOP1.P(86) := 1.74645e+006 ; # 308
311 PLANT.LOOP1.P(87) := 1.74518e+006 ; # 309
312 PLANT.LOOP1.P(88) := 1.74392e+006 ; # 310
313 PLANT.LOOP1.P(89) := 1.74267e+006 ; # 311
314 PLANT.LOOP1.P(90) := 1.74145e+006 ; # 312
315 PLANT.LOOP1.P(91) := 1.74025e+006 ; # 313
316 PLANT.LOOP1.P(92) := 1.73907e+006 ; # 314
317 PLANT.LOOP1.P(93) := 1.73791e+006 ; # 315
318 PLANT.LOOP1.P(94) := 1.73677e+006 ; # 316
319 PLANT.LOOP1.P(95) := 1.73566e+006 ; # 317
320 PLANT.LOOP1.P(96) := 1.73458e+006 ; # 318
321 PLANT.LOOP1.P(97) := 1.73353e+006 ; # 319
322 PLANT.LOOP1.P(98) := 1.7325e+006 ; # 320
323 PLANT.LOOP1.P(99) := 1.73151e+006 ; # 321
324 PLANT.LOOP1.P(100) := 1.73056e+006 ; # 322
325 PLANT.LOOP1.P_OUT := 1.73003e+006 ; # 323
326 PLANT.LOOP1.H(1) := 2.81232e+006 ; # 324
327 PLANT.LOOP1.H(2) := 2.81015e+006 ; # 325
328 PLANT.LOOP1.H(3) := 2.80798e+006 ; # 326
329 PLANT.LOOP1.H(4) := 2.80581e+006 ; # 327
330 PLANT.LOOP1.H(5) := 2.80364e+006 ; # 328
331 PLANT.LOOP1.H(6) := 2.80148e+006 ; # 329
332 PLANT.LOOP1.H(7) := 2.79931e+006 ; # 330
333 PLANT.LOOP1.H(8) := 2.79715e+006 ; # 331
334 PLANT.LOOP1.H(9) := 2.79499e+006 ; # 332
335 PLANT.LOOP1.H(10) := 2.79283e+006 ; # 333
336 PLANT.LOOP1.H(11) := 2.86435e+006 ; # 334
337 PLANT.LOOP1.H(12) := 2.93349e+006 ; # 335
338 PLANT.LOOP1.H(13) := 3.00048e+006 ; # 336
339 PLANT.LOOP1.H(14) := 3.06539e+006 ; # 337
340 PLANT.LOOP1.H(15) := 3.12828e+006 ; # 338
341 PLANT.LOOP1.H(16) := 3.18921e+006 ; # 339
342 PLANT.LOOP1.H(17) := 3.24824e+006 ; # 340
343 PLANT.LOOP1.H(18) := 3.30545e+006 ; # 341
344 PLANT.LOOP1.H(19) := 3.36087e+006 ; # 342
345 PLANT.LOOP1.H(20) := 3.41457e+006 ; # 343
346 PLANT.LOOP1.H(21) := 3.4666e+006 ; # 344
347 PLANT.LOOP1.H(22) := 3.51701e+006 ; # 345
348 PLANT.LOOP1.H(23) := 3.56585e+006 ; # 346
349 PLANT.LOOP1.H(24) := 3.61317e+006 ; # 347
350 PLANT.LOOP1.H(25) := 3.65903e+006 ; # 348
351 PLANT.LOOP1.H(26) := 3.70345e+006 ; # 349
352 PLANT.LOOP1.H(27) := 3.7465e+006 ; # 350
353 PLANT.LOOP1.H(28) := 3.78821e+006 ; # 351
354 PLANT.LOOP1.H(29) := 3.82862e+006 ; # 352
355 PLANT.LOOP1.H(30) := 3.86777e+006 ; # 353
356 PLANT.LOOP1.H(31) := 3.90571e+006 ; # 354
357 PLANT.LOOP1.H(32) := 3.94246e+006 ; # 355
358 PLANT.LOOP1.H(33) := 3.97808e+006 ; # 356
359 PLANT.LOOP1.H(34) := 4.01258e+006 ; # 357
360 PLANT.LOOP1.H(35) := 4.04601e+006 ; # 358
361 PLANT.LOOP1.H(36) := 4.07841e+006 ; # 359
362 PLANT.LOOP1.H(37) := 4.10979e+006 ; # 360
363 PLANT.LOOP1.H(38) := 4.1402e+006 ; # 361
364 PLANT.LOOP1.H(39) := 4.16967e+006 ; # 362
365 PLANT.LOOP1.H(40) := 4.19822e+006 ; # 363
366 PLANT.LOOP1.H(41) := 4.22588e+006 ; # 364
367 PLANT.LOOP1.H(42) := 4.25268e+006 ; # 365
368 PLANT.LOOP1.H(43) := 4.27864e+006 ; # 366
369 PLANT.LOOP1.H(44) := 4.3038e+006 ; # 367
370 PLANT.LOOP1.H(45) := 4.32818e+006 ; # 368
371 PLANT.LOOP1.H(46) := 4.3518e+006 ; # 369
372 PLANT.LOOP1.H(47) := 4.37468e+006 ; # 370
373 PLANT.LOOP1.H(48) := 4.39685e+006 ; # 371
374 PLANT.LOOP1.H(49) := 4.41834e+006 ; # 372
375 PLANT.LOOP1.H(50) := 4.43912e+006 ; # 373
376 PLANT.LOOP1.H(51) := 4.43487e+006 ; # 374
377 PLANT.LOOP1.H(52) := 4.43062e+006 ; # 375
378 PLANT.LOOP1.H(53) := 4.42637e+006 ; # 376
379 PLANT.LOOP1.H(54) := 4.42213e+006 ; # 377
380 PLANT.LOOP1.H(55) := 4.41789e+006 ; # 378
381 PLANT.LOOP1.H(56) := 4.41366e+006 ; # 379
382 PLANT.LOOP1.H(57) := 4.40943e+006 ; # 380
383 PLANT.LOOP1.H(58) := 4.40521e+006 ; # 381
384 PLANT.LOOP1.H(59) := 4.40099e+006 ; # 382
385 PLANT.LOOP1.H(60) := 4.39677e+006 ; # 383
386 PLANT.LOOP1.H(61) := 4.38421e+006 ; # 384
387 PLANT.LOOP1.H(62) := 4.37092e+006 ; # 385
388 PLANT.LOOP1.H(63) := 4.35686e+006 ; # 386
389 PLANT.LOOP1.H(64) := 4.34197e+006 ; # 387
390 PLANT.LOOP1.H(65) := 4.32623e+006 ; # 388
391 PLANT.LOOP1.H(66) := 4.30957e+006 ; # 389
392 PLANT.LOOP1.H(67) := 4.29193e+006 ; # 390

```

```

393 PLANT.LOOP1.H(68) := 4.27328e+006 ; # 391
394 PLANT.LOOP1.H(69) := 4.25354e+006 ; # 392
395 PLANT.LOOP1.H(70) := 4.23265e+006 ; # 393
396 PLANT.LOOP1.H(71) := 4.21054e+006 ; # 394
397 PLANT.LOOP1.H(72) := 4.18715e+006 ; # 395
398 PLANT.LOOP1.H(73) := 4.1624e+006 ; # 396
399 PLANT.LOOP1.H(74) := 4.13621e+006 ; # 397
400 PLANT.LOOP1.H(75) := 4.1085e+006 ; # 398
401 PLANT.LOOP1.H(76) := 4.07917e+006 ; # 399
402 PLANT.LOOP1.H(77) := 4.04814e+006 ; # 400
403 PLANT.LOOP1.H(78) := 4.01531e+006 ; # 401
404 PLANT.LOOP1.H(79) := 3.98056e+006 ; # 402
405 PLANT.LOOP1.H(80) := 3.9438e+006 ; # 403
406 PLANT.LOOP1.H(81) := 3.90489e+006 ; # 404
407 PLANT.LOOP1.H(82) := 3.86373e+006 ; # 405
408 PLANT.LOOP1.H(83) := 3.82017e+006 ; # 406
409 PLANT.LOOP1.H(84) := 3.77408e+006 ; # 407
410 PLANT.LOOP1.H(85) := 3.7253e+006 ; # 408
411 PLANT.LOOP1.H(86) := 3.67369e+006 ; # 409
412 PLANT.LOOP1.H(87) := 3.61908e+006 ; # 410
413 PLANT.LOOP1.H(88) := 3.5613e+006 ; # 411
414 PLANT.LOOP1.H(89) := 3.50015e+006 ; # 412
415 PLANT.LOOP1.H(90) := 3.43544e+006 ; # 413
416 PLANT.LOOP1.H(91) := 3.36698e+006 ; # 414
417 PLANT.LOOP1.H(92) := 3.29453e+006 ; # 415
418 PLANT.LOOP1.H(93) := 3.21787e+006 ; # 416
419 PLANT.LOOP1.H(94) := 3.13674e+006 ; # 417
420 PLANT.LOOP1.H(95) := 3.05091e+006 ; # 418
421 PLANT.LOOP1.H(96) := 2.96008e+006 ; # 419
422 PLANT.LOOP1.H(97) := 2.86396e+006 ; # 420
423 PLANT.LOOP1.H(98) := 2.76226e+006 ; # 421
424 PLANT.LOOP1.H(99) := 2.65465e+006 ; # 422
425 PLANT.LOOP1.H(100) := 2.54078e+006 ; # 423
426 PLANT.LOOP1.HO := 2.81449e+006 ; # 424
427 PLANT.LOOP1.T(1) := 839.351 ; # 425
428 PLANT.LOOP1.T(2) := 838.933 ; # 426
429 PLANT.LOOP1.T(3) := 838.515 ; # 427
430 PLANT.LOOP1.T(4) := 838.098 ; # 428
431 PLANT.LOOP1.T(5) := 837.681 ; # 429
432 PLANT.LOOP1.T(6) := 837.264 ; # 430
433 PLANT.LOOP1.T(7) := 836.847 ; # 431
434 PLANT.LOOP1.T(8) := 836.431 ; # 432
435 PLANT.LOOP1.T(9) := 836.015 ; # 433
436 PLANT.LOOP1.T(10) := 835.6 ; # 434
437 PLANT.LOOP1.T(11) := 849.368 ; # 435
438 PLANT.LOOP1.T(12) := 862.676 ; # 436
439 PLANT.LOOP1.T(13) := 875.571 ; # 437
440 PLANT.LOOP1.T(14) := 888.065 ; # 438
441 PLANT.LOOP1.T(15) := 900.17 ; # 439
442 PLANT.LOOP1.T(16) := 911.899 ; # 440
443 PLANT.LOOP1.T(17) := 923.264 ; # 441
444 PLANT.LOOP1.T(18) := 934.274 ; # 442
445 PLANT.LOOP1.T(19) := 944.943 ; # 443
446 PLANT.LOOP1.T(20) := 955.279 ; # 444
447 PLANT.LOOP1.T(21) := 965.295 ; # 445
448 PLANT.LOOP1.T(22) := 974.998 ; # 446
449 PLANT.LOOP1.T(23) := 984.4 ; # 447
450 PLANT.LOOP1.T(24) := 993.51 ; # 448
451 PLANT.LOOP1.T(25) := 1002.34 ; # 449
452 PLANT.LOOP1.T(26) := 1010.89 ; # 450
453 PLANT.LOOP1.T(27) := 1019.17 ; # 451
454 PLANT.LOOP1.T(28) := 1027.2 ; # 452
455 PLANT.LOOP1.T(29) := 1034.98 ; # 453
456 PLANT.LOOP1.T(30) := 1042.52 ; # 454
457 PLANT.LOOP1.T(31) := 1049.82 ; # 455
458 PLANT.LOOP1.T(32) := 1056.9 ; # 456
459 PLANT.LOOP1.T(33) := 1063.75 ; # 457
460 PLANT.LOOP1.T(34) := 1070.39 ; # 458
461 PLANT.LOOP1.T(35) := 1076.83 ; # 459
462 PLANT.LOOP1.T(36) := 1083.06 ; # 460
463 PLANT.LOOP1.T(37) := 1089.11 ; # 461
464 PLANT.LOOP1.T(38) := 1094.96 ; # 462
465 PLANT.LOOP1.T(39) := 1100.63 ; # 463
466 PLANT.LOOP1.T(40) := 1106.13 ; # 464
467 PLANT.LOOP1.T(41) := 1111.45 ; # 465
468 PLANT.LOOP1.T(42) := 1116.61 ; # 466
469 PLANT.LOOP1.T(43) := 1121.61 ; # 467
470 PLANT.LOOP1.T(44) := 1126.45 ; # 468
471 PLANT.LOOP1.T(45) := 1131.14 ; # 469
472 PLANT.LOOP1.T(46) := 1135.69 ; # 470
473 PLANT.LOOP1.T(47) := 1140.09 ; # 471
474 PLANT.LOOP1.T(48) := 1144.36 ; # 472
475 PLANT.LOOP1.T(49) := 1148.5 ; # 473
476 PLANT.LOOP1.T(50) := 1152.5 ; # 474
477 PLANT.LOOP1.T(51) := 1151.68 ; # 475
478 PLANT.LOOP1.T(52) := 1150.86 ; # 476
479 PLANT.LOOP1.T(53) := 1150.04 ; # 477
480 PLANT.LOOP1.T(54) := 1149.23 ; # 478
481 PLANT.LOOP1.T(55) := 1148.41 ; # 479
482 PLANT.LOOP1.T(56) := 1147.6 ; # 480
483 PLANT.LOOP1.T(57) := 1146.78 ; # 481
484 PLANT.LOOP1.T(58) := 1145.97 ; # 482

```

```

485 PLANT.LOOP1.T(59) := 1145.16 ; # 483
486 PLANT.LOOP1.T(60) := 1144.35 ; # 484
487 PLANT.LOOP1.T(61) := 1141.93 ; # 485
488 PLANT.LOOP1.T(62) := 1139.37 ; # 486
489 PLANT.LOOP1.T(63) := 1136.66 ; # 487
490 PLANT.LOOP1.T(64) := 1133.8 ; # 488
491 PLANT.LOOP1.T(65) := 1130.77 ; # 489
492 PLANT.LOOP1.T(66) := 1127.56 ; # 490
493 PLANT.LOOP1.T(67) := 1124.17 ; # 491
494 PLANT.LOOP1.T(68) := 1120.57 ; # 492
495 PLANT.LOOP1.T(69) := 1116.77 ; # 493
496 PLANT.LOOP1.T(70) := 1112.75 ; # 494
497 PLANT.LOOP1.T(71) := 1108.5 ; # 495
498 PLANT.LOOP1.T(72) := 1104 ; # 496
499 PLANT.LOOP1.T(73) := 1099.23 ; # 497
500 PLANT.LOOP1.T(74) := 1094.19 ; # 498
501 PLANT.LOOP1.T(75) := 1088.86 ; # 499
502 PLANT.LOOP1.T(76) := 1083.21 ; # 500
503 PLANT.LOOP1.T(77) := 1077.24 ; # 501
504 PLANT.LOOP1.T(78) := 1070.92 ; # 502
505 PLANT.LOOP1.T(79) := 1064.23 ; # 503
506 PLANT.LOOP1.T(80) := 1057.15 ; # 504
507 PLANT.LOOP1.T(81) := 1049.66 ; # 505
508 PLANT.LOOP1.T(82) := 1041.74 ; # 506
509 PLANT.LOOP1.T(83) := 1033.36 ; # 507
510 PLANT.LOOP1.T(84) := 1024.48 ; # 508
511 PLANT.LOOP1.T(85) := 1015.09 ; # 509
512 PLANT.LOOP1.T(86) := 1005.16 ; # 510
513 PLANT.LOOP1.T(87) := 994.647 ; # 511
514 PLANT.LOOP1.T(88) := 983.524 ; # 512
515 PLANT.LOOP1.T(89) := 971.753 ; # 513
516 PLANT.LOOP1.T(90) := 959.298 ; # 514
517 PLANT.LOOP1.T(91) := 946.119 ; # 515
518 PLANT.LOOP1.T(92) := 932.173 ; # 516
519 PLANT.LOOP1.T(93) := 917.416 ; # 517
520 PLANT.LOOP1.T(94) := 901.801 ; # 518
521 PLANT.LOOP1.T(95) := 885.278 ; # 519
522 PLANT.LOOP1.T(96) := 867.793 ; # 520
523 PLANT.LOOP1.T(97) := 849.292 ; # 521
524 PLANT.LOOP1.T(98) := 829.715 ; # 522
525 PLANT.LOOP1.T(99) := 809 ; # 523
526 PLANT.LOOP1.T(100) := 787.081 ; # 524
527 PLANT.LOOP1.TO := 839.77 ; # 525
528 PLANT.LOOP1.TEXTRNL(1) := 291.15 ; # 526
529 PLANT.LOOP1.TEXTRNL(2) := 291.15 ; # 527
530 PLANT.LOOP1.TEXTRNL(3) := 291.15 ; # 528
531 PLANT.LOOP1.TEXTRNL(4) := 291.15 ; # 529
532 PLANT.LOOP1.TEXTRNL(5) := 291.15 ; # 530
533 PLANT.LOOP1.TEXTRNL(6) := 291.15 ; # 531
534 PLANT.LOOP1.TEXTRNL(7) := 291.15 ; # 532
535 PLANT.LOOP1.TEXTRNL(8) := 291.15 ; # 533
536 PLANT.LOOP1.TEXTRNL(9) := 291.15 ; # 534
537 PLANT.LOOP1.TEXTRNL(10) := 291.15 ; # 535
538 PLANT.LOOP1.TEXTRNL(11) := 879.893 ; # 536
539 PLANT.LOOP1.TEXTRNL(12) := 892.184 ; # 537
540 PLANT.LOOP1.TEXTRNL(13) := 904.161 ; # 538
541 PLANT.LOOP1.TEXTRNL(14) := 915.766 ; # 539
542 PLANT.LOOP1.TEXTRNL(15) := 927.009 ; # 540
543 PLANT.LOOP1.TEXTRNL(16) := 937.904 ; # 541
544 PLANT.LOOP1.TEXTRNL(17) := 948.459 ; # 542
545 PLANT.LOOP1.TEXTRNL(18) := 958.687 ; # 543
546 PLANT.LOOP1.TEXTRNL(19) := 968.596 ; # 544
547 PLANT.LOOP1.TEXTRNL(20) := 978.197 ; # 545
548 PLANT.LOOP1.TEXTRNL(21) := 987.5 ; # 546
549 PLANT.LOOP1.TEXTRNL(22) := 996.513 ; # 547
550 PLANT.LOOP1.TEXTRNL(23) := 1005.25 ; # 548
551 PLANT.LOOP1.TEXTRNL(24) := 1013.71 ; # 549
552 PLANT.LOOP1.TEXTRNL(25) := 1021.91 ; # 550
553 PLANT.LOOP1.TEXTRNL(26) := 1029.85 ; # 551
554 PLANT.LOOP1.TEXTRNL(27) := 1037.55 ; # 552
555 PLANT.LOOP1.TEXTRNL(28) := 1045 ; # 553
556 PLANT.LOOP1.TEXTRNL(29) := 1052.23 ; # 554
557 PLANT.LOOP1.TEXTRNL(30) := 1059.23 ; # 555
558 PLANT.LOOP1.TEXTRNL(31) := 1066.01 ; # 556
559 PLANT.LOOP1.TEXTRNL(32) := 1072.58 ; # 557
560 PLANT.LOOP1.TEXTRNL(33) := 1078.95 ; # 558
561 PLANT.LOOP1.TEXTRNL(34) := 1085.12 ; # 559
562 PLANT.LOOP1.TEXTRNL(35) := 1091.1 ; # 560
563 PLANT.LOOP1.TEXTRNL(36) := 1096.89 ; # 561
564 PLANT.LOOP1.TEXTRNL(37) := 1102.5 ; # 562
565 PLANT.LOOP1.TEXTRNL(38) := 1107.94 ; # 563
566 PLANT.LOOP1.TEXTRNL(39) := 1113.21 ; # 564
567 PLANT.LOOP1.TEXTRNL(40) := 1118.31 ; # 565
568 PLANT.LOOP1.TEXTRNL(41) := 1123.26 ; # 566
569 PLANT.LOOP1.TEXTRNL(42) := 1128.05 ; # 567
570 PLANT.LOOP1.TEXTRNL(43) := 1132.69 ; # 568
571 PLANT.LOOP1.TEXTRNL(44) := 1137.19 ; # 569
572 PLANT.LOOP1.TEXTRNL(45) := 1141.55 ; # 570
573 PLANT.LOOP1.TEXTRNL(46) := 1145.77 ; # 571
574 PLANT.LOOP1.TEXTRNL(47) := 1149.86 ; # 572
575 PLANT.LOOP1.TEXTRNL(48) := 1153.83 ; # 573
576 PLANT.LOOP1.TEXTRNL(49) := 1157.67 ; # 574

```

```

577 PLANT.LOOP1.TEXTRNL(50) := 1161.37 ; # 575
578 PLANT.LOOP1.TEXTRNL(51) := 291.15 ; # 576
579 PLANT.LOOP1.TEXTRNL(52) := 291.15 ; # 577
580 PLANT.LOOP1.TEXTRNL(53) := 291.15 ; # 578
581 PLANT.LOOP1.TEXTRNL(54) := 291.15 ; # 579
582 PLANT.LOOP1.TEXTRNL(55) := 291.15 ; # 580
583 PLANT.LOOP1.TEXTRNL(56) := 291.15 ; # 581
584 PLANT.LOOP1.TEXTRNL(57) := 291.15 ; # 582
585 PLANT.LOOP1.TEXTRNL(58) := 291.15 ; # 583
586 PLANT.LOOP1.TEXTRNL(59) := 291.15 ; # 584
587 PLANT.LOOP1.TEXTRNL(60) := 291.15 ; # 585
588 PLANT.LOOP1.TEXTRNL(61) := 1133.71 ; # 586
589 PLANT.LOOP1.TEXTRNL(62) := 1130.67 ; # 587
590 PLANT.LOOP1.TEXTRNL(63) := 1127.46 ; # 588
591 PLANT.LOOP1.TEXTRNL(64) := 1124.06 ; # 589
592 PLANT.LOOP1.TEXTRNL(65) := 1120.46 ; # 590
593 PLANT.LOOP1.TEXTRNL(66) := 1116.65 ; # 591
594 PLANT.LOOP1.TEXTRNL(67) := 1112.63 ; # 592
595 PLANT.LOOP1.TEXTRNL(68) := 1108.36 ; # 593
596 PLANT.LOOP1.TEXTRNL(69) := 1103.85 ; # 594
597 PLANT.LOOP1.TEXTRNL(70) := 1099.08 ; # 595
598 PLANT.LOOP1.TEXTRNL(71) := 1094.03 ; # 596
599 PLANT.LOOP1.TEXTRNL(72) := 1088.69 ; # 597
600 PLANT.LOOP1.TEXTRNL(73) := 1083.03 ; # 598
601 PLANT.LOOP1.TEXTRNL(74) := 1077.05 ; # 599
602 PLANT.LOOP1.TEXTRNL(75) := 1070.72 ; # 600
603 PLANT.LOOP1.TEXTRNL(76) := 1064.02 ; # 601
604 PLANT.LOOP1.TEXTRNL(77) := 1056.93 ; # 602
605 PLANT.LOOP1.TEXTRNL(78) := 1049.43 ; # 603
606 PLANT.LOOP1.TEXTRNL(79) := 1041.49 ; # 604
607 PLANT.LOOP1.TEXTRNL(80) := 1033.09 ; # 605
608 PLANT.LOOP1.TEXTRNL(81) := 1024.2 ; # 606
609 PLANT.LOOP1.TEXTRNL(82) := 1014.8 ; # 607
610 PLANT.LOOP1.TEXTRNL(83) := 1004.84 ; # 608
611 PLANT.LOOP1.TEXTRNL(84) := 994.314 ; # 609
612 PLANT.LOOP1.TEXTRNL(85) := 983.171 ; # 610
613 PLANT.LOOP1.TEXTRNL(86) := 971.38 ; # 611
614 PLANT.LOOP1.TEXTRNL(87) := 958.903 ; # 612
615 PLANT.LOOP1.TEXTRNL(88) := 945.701 ; # 613
616 PLANT.LOOP1.TEXTRNL(89) := 931.731 ; # 614
617 PLANT.LOOP1.TEXTRNL(90) := 916.948 ; # 615
618 PLANT.LOOP1.TEXTRNL(91) := 901.306 ; # 616
619 PLANT.LOOP1.TEXTRNL(92) := 884.754 ; # 617
620 PLANT.LOOP1.TEXTRNL(93) := 867.239 ; # 618
621 PLANT.LOOP1.TEXTRNL(94) := 848.706 ; # 619
622 PLANT.LOOP1.TEXTRNL(95) := 829.095 ; # 620
623 PLANT.LOOP1.TEXTRNL(96) := 808.344 ; # 621
624 PLANT.LOOP1.TEXTRNL(97) := 786.385 ; # 622
625 PLANT.LOOP1.TEXTRNL(98) := 763.15 ; # 623
626 PLANT.LOOP1.TEXTRNL(99) := 738.563 ; # 624
627 PLANT.LOOP1.TEXTRNL(100) := 712.554 ; # 625
628 PLANT.LOOP1.PSI(1) := 1.23127e+006 ; # 626
629 PLANT.LOOP1.PSI(2) := 1.22711e+006 ; # 627
630 PLANT.LOOP1.PSI(3) := 1.22294e+006 ; # 628
631 PLANT.LOOP1.PSI(4) := 1.21877e+006 ; # 629
632 PLANT.LOOP1.PSI(5) := 1.2146e+006 ; # 630
633 PLANT.LOOP1.PSI(6) := 1.21042e+006 ; # 631
634 PLANT.LOOP1.PSI(7) := 1.20624e+006 ; # 632
635 PLANT.LOOP1.PSI(8) := 1.20206e+006 ; # 633
636 PLANT.LOOP1.PSI(9) := 1.19787e+006 ; # 634
637 PLANT.LOOP1.PSI(10) := 1.19368e+006 ; # 635
638 PLANT.LOOP1.PSI(11) := 1.23208e+006 ; # 636
639 PLANT.LOOP1.PSI(12) := 1.25743e+006 ; # 637
640 PLANT.LOOP1.PSI(13) := 1.28069e+006 ; # 638
641 PLANT.LOOP1.PSI(14) := 1.30237e+006 ; # 639
642 PLANT.LOOP1.PSI(15) := 1.32259e+006 ; # 640
643 PLANT.LOOP1.PSI(16) := 1.34148e+006 ; # 641
644 PLANT.LOOP1.PSI(17) := 1.35911e+006 ; # 642
645 PLANT.LOOP1.PSI(18) := 1.37558e+006 ; # 643
646 PLANT.LOOP1.PSI(19) := 1.39098e+006 ; # 644
647 PLANT.LOOP1.PSI(20) := 1.40537e+006 ; # 645
648 PLANT.LOOP1.PSI(21) := 1.41883e+006 ; # 646
649 PLANT.LOOP1.PSI(22) := 1.4314e+006 ; # 647
650 PLANT.LOOP1.PSI(23) := 1.44316e+006 ; # 648
651 PLANT.LOOP1.PSI(24) := 1.45415e+006 ; # 649
652 PLANT.LOOP1.PSI(25) := 1.46441e+006 ; # 650
653 PLANT.LOOP1.PSI(26) := 1.474e+006 ; # 651
654 PLANT.LOOP1.PSI(27) := 1.48294e+006 ; # 652
655 PLANT.LOOP1.PSI(28) := 1.49129e+006 ; # 653
656 PLANT.LOOP1.PSI(29) := 1.49907e+006 ; # 654
657 PLANT.LOOP1.PSI(30) := 1.50631e+006 ; # 655
658 PLANT.LOOP1.PSI(31) := 1.51304e+006 ; # 656
659 PLANT.LOOP1.PSI(32) := 1.5193e+006 ; # 657
660 PLANT.LOOP1.PSI(33) := 1.5251e+006 ; # 658
661 PLANT.LOOP1.PSI(34) := 1.53047e+006 ; # 659
662 PLANT.LOOP1.PSI(35) := 1.53543e+006 ; # 660
663 PLANT.LOOP1.PSI(36) := 1.54001e+006 ; # 661
664 PLANT.LOOP1.PSI(37) := 1.54421e+006 ; # 662
665 PLANT.LOOP1.PSI(38) := 1.54807e+006 ; # 663
666 PLANT.LOOP1.PSI(39) := 1.5516e+006 ; # 664
667 PLANT.LOOP1.PSI(40) := 1.5548e+006 ; # 665
668 PLANT.LOOP1.PSI(41) := 1.55771e+006 ; # 666

```

```

669 PLANT.LOOP1.PSI(42) := 1.56032e+006 ; # 667
670 PLANT.LOOP1.PSI(43) := 1.56266e+006 ; # 668
671 PLANT.LOOP1.PSI(44) := 1.56474e+006 ; # 669
672 PLANT.LOOP1.PSI(45) := 1.56657e+006 ; # 670
673 PLANT.LOOP1.PSI(46) := 1.56816e+006 ; # 671
674 PLANT.LOOP1.PSI(47) := 1.56951e+006 ; # 672
675 PLANT.LOOP1.PSI(48) := 1.57065e+006 ; # 673
676 PLANT.LOOP1.PSI(49) := 1.57158e+006 ; # 674
677 PLANT.LOOP1.PSI(50) := 1.5723e+006 ; # 675
678 PLANT.LOOP1.PSI(51) := 1.54707e+006 ; # 676
679 PLANT.LOOP1.PSI(52) := 1.54135e+006 ; # 677
680 PLANT.LOOP1.PSI(53) := 1.53567e+006 ; # 678
681 PLANT.LOOP1.PSI(54) := 1.52997e+006 ; # 679
682 PLANT.LOOP1.PSI(55) := 1.52427e+006 ; # 680
683 PLANT.LOOP1.PSI(56) := 1.51856e+006 ; # 681
684 PLANT.LOOP1.PSI(57) := 1.51284e+006 ; # 682
685 PLANT.LOOP1.PSI(58) := 1.50712e+006 ; # 683
686 PLANT.LOOP1.PSI(59) := 1.50138e+006 ; # 684
687 PLANT.LOOP1.PSI(60) := 1.49564e+006 ; # 685
688 PLANT.LOOP1.PSI(61) := 1.50921e+006 ; # 686
689 PLANT.LOOP1.PSI(62) := 1.50544e+006 ; # 687
690 PLANT.LOOP1.PSI(63) := 1.50142e+006 ; # 688
691 PLANT.LOOP1.PSI(64) := 1.49724e+006 ; # 689
692 PLANT.LOOP1.PSI(65) := 1.49288e+006 ; # 690
693 PLANT.LOOP1.PSI(66) := 1.48832e+006 ; # 691
694 PLANT.LOOP1.PSI(67) := 1.48357e+006 ; # 692
695 PLANT.LOOP1.PSI(68) := 1.47859e+006 ; # 693
696 PLANT.LOOP1.PSI(69) := 1.47338e+006 ; # 694
697 PLANT.LOOP1.PSI(70) := 1.46791e+006 ; # 695
698 PLANT.LOOP1.PSI(71) := 1.46218e+006 ; # 696
699 PLANT.LOOP1.PSI(72) := 1.45616e+006 ; # 697
700 PLANT.LOOP1.PSI(73) := 1.44982e+006 ; # 698
701 PLANT.LOOP1.PSI(74) := 1.44315e+006 ; # 699
702 PLANT.LOOP1.PSI(75) := 1.43612e+006 ; # 700
703 PLANT.LOOP1.PSI(76) := 1.4287e+006 ; # 701
704 PLANT.LOOP1.PSI(77) := 1.42087e+006 ; # 702
705 PLANT.LOOP1.PSI(78) := 1.41258e+006 ; # 703
706 PLANT.LOOP1.PSI(79) := 1.40379e+006 ; # 704
707 PLANT.LOOP1.PSI(80) := 1.39448e+006 ; # 705
708 PLANT.LOOP1.PSI(81) := 1.38459e+006 ; # 706
709 PLANT.LOOP1.PSI(82) := 1.37407e+006 ; # 707
710 PLANT.LOOP1.PSI(83) := 1.36287e+006 ; # 708
711 PLANT.LOOP1.PSI(84) := 1.35093e+006 ; # 709
712 PLANT.LOOP1.PSI(85) := 1.33817e+006 ; # 710
713 PLANT.LOOP1.PSI(86) := 1.32451e+006 ; # 711
714 PLANT.LOOP1.PSI(87) := 1.30988e+006 ; # 712
715 PLANT.LOOP1.PSI(88) := 1.29416e+006 ; # 713
716 PLANT.LOOP1.PSI(89) := 1.27725e+006 ; # 714
717 PLANT.LOOP1.PSI(90) := 1.25903e+006 ; # 715
718 PLANT.LOOP1.PSI(91) := 1.23934e+006 ; # 716
719 PLANT.LOOP1.PSI(92) := 1.21801e+006 ; # 717
720 PLANT.LOOP1.PSI(93) := 1.19486e+006 ; # 718
721 PLANT.LOOP1.PSI(94) := 1.16967e+006 ; # 719
722 PLANT.LOOP1.PSI(95) := 1.14217e+006 ; # 720
723 PLANT.LOOP1.PSI(96) := 1.11205e+006 ; # 721
724 PLANT.LOOP1.PSI(97) := 1.07896e+006 ; # 722
725 PLANT.LOOP1.PSI(98) := 1.04248e+006 ; # 723
726 PLANT.LOOP1.PSI(99) := 1.00208e+006 ; # 724
727 PLANT.LOOP1.PSI(100) := 957155 ; # 725
728 PLANT.LOOP1.F(1) := 26.308 ; # 726
729 PLANT.LOOP1.F(2) := 26.308 ; # 727
730 PLANT.LOOP1.F(3) := 26.308 ; # 728
731 PLANT.LOOP1.F(4) := 26.308 ; # 729
732 PLANT.LOOP1.F(5) := 26.308 ; # 730
733 PLANT.LOOP1.F(6) := 26.308 ; # 731
734 PLANT.LOOP1.F(7) := 26.308 ; # 732
735 PLANT.LOOP1.F(8) := 26.308 ; # 733
736 PLANT.LOOP1.F(9) := 26.308 ; # 734
737 PLANT.LOOP1.F(10) := 26.308 ; # 735
738 PLANT.LOOP1.F(11) := 26.308 ; # 736
739 PLANT.LOOP1.F(12) := 26.308 ; # 737
740 PLANT.LOOP1.F(13) := 26.308 ; # 738
741 PLANT.LOOP1.F(14) := 26.308 ; # 739
742 PLANT.LOOP1.F(15) := 26.308 ; # 740
743 PLANT.LOOP1.F(16) := 26.308 ; # 741
744 PLANT.LOOP1.F(17) := 26.308 ; # 742
745 PLANT.LOOP1.F(18) := 26.308 ; # 743
746 PLANT.LOOP1.F(19) := 26.308 ; # 744
747 PLANT.LOOP1.F(20) := 26.308 ; # 745
748 PLANT.LOOP1.F(21) := 26.308 ; # 746
749 PLANT.LOOP1.F(22) := 26.308 ; # 747
750 PLANT.LOOP1.F(23) := 26.308 ; # 748
751 PLANT.LOOP1.F(24) := 26.308 ; # 749
752 PLANT.LOOP1.F(25) := 26.308 ; # 750
753 PLANT.LOOP1.F(26) := 26.308 ; # 751
754 PLANT.LOOP1.F(27) := 26.308 ; # 752
755 PLANT.LOOP1.F(28) := 26.308 ; # 753
756 PLANT.LOOP1.F(29) := 26.308 ; # 754
757 PLANT.LOOP1.F(30) := 26.308 ; # 755
758 PLANT.LOOP1.F(31) := 26.308 ; # 756
759 PLANT.LOOP1.F(32) := 26.308 ; # 757
760 PLANT.LOOP1.F(33) := 26.308 ; # 758

```


761 PLANT.LOOP1.F(34) := 26.308 ; # 759
762 PLANT.LOOP1.F(35) := 26.308 ; # 760
763 PLANT.LOOP1.F(36) := 26.308 ; # 761
764 PLANT.LOOP1.F(37) := 26.308 ; # 762
765 PLANT.LOOP1.F(38) := 26.308 ; # 763
766 PLANT.LOOP1.F(39) := 26.308 ; # 764
767 PLANT.LOOP1.F(40) := 26.308 ; # 765
768 PLANT.LOOP1.F(41) := 26.308 ; # 766
769 PLANT.LOOP1.F(42) := 26.308 ; # 767
770 PLANT.LOOP1.F(43) := 26.308 ; # 768
771 PLANT.LOOP1.F(44) := 26.308 ; # 769
772 PLANT.LOOP1.F(45) := 26.308 ; # 770
773 PLANT.LOOP1.F(46) := 26.308 ; # 771
774 PLANT.LOOP1.F(47) := 26.308 ; # 772
775 PLANT.LOOP1.F(48) := 26.308 ; # 773
776 PLANT.LOOP1.F(49) := 26.308 ; # 774
777 PLANT.LOOP1.F(50) := 26.308 ; # 775
778 PLANT.LOOP1.F(51) := 26.308 ; # 776
779 PLANT.LOOP1.F(52) := 26.308 ; # 777
780 PLANT.LOOP1.F(53) := 26.308 ; # 778
781 PLANT.LOOP1.F(54) := 26.308 ; # 779
782 PLANT.LOOP1.F(55) := 26.308 ; # 780
783 PLANT.LOOP1.F(56) := 26.308 ; # 781
784 PLANT.LOOP1.F(57) := 26.308 ; # 782
785 PLANT.LOOP1.F(58) := 26.308 ; # 783
786 PLANT.LOOP1.F(59) := 26.308 ; # 784
787 PLANT.LOOP1.F(60) := 26.308 ; # 785
788 PLANT.LOOP1.F(61) := 26.308 ; # 786
789 PLANT.LOOP1.F(62) := 26.308 ; # 787
790 PLANT.LOOP1.F(63) := 26.308 ; # 788
791 PLANT.LOOP1.F(64) := 26.308 ; # 789
792 PLANT.LOOP1.F(65) := 26.308 ; # 790
793 PLANT.LOOP1.F(66) := 26.308 ; # 791
794 PLANT.LOOP1.F(67) := 26.308 ; # 792
795 PLANT.LOOP1.F(68) := 26.308 ; # 793
796 PLANT.LOOP1.F(69) := 26.308 ; # 794
797 PLANT.LOOP1.F(70) := 26.308 ; # 795
798 PLANT.LOOP1.F(71) := 26.308 ; # 796
799 PLANT.LOOP1.F(72) := 26.308 ; # 797
800 PLANT.LOOP1.F(73) := 26.308 ; # 798
801 PLANT.LOOP1.F(74) := 26.308 ; # 799
802 PLANT.LOOP1.F(75) := 26.308 ; # 800
803 PLANT.LOOP1.F(76) := 26.308 ; # 801
804 PLANT.LOOP1.F(77) := 26.308 ; # 802
805 PLANT.LOOP1.F(78) := 26.308 ; # 803
806 PLANT.LOOP1.F(79) := 26.308 ; # 804
807 PLANT.LOOP1.F(80) := 26.308 ; # 805
808 PLANT.LOOP1.F(81) := 26.308 ; # 806
809 PLANT.LOOP1.F(82) := 26.308 ; # 807
810 PLANT.LOOP1.F(83) := 26.308 ; # 808
811 PLANT.LOOP1.F(84) := 26.308 ; # 809
812 PLANT.LOOP1.F(85) := 26.308 ; # 810
813 PLANT.LOOP1.F(86) := 26.308 ; # 811
814 PLANT.LOOP1.F(87) := 26.308 ; # 812
815 PLANT.LOOP1.F(88) := 26.308 ; # 813
816 PLANT.LOOP1.F(89) := 26.308 ; # 814
817 PLANT.LOOP1.F(90) := 26.308 ; # 815
818 PLANT.LOOP1.F(91) := 26.308 ; # 816
819 PLANT.LOOP1.F(92) := 26.308 ; # 817
820 PLANT.LOOP1.F(93) := 26.308 ; # 818
821 PLANT.LOOP1.F(94) := 26.308 ; # 819
822 PLANT.LOOP1.F(95) := 26.308 ; # 820
823 PLANT.LOOP1.F(96) := 26.308 ; # 821
824 PLANT.LOOP1.F(97) := 26.308 ; # 822
825 PLANT.LOOP1.F(98) := 26.308 ; # 823
826 PLANT.LOOP1.F(99) := 26.308 ; # 824
827 PLANT.LOOP1.F(100) := 26.308 ; # 825
828 PLANT.LOOP1.F_IN := 26.308 ; # 826
829 PLANT.LOOP1.RHO_AVG := 0.919789 ; # 827
830 PLANT.LOOP1.TOTALMASS := 27.4242 ; # 828
831 PLANT.LOOP1.RHOEXTRA(1) := 1.1654 ; # 829
832 PLANT.LOOP1.RHOEXTRA(2) := 1.1654 ; # 830
833 PLANT.LOOP1.PEXTRA(1) := 2.03415e+006 ; # 831
834 PLANT.LOOP1.PEXTRA(2) := 2.03415e+006 ; # 832
835 PLANT.LOOP1.HEXTRA(1) := 2.81449e+006 ; # 833
836 PLANT.LOOP1.HEXTRA(2) := 2.81449e+006 ; # 834
837 PLANT.LOOP1.TEXTRA(1) := 839.77 ; # 835
838 PLANT.LOOP1.TEXTRA(2) := 839.77 ; # 836
839 PLANT.LOOP1.PSIEXTRA(1) := 1.24585e+006 ; # 837
840 PLANT.LOOP1.PSIEXTRA(2) := 1.24585e+006 ; # 838
841 PLANT.LOOP1.FEXTRA(1) := 26.308 ; # 839
842 PLANT.LOOP1.FEXTRA(2) := 26.308 ; # 840
843 PLANT.LOOP1.HT1.H2 := 17.344 ; # 841
844 PLANT.LOOP1.HT1.RHOPIPEHE := 1.14182 ; # 842
845 PLANT.LOOP1.HT1.VPIPE := 171.996 ; # 843
846 PLANT.LOOP1.HT1.HO := 1500.09 ; # 844
847 PLANT.LOOP1.HT1.U := 8.93421 ; # 845
848 PLANT.LOOP1.HT2.RHOPIPEHE := 0.902801 ; # 846
849 PLANT.LOOP1.HT2.VPIPE := 84.86 ; # 847
850 PLANT.LOOP1.HT2.HO := 1665.62 ; # 848
851 PLANT.LOOP1.HT2.U := 1645.45 ; # 849
852 PLANT.LOOP1.HT3.H2 := 17.344 ; # 850

853 PLANT.LOOP1.HT3.RHOPIPEHE := 0.749559 ; # 851
854 PLANT.LOOP1.HT3.VPIPE := 226.698 ; # 852
855 PLANT.LOOP1.HT3.HO := 1316.87 ; # 853
856 PLANT.LOOP1.HT3.U := 10.3572 ; # 854
857 PLANT.LOOP1.HT4.RHOPIPEHE := 0.833125 ; # 855
858 PLANT.LOOP1.HT4.VPIPE := 79.4405 ; # 856
859 PLANT.LOOP1.HT4.U := 1299.78 ; # 857
860 PLANT.PIPEH.RHO(1) := 2.87869 ; # 858
861 PLANT.PIPEH.RHO(2) := 2.88664 ; # 859
862 PLANT.PIPEH.RHO(3) := 2.89491 ; # 860
863 PLANT.PIPEH.RHO(4) := 2.90353 ; # 861
864 PLANT.PIPEH.RHO(5) := 2.9125 ; # 862
865 PLANT.PIPEH.RHO(6) := 2.92184 ; # 863
866 PLANT.PIPEH.RHO(7) := 2.93156 ; # 864
867 PLANT.PIPEH.RHO(8) := 2.9417 ; # 865
868 PLANT.PIPEH.RHO(9) := 2.95225 ; # 866
869 PLANT.PIPEH.RHO(10) := 2.96325 ; # 867
870 PLANT.PIPEH.RHO(11) := 2.97471 ; # 868
871 PLANT.PIPEH.RHO(12) := 2.98666 ; # 869
872 PLANT.PIPEH.RHO(13) := 2.99912 ; # 870
873 PLANT.PIPEH.RHO(14) := 3.01211 ; # 871
874 PLANT.PIPEH.RHO(15) := 3.02567 ; # 872
875 PLANT.PIPEH.RHO(16) := 3.03982 ; # 873
876 PLANT.PIPEH.RHO(17) := 3.05458 ; # 874
877 PLANT.PIPEH.RHO(18) := 3.07 ; # 875
878 PLANT.PIPEH.RHO(19) := 3.08611 ; # 876
879 PLANT.PIPEH.RHO(20) := 3.10294 ; # 877
880 PLANT.PIPEH.RHO(21) := 3.12053 ; # 878
881 PLANT.PIPEH.RHO(22) := 3.13892 ; # 879
882 PLANT.PIPEH.RHO(23) := 3.15816 ; # 880
883 PLANT.PIPEH.RHO(24) := 3.1783 ; # 881
884 PLANT.PIPEH.RHO(25) := 3.19939 ; # 882
885 PLANT.PIPEH.RHO(26) := 3.22148 ; # 883
886 PLANT.PIPEH.RHO(27) := 3.24463 ; # 884
887 PLANT.PIPEH.RHO(28) := 3.2689 ; # 885
888 PLANT.PIPEH.RHO(29) := 3.29437 ; # 886
889 PLANT.PIPEH.RHO(30) := 3.32112 ; # 887
890 PLANT.PIPEH.RHO(31) := 3.34921 ; # 888
891 PLANT.PIPEH.RHO(32) := 3.37874 ; # 889
892 PLANT.PIPEH.RHO(33) := 3.4098 ; # 890
893 PLANT.PIPEH.RHO(34) := 3.4425 ; # 891
894 PLANT.PIPEH.RHO(35) := 3.47695 ; # 892
895 PLANT.PIPEH.RHO(36) := 3.51328 ; # 893
896 PLANT.PIPEH.RHO(37) := 3.55161 ; # 894
897 PLANT.PIPEH.RHO(38) := 3.59209 ; # 895
898 PLANT.PIPEH.RHO(39) := 3.6349 ; # 896
899 PLANT.PIPEH.RHO(40) := 3.68012 ; # 897
900 PLANT.PIPEH.P(1) := 6.99931e+006 ; # 898
901 PLANT.PIPEH.P(2) := 6.99793e+006 ; # 899
902 PLANT.PIPEH.P(3) := 6.99656e+006 ; # 900
903 PLANT.PIPEH.P(4) := 6.99519e+006 ; # 901
904 PLANT.PIPEH.P(5) := 6.99383e+006 ; # 902
905 PLANT.PIPEH.P(6) := 6.99247e+006 ; # 903
906 PLANT.PIPEH.P(7) := 6.99111e+006 ; # 904
907 PLANT.PIPEH.P(8) := 6.98977e+006 ; # 905
908 PLANT.PIPEH.P(9) := 6.98842e+006 ; # 906
909 PLANT.PIPEH.P(10) := 6.98708e+006 ; # 907
910 PLANT.PIPEH.P(11) := 6.98575e+006 ; # 908
911 PLANT.PIPEH.P(12) := 6.98442e+006 ; # 909
912 PLANT.PIPEH.P(13) := 6.9831e+006 ; # 910
913 PLANT.PIPEH.P(14) := 6.98179e+006 ; # 911
914 PLANT.PIPEH.P(15) := 6.98048e+006 ; # 912
915 PLANT.PIPEH.P(16) := 6.97917e+006 ; # 913
916 PLANT.PIPEH.P(17) := 6.97788e+006 ; # 914
917 PLANT.PIPEH.P(18) := 6.97659e+006 ; # 915
918 PLANT.PIPEH.P(19) := 6.97531e+006 ; # 916
919 PLANT.PIPEH.P(20) := 6.97403e+006 ; # 917
920 PLANT.PIPEH.P(21) := 6.97276e+006 ; # 918
921 PLANT.PIPEH.P(22) := 6.97151e+006 ; # 919
922 PLANT.PIPEH.P(23) := 6.97025e+006 ; # 920
923 PLANT.PIPEH.P(24) := 6.96901e+006 ; # 921
924 PLANT.PIPEH.P(25) := 6.96778e+006 ; # 922
925 PLANT.PIPEH.P(26) := 6.96655e+006 ; # 923
926 PLANT.PIPEH.P(27) := 6.96534e+006 ; # 924
927 PLANT.PIPEH.P(28) := 6.96413e+006 ; # 925
928 PLANT.PIPEH.P(29) := 6.96294e+006 ; # 926
929 PLANT.PIPEH.P(30) := 6.96175e+006 ; # 927
930 PLANT.PIPEH.P(31) := 6.96058e+006 ; # 928
931 PLANT.PIPEH.P(32) := 6.95941e+006 ; # 929
932 PLANT.PIPEH.P(33) := 6.95826e+006 ; # 930
933 PLANT.PIPEH.P(34) := 6.95712e+006 ; # 931
934 PLANT.PIPEH.P(35) := 6.95599e+006 ; # 932
935 PLANT.PIPEH.P(36) := 6.95487e+006 ; # 933
936 PLANT.PIPEH.P(37) := 6.95377e+006 ; # 934
937 PLANT.PIPEH.P(38) := 6.95268e+006 ; # 935
938 PLANT.PIPEH.P(39) := 6.9516e+006 ; # 936
939 PLANT.PIPEH.P(40) := 6.95054e+006 ; # 937
940 PLANT.PIPEH.H(1) := 4.52899e+006 ; # 938
941 PLANT.PIPEH.H(2) := 4.51106e+006 ; # 939
942 PLANT.PIPEH.H(3) := 4.49255e+006 ; # 940
943 PLANT.PIPEH.H(4) := 4.47345e+006 ; # 941
944 PLANT.PIPEH.H(5) := 4.45373e+006 ; # 942

945 PLANT.PIPEH.H(6) := 4.43339e+006 ; # 943
 946 PLANT.PIPEH.H(7) := 4.41239e+006 ; # 944
 947 PLANT.PIPEH.H(8) := 4.39071e+006 ; # 945
 948 PLANT.PIPEH.H(9) := 4.36834e+006 ; # 946
 949 PLANT.PIPEH.H(10) := 4.34525e+006 ; # 947
 950 PLANT.PIPEH.H(11) := 4.32143e+006 ; # 948
 951 PLANT.PIPEH.H(12) := 4.29683e+006 ; # 949
 952 PLANT.PIPEH.H(13) := 4.27145e+006 ; # 950
 953 PLANT.PIPEH.H(14) := 4.24525e+006 ; # 951
 954 PLANT.PIPEH.H(15) := 4.21821e+006 ; # 952
 955 PLANT.PIPEH.H(16) := 4.19031e+006 ; # 953
 956 PLANT.PIPEH.H(17) := 4.16151e+006 ; # 954
 957 PLANT.PIPEH.H(18) := 4.13178e+006 ; # 955
 958 PLANT.PIPEH.H(19) := 4.1011e+006 ; # 956
 959 PLANT.PIPEH.H(20) := 4.06944e+006 ; # 957
 960 PLANT.PIPEH.H(21) := 4.03675e+006 ; # 958
 961 PLANT.PIPEH.H(22) := 4.00302e+006 ; # 959
 962 PLANT.PIPEH.H(23) := 3.96821e+006 ; # 960
 963 PLANT.PIPEH.H(24) := 3.93228e+006 ; # 961
 964 PLANT.PIPEH.H(25) := 3.8952e+006 ; # 962
 965 PLANT.PIPEH.H(26) := 3.85693e+006 ; # 963
 966 PLANT.PIPEH.H(27) := 3.81742e+006 ; # 964
 967 PLANT.PIPEH.H(28) := 3.77666e+006 ; # 965
 968 PLANT.PIPEH.H(29) := 3.73458e+006 ; # 966
 969 PLANT.PIPEH.H(30) := 3.69115e+006 ; # 967
 970 PLANT.PIPEH.H(31) := 3.64633e+006 ; # 968
 971 PLANT.PIPEH.H(32) := 3.60007e+006 ; # 969
 972 PLANT.PIPEH.H(33) := 3.55232e+006 ; # 970
 973 PLANT.PIPEH.H(34) := 3.50304e+006 ; # 971
 974 PLANT.PIPEH.H(35) := 3.45219e+006 ; # 972
 975 PLANT.PIPEH.H(36) := 3.39969e+006 ; # 973
 976 PLANT.PIPEH.H(37) := 3.34552e+006 ; # 974
 977 PLANT.PIPEH.H(38) := 3.2896e+006 ; # 975
 978 PLANT.PIPEH.H(39) := 3.23189e+006 ; # 976
 979 PLANT.PIPEH.H(40) := 3.17244e+006 ; # 977
 980 PLANT.PIPEH.HO := 4.5464e+006 ; # 978
 981 PLANT.PIPEH.T(1) := 1169.8 ; # 979
 982 PLANT.PIPEH.T(2) := 1166.35 ; # 980
 983 PLANT.PIPEH.T(3) := 1162.78 ; # 981
 984 PLANT.PIPEH.T(4) := 1159.11 ; # 982
 985 PLANT.PIPEH.T(5) := 1155.31 ; # 983
 986 PLANT.PIPEH.T(6) := 1151.39 ; # 984
 987 PLANT.PIPEH.T(7) := 1147.35 ; # 985
 988 PLANT.PIPEH.T(8) := 1143.18 ; # 986
 989 PLANT.PIPEH.T(9) := 1138.87 ; # 987
 990 PLANT.PIPEH.T(10) := 1134.43 ; # 988
 991 PLANT.PIPEH.T(11) := 1129.84 ; # 989
 992 PLANT.PIPEH.T(12) := 1125.11 ; # 990
 993 PLANT.PIPEH.T(13) := 1120.22 ; # 991
 994 PLANT.PIPEH.T(14) := 1115.18 ; # 992
 995 PLANT.PIPEH.T(15) := 1109.98 ; # 993
 996 PLANT.PIPEH.T(16) := 1104.6 ; # 994
 997 PLANT.PIPEH.T(17) := 1099.06 ; # 995
 998 PLANT.PIPEH.T(18) := 1093.34 ; # 996
 999 PLANT.PIPEH.T(19) := 1087.43 ; # 997
 1000 PLANT.PIPEH.T(20) := 1081.34 ; # 998
 1001 PLANT.PIPEH.T(21) := 1075.05 ; # 999
 1002 PLANT.PIPEH.T(22) := 1068.55 ; # 1000
 1003 PLANT.PIPEH.T(23) := 1061.85 ; # 1001
 1004 PLANT.PIPEH.T(24) := 1054.94 ; # 1002
 1005 PLANT.PIPEH.T(25) := 1047.8 ; # 1003
 1006 PLANT.PIPEH.T(26) := 1040.43 ; # 1004
 1007 PLANT.PIPEH.T(27) := 1032.83 ; # 1005
 1008 PLANT.PIPEH.T(28) := 1024.98 ; # 1006
 1009 PLANT.PIPEH.T(29) := 1016.88 ; # 1007
 1010 PLANT.PIPEH.T(30) := 1008.52 ; # 1008
 1011 PLANT.PIPEH.T(31) := 999.892 ; # 1009
 1012 PLANT.PIPEH.T(32) := 990.987 ; # 1010
 1013 PLANT.PIPEH.T(33) := 981.796 ; # 1011
 1014 PLANT.PIPEH.T(34) := 972.311 ; # 1012
 1015 PLANT.PIPEH.T(35) := 962.521 ; # 1013
 1016 PLANT.PIPEH.T(36) := 952.416 ; # 1014
 1017 PLANT.PIPEH.T(37) := 941.988 ; # 1015
 1018 PLANT.PIPEH.T(38) := 931.225 ; # 1016
 1019 PLANT.PIPEH.T(39) := 920.116 ; # 1017
 1020 PLANT.PIPEH.T(40) := 908.671 ; # 1018
 1021 PLANT.PIPEH.TEXTRNL(1) := 1161.37 ; # 1019
 1022 PLANT.PIPEH.TEXTRNL(2) := 1157.67 ; # 1020
 1023 PLANT.PIPEH.TEXTRNL(3) := 1153.83 ; # 1021
 1024 PLANT.PIPEH.TEXTRNL(4) := 1149.86 ; # 1022
 1025 PLANT.PIPEH.TEXTRNL(5) := 1145.77 ; # 1023
 1026 PLANT.PIPEH.TEXTRNL(6) := 1141.55 ; # 1024
 1027 PLANT.PIPEH.TEXTRNL(7) := 1137.19 ; # 1025
 1028 PLANT.PIPEH.TEXTRNL(8) := 1132.69 ; # 1026
 1029 PLANT.PIPEH.TEXTRNL(9) := 1128.05 ; # 1027
 1030 PLANT.PIPEH.TEXTRNL(10) := 1123.26 ; # 1028
 1031 PLANT.PIPEH.TEXTRNL(11) := 1118.31 ; # 1029
 1032 PLANT.PIPEH.TEXTRNL(12) := 1113.21 ; # 1030
 1033 PLANT.PIPEH.TEXTRNL(13) := 1107.94 ; # 1031
 1034 PLANT.PIPEH.TEXTRNL(14) := 1102.5 ; # 1032
 1035 PLANT.PIPEH.TEXTRNL(15) := 1096.89 ; # 1033
 1036 PLANT.PIPEH.TEXTRNL(16) := 1091.1 ; # 1034

1037 PLANT.PIPEH.TEXTRNL(17) := 1085.12 ; # 1035
1038 PLANT.PIPEH.TEXTRNL(18) := 1078.95 ; # 1036
1039 PLANT.PIPEH.TEXTRNL(19) := 1072.58 ; # 1037
1040 PLANT.PIPEH.TEXTRNL(20) := 1066.01 ; # 1038
1041 PLANT.PIPEH.TEXTRNL(21) := 1059.23 ; # 1039
1042 PLANT.PIPEH.TEXTRNL(22) := 1052.23 ; # 1040
1043 PLANT.PIPEH.TEXTRNL(23) := 1045 ; # 1041
1044 PLANT.PIPEH.TEXTRNL(24) := 1037.55 ; # 1042
1045 PLANT.PIPEH.TEXTRNL(25) := 1029.85 ; # 1043
1046 PLANT.PIPEH.TEXTRNL(26) := 1021.91 ; # 1044
1047 PLANT.PIPEH.TEXTRNL(27) := 1013.71 ; # 1045
1048 PLANT.PIPEH.TEXTRNL(28) := 1005.25 ; # 1046
1049 PLANT.PIPEH.TEXTRNL(29) := 996.513 ; # 1047
1050 PLANT.PIPEH.TEXTRNL(30) := 987.5 ; # 1048
1051 PLANT.PIPEH.TEXTRNL(31) := 978.197 ; # 1049
1052 PLANT.PIPEH.TEXTRNL(32) := 968.596 ; # 1050
1053 PLANT.PIPEH.TEXTRNL(33) := 958.687 ; # 1051
1054 PLANT.PIPEH.TEXTRNL(34) := 948.459 ; # 1052
1055 PLANT.PIPEH.TEXTRNL(35) := 937.904 ; # 1053
1056 PLANT.PIPEH.TEXTRNL(36) := 927.009 ; # 1054
1057 PLANT.PIPEH.TEXTRNL(37) := 915.766 ; # 1055
1058 PLANT.PIPEH.TEXTRNL(38) := 904.161 ; # 1056
1059 PLANT.PIPEH.TEXTRNL(39) := 892.184 ; # 1057
1060 PLANT.PIPEH.TEXTRNL(40) := 879.893 ; # 1058
1061 PLANT.PIPEH.F(1) := 32.3305 ; # 1059
1062 PLANT.PIPEH.F(2) := 32.3305 ; # 1060
1063 PLANT.PIPEH.F(3) := 32.3305 ; # 1061
1064 PLANT.PIPEH.F(4) := 32.3305 ; # 1062
1065 PLANT.PIPEH.F(5) := 32.3305 ; # 1063
1066 PLANT.PIPEH.F(6) := 32.3305 ; # 1064
1067 PLANT.PIPEH.F(7) := 32.3305 ; # 1065
1068 PLANT.PIPEH.F(8) := 32.3305 ; # 1066
1069 PLANT.PIPEH.F(9) := 32.3305 ; # 1067
1070 PLANT.PIPEH.F(10) := 32.3305 ; # 1068
1071 PLANT.PIPEH.F(11) := 32.3305 ; # 1069
1072 PLANT.PIPEH.F(12) := 32.3305 ; # 1070
1073 PLANT.PIPEH.F(13) := 32.3305 ; # 1071
1074 PLANT.PIPEH.F(14) := 32.3305 ; # 1072
1075 PLANT.PIPEH.F(15) := 32.3305 ; # 1073
1076 PLANT.PIPEH.F(16) := 32.3305 ; # 1074
1077 PLANT.PIPEH.F(17) := 32.3305 ; # 1075
1078 PLANT.PIPEH.F(18) := 32.3305 ; # 1076
1079 PLANT.PIPEH.F(19) := 32.3305 ; # 1077
1080 PLANT.PIPEH.F(20) := 32.3305 ; # 1078
1081 PLANT.PIPEH.F(21) := 32.3305 ; # 1079
1082 PLANT.PIPEH.F(22) := 32.3305 ; # 1080
1083 PLANT.PIPEH.F(23) := 32.3305 ; # 1081
1084 PLANT.PIPEH.F(24) := 32.3305 ; # 1082
1085 PLANT.PIPEH.F(25) := 32.3305 ; # 1083
1086 PLANT.PIPEH.F(26) := 32.3305 ; # 1084
1087 PLANT.PIPEH.F(27) := 32.3305 ; # 1085
1088 PLANT.PIPEH.F(28) := 32.3305 ; # 1086
1089 PLANT.PIPEH.F(29) := 32.3305 ; # 1087
1090 PLANT.PIPEH.F(30) := 32.3305 ; # 1088
1091 PLANT.PIPEH.F(31) := 32.3305 ; # 1089
1092 PLANT.PIPEH.F(32) := 32.3305 ; # 1090
1093 PLANT.PIPEH.F(33) := 32.3305 ; # 1091
1094 PLANT.PIPEH.F(34) := 32.3305 ; # 1092
1095 PLANT.PIPEH.F(35) := 32.3305 ; # 1093
1096 PLANT.PIPEH.F(36) := 32.3305 ; # 1094
1097 PLANT.PIPEH.F(37) := 32.3305 ; # 1095
1098 PLANT.PIPEH.F(38) := 32.3305 ; # 1096
1099 PLANT.PIPEH.F(39) := 32.3305 ; # 1097
1100 PLANT.PIPEH.F(40) := 32.3305 ; # 1098
1101 PLANT.PIPEH.F_IN := 32.3305 ; # 1099
1102 PLANT.PIPEH.PSI(1) := 6.03823e+006 ; # 1100
1103 PLANT.PIPEH.PSI(2) := 6.02385e+006 ; # 1101
1104 PLANT.PIPEH.PSI(3) := 6.00898e+006 ; # 1102
1105 PLANT.PIPEH.PSI(4) := 5.9936e+006 ; # 1103
1106 PLANT.PIPEH.PSI(5) := 5.97767e+006 ; # 1104
1107 PLANT.PIPEH.PSI(6) := 5.96117e+006 ; # 1105
1108 PLANT.PIPEH.PSI(7) := 5.94408e+006 ; # 1106
1109 PLANT.PIPEH.PSI(8) := 5.92638e+006 ; # 1107
1110 PLANT.PIPEH.PSI(9) := 5.90802e+006 ; # 1108
1111 PLANT.PIPEH.PSI(10) := 5.88899e+006 ; # 1109
1112 PLANT.PIPEH.PSI(11) := 5.86924e+006 ; # 1110
1113 PLANT.PIPEH.PSI(12) := 5.84876e+006 ; # 1111
1114 PLANT.PIPEH.PSI(13) := 5.82749e+006 ; # 1112
1115 PLANT.PIPEH.PSI(14) := 5.8054e+006 ; # 1113
1116 PLANT.PIPEH.PSI(15) := 5.78245e+006 ; # 1114
1117 PLANT.PIPEH.PSI(16) := 5.75859e+006 ; # 1115
1118 PLANT.PIPEH.PSI(17) := 5.73379e+006 ; # 1116
1119 PLANT.PIPEH.PSI(18) := 5.70799e+006 ; # 1117
1120 PLANT.PIPEH.PSI(19) := 5.68113e+006 ; # 1118
1121 PLANT.PIPEH.PSI(20) := 5.65317e+006 ; # 1119
1122 PLANT.PIPEH.PSI(21) := 5.62404e+006 ; # 1120
1123 PLANT.PIPEH.PSI(22) := 5.59367e+006 ; # 1121
1124 PLANT.PIPEH.PSI(23) := 5.56201e+006 ; # 1122
1125 PLANT.PIPEH.PSI(24) := 5.52897e+006 ; # 1123
1126 PLANT.PIPEH.PSI(25) := 5.49447e+006 ; # 1124
1127 PLANT.PIPEH.PSI(26) := 5.45844e+006 ; # 1125
1128 PLANT.PIPEH.PSI(27) := 5.42078e+006 ; # 1126

1129 PLANT.PIPEH.PSI(28) := 5.38139e+006 ; # 1127
1130 PLANT.PIPEH.PSI(29) := 5.34016e+006 ; # 1128
1131 PLANT.PIPEH.PSI(30) := 5.29699e+006 ; # 1129
1132 PLANT.PIPEH.PSI(31) := 5.25174e+006 ; # 1130
1133 PLANT.PIPEH.PSI(32) := 5.20427e+006 ; # 1131
1134 PLANT.PIPEH.PSI(33) := 5.15446e+006 ; # 1132
1135 PLANT.PIPEH.PSI(34) := 5.10212e+006 ; # 1133
1136 PLANT.PIPEH.PSI(35) := 5.0471e+006 ; # 1134
1137 PLANT.PIPEH.PSI(36) := 4.98919e+006 ; # 1135
1138 PLANT.PIPEH.PSI(37) := 4.92819e+006 ; # 1136
1139 PLANT.PIPEH.PSI(38) := 4.86388e+006 ; # 1137
1140 PLANT.PIPEH.PSI(39) := 4.796e+006 ; # 1138
1141 PLANT.PIPEH.PSI(40) := 4.7244e+006 ; # 1139
1142 PLANT.PIPEH.HT.RHOPIPEHE := 3.09587 ; # 1140
1143 PLANT.PIPEH.HT.VPIPE := 28.7109 ; # 1141
1144 PLANT.PIPEH.HT.HO := 1760.94 ; # 1142
1145 PLANT.PIPEH.HT.U := 1738.41 ; # 1143
1146 PLANT.HX2.TGASHOT(1) := 1141.93 ; # 1144
1147 PLANT.HX2.TGASHOT(2) := 1139.37 ; # 1145
1148 PLANT.HX2.TGASHOT(3) := 1136.66 ; # 1146
1149 PLANT.HX2.TGASHOT(4) := 1133.8 ; # 1147
1150 PLANT.HX2.TGASHOT(5) := 1130.77 ; # 1148
1151 PLANT.HX2.TGASHOT(6) := 1127.56 ; # 1149
1152 PLANT.HX2.TGASHOT(7) := 1124.17 ; # 1150
1153 PLANT.HX2.TGASHOT(8) := 1120.57 ; # 1151
1154 PLANT.HX2.TGASHOT(9) := 1116.77 ; # 1152
1155 PLANT.HX2.TGASHOT(10) := 1112.75 ; # 1153
1156 PLANT.HX2.TGASHOT(11) := 1108.5 ; # 1154
1157 PLANT.HX2.TGASHOT(12) := 1104 ; # 1155
1158 PLANT.HX2.TGASHOT(13) := 1099.23 ; # 1156
1159 PLANT.HX2.TGASHOT(14) := 1094.19 ; # 1157
1160 PLANT.HX2.TGASHOT(15) := 1088.86 ; # 1158
1161 PLANT.HX2.TGASHOT(16) := 1083.21 ; # 1159
1162 PLANT.HX2.TGASHOT(17) := 1077.24 ; # 1160
1163 PLANT.HX2.TGASHOT(18) := 1070.92 ; # 1161
1164 PLANT.HX2.TGASHOT(19) := 1064.23 ; # 1162
1165 PLANT.HX2.TGASHOT(20) := 1057.15 ; # 1163
1166 PLANT.HX2.TGASHOT(21) := 1049.66 ; # 1164
1167 PLANT.HX2.TGASHOT(22) := 1041.74 ; # 1165
1168 PLANT.HX2.TGASHOT(23) := 1033.36 ; # 1166
1169 PLANT.HX2.TGASHOT(24) := 1024.48 ; # 1167
1170 PLANT.HX2.TGASHOT(25) := 1015.09 ; # 1168
1171 PLANT.HX2.TGASHOT(26) := 1005.16 ; # 1169
1172 PLANT.HX2.TGASHOT(27) := 994.647 ; # 1170
1173 PLANT.HX2.TGASHOT(28) := 983.524 ; # 1171
1174 PLANT.HX2.TGASHOT(29) := 971.753 ; # 1172
1175 PLANT.HX2.TGASHOT(30) := 959.298 ; # 1173
1176 PLANT.HX2.TGASHOT(31) := 946.119 ; # 1174
1177 PLANT.HX2.TGASHOT(32) := 932.173 ; # 1175
1178 PLANT.HX2.TGASHOT(33) := 917.416 ; # 1176
1179 PLANT.HX2.TGASHOT(34) := 901.801 ; # 1177
1180 PLANT.HX2.TGASHOT(35) := 885.278 ; # 1178
1181 PLANT.HX2.TGASHOT(36) := 867.793 ; # 1179
1182 PLANT.HX2.TGASHOT(37) := 849.292 ; # 1180
1183 PLANT.HX2.TGASHOT(38) := 829.715 ; # 1181
1184 PLANT.HX2.TGASHOT(39) := 809 ; # 1182
1185 PLANT.HX2.TGASHOT(40) := 787.081 ; # 1183
1186 PLANT.HX2.TGASCOLD(1) := 1126.32 ; # 1184
1187 PLANT.HX2.TGASCOLD(2) := 1122.86 ; # 1185
1188 PLANT.HX2.TGASCOLD(3) := 1119.19 ; # 1186
1189 PLANT.HX2.TGASCOLD(4) := 1115.31 ; # 1187
1190 PLANT.HX2.TGASCOLD(5) := 1111.2 ; # 1188
1191 PLANT.HX2.TGASCOLD(6) := 1106.86 ; # 1189
1192 PLANT.HX2.TGASCOLD(7) := 1102.26 ; # 1190
1193 PLANT.HX2.TGASCOLD(8) := 1097.39 ; # 1191
1194 PLANT.HX2.TGASCOLD(9) := 1092.24 ; # 1192
1195 PLANT.HX2.TGASCOLD(10) := 1086.8 ; # 1193
1196 PLANT.HX2.TGASCOLD(11) := 1081.03 ; # 1194
1197 PLANT.HX2.TGASCOLD(12) := 1074.93 ; # 1195
1198 PLANT.HX2.TGASCOLD(13) := 1068.48 ; # 1196
1199 PLANT.HX2.TGASCOLD(14) := 1061.65 ; # 1197
1200 PLANT.HX2.TGASCOLD(15) := 1054.42 ; # 1198
1201 PLANT.HX2.TGASCOLD(16) := 1046.77 ; # 1199
1202 PLANT.HX2.TGASCOLD(17) := 1038.68 ; # 1200
1203 PLANT.HX2.TGASCOLD(18) := 1030.12 ; # 1201
1204 PLANT.HX2.TGASCOLD(19) := 1021.06 ; # 1202
1205 PLANT.HX2.TGASCOLD(20) := 1011.47 ; # 1203
1206 PLANT.HX2.TGASCOLD(21) := 1001.32 ; # 1204
1207 PLANT.HX2.TGASCOLD(22) := 990.587 ; # 1205
1208 PLANT.HX2.TGASCOLD(23) := 979.228 ; # 1206
1209 PLANT.HX2.TGASCOLD(24) := 967.207 ; # 1207
1210 PLANT.HX2.TGASCOLD(25) := 954.488 ; # 1208
1211 PLANT.HX2.TGASCOLD(26) := 941.029 ; # 1209
1212 PLANT.HX2.TGASCOLD(27) := 926.787 ; # 1210
1213 PLANT.HX2.TGASCOLD(28) := 911.717 ; # 1211
1214 PLANT.HX2.TGASCOLD(29) := 895.77 ; # 1212
1215 PLANT.HX2.TGASCOLD(30) := 878.896 ; # 1213
1216 PLANT.HX2.TGASCOLD(31) := 861.041 ; # 1214
1217 PLANT.HX2.TGASCOLD(32) := 842.147 ; # 1215
1218 PLANT.HX2.TGASCOLD(33) := 822.155 ; # 1216
1219 PLANT.HX2.TGASCOLD(34) := 801 ; # 1217
1220 PLANT.HX2.TGASCOLD(35) := 778.614 ; # 1218

1221 PLANT.HX2.TGASCOLD(36) := 754.927 ; # 1219
1222 PLANT.HX2.TGASCOLD(37) := 729.862 ; # 1220
1223 PLANT.HX2.TGASCOLD(38) := 703.34 ; # 1221
1224 PLANT.HX2.TGASCOLD(39) := 675.275 ; # 1222
1225 PLANT.HX2.TGASCOLD(40) := 645.577 ; # 1223
1226 PLANT.HX2.UHOT := 1299.78 ; # 1224
1227 PLANT.HX2.UCOLD := 1880.53 ; # 1225
1228 PLANT.HX2.THX(1) := 1133.71 ; # 1226
1229 PLANT.HX2.THX(2) := 1130.67 ; # 1227
1230 PLANT.HX2.THX(3) := 1127.46 ; # 1228
1231 PLANT.HX2.THX(4) := 1124.06 ; # 1229
1232 PLANT.HX2.THX(5) := 1120.46 ; # 1230
1233 PLANT.HX2.THX(6) := 1116.65 ; # 1231
1234 PLANT.HX2.THX(7) := 1112.63 ; # 1232
1235 PLANT.HX2.THX(8) := 1108.36 ; # 1233
1236 PLANT.HX2.THX(9) := 1103.85 ; # 1234
1237 PLANT.HX2.THX(10) := 1099.08 ; # 1235
1238 PLANT.HX2.THX(11) := 1094.03 ; # 1236
1239 PLANT.HX2.THX(12) := 1088.69 ; # 1237
1240 PLANT.HX2.THX(13) := 1083.03 ; # 1238
1241 PLANT.HX2.THX(14) := 1077.05 ; # 1239
1242 PLANT.HX2.THX(15) := 1070.72 ; # 1240
1243 PLANT.HX2.THX(16) := 1064.02 ; # 1241
1244 PLANT.HX2.THX(17) := 1056.93 ; # 1242
1245 PLANT.HX2.THX(18) := 1049.43 ; # 1243
1246 PLANT.HX2.THX(19) := 1041.49 ; # 1244
1247 PLANT.HX2.THX(20) := 1033.09 ; # 1245
1248 PLANT.HX2.THX(21) := 1024.2 ; # 1246
1249 PLANT.HX2.THX(22) := 1014.8 ; # 1247
1250 PLANT.HX2.THX(23) := 1004.84 ; # 1248
1251 PLANT.HX2.THX(24) := 994.314 ; # 1249
1252 PLANT.HX2.THX(25) := 983.171 ; # 1250
1253 PLANT.HX2.THX(26) := 971.38 ; # 1251
1254 PLANT.HX2.THX(27) := 958.903 ; # 1252
1255 PLANT.HX2.THX(28) := 945.701 ; # 1253
1256 PLANT.HX2.THX(29) := 931.731 ; # 1254
1257 PLANT.HX2.THX(30) := 916.948 ; # 1255
1258 PLANT.HX2.THX(31) := 901.306 ; # 1256
1259 PLANT.HX2.THX(32) := 884.754 ; # 1257
1260 PLANT.HX2.THX(33) := 867.239 ; # 1258
1261 PLANT.HX2.THX(34) := 848.706 ; # 1259
1262 PLANT.HX2.THX(35) := 829.095 ; # 1260
1263 PLANT.HX2.THX(36) := 808.344 ; # 1261
1264 PLANT.HX2.THX(37) := 786.385 ; # 1262
1265 PLANT.HX2.THX(38) := 763.15 ; # 1263
1266 PLANT.HX2.THX(39) := 738.563 ; # 1264
1267 PLANT.HX2.THX(40) := 712.554 ; # 1265
1268 PLANT.PIPEC2.RHO(1) := 3.72389 ; # 1266
1269 PLANT.PIPEC2.RHO(2) := 3.55368 ; # 1267
1270 PLANT.PIPEC2.RHO(3) := 3.4055 ; # 1268
1271 PLANT.PIPEC2.RHO(4) := 3.27543 ; # 1269
1272 PLANT.PIPEC2.RHO(5) := 3.16041 ; # 1270
1273 PLANT.PIPEC2.RHO(6) := 3.05803 ; # 1271
1274 PLANT.PIPEC2.RHO(7) := 2.96638 ; # 1272
1275 PLANT.PIPEC2.RHO(8) := 2.88388 ; # 1273
1276 PLANT.PIPEC2.RHO(9) := 2.80928 ; # 1274
1277 PLANT.PIPEC2.RHO(10) := 2.74152 ; # 1275
1278 PLANT.PIPEC2.RHO(11) := 2.67973 ; # 1276
1279 PLANT.PIPEC2.RHO(12) := 2.62316 ; # 1277
1280 PLANT.PIPEC2.RHO(13) := 2.57121 ; # 1278
1281 PLANT.PIPEC2.RHO(14) := 2.52333 ; # 1279
1282 PLANT.PIPEC2.RHO(15) := 2.47909 ; # 1280
1283 PLANT.PIPEC2.RHO(16) := 2.43808 ; # 1281
1284 PLANT.PIPEC2.RHO(17) := 2.39997 ; # 1282
1285 PLANT.PIPEC2.RHO(18) := 2.36446 ; # 1283
1286 PLANT.PIPEC2.RHO(19) := 2.3313 ; # 1284
1287 PLANT.PIPEC2.RHO(20) := 2.30026 ; # 1285
1288 PLANT.PIPEC2.RHO(21) := 2.27113 ; # 1286
1289 PLANT.PIPEC2.RHO(22) := 2.24375 ; # 1287
1290 PLANT.PIPEC2.RHO(23) := 2.21796 ; # 1288
1291 PLANT.PIPEC2.RHO(24) := 2.19361 ; # 1289
1292 PLANT.PIPEC2.RHO(25) := 2.17058 ; # 1290
1293 PLANT.PIPEC2.RHO(26) := 2.14875 ; # 1291
1294 PLANT.PIPEC2.RHO(27) := 2.12804 ; # 1292
1295 PLANT.PIPEC2.RHO(28) := 2.10834 ; # 1293
1296 PLANT.PIPEC2.RHO(29) := 2.08957 ; # 1294
1297 PLANT.PIPEC2.RHO(30) := 2.07166 ; # 1295
1298 PLANT.PIPEC2.RHO(31) := 2.05454 ; # 1296
1299 PLANT.PIPEC2.RHO(32) := 2.03814 ; # 1297
1300 PLANT.PIPEC2.RHO(33) := 2.02242 ; # 1298
1301 PLANT.PIPEC2.RHO(34) := 2.00733 ; # 1299
1302 PLANT.PIPEC2.RHO(35) := 1.9928 ; # 1300
1303 PLANT.PIPEC2.RHO(36) := 1.97881 ; # 1301
1304 PLANT.PIPEC2.RHO(37) := 1.96531 ; # 1302
1305 PLANT.PIPEC2.RHO(38) := 1.95226 ; # 1303
1306 PLANT.PIPEC2.RHO(39) := 1.93964 ; # 1304
1307 PLANT.PIPEC2.RHO(40) := 1.92741 ; # 1305
1308 PLANT.PIPEC2.P(1) := 1.10918e+006 ; # 1306
1309 PLANT.PIPEC2.P(2) := 1.10717e+006 ; # 1307
1310 PLANT.PIPEC2.P(3) := 1.1051e+006 ; # 1308
1311 PLANT.PIPEC2.P(4) := 1.10297e+006 ; # 1309
1312 PLANT.PIPEC2.P(5) := 1.10079e+006 ; # 1310

1313 PLANT.PIPEC2.P(6) := 1.09855e+006 ; # 1311
1314 PLANT.PIPEC2.P(7) := 1.09626e+006 ; # 1312
1315 PLANT.PIPEC2.P(8) := 1.09392e+006 ; # 1313
1316 PLANT.PIPEC2.P(9) := 1.09154e+006 ; # 1314
1317 PLANT.PIPEC2.P(10) := 1.08911e+006 ; # 1315
1318 PLANT.PIPEC2.P(11) := 1.08663e+006 ; # 1316
1319 PLANT.PIPEC2.P(12) := 1.08412e+006 ; # 1317
1320 PLANT.PIPEC2.P(13) := 1.08156e+006 ; # 1318
1321 PLANT.PIPEC2.P(14) := 1.07897e+006 ; # 1319
1322 PLANT.PIPEC2.P(15) := 1.07634e+006 ; # 1320
1323 PLANT.PIPEC2.P(16) := 1.07368e+006 ; # 1321
1324 PLANT.PIPEC2.P(17) := 1.07098e+006 ; # 1322
1325 PLANT.PIPEC2.P(18) := 1.06825e+006 ; # 1323
1326 PLANT.PIPEC2.P(19) := 1.06548e+006 ; # 1324
1327 PLANT.PIPEC2.P(20) := 1.06269e+006 ; # 1325
1328 PLANT.PIPEC2.P(21) := 1.05986e+006 ; # 1326
1329 PLANT.PIPEC2.P(22) := 1.05701e+006 ; # 1327
1330 PLANT.PIPEC2.P(23) := 1.05413e+006 ; # 1328
1331 PLANT.PIPEC2.P(24) := 1.05123e+006 ; # 1329
1332 PLANT.PIPEC2.P(25) := 1.04829e+006 ; # 1330
1333 PLANT.PIPEC2.P(26) := 1.04533e+006 ; # 1331
1334 PLANT.PIPEC2.P(27) := 1.04235e+006 ; # 1332
1335 PLANT.PIPEC2.P(28) := 1.03935e+006 ; # 1333
1336 PLANT.PIPEC2.P(29) := 1.03632e+006 ; # 1334
1337 PLANT.PIPEC2.P(30) := 1.03326e+006 ; # 1335
1338 PLANT.PIPEC2.P(31) := 1.03019e+006 ; # 1336
1339 PLANT.PIPEC2.P(32) := 1.02709e+006 ; # 1337
1340 PLANT.PIPEC2.P(33) := 1.02398e+006 ; # 1338
1341 PLANT.PIPEC2.P(34) := 1.02084e+006 ; # 1339
1342 PLANT.PIPEC2.P(35) := 1.01768e+006 ; # 1340
1343 PLANT.PIPEC2.P(36) := 1.0145e+006 ; # 1341
1344 PLANT.PIPEC2.P(37) := 1.0113e+006 ; # 1342
1345 PLANT.PIPEC2.P(38) := 1.00808e+006 ; # 1343
1346 PLANT.PIPEC2.P(39) := 1.00485e+006 ; # 1344
1347 PLANT.PIPEC2.P(40) := 1.00159e+006 ; # 1345
1348 PLANT.PIPEC2.H(1) := 784075 ; # 1346
1349 PLANT.PIPEC2.H(2) := 851066 ; # 1347
1350 PLANT.PIPEC2.H(3) := 914376 ; # 1348
1351 PLANT.PIPEC2.H(4) := 974206 ; # 1349
1352 PLANT.PIPEC2.H(5) := 1.03075e+006 ; # 1350
1353 PLANT.PIPEC2.H(6) := 1.08418e+006 ; # 1351
1354 PLANT.PIPEC2.H(7) := 1.13468e+006 ; # 1352
1355 PLANT.PIPEC2.H(8) := 1.1824e+006 ; # 1353
1356 PLANT.PIPEC2.H(9) := 1.2275e+006 ; # 1354
1357 PLANT.PIPEC2.H(10) := 1.27012e+006 ; # 1355
1358 PLANT.PIPEC2.H(11) := 1.3104e+006 ; # 1356
1359 PLANT.PIPEC2.H(12) := 1.34847e+006 ; # 1357
1360 PLANT.PIPEC2.H(13) := 1.38444e+006 ; # 1358
1361 PLANT.PIPEC2.H(14) := 1.41843e+006 ; # 1359
1362 PLANT.PIPEC2.H(15) := 1.45056e+006 ; # 1360
1363 PLANT.PIPEC2.H(16) := 1.48092e+006 ; # 1361
1364 PLANT.PIPEC2.H(17) := 1.50962e+006 ; # 1362
1365 PLANT.PIPEC2.H(18) := 1.53673e+006 ; # 1363
1366 PLANT.PIPEC2.H(19) := 1.56236e+006 ; # 1364
1367 PLANT.PIPEC2.H(20) := 1.58657e+006 ; # 1365
1368 PLANT.PIPEC2.H(21) := 1.60946e+006 ; # 1366
1369 PLANT.PIPEC2.H(22) := 1.63109e+006 ; # 1367
1370 PLANT.PIPEC2.H(23) := 1.65153e+006 ; # 1368
1371 PLANT.PIPEC2.H(24) := 1.67085e+006 ; # 1369
1372 PLANT.PIPEC2.H(25) := 1.6891e+006 ; # 1370
1373 PLANT.PIPEC2.H(26) := 1.70635e+006 ; # 1371
1374 PLANT.PIPEC2.H(27) := 1.72265e+006 ; # 1372
1375 PLANT.PIPEC2.H(28) := 1.73806e+006 ; # 1373
1376 PLANT.PIPEC2.H(29) := 1.75262e+006 ; # 1374
1377 PLANT.PIPEC2.H(30) := 1.76638e+006 ; # 1375
1378 PLANT.PIPEC2.H(31) := 1.77939e+006 ; # 1376
1379 PLANT.PIPEC2.H(32) := 1.79168e+006 ; # 1377
1380 PLANT.PIPEC2.H(33) := 1.80329e+006 ; # 1378
1381 PLANT.PIPEC2.H(34) := 1.81427e+006 ; # 1379
1382 PLANT.PIPEC2.H(35) := 1.82464e+006 ; # 1380
1383 PLANT.PIPEC2.H(36) := 1.83444e+006 ; # 1381
1384 PLANT.PIPEC2.H(37) := 1.8437e+006 ; # 1382
1385 PLANT.PIPEC2.H(38) := 1.85246e+006 ; # 1383
1386 PLANT.PIPEC2.H(39) := 1.86073e+006 ; # 1384
1387 PLANT.PIPEC2.H(40) := 1.86855e+006 ; # 1385
1388 PLANT.PIPEC2.H0 := 713180 ; # 1386
1389 PLANT.PIPEC2.T(1) := 645.577 ; # 1387
1390 PLANT.PIPEC2.T(2) := 675.275 ; # 1388
1391 PLANT.PIPEC2.T(3) := 703.34 ; # 1389
1392 PLANT.PIPEC2.T(4) := 729.862 ; # 1390
1393 PLANT.PIPEC2.T(5) := 754.927 ; # 1391
1394 PLANT.PIPEC2.T(6) := 778.614 ; # 1392
1395 PLANT.PIPEC2.T(7) := 801 ; # 1393
1396 PLANT.PIPEC2.T(8) := 822.155 ; # 1394
1397 PLANT.PIPEC2.T(9) := 842.147 ; # 1395
1398 PLANT.PIPEC2.T(10) := 861.041 ; # 1396
1399 PLANT.PIPEC2.T(11) := 878.896 ; # 1397
1400 PLANT.PIPEC2.T(12) := 895.77 ; # 1398
1401 PLANT.PIPEC2.T(13) := 911.717 ; # 1399
1402 PLANT.PIPEC2.T(14) := 926.787 ; # 1400
1403 PLANT.PIPEC2.T(15) := 941.029 ; # 1401
1404 PLANT.PIPEC2.T(16) := 954.488 ; # 1402

1405 PLANT.PIPEC2.T(17) := 967.207 ; # 1403
1406 PLANT.PIPEC2.T(18) := 979.228 ; # 1404
1407 PLANT.PIPEC2.T(19) := 990.587 ; # 1405
1408 PLANT.PIPEC2.T(20) := 1001.32 ; # 1406
1409 PLANT.PIPEC2.T(21) := 1011.47 ; # 1407
1410 PLANT.PIPEC2.T(22) := 1021.06 ; # 1408
1411 PLANT.PIPEC2.T(23) := 1030.12 ; # 1409
1412 PLANT.PIPEC2.T(24) := 1038.68 ; # 1410
1413 PLANT.PIPEC2.T(25) := 1046.77 ; # 1411
1414 PLANT.PIPEC2.T(26) := 1054.42 ; # 1412
1415 PLANT.PIPEC2.T(27) := 1061.65 ; # 1413
1416 PLANT.PIPEC2.T(28) := 1068.48 ; # 1414
1417 PLANT.PIPEC2.T(29) := 1074.93 ; # 1415
1418 PLANT.PIPEC2.T(30) := 1081.03 ; # 1416
1419 PLANT.PIPEC2.T(31) := 1086.8 ; # 1417
1420 PLANT.PIPEC2.T(32) := 1092.24 ; # 1418
1421 PLANT.PIPEC2.T(33) := 1097.39 ; # 1419
1422 PLANT.PIPEC2.T(34) := 1102.26 ; # 1420
1423 PLANT.PIPEC2.T(35) := 1106.86 ; # 1421
1424 PLANT.PIPEC2.T(36) := 1111.2 ; # 1422
1425 PLANT.PIPEC2.T(37) := 1115.31 ; # 1423
1426 PLANT.PIPEC2.T(38) := 1119.19 ; # 1424
1427 PLANT.PIPEC2.T(39) := 1122.86 ; # 1425
1428 PLANT.PIPEC2.T(40) := 1126.32 ; # 1426
1429 PLANT.PIPEC2.TEXTRNL(1) := 712.554 ; # 1427
1430 PLANT.PIPEC2.TEXTRNL(2) := 738.563 ; # 1428
1431 PLANT.PIPEC2.TEXTRNL(3) := 763.15 ; # 1429
1432 PLANT.PIPEC2.TEXTRNL(4) := 786.385 ; # 1430
1433 PLANT.PIPEC2.TEXTRNL(5) := 808.344 ; # 1431
1434 PLANT.PIPEC2.TEXTRNL(6) := 829.095 ; # 1432
1435 PLANT.PIPEC2.TEXTRNL(7) := 848.706 ; # 1433
1436 PLANT.PIPEC2.TEXTRNL(8) := 867.239 ; # 1434
1437 PLANT.PIPEC2.TEXTRNL(9) := 884.754 ; # 1435
1438 PLANT.PIPEC2.TEXTRNL(10) := 901.306 ; # 1436
1439 PLANT.PIPEC2.TEXTRNL(11) := 916.948 ; # 1437
1440 PLANT.PIPEC2.TEXTRNL(12) := 931.731 ; # 1438
1441 PLANT.PIPEC2.TEXTRNL(13) := 945.701 ; # 1439
1442 PLANT.PIPEC2.TEXTRNL(14) := 958.903 ; # 1440
1443 PLANT.PIPEC2.TEXTRNL(15) := 971.38 ; # 1441
1444 PLANT.PIPEC2.TEXTRNL(16) := 983.171 ; # 1442
1445 PLANT.PIPEC2.TEXTRNL(17) := 994.314 ; # 1443
1446 PLANT.PIPEC2.TEXTRNL(18) := 1004.84 ; # 1444
1447 PLANT.PIPEC2.TEXTRNL(19) := 1014.8 ; # 1445
1448 PLANT.PIPEC2.TEXTRNL(20) := 1024.2 ; # 1446
1449 PLANT.PIPEC2.TEXTRNL(21) := 1033.09 ; # 1447
1450 PLANT.PIPEC2.TEXTRNL(22) := 1041.49 ; # 1448
1451 PLANT.PIPEC2.TEXTRNL(23) := 1049.43 ; # 1449
1452 PLANT.PIPEC2.TEXTRNL(24) := 1056.93 ; # 1450
1453 PLANT.PIPEC2.TEXTRNL(25) := 1064.02 ; # 1451
1454 PLANT.PIPEC2.TEXTRNL(26) := 1070.72 ; # 1452
1455 PLANT.PIPEC2.TEXTRNL(27) := 1077.05 ; # 1453
1456 PLANT.PIPEC2.TEXTRNL(28) := 1083.03 ; # 1454
1457 PLANT.PIPEC2.TEXTRNL(29) := 1088.69 ; # 1455
1458 PLANT.PIPEC2.TEXTRNL(30) := 1094.03 ; # 1456
1459 PLANT.PIPEC2.TEXTRNL(31) := 1099.08 ; # 1457
1460 PLANT.PIPEC2.TEXTRNL(32) := 1103.85 ; # 1458
1461 PLANT.PIPEC2.TEXTRNL(33) := 1108.36 ; # 1459
1462 PLANT.PIPEC2.TEXTRNL(34) := 1112.63 ; # 1460
1463 PLANT.PIPEC2.TEXTRNL(35) := 1116.65 ; # 1461
1464 PLANT.PIPEC2.TEXTRNL(36) := 1120.46 ; # 1462
1465 PLANT.PIPEC2.TEXTRNL(37) := 1124.06 ; # 1463
1466 PLANT.PIPEC2.TEXTRNL(38) := 1127.46 ; # 1464
1467 PLANT.PIPEC2.TEXTRNL(39) := 1130.67 ; # 1465
1468 PLANT.PIPEC2.TEXTRNL(40) := 1133.71 ; # 1466
1469 PLANT.PIPEC2.F(1) := 43.3743 ; # 1467
1470 PLANT.PIPEC2.F(2) := 43.3743 ; # 1468
1471 PLANT.PIPEC2.F(3) := 43.3743 ; # 1469
1472 PLANT.PIPEC2.F(4) := 43.3743 ; # 1470
1473 PLANT.PIPEC2.F(5) := 43.3743 ; # 1471
1474 PLANT.PIPEC2.F(6) := 43.3743 ; # 1472
1475 PLANT.PIPEC2.F(7) := 43.3743 ; # 1473
1476 PLANT.PIPEC2.F(8) := 43.3743 ; # 1474
1477 PLANT.PIPEC2.F(9) := 43.3743 ; # 1475
1478 PLANT.PIPEC2.F(10) := 43.3743 ; # 1476
1479 PLANT.PIPEC2.F(11) := 43.3743 ; # 1477
1480 PLANT.PIPEC2.F(12) := 43.3743 ; # 1478
1481 PLANT.PIPEC2.F(13) := 43.3743 ; # 1479
1482 PLANT.PIPEC2.F(14) := 43.3743 ; # 1480
1483 PLANT.PIPEC2.F(15) := 43.3743 ; # 1481
1484 PLANT.PIPEC2.F(16) := 43.3743 ; # 1482
1485 PLANT.PIPEC2.F(17) := 43.3743 ; # 1483
1486 PLANT.PIPEC2.F(18) := 43.3743 ; # 1484
1487 PLANT.PIPEC2.F(19) := 43.3743 ; # 1485
1488 PLANT.PIPEC2.F(20) := 43.3743 ; # 1486
1489 PLANT.PIPEC2.F(21) := 43.3743 ; # 1487
1490 PLANT.PIPEC2.F(22) := 43.3743 ; # 1488
1491 PLANT.PIPEC2.F(23) := 43.3743 ; # 1489
1492 PLANT.PIPEC2.F(24) := 43.3743 ; # 1490
1493 PLANT.PIPEC2.F(25) := 43.3743 ; # 1491
1494 PLANT.PIPEC2.F(26) := 43.3743 ; # 1492
1495 PLANT.PIPEC2.F(27) := 43.3743 ; # 1493
1496 PLANT.PIPEC2.F(28) := 43.3743 ; # 1494


```

1497 PLANT.PIPEC2.F(29) := 43.3743 ; # 1495
1498 PLANT.PIPEC2.F(30) := 43.3743 ; # 1496
1499 PLANT.PIPEC2.F(31) := 43.3743 ; # 1497
1500 PLANT.PIPEC2.F(32) := 43.3743 ; # 1498
1501 PLANT.PIPEC2.F(33) := 43.3743 ; # 1499
1502 PLANT.PIPEC2.F(34) := 43.3743 ; # 1500
1503 PLANT.PIPEC2.F(35) := 43.3743 ; # 1501
1504 PLANT.PIPEC2.F(36) := 43.3743 ; # 1502
1505 PLANT.PIPEC2.F(37) := 43.3743 ; # 1503
1506 PLANT.PIPEC2.F(38) := 43.3743 ; # 1504
1507 PLANT.PIPEC2.F(39) := 43.3743 ; # 1505
1508 PLANT.PIPEC2.F(40) := 43.3743 ; # 1506
1509 PLANT.PIPEC2.F_IN := 43.3743 ; # 1507
1510 PLANT.PIPEC2.PSI(1) := 1.81063e+006 ; # 1508
1511 PLANT.PIPEC2.PSI(2) := 1.91725e+006 ; # 1509
1512 PLANT.PIPEC2.PSI(3) := 2.00881e+006 ; # 1510
1513 PLANT.PIPEC2.PSI(4) := 2.08797e+006 ; # 1511
1514 PLANT.PIPEC2.PSI(5) := 2.1568e+006 ; # 1512
1515 PLANT.PIPEC2.PSI(6) := 2.21692e+006 ; # 1513
1516 PLANT.PIPEC2.PSI(7) := 2.26963e+006 ; # 1514
1517 PLANT.PIPEC2.PSI(8) := 2.31599e+006 ; # 1515
1518 PLANT.PIPEC2.PSI(9) := 2.35686e+006 ; # 1516
1519 PLANT.PIPEC2.PSI(10) := 2.39296e+006 ; # 1517
1520 PLANT.PIPEC2.PSI(11) := 2.42488e+006 ; # 1518
1521 PLANT.PIPEC2.PSI(12) := 2.45312e+006 ; # 1519
1522 PLANT.PIPEC2.PSI(13) := 2.47811e+006 ; # 1520
1523 PLANT.PIPEC2.PSI(14) := 2.50021e+006 ; # 1521
1524 PLANT.PIPEC2.PSI(15) := 2.51973e+006 ; # 1522
1525 PLANT.PIPEC2.PSI(16) := 2.53693e+006 ; # 1523
1526 PLANT.PIPEC2.PSI(17) := 2.55205e+006 ; # 1524
1527 PLANT.PIPEC2.PSI(18) := 2.5653e+006 ; # 1525
1528 PLANT.PIPEC2.PSI(19) := 2.57684e+006 ; # 1526
1529 PLANT.PIPEC2.PSI(20) := 2.58684e+006 ; # 1527
1530 PLANT.PIPEC2.PSI(21) := 2.59544e+006 ; # 1528
1531 PLANT.PIPEC2.PSI(22) := 2.60275e+006 ; # 1529
1532 PLANT.PIPEC2.PSI(23) := 2.60889e+006 ; # 1530
1533 PLANT.PIPEC2.PSI(24) := 2.61395e+006 ; # 1531
1534 PLANT.PIPEC2.PSI(25) := 2.61803e+006 ; # 1532
1535 PLANT.PIPEC2.PSI(26) := 2.62119e+006 ; # 1533
1536 PLANT.PIPEC2.PSI(27) := 2.62352e+006 ; # 1534
1537 PLANT.PIPEC2.PSI(28) := 2.62507e+006 ; # 1535
1538 PLANT.PIPEC2.PSI(29) := 2.62591e+006 ; # 1536
1539 PLANT.PIPEC2.PSI(30) := 2.62607e+006 ; # 1537
1540 PLANT.PIPEC2.PSI(31) := 2.62562e+006 ; # 1538
1541 PLANT.PIPEC2.PSI(32) := 2.6246e+006 ; # 1539
1542 PLANT.PIPEC2.PSI(33) := 2.62304e+006 ; # 1540
1543 PLANT.PIPEC2.PSI(34) := 2.62099e+006 ; # 1541
1544 PLANT.PIPEC2.PSI(35) := 2.61847e+006 ; # 1542
1545 PLANT.PIPEC2.PSI(36) := 2.61551e+006 ; # 1543
1546 PLANT.PIPEC2.PSI(37) := 2.61215e+006 ; # 1544
1547 PLANT.PIPEC2.PSI(38) := 2.6084e+006 ; # 1545
1548 PLANT.PIPEC2.PSI(39) := 2.6043e+006 ; # 1546
1549 PLANT.PIPEC2.PSI(40) := 2.59986e+006 ; # 1547
1550 PLANT.PIPEC2.HT.RHOPIPEHE := 2.35217 ; # 1548
1551 PLANT.PIPEC2.HT.VPIPE := 65.6203 ; # 1549
1552 PLANT.PIPEC2.HT.U := 1880.53 ; # 1550

```

HTLOMACH_SS_IN_INI.INITIAL

```

1 # Values for differential variables in computation HTLOMACH_SS
2 # Saved at time 1000
3 PLANT.HX.THX(1) = 879.893 ; # 1
4 PLANT.HX.THX(2) = 892.184 ; # 2
5 PLANT.HX.THX(3) = 904.161 ; # 3
6 PLANT.HX.THX(4) = 915.766 ; # 4
7 PLANT.HX.THX(5) = 927.009 ; # 5
8 PLANT.HX.THX(6) = 937.904 ; # 6
9 PLANT.HX.THX(7) = 948.459 ; # 7
10 PLANT.HX.THX(8) = 958.687 ; # 8
11 PLANT.HX.THX(9) = 968.596 ; # 9
12 PLANT.HX.THX(10) = 978.197 ; # 10
13 PLANT.HX.THX(11) = 987.5 ; # 11
14 PLANT.HX.THX(12) = 996.513 ; # 12
15 PLANT.HX.THX(13) = 1005.25 ; # 13
16 PLANT.HX.THX(14) = 1013.71 ; # 14
17 PLANT.HX.THX(15) = 1021.91 ; # 15
18 PLANT.HX.THX(16) = 1029.85 ; # 16
19 PLANT.HX.THX(17) = 1037.55 ; # 17
20 PLANT.HX.THX(18) = 1045 ; # 18
21 PLANT.HX.THX(19) = 1052.23 ; # 19
22 PLANT.HX.THX(20) = 1059.23 ; # 20
23 PLANT.HX.THX(21) = 1066.01 ; # 21
24 PLANT.HX.THX(22) = 1072.58 ; # 22

```

25 PLANT.HX.THX(23) = 1078.95 ; # 23
26 PLANT.HX.THX(24) = 1085.12 ; # 24
27 PLANT.HX.THX(25) = 1091.1 ; # 25
28 PLANT.HX.THX(26) = 1096.89 ; # 26
29 PLANT.HX.THX(27) = 1102.5 ; # 27
30 PLANT.HX.THX(28) = 1107.94 ; # 28
31 PLANT.HX.THX(29) = 1113.21 ; # 29
32 PLANT.HX.THX(30) = 1118.31 ; # 30
33 PLANT.HX.THX(31) = 1123.26 ; # 31
34 PLANT.HX.THX(32) = 1128.05 ; # 32
35 PLANT.HX.THX(33) = 1132.69 ; # 33
36 PLANT.HX.THX(34) = 1137.19 ; # 34
37 PLANT.HX.THX(35) = 1141.55 ; # 35
38 PLANT.HX.THX(36) = 1145.77 ; # 36
39 PLANT.HX.THX(37) = 1149.86 ; # 37
40 PLANT.HX.THX(38) = 1153.83 ; # 38
41 PLANT.HX.THX(39) = 1157.67 ; # 39
42 PLANT.HX.THX(40) = 1161.37 ; # 40
43 PLANT.LOOP1.RHO(1) = 1.15317 ; # 41
44 PLANT.LOOP1.RHO(2) = 1.15067 ; # 42
45 PLANT.LOOP1.RHO(3) = 1.14817 ; # 43
46 PLANT.LOOP1.RHO(4) = 1.14565 ; # 44
47 PLANT.LOOP1.RHO(5) = 1.14313 ; # 45
48 PLANT.LOOP1.RHO(6) = 1.14059 ; # 46
49 PLANT.LOOP1.RHO(7) = 1.13804 ; # 47
50 PLANT.LOOP1.RHO(8) = 1.13549 ; # 48
51 PLANT.LOOP1.RHO(9) = 1.13292 ; # 49
52 PLANT.LOOP1.RHO(10) = 1.13034 ; # 50
53 PLANT.LOOP1.RHO(11) = 1.12115 ; # 51
54 PLANT.LOOP1.RHO(12) = 1.1026 ; # 52
55 PLANT.LOOP1.RHO(13) = 1.08477 ; # 53
56 PLANT.LOOP1.RHO(14) = 1.06791 ; # 54
57 PLANT.LOOP1.RHO(15) = 1.05196 ; # 55
58 PLANT.LOOP1.RHO(16) = 1.03683 ; # 56
59 PLANT.LOOP1.RHO(17) = 1.02247 ; # 57
60 PLANT.LOOP1.RHO(18) = 1.00882 ; # 58
61 PLANT.LOOP1.RHO(19) = 0.995831 ; # 59
62 PLANT.LOOP1.RHO(20) = 0.983453 ; # 60
63 PLANT.LOOP1.RHO(21) = 0.971645 ; # 61
64 PLANT.LOOP1.RHO(22) = 0.960369 ; # 62
65 PLANT.LOOP1.RHO(23) = 0.949588 ; # 63
66 PLANT.LOOP1.RHO(24) = 0.939272 ; # 64
67 PLANT.LOOP1.RHO(25) = 0.929389 ; # 65
68 PLANT.LOOP1.RHO(26) = 0.919912 ; # 66
69 PLANT.LOOP1.RHO(27) = 0.910817 ; # 67
70 PLANT.LOOP1.RHO(28) = 0.90208 ; # 68
71 PLANT.LOOP1.RHO(29) = 0.89368 ; # 69
72 PLANT.LOOP1.RHO(30) = 0.885596 ; # 70
73 PLANT.LOOP1.RHO(31) = 0.87781 ; # 71
74 PLANT.LOOP1.RHO(32) = 0.870305 ; # 72
75 PLANT.LOOP1.RHO(33) = 0.863066 ; # 73
76 PLANT.LOOP1.RHO(34) = 0.856077 ; # 74
77 PLANT.LOOP1.RHO(35) = 0.849325 ; # 75
78 PLANT.LOOP1.RHO(36) = 0.842796 ; # 76
79 PLANT.LOOP1.RHO(37) = 0.83648 ; # 77
80 PLANT.LOOP1.RHO(38) = 0.830364 ; # 78
81 PLANT.LOOP1.RHO(39) = 0.824437 ; # 79
82 PLANT.LOOP1.RHO(40) = 0.818691 ; # 80
83 PLANT.LOOP1.RHO(41) = 0.813116 ; # 81
84 PLANT.LOOP1.RHO(42) = 0.807703 ; # 82
85 PLANT.LOOP1.RHO(43) = 0.802444 ; # 83
86 PLANT.LOOP1.RHO(44) = 0.797332 ; # 84
87 PLANT.LOOP1.RHO(45) = 0.792359 ; # 85
88 PLANT.LOOP1.RHO(46) = 0.787518 ; # 86
89 PLANT.LOOP1.RHO(47) = 0.782803 ; # 87
90 PLANT.LOOP1.RHO(48) = 0.778208 ; # 88
91 PLANT.LOOP1.RHO(49) = 0.773727 ; # 89
92 PLANT.LOOP1.RHO(50) = 0.769359 ; # 90
93 PLANT.LOOP1.RHO(51) = 0.7657959 ; # 91
94 PLANT.LOOP1.RHO(52) = 0.761103 ; # 92
95 PLANT.LOOP1.RHO(53) = 0.754256 ; # 93
96 PLANT.LOOP1.RHO(54) = 0.752399 ; # 94
97 PLANT.LOOP1.RHO(55) = 0.750533 ; # 95
98 PLANT.LOOP1.RHO(56) = 0.748658 ; # 96
99 PLANT.LOOP1.RHO(57) = 0.746773 ; # 97
100 PLANT.LOOP1.RHO(58) = 0.744879 ; # 98
101 PLANT.LOOP1.RHO(59) = 0.742975 ; # 99
102 PLANT.LOOP1.RHO(60) = 0.741061 ; # 100
103 PLANT.LOOP1.RHO(61) = 0.750585 ; # 101
104 PLANT.LOOP1.RHO(62) = 0.751689 ; # 102
105 PLANT.LOOP1.RHO(63) = 0.752856 ; # 103
106 PLANT.LOOP1.RHO(64) = 0.754135 ; # 104
107 PLANT.LOOP1.RHO(65) = 0.755533 ; # 105
108 PLANT.LOOP1.RHO(66) = 0.757059 ; # 106
109 PLANT.LOOP1.RHO(67) = 0.75872 ; # 107
110 PLANT.LOOP1.RHO(68) = 0.760528 ; # 108
111 PLANT.LOOP1.RHO(69) = 0.762492 ; # 109
112 PLANT.LOOP1.RHO(70) = 0.764623 ; # 110
113 PLANT.LOOP1.RHO(71) = 0.766934 ; # 111
114 PLANT.LOOP1.RHO(72) = 0.769438 ; # 112
115 PLANT.LOOP1.RHO(73) = 0.772149 ; # 113
116 PLANT.LOOP1.RHO(74) = 0.775083 ; # 114

117 PLANT.LOOP1.RHO(75) = 0.778256 ; # 115
118 PLANT.LOOP1.RHO(76) = 0.781688 ; # 116
119 PLANT.LOOP1.RHO(77) = 0.785399 ; # 117
120 PLANT.LOOP1.RHO(78) = 0.789411 ; # 118
121 PLANT.LOOP1.RHO(79) = 0.793749 ; # 119
122 PLANT.LOOP1.RHO(80) = 0.798441 ; # 120
123 PLANT.LOOP1.RHO(81) = 0.803515 ; # 121
124 PLANT.LOOP1.RHO(82) = 0.809005 ; # 122
125 PLANT.LOOP1.RHO(83) = 0.814949 ; # 123
126 PLANT.LOOP1.RHO(84) = 0.821387 ; # 124
127 PLANT.LOOP1.RHO(85) = 0.828365 ; # 125
128 PLANT.LOOP1.RHO(86) = 0.835933 ; # 126
129 PLANT.LOOP1.RHO(87) = 0.844151 ; # 127
130 PLANT.LOOP1.RHO(88) = 0.853082 ; # 128
131 PLANT.LOOP1.RHO(89) = 0.8628 ; # 129
132 PLANT.LOOP1.RHO(90) = 0.873389 ; # 130
133 PLANT.LOOP1.RHO(91) = 0.884944 ; # 131
134 PLANT.LOOP1.RHO(92) = 0.897573 ; # 132
135 PLANT.LOOP1.RHO(93) = 0.911403 ; # 133
136 PLANT.LOOP1.RHO(94) = 0.926579 ; # 134
137 PLANT.LOOP1.RHO(95) = 0.94327 ; # 135
138 PLANT.LOOP1.RHO(96) = 0.961674 ; # 136
139 PLANT.LOOP1.RHO(97) = 0.982027 ; # 137
140 PLANT.LOOP1.RHO(98) = 1.0046 ; # 138
141 PLANT.LOOP1.RHO(99) = 1.02974 ; # 139
142 PLANT.LOOP1.RHO(100) = 1.05783 ; # 140
143 PLANT.LOOP1.PSI(1) = 1.23127e+006 ; # 141
144 PLANT.LOOP1.PSI(2) = 1.22711e+006 ; # 142
145 PLANT.LOOP1.PSI(3) = 1.22294e+006 ; # 143
146 PLANT.LOOP1.PSI(4) = 1.21877e+006 ; # 144
147 PLANT.LOOP1.PSI(5) = 1.2146e+006 ; # 145
148 PLANT.LOOP1.PSI(6) = 1.21042e+006 ; # 146
149 PLANT.LOOP1.PSI(7) = 1.20624e+006 ; # 147
150 PLANT.LOOP1.PSI(8) = 1.20206e+006 ; # 148
151 PLANT.LOOP1.PSI(9) = 1.19787e+006 ; # 149
152 PLANT.LOOP1.PSI(10) = 1.19368e+006 ; # 150
153 PLANT.LOOP1.PSI(11) = 1.23208e+006 ; # 151
154 PLANT.LOOP1.PSI(12) = 1.25743e+006 ; # 152
155 PLANT.LOOP1.PSI(13) = 1.28069e+006 ; # 153
156 PLANT.LOOP1.PSI(14) = 1.30237e+006 ; # 154
157 PLANT.LOOP1.PSI(15) = 1.3226e+006 ; # 155
158 PLANT.LOOP1.PSI(16) = 1.34148e+006 ; # 156
159 PLANT.LOOP1.PSI(17) = 1.35911e+006 ; # 157
160 PLANT.LOOP1.PSI(18) = 1.37558e+006 ; # 158
161 PLANT.LOOP1.PSI(19) = 1.39098e+006 ; # 159
162 PLANT.LOOP1.PSI(20) = 1.40537e+006 ; # 160
163 PLANT.LOOP1.PSI(21) = 1.41883e+006 ; # 161
164 PLANT.LOOP1.PSI(22) = 1.4314e+006 ; # 162
165 PLANT.LOOP1.PSI(23) = 1.44316e+006 ; # 163
166 PLANT.LOOP1.PSI(24) = 1.45415e+006 ; # 164
167 PLANT.LOOP1.PSI(25) = 1.46441e+006 ; # 165
168 PLANT.LOOP1.PSI(26) = 1.474e+006 ; # 166
169 PLANT.LOOP1.PSI(27) = 1.48294e+006 ; # 167
170 PLANT.LOOP1.PSI(28) = 1.49129e+006 ; # 168
171 PLANT.LOOP1.PSI(29) = 1.49907e+006 ; # 169
172 PLANT.LOOP1.PSI(30) = 1.50631e+006 ; # 170
173 PLANT.LOOP1.PSI(31) = 1.51304e+006 ; # 171
174 PLANT.LOOP1.PSI(32) = 1.5193e+006 ; # 172
175 PLANT.LOOP1.PSI(33) = 1.5251e+006 ; # 173
176 PLANT.LOOP1.PSI(34) = 1.53047e+006 ; # 174
177 PLANT.LOOP1.PSI(35) = 1.53543e+006 ; # 175
178 PLANT.LOOP1.PSI(36) = 1.54001e+006 ; # 176
179 PLANT.LOOP1.PSI(37) = 1.54421e+006 ; # 177
180 PLANT.LOOP1.PSI(38) = 1.54807e+006 ; # 178
181 PLANT.LOOP1.PSI(39) = 1.5516e+006 ; # 179
182 PLANT.LOOP1.PSI(40) = 1.5548e+006 ; # 180
183 PLANT.LOOP1.PSI(41) = 1.55771e+006 ; # 181
184 PLANT.LOOP1.PSI(42) = 1.56032e+006 ; # 182
185 PLANT.LOOP1.PSI(43) = 1.56266e+006 ; # 183
186 PLANT.LOOP1.PSI(44) = 1.56474e+006 ; # 184
187 PLANT.LOOP1.PSI(45) = 1.56657e+006 ; # 185
188 PLANT.LOOP1.PSI(46) = 1.56816e+006 ; # 186
189 PLANT.LOOP1.PSI(47) = 1.56951e+006 ; # 187
190 PLANT.LOOP1.PSI(48) = 1.57065e+006 ; # 188
191 PLANT.LOOP1.PSI(49) = 1.57158e+006 ; # 189
192 PLANT.LOOP1.PSI(50) = 1.5723e+006 ; # 190
193 PLANT.LOOP1.PSI(51) = 1.57307e+006 ; # 191
194 PLANT.LOOP1.PSI(52) = 1.5738e+006 ; # 192
195 PLANT.LOOP1.PSI(53) = 1.57457e+006 ; # 193
196 PLANT.LOOP1.PSI(54) = 1.57534e+006 ; # 194
197 PLANT.LOOP1.PSI(55) = 1.57611e+006 ; # 195
198 PLANT.LOOP1.PSI(56) = 1.57688e+006 ; # 196
199 PLANT.LOOP1.PSI(57) = 1.57765e+006 ; # 197
200 PLANT.LOOP1.PSI(58) = 1.57842e+006 ; # 198
201 PLANT.LOOP1.PSI(59) = 1.57919e+006 ; # 199
202 PLANT.LOOP1.PSI(60) = 1.57996e+006 ; # 200
203 PLANT.LOOP1.PSI(61) = 1.58073e+006 ; # 201
204 PLANT.LOOP1.PSI(62) = 1.5815e+006 ; # 202
205 PLANT.LOOP1.PSI(63) = 1.58227e+006 ; # 203
206 PLANT.LOOP1.PSI(64) = 1.58304e+006 ; # 204
207 PLANT.LOOP1.PSI(65) = 1.58381e+006 ; # 205
208 PLANT.LOOP1.PSI(66) = 1.58458e+006 ; # 206

209 PLANT.LOOP1.PSI(67) = 1.48357e+006 ; # 207
 210 PLANT.LOOP1.PSI(68) = 1.47859e+006 ; # 208
 211 PLANT.LOOP1.PSI(69) = 1.47338e+006 ; # 209
 212 PLANT.LOOP1.PSI(70) = 1.46791e+006 ; # 210
 213 PLANT.LOOP1.PSI(71) = 1.46218e+006 ; # 211
 214 PLANT.LOOP1.PSI(72) = 1.45616e+006 ; # 212
 215 PLANT.LOOP1.PSI(73) = 1.44982e+006 ; # 213
 216 PLANT.LOOP1.PSI(74) = 1.44315e+006 ; # 214
 217 PLANT.LOOP1.PSI(75) = 1.43612e+006 ; # 215
 218 PLANT.LOOP1.PSI(76) = 1.4287e+006 ; # 216
 219 PLANT.LOOP1.PSI(77) = 1.42087e+006 ; # 217
 220 PLANT.LOOP1.PSI(78) = 1.41258e+006 ; # 218
 221 PLANT.LOOP1.PSI(79) = 1.40379e+006 ; # 219
 222 PLANT.LOOP1.PSI(80) = 1.39448e+006 ; # 220
 223 PLANT.LOOP1.PSI(81) = 1.38459e+006 ; # 221
 224 PLANT.LOOP1.PSI(82) = 1.37407e+006 ; # 222
 225 PLANT.LOOP1.PSI(83) = 1.36287e+006 ; # 223
 226 PLANT.LOOP1.PSI(84) = 1.35093e+006 ; # 224
 227 PLANT.LOOP1.PSI(85) = 1.33817e+006 ; # 225
 228 PLANT.LOOP1.PSI(86) = 1.32451e+006 ; # 226
 229 PLANT.LOOP1.PSI(87) = 1.30988e+006 ; # 227
 230 PLANT.LOOP1.PSI(88) = 1.29416e+006 ; # 228
 231 PLANT.LOOP1.PSI(89) = 1.27725e+006 ; # 229
 232 PLANT.LOOP1.PSI(90) = 1.25903e+006 ; # 230
 233 PLANT.LOOP1.PSI(91) = 1.23934e+006 ; # 231
 234 PLANT.LOOP1.PSI(92) = 1.21801e+006 ; # 232
 235 PLANT.LOOP1.PSI(93) = 1.19486e+006 ; # 233
 236 PLANT.LOOP1.PSI(94) = 1.16967e+006 ; # 234
 237 PLANT.LOOP1.PSI(95) = 1.14217e+006 ; # 235
 238 PLANT.LOOP1.PSI(96) = 1.11205e+006 ; # 236
 239 PLANT.LOOP1.PSI(97) = 1.07896e+006 ; # 237
 240 PLANT.LOOP1.PSI(98) = 1.04248e+006 ; # 238
 241 PLANT.LOOP1.PSI(99) = 1.00208e+006 ; # 239
 242 PLANT.LOOP1.PSI(100) = 957156 ; # 240
 243 PLANT.LOOP1.RHOEXTRA(1) = 1.1654 ; # 241
 244 PLANT.LOOP1.RHOEXTRA(2) = 1.1654 ; # 242
 245 PLANT.LOOP1.PSIEXTRA(1) = 1.24585e+006 ; # 243
 246 PLANT.LOOP1.PSIEXTRA(2) = 1.24585e+006 ; # 244
 247 PLANT.PIPEH.RHO(1) = 2.87869 ; # 245
 248 PLANT.PIPEH.RHO(2) = 2.88664 ; # 246
 249 PLANT.PIPEH.RHO(3) = 2.89491 ; # 247
 250 PLANT.PIPEH.RHO(4) = 2.90353 ; # 248
 251 PLANT.PIPEH.RHO(5) = 2.9125 ; # 249
 252 PLANT.PIPEH.RHO(6) = 2.92184 ; # 250
 253 PLANT.PIPEH.RHO(7) = 2.93156 ; # 251
 254 PLANT.PIPEH.RHO(8) = 2.9417 ; # 252
 255 PLANT.PIPEH.RHO(9) = 2.95225 ; # 253
 256 PLANT.PIPEH.RHO(10) = 2.96325 ; # 254
 257 PLANT.PIPEH.RHO(11) = 2.97471 ; # 255
 258 PLANT.PIPEH.RHO(12) = 2.98666 ; # 256
 259 PLANT.PIPEH.RHO(13) = 2.99912 ; # 257
 260 PLANT.PIPEH.RHO(14) = 3.01211 ; # 258
 261 PLANT.PIPEH.RHO(15) = 3.02567 ; # 259
 262 PLANT.PIPEH.RHO(16) = 3.03982 ; # 260
 263 PLANT.PIPEH.RHO(17) = 3.05458 ; # 261
 264 PLANT.PIPEH.RHO(18) = 3.07 ; # 262
 265 PLANT.PIPEH.RHO(19) = 3.08611 ; # 263
 266 PLANT.PIPEH.RHO(20) = 3.10294 ; # 264
 267 PLANT.PIPEH.RHO(21) = 3.12053 ; # 265
 268 PLANT.PIPEH.RHO(22) = 3.13892 ; # 266
 269 PLANT.PIPEH.RHO(23) = 3.15816 ; # 267
 270 PLANT.PIPEH.RHO(24) = 3.1783 ; # 268
 271 PLANT.PIPEH.RHO(25) = 3.19939 ; # 269
 272 PLANT.PIPEH.RHO(26) = 3.22148 ; # 270
 273 PLANT.PIPEH.RHO(27) = 3.24463 ; # 271
 274 PLANT.PIPEH.RHO(28) = 3.2689 ; # 272
 275 PLANT.PIPEH.RHO(29) = 3.29437 ; # 273
 276 PLANT.PIPEH.RHO(30) = 3.32112 ; # 274
 277 PLANT.PIPEH.RHO(31) = 3.34921 ; # 275
 278 PLANT.PIPEH.RHO(32) = 3.37874 ; # 276
 279 PLANT.PIPEH.RHO(33) = 3.4098 ; # 277
 280 PLANT.PIPEH.RHO(34) = 3.4425 ; # 278
 281 PLANT.PIPEH.RHO(35) = 3.47695 ; # 279
 282 PLANT.PIPEH.RHO(36) = 3.51328 ; # 280
 283 PLANT.PIPEH.RHO(37) = 3.55161 ; # 281
 284 PLANT.PIPEH.RHO(38) = 3.59209 ; # 282
 285 PLANT.PIPEH.RHO(39) = 3.6349 ; # 283
 286 PLANT.PIPEH.RHO(40) = 3.68012 ; # 284
 287 PLANT.PIPEH.F(1) = 32.3305 ; # 285
 288 PLANT.PIPEH.F(2) = 32.3305 ; # 286
 289 PLANT.PIPEH.F(3) = 32.3305 ; # 287
 290 PLANT.PIPEH.F(4) = 32.3305 ; # 288
 291 PLANT.PIPEH.F(5) = 32.3305 ; # 289
 292 PLANT.PIPEH.F(6) = 32.3305 ; # 290
 293 PLANT.PIPEH.F(7) = 32.3305 ; # 291
 294 PLANT.PIPEH.F(8) = 32.3305 ; # 292
 295 PLANT.PIPEH.F(9) = 32.3305 ; # 293
 296 PLANT.PIPEH.F(10) = 32.3305 ; # 294
 297 PLANT.PIPEH.F(11) = 32.3305 ; # 295
 298 PLANT.PIPEH.F(12) = 32.3305 ; # 296
 299 PLANT.PIPEH.F(13) = 32.3305 ; # 297
 300 PLANT.PIPEH.F(14) = 32.3305 ; # 298

301 PLANT.PIPEH.F(15) = 32.3305 ; # 299
302 PLANT.PIPEH.F(16) = 32.3305 ; # 300
303 PLANT.PIPEH.F(17) = 32.3305 ; # 301
304 PLANT.PIPEH.F(18) = 32.3305 ; # 302
305 PLANT.PIPEH.F(19) = 32.3305 ; # 303
306 PLANT.PIPEH.F(20) = 32.3305 ; # 304
307 PLANT.PIPEH.F(21) = 32.3305 ; # 305
308 PLANT.PIPEH.F(22) = 32.3305 ; # 306
309 PLANT.PIPEH.F(23) = 32.3305 ; # 307
310 PLANT.PIPEH.F(24) = 32.3305 ; # 308
311 PLANT.PIPEH.F(25) = 32.3305 ; # 309
312 PLANT.PIPEH.F(26) = 32.3305 ; # 310
313 PLANT.PIPEH.F(27) = 32.3305 ; # 311
314 PLANT.PIPEH.F(28) = 32.3305 ; # 312
315 PLANT.PIPEH.F(29) = 32.3305 ; # 313
316 PLANT.PIPEH.F(30) = 32.3305 ; # 314
317 PLANT.PIPEH.F(31) = 32.3305 ; # 315
318 PLANT.PIPEH.F(32) = 32.3305 ; # 316
319 PLANT.PIPEH.F(33) = 32.3305 ; # 317
320 PLANT.PIPEH.F(34) = 32.3305 ; # 318
321 PLANT.PIPEH.F(35) = 32.3305 ; # 319
322 PLANT.PIPEH.F(36) = 32.3305 ; # 320
323 PLANT.PIPEH.F(37) = 32.3305 ; # 321
324 PLANT.PIPEH.F(38) = 32.3305 ; # 322
325 PLANT.PIPEH.F(39) = 32.3305 ; # 323
326 PLANT.PIPEH.F(40) = 32.3305 ; # 324
327 PLANT.PIPEH.F_IN = 32.3305 ; # 325
328 PLANT.PIPEH.PSI(1) = 6.03823e+006 ; # 326
329 PLANT.PIPEH.PSI(2) = 6.02385e+006 ; # 327
330 PLANT.PIPEH.PSI(3) = 6.00898e+006 ; # 328
331 PLANT.PIPEH.PSI(4) = 5.9936e+006 ; # 329
332 PLANT.PIPEH.PSI(5) = 5.97767e+006 ; # 330
333 PLANT.PIPEH.PSI(6) = 5.96117e+006 ; # 331
334 PLANT.PIPEH.PSI(7) = 5.94408e+006 ; # 332
335 PLANT.PIPEH.PSI(8) = 5.92638e+006 ; # 333
336 PLANT.PIPEH.PSI(9) = 5.90802e+006 ; # 334
337 PLANT.PIPEH.PSI(10) = 5.88899e+006 ; # 335
338 PLANT.PIPEH.PSI(11) = 5.86924e+006 ; # 336
339 PLANT.PIPEH.PSI(12) = 5.84876e+006 ; # 337
340 PLANT.PIPEH.PSI(13) = 5.82749e+006 ; # 338
341 PLANT.PIPEH.PSI(14) = 5.8054e+006 ; # 339
342 PLANT.PIPEH.PSI(15) = 5.78245e+006 ; # 340
343 PLANT.PIPEH.PSI(16) = 5.75859e+006 ; # 341
344 PLANT.PIPEH.PSI(17) = 5.73379e+006 ; # 342
345 PLANT.PIPEH.PSI(18) = 5.70799e+006 ; # 343
346 PLANT.PIPEH.PSI(19) = 5.68113e+006 ; # 344
347 PLANT.PIPEH.PSI(20) = 5.65317e+006 ; # 345
348 PLANT.PIPEH.PSI(21) = 5.62404e+006 ; # 346
349 PLANT.PIPEH.PSI(22) = 5.59367e+006 ; # 347
350 PLANT.PIPEH.PSI(23) = 5.56201e+006 ; # 348
351 PLANT.PIPEH.PSI(24) = 5.52897e+006 ; # 349
352 PLANT.PIPEH.PSI(25) = 5.49447e+006 ; # 350
353 PLANT.PIPEH.PSI(26) = 5.45844e+006 ; # 351
354 PLANT.PIPEH.PSI(27) = 5.42078e+006 ; # 352
355 PLANT.PIPEH.PSI(28) = 5.38139e+006 ; # 353
356 PLANT.PIPEH.PSI(29) = 5.34016e+006 ; # 354
357 PLANT.PIPEH.PSI(30) = 5.29699e+006 ; # 355
358 PLANT.PIPEH.PSI(31) = 5.25174e+006 ; # 356
359 PLANT.PIPEH.PSI(32) = 5.20427e+006 ; # 357
360 PLANT.PIPEH.PSI(33) = 5.15446e+006 ; # 358
361 PLANT.PIPEH.PSI(34) = 5.10212e+006 ; # 359
362 PLANT.PIPEH.PSI(35) = 5.0471e+006 ; # 360
363 PLANT.PIPEH.PSI(36) = 4.98919e+006 ; # 361
364 PLANT.PIPEH.PSI(37) = 4.92819e+006 ; # 362
365 PLANT.PIPEH.PSI(38) = 4.86388e+006 ; # 363
366 PLANT.PIPEH.PSI(39) = 4.796e+006 ; # 364
367 PLANT.PIPEH.PSI(40) = 4.7244e+006 ; # 365
368 PLANT.HX2.TH(1) = 1133.71 ; # 366
369 PLANT.HX2.TH(2) = 1130.67 ; # 367
370 PLANT.HX2.TH(3) = 1127.46 ; # 368
371 PLANT.HX2.TH(4) = 1124.06 ; # 369
372 PLANT.HX2.TH(5) = 1120.46 ; # 370
373 PLANT.HX2.TH(6) = 1116.65 ; # 371
374 PLANT.HX2.TH(7) = 1112.63 ; # 372
375 PLANT.HX2.TH(8) = 1108.36 ; # 373
376 PLANT.HX2.TH(9) = 1103.85 ; # 374
377 PLANT.HX2.TH(10) = 1099.08 ; # 375
378 PLANT.HX2.TH(11) = 1094.03 ; # 376
379 PLANT.HX2.TH(12) = 1088.69 ; # 377
380 PLANT.HX2.TH(13) = 1083.03 ; # 378
381 PLANT.HX2.TH(14) = 1077.05 ; # 379
382 PLANT.HX2.TH(15) = 1070.72 ; # 380
383 PLANT.HX2.TH(16) = 1064.02 ; # 381
384 PLANT.HX2.TH(17) = 1056.93 ; # 382
385 PLANT.HX2.TH(18) = 1049.43 ; # 383
386 PLANT.HX2.TH(19) = 1041.49 ; # 384
387 PLANT.HX2.TH(20) = 1033.09 ; # 385
388 PLANT.HX2.TH(21) = 1024.2 ; # 386
389 PLANT.HX2.TH(22) = 1014.8 ; # 387
390 PLANT.HX2.TH(23) = 1004.84 ; # 388
391 PLANT.HX2.TH(24) = 994.314 ; # 389
392 PLANT.HX2.TH(25) = 983.171 ; # 390

393 PLANT.HX2.THX(26) = 971.38 ; # 391
394 PLANT.HX2.THX(27) = 958.903 ; # 392
395 PLANT.HX2.THX(28) = 945.701 ; # 393
396 PLANT.HX2.THX(29) = 931.731 ; # 394
397 PLANT.HX2.THX(30) = 916.948 ; # 395
398 PLANT.HX2.THX(31) = 901.306 ; # 396
399 PLANT.HX2.THX(32) = 884.754 ; # 397
400 PLANT.HX2.THX(33) = 867.239 ; # 398
401 PLANT.HX2.THX(34) = 848.706 ; # 399
402 PLANT.HX2.THX(35) = 829.095 ; # 400
403 PLANT.HX2.THX(36) = 808.344 ; # 401
404 PLANT.HX2.THX(37) = 786.385 ; # 402
405 PLANT.HX2.THX(38) = 763.15 ; # 403
406 PLANT.HX2.THX(39) = 738.563 ; # 404
407 PLANT.HX2.THX(40) = 712.554 ; # 405
408 PLANT.PIPEC2.RHO(1) = 3.72389 ; # 406
409 PLANT.PIPEC2.RHO(2) = 3.55368 ; # 407
410 PLANT.PIPEC2.RHO(3) = 3.4055 ; # 408
411 PLANT.PIPEC2.RHO(4) = 3.27543 ; # 409
412 PLANT.PIPEC2.RHO(5) = 3.16041 ; # 410
413 PLANT.PIPEC2.RHO(6) = 3.05803 ; # 411
414 PLANT.PIPEC2.RHO(7) = 2.96638 ; # 412
415 PLANT.PIPEC2.RHO(8) = 2.88388 ; # 413
416 PLANT.PIPEC2.RHO(9) = 2.80928 ; # 414
417 PLANT.PIPEC2.RHO(10) = 2.74152 ; # 415
418 PLANT.PIPEC2.RHO(11) = 2.67973 ; # 416
419 PLANT.PIPEC2.RHO(12) = 2.62316 ; # 417
420 PLANT.PIPEC2.RHO(13) = 2.57121 ; # 418
421 PLANT.PIPEC2.RHO(14) = 2.52333 ; # 419
422 PLANT.PIPEC2.RHO(15) = 2.47909 ; # 420
423 PLANT.PIPEC2.RHO(16) = 2.43808 ; # 421
424 PLANT.PIPEC2.RHO(17) = 2.39997 ; # 422
425 PLANT.PIPEC2.RHO(18) = 2.36446 ; # 423
426 PLANT.PIPEC2.RHO(19) = 2.3313 ; # 424
427 PLANT.PIPEC2.RHO(20) = 2.30026 ; # 425
428 PLANT.PIPEC2.RHO(21) = 2.27113 ; # 426
429 PLANT.PIPEC2.RHO(22) = 2.24375 ; # 427
430 PLANT.PIPEC2.RHO(23) = 2.21796 ; # 428
431 PLANT.PIPEC2.RHO(24) = 2.19361 ; # 429
432 PLANT.PIPEC2.RHO(25) = 2.17058 ; # 430
433 PLANT.PIPEC2.RHO(26) = 2.14875 ; # 431
434 PLANT.PIPEC2.RHO(27) = 2.12804 ; # 432
435 PLANT.PIPEC2.RHO(28) = 2.10834 ; # 433
436 PLANT.PIPEC2.RHO(29) = 2.08957 ; # 434
437 PLANT.PIPEC2.RHO(30) = 2.07166 ; # 435
438 PLANT.PIPEC2.RHO(31) = 2.05454 ; # 436
439 PLANT.PIPEC2.RHO(32) = 2.03814 ; # 437
440 PLANT.PIPEC2.RHO(33) = 2.02242 ; # 438
441 PLANT.PIPEC2.RHO(34) = 2.00733 ; # 439
442 PLANT.PIPEC2.RHO(35) = 1.9928 ; # 440
443 PLANT.PIPEC2.RHO(36) = 1.97881 ; # 441
444 PLANT.PIPEC2.RHO(37) = 1.96531 ; # 442
445 PLANT.PIPEC2.RHO(38) = 1.95226 ; # 443
446 PLANT.PIPEC2.RHO(39) = 1.93964 ; # 444
447 PLANT.PIPEC2.RHO(40) = 1.92741 ; # 445
448 PLANT.PIPEC2.F(1) = 43.3743 ; # 446
449 PLANT.PIPEC2.F(2) = 43.3743 ; # 447
450 PLANT.PIPEC2.F(3) = 43.3743 ; # 448
451 PLANT.PIPEC2.F(4) = 43.3743 ; # 449
452 PLANT.PIPEC2.F(5) = 43.3743 ; # 450
453 PLANT.PIPEC2.F(6) = 43.3743 ; # 451
454 PLANT.PIPEC2.F(7) = 43.3743 ; # 452
455 PLANT.PIPEC2.F(8) = 43.3743 ; # 453
456 PLANT.PIPEC2.F(9) = 43.3743 ; # 454
457 PLANT.PIPEC2.F(10) = 43.3743 ; # 455
458 PLANT.PIPEC2.F(11) = 43.3743 ; # 456
459 PLANT.PIPEC2.F(12) = 43.3743 ; # 457
460 PLANT.PIPEC2.F(13) = 43.3743 ; # 458
461 PLANT.PIPEC2.F(14) = 43.3743 ; # 459
462 PLANT.PIPEC2.F(15) = 43.3743 ; # 460
463 PLANT.PIPEC2.F(16) = 43.3743 ; # 461
464 PLANT.PIPEC2.F(17) = 43.3743 ; # 462
465 PLANT.PIPEC2.F(18) = 43.3743 ; # 463
466 PLANT.PIPEC2.F(19) = 43.3743 ; # 464
467 PLANT.PIPEC2.F(20) = 43.3743 ; # 465
468 PLANT.PIPEC2.F(21) = 43.3743 ; # 466
469 PLANT.PIPEC2.F(22) = 43.3743 ; # 467
470 PLANT.PIPEC2.F(23) = 43.3743 ; # 468
471 PLANT.PIPEC2.F(24) = 43.3743 ; # 469
472 PLANT.PIPEC2.F(25) = 43.3743 ; # 470
473 PLANT.PIPEC2.F(26) = 43.3743 ; # 471
474 PLANT.PIPEC2.F(27) = 43.3743 ; # 472
475 PLANT.PIPEC2.F(28) = 43.3743 ; # 473
476 PLANT.PIPEC2.F(29) = 43.3743 ; # 474
477 PLANT.PIPEC2.F(30) = 43.3743 ; # 475
478 PLANT.PIPEC2.F(31) = 43.3743 ; # 476
479 PLANT.PIPEC2.F(32) = 43.3743 ; # 477
480 PLANT.PIPEC2.F(33) = 43.3743 ; # 478
481 PLANT.PIPEC2.F(34) = 43.3743 ; # 479
482 PLANT.PIPEC2.F(35) = 43.3743 ; # 480
483 PLANT.PIPEC2.F(36) = 43.3743 ; # 481
484 PLANT.PIPEC2.F(37) = 43.3743 ; # 482

```

485 PLANT.PIPEC2.F(38) = 43.3743 ; # 483
486 PLANT.PIPEC2.F(39) = 43.3743 ; # 484
487 PLANT.PIPEC2.F(40) = 43.3743 ; # 485
488 PLANT.PIPEC2.F_IN = 43.3743 ; # 486
489 PLANT.PIPEC2.PSI(1) = 1.81063e+006 ; # 487
490 PLANT.PIPEC2.PSI(2) = 1.91725e+006 ; # 488
491 PLANT.PIPEC2.PSI(3) = 2.00881e+006 ; # 489
492 PLANT.PIPEC2.PSI(4) = 2.08797e+006 ; # 490
493 PLANT.PIPEC2.PSI(5) = 2.1568e+006 ; # 491
494 PLANT.PIPEC2.PSI(6) = 2.21692e+006 ; # 492
495 PLANT.PIPEC2.PSI(7) = 2.26963e+006 ; # 493
496 PLANT.PIPEC2.PSI(8) = 2.31599e+006 ; # 494
497 PLANT.PIPEC2.PSI(9) = 2.35686e+006 ; # 495
498 PLANT.PIPEC2.PSI(10) = 2.39296e+006 ; # 496
499 PLANT.PIPEC2.PSI(11) = 2.42488e+006 ; # 497
500 PLANT.PIPEC2.PSI(12) = 2.45312e+006 ; # 498
501 PLANT.PIPEC2.PSI(13) = 2.47811e+006 ; # 499
502 PLANT.PIPEC2.PSI(14) = 2.50021e+006 ; # 500
503 PLANT.PIPEC2.PSI(15) = 2.51973e+006 ; # 501
504 PLANT.PIPEC2.PSI(16) = 2.53693e+006 ; # 502
505 PLANT.PIPEC2.PSI(17) = 2.55205e+006 ; # 503
506 PLANT.PIPEC2.PSI(18) = 2.5653e+006 ; # 504
507 PLANT.PIPEC2.PSI(19) = 2.57684e+006 ; # 505
508 PLANT.PIPEC2.PSI(20) = 2.58684e+006 ; # 506
509 PLANT.PIPEC2.PSI(21) = 2.59544e+006 ; # 507
510 PLANT.PIPEC2.PSI(22) = 2.60275e+006 ; # 508
511 PLANT.PIPEC2.PSI(23) = 2.60889e+006 ; # 509
512 PLANT.PIPEC2.PSI(24) = 2.61395e+006 ; # 510
513 PLANT.PIPEC2.PSI(25) = 2.61803e+006 ; # 511
514 PLANT.PIPEC2.PSI(26) = 2.62119e+006 ; # 512
515 PLANT.PIPEC2.PSI(27) = 2.62352e+006 ; # 513
516 PLANT.PIPEC2.PSI(28) = 2.62507e+006 ; # 514
517 PLANT.PIPEC2.PSI(29) = 2.62591e+006 ; # 515
518 PLANT.PIPEC2.PSI(30) = 2.62607e+006 ; # 516
519 PLANT.PIPEC2.PSI(31) = 2.62562e+006 ; # 517
520 PLANT.PIPEC2.PSI(32) = 2.6246e+006 ; # 518
521 PLANT.PIPEC2.PSI(33) = 2.62304e+006 ; # 519
522 PLANT.PIPEC2.PSI(34) = 2.62099e+006 ; # 520
523 PLANT.PIPEC2.PSI(35) = 2.61847e+006 ; # 521
524 PLANT.PIPEC2.PSI(36) = 2.61551e+006 ; # 522
525 PLANT.PIPEC2.PSI(37) = 2.61215e+006 ; # 523
526 PLANT.PIPEC2.PSI(38) = 2.6084e+006 ; # 524
527 PLANT.PIPEC2.PSI(39) = 2.6043e+006 ; # 525
528 PLANT.PIPEC2.PSI(40) = 2.59986e+006 ; # 526

```

HTL0MACH_SS_IN_PRE.PRESETS

```

1 # Values for computation HTL0MACH_SS
2 # Saved at time 1000
3 PLANT.HX.TGASHOT(1) := 908.671 ; # 1
4 PLANT.HX.TGASHOT(2) := 920.116 ; # 2
5 PLANT.HX.TGASHOT(3) := 931.225 ; # 3
6 PLANT.HX.TGASHOT(4) := 941.988 ; # 4
7 PLANT.HX.TGASHOT(5) := 952.416 ; # 5
8 PLANT.HX.TGASHOT(6) := 962.521 ; # 6
9 PLANT.HX.TGASHOT(7) := 972.311 ; # 7
10 PLANT.HX.TGASHOT(8) := 981.796 ; # 8
11 PLANT.HX.TGASHOT(9) := 990.987 ; # 9
12 PLANT.HX.TGASHOT(10) := 999.892 ; # 10
13 PLANT.HX.TGASHOT(11) := 1008.52 ; # 11
14 PLANT.HX.TGASHOT(12) := 1016.88 ; # 12
15 PLANT.HX.TGASHOT(13) := 1024.98 ; # 13
16 PLANT.HX.TGASHOT(14) := 1032.83 ; # 14
17 PLANT.HX.TGASHOT(15) := 1040.43 ; # 15
18 PLANT.HX.TGASHOT(16) := 1047.8 ; # 16
19 PLANT.HX.TGASHOT(17) := 1054.94 ; # 17
20 PLANT.HX.TGASHOT(18) := 1061.85 ; # 18
21 PLANT.HX.TGASHOT(19) := 1068.55 ; # 19
22 PLANT.HX.TGASHOT(20) := 1075.05 ; # 20
23 PLANT.HX.TGASHOT(21) := 1081.34 ; # 21
24 PLANT.HX.TGASHOT(22) := 1087.43 ; # 22
25 PLANT.HX.TGASHOT(23) := 1093.34 ; # 23
26 PLANT.HX.TGASHOT(24) := 1099.06 ; # 24
27 PLANT.HX.TGASHOT(25) := 1104.6 ; # 25
28 PLANT.HX.TGASHOT(26) := 1109.98 ; # 26
29 PLANT.HX.TGASHOT(27) := 1115.18 ; # 27
30 PLANT.HX.TGASHOT(28) := 1120.22 ; # 28
31 PLANT.HX.TGASHOT(29) := 1125.11 ; # 29
32 PLANT.HX.TGASHOT(30) := 1129.84 ; # 30
33 PLANT.HX.TGASHOT(31) := 1134.43 ; # 31
34 PLANT.HX.TGASHOT(32) := 1138.87 ; # 32
35 PLANT.HX.TGASHOT(33) := 1143.18 ; # 33
36 PLANT.HX.TGASHOT(34) := 1147.35 ; # 34

```

37 PLANT.HX.TGASHOT(35) := 1151.39 ; # 35
38 PLANT.HX.TGASHOT(36) := 1155.31 ; # 36
39 PLANT.HX.TGASHOT(37) := 1159.11 ; # 37
40 PLANT.HX.TGASHOT(38) := 1162.78 ; # 38
41 PLANT.HX.TGASHOT(39) := 1166.35 ; # 39
42 PLANT.HX.TGASHOT(40) := 1169.8 ; # 40
43 PLANT.HX.TGASCOLD(1) := 849.368 ; # 41
44 PLANT.HX.TGASCOLD(2) := 862.676 ; # 42
45 PLANT.HX.TGASCOLD(3) := 875.571 ; # 43
46 PLANT.HX.TGASCOLD(4) := 888.065 ; # 44
47 PLANT.HX.TGASCOLD(5) := 900.17 ; # 45
48 PLANT.HX.TGASCOLD(6) := 911.899 ; # 46
49 PLANT.HX.TGASCOLD(7) := 923.264 ; # 47
50 PLANT.HX.TGASCOLD(8) := 934.274 ; # 48
51 PLANT.HX.TGASCOLD(9) := 944.943 ; # 49
52 PLANT.HX.TGASCOLD(10) := 955.279 ; # 50
53 PLANT.HX.TGASCOLD(11) := 965.295 ; # 51
54 PLANT.HX.TGASCOLD(12) := 974.998 ; # 52
55 PLANT.HX.TGASCOLD(13) := 984.4 ; # 53
56 PLANT.HX.TGASCOLD(14) := 993.51 ; # 54
57 PLANT.HX.TGASCOLD(15) := 1002.34 ; # 55
58 PLANT.HX.TGASCOLD(16) := 1010.89 ; # 56
59 PLANT.HX.TGASCOLD(17) := 1019.17 ; # 57
60 PLANT.HX.TGASCOLD(18) := 1027.2 ; # 58
61 PLANT.HX.TGASCOLD(19) := 1034.98 ; # 59
62 PLANT.HX.TGASCOLD(20) := 1042.52 ; # 60
63 PLANT.HX.TGASCOLD(21) := 1049.82 ; # 61
64 PLANT.HX.TGASCOLD(22) := 1056.9 ; # 62
65 PLANT.HX.TGASCOLD(23) := 1063.75 ; # 63
66 PLANT.HX.TGASCOLD(24) := 1070.39 ; # 64
67 PLANT.HX.TGASCOLD(25) := 1076.83 ; # 65
68 PLANT.HX.TGASCOLD(26) := 1083.06 ; # 66
69 PLANT.HX.TGASCOLD(27) := 1089.11 ; # 67
70 PLANT.HX.TGASCOLD(28) := 1094.96 ; # 68
71 PLANT.HX.TGASCOLD(29) := 1100.63 ; # 69
72 PLANT.HX.TGASCOLD(30) := 1106.13 ; # 70
73 PLANT.HX.TGASCOLD(31) := 1111.45 ; # 71
74 PLANT.HX.TGASCOLD(32) := 1116.61 ; # 72
75 PLANT.HX.TGASCOLD(33) := 1121.61 ; # 73
76 PLANT.HX.TGASCOLD(34) := 1126.45 ; # 74
77 PLANT.HX.TGASCOLD(35) := 1131.14 ; # 75
78 PLANT.HX.TGASCOLD(36) := 1135.69 ; # 76
79 PLANT.HX.TGASCOLD(37) := 1140.09 ; # 77
80 PLANT.HX.TGASCOLD(38) := 1144.36 ; # 78
81 PLANT.HX.TGASCOLD(39) := 1148.5 ; # 79
82 PLANT.HX.TGASCOLD(40) := 1152.5 ; # 80
83 PLANT.HX.UHOT := 1738.41 ; # 81
84 PLANT.HX.UCOLD := 1645.45 ; # 82
85 PLANT.HX.TH(1) := 879.893 ; # 83
86 PLANT.HX.TH(2) := 892.184 ; # 84
87 PLANT.HX.TH(3) := 904.161 ; # 85
88 PLANT.HX.TH(4) := 915.766 ; # 86
89 PLANT.HX.TH(5) := 927.009 ; # 87
90 PLANT.HX.TH(6) := 937.904 ; # 88
91 PLANT.HX.TH(7) := 948.459 ; # 89
92 PLANT.HX.TH(8) := 958.687 ; # 90
93 PLANT.HX.TH(9) := 968.596 ; # 91
94 PLANT.HX.TH(10) := 978.197 ; # 92
95 PLANT.HX.TH(11) := 987.5 ; # 93
96 PLANT.HX.TH(12) := 996.513 ; # 94
97 PLANT.HX.TH(13) := 1005.25 ; # 95
98 PLANT.HX.TH(14) := 1013.71 ; # 96
99 PLANT.HX.TH(15) := 1021.91 ; # 97
100 PLANT.HX.TH(16) := 1029.85 ; # 98
101 PLANT.HX.TH(17) := 1037.55 ; # 99
102 PLANT.HX.TH(18) := 1045 ; # 100
103 PLANT.HX.TH(19) := 1052.23 ; # 101
104 PLANT.HX.TH(20) := 1059.23 ; # 102
105 PLANT.HX.TH(21) := 1066.01 ; # 103
106 PLANT.HX.TH(22) := 1072.58 ; # 104
107 PLANT.HX.TH(23) := 1078.95 ; # 105
108 PLANT.HX.TH(24) := 1085.12 ; # 106
109 PLANT.HX.TH(25) := 1091.1 ; # 107
110 PLANT.HX.TH(26) := 1096.89 ; # 108
111 PLANT.HX.TH(27) := 1102.5 ; # 109
112 PLANT.HX.TH(28) := 1107.94 ; # 110
113 PLANT.HX.TH(29) := 1113.21 ; # 111
114 PLANT.HX.TH(30) := 1118.31 ; # 112
115 PLANT.HX.TH(31) := 1123.26 ; # 113
116 PLANT.HX.TH(32) := 1128.05 ; # 114
117 PLANT.HX.TH(33) := 1132.69 ; # 115
118 PLANT.HX.TH(34) := 1137.19 ; # 116
119 PLANT.HX.TH(35) := 1141.55 ; # 117
120 PLANT.HX.TH(36) := 1145.77 ; # 118
121 PLANT.HX.TH(37) := 1149.86 ; # 119
122 PLANT.HX.TH(38) := 1153.83 ; # 120
123 PLANT.HX.TH(39) := 1157.67 ; # 121
124 PLANT.HX.TH(40) := 1161.37 ; # 122
125 PLANT.LOOP1.RHO(1) := 1.15317 ; # 123
126 PLANT.LOOP1.RHO(2) := 1.15067 ; # 124
127 PLANT.LOOP1.RHO(3) := 1.14817 ; # 125
128 PLANT.LOOP1.RHO(4) := 1.14565 ; # 126

129 PLANT.LOOP1.RHO(5) := 1.14313 ; # 127
130 PLANT.LOOP1.RHO(6) := 1.14059 ; # 128
131 PLANT.LOOP1.RHO(7) := 1.13804 ; # 129
132 PLANT.LOOP1.RHO(8) := 1.13549 ; # 130
133 PLANT.LOOP1.RHO(9) := 1.13292 ; # 131
134 PLANT.LOOP1.RHO(10) := 1.13034 ; # 132
135 PLANT.LOOP1.RHO(11) := 1.12115 ; # 133
136 PLANT.LOOP1.RHO(12) := 1.1026 ; # 134
137 PLANT.LOOP1.RHO(13) := 1.08477 ; # 135
138 PLANT.LOOP1.RHO(14) := 1.06791 ; # 136
139 PLANT.LOOP1.RHO(15) := 1.05196 ; # 137
140 PLANT.LOOP1.RHO(16) := 1.03683 ; # 138
141 PLANT.LOOP1.RHO(17) := 1.02247 ; # 139
142 PLANT.LOOP1.RHO(18) := 1.00882 ; # 140
143 PLANT.LOOP1.RHO(19) := 0.995831 ; # 141
144 PLANT.LOOP1.RHO(20) := 0.983453 ; # 142
145 PLANT.LOOP1.RHO(21) := 0.971645 ; # 143
146 PLANT.LOOP1.RHO(22) := 0.960369 ; # 144
147 PLANT.LOOP1.RHO(23) := 0.949588 ; # 145
148 PLANT.LOOP1.RHO(24) := 0.939272 ; # 146
149 PLANT.LOOP1.RHO(25) := 0.929389 ; # 147
150 PLANT.LOOP1.RHO(26) := 0.919912 ; # 148
151 PLANT.LOOP1.RHO(27) := 0.910817 ; # 149
152 PLANT.LOOP1.RHO(28) := 0.90208 ; # 150
153 PLANT.LOOP1.RHO(29) := 0.89368 ; # 151
154 PLANT.LOOP1.RHO(30) := 0.885596 ; # 152
155 PLANT.LOOP1.RHO(31) := 0.87781 ; # 153
156 PLANT.LOOP1.RHO(32) := 0.870305 ; # 154
157 PLANT.LOOP1.RHO(33) := 0.863066 ; # 155
158 PLANT.LOOP1.RHO(34) := 0.856077 ; # 156
159 PLANT.LOOP1.RHO(35) := 0.849325 ; # 157
160 PLANT.LOOP1.RHO(36) := 0.842796 ; # 158
161 PLANT.LOOP1.RHO(37) := 0.83648 ; # 159
162 PLANT.LOOP1.RHO(38) := 0.830364 ; # 160
163 PLANT.LOOP1.RHO(39) := 0.824437 ; # 161
164 PLANT.LOOP1.RHO(40) := 0.818691 ; # 162
165 PLANT.LOOP1.RHO(41) := 0.813116 ; # 163
166 PLANT.LOOP1.RHO(42) := 0.807703 ; # 164
167 PLANT.LOOP1.RHO(43) := 0.802444 ; # 165
168 PLANT.LOOP1.RHO(44) := 0.797332 ; # 166
169 PLANT.LOOP1.RHO(45) := 0.792359 ; # 167
170 PLANT.LOOP1.RHO(46) := 0.787518 ; # 168
171 PLANT.LOOP1.RHO(47) := 0.782803 ; # 169
172 PLANT.LOOP1.RHO(48) := 0.778208 ; # 170
173 PLANT.LOOP1.RHO(49) := 0.773727 ; # 171
174 PLANT.LOOP1.RHO(50) := 0.769359 ; # 172
175 PLANT.LOOP1.RHO(51) := 0.765795 ; # 173
176 PLANT.LOOP1.RHO(52) := 0.761103 ; # 174
177 PLANT.LOOP1.RHO(53) := 0.754256 ; # 175
178 PLANT.LOOP1.RHO(54) := 0.752399 ; # 176
179 PLANT.LOOP1.RHO(55) := 0.750533 ; # 177
180 PLANT.LOOP1.RHO(56) := 0.748658 ; # 178
181 PLANT.LOOP1.RHO(57) := 0.746773 ; # 179
182 PLANT.LOOP1.RHO(58) := 0.744879 ; # 180
183 PLANT.LOOP1.RHO(59) := 0.742975 ; # 181
184 PLANT.LOOP1.RHO(60) := 0.741061 ; # 182
185 PLANT.LOOP1.RHO(61) := 0.750585 ; # 183
186 PLANT.LOOP1.RHO(62) := 0.751689 ; # 184
187 PLANT.LOOP1.RHO(63) := 0.752856 ; # 185
188 PLANT.LOOP1.RHO(64) := 0.754135 ; # 186
189 PLANT.LOOP1.RHO(65) := 0.755533 ; # 187
190 PLANT.LOOP1.RHO(66) := 0.757059 ; # 188
191 PLANT.LOOP1.RHO(67) := 0.75872 ; # 189
192 PLANT.LOOP1.RHO(68) := 0.760528 ; # 190
193 PLANT.LOOP1.RHO(69) := 0.762492 ; # 191
194 PLANT.LOOP1.RHO(70) := 0.764623 ; # 192
195 PLANT.LOOP1.RHO(71) := 0.766934 ; # 193
196 PLANT.LOOP1.RHO(72) := 0.769438 ; # 194
197 PLANT.LOOP1.RHO(73) := 0.772149 ; # 195
198 PLANT.LOOP1.RHO(74) := 0.775083 ; # 196
199 PLANT.LOOP1.RHO(75) := 0.778256 ; # 197
200 PLANT.LOOP1.RHO(76) := 0.781688 ; # 198
201 PLANT.LOOP1.RHO(77) := 0.785399 ; # 199
202 PLANT.LOOP1.RHO(78) := 0.789411 ; # 200
203 PLANT.LOOP1.RHO(79) := 0.793749 ; # 201
204 PLANT.LOOP1.RHO(80) := 0.798441 ; # 202
205 PLANT.LOOP1.RHO(81) := 0.803515 ; # 203
206 PLANT.LOOP1.RHO(82) := 0.809005 ; # 204
207 PLANT.LOOP1.RHO(83) := 0.814949 ; # 205
208 PLANT.LOOP1.RHO(84) := 0.821387 ; # 206
209 PLANT.LOOP1.RHO(85) := 0.828365 ; # 207
210 PLANT.LOOP1.RHO(86) := 0.835933 ; # 208
211 PLANT.LOOP1.RHO(87) := 0.844151 ; # 209
212 PLANT.LOOP1.RHO(88) := 0.853082 ; # 210
213 PLANT.LOOP1.RHO(89) := 0.8628 ; # 211
214 PLANT.LOOP1.RHO(90) := 0.873389 ; # 212
215 PLANT.LOOP1.RHO(91) := 0.884944 ; # 213
216 PLANT.LOOP1.RHO(92) := 0.897573 ; # 214
217 PLANT.LOOP1.RHO(93) := 0.911403 ; # 215
218 PLANT.LOOP1.RHO(94) := 0.926579 ; # 216
219 PLANT.LOOP1.RHO(95) := 0.94327 ; # 217
220 PLANT.LOOP1.RHO(96) := 0.961674 ; # 218

```

221 PLANT.LOOP1.RHO(97) := 0.982027 ; # 219
222 PLANT.LOOP1.RHO(98) := 1.0046 ; # 220
223 PLANT.LOOP1.RHO(99) := 1.02974 ; # 221
224 PLANT.LOOP1.RHO(100) := 1.05783 ; # 222
225 PLANT.LOOP1.P(1) := 2.01181e+006 ; # 223
226 PLANT.LOOP1.P(2) := 2.00646e+006 ; # 224
227 PLANT.LOOP1.P(3) := 2.00109e+006 ; # 225
228 PLANT.LOOP1.P(4) := 1.99571e+006 ; # 226
229 PLANT.LOOP1.P(5) := 1.99032e+006 ; # 227
230 PLANT.LOOP1.P(6) := 1.98491e+006 ; # 228
231 PLANT.LOOP1.P(7) := 1.9795e+006 ; # 229
232 PLANT.LOOP1.P(8) := 1.97407e+006 ; # 230
233 PLANT.LOOP1.P(9) := 1.96863e+006 ; # 231
234 PLANT.LOOP1.P(10) := 1.96317e+006 ; # 232
235 PLANT.LOOP1.P(11) := 1.97929e+006 ; # 233
236 PLANT.LOOP1.P(12) := 1.97704e+006 ; # 234
237 PLANT.LOOP1.P(13) := 1.97414e+006 ; # 235
238 PLANT.LOOP1.P(14) := 1.9712e+006 ; # 236
239 PLANT.LOOP1.P(15) := 1.96822e+006 ; # 237
240 PLANT.LOOP1.P(16) := 1.96519e+006 ; # 238
241 PLANT.LOOP1.P(17) := 1.96212e+006 ; # 239
242 PLANT.LOOP1.P(18) := 1.95902e+006 ; # 240
243 PLANT.LOOP1.P(19) := 1.95587e+006 ; # 241
244 PLANT.LOOP1.P(20) := 1.95269e+006 ; # 242
245 PLANT.LOOP1.P(21) := 1.94947e+006 ; # 243
246 PLANT.LOOP1.P(22) := 1.94622e+006 ; # 244
247 PLANT.LOOP1.P(23) := 1.94293e+006 ; # 245
248 PLANT.LOOP1.P(24) := 1.93961e+006 ; # 246
249 PLANT.LOOP1.P(25) := 1.93625e+006 ; # 247
250 PLANT.LOOP1.P(26) := 1.93286e+006 ; # 248
251 PLANT.LOOP1.P(27) := 1.92943e+006 ; # 249
252 PLANT.LOOP1.P(28) := 1.92598e+006 ; # 250
253 PLANT.LOOP1.P(29) := 1.92249e+006 ; # 251
254 PLANT.LOOP1.P(30) := 1.91897e+006 ; # 252
255 PLANT.LOOP1.P(31) := 1.91543e+006 ; # 253
256 PLANT.LOOP1.P(32) := 1.91185e+006 ; # 254
257 PLANT.LOOP1.P(33) := 1.90824e+006 ; # 255
258 PLANT.LOOP1.P(34) := 1.90461e+006 ; # 256
259 PLANT.LOOP1.P(35) := 1.90095e+006 ; # 257
260 PLANT.LOOP1.P(36) := 1.89726e+006 ; # 258
261 PLANT.LOOP1.P(37) := 1.89354e+006 ; # 259
262 PLANT.LOOP1.P(38) := 1.8898e+006 ; # 260
263 PLANT.LOOP1.P(39) := 1.88603e+006 ; # 261
264 PLANT.LOOP1.P(40) := 1.88224e+006 ; # 262
265 PLANT.LOOP1.P(41) := 1.87842e+006 ; # 263
266 PLANT.LOOP1.P(42) := 1.87458e+006 ; # 264
267 PLANT.LOOP1.P(43) := 1.87071e+006 ; # 265
268 PLANT.LOOP1.P(44) := 1.86682e+006 ; # 266
269 PLANT.LOOP1.P(45) := 1.8629e+006 ; # 267
270 PLANT.LOOP1.P(46) := 1.85896e+006 ; # 268
271 PLANT.LOOP1.P(47) := 1.855e+006 ; # 269
272 PLANT.LOOP1.P(48) := 1.85101e+006 ; # 270
273 PLANT.LOOP1.P(49) := 1.847e+006 ; # 271
274 PLANT.LOOP1.P(50) := 1.84297e+006 ; # 272
275 PLANT.LOOP1.P(51) := 1.81438e+006 ; # 273
276 PLANT.LOOP1.P(52) := 1.80865e+006 ; # 274
277 PLANT.LOOP1.P(53) := 1.80295e+006 ; # 275
278 PLANT.LOOP1.P(54) := 1.79723e+006 ; # 276
279 PLANT.LOOP1.P(55) := 1.7915e+006 ; # 277
280 PLANT.LOOP1.P(56) := 1.78576e+006 ; # 278
281 PLANT.LOOP1.P(57) := 1.78e+006 ; # 279
282 PLANT.LOOP1.P(58) := 1.77423e+006 ; # 280
283 PLANT.LOOP1.P(59) := 1.76844e+006 ; # 281
284 PLANT.LOOP1.P(60) := 1.76263e+006 ; # 282
285 PLANT.LOOP1.P(61) := 1.78151e+006 ; # 283
286 PLANT.LOOP1.P(62) := 1.78014e+006 ; # 284
287 PLANT.LOOP1.P(63) := 1.77866e+006 ; # 285
288 PLANT.LOOP1.P(64) := 1.7772e+006 ; # 286
289 PLANT.LOOP1.P(65) := 1.77573e+006 ; # 287
290 PLANT.LOOP1.P(66) := 1.77427e+006 ; # 288
291 PLANT.LOOP1.P(67) := 1.77281e+006 ; # 289
292 PLANT.LOOP1.P(68) := 1.77136e+006 ; # 290
293 PLANT.LOOP1.P(69) := 1.76991e+006 ; # 291
294 PLANT.LOOP1.P(70) := 1.76847e+006 ; # 292
295 PLANT.LOOP1.P(71) := 1.76703e+006 ; # 293
296 PLANT.LOOP1.P(72) := 1.7656e+006 ; # 294
297 PLANT.LOOP1.P(73) := 1.76417e+006 ; # 295
298 PLANT.LOOP1.P(74) := 1.76275e+006 ; # 296
299 PLANT.LOOP1.P(75) := 1.76134e+006 ; # 297
300 PLANT.LOOP1.P(76) := 1.75993e+006 ; # 298
301 PLANT.LOOP1.P(77) := 1.75854e+006 ; # 299
302 PLANT.LOOP1.P(78) := 1.75715e+006 ; # 300
303 PLANT.LOOP1.P(79) := 1.75577e+006 ; # 301
304 PLANT.LOOP1.P(80) := 1.75441e+006 ; # 302
305 PLANT.LOOP1.P(81) := 1.75305e+006 ; # 303
306 PLANT.LOOP1.P(82) := 1.7517e+006 ; # 304
307 PLANT.LOOP1.P(83) := 1.75037e+006 ; # 305
308 PLANT.LOOP1.P(84) := 1.74905e+006 ; # 306
309 PLANT.LOOP1.P(85) := 1.74774e+006 ; # 307
310 PLANT.LOOP1.P(86) := 1.74645e+006 ; # 308
311 PLANT.LOOP1.P(87) := 1.74518e+006 ; # 309
312 PLANT.LOOP1.P(88) := 1.74392e+006 ; # 310

```

```

313 PLANT.LOOP1.P(89) := 1.74267e+006 ; # 311
314 PLANT.LOOP1.P(90) := 1.74145e+006 ; # 312
315 PLANT.LOOP1.P(91) := 1.74025e+006 ; # 313
316 PLANT.LOOP1.P(92) := 1.73907e+006 ; # 314
317 PLANT.LOOP1.P(93) := 1.73791e+006 ; # 315
318 PLANT.LOOP1.P(94) := 1.73677e+006 ; # 316
319 PLANT.LOOP1.P(95) := 1.73566e+006 ; # 317
320 PLANT.LOOP1.P(96) := 1.73458e+006 ; # 318
321 PLANT.LOOP1.P(97) := 1.73353e+006 ; # 319
322 PLANT.LOOP1.P(98) := 1.7325e+006 ; # 320
323 PLANT.LOOP1.P(99) := 1.73151e+006 ; # 321
324 PLANT.LOOP1.P(100) := 1.73056e+006 ; # 322
325 PLANT.LOOP1.P_OUT := 1.73003e+006 ; # 323
326 PLANT.LOOP1.H(1) := 2.81232e+006 ; # 324
327 PLANT.LOOP1.H(2) := 2.81015e+006 ; # 325
328 PLANT.LOOP1.H(3) := 2.80798e+006 ; # 326
329 PLANT.LOOP1.H(4) := 2.80581e+006 ; # 327
330 PLANT.LOOP1.H(5) := 2.80364e+006 ; # 328
331 PLANT.LOOP1.H(6) := 2.80148e+006 ; # 329
332 PLANT.LOOP1.H(7) := 2.79931e+006 ; # 330
333 PLANT.LOOP1.H(8) := 2.79715e+006 ; # 331
334 PLANT.LOOP1.H(9) := 2.79499e+006 ; # 332
335 PLANT.LOOP1.H(10) := 2.79283e+006 ; # 333
336 PLANT.LOOP1.H(11) := 2.86435e+006 ; # 334
337 PLANT.LOOP1.H(12) := 2.93349e+006 ; # 335
338 PLANT.LOOP1.H(13) := 3.00048e+006 ; # 336
339 PLANT.LOOP1.H(14) := 3.06539e+006 ; # 337
340 PLANT.LOOP1.H(15) := 3.12828e+006 ; # 338
341 PLANT.LOOP1.H(16) := 3.18921e+006 ; # 339
342 PLANT.LOOP1.H(17) := 3.24824e+006 ; # 340
343 PLANT.LOOP1.H(18) := 3.30545e+006 ; # 341
344 PLANT.LOOP1.H(19) := 3.36087e+006 ; # 342
345 PLANT.LOOP1.H(20) := 3.41457e+006 ; # 343
346 PLANT.LOOP1.H(21) := 3.4666e+006 ; # 344
347 PLANT.LOOP1.H(22) := 3.51701e+006 ; # 345
348 PLANT.LOOP1.H(23) := 3.56585e+006 ; # 346
349 PLANT.LOOP1.H(24) := 3.61317e+006 ; # 347
350 PLANT.LOOP1.H(25) := 3.65903e+006 ; # 348
351 PLANT.LOOP1.H(26) := 3.70345e+006 ; # 349
352 PLANT.LOOP1.H(27) := 3.7465e+006 ; # 350
353 PLANT.LOOP1.H(28) := 3.78821e+006 ; # 351
354 PLANT.LOOP1.H(29) := 3.82862e+006 ; # 352
355 PLANT.LOOP1.H(30) := 3.86777e+006 ; # 353
356 PLANT.LOOP1.H(31) := 3.90571e+006 ; # 354
357 PLANT.LOOP1.H(32) := 3.94246e+006 ; # 355
358 PLANT.LOOP1.H(33) := 3.97808e+006 ; # 356
359 PLANT.LOOP1.H(34) := 4.01258e+006 ; # 357
360 PLANT.LOOP1.H(35) := 4.04601e+006 ; # 358
361 PLANT.LOOP1.H(36) := 4.07841e+006 ; # 359
362 PLANT.LOOP1.H(37) := 4.10979e+006 ; # 360
363 PLANT.LOOP1.H(38) := 4.1402e+006 ; # 361
364 PLANT.LOOP1.H(39) := 4.16967e+006 ; # 362
365 PLANT.LOOP1.H(40) := 4.19821e+006 ; # 363
366 PLANT.LOOP1.H(41) := 4.22588e+006 ; # 364
367 PLANT.LOOP1.H(42) := 4.25268e+006 ; # 365
368 PLANT.LOOP1.H(43) := 4.27864e+006 ; # 366
369 PLANT.LOOP1.H(44) := 4.3038e+006 ; # 367
370 PLANT.LOOP1.H(45) := 4.32818e+006 ; # 368
371 PLANT.LOOP1.H(46) := 4.3518e+006 ; # 369
372 PLANT.LOOP1.H(47) := 4.37468e+006 ; # 370
373 PLANT.LOOP1.H(48) := 4.39685e+006 ; # 371
374 PLANT.LOOP1.H(49) := 4.41834e+006 ; # 372
375 PLANT.LOOP1.H(50) := 4.43912e+006 ; # 373
376 PLANT.LOOP1.H(51) := 4.43487e+006 ; # 374
377 PLANT.LOOP1.H(52) := 4.43062e+006 ; # 375
378 PLANT.LOOP1.H(53) := 4.42637e+006 ; # 376
379 PLANT.LOOP1.H(54) := 4.42213e+006 ; # 377
380 PLANT.LOOP1.H(55) := 4.41789e+006 ; # 378
381 PLANT.LOOP1.H(56) := 4.41366e+006 ; # 379
382 PLANT.LOOP1.H(57) := 4.40943e+006 ; # 380
383 PLANT.LOOP1.H(58) := 4.40521e+006 ; # 381
384 PLANT.LOOP1.H(59) := 4.40099e+006 ; # 382
385 PLANT.LOOP1.H(60) := 4.39677e+006 ; # 383
386 PLANT.LOOP1.H(61) := 4.38421e+006 ; # 384
387 PLANT.LOOP1.H(62) := 4.37092e+006 ; # 385
388 PLANT.LOOP1.H(63) := 4.35686e+006 ; # 386
389 PLANT.LOOP1.H(64) := 4.34197e+006 ; # 387
390 PLANT.LOOP1.H(65) := 4.32623e+006 ; # 388
391 PLANT.LOOP1.H(66) := 4.30957e+006 ; # 389
392 PLANT.LOOP1.H(67) := 4.29193e+006 ; # 390
393 PLANT.LOOP1.H(68) := 4.27328e+006 ; # 391
394 PLANT.LOOP1.H(69) := 4.25354e+006 ; # 392
395 PLANT.LOOP1.H(70) := 4.23265e+006 ; # 393
396 PLANT.LOOP1.H(71) := 4.21054e+006 ; # 394
397 PLANT.LOOP1.H(72) := 4.18715e+006 ; # 395
398 PLANT.LOOP1.H(73) := 4.1624e+006 ; # 396
399 PLANT.LOOP1.H(74) := 4.13621e+006 ; # 397
400 PLANT.LOOP1.H(75) := 4.1085e+006 ; # 398
401 PLANT.LOOP1.H(76) := 4.07917e+006 ; # 399
402 PLANT.LOOP1.H(77) := 4.04814e+006 ; # 400
403 PLANT.LOOP1.H(78) := 4.01531e+006 ; # 401
404 PLANT.LOOP1.H(79) := 3.98056e+006 ; # 402

```

```

405 PLANT.LOOP1.H(80) := 3.9438e+006 ; # 403
406 PLANT.LOOP1.H(81) := 3.90489e+006 ; # 404
407 PLANT.LOOP1.H(82) := 3.86373e+006 ; # 405
408 PLANT.LOOP1.H(83) := 3.82017e+006 ; # 406
409 PLANT.LOOP1.H(84) := 3.77408e+006 ; # 407
410 PLANT.LOOP1.H(85) := 3.7253e+006 ; # 408
411 PLANT.LOOP1.H(86) := 3.67369e+006 ; # 409
412 PLANT.LOOP1.H(87) := 3.61908e+006 ; # 410
413 PLANT.LOOP1.H(88) := 3.5613e+006 ; # 411
414 PLANT.LOOP1.H(89) := 3.50015e+006 ; # 412
415 PLANT.LOOP1.H(90) := 3.43544e+006 ; # 413
416 PLANT.LOOP1.H(91) := 3.36698e+006 ; # 414
417 PLANT.LOOP1.H(92) := 3.29453e+006 ; # 415
418 PLANT.LOOP1.H(93) := 3.21787e+006 ; # 416
419 PLANT.LOOP1.H(94) := 3.13675e+006 ; # 417
420 PLANT.LOOP1.H(95) := 3.05091e+006 ; # 418
421 PLANT.LOOP1.H(96) := 2.96008e+006 ; # 419
422 PLANT.LOOP1.H(97) := 2.86396e+006 ; # 420
423 PLANT.LOOP1.H(98) := 2.76226e+006 ; # 421
424 PLANT.LOOP1.H(99) := 2.65465e+006 ; # 422
425 PLANT.LOOP1.H(100) := 2.54078e+006 ; # 423
426 PLANT.LOOP1.H0 := 2.81449e+006 ; # 424
427 PLANT.LOOP1.T(1) := 839.351 ; # 425
428 PLANT.LOOP1.T(2) := 838.933 ; # 426
429 PLANT.LOOP1.T(3) := 838.516 ; # 427
430 PLANT.LOOP1.T(4) := 838.098 ; # 428
431 PLANT.LOOP1.T(5) := 837.681 ; # 429
432 PLANT.LOOP1.T(6) := 837.264 ; # 430
433 PLANT.LOOP1.T(7) := 836.847 ; # 431
434 PLANT.LOOP1.T(8) := 836.431 ; # 432
435 PLANT.LOOP1.T(9) := 836.015 ; # 433
436 PLANT.LOOP1.T(10) := 835.6 ; # 434
437 PLANT.LOOP1.T(11) := 849.368 ; # 435
438 PLANT.LOOP1.T(12) := 862.676 ; # 436
439 PLANT.LOOP1.T(13) := 875.571 ; # 437
440 PLANT.LOOP1.T(14) := 888.065 ; # 438
441 PLANT.LOOP1.T(15) := 900.17 ; # 439
442 PLANT.LOOP1.T(16) := 911.899 ; # 440
443 PLANT.LOOP1.T(17) := 923.264 ; # 441
444 PLANT.LOOP1.T(18) := 934.274 ; # 442
445 PLANT.LOOP1.T(19) := 944.943 ; # 443
446 PLANT.LOOP1.T(20) := 955.279 ; # 444
447 PLANT.LOOP1.T(21) := 965.295 ; # 445
448 PLANT.LOOP1.T(22) := 974.998 ; # 446
449 PLANT.LOOP1.T(23) := 984.4 ; # 447
450 PLANT.LOOP1.T(24) := 993.51 ; # 448
451 PLANT.LOOP1.T(25) := 1002.34 ; # 449
452 PLANT.LOOP1.T(26) := 1010.89 ; # 450
453 PLANT.LOOP1.T(27) := 1019.17 ; # 451
454 PLANT.LOOP1.T(28) := 1027.2 ; # 452
455 PLANT.LOOP1.T(29) := 1034.98 ; # 453
456 PLANT.LOOP1.T(30) := 1042.52 ; # 454
457 PLANT.LOOP1.T(31) := 1049.82 ; # 455
458 PLANT.LOOP1.T(32) := 1056.9 ; # 456
459 PLANT.LOOP1.T(33) := 1063.75 ; # 457
460 PLANT.LOOP1.T(34) := 1070.39 ; # 458
461 PLANT.LOOP1.T(35) := 1076.83 ; # 459
462 PLANT.LOOP1.T(36) := 1083.06 ; # 460
463 PLANT.LOOP1.T(37) := 1089.11 ; # 461
464 PLANT.LOOP1.T(38) := 1094.96 ; # 462
465 PLANT.LOOP1.T(39) := 1100.63 ; # 463
466 PLANT.LOOP1.T(40) := 1106.13 ; # 464
467 PLANT.LOOP1.T(41) := 1111.45 ; # 465
468 PLANT.LOOP1.T(42) := 1116.61 ; # 466
469 PLANT.LOOP1.T(43) := 1121.61 ; # 467
470 PLANT.LOOP1.T(44) := 1126.45 ; # 468
471 PLANT.LOOP1.T(45) := 1131.14 ; # 469
472 PLANT.LOOP1.T(46) := 1135.69 ; # 470
473 PLANT.LOOP1.T(47) := 1140.09 ; # 471
474 PLANT.LOOP1.T(48) := 1144.36 ; # 472
475 PLANT.LOOP1.T(49) := 1148.5 ; # 473
476 PLANT.LOOP1.T(50) := 1152.5 ; # 474
477 PLANT.LOOP1.T(51) := 1151.68 ; # 475
478 PLANT.LOOP1.T(52) := 1150.86 ; # 476
479 PLANT.LOOP1.T(53) := 1150.04 ; # 477
480 PLANT.LOOP1.T(54) := 1149.23 ; # 478
481 PLANT.LOOP1.T(55) := 1148.41 ; # 479
482 PLANT.LOOP1.T(56) := 1147.6 ; # 480
483 PLANT.LOOP1.T(57) := 1146.78 ; # 481
484 PLANT.LOOP1.T(58) := 1145.97 ; # 482
485 PLANT.LOOP1.T(59) := 1145.16 ; # 483
486 PLANT.LOOP1.T(60) := 1144.35 ; # 484
487 PLANT.LOOP1.T(61) := 1141.93 ; # 485
488 PLANT.LOOP1.T(62) := 1139.37 ; # 486
489 PLANT.LOOP1.T(63) := 1136.66 ; # 487
490 PLANT.LOOP1.T(64) := 1133.8 ; # 488
491 PLANT.LOOP1.T(65) := 1130.77 ; # 489
492 PLANT.LOOP1.T(66) := 1127.56 ; # 490
493 PLANT.LOOP1.T(67) := 1124.17 ; # 491
494 PLANT.LOOP1.T(68) := 1120.57 ; # 492
495 PLANT.LOOP1.T(69) := 1116.77 ; # 493
496 PLANT.LOOP1.T(70) := 1112.75 ; # 494

```

497 PLANT.LOOP1.T(71) := 1108.5 ; # 495
498 PLANT.LOOP1.T(72) := 1104 ; # 496
499 PLANT.LOOP1.T(73) := 1099.23 ; # 497
500 PLANT.LOOP1.T(74) := 1094.19 ; # 498
501 PLANT.LOOP1.T(75) := 1088.86 ; # 499
502 PLANT.LOOP1.T(76) := 1083.21 ; # 500
503 PLANT.LOOP1.T(77) := 1077.24 ; # 501
504 PLANT.LOOP1.T(78) := 1070.92 ; # 502
505 PLANT.LOOP1.T(79) := 1064.23 ; # 503
506 PLANT.LOOP1.T(80) := 1057.15 ; # 504
507 PLANT.LOOP1.T(81) := 1049.66 ; # 505
508 PLANT.LOOP1.T(82) := 1041.74 ; # 506
509 PLANT.LOOP1.T(83) := 1033.36 ; # 507
510 PLANT.LOOP1.T(84) := 1024.48 ; # 508
511 PLANT.LOOP1.T(85) := 1015.09 ; # 509
512 PLANT.LOOP1.T(86) := 1005.16 ; # 510
513 PLANT.LOOP1.T(87) := 994.647 ; # 511
514 PLANT.LOOP1.T(88) := 983.524 ; # 512
515 PLANT.LOOP1.T(89) := 971.753 ; # 513
516 PLANT.LOOP1.T(90) := 959.298 ; # 514
517 PLANT.LOOP1.T(91) := 946.119 ; # 515
518 PLANT.LOOP1.T(92) := 932.173 ; # 516
519 PLANT.LOOP1.T(93) := 917.416 ; # 517
520 PLANT.LOOP1.T(94) := 901.801 ; # 518
521 PLANT.LOOP1.T(95) := 885.278 ; # 519
522 PLANT.LOOP1.T(96) := 867.793 ; # 520
523 PLANT.LOOP1.T(97) := 849.292 ; # 521
524 PLANT.LOOP1.T(98) := 829.716 ; # 522
525 PLANT.LOOP1.T(99) := 809 ; # 523
526 PLANT.LOOP1.T(100) := 787.082 ; # 524
527 PLANT.LOOP1.T0 := 839.77 ; # 525
528 PLANT.LOOP1.TEXTRNL(1) := 291.15 ; # 526
529 PLANT.LOOP1.TEXTRNL(2) := 291.15 ; # 527
530 PLANT.LOOP1.TEXTRNL(3) := 291.15 ; # 528
531 PLANT.LOOP1.TEXTRNL(4) := 291.15 ; # 529
532 PLANT.LOOP1.TEXTRNL(5) := 291.15 ; # 530
533 PLANT.LOOP1.TEXTRNL(6) := 291.15 ; # 531
534 PLANT.LOOP1.TEXTRNL(7) := 291.15 ; # 532
535 PLANT.LOOP1.TEXTRNL(8) := 291.15 ; # 533
536 PLANT.LOOP1.TEXTRNL(9) := 291.15 ; # 534
537 PLANT.LOOP1.TEXTRNL(10) := 291.15 ; # 535
538 PLANT.LOOP1.TEXTRNL(11) := 879.893 ; # 536
539 PLANT.LOOP1.TEXTRNL(12) := 892.184 ; # 537
540 PLANT.LOOP1.TEXTRNL(13) := 904.161 ; # 538
541 PLANT.LOOP1.TEXTRNL(14) := 915.766 ; # 539
542 PLANT.LOOP1.TEXTRNL(15) := 927.009 ; # 540
543 PLANT.LOOP1.TEXTRNL(16) := 937.904 ; # 541
544 PLANT.LOOP1.TEXTRNL(17) := 948.459 ; # 542
545 PLANT.LOOP1.TEXTRNL(18) := 958.687 ; # 543
546 PLANT.LOOP1.TEXTRNL(19) := 968.596 ; # 544
547 PLANT.LOOP1.TEXTRNL(20) := 978.197 ; # 545
548 PLANT.LOOP1.TEXTRNL(21) := 987.5 ; # 546
549 PLANT.LOOP1.TEXTRNL(22) := 996.513 ; # 547
550 PLANT.LOOP1.TEXTRNL(23) := 1005.25 ; # 548
551 PLANT.LOOP1.TEXTRNL(24) := 1013.71 ; # 549
552 PLANT.LOOP1.TEXTRNL(25) := 1021.91 ; # 550
553 PLANT.LOOP1.TEXTRNL(26) := 1029.85 ; # 551
554 PLANT.LOOP1.TEXTRNL(27) := 1037.55 ; # 552
555 PLANT.LOOP1.TEXTRNL(28) := 1045 ; # 553
556 PLANT.LOOP1.TEXTRNL(29) := 1052.23 ; # 554
557 PLANT.LOOP1.TEXTRNL(30) := 1059.23 ; # 555
558 PLANT.LOOP1.TEXTRNL(31) := 1066.01 ; # 556
559 PLANT.LOOP1.TEXTRNL(32) := 1072.58 ; # 557
560 PLANT.LOOP1.TEXTRNL(33) := 1078.95 ; # 558
561 PLANT.LOOP1.TEXTRNL(34) := 1085.12 ; # 559
562 PLANT.LOOP1.TEXTRNL(35) := 1091.1 ; # 560
563 PLANT.LOOP1.TEXTRNL(36) := 1096.89 ; # 561
564 PLANT.LOOP1.TEXTRNL(37) := 1102.5 ; # 562
565 PLANT.LOOP1.TEXTRNL(38) := 1107.94 ; # 563
566 PLANT.LOOP1.TEXTRNL(39) := 1113.21 ; # 564
567 PLANT.LOOP1.TEXTRNL(40) := 1118.31 ; # 565
568 PLANT.LOOP1.TEXTRNL(41) := 1123.26 ; # 566
569 PLANT.LOOP1.TEXTRNL(42) := 1128.05 ; # 567
570 PLANT.LOOP1.TEXTRNL(43) := 1132.69 ; # 568
571 PLANT.LOOP1.TEXTRNL(44) := 1137.19 ; # 569
572 PLANT.LOOP1.TEXTRNL(45) := 1141.55 ; # 570
573 PLANT.LOOP1.TEXTRNL(46) := 1145.77 ; # 571
574 PLANT.LOOP1.TEXTRNL(47) := 1149.86 ; # 572
575 PLANT.LOOP1.TEXTRNL(48) := 1153.83 ; # 573
576 PLANT.LOOP1.TEXTRNL(49) := 1157.67 ; # 574
577 PLANT.LOOP1.TEXTRNL(50) := 1161.37 ; # 575
578 PLANT.LOOP1.TEXTRNL(51) := 291.15 ; # 576
579 PLANT.LOOP1.TEXTRNL(52) := 291.15 ; # 577
580 PLANT.LOOP1.TEXTRNL(53) := 291.15 ; # 578
581 PLANT.LOOP1.TEXTRNL(54) := 291.15 ; # 579
582 PLANT.LOOP1.TEXTRNL(55) := 291.15 ; # 580
583 PLANT.LOOP1.TEXTRNL(56) := 291.15 ; # 581
584 PLANT.LOOP1.TEXTRNL(57) := 291.15 ; # 582
585 PLANT.LOOP1.TEXTRNL(58) := 291.15 ; # 583
586 PLANT.LOOP1.TEXTRNL(59) := 291.15 ; # 584
587 PLANT.LOOP1.TEXTRNL(60) := 291.15 ; # 585
588 PLANT.LOOP1.TEXTRNL(61) := 1133.71 ; # 586

```

589 PLANT.LOOP1.TEXTRNL(62) := 1130.67 ; # 587
590 PLANT.LOOP1.TEXTRNL(63) := 1127.46 ; # 588
591 PLANT.LOOP1.TEXTRNL(64) := 1124.06 ; # 589
592 PLANT.LOOP1.TEXTRNL(65) := 1120.46 ; # 590
593 PLANT.LOOP1.TEXTRNL(66) := 1116.65 ; # 591
594 PLANT.LOOP1.TEXTRNL(67) := 1112.63 ; # 592
595 PLANT.LOOP1.TEXTRNL(68) := 1108.36 ; # 593
596 PLANT.LOOP1.TEXTRNL(69) := 1103.85 ; # 594
597 PLANT.LOOP1.TEXTRNL(70) := 1099.08 ; # 595
598 PLANT.LOOP1.TEXTRNL(71) := 1094.03 ; # 596
599 PLANT.LOOP1.TEXTRNL(72) := 1088.69 ; # 597
600 PLANT.LOOP1.TEXTRNL(73) := 1083.03 ; # 598
601 PLANT.LOOP1.TEXTRNL(74) := 1077.05 ; # 599
602 PLANT.LOOP1.TEXTRNL(75) := 1070.72 ; # 600
603 PLANT.LOOP1.TEXTRNL(76) := 1064.02 ; # 601
604 PLANT.LOOP1.TEXTRNL(77) := 1056.93 ; # 602
605 PLANT.LOOP1.TEXTRNL(78) := 1049.43 ; # 603
606 PLANT.LOOP1.TEXTRNL(79) := 1041.49 ; # 604
607 PLANT.LOOP1.TEXTRNL(80) := 1033.09 ; # 605
608 PLANT.LOOP1.TEXTRNL(81) := 1024.2 ; # 606
609 PLANT.LOOP1.TEXTRNL(82) := 1014.8 ; # 607
610 PLANT.LOOP1.TEXTRNL(83) := 1004.84 ; # 608
611 PLANT.LOOP1.TEXTRNL(84) := 994.314 ; # 609
612 PLANT.LOOP1.TEXTRNL(85) := 983.171 ; # 610
613 PLANT.LOOP1.TEXTRNL(86) := 971.38 ; # 611
614 PLANT.LOOP1.TEXTRNL(87) := 958.903 ; # 612
615 PLANT.LOOP1.TEXTRNL(88) := 945.701 ; # 613
616 PLANT.LOOP1.TEXTRNL(89) := 931.731 ; # 614
617 PLANT.LOOP1.TEXTRNL(90) := 916.948 ; # 615
618 PLANT.LOOP1.TEXTRNL(91) := 901.306 ; # 616
619 PLANT.LOOP1.TEXTRNL(92) := 884.754 ; # 617
620 PLANT.LOOP1.TEXTRNL(93) := 867.239 ; # 618
621 PLANT.LOOP1.TEXTRNL(94) := 848.706 ; # 619
622 PLANT.LOOP1.TEXTRNL(95) := 829.095 ; # 620
623 PLANT.LOOP1.TEXTRNL(96) := 808.344 ; # 621
624 PLANT.LOOP1.TEXTRNL(97) := 786.385 ; # 622
625 PLANT.LOOP1.TEXTRNL(98) := 763.15 ; # 623
626 PLANT.LOOP1.TEXTRNL(99) := 738.563 ; # 624
627 PLANT.LOOP1.TEXTRNL(100) := 712.554 ; # 625
628 PLANT.LOOP1.PSI(1) := 1.23127e+006 ; # 626
629 PLANT.LOOP1.PSI(2) := 1.22711e+006 ; # 627
630 PLANT.LOOP1.PSI(3) := 1.22294e+006 ; # 628
631 PLANT.LOOP1.PSI(4) := 1.21877e+006 ; # 629
632 PLANT.LOOP1.PSI(5) := 1.2146e+006 ; # 630
633 PLANT.LOOP1.PSI(6) := 1.21042e+006 ; # 631
634 PLANT.LOOP1.PSI(7) := 1.20624e+006 ; # 632
635 PLANT.LOOP1.PSI(8) := 1.20206e+006 ; # 633
636 PLANT.LOOP1.PSI(9) := 1.19787e+006 ; # 634
637 PLANT.LOOP1.PSI(10) := 1.19368e+006 ; # 635
638 PLANT.LOOP1.PSI(11) := 1.23208e+006 ; # 636
639 PLANT.LOOP1.PSI(12) := 1.25743e+006 ; # 637
640 PLANT.LOOP1.PSI(13) := 1.28069e+006 ; # 638
641 PLANT.LOOP1.PSI(14) := 1.30237e+006 ; # 639
642 PLANT.LOOP1.PSI(15) := 1.3226e+006 ; # 640
643 PLANT.LOOP1.PSI(16) := 1.34148e+006 ; # 641
644 PLANT.LOOP1.PSI(17) := 1.35911e+006 ; # 642
645 PLANT.LOOP1.PSI(18) := 1.37558e+006 ; # 643
646 PLANT.LOOP1.PSI(19) := 1.39098e+006 ; # 644
647 PLANT.LOOP1.PSI(20) := 1.40537e+006 ; # 645
648 PLANT.LOOP1.PSI(21) := 1.41883e+006 ; # 646
649 PLANT.LOOP1.PSI(22) := 1.4314e+006 ; # 647
650 PLANT.LOOP1.PSI(23) := 1.44316e+006 ; # 648
651 PLANT.LOOP1.PSI(24) := 1.45415e+006 ; # 649
652 PLANT.LOOP1.PSI(25) := 1.46441e+006 ; # 650
653 PLANT.LOOP1.PSI(26) := 1.474e+006 ; # 651
654 PLANT.LOOP1.PSI(27) := 1.48294e+006 ; # 652
655 PLANT.LOOP1.PSI(28) := 1.49129e+006 ; # 653
656 PLANT.LOOP1.PSI(29) := 1.49907e+006 ; # 654
657 PLANT.LOOP1.PSI(30) := 1.50631e+006 ; # 655
658 PLANT.LOOP1.PSI(31) := 1.51304e+006 ; # 656
659 PLANT.LOOP1.PSI(32) := 1.5193e+006 ; # 657
660 PLANT.LOOP1.PSI(33) := 1.5251e+006 ; # 658
661 PLANT.LOOP1.PSI(34) := 1.53047e+006 ; # 659
662 PLANT.LOOP1.PSI(35) := 1.53543e+006 ; # 660
663 PLANT.LOOP1.PSI(36) := 1.54001e+006 ; # 661
664 PLANT.LOOP1.PSI(37) := 1.54421e+006 ; # 662
665 PLANT.LOOP1.PSI(38) := 1.54807e+006 ; # 663
666 PLANT.LOOP1.PSI(39) := 1.5516e+006 ; # 664
667 PLANT.LOOP1.PSI(40) := 1.5548e+006 ; # 665
668 PLANT.LOOP1.PSI(41) := 1.55771e+006 ; # 666
669 PLANT.LOOP1.PSI(42) := 1.56032e+006 ; # 667
670 PLANT.LOOP1.PSI(43) := 1.56266e+006 ; # 668
671 PLANT.LOOP1.PSI(44) := 1.56474e+006 ; # 669
672 PLANT.LOOP1.PSI(45) := 1.56657e+006 ; # 670
673 PLANT.LOOP1.PSI(46) := 1.56816e+006 ; # 671
674 PLANT.LOOP1.PSI(47) := 1.56951e+006 ; # 672
675 PLANT.LOOP1.PSI(48) := 1.57065e+006 ; # 673
676 PLANT.LOOP1.PSI(49) := 1.57158e+006 ; # 674
677 PLANT.LOOP1.PSI(50) := 1.5723e+006 ; # 675
678 PLANT.LOOP1.PSI(51) := 1.54707e+006 ; # 676
679 PLANT.LOOP1.PSI(52) := 1.54135e+006 ; # 677
680 PLANT.LOOP1.PSI(53) := 1.53567e+006 ; # 678

```

881 PLANT.LOOP1.PSI (54) : = 1.5297e+006 ; # 679
882 PLANT.LOOP1.PSI (55) : = 1.52427e+006 ; # 680
883 PLANT.LOOP1.PSI (56) : = 1.51856e+006 ; # 681
884 PLANT.LOOP1.PSI (57) : = 1.51284e+006 ; # 682
885 PLANT.LOOP1.PSI (58) : = 1.50712e+006 ; # 683
886 PLANT.LOOP1.PSI (59) : = 1.50138e+006 ; # 684
887 PLANT.LOOP1.PSI (60) : = 1.49564e+006 ; # 685
888 PLANT.LOOP1.PSI (61) : = 1.50921e+006 ; # 686
889 PLANT.LOOP1.PSI (62) : = 1.50544e+006 ; # 687
890 PLANT.LOOP1.PSI (63) : = 1.50142e+006 ; # 688
891 PLANT.LOOP1.PSI (64) : = 1.49724e+006 ; # 689
892 PLANT.LOOP1.PSI (65) : = 1.49288e+006 ; # 690
893 PLANT.LOOP1.PSI (66) : = 1.48833e+006 ; # 691
894 PLANT.LOOP1.PSI (67) : = 1.48357e+006 ; # 692
895 PLANT.LOOP1.PSI (68) : = 1.47859e+006 ; # 693
896 PLANT.LOOP1.PSI (69) : = 1.47338e+006 ; # 694
897 PLANT.LOOP1.PSI (70) : = 1.46791e+006 ; # 695
898 PLANT.LOOP1.PSI (71) : = 1.46218e+006 ; # 696
899 PLANT.LOOP1.PSI (72) : = 1.45616e+006 ; # 697
900 PLANT.LOOP1.PSI (73) : = 1.44982e+006 ; # 698
901 PLANT.LOOP1.PSI (74) : = 1.44315e+006 ; # 699
902 PLANT.LOOP1.PSI (75) : = 1.43612e+006 ; # 700
903 PLANT.LOOP1.PSI (76) : = 1.4287e+006 ; # 701
904 PLANT.LOOP1.PSI (77) : = 1.42087e+006 ; # 702
905 PLANT.LOOP1.PSI (78) : = 1.41258e+006 ; # 703
906 PLANT.LOOP1.PSI (79) : = 1.40379e+006 ; # 704
907 PLANT.LOOP1.PSI (80) : = 1.39448e+006 ; # 705
908 PLANT.LOOP1.PSI (81) : = 1.38459e+006 ; # 706
909 PLANT.LOOP1.PSI (82) : = 1.37407e+006 ; # 707
910 PLANT.LOOP1.PSI (83) : = 1.36287e+006 ; # 708
911 PLANT.LOOP1.PSI (84) : = 1.35093e+006 ; # 709
912 PLANT.LOOP1.PSI (85) : = 1.33817e+006 ; # 710
913 PLANT.LOOP1.PSI (86) : = 1.32451e+006 ; # 711
914 PLANT.LOOP1.PSI (87) : = 1.30988e+006 ; # 712
915 PLANT.LOOP1.PSI (88) : = 1.29416e+006 ; # 713
916 PLANT.LOOP1.PSI (89) : = 1.27725e+006 ; # 714
917 PLANT.LOOP1.PSI (90) : = 1.25903e+006 ; # 715
918 PLANT.LOOP1.PSI (91) : = 1.23934e+006 ; # 716
919 PLANT.LOOP1.PSI (92) : = 1.21801e+006 ; # 717
920 PLANT.LOOP1.PSI (93) : = 1.19486e+006 ; # 718
921 PLANT.LOOP1.PSI (94) : = 1.16967e+006 ; # 719
922 PLANT.LOOP1.PSI (95) : = 1.14217e+006 ; # 720
923 PLANT.LOOP1.PSI (96) : = 1.11205e+006 ; # 721
924 PLANT.LOOP1.PSI (97) : = 1.07896e+006 ; # 722
925 PLANT.LOOP1.PSI (98) : = 1.04248e+006 ; # 723
926 PLANT.LOOP1.PSI (99) : = 1.00208e+006 ; # 724
927 PLANT.LOOP1.PSI (100) : = 957156 ; # 725
728 PLANT.LOOP1.F (1) : = 26.308 ; # 726
729 PLANT.LOOP1.F (2) : = 26.308 ; # 727
730 PLANT.LOOP1.F (3) : = 26.308 ; # 728
731 PLANT.LOOP1.F (4) : = 26.308 ; # 729
732 PLANT.LOOP1.F (5) : = 26.308 ; # 730
733 PLANT.LOOP1.F (6) : = 26.308 ; # 731
734 PLANT.LOOP1.F (7) : = 26.308 ; # 732
735 PLANT.LOOP1.F (8) : = 26.308 ; # 733
736 PLANT.LOOP1.F (9) : = 26.308 ; # 734
737 PLANT.LOOP1.F (10) : = 26.308 ; # 735
738 PLANT.LOOP1.F (11) : = 26.308 ; # 736
739 PLANT.LOOP1.F (12) : = 26.308 ; # 737
740 PLANT.LOOP1.F (13) : = 26.308 ; # 738
741 PLANT.LOOP1.F (14) : = 26.308 ; # 739
742 PLANT.LOOP1.F (15) : = 26.308 ; # 740
743 PLANT.LOOP1.F (16) : = 26.308 ; # 741
744 PLANT.LOOP1.F (17) : = 26.308 ; # 742
745 PLANT.LOOP1.F (18) : = 26.308 ; # 743
746 PLANT.LOOP1.F (19) : = 26.308 ; # 744
747 PLANT.LOOP1.F (20) : = 26.308 ; # 745
748 PLANT.LOOP1.F (21) : = 26.308 ; # 746
749 PLANT.LOOP1.F (22) : = 26.308 ; # 747
750 PLANT.LOOP1.F (23) : = 26.308 ; # 748
751 PLANT.LOOP1.F (24) : = 26.308 ; # 749
752 PLANT.LOOP1.F (25) : = 26.308 ; # 750
753 PLANT.LOOP1.F (26) : = 26.308 ; # 751
754 PLANT.LOOP1.F (27) : = 26.308 ; # 752
755 PLANT.LOOP1.F (28) : = 26.308 ; # 753
756 PLANT.LOOP1.F (29) : = 26.308 ; # 754
757 PLANT.LOOP1.F (30) : = 26.308 ; # 755
758 PLANT.LOOP1.F (31) : = 26.308 ; # 756
759 PLANT.LOOP1.F (32) : = 26.308 ; # 757
760 PLANT.LOOP1.F (33) : = 26.308 ; # 758
761 PLANT.LOOP1.F (34) : = 26.308 ; # 759
762 PLANT.LOOP1.F (35) : = 26.308 ; # 760
763 PLANT.LOOP1.F (36) : = 26.308 ; # 761
764 PLANT.LOOP1.F (37) : = 26.308 ; # 762
765 PLANT.LOOP1.F (38) : = 26.308 ; # 763
766 PLANT.LOOP1.F (39) : = 26.308 ; # 764
767 PLANT.LOOP1.F (40) : = 26.308 ; # 765
768 PLANT.LOOP1.F (41) : = 26.308 ; # 766
769 PLANT.LOOP1.F (42) : = 26.308 ; # 767
770 PLANT.LOOP1.F (43) : = 26.308 ; # 768
771 PLANT.LOOP1.F (44) : = 26.308 ; # 769
772 PLANT.LOOP1.F (45) : = 26.308 ; # 770

```

773 PLANT.LOOP1.F(46) := 26.308 ; # 771
774 PLANT.LOOP1.F(47) := 26.308 ; # 772
775 PLANT.LOOP1.F(48) := 26.308 ; # 773
776 PLANT.LOOP1.F(49) := 26.308 ; # 774
777 PLANT.LOOP1.F(50) := 26.308 ; # 775
778 PLANT.LOOP1.F(51) := 26.308 ; # 776
779 PLANT.LOOP1.F(52) := 26.308 ; # 777
780 PLANT.LOOP1.F(53) := 26.308 ; # 778
781 PLANT.LOOP1.F(54) := 26.308 ; # 779
782 PLANT.LOOP1.F(55) := 26.308 ; # 780
783 PLANT.LOOP1.F(56) := 26.308 ; # 781
784 PLANT.LOOP1.F(57) := 26.308 ; # 782
785 PLANT.LOOP1.F(58) := 26.308 ; # 783
786 PLANT.LOOP1.F(59) := 26.308 ; # 784
787 PLANT.LOOP1.F(60) := 26.308 ; # 785
788 PLANT.LOOP1.F(61) := 26.308 ; # 786
789 PLANT.LOOP1.F(62) := 26.308 ; # 787
790 PLANT.LOOP1.F(63) := 26.308 ; # 788
791 PLANT.LOOP1.F(64) := 26.308 ; # 789
792 PLANT.LOOP1.F(65) := 26.308 ; # 790
793 PLANT.LOOP1.F(66) := 26.308 ; # 791
794 PLANT.LOOP1.F(67) := 26.308 ; # 792
795 PLANT.LOOP1.F(68) := 26.308 ; # 793
796 PLANT.LOOP1.F(69) := 26.308 ; # 794
797 PLANT.LOOP1.F(70) := 26.308 ; # 795
798 PLANT.LOOP1.F(71) := 26.308 ; # 796
799 PLANT.LOOP1.F(72) := 26.308 ; # 797
800 PLANT.LOOP1.F(73) := 26.308 ; # 798
801 PLANT.LOOP1.F(74) := 26.308 ; # 799
802 PLANT.LOOP1.F(75) := 26.308 ; # 800
803 PLANT.LOOP1.F(76) := 26.308 ; # 801
804 PLANT.LOOP1.F(77) := 26.308 ; # 802
805 PLANT.LOOP1.F(78) := 26.308 ; # 803
806 PLANT.LOOP1.F(79) := 26.308 ; # 804
807 PLANT.LOOP1.F(80) := 26.308 ; # 805
808 PLANT.LOOP1.F(81) := 26.308 ; # 806
809 PLANT.LOOP1.F(82) := 26.308 ; # 807
810 PLANT.LOOP1.F(83) := 26.308 ; # 808
811 PLANT.LOOP1.F(84) := 26.308 ; # 809
812 PLANT.LOOP1.F(85) := 26.308 ; # 810
813 PLANT.LOOP1.F(86) := 26.308 ; # 811
814 PLANT.LOOP1.F(87) := 26.308 ; # 812
815 PLANT.LOOP1.F(88) := 26.308 ; # 813
816 PLANT.LOOP1.F(89) := 26.308 ; # 814
817 PLANT.LOOP1.F(90) := 26.308 ; # 815
818 PLANT.LOOP1.F(91) := 26.308 ; # 816
819 PLANT.LOOP1.F(92) := 26.308 ; # 817
820 PLANT.LOOP1.F(93) := 26.308 ; # 818
821 PLANT.LOOP1.F(94) := 26.308 ; # 819
822 PLANT.LOOP1.F(95) := 26.308 ; # 820
823 PLANT.LOOP1.F(96) := 26.308 ; # 821
824 PLANT.LOOP1.F(97) := 26.308 ; # 822
825 PLANT.LOOP1.F(98) := 26.308 ; # 823
826 PLANT.LOOP1.F(99) := 26.308 ; # 824
827 PLANT.LOOP1.F(100) := 26.308 ; # 825
828 PLANT.LOOP1.F_IN := 26.308 ; # 826
829 PLANT.LOOP1.RHO_AVG := 0.91979 ; # 827
830 PLANT.LOOP1.TOTALMASS := 27.4242 ; # 828
831 PLANT.LOOP1.RHOEXTRA(1) := 1.1654 ; # 829
832 PLANT.LOOP1.RHOEXTRA(2) := 1.1654 ; # 830
833 PLANT.LOOP1.PEXTRA(1) := 2.03415e+006 ; # 831
834 PLANT.LOOP1.PEXTRA(2) := 2.03415e+006 ; # 832
835 PLANT.LOOP1.HEXTRA(1) := 2.81449e+006 ; # 833
836 PLANT.LOOP1.HEXTRA(2) := 2.81449e+006 ; # 834
837 PLANT.LOOP1.TEXTRA(1) := 839.77 ; # 835
838 PLANT.LOOP1.TEXTRA(2) := 839.77 ; # 836
839 PLANT.LOOP1.PSIEXTRA(1) := 1.24585e+006 ; # 837
840 PLANT.LOOP1.PSIEXTRA(2) := 1.24585e+006 ; # 838
841 PLANT.LOOP1.FEXTRA(1) := 26.308 ; # 839
842 PLANT.LOOP1.FEXTRA(2) := 26.308 ; # 840
843 PLANT.LOOP1.HT1.H2 := 17.344 ; # 841
844 PLANT.LOOP1.HT1.RHOPIPEHE := 1.14182 ; # 842
845 PLANT.LOOP1.HT1.VPIPE := 171.996 ; # 843
846 PLANT.LOOP1.HT1.HO := 1500.09 ; # 844
847 PLANT.LOOP1.HT1.U := 8.93421 ; # 845
848 PLANT.LOOP1.HT2.RHOPIPEHE := 0.902801 ; # 846
849 PLANT.LOOP1.HT2.VPIPE := 84.86 ; # 847
850 PLANT.LOOP1.HT2.HO := 1665.62 ; # 848
851 PLANT.LOOP1.HT2.U := 1645.45 ; # 849
852 PLANT.LOOP1.HT3.H2 := 17.344 ; # 850
853 PLANT.LOOP1.HT3.RHOPIPEHE := 0.74956 ; # 851
854 PLANT.LOOP1.HT3.VPIPE := 226.698 ; # 852
855 PLANT.LOOP1.HT3.HO := 1316.87 ; # 853
856 PLANT.LOOP1.HT3.U := 10.3572 ; # 854
857 PLANT.LOOP1.HT4.RHOPIPEHE := 0.833125 ; # 855
858 PLANT.LOOP1.HT4.VPIPE := 79.4405 ; # 856
859 PLANT.LOOP1.HT4.U := 1299.78 ; # 857
860 PLANT.PIPEH.RHO(1) := 2.87869 ; # 858
861 PLANT.PIPEH.RHO(2) := 2.88664 ; # 859
862 PLANT.PIPEH.RHO(3) := 2.89491 ; # 860
863 PLANT.PIPEH.RHO(4) := 2.90353 ; # 861
864 PLANT.PIPEH.RHO(5) := 2.9125 ; # 862

```



```

865 PLANT.PIPEH.RHO(6) := 2.92184 ; # 863
866 PLANT.PIPEH.RHO(7) := 2.93156 ; # 864
867 PLANT.PIPEH.RHO(8) := 2.9417 ; # 865
868 PLANT.PIPEH.RHO(9) := 2.95225 ; # 866
869 PLANT.PIPEH.RHO(10) := 2.96325 ; # 867
870 PLANT.PIPEH.RHO(11) := 2.97471 ; # 868
871 PLANT.PIPEH.RHO(12) := 2.98666 ; # 869
872 PLANT.PIPEH.RHO(13) := 2.99912 ; # 870
873 PLANT.PIPEH.RHO(14) := 3.01211 ; # 871
874 PLANT.PIPEH.RHO(15) := 3.02567 ; # 872
875 PLANT.PIPEH.RHO(16) := 3.03982 ; # 873
876 PLANT.PIPEH.RHO(17) := 3.05458 ; # 874
877 PLANT.PIPEH.RHO(18) := 3.07 ; # 875
878 PLANT.PIPEH.RHO(19) := 3.08611 ; # 876
879 PLANT.PIPEH.RHO(20) := 3.10294 ; # 877
880 PLANT.PIPEH.RHO(21) := 3.12053 ; # 878
881 PLANT.PIPEH.RHO(22) := 3.13892 ; # 879
882 PLANT.PIPEH.RHO(23) := 3.15816 ; # 880
883 PLANT.PIPEH.RHO(24) := 3.1783 ; # 881
884 PLANT.PIPEH.RHO(25) := 3.19939 ; # 882
885 PLANT.PIPEH.RHO(26) := 3.22148 ; # 883
886 PLANT.PIPEH.RHO(27) := 3.24463 ; # 884
887 PLANT.PIPEH.RHO(28) := 3.2689 ; # 885
888 PLANT.PIPEH.RHO(29) := 3.29437 ; # 886
889 PLANT.PIPEH.RHO(30) := 3.32112 ; # 887
890 PLANT.PIPEH.RHO(31) := 3.34921 ; # 888
891 PLANT.PIPEH.RHO(32) := 3.37874 ; # 889
892 PLANT.PIPEH.RHO(33) := 3.4098 ; # 890
893 PLANT.PIPEH.RHO(34) := 3.4425 ; # 891
894 PLANT.PIPEH.RHO(35) := 3.47695 ; # 892
895 PLANT.PIPEH.RHO(36) := 3.51328 ; # 893
896 PLANT.PIPEH.RHO(37) := 3.55161 ; # 894
897 PLANT.PIPEH.RHO(38) := 3.59209 ; # 895
898 PLANT.PIPEH.RHO(39) := 3.6349 ; # 896
899 PLANT.PIPEH.RHO(40) := 3.68012 ; # 897
900 PLANT.PIPEH.P(1) := 6.99931e+006 ; # 898
901 PLANT.PIPEH.P(2) := 6.99793e+006 ; # 899
902 PLANT.PIPEH.P(3) := 6.99656e+006 ; # 900
903 PLANT.PIPEH.P(4) := 6.99519e+006 ; # 901
904 PLANT.PIPEH.P(5) := 6.99383e+006 ; # 902
905 PLANT.PIPEH.P(6) := 6.99247e+006 ; # 903
906 PLANT.PIPEH.P(7) := 6.99111e+006 ; # 904
907 PLANT.PIPEH.P(8) := 6.98977e+006 ; # 905
908 PLANT.PIPEH.P(9) := 6.98842e+006 ; # 906
909 PLANT.PIPEH.P(10) := 6.98708e+006 ; # 907
910 PLANT.PIPEH.P(11) := 6.98575e+006 ; # 908
911 PLANT.PIPEH.P(12) := 6.98442e+006 ; # 909
912 PLANT.PIPEH.P(13) := 6.9831e+006 ; # 910
913 PLANT.PIPEH.P(14) := 6.98179e+006 ; # 911
914 PLANT.PIPEH.P(15) := 6.98048e+006 ; # 912
915 PLANT.PIPEH.P(16) := 6.97917e+006 ; # 913
916 PLANT.PIPEH.P(17) := 6.97788e+006 ; # 914
917 PLANT.PIPEH.P(18) := 6.97659e+006 ; # 915
918 PLANT.PIPEH.P(19) := 6.97531e+006 ; # 916
919 PLANT.PIPEH.P(20) := 6.97403e+006 ; # 917
920 PLANT.PIPEH.P(21) := 6.97276e+006 ; # 918
921 PLANT.PIPEH.P(22) := 6.97151e+006 ; # 919
922 PLANT.PIPEH.P(23) := 6.97025e+006 ; # 920
923 PLANT.PIPEH.P(24) := 6.96901e+006 ; # 921
924 PLANT.PIPEH.P(25) := 6.96778e+006 ; # 922
925 PLANT.PIPEH.P(26) := 6.96655e+006 ; # 923
926 PLANT.PIPEH.P(27) := 6.96534e+006 ; # 924
927 PLANT.PIPEH.P(28) := 6.96413e+006 ; # 925
928 PLANT.PIPEH.P(29) := 6.96294e+006 ; # 926
929 PLANT.PIPEH.P(30) := 6.96175e+006 ; # 927
930 PLANT.PIPEH.P(31) := 6.96058e+006 ; # 928
931 PLANT.PIPEH.P(32) := 6.95941e+006 ; # 929
932 PLANT.PIPEH.P(33) := 6.95826e+006 ; # 930
933 PLANT.PIPEH.P(34) := 6.95712e+006 ; # 931
934 PLANT.PIPEH.P(35) := 6.95599e+006 ; # 932
935 PLANT.PIPEH.P(36) := 6.95487e+006 ; # 933
936 PLANT.PIPEH.P(37) := 6.95377e+006 ; # 934
937 PLANT.PIPEH.P(38) := 6.95268e+006 ; # 935
938 PLANT.PIPEH.P(39) := 6.9516e+006 ; # 936
939 PLANT.PIPEH.P(40) := 6.95054e+006 ; # 937
940 PLANT.PIPEH.H(1) := 4.52899e+006 ; # 938
941 PLANT.PIPEH.H(2) := 4.51106e+006 ; # 939
942 PLANT.PIPEH.H(3) := 4.49255e+006 ; # 940
943 PLANT.PIPEH.H(4) := 4.47345e+006 ; # 941
944 PLANT.PIPEH.H(5) := 4.45373e+006 ; # 942
945 PLANT.PIPEH.H(6) := 4.43339e+006 ; # 943
946 PLANT.PIPEH.H(7) := 4.41239e+006 ; # 944
947 PLANT.PIPEH.H(8) := 4.39071e+006 ; # 945
948 PLANT.PIPEH.H(9) := 4.36834e+006 ; # 946
949 PLANT.PIPEH.H(10) := 4.34525e+006 ; # 947
950 PLANT.PIPEH.H(11) := 4.32143e+006 ; # 948
951 PLANT.PIPEH.H(12) := 4.29683e+006 ; # 949
952 PLANT.PIPEH.H(13) := 4.27145e+006 ; # 950
953 PLANT.PIPEH.H(14) := 4.24525e+006 ; # 951
954 PLANT.PIPEH.H(15) := 4.21821e+006 ; # 952
955 PLANT.PIPEH.H(16) := 4.19031e+006 ; # 953
956 PLANT.PIPEH.H(17) := 4.16151e+006 ; # 954

```

957 PLANT.PIPEH.H(18) := 4.13178e+006 ; # 955
 958 PLANT.PIPEH.H(19) := 4.1011e+006 ; # 956
 959 PLANT.PIPEH.H(20) := 4.06944e+006 ; # 957
 960 PLANT.PIPEH.H(21) := 4.03675e+006 ; # 958
 961 PLANT.PIPEH.H(22) := 4.00302e+006 ; # 959
 962 PLANT.PIPEH.H(23) := 3.96821e+006 ; # 960
 963 PLANT.PIPEH.H(24) := 3.93228e+006 ; # 961
 964 PLANT.PIPEH.H(25) := 3.8952e+006 ; # 962
 965 PLANT.PIPEH.H(26) := 3.85693e+006 ; # 963
 966 PLANT.PIPEH.H(27) := 3.81742e+006 ; # 964
 967 PLANT.PIPEH.H(28) := 3.77666e+006 ; # 965
 968 PLANT.PIPEH.H(29) := 3.73458e+006 ; # 966
 969 PLANT.PIPEH.H(30) := 3.69115e+006 ; # 967
 970 PLANT.PIPEH.H(31) := 3.64633e+006 ; # 968
 971 PLANT.PIPEH.H(32) := 3.60007e+006 ; # 969
 972 PLANT.PIPEH.H(33) := 3.55232e+006 ; # 970
 973 PLANT.PIPEH.H(34) := 3.50304e+006 ; # 971
 974 PLANT.PIPEH.H(35) := 3.45219e+006 ; # 972
 975 PLANT.PIPEH.H(36) := 3.39969e+006 ; # 973
 976 PLANT.PIPEH.H(37) := 3.34552e+006 ; # 974
 977 PLANT.PIPEH.H(38) := 3.2896e+006 ; # 975
 978 PLANT.PIPEH.H(39) := 3.23189e+006 ; # 976
 979 PLANT.PIPEH.H(40) := 3.17244e+006 ; # 977
 980 PLANT.PIPEH.H0 := 4.5464e+006 ; # 978
 981 PLANT.PIPEH.T(1) := 1169.8 ; # 979
 982 PLANT.PIPEH.T(2) := 1166.35 ; # 980
 983 PLANT.PIPEH.T(3) := 1162.78 ; # 981
 984 PLANT.PIPEH.T(4) := 1159.11 ; # 982
 985 PLANT.PIPEH.T(5) := 1155.31 ; # 983
 986 PLANT.PIPEH.T(6) := 1151.39 ; # 984
 987 PLANT.PIPEH.T(7) := 1147.35 ; # 985
 988 PLANT.PIPEH.T(8) := 1143.18 ; # 986
 989 PLANT.PIPEH.T(9) := 1138.87 ; # 987
 990 PLANT.PIPEH.T(10) := 1134.43 ; # 988
 991 PLANT.PIPEH.T(11) := 1129.84 ; # 989
 992 PLANT.PIPEH.T(12) := 1125.11 ; # 990
 993 PLANT.PIPEH.T(13) := 1120.22 ; # 991
 994 PLANT.PIPEH.T(14) := 1115.18 ; # 992
 995 PLANT.PIPEH.T(15) := 1109.98 ; # 993
 996 PLANT.PIPEH.T(16) := 1104.6 ; # 994
 997 PLANT.PIPEH.T(17) := 1099.06 ; # 995
 998 PLANT.PIPEH.T(18) := 1093.34 ; # 996
 999 PLANT.PIPEH.T(19) := 1087.43 ; # 997
 1000 PLANT.PIPEH.T(20) := 1081.34 ; # 998
 1001 PLANT.PIPEH.T(21) := 1075.05 ; # 999
 1002 PLANT.PIPEH.T(22) := 1068.55 ; # 1000
 1003 PLANT.PIPEH.T(23) := 1061.85 ; # 1001
 1004 PLANT.PIPEH.T(24) := 1054.94 ; # 1002
 1005 PLANT.PIPEH.T(25) := 1047.8 ; # 1003
 1006 PLANT.PIPEH.T(26) := 1040.43 ; # 1004
 1007 PLANT.PIPEH.T(27) := 1032.83 ; # 1005
 1008 PLANT.PIPEH.T(28) := 1024.98 ; # 1006
 1009 PLANT.PIPEH.T(29) := 1016.88 ; # 1007
 1010 PLANT.PIPEH.T(30) := 1008.52 ; # 1008
 1011 PLANT.PIPEH.T(31) := 999.892 ; # 1009
 1012 PLANT.PIPEH.T(32) := 990.987 ; # 1010
 1013 PLANT.PIPEH.T(33) := 981.796 ; # 1011
 1014 PLANT.PIPEH.T(34) := 972.311 ; # 1012
 1015 PLANT.PIPEH.T(35) := 962.521 ; # 1013
 1016 PLANT.PIPEH.T(36) := 952.416 ; # 1014
 1017 PLANT.PIPEH.T(37) := 941.988 ; # 1015
 1018 PLANT.PIPEH.T(38) := 931.225 ; # 1016
 1019 PLANT.PIPEH.T(39) := 920.116 ; # 1017
 1020 PLANT.PIPEH.T(40) := 908.671 ; # 1018
 1021 PLANT.PIPEH.TEXTRNL(1) := 1161.37 ; # 1019
 1022 PLANT.PIPEH.TEXTRNL(2) := 1157.67 ; # 1020
 1023 PLANT.PIPEH.TEXTRNL(3) := 1153.83 ; # 1021
 1024 PLANT.PIPEH.TEXTRNL(4) := 1149.86 ; # 1022
 1025 PLANT.PIPEH.TEXTRNL(5) := 1145.77 ; # 1023
 1026 PLANT.PIPEH.TEXTRNL(6) := 1141.55 ; # 1024
 1027 PLANT.PIPEH.TEXTRNL(7) := 1137.19 ; # 1025
 1028 PLANT.PIPEH.TEXTRNL(8) := 1132.69 ; # 1026
 1029 PLANT.PIPEH.TEXTRNL(9) := 1128.05 ; # 1027
 1030 PLANT.PIPEH.TEXTRNL(10) := 1123.26 ; # 1028
 1031 PLANT.PIPEH.TEXTRNL(11) := 1118.31 ; # 1029
 1032 PLANT.PIPEH.TEXTRNL(12) := 1113.21 ; # 1030
 1033 PLANT.PIPEH.TEXTRNL(13) := 1107.94 ; # 1031
 1034 PLANT.PIPEH.TEXTRNL(14) := 1102.5 ; # 1032
 1035 PLANT.PIPEH.TEXTRNL(15) := 1096.89 ; # 1033
 1036 PLANT.PIPEH.TEXTRNL(16) := 1091.1 ; # 1034
 1037 PLANT.PIPEH.TEXTRNL(17) := 1085.12 ; # 1035
 1038 PLANT.PIPEH.TEXTRNL(18) := 1078.95 ; # 1036
 1039 PLANT.PIPEH.TEXTRNL(19) := 1072.58 ; # 1037
 1040 PLANT.PIPEH.TEXTRNL(20) := 1066.01 ; # 1038
 1041 PLANT.PIPEH.TEXTRNL(21) := 1059.23 ; # 1039
 1042 PLANT.PIPEH.TEXTRNL(22) := 1052.23 ; # 1040
 1043 PLANT.PIPEH.TEXTRNL(23) := 1045 ; # 1041
 1044 PLANT.PIPEH.TEXTRNL(24) := 1037.55 ; # 1042
 1045 PLANT.PIPEH.TEXTRNL(25) := 1029.85 ; # 1043
 1046 PLANT.PIPEH.TEXTRNL(26) := 1021.91 ; # 1044
 1047 PLANT.PIPEH.TEXTRNL(27) := 1013.71 ; # 1045
 1048 PLANT.PIPEH.TEXTRNL(28) := 1005.25 ; # 1046

1049 PLANT.PIPEH.TEXTRNL(29) := 996.513 ; # 1047
1050 PLANT.PIPEH.TEXTRNL(30) := 987.5 ; # 1048
1051 PLANT.PIPEH.TEXTRNL(31) := 978.197 ; # 1049
1052 PLANT.PIPEH.TEXTRNL(32) := 968.596 ; # 1050
1053 PLANT.PIPEH.TEXTRNL(33) := 958.687 ; # 1051
1054 PLANT.PIPEH.TEXTRNL(34) := 948.459 ; # 1052
1055 PLANT.PIPEH.TEXTRNL(35) := 937.904 ; # 1053
1056 PLANT.PIPEH.TEXTRNL(36) := 927.009 ; # 1054
1057 PLANT.PIPEH.TEXTRNL(37) := 915.766 ; # 1055
1058 PLANT.PIPEH.TEXTRNL(38) := 904.161 ; # 1056
1059 PLANT.PIPEH.TEXTRNL(39) := 892.184 ; # 1057
1060 PLANT.PIPEH.TEXTRNL(40) := 879.893 ; # 1058
1061 PLANT.PIPEH.F(1) := 32.3305 ; # 1059
1062 PLANT.PIPEH.F(2) := 32.3305 ; # 1060
1063 PLANT.PIPEH.F(3) := 32.3305 ; # 1061
1064 PLANT.PIPEH.F(4) := 32.3305 ; # 1062
1065 PLANT.PIPEH.F(5) := 32.3305 ; # 1063
1066 PLANT.PIPEH.F(6) := 32.3305 ; # 1064
1067 PLANT.PIPEH.F(7) := 32.3305 ; # 1065
1068 PLANT.PIPEH.F(8) := 32.3305 ; # 1066
1069 PLANT.PIPEH.F(9) := 32.3305 ; # 1067
1070 PLANT.PIPEH.F(10) := 32.3305 ; # 1068
1071 PLANT.PIPEH.F(11) := 32.3305 ; # 1069
1072 PLANT.PIPEH.F(12) := 32.3305 ; # 1070
1073 PLANT.PIPEH.F(13) := 32.3305 ; # 1071
1074 PLANT.PIPEH.F(14) := 32.3305 ; # 1072
1075 PLANT.PIPEH.F(15) := 32.3305 ; # 1073
1076 PLANT.PIPEH.F(16) := 32.3305 ; # 1074
1077 PLANT.PIPEH.F(17) := 32.3305 ; # 1075
1078 PLANT.PIPEH.F(18) := 32.3305 ; # 1076
1079 PLANT.PIPEH.F(19) := 32.3305 ; # 1077
1080 PLANT.PIPEH.F(20) := 32.3305 ; # 1078
1081 PLANT.PIPEH.F(21) := 32.3305 ; # 1079
1082 PLANT.PIPEH.F(22) := 32.3305 ; # 1080
1083 PLANT.PIPEH.F(23) := 32.3305 ; # 1081
1084 PLANT.PIPEH.F(24) := 32.3305 ; # 1082
1085 PLANT.PIPEH.F(25) := 32.3305 ; # 1083
1086 PLANT.PIPEH.F(26) := 32.3305 ; # 1084
1087 PLANT.PIPEH.F(27) := 32.3305 ; # 1085
1088 PLANT.PIPEH.F(28) := 32.3305 ; # 1086
1089 PLANT.PIPEH.F(29) := 32.3305 ; # 1087
1090 PLANT.PIPEH.F(30) := 32.3305 ; # 1088
1091 PLANT.PIPEH.F(31) := 32.3305 ; # 1089
1092 PLANT.PIPEH.F(32) := 32.3305 ; # 1090
1093 PLANT.PIPEH.F(33) := 32.3305 ; # 1091
1094 PLANT.PIPEH.F(34) := 32.3305 ; # 1092
1095 PLANT.PIPEH.F(35) := 32.3305 ; # 1093
1096 PLANT.PIPEH.F(36) := 32.3305 ; # 1094
1097 PLANT.PIPEH.F(37) := 32.3305 ; # 1095
1098 PLANT.PIPEH.F(38) := 32.3305 ; # 1096
1099 PLANT.PIPEH.F(39) := 32.3305 ; # 1097
1100 PLANT.PIPEH.F(40) := 32.3305 ; # 1098
1101 PLANT.PIPEH.F_IN := 32.3305 ; # 1099
1102 PLANT.PIPEH.PSI(1) := 6.03823e+006 ; # 1100
1103 PLANT.PIPEH.PSI(2) := 6.02385e+006 ; # 1101
1104 PLANT.PIPEH.PSI(3) := 6.00898e+006 ; # 1102
1105 PLANT.PIPEH.PSI(4) := 5.9936e+006 ; # 1103
1106 PLANT.PIPEH.PSI(5) := 5.97767e+006 ; # 1104
1107 PLANT.PIPEH.PSI(6) := 5.96117e+006 ; # 1105
1108 PLANT.PIPEH.PSI(7) := 5.94408e+006 ; # 1106
1109 PLANT.PIPEH.PSI(8) := 5.92638e+006 ; # 1107
1110 PLANT.PIPEH.PSI(9) := 5.90802e+006 ; # 1108
1111 PLANT.PIPEH.PSI(10) := 5.88899e+006 ; # 1109
1112 PLANT.PIPEH.PSI(11) := 5.86924e+006 ; # 1110
1113 PLANT.PIPEH.PSI(12) := 5.84876e+006 ; # 1111
1114 PLANT.PIPEH.PSI(13) := 5.82749e+006 ; # 1112
1115 PLANT.PIPEH.PSI(14) := 5.8054e+006 ; # 1113
1116 PLANT.PIPEH.PSI(15) := 5.78245e+006 ; # 1114
1117 PLANT.PIPEH.PSI(16) := 5.75859e+006 ; # 1115
1118 PLANT.PIPEH.PSI(17) := 5.73379e+006 ; # 1116
1119 PLANT.PIPEH.PSI(18) := 5.70799e+006 ; # 1117
1120 PLANT.PIPEH.PSI(19) := 5.68113e+006 ; # 1118
1121 PLANT.PIPEH.PSI(20) := 5.65317e+006 ; # 1119
1122 PLANT.PIPEH.PSI(21) := 5.62404e+006 ; # 1120
1123 PLANT.PIPEH.PSI(22) := 5.59367e+006 ; # 1121
1124 PLANT.PIPEH.PSI(23) := 5.56201e+006 ; # 1122
1125 PLANT.PIPEH.PSI(24) := 5.52897e+006 ; # 1123
1126 PLANT.PIPEH.PSI(25) := 5.49447e+006 ; # 1124
1127 PLANT.PIPEH.PSI(26) := 5.45844e+006 ; # 1125
1128 PLANT.PIPEH.PSI(27) := 5.42078e+006 ; # 1126
1129 PLANT.PIPEH.PSI(28) := 5.38139e+006 ; # 1127
1130 PLANT.PIPEH.PSI(29) := 5.34016e+006 ; # 1128
1131 PLANT.PIPEH.PSI(30) := 5.29699e+006 ; # 1129
1132 PLANT.PIPEH.PSI(31) := 5.25174e+006 ; # 1130
1133 PLANT.PIPEH.PSI(32) := 5.20427e+006 ; # 1131
1134 PLANT.PIPEH.PSI(33) := 5.15446e+006 ; # 1132
1135 PLANT.PIPEH.PSI(34) := 5.10212e+006 ; # 1133
1136 PLANT.PIPEH.PSI(35) := 5.0471e+006 ; # 1134
1137 PLANT.PIPEH.PSI(36) := 4.98919e+006 ; # 1135
1138 PLANT.PIPEH.PSI(37) := 4.92819e+006 ; # 1136
1139 PLANT.PIPEH.PSI(38) := 4.86388e+006 ; # 1137
1140 PLANT.PIPEH.PSI(39) := 4.796e+006 ; # 1138

1141 PLANT.PIPEH.PSI(40) := 4.7244e+006 ; # 1139
1142 PLANT.PIPEH.HT.RHOPIPEHE := 3.09587 ; # 1140
1143 PLANT.PIPEH.HT.VPIPE := 28.7109 ; # 1141
1144 PLANT.PIPEH.HT.HO := 1760.94 ; # 1142
1145 PLANT.PIPEH.HT.U := 1738.41 ; # 1143
1146 PLANT.HX2.TGASHOT(1) := 1141.93 ; # 1144
1147 PLANT.HX2.TGASHOT(2) := 1139.37 ; # 1145
1148 PLANT.HX2.TGASHOT(3) := 1136.66 ; # 1146
1149 PLANT.HX2.TGASHOT(4) := 1133.8 ; # 1147
1150 PLANT.HX2.TGASHOT(5) := 1130.77 ; # 1148
1151 PLANT.HX2.TGASHOT(6) := 1127.56 ; # 1149
1152 PLANT.HX2.TGASHOT(7) := 1124.17 ; # 1150
1153 PLANT.HX2.TGASHOT(8) := 1120.57 ; # 1151
1154 PLANT.HX2.TGASHOT(9) := 1116.77 ; # 1152
1155 PLANT.HX2.TGASHOT(10) := 1112.75 ; # 1153
1156 PLANT.HX2.TGASHOT(11) := 1108.5 ; # 1154
1157 PLANT.HX2.TGASHOT(12) := 1104 ; # 1155
1158 PLANT.HX2.TGASHOT(13) := 1099.23 ; # 1156
1159 PLANT.HX2.TGASHOT(14) := 1094.19 ; # 1157
1160 PLANT.HX2.TGASHOT(15) := 1088.86 ; # 1158
1161 PLANT.HX2.TGASHOT(16) := 1083.21 ; # 1159
1162 PLANT.HX2.TGASHOT(17) := 1077.24 ; # 1160
1163 PLANT.HX2.TGASHOT(18) := 1070.92 ; # 1161
1164 PLANT.HX2.TGASHOT(19) := 1064.23 ; # 1162
1165 PLANT.HX2.TGASHOT(20) := 1057.15 ; # 1163
1166 PLANT.HX2.TGASHOT(21) := 1049.66 ; # 1164
1167 PLANT.HX2.TGASHOT(22) := 1041.74 ; # 1165
1168 PLANT.HX2.TGASHOT(23) := 1033.36 ; # 1166
1169 PLANT.HX2.TGASHOT(24) := 1024.48 ; # 1167
1170 PLANT.HX2.TGASHOT(25) := 1015.09 ; # 1168
1171 PLANT.HX2.TGASHOT(26) := 1005.16 ; # 1169
1172 PLANT.HX2.TGASHOT(27) := 994.647 ; # 1170
1173 PLANT.HX2.TGASHOT(28) := 983.524 ; # 1171
1174 PLANT.HX2.TGASHOT(29) := 971.753 ; # 1172
1175 PLANT.HX2.TGASHOT(30) := 959.298 ; # 1173
1176 PLANT.HX2.TGASHOT(31) := 946.119 ; # 1174
1177 PLANT.HX2.TGASHOT(32) := 932.173 ; # 1175
1178 PLANT.HX2.TGASHOT(33) := 917.416 ; # 1176
1179 PLANT.HX2.TGASHOT(34) := 901.801 ; # 1177
1180 PLANT.HX2.TGASHOT(35) := 885.278 ; # 1178
1181 PLANT.HX2.TGASHOT(36) := 867.793 ; # 1179
1182 PLANT.HX2.TGASHOT(37) := 849.292 ; # 1180
1183 PLANT.HX2.TGASHOT(38) := 829.716 ; # 1181
1184 PLANT.HX2.TGASHOT(39) := 809 ; # 1182
1185 PLANT.HX2.TGASHOT(40) := 787.082 ; # 1183
1186 PLANT.HX2.TGASCOLD(1) := 1126.32 ; # 1184
1187 PLANT.HX2.TGASCOLD(2) := 1122.86 ; # 1185
1188 PLANT.HX2.TGASCOLD(3) := 1119.19 ; # 1186
1189 PLANT.HX2.TGASCOLD(4) := 1115.31 ; # 1187
1190 PLANT.HX2.TGASCOLD(5) := 1111.2 ; # 1188
1191 PLANT.HX2.TGASCOLD(6) := 1106.86 ; # 1189
1192 PLANT.HX2.TGASCOLD(7) := 1102.26 ; # 1190
1193 PLANT.HX2.TGASCOLD(8) := 1097.39 ; # 1191
1194 PLANT.HX2.TGASCOLD(9) := 1092.24 ; # 1192
1195 PLANT.HX2.TGASCOLD(10) := 1086.8 ; # 1193
1196 PLANT.HX2.TGASCOLD(11) := 1081.03 ; # 1194
1197 PLANT.HX2.TGASCOLD(12) := 1074.93 ; # 1195
1198 PLANT.HX2.TGASCOLD(13) := 1068.48 ; # 1196
1199 PLANT.HX2.TGASCOLD(14) := 1061.65 ; # 1197
1200 PLANT.HX2.TGASCOLD(15) := 1054.42 ; # 1198
1201 PLANT.HX2.TGASCOLD(16) := 1046.77 ; # 1199
1202 PLANT.HX2.TGASCOLD(17) := 1038.68 ; # 1200
1203 PLANT.HX2.TGASCOLD(18) := 1030.12 ; # 1201
1204 PLANT.HX2.TGASCOLD(19) := 1021.06 ; # 1202
1205 PLANT.HX2.TGASCOLD(20) := 1011.47 ; # 1203
1206 PLANT.HX2.TGASCOLD(21) := 1001.32 ; # 1204
1207 PLANT.HX2.TGASCOLD(22) := 990.587 ; # 1205
1208 PLANT.HX2.TGASCOLD(23) := 979.228 ; # 1206
1209 PLANT.HX2.TGASCOLD(24) := 967.207 ; # 1207
1210 PLANT.HX2.TGASCOLD(25) := 954.488 ; # 1208
1211 PLANT.HX2.TGASCOLD(26) := 941.029 ; # 1209
1212 PLANT.HX2.TGASCOLD(27) := 926.787 ; # 1210
1213 PLANT.HX2.TGASCOLD(28) := 911.717 ; # 1211
1214 PLANT.HX2.TGASCOLD(29) := 895.77 ; # 1212
1215 PLANT.HX2.TGASCOLD(30) := 878.896 ; # 1213
1216 PLANT.HX2.TGASCOLD(31) := 861.041 ; # 1214
1217 PLANT.HX2.TGASCOLD(32) := 842.147 ; # 1215
1218 PLANT.HX2.TGASCOLD(33) := 822.155 ; # 1216
1219 PLANT.HX2.TGASCOLD(34) := 801 ; # 1217
1220 PLANT.HX2.TGASCOLD(35) := 778.614 ; # 1218
1221 PLANT.HX2.TGASCOLD(36) := 754.927 ; # 1219
1222 PLANT.HX2.TGASCOLD(37) := 729.862 ; # 1220
1223 PLANT.HX2.TGASCOLD(38) := 703.34 ; # 1221
1224 PLANT.HX2.TGASCOLD(39) := 675.275 ; # 1222
1225 PLANT.HX2.TGASCOLD(40) := 645.577 ; # 1223
1226 PLANT.HX2.UHOT := 1299.78 ; # 1224
1227 PLANT.HX2.UCOLD := 1880.53 ; # 1225
1228 PLANT.HX2.THX(1) := 1133.71 ; # 1226
1229 PLANT.HX2.THX(2) := 1130.67 ; # 1227
1230 PLANT.HX2.THX(3) := 1127.46 ; # 1228
1231 PLANT.HX2.THX(4) := 1124.06 ; # 1229
1232 PLANT.HX2.THX(5) := 1120.46 ; # 1230

1233 PLANT.HX2.THX(6) := 1116.65 ; # 1231
1234 PLANT.HX2.THX(7) := 1112.63 ; # 1232
1235 PLANT.HX2.THX(8) := 1108.36 ; # 1233
1236 PLANT.HX2.THX(9) := 1103.85 ; # 1234
1237 PLANT.HX2.THX(10) := 1099.08 ; # 1235
1238 PLANT.HX2.THX(11) := 1094.03 ; # 1236
1239 PLANT.HX2.THX(12) := 1088.69 ; # 1237
1240 PLANT.HX2.THX(13) := 1083.03 ; # 1238
1241 PLANT.HX2.THX(14) := 1077.05 ; # 1239
1242 PLANT.HX2.THX(15) := 1070.72 ; # 1240
1243 PLANT.HX2.THX(16) := 1064.02 ; # 1241
1244 PLANT.HX2.THX(17) := 1056.93 ; # 1242
1245 PLANT.HX2.THX(18) := 1049.43 ; # 1243
1246 PLANT.HX2.THX(19) := 1041.49 ; # 1244
1247 PLANT.HX2.THX(20) := 1033.09 ; # 1245
1248 PLANT.HX2.THX(21) := 1024.2 ; # 1246
1249 PLANT.HX2.THX(22) := 1014.8 ; # 1247
1250 PLANT.HX2.THX(23) := 1004.84 ; # 1248
1251 PLANT.HX2.THX(24) := 994.314 ; # 1249
1252 PLANT.HX2.THX(25) := 983.171 ; # 1250
1253 PLANT.HX2.THX(26) := 971.38 ; # 1251
1254 PLANT.HX2.THX(27) := 958.903 ; # 1252
1255 PLANT.HX2.THX(28) := 945.701 ; # 1253
1256 PLANT.HX2.THX(29) := 931.731 ; # 1254
1257 PLANT.HX2.THX(30) := 916.948 ; # 1255
1258 PLANT.HX2.THX(31) := 901.306 ; # 1256
1259 PLANT.HX2.THX(32) := 884.754 ; # 1257
1260 PLANT.HX2.THX(33) := 867.239 ; # 1258
1261 PLANT.HX2.THX(34) := 848.706 ; # 1259
1262 PLANT.HX2.THX(35) := 829.095 ; # 1260
1263 PLANT.HX2.THX(36) := 808.344 ; # 1261
1264 PLANT.HX2.THX(37) := 786.385 ; # 1262
1265 PLANT.HX2.THX(38) := 763.15 ; # 1263
1266 PLANT.HX2.THX(39) := 738.563 ; # 1264
1267 PLANT.HX2.THX(40) := 712.554 ; # 1265
1268 PLANT.PIPEC2.RHO(1) := 3.72389 ; # 1266
1269 PLANT.PIPEC2.RHO(2) := 3.55368 ; # 1267
1270 PLANT.PIPEC2.RHO(3) := 3.4055 ; # 1268
1271 PLANT.PIPEC2.RHO(4) := 3.27543 ; # 1269
1272 PLANT.PIPEC2.RHO(5) := 3.16041 ; # 1270
1273 PLANT.PIPEC2.RHO(6) := 3.05803 ; # 1271
1274 PLANT.PIPEC2.RHO(7) := 2.96638 ; # 1272
1275 PLANT.PIPEC2.RHO(8) := 2.88388 ; # 1273
1276 PLANT.PIPEC2.RHO(9) := 2.80928 ; # 1274
1277 PLANT.PIPEC2.RHO(10) := 2.74152 ; # 1275
1278 PLANT.PIPEC2.RHO(11) := 2.67973 ; # 1276
1279 PLANT.PIPEC2.RHO(12) := 2.62316 ; # 1277
1280 PLANT.PIPEC2.RHO(13) := 2.57121 ; # 1278
1281 PLANT.PIPEC2.RHO(14) := 2.52333 ; # 1279
1282 PLANT.PIPEC2.RHO(15) := 2.47909 ; # 1280
1283 PLANT.PIPEC2.RHO(16) := 2.43808 ; # 1281
1284 PLANT.PIPEC2.RHO(17) := 2.39997 ; # 1282
1285 PLANT.PIPEC2.RHO(18) := 2.36446 ; # 1283
1286 PLANT.PIPEC2.RHO(19) := 2.3313 ; # 1284
1287 PLANT.PIPEC2.RHO(20) := 2.30026 ; # 1285
1288 PLANT.PIPEC2.RHO(21) := 2.27113 ; # 1286
1289 PLANT.PIPEC2.RHO(22) := 2.24375 ; # 1287
1290 PLANT.PIPEC2.RHO(23) := 2.21796 ; # 1288
1291 PLANT.PIPEC2.RHO(24) := 2.19361 ; # 1289
1292 PLANT.PIPEC2.RHO(25) := 2.17058 ; # 1290
1293 PLANT.PIPEC2.RHO(26) := 2.14875 ; # 1291
1294 PLANT.PIPEC2.RHO(27) := 2.12804 ; # 1292
1295 PLANT.PIPEC2.RHO(28) := 2.10834 ; # 1293
1296 PLANT.PIPEC2.RHO(29) := 2.08957 ; # 1294
1297 PLANT.PIPEC2.RHO(30) := 2.07166 ; # 1295
1298 PLANT.PIPEC2.RHO(31) := 2.05454 ; # 1296
1299 PLANT.PIPEC2.RHO(32) := 2.03814 ; # 1297
1300 PLANT.PIPEC2.RHO(33) := 2.02242 ; # 1298
1301 PLANT.PIPEC2.RHO(34) := 2.00733 ; # 1299
1302 PLANT.PIPEC2.RHO(35) := 1.9928 ; # 1300
1303 PLANT.PIPEC2.RHO(36) := 1.97881 ; # 1301
1304 PLANT.PIPEC2.RHO(37) := 1.96531 ; # 1302
1305 PLANT.PIPEC2.RHO(38) := 1.95226 ; # 1303
1306 PLANT.PIPEC2.RHO(39) := 1.93964 ; # 1304
1307 PLANT.PIPEC2.RHO(40) := 1.92741 ; # 1305
1308 PLANT.PIPEC2.P(1) := 1.10918e+006 ; # 1306
1309 PLANT.PIPEC2.P(2) := 1.10717e+006 ; # 1307
1310 PLANT.PIPEC2.P(3) := 1.1051e+006 ; # 1308
1311 PLANT.PIPEC2.P(4) := 1.10297e+006 ; # 1309
1312 PLANT.PIPEC2.P(5) := 1.10079e+006 ; # 1310
1313 PLANT.PIPEC2.P(6) := 1.09855e+006 ; # 1311
1314 PLANT.PIPEC2.P(7) := 1.09626e+006 ; # 1312
1315 PLANT.PIPEC2.P(8) := 1.09392e+006 ; # 1313
1316 PLANT.PIPEC2.P(9) := 1.09154e+006 ; # 1314
1317 PLANT.PIPEC2.P(10) := 1.08911e+006 ; # 1315
1318 PLANT.PIPEC2.P(11) := 1.08663e+006 ; # 1316
1319 PLANT.PIPEC2.P(12) := 1.08412e+006 ; # 1317
1320 PLANT.PIPEC2.P(13) := 1.08156e+006 ; # 1318
1321 PLANT.PIPEC2.P(14) := 1.07897e+006 ; # 1319
1322 PLANT.PIPEC2.P(15) := 1.07634e+006 ; # 1320
1323 PLANT.PIPEC2.P(16) := 1.07368e+006 ; # 1321
1324 PLANT.PIPEC2.P(17) := 1.07098e+006 ; # 1322

1325 PLANT.PIPEC2.P(18) := 1.06825e+006 ; # 1323
1326 PLANT.PIPEC2.P(19) := 1.06548e+006 ; # 1324
1327 PLANT.PIPEC2.P(20) := 1.06269e+006 ; # 1325
1328 PLANT.PIPEC2.P(21) := 1.05986e+006 ; # 1326
1329 PLANT.PIPEC2.P(22) := 1.05701e+006 ; # 1327
1330 PLANT.PIPEC2.P(23) := 1.05413e+006 ; # 1328
1331 PLANT.PIPEC2.P(24) := 1.05123e+006 ; # 1329
1332 PLANT.PIPEC2.P(25) := 1.04829e+006 ; # 1330
1333 PLANT.PIPEC2.P(26) := 1.04533e+006 ; # 1331
1334 PLANT.PIPEC2.P(27) := 1.04235e+006 ; # 1332
1335 PLANT.PIPEC2.P(28) := 1.03935e+006 ; # 1333
1336 PLANT.PIPEC2.P(29) := 1.03632e+006 ; # 1334
1337 PLANT.PIPEC2.P(30) := 1.03326e+006 ; # 1335
1338 PLANT.PIPEC2.P(31) := 1.03019e+006 ; # 1336
1339 PLANT.PIPEC2.P(32) := 1.02709e+006 ; # 1337
1340 PLANT.PIPEC2.P(33) := 1.02398e+006 ; # 1338
1341 PLANT.PIPEC2.P(34) := 1.02084e+006 ; # 1339
1342 PLANT.PIPEC2.P(35) := 1.01768e+006 ; # 1340
1343 PLANT.PIPEC2.P(36) := 1.0145e+006 ; # 1341
1344 PLANT.PIPEC2.P(37) := 1.0113e+006 ; # 1342
1345 PLANT.PIPEC2.P(38) := 1.00808e+006 ; # 1343
1346 PLANT.PIPEC2.P(39) := 1.00485e+006 ; # 1344
1347 PLANT.PIPEC2.P(40) := 1.00159e+006 ; # 1345
1348 PLANT.PIPEC2.H(1) := 784075 ; # 1346
1349 PLANT.PIPEC2.H(2) := 851066 ; # 1347
1350 PLANT.PIPEC2.H(3) := 914376 ; # 1348
1351 PLANT.PIPEC2.H(4) := 974206 ; # 1349
1352 PLANT.PIPEC2.H(5) := 1.03075e+006 ; # 1350
1353 PLANT.PIPEC2.H(6) := 1.08418e+006 ; # 1351
1354 PLANT.PIPEC2.H(7) := 1.13468e+006 ; # 1352
1355 PLANT.PIPEC2.H(8) := 1.1824e+006 ; # 1353
1356 PLANT.PIPEC2.H(9) := 1.2275e+006 ; # 1354
1357 PLANT.PIPEC2.H(10) := 1.27012e+006 ; # 1355
1358 PLANT.PIPEC2.H(11) := 1.3104e+006 ; # 1356
1359 PLANT.PIPEC2.H(12) := 1.34847e+006 ; # 1357
1360 PLANT.PIPEC2.H(13) := 1.38444e+006 ; # 1358
1361 PLANT.PIPEC2.H(14) := 1.41843e+006 ; # 1359
1362 PLANT.PIPEC2.H(15) := 1.45056e+006 ; # 1360
1363 PLANT.PIPEC2.H(16) := 1.48092e+006 ; # 1361
1364 PLANT.PIPEC2.H(17) := 1.50962e+006 ; # 1362
1365 PLANT.PIPEC2.H(18) := 1.53673e+006 ; # 1363
1366 PLANT.PIPEC2.H(19) := 1.56236e+006 ; # 1364
1367 PLANT.PIPEC2.H(20) := 1.58657e+006 ; # 1365
1368 PLANT.PIPEC2.H(21) := 1.60946e+006 ; # 1366
1369 PLANT.PIPEC2.H(22) := 1.63109e+006 ; # 1367
1370 PLANT.PIPEC2.H(23) := 1.65153e+006 ; # 1368
1371 PLANT.PIPEC2.H(24) := 1.67085e+006 ; # 1369
1372 PLANT.PIPEC2.H(25) := 1.6891e+006 ; # 1370
1373 PLANT.PIPEC2.H(26) := 1.70635e+006 ; # 1371
1374 PLANT.PIPEC2.H(27) := 1.72265e+006 ; # 1372
1375 PLANT.PIPEC2.H(28) := 1.73806e+006 ; # 1373
1376 PLANT.PIPEC2.H(29) := 1.75262e+006 ; # 1374
1377 PLANT.PIPEC2.H(30) := 1.76638e+006 ; # 1375
1378 PLANT.PIPEC2.H(31) := 1.77939e+006 ; # 1376
1379 PLANT.PIPEC2.H(32) := 1.79168e+006 ; # 1377
1380 PLANT.PIPEC2.H(33) := 1.80329e+006 ; # 1378
1381 PLANT.PIPEC2.H(34) := 1.81427e+006 ; # 1379
1382 PLANT.PIPEC2.H(35) := 1.82464e+006 ; # 1380
1383 PLANT.PIPEC2.H(36) := 1.83444e+006 ; # 1381
1384 PLANT.PIPEC2.H(37) := 1.8437e+006 ; # 1382
1385 PLANT.PIPEC2.H(38) := 1.85246e+006 ; # 1383
1386 PLANT.PIPEC2.H(39) := 1.86073e+006 ; # 1384
1387 PLANT.PIPEC2.H(40) := 1.86855e+006 ; # 1385
1388 PLANT.PIPEC2.H0 := 713180 ; # 1386
1389 PLANT.PIPEC2.T(1) := 645.577 ; # 1387
1390 PLANT.PIPEC2.T(2) := 675.275 ; # 1388
1391 PLANT.PIPEC2.T(3) := 703.34 ; # 1389
1392 PLANT.PIPEC2.T(4) := 729.862 ; # 1390
1393 PLANT.PIPEC2.T(5) := 754.927 ; # 1391
1394 PLANT.PIPEC2.T(6) := 778.614 ; # 1392
1395 PLANT.PIPEC2.T(7) := 801 ; # 1393
1396 PLANT.PIPEC2.T(8) := 822.155 ; # 1394
1397 PLANT.PIPEC2.T(9) := 842.147 ; # 1395
1398 PLANT.PIPEC2.T(10) := 861.041 ; # 1396
1399 PLANT.PIPEC2.T(11) := 878.896 ; # 1397
1400 PLANT.PIPEC2.T(12) := 895.77 ; # 1398
1401 PLANT.PIPEC2.T(13) := 911.717 ; # 1399
1402 PLANT.PIPEC2.T(14) := 926.787 ; # 1400
1403 PLANT.PIPEC2.T(15) := 941.029 ; # 1401
1404 PLANT.PIPEC2.T(16) := 954.488 ; # 1402
1405 PLANT.PIPEC2.T(17) := 967.207 ; # 1403
1406 PLANT.PIPEC2.T(18) := 979.228 ; # 1404
1407 PLANT.PIPEC2.T(19) := 990.587 ; # 1405
1408 PLANT.PIPEC2.T(20) := 1001.32 ; # 1406
1409 PLANT.PIPEC2.T(21) := 1011.47 ; # 1407
1410 PLANT.PIPEC2.T(22) := 1021.06 ; # 1408
1411 PLANT.PIPEC2.T(23) := 1030.12 ; # 1409
1412 PLANT.PIPEC2.T(24) := 1038.68 ; # 1410
1413 PLANT.PIPEC2.T(25) := 1046.77 ; # 1411
1414 PLANT.PIPEC2.T(26) := 1054.42 ; # 1412
1415 PLANT.PIPEC2.T(27) := 1061.65 ; # 1413
1416 PLANT.PIPEC2.T(28) := 1068.48 ; # 1414

1417 PLANT.PIPEC2.T(29) := 1074.93 ; # 1415
1418 PLANT.PIPEC2.T(30) := 1081.03 ; # 1416
1419 PLANT.PIPEC2.T(31) := 1086.8 ; # 1417
1420 PLANT.PIPEC2.T(32) := 1092.24 ; # 1418
1421 PLANT.PIPEC2.T(33) := 1097.39 ; # 1419
1422 PLANT.PIPEC2.T(34) := 1102.26 ; # 1420
1423 PLANT.PIPEC2.T(35) := 1106.86 ; # 1421
1424 PLANT.PIPEC2.T(36) := 1111.2 ; # 1422
1425 PLANT.PIPEC2.T(37) := 1115.31 ; # 1423
1426 PLANT.PIPEC2.T(38) := 1119.19 ; # 1424
1427 PLANT.PIPEC2.T(39) := 1122.86 ; # 1425
1428 PLANT.PIPEC2.T(40) := 1126.32 ; # 1426
1429 PLANT.PIPEC2.TEXTRNL(1) := 712.554 ; # 1427
1430 PLANT.PIPEC2.TEXTRNL(2) := 738.563 ; # 1428
1431 PLANT.PIPEC2.TEXTRNL(3) := 763.15 ; # 1429
1432 PLANT.PIPEC2.TEXTRNL(4) := 786.385 ; # 1430
1433 PLANT.PIPEC2.TEXTRNL(5) := 808.344 ; # 1431
1434 PLANT.PIPEC2.TEXTRNL(6) := 829.095 ; # 1432
1435 PLANT.PIPEC2.TEXTRNL(7) := 848.706 ; # 1433
1436 PLANT.PIPEC2.TEXTRNL(8) := 867.239 ; # 1434
1437 PLANT.PIPEC2.TEXTRNL(9) := 884.754 ; # 1435
1438 PLANT.PIPEC2.TEXTRNL(10) := 901.306 ; # 1436
1439 PLANT.PIPEC2.TEXTRNL(11) := 916.948 ; # 1437
1440 PLANT.PIPEC2.TEXTRNL(12) := 931.731 ; # 1438
1441 PLANT.PIPEC2.TEXTRNL(13) := 945.701 ; # 1439
1442 PLANT.PIPEC2.TEXTRNL(14) := 958.903 ; # 1440
1443 PLANT.PIPEC2.TEXTRNL(15) := 971.38 ; # 1441
1444 PLANT.PIPEC2.TEXTRNL(16) := 983.171 ; # 1442
1445 PLANT.PIPEC2.TEXTRNL(17) := 994.314 ; # 1443
1446 PLANT.PIPEC2.TEXTRNL(18) := 1004.84 ; # 1444
1447 PLANT.PIPEC2.TEXTRNL(19) := 1014.8 ; # 1445
1448 PLANT.PIPEC2.TEXTRNL(20) := 1024.2 ; # 1446
1449 PLANT.PIPEC2.TEXTRNL(21) := 1033.09 ; # 1447
1450 PLANT.PIPEC2.TEXTRNL(22) := 1041.49 ; # 1448
1451 PLANT.PIPEC2.TEXTRNL(23) := 1049.43 ; # 1449
1452 PLANT.PIPEC2.TEXTRNL(24) := 1056.93 ; # 1450
1453 PLANT.PIPEC2.TEXTRNL(25) := 1064.02 ; # 1451
1454 PLANT.PIPEC2.TEXTRNL(26) := 1070.72 ; # 1452
1455 PLANT.PIPEC2.TEXTRNL(27) := 1077.05 ; # 1453
1456 PLANT.PIPEC2.TEXTRNL(28) := 1083.03 ; # 1454
1457 PLANT.PIPEC2.TEXTRNL(29) := 1088.69 ; # 1455
1458 PLANT.PIPEC2.TEXTRNL(30) := 1094.03 ; # 1456
1459 PLANT.PIPEC2.TEXTRNL(31) := 1099.08 ; # 1457
1460 PLANT.PIPEC2.TEXTRNL(32) := 1103.85 ; # 1458
1461 PLANT.PIPEC2.TEXTRNL(33) := 1108.36 ; # 1459
1462 PLANT.PIPEC2.TEXTRNL(34) := 1112.63 ; # 1460
1463 PLANT.PIPEC2.TEXTRNL(35) := 1116.65 ; # 1461
1464 PLANT.PIPEC2.TEXTRNL(36) := 1120.46 ; # 1462
1465 PLANT.PIPEC2.TEXTRNL(37) := 1124.06 ; # 1463
1466 PLANT.PIPEC2.TEXTRNL(38) := 1127.46 ; # 1464
1467 PLANT.PIPEC2.TEXTRNL(39) := 1130.67 ; # 1465
1468 PLANT.PIPEC2.TEXTRNL(40) := 1133.71 ; # 1466
1469 PLANT.PIPEC2.F(1) := 43.3743 ; # 1467
1470 PLANT.PIPEC2.F(2) := 43.3743 ; # 1468
1471 PLANT.PIPEC2.F(3) := 43.3743 ; # 1469
1472 PLANT.PIPEC2.F(4) := 43.3743 ; # 1470
1473 PLANT.PIPEC2.F(5) := 43.3743 ; # 1471
1474 PLANT.PIPEC2.F(6) := 43.3743 ; # 1472
1475 PLANT.PIPEC2.F(7) := 43.3743 ; # 1473
1476 PLANT.PIPEC2.F(8) := 43.3743 ; # 1474
1477 PLANT.PIPEC2.F(9) := 43.3743 ; # 1475
1478 PLANT.PIPEC2.F(10) := 43.3743 ; # 1476
1479 PLANT.PIPEC2.F(11) := 43.3743 ; # 1477
1480 PLANT.PIPEC2.F(12) := 43.3743 ; # 1478
1481 PLANT.PIPEC2.F(13) := 43.3743 ; # 1479
1482 PLANT.PIPEC2.F(14) := 43.3743 ; # 1480
1483 PLANT.PIPEC2.F(15) := 43.3743 ; # 1481
1484 PLANT.PIPEC2.F(16) := 43.3743 ; # 1482
1485 PLANT.PIPEC2.F(17) := 43.3743 ; # 1483
1486 PLANT.PIPEC2.F(18) := 43.3743 ; # 1484
1487 PLANT.PIPEC2.F(19) := 43.3743 ; # 1485
1488 PLANT.PIPEC2.F(20) := 43.3743 ; # 1486
1489 PLANT.PIPEC2.F(21) := 43.3743 ; # 1487
1490 PLANT.PIPEC2.F(22) := 43.3743 ; # 1488
1491 PLANT.PIPEC2.F(23) := 43.3743 ; # 1489
1492 PLANT.PIPEC2.F(24) := 43.3743 ; # 1490
1493 PLANT.PIPEC2.F(25) := 43.3743 ; # 1491
1494 PLANT.PIPEC2.F(26) := 43.3743 ; # 1492
1495 PLANT.PIPEC2.F(27) := 43.3743 ; # 1493
1496 PLANT.PIPEC2.F(28) := 43.3743 ; # 1494
1497 PLANT.PIPEC2.F(29) := 43.3743 ; # 1495
1498 PLANT.PIPEC2.F(30) := 43.3743 ; # 1496
1499 PLANT.PIPEC2.F(31) := 43.3743 ; # 1497
1500 PLANT.PIPEC2.F(32) := 43.3743 ; # 1498
1501 PLANT.PIPEC2.F(33) := 43.3743 ; # 1499
1502 PLANT.PIPEC2.F(34) := 43.3743 ; # 1500
1503 PLANT.PIPEC2.F(35) := 43.3743 ; # 1501
1504 PLANT.PIPEC2.F(36) := 43.3743 ; # 1502
1505 PLANT.PIPEC2.F(37) := 43.3743 ; # 1503
1506 PLANT.PIPEC2.F(38) := 43.3743 ; # 1504
1507 PLANT.PIPEC2.F(39) := 43.3743 ; # 1505
1508 PLANT.PIPEC2.F(40) := 43.3743 ; # 1506

```

1509 PLANT.PIPEC2.F_IN := 43.3743 ; # 1507
1510 PLANT.PIPEC2.PSI(1) := 1.81063e+006 ; # 1508
1511 PLANT.PIPEC2.PSI(2) := 1.91725e+006 ; # 1509
1512 PLANT.PIPEC2.PSI(3) := 2.00881e+006 ; # 1510
1513 PLANT.PIPEC2.PSI(4) := 2.08797e+006 ; # 1511
1514 PLANT.PIPEC2.PSI(5) := 2.1568e+006 ; # 1512
1515 PLANT.PIPEC2.PSI(6) := 2.21692e+006 ; # 1513
1516 PLANT.PIPEC2.PSI(7) := 2.26963e+006 ; # 1514
1517 PLANT.PIPEC2.PSI(8) := 2.31599e+006 ; # 1515
1518 PLANT.PIPEC2.PSI(9) := 2.35686e+006 ; # 1516
1519 PLANT.PIPEC2.PSI(10) := 2.39296e+006 ; # 1517
1520 PLANT.PIPEC2.PSI(11) := 2.42488e+006 ; # 1518
1521 PLANT.PIPEC2.PSI(12) := 2.45312e+006 ; # 1519
1522 PLANT.PIPEC2.PSI(13) := 2.47811e+006 ; # 1520
1523 PLANT.PIPEC2.PSI(14) := 2.50021e+006 ; # 1521
1524 PLANT.PIPEC2.PSI(15) := 2.51973e+006 ; # 1522
1525 PLANT.PIPEC2.PSI(16) := 2.53693e+006 ; # 1523
1526 PLANT.PIPEC2.PSI(17) := 2.55205e+006 ; # 1524
1527 PLANT.PIPEC2.PSI(18) := 2.5653e+006 ; # 1525
1528 PLANT.PIPEC2.PSI(19) := 2.57684e+006 ; # 1526
1529 PLANT.PIPEC2.PSI(20) := 2.58684e+006 ; # 1527
1530 PLANT.PIPEC2.PSI(21) := 2.59544e+006 ; # 1528
1531 PLANT.PIPEC2.PSI(22) := 2.60275e+006 ; # 1529
1532 PLANT.PIPEC2.PSI(23) := 2.60889e+006 ; # 1530
1533 PLANT.PIPEC2.PSI(24) := 2.61395e+006 ; # 1531
1534 PLANT.PIPEC2.PSI(25) := 2.61803e+006 ; # 1532
1535 PLANT.PIPEC2.PSI(26) := 2.62119e+006 ; # 1533
1536 PLANT.PIPEC2.PSI(27) := 2.62352e+006 ; # 1534
1537 PLANT.PIPEC2.PSI(28) := 2.62507e+006 ; # 1535
1538 PLANT.PIPEC2.PSI(29) := 2.62591e+006 ; # 1536
1539 PLANT.PIPEC2.PSI(30) := 2.62607e+006 ; # 1537
1540 PLANT.PIPEC2.PSI(31) := 2.62562e+006 ; # 1538
1541 PLANT.PIPEC2.PSI(32) := 2.6246e+006 ; # 1539
1542 PLANT.PIPEC2.PSI(33) := 2.62304e+006 ; # 1540
1543 PLANT.PIPEC2.PSI(34) := 2.62099e+006 ; # 1541
1544 PLANT.PIPEC2.PSI(35) := 2.61847e+006 ; # 1542
1545 PLANT.PIPEC2.PSI(36) := 2.61551e+006 ; # 1543
1546 PLANT.PIPEC2.PSI(37) := 2.61215e+006 ; # 1544
1547 PLANT.PIPEC2.PSI(38) := 2.6084e+006 ; # 1545
1548 PLANT.PIPEC2.PSI(39) := 2.6043e+006 ; # 1546
1549 PLANT.PIPEC2.PSI(40) := 2.59986e+006 ; # 1547
1550 PLANT.PIPEC2.HT.RHOPIPEHE := 2.35217 ; # 1548
1551 PLANT.PIPEC2.HT.VPIPE := 65.6203 ; # 1549
1552 PLANT.PIPEC2.HT.U := 1880.53 ; # 1550

```

HTLQSS_SS_IN_INI.INITIAL

```

1 # Values for differential variables in computation HTLFULLDYN_SS
2 # Saved at time 1000
3 PLANT.HX.TH(1) = 889.835 ; # 1
4 PLANT.HX.TH(2) = 900.086 ; # 2
5 PLANT.HX.TH(3) = 910.162 ; # 3
6 PLANT.HX.TH(4) = 920.011 ; # 4
7 PLANT.HX.TH(5) = 929.638 ; # 5
8 PLANT.HX.TH(6) = 939.048 ; # 6
9 PLANT.HX.TH(7) = 948.245 ; # 7
10 PLANT.HX.TH(8) = 957.235 ; # 8
11 PLANT.HX.TH(9) = 966.021 ; # 9
12 PLANT.HX.TH(10) = 974.61 ; # 10
13 PLANT.HX.TH(11) = 983.004 ; # 11
14 PLANT.HX.TH(12) = 991.209 ; # 12
15 PLANT.HX.TH(13) = 999.229 ; # 13
16 PLANT.HX.TH(14) = 1007.07 ; # 14
17 PLANT.HX.TH(15) = 1014.73 ; # 15
18 PLANT.HX.TH(16) = 1022.22 ; # 16
19 PLANT.HX.TH(17) = 1029.54 ; # 17
20 PLANT.HX.TH(18) = 1036.69 ; # 18
21 PLANT.HX.TH(19) = 1043.69 ; # 19
22 PLANT.HX.TH(20) = 1050.52 ; # 20
23 PLANT.HX.TH(21) = 1057.2 ; # 21
24 PLANT.HX.TH(22) = 1063.73 ; # 22
25 PLANT.HX.TH(23) = 1070.12 ; # 23
26 PLANT.HX.TH(24) = 1076.36 ; # 24
27 PLANT.HX.TH(25) = 1082.45 ; # 25
28 PLANT.HX.TH(26) = 1088.41 ; # 26
29 PLANT.HX.TH(27) = 1094.24 ; # 27
30 PLANT.HX.TH(28) = 1099.93 ; # 28
31 PLANT.HX.TH(29) = 1105.5 ; # 29
32 PLANT.HX.TH(30) = 1110.94 ; # 30
33 PLANT.HX.TH(31) = 1116.26 ; # 31
34 PLANT.HX.TH(32) = 1121.45 ; # 32
35 PLANT.HX.TH(33) = 1126.53 ; # 33
36 PLANT.HX.TH(34) = 1131.5 ; # 34

```


37 PLANT.HX.THX(35) = 1136.35 ; # 35
38 PLANT.HX.THX(36) = 1141.1 ; # 36
39 PLANT.HX.THX(37) = 1145.73 ; # 37
40 PLANT.HX.THX(38) = 1150.27 ; # 38
41 PLANT.HX.THX(39) = 1154.7 ; # 39
42 PLANT.HX.THX(40) = 1159 ; # 40
43 PLANT.LOOP1.PSIEXTRA(1) = 1.28551e+006 ; # 141
44 PLANT.LOOP1.PSIEXTRA(2) = 1.28551e+006 ; # 141
45 PLANT.LOOP1.PSI(1) = 1.28551e+006 ; # 141
46 PLANT.LOOP1.PSI(2) = 1.27902e+006 ; # 142
47 PLANT.LOOP1.PSI(3) = 1.27441e+006 ; # 143
48 PLANT.LOOP1.PSI(4) = 1.26979e+006 ; # 144
49 PLANT.LOOP1.PSI(5) = 1.26517e+006 ; # 145
50 PLANT.LOOP1.PSI(6) = 1.26054e+006 ; # 146
51 PLANT.LOOP1.PSI(7) = 1.25591e+006 ; # 147
52 PLANT.LOOP1.PSI(8) = 1.25127e+006 ; # 148
53 PLANT.LOOP1.PSI(9) = 1.24663e+006 ; # 149
54 PLANT.LOOP1.PSI(10) = 1.24198e+006 ; # 150
55 PLANT.LOOP1.PSI(11) = 1.23734e+006 ; # 151
56 PLANT.LOOP1.PSI(12) = 1.23270e+006 ; # 152
57 PLANT.LOOP1.PSI(13) = 1.22806e+006 ; # 153
58 PLANT.LOOP1.PSI(14) = 1.22342e+006 ; # 154
59 PLANT.LOOP1.PSI(15) = 1.21878e+006 ; # 155
60 PLANT.LOOP1.PSI(16) = 1.21414e+006 ; # 156
61 PLANT.LOOP1.PSI(17) = 1.20950e+006 ; # 157
62 PLANT.LOOP1.PSI(18) = 1.20486e+006 ; # 158
63 PLANT.LOOP1.PSI(19) = 1.20022e+006 ; # 159
64 PLANT.LOOP1.PSI(20) = 1.19558e+006 ; # 160
65 PLANT.LOOP1.PSI(21) = 1.19094e+006 ; # 161
66 PLANT.LOOP1.PSI(22) = 1.18630e+006 ; # 162
67 PLANT.LOOP1.PSI(23) = 1.18166e+006 ; # 163
68 PLANT.LOOP1.PSI(24) = 1.17702e+006 ; # 164
69 PLANT.LOOP1.PSI(25) = 1.17238e+006 ; # 165
70 PLANT.LOOP1.PSI(26) = 1.16774e+006 ; # 166
71 PLANT.LOOP1.PSI(27) = 1.16310e+006 ; # 167
72 PLANT.LOOP1.PSI(28) = 1.15846e+006 ; # 168
73 PLANT.LOOP1.PSI(29) = 1.15382e+006 ; # 169
74 PLANT.LOOP1.PSI(30) = 1.14918e+006 ; # 170
75 PLANT.LOOP1.PSI(31) = 1.14454e+006 ; # 171
76 PLANT.LOOP1.PSI(32) = 1.13990e+006 ; # 172
77 PLANT.LOOP1.PSI(33) = 1.13526e+006 ; # 173
78 PLANT.LOOP1.PSI(34) = 1.13062e+006 ; # 174
79 PLANT.LOOP1.PSI(35) = 1.12598e+006 ; # 175
80 PLANT.LOOP1.PSI(36) = 1.12134e+006 ; # 176
81 PLANT.LOOP1.PSI(37) = 1.11670e+006 ; # 177
82 PLANT.LOOP1.PSI(38) = 1.11206e+006 ; # 178
83 PLANT.LOOP1.PSI(39) = 1.10742e+006 ; # 179
84 PLANT.LOOP1.PSI(40) = 1.10278e+006 ; # 180
85 PLANT.LOOP1.PSI(41) = 1.09814e+006 ; # 181
86 PLANT.LOOP1.PSI(42) = 1.09350e+006 ; # 182
87 PLANT.LOOP1.PSI(43) = 1.08886e+006 ; # 183
88 PLANT.LOOP1.PSI(44) = 1.08422e+006 ; # 184
89 PLANT.LOOP1.PSI(45) = 1.07958e+006 ; # 185
90 PLANT.LOOP1.PSI(46) = 1.07494e+006 ; # 186
91 PLANT.LOOP1.PSI(47) = 1.07030e+006 ; # 187
92 PLANT.LOOP1.PSI(48) = 1.06566e+006 ; # 188
93 PLANT.LOOP1.PSI(49) = 1.06102e+006 ; # 189
94 PLANT.LOOP1.PSI(50) = 1.05638e+006 ; # 190
95 PLANT.LOOP1.PSI(51) = 1.05174e+006 ; # 191
96 PLANT.LOOP1.PSI(52) = 1.04710e+006 ; # 192
97 PLANT.LOOP1.PSI(53) = 1.04246e+006 ; # 193
98 PLANT.LOOP1.PSI(54) = 1.03782e+006 ; # 194
99 PLANT.LOOP1.PSI(55) = 1.03318e+006 ; # 195
100 PLANT.LOOP1.PSI(56) = 1.02854e+006 ; # 196
101 PLANT.LOOP1.PSI(57) = 1.02390e+006 ; # 197
102 PLANT.LOOP1.PSI(58) = 1.01926e+006 ; # 198
103 PLANT.LOOP1.PSI(59) = 1.01462e+006 ; # 199
104 PLANT.LOOP1.PSI(60) = 1.01000e+006 ; # 200
105 PLANT.LOOP1.PSI(61) = 1.00536e+006 ; # 201
106 PLANT.LOOP1.PSI(62) = 1.00072e+006 ; # 202
107 PLANT.LOOP1.PSI(63) = 0.99608e+006 ; # 203
108 PLANT.LOOP1.PSI(64) = 0.99144e+006 ; # 204
109 PLANT.LOOP1.PSI(65) = 0.98680e+006 ; # 205
110 PLANT.LOOP1.PSI(66) = 0.98216e+006 ; # 206
111 PLANT.LOOP1.PSI(67) = 0.97752e+006 ; # 207
112 PLANT.LOOP1.PSI(68) = 0.97288e+006 ; # 208
113 PLANT.LOOP1.PSI(69) = 0.96824e+006 ; # 209
114 PLANT.LOOP1.PSI(70) = 0.96360e+006 ; # 210
115 PLANT.LOOP1.PSI(71) = 0.95896e+006 ; # 211
116 PLANT.LOOP1.PSI(72) = 0.95432e+006 ; # 212
117 PLANT.LOOP1.PSI(73) = 0.94968e+006 ; # 213
118 PLANT.LOOP1.PSI(74) = 0.94504e+006 ; # 214
119 PLANT.LOOP1.PSI(75) = 0.94040e+006 ; # 215
120 PLANT.LOOP1.PSI(76) = 0.93576e+006 ; # 216
121 PLANT.LOOP1.PSI(77) = 0.93112e+006 ; # 217
122 PLANT.LOOP1.PSI(78) = 0.92648e+006 ; # 218
123 PLANT.LOOP1.PSI(79) = 0.92184e+006 ; # 219
124 PLANT.LOOP1.PSI(80) = 0.91720e+006 ; # 220
125 PLANT.LOOP1.PSI(81) = 0.91256e+006 ; # 221
126 PLANT.LOOP1.PSI(82) = 0.90792e+006 ; # 222
127 PLANT.LOOP1.PSI(83) = 0.90328e+006 ; # 223
128 PLANT.LOOP1.PSI(84) = 0.89864e+006 ; # 224

129 PLANT.LOOP1.PSI(85) = 1.36326e+006 ; # 225
130 PLANT.LOOP1.PSI(86) = 1.35062e+006 ; # 226
131 PLANT.LOOP1.PSI(87) = 1.33702e+006 ; # 227
132 PLANT.LOOP1.PSI(88) = 1.32234e+006 ; # 228
133 PLANT.LOOP1.PSI(89) = 1.30649e+006 ; # 229
134 PLANT.LOOP1.PSI(90) = 1.28931e+006 ; # 230
135 PLANT.LOOP1.PSI(91) = 1.27066e+006 ; # 231
136 PLANT.LOOP1.PSI(92) = 1.25037e+006 ; # 232
137 PLANT.LOOP1.PSI(93) = 1.22822e+006 ; # 233
138 PLANT.LOOP1.PSI(94) = 1.20397e+006 ; # 234
139 PLANT.LOOP1.PSI(95) = 1.17735e+006 ; # 235
140 PLANT.LOOP1.PSI(96) = 1.14802e+006 ; # 236
141 PLANT.LOOP1.PSI(97) = 1.11558e+006 ; # 237
142 PLANT.LOOP1.PSI(98) = 1.07957e+006 ; # 238
143 PLANT.LOOP1.PSI(99) = 1.03941e+006 ; # 239
144 PLANT.LOOP1.PSI(100) = 994398 ; # 240
145 PLANT.PIPEH.RHO(1) = 2.88031 ; # 341
146 PLANT.PIPEH.RHO(2) = 2.88987 ; # 342
147 PLANT.PIPEH.RHO(3) = 2.89973 ; # 343
148 PLANT.PIPEH.RHO(4) = 2.90991 ; # 344
149 PLANT.PIPEH.RHO(5) = 2.92042 ; # 345
150 PLANT.PIPEH.RHO(6) = 2.93127 ; # 346
151 PLANT.PIPEH.RHO(7) = 2.94248 ; # 347
152 PLANT.PIPEH.RHO(8) = 2.95405 ; # 348
153 PLANT.PIPEH.RHO(9) = 2.96601 ; # 349
154 PLANT.PIPEH.RHO(10) = 2.97836 ; # 350
155 PLANT.PIPEH.RHO(11) = 2.99112 ; # 351
156 PLANT.PIPEH.RHO(12) = 3.00432 ; # 352
157 PLANT.PIPEH.RHO(13) = 3.01796 ; # 353
158 PLANT.PIPEH.RHO(14) = 3.03206 ; # 354
159 PLANT.PIPEH.RHO(15) = 3.04666 ; # 355
160 PLANT.PIPEH.RHO(16) = 3.06175 ; # 356
161 PLANT.PIPEH.RHO(17) = 3.07737 ; # 357
162 PLANT.PIPEH.RHO(18) = 3.09354 ; # 358
163 PLANT.PIPEH.RHO(19) = 3.11029 ; # 359
164 PLANT.PIPEH.RHO(20) = 3.12763 ; # 360
165 PLANT.PIPEH.RHO(21) = 3.1456 ; # 361
166 PLANT.PIPEH.RHO(22) = 3.16422 ; # 362
167 PLANT.PIPEH.RHO(23) = 3.18352 ; # 363
168 PLANT.PIPEH.RHO(24) = 3.20354 ; # 364
169 PLANT.PIPEH.RHO(25) = 3.22431 ; # 365
170 PLANT.PIPEH.RHO(26) = 3.24587 ; # 366
171 PLANT.PIPEH.RHO(27) = 3.26824 ; # 367
172 PLANT.PIPEH.RHO(28) = 3.29149 ; # 368
173 PLANT.PIPEH.RHO(29) = 3.31563 ; # 369
174 PLANT.PIPEH.RHO(30) = 3.34074 ; # 370
175 PLANT.PIPEH.RHO(31) = 3.36684 ; # 371
176 PLANT.PIPEH.RHO(32) = 3.394 ; # 372
177 PLANT.PIPEH.RHO(33) = 3.42228 ; # 373
178 PLANT.PIPEH.RHO(34) = 3.45173 ; # 374
179 PLANT.PIPEH.RHO(35) = 3.48241 ; # 375
180 PLANT.PIPEH.RHO(36) = 3.5144 ; # 376
181 PLANT.PIPEH.RHO(37) = 3.54778 ; # 377
182 PLANT.PIPEH.RHO(38) = 3.58262 ; # 378
183 PLANT.PIPEH.RHO(39) = 3.61901 ; # 379
184 PLANT.PIPEH.RHO(40) = 3.65698 ; # 380
185 PLANT.PIPEH.F(1) = 32.4687 ; # 381
186 PLANT.PIPEH.F(2) = 32.4687 ; # 382
187 PLANT.PIPEH.F(3) = 32.4687 ; # 383
188 PLANT.PIPEH.F(4) = 32.4687 ; # 384
189 PLANT.PIPEH.F(5) = 32.4687 ; # 385
190 PLANT.PIPEH.F(6) = 32.4687 ; # 386
191 PLANT.PIPEH.F(7) = 32.4687 ; # 387
192 PLANT.PIPEH.F(8) = 32.4687 ; # 388
193 PLANT.PIPEH.F(9) = 32.4687 ; # 389
194 PLANT.PIPEH.F(10) = 32.4687 ; # 390
195 PLANT.PIPEH.F(11) = 32.4687 ; # 391
196 PLANT.PIPEH.F(12) = 32.4687 ; # 392
197 PLANT.PIPEH.F(13) = 32.4687 ; # 393
198 PLANT.PIPEH.F(14) = 32.4687 ; # 394
199 PLANT.PIPEH.F(15) = 32.4687 ; # 395
200 PLANT.PIPEH.F(16) = 32.4687 ; # 396
201 PLANT.PIPEH.F(17) = 32.4687 ; # 397
202 PLANT.PIPEH.F(18) = 32.4687 ; # 398
203 PLANT.PIPEH.F(19) = 32.4687 ; # 399
204 PLANT.PIPEH.F(20) = 32.4687 ; # 400
205 PLANT.PIPEH.F(21) = 32.4687 ; # 401
206 PLANT.PIPEH.F(22) = 32.4687 ; # 402
207 PLANT.PIPEH.F(23) = 32.4687 ; # 403
208 PLANT.PIPEH.F(24) = 32.4687 ; # 404
209 PLANT.PIPEH.F(25) = 32.4687 ; # 405
210 PLANT.PIPEH.F(26) = 32.4687 ; # 406
211 PLANT.PIPEH.F(27) = 32.4687 ; # 407
212 PLANT.PIPEH.F(28) = 32.4687 ; # 408
213 PLANT.PIPEH.F(29) = 32.4687 ; # 409
214 PLANT.PIPEH.F(30) = 32.4687 ; # 410
215 PLANT.PIPEH.F(31) = 32.4687 ; # 411
216 PLANT.PIPEH.F(32) = 32.4687 ; # 412
217 PLANT.PIPEH.F(33) = 32.4687 ; # 413
218 PLANT.PIPEH.F(34) = 32.4687 ; # 414
219 PLANT.PIPEH.F(35) = 32.4687 ; # 415
220 PLANT.PIPEH.F(36) = 32.4687 ; # 416

221 PLANT.PIPEH.F(37) = 32.4687 ; # 417
222 PLANT.PIPEH.F(38) = 32.4687 ; # 418
223 PLANT.PIPEH.F(39) = 32.4687 ; # 419
224 PLANT.PIPEH.F(40) = 32.4687 ; # 420
225 PLANT.PIPEH.F_IN = 32.4687 ; # 421
226 PLANT.PIPEH.PSI(1) = 6.03571e+006 ; # 422
227 PLANT.PIPEH.PSI(2) = 6.01884e+006 ; # 423
228 PLANT.PIPEH.PSI(3) = 6.00151e+006 ; # 424
229 PLANT.PIPEH.PSI(4) = 5.9837e+006 ; # 425
230 PLANT.PIPEH.PSI(5) = 5.96538e+006 ; # 426
231 PLANT.PIPEH.PSI(6) = 5.94655e+006 ; # 427
232 PLANT.PIPEH.PSI(7) = 5.92717e+006 ; # 428
233 PLANT.PIPEH.PSI(8) = 5.90723e+006 ; # 429
234 PLANT.PIPEH.PSI(9) = 5.88672e+006 ; # 430
235 PLANT.PIPEH.PSI(10) = 5.86559e+006 ; # 431
236 PLANT.PIPEH.PSI(11) = 5.84383e+006 ; # 432
237 PLANT.PIPEH.PSI(12) = 5.82142e+006 ; # 433
238 PLANT.PIPEH.PSI(13) = 5.79833e+006 ; # 434
239 PLANT.PIPEH.PSI(14) = 5.77452e+006 ; # 435
240 PLANT.PIPEH.PSI(15) = 5.74998e+006 ; # 436
241 PLANT.PIPEH.PSI(16) = 5.72466e+006 ; # 437
242 PLANT.PIPEH.PSI(17) = 5.69854e+006 ; # 438
243 PLANT.PIPEH.PSI(18) = 5.67158e+006 ; # 439
244 PLANT.PIPEH.PSI(19) = 5.64374e+006 ; # 440
245 PLANT.PIPEH.PSI(20) = 5.61499e+006 ; # 441
246 PLANT.PIPEH.PSI(21) = 5.58528e+006 ; # 442
247 PLANT.PIPEH.PSI(22) = 5.55457e+006 ; # 443
248 PLANT.PIPEH.PSI(23) = 5.52282e+006 ; # 444
249 PLANT.PIPEH.PSI(24) = 5.48997e+006 ; # 445
250 PLANT.PIPEH.PSI(25) = 5.45597e+006 ; # 446
251 PLANT.PIPEH.PSI(26) = 5.42078e+006 ; # 447
252 PLANT.PIPEH.PSI(27) = 5.38432e+006 ; # 448
253 PLANT.PIPEH.PSI(28) = 5.34653e+006 ; # 449
254 PLANT.PIPEH.PSI(29) = 5.30735e+006 ; # 450
255 PLANT.PIPEH.PSI(30) = 5.26672e+006 ; # 451
256 PLANT.PIPEH.PSI(31) = 5.22454e+006 ; # 452
257 PLANT.PIPEH.PSI(32) = 5.18075e+006 ; # 453
258 PLANT.PIPEH.PSI(33) = 5.13524e+006 ; # 454
259 PLANT.PIPEH.PSI(34) = 5.08794e+006 ; # 455
260 PLANT.PIPEH.PSI(35) = 5.03874e+006 ; # 456
261 PLANT.PIPEH.PSI(36) = 4.98752e+006 ; # 457
262 PLANT.PIPEH.PSI(37) = 4.93419e+006 ; # 458
263 PLANT.PIPEH.PSI(38) = 4.8786e+006 ; # 459
264 PLANT.PIPEH.PSI(39) = 4.82064e+006 ; # 460
265 PLANT.PIPEH.PSI(40) = 4.76024e+006 ; # 461
266 PLANT.HX2.THX(1) = 1132.12 ; # 462
267 PLANT.HX2.THX(2) = 1129.7 ; # 463
268 PLANT.HX2.THX(3) = 1127.12 ; # 464
269 PLANT.HX2.THX(4) = 1124.36 ; # 465
270 PLANT.HX2.THX(5) = 1121.43 ; # 466
271 PLANT.HX2.THX(6) = 1118.29 ; # 467
272 PLANT.HX2.THX(7) = 1114.96 ; # 468
273 PLANT.HX2.THX(8) = 1111.4 ; # 469
274 PLANT.HX2.THX(9) = 1107.6 ; # 470
275 PLANT.HX2.THX(10) = 1103.55 ; # 471
276 PLANT.HX2.THX(11) = 1099.23 ; # 472
277 PLANT.HX2.THX(12) = 1094.63 ; # 473
278 PLANT.HX2.THX(13) = 1089.72 ; # 474
279 PLANT.HX2.THX(14) = 1084.49 ; # 475
280 PLANT.HX2.THX(15) = 1078.91 ; # 476
281 PLANT.HX2.THX(16) = 1072.96 ; # 477
282 PLANT.HX2.THX(17) = 1066.61 ; # 478
283 PLANT.HX2.THX(18) = 1059.84 ; # 479
284 PLANT.HX2.THX(19) = 1052.63 ; # 480
285 PLANT.HX2.THX(20) = 1044.93 ; # 481
286 PLANT.HX2.THX(21) = 1036.73 ; # 482
287 PLANT.HX2.THX(22) = 1027.98 ; # 483
288 PLANT.HX2.THX(23) = 1018.65 ; # 484
289 PLANT.HX2.THX(24) = 1008.7 ; # 485
290 PLANT.HX2.THX(25) = 998.095 ; # 486
291 PLANT.HX2.THX(26) = 986.784 ; # 487
292 PLANT.HX2.THX(27) = 974.722 ; # 488
293 PLANT.HX2.THX(28) = 961.86 ; # 489
294 PLANT.HX2.THX(29) = 948.145 ; # 490
295 PLANT.HX2.THX(30) = 933.521 ; # 491
296 PLANT.HX2.THX(31) = 917.926 ; # 492
297 PLANT.HX2.THX(32) = 901.297 ; # 493
298 PLANT.HX2.THX(33) = 883.565 ; # 494
299 PLANT.HX2.THX(34) = 864.657 ; # 495
300 PLANT.HX2.THX(35) = 844.495 ; # 496
301 PLANT.HX2.THX(36) = 822.996 ; # 497
302 PLANT.HX2.THX(37) = 800.07 ; # 498
303 PLANT.HX2.THX(38) = 775.624 ; # 499
304 PLANT.HX2.THX(39) = 749.557 ; # 500
305 PLANT.HX2.THX(40) = 721.768 ; # 501
306 PLANT.PIPEC2.RHO(1) = 3.7063 ; # 502
307 PLANT.PIPEC2.RHO(2) = 3.52381 ; # 503
308 PLANT.PIPEC2.RHO(3) = 3.36718 ; # 504
309 PLANT.PIPEC2.RHO(4) = 3.2314 ; # 505
310 PLANT.PIPEC2.RHO(5) = 3.11269 ; # 506
311 PLANT.PIPEC2.RHO(6) = 3.0081 ; # 507
312 PLANT.PIPEC2.RHO(7) = 2.91535 ; # 508

313 PLANT.PIPEC2.RHO(8) = 2.83259 ; # 509
314 PLANT.PIPEC2.RHO(9) = 2.75835 ; # 510
315 PLANT.PIPEC2.RHO(10) = 2.69142 ; # 511
316 PLANT.PIPEC2.RHO(11) = 2.63081 ; # 512
317 PLANT.PIPEC2.RHO(12) = 2.5757 ; # 513
318 PLANT.PIPEC2.RHO(13) = 2.52539 ; # 514
319 PLANT.PIPEC2.RHO(14) = 2.47931 ; # 515
320 PLANT.PIPEC2.RHO(15) = 2.43696 ; # 516
321 PLANT.PIPEC2.RHO(16) = 2.39791 ; # 517
322 PLANT.PIPEC2.RHO(17) = 2.3618 ; # 518
323 PLANT.PIPEC2.RHO(18) = 2.32832 ; # 519
324 PLANT.PIPEC2.RHO(19) = 2.29719 ; # 520
325 PLANT.PIPEC2.RHO(20) = 2.26818 ; # 521
326 PLANT.PIPEC2.RHO(21) = 2.24106 ; # 522
327 PLANT.PIPEC2.RHO(22) = 2.21566 ; # 523
328 PLANT.PIPEC2.RHO(23) = 2.19182 ; # 524
329 PLANT.PIPEC2.RHO(24) = 2.16939 ; # 525
330 PLANT.PIPEC2.RHO(25) = 2.14823 ; # 526
331 PLANT.PIPEC2.RHO(26) = 2.12824 ; # 527
332 PLANT.PIPEC2.RHO(27) = 2.10932 ; # 528
333 PLANT.PIPEC2.RHO(28) = 2.09136 ; # 529
334 PLANT.PIPEC2.RHO(29) = 2.07429 ; # 530
335 PLANT.PIPEC2.RHO(30) = 2.05802 ; # 531
336 PLANT.PIPEC2.RHO(31) = 2.0425 ; # 532
337 PLANT.PIPEC2.RHO(32) = 2.02766 ; # 533
338 PLANT.PIPEC2.RHO(33) = 2.01345 ; # 534
339 PLANT.PIPEC2.RHO(34) = 1.99981 ; # 535
340 PLANT.PIPEC2.RHO(35) = 1.9867 ; # 536
341 PLANT.PIPEC2.RHO(36) = 1.97407 ; # 537
342 PLANT.PIPEC2.RHO(37) = 1.96189 ; # 538
343 PLANT.PIPEC2.RHO(38) = 1.95011 ; # 539
344 PLANT.PIPEC2.RHO(39) = 1.93872 ; # 540
345 PLANT.PIPEC2.RHO(40) = 1.92768 ; # 541
346 PLANT.PIPEC2.F(1) = 43.1466 ; # 542
347 PLANT.PIPEC2.F(2) = 43.1466 ; # 543
348 PLANT.PIPEC2.F(3) = 43.1466 ; # 544
349 PLANT.PIPEC2.F(4) = 43.1466 ; # 545
350 PLANT.PIPEC2.F(5) = 43.1466 ; # 546
351 PLANT.PIPEC2.F(6) = 43.1466 ; # 547
352 PLANT.PIPEC2.F(7) = 43.1466 ; # 548
353 PLANT.PIPEC2.F(8) = 43.1466 ; # 549
354 PLANT.PIPEC2.F(9) = 43.1466 ; # 550
355 PLANT.PIPEC2.F(10) = 43.1466 ; # 551
356 PLANT.PIPEC2.F(11) = 43.1466 ; # 552
357 PLANT.PIPEC2.F(12) = 43.1466 ; # 553
358 PLANT.PIPEC2.F(13) = 43.1466 ; # 554
359 PLANT.PIPEC2.F(14) = 43.1466 ; # 555
360 PLANT.PIPEC2.F(15) = 43.1466 ; # 556
361 PLANT.PIPEC2.F(16) = 43.1466 ; # 557
362 PLANT.PIPEC2.F(17) = 43.1466 ; # 558
363 PLANT.PIPEC2.F(18) = 43.1466 ; # 559
364 PLANT.PIPEC2.F(19) = 43.1466 ; # 560
365 PLANT.PIPEC2.F(20) = 43.1466 ; # 561
366 PLANT.PIPEC2.F(21) = 43.1466 ; # 562
367 PLANT.PIPEC2.F(22) = 43.1466 ; # 563
368 PLANT.PIPEC2.F(23) = 43.1466 ; # 564
369 PLANT.PIPEC2.F(24) = 43.1466 ; # 565
370 PLANT.PIPEC2.F(25) = 43.1466 ; # 566
371 PLANT.PIPEC2.F(26) = 43.1466 ; # 567
372 PLANT.PIPEC2.F(27) = 43.1466 ; # 568
373 PLANT.PIPEC2.F(28) = 43.1466 ; # 569
374 PLANT.PIPEC2.F(29) = 43.1466 ; # 570
375 PLANT.PIPEC2.F(30) = 43.1466 ; # 571
376 PLANT.PIPEC2.F(31) = 43.1466 ; # 572
377 PLANT.PIPEC2.F(32) = 43.1466 ; # 573
378 PLANT.PIPEC2.F(33) = 43.1466 ; # 574
379 PLANT.PIPEC2.F(34) = 43.1466 ; # 575
380 PLANT.PIPEC2.F(35) = 43.1466 ; # 576
381 PLANT.PIPEC2.F(36) = 43.1466 ; # 577
382 PLANT.PIPEC2.F(37) = 43.1466 ; # 578
383 PLANT.PIPEC2.F(38) = 43.1466 ; # 579
384 PLANT.PIPEC2.F(39) = 43.1466 ; # 580
385 PLANT.PIPEC2.F(40) = 43.1466 ; # 581
386 PLANT.PIPEC2.F_IN = 43.1466 ; # 582
387 PLANT.PIPEC2.PSI(1) = 1.82247e+006 ; # 583
388 PLANT.PIPEC2.PSI(2) = 1.93726e+006 ; # 584
389 PLANT.PIPEC2.PSI(3) = 2.03443e+006 ; # 585
390 PLANT.PIPEC2.PSI(4) = 2.11734e+006 ; # 586
391 PLANT.PIPEC2.PSI(5) = 2.18855e+006 ; # 587
392 PLANT.PIPEC2.PSI(6) = 2.25006e+006 ; # 588
393 PLANT.PIPEC2.PSI(7) = 2.30342e+006 ; # 589
394 PLANT.PIPEC2.PSI(8) = 2.34986e+006 ; # 590
395 PLANT.PIPEC2.PSI(9) = 2.3904e+006 ; # 591
396 PLANT.PIPEC2.PSI(10) = 2.42585e+006 ; # 592
397 PLANT.PIPEC2.PSI(11) = 2.45689e+006 ; # 593
398 PLANT.PIPEC2.PSI(12) = 2.48407e+006 ; # 594
399 PLANT.PIPEC2.PSI(13) = 2.50788e+006 ; # 595
400 PLANT.PIPEC2.PSI(14) = 2.5287e+006 ; # 596
401 PLANT.PIPEC2.PSI(15) = 2.54688e+006 ; # 597
402 PLANT.PIPEC2.PSI(16) = 2.56271e+006 ; # 598
403 PLANT.PIPEC2.PSI(17) = 2.57643e+006 ; # 599
404 PLANT.PIPEC2.PSI(18) = 2.58827e+006 ; # 600

```

405 PLANT.PIPEC2.PSI(19) = 2.59842e+006 ; # 601
406 PLANT.PIPEC2.PSI(20) = 2.60703e+006 ; # 602
407 PLANT.PIPEC2.PSI(21) = 2.61426e+006 ; # 603
408 PLANT.PIPEC2.PSI(22) = 2.62023e+006 ; # 604
409 PLANT.PIPEC2.PSI(23) = 2.62506e+006 ; # 605
410 PLANT.PIPEC2.PSI(24) = 2.62884e+006 ; # 606
411 PLANT.PIPEC2.PSI(25) = 2.63167e+006 ; # 607
412 PLANT.PIPEC2.PSI(26) = 2.63363e+006 ; # 608
413 PLANT.PIPEC2.PSI(27) = 2.63479e+006 ; # 609
414 PLANT.PIPEC2.PSI(28) = 2.63522e+006 ; # 610
415 PLANT.PIPEC2.PSI(29) = 2.63496e+006 ; # 611
416 PLANT.PIPEC2.PSI(30) = 2.63409e+006 ; # 612
417 PLANT.PIPEC2.PSI(31) = 2.63263e+006 ; # 613
418 PLANT.PIPEC2.PSI(32) = 2.63064e+006 ; # 614
419 PLANT.PIPEC2.PSI(33) = 2.62816e+006 ; # 615
420 PLANT.PIPEC2.PSI(34) = 2.62522e+006 ; # 616
421 PLANT.PIPEC2.PSI(35) = 2.62186e+006 ; # 617
422 PLANT.PIPEC2.PSI(36) = 2.6181e+006 ; # 618
423 PLANT.PIPEC2.PSI(37) = 2.61397e+006 ; # 619
424 PLANT.PIPEC2.PSI(38) = 2.6095e+006 ; # 620
425 PLANT.PIPEC2.PSI(39) = 2.60471e+006 ; # 621
426 PLANT.PIPEC2.PSI(40) = 2.59962e+006 ; # 622

```

HTLQSS_SS_IN_PRE.PRESETS

```

1 # Values for computation HTLFULLDYN_SS
2 # Saved at time 1000
3 PLANT.HX.TGASHOT(1) := 914.423 ; # 1
4 PLANT.HX.TGASHOT(2) := 924.159 ; # 2
5 PLANT.HX.TGASHOT(3) := 933.692 ; # 3
6 PLANT.HX.TGASHOT(4) := 943.011 ; # 4
7 PLANT.HX.TGASHOT(5) := 952.118 ; # 5
8 PLANT.HX.TGASHOT(6) := 961.02 ; # 6
9 PLANT.HX.TGASHOT(7) := 969.722 ; # 7
10 PLANT.HX.TGASHOT(8) := 978.227 ; # 8
11 PLANT.HX.TGASHOT(9) := 986.539 ; # 9
12 PLANT.HX.TGASHOT(10) := 994.665 ; # 10
13 PLANT.HX.TGASHOT(11) := 1002.61 ; # 11
14 PLANT.HX.TGASHOT(12) := 1010.37 ; # 12
15 PLANT.HX.TGASHOT(13) := 1017.96 ; # 13
16 PLANT.HX.TGASHOT(14) := 1025.37 ; # 14
17 PLANT.HX.TGASHOT(15) := 1032.62 ; # 15
18 PLANT.HX.TGASHOT(16) := 1039.71 ; # 16
19 PLANT.HX.TGASHOT(17) := 1046.63 ; # 17
20 PLANT.HX.TGASHOT(18) := 1053.4 ; # 18
21 PLANT.HX.TGASHOT(19) := 1060.02 ; # 19
22 PLANT.HX.TGASHOT(20) := 1066.48 ; # 20
23 PLANT.HX.TGASHOT(21) := 1072.8 ; # 21
24 PLANT.HX.TGASHOT(22) := 1078.98 ; # 22
25 PLANT.HX.TGASHOT(23) := 1085.02 ; # 23
26 PLANT.HX.TGASHOT(24) := 1090.92 ; # 24
27 PLANT.HX.TGASHOT(25) := 1096.69 ; # 25
28 PLANT.HX.TGASHOT(26) := 1102.33 ; # 26
29 PLANT.HX.TGASHOT(27) := 1107.84 ; # 27
30 PLANT.HX.TGASHOT(28) := 1113.23 ; # 28
31 PLANT.HX.TGASHOT(29) := 1118.5 ; # 29
32 PLANT.HX.TGASHOT(30) := 1123.64 ; # 30
33 PLANT.HX.TGASHOT(31) := 1128.67 ; # 31
34 PLANT.HX.TGASHOT(32) := 1133.59 ; # 32
35 PLANT.HX.TGASHOT(33) := 1138.4 ; # 33
36 PLANT.HX.TGASHOT(34) := 1143.1 ; # 34
37 PLANT.HX.TGASHOT(35) := 1147.69 ; # 35
38 PLANT.HX.TGASHOT(36) := 1152.18 ; # 36
39 PLANT.HX.TGASHOT(37) := 1156.56 ; # 37
40 PLANT.HX.TGASHOT(38) := 1160.85 ; # 38
41 PLANT.HX.TGASHOT(39) := 1165.04 ; # 39
42 PLANT.HX.TGASHOT(40) := 1169.14 ; # 40
43 PLANT.HX.TGASCOLD(1) := 863.757 ; # 41
44 PLANT.HX.TGASCOLD(2) := 874.654 ; # 42
45 PLANT.HX.TGASCOLD(3) := 885.305 ; # 43
46 PLANT.HX.TGASCOLD(4) := 895.715 ; # 44
47 PLANT.HX.TGASCOLD(5) := 905.89 ; # 45
48 PLANT.HX.TGASCOLD(6) := 915.836 ; # 46
49 PLANT.HX.TGASCOLD(7) := 925.557 ; # 47
50 PLANT.HX.TGASCOLD(8) := 935.058 ; # 48
51 PLANT.HX.TGASCOLD(9) := 944.346 ; # 49
52 PLANT.HX.TGASCOLD(10) := 953.423 ; # 50
53 PLANT.HX.TGASCOLD(11) := 962.296 ; # 51
54 PLANT.HX.TGASCOLD(12) := 970.968 ; # 52
55 PLANT.HX.TGASCOLD(13) := 979.445 ; # 53
56 PLANT.HX.TGASCOLD(14) := 987.731 ; # 54
57 PLANT.HX.TGASCOLD(15) := 995.829 ; # 55
58 PLANT.HX.TGASCOLD(16) := 1003.74 ; # 56

```

59 PLANT.HX.TGASCOLD(17) := 1011.48 ; # 57
60 PLANT.HX.TGASCOLD(18) := 1019.04 ; # 58
61 PLANT.HX.TGASCOLD(19) := 1026.44 ; # 59
62 PLANT.HX.TGASCOLD(20) := 1033.66 ; # 60
63 PLANT.HX.TGASCOLD(21) := 1040.72 ; # 61
64 PLANT.HX.TGASCOLD(22) := 1047.62 ; # 62
65 PLANT.HX.TGASCOLD(23) := 1054.37 ; # 63
66 PLANT.HX.TGASCOLD(24) := 1060.96 ; # 64
67 PLANT.HX.TGASCOLD(25) := 1067.41 ; # 65
68 PLANT.HX.TGASCOLD(26) := 1073.71 ; # 66
69 PLANT.HX.TGASCOLD(27) := 1079.87 ; # 67
70 PLANT.HX.TGASCOLD(28) := 1085.89 ; # 68
71 PLANT.HX.TGASCOLD(29) := 1091.77 ; # 69
72 PLANT.HX.TGASCOLD(30) := 1097.52 ; # 70
73 PLANT.HX.TGASCOLD(31) := 1103.14 ; # 71
74 PLANT.HX.TGASCOLD(32) := 1108.63 ; # 72
75 PLANT.HX.TGASCOLD(33) := 1114 ; # 73
76 PLANT.HX.TGASCOLD(34) := 1119.25 ; # 74
77 PLANT.HX.TGASCOLD(35) := 1124.38 ; # 75
78 PLANT.HX.TGASCOLD(36) := 1129.4 ; # 76
79 PLANT.HX.TGASCOLD(37) := 1134.3 ; # 77
80 PLANT.HX.TGASCOLD(38) := 1139.09 ; # 78
81 PLANT.HX.TGASCOLD(39) := 1143.77 ; # 79
82 PLANT.HX.TGASCOLD(40) := 1148.34 ; # 80
83 PLANT.HX.UHOT := 1738.41 ; # 81
84 PLANT.HX.UCOLD := 1645.45 ; # 82
85 PLANT.HX.TH(1) := 889.835 ; # 83
86 PLANT.HX.TH(2) := 900.086 ; # 84
87 PLANT.HX.TH(3) := 910.162 ; # 85
88 PLANT.HX.TH(4) := 920.011 ; # 86
89 PLANT.HX.TH(5) := 929.638 ; # 87
90 PLANT.HX.TH(6) := 939.048 ; # 88
91 PLANT.HX.TH(7) := 948.245 ; # 89
92 PLANT.HX.TH(8) := 957.235 ; # 90
93 PLANT.HX.TH(9) := 966.021 ; # 91
94 PLANT.HX.TH(10) := 974.61 ; # 92
95 PLANT.HX.TH(11) := 983.004 ; # 93
96 PLANT.HX.TH(12) := 991.209 ; # 94
97 PLANT.HX.TH(13) := 999.229 ; # 95
98 PLANT.HX.TH(14) := 1007.07 ; # 96
99 PLANT.HX.TH(15) := 1014.73 ; # 97
100 PLANT.HX.TH(16) := 1022.22 ; # 98
101 PLANT.HX.TH(17) := 1029.54 ; # 99
102 PLANT.HX.TH(18) := 1036.69 ; # 100
103 PLANT.HX.TH(19) := 1043.69 ; # 101
104 PLANT.HX.TH(20) := 1050.52 ; # 102
105 PLANT.HX.TH(21) := 1057.2 ; # 103
106 PLANT.HX.TH(22) := 1063.73 ; # 104
107 PLANT.HX.TH(23) := 1070.12 ; # 105
108 PLANT.HX.TH(24) := 1076.36 ; # 106
109 PLANT.HX.TH(25) := 1082.45 ; # 107
110 PLANT.HX.TH(26) := 1088.41 ; # 108
111 PLANT.HX.TH(27) := 1094.24 ; # 109
112 PLANT.HX.TH(28) := 1099.93 ; # 110
113 PLANT.HX.TH(29) := 1105.5 ; # 111
114 PLANT.HX.TH(30) := 1110.94 ; # 112
115 PLANT.HX.TH(31) := 1116.26 ; # 113
116 PLANT.HX.TH(32) := 1121.45 ; # 114
117 PLANT.HX.TH(33) := 1126.53 ; # 115
118 PLANT.HX.TH(34) := 1131.5 ; # 116
119 PLANT.HX.TH(35) := 1136.35 ; # 117
120 PLANT.HX.TH(36) := 1141.1 ; # 118
121 PLANT.HX.TH(37) := 1145.73 ; # 119
122 PLANT.HX.TH(38) := 1150.27 ; # 120
123 PLANT.HX.TH(39) := 1154.7 ; # 121
124 PLANT.HX.TH(40) := 1159 ; # 122
125 PLANT.LOOP1.RHOEXTRA(1) := 1.14734 ; # 123
126 PLANT.LOOP1.RHOEXTRA(2) := 1.14734 ; # 123
127 PLANT.LOOP1.RHO(1) := 1.14734 ; # 123
128 PLANT.LOOP1.RHO(2) := 1.14286 ; # 124
129 PLANT.LOOP1.RHO(3) := 1.14003 ; # 125
130 PLANT.LOOP1.RHO(4) := 1.1372 ; # 126
131 PLANT.LOOP1.RHO(5) := 1.13435 ; # 127
132 PLANT.LOOP1.RHO(6) := 1.1315 ; # 128
133 PLANT.LOOP1.RHO(7) := 1.12862 ; # 129
134 PLANT.LOOP1.RHO(8) := 1.12574 ; # 130
135 PLANT.LOOP1.RHO(9) := 1.12285 ; # 131
136 PLANT.LOOP1.RHO(10) := 1.11994 ; # 132
137 PLANT.LOOP1.RHO(11) := 1.1156 ; # 133
138 PLANT.LOOP1.RHO(12) := 1.1004 ; # 134
139 PLANT.LOOP1.RHO(13) := 1.08551 ; # 135
140 PLANT.LOOP1.RHO(14) := 1.07124 ; # 136
141 PLANT.LOOP1.RHO(15) := 1.05755 ; # 137
142 PLANT.LOOP1.RHO(16) := 1.0444 ; # 138
143 PLANT.LOOP1.RHO(17) := 1.03177 ; # 139
144 PLANT.LOOP1.RHO(18) := 1.01963 ; # 140
145 PLANT.LOOP1.RHO(19) := 1.00793 ; # 141
146 PLANT.LOOP1.RHO(20) := 0.996671 ; # 142
147 PLANT.LOOP1.RHO(21) := 0.985813 ; # 143
148 PLANT.LOOP1.RHO(22) := 0.975337 ; # 144
149 PLANT.LOOP1.RHO(23) := 0.965222 ; # 145
150 PLANT.LOOP1.RHO(24) := 0.95545 ; # 146

```

151 PLANT.LOOP1.RHO(25) := 0.946002 ; # 147
152 PLANT.LOOP1.RHO(26) := 0.936861 ; # 148
153 PLANT.LOOP1.RHO(27) := 0.928012 ; # 149
154 PLANT.LOOP1.RHO(28) := 0.91944 ; # 150
155 PLANT.LOOP1.RHO(29) := 0.91113 ; # 151
156 PLANT.LOOP1.RHO(30) := 0.903071 ; # 152
157 PLANT.LOOP1.RHO(31) := 0.89525 ; # 153
158 PLANT.LOOP1.RHO(32) := 0.887655 ; # 154
159 PLANT.LOOP1.RHO(33) := 0.880276 ; # 155
160 PLANT.LOOP1.RHO(34) := 0.873102 ; # 156
161 PLANT.LOOP1.RHO(35) := 0.866125 ; # 157
162 PLANT.LOOP1.RHO(36) := 0.859335 ; # 158
163 PLANT.LOOP1.RHO(37) := 0.852723 ; # 159
164 PLANT.LOOP1.RHO(38) := 0.846282 ; # 160
165 PLANT.LOOP1.RHO(39) := 0.840005 ; # 161
166 PLANT.LOOP1.RHO(40) := 0.833883 ; # 162
167 PLANT.LOOP1.RHO(41) := 0.82791 ; # 163
168 PLANT.LOOP1.RHO(42) := 0.82208 ; # 164
169 PLANT.LOOP1.RHO(43) := 0.816387 ; # 165
170 PLANT.LOOP1.RHO(44) := 0.810825 ; # 166
171 PLANT.LOOP1.RHO(45) := 0.805388 ; # 167
172 PLANT.LOOP1.RHO(46) := 0.800071 ; # 168
173 PLANT.LOOP1.RHO(47) := 0.794869 ; # 169
174 PLANT.LOOP1.RHO(48) := 0.789778 ; # 170
175 PLANT.LOOP1.RHO(49) := 0.784793 ; # 171
176 PLANT.LOOP1.RHO(50) := 0.779915 ; # 172
177 PLANT.LOOP1.RHO(51) := 0.775148 ; # 173
178 PLANT.LOOP1.RHO(52) := 0.770306 ; # 174
179 PLANT.LOOP1.RHO(53) := 0.765302 ; # 175
180 PLANT.LOOP1.RHO(54) := 0.761087 ; # 176
181 PLANT.LOOP1.RHO(55) := 0.758961 ; # 177
182 PLANT.LOOP1.RHO(56) := 0.756824 ; # 178
183 PLANT.LOOP1.RHO(57) := 0.754676 ; # 179
184 PLANT.LOOP1.RHO(58) := 0.752516 ; # 180
185 PLANT.LOOP1.RHO(59) := 0.750345 ; # 181
186 PLANT.LOOP1.RHO(60) := 0.748162 ; # 182
187 PLANT.LOOP1.RHO(61) := 0.758154 ; # 183
188 PLANT.LOOP1.RHO(62) := 0.758842 ; # 184
189 PLANT.LOOP1.RHO(63) := 0.759576 ; # 185
190 PLANT.LOOP1.RHO(64) := 0.760408 ; # 186
191 PLANT.LOOP1.RHO(65) := 0.761346 ; # 187
192 PLANT.LOOP1.RHO(66) := 0.762396 ; # 188
193 PLANT.LOOP1.RHO(67) := 0.763568 ; # 189
194 PLANT.LOOP1.RHO(68) := 0.76487 ; # 190
195 PLANT.LOOP1.RHO(69) := 0.766313 ; # 191
196 PLANT.LOOP1.RHO(70) := 0.767908 ; # 192
197 PLANT.LOOP1.RHO(71) := 0.769667 ; # 193
198 PLANT.LOOP1.RHO(72) := 0.771602 ; # 194
199 PLANT.LOOP1.RHO(73) := 0.773727 ; # 195
200 PLANT.LOOP1.RHO(74) := 0.776059 ; # 196
201 PLANT.LOOP1.RHO(75) := 0.778613 ; # 197
202 PLANT.LOOP1.RHO(76) := 0.781409 ; # 198
203 PLANT.LOOP1.RHO(77) := 0.784467 ; # 199
204 PLANT.LOOP1.RHO(78) := 0.787809 ; # 200
205 PLANT.LOOP1.RHO(79) := 0.79146 ; # 201
206 PLANT.LOOP1.RHO(80) := 0.795447 ; # 202
207 PLANT.LOOP1.RHO(81) := 0.799801 ; # 203
208 PLANT.LOOP1.RHO(82) := 0.804555 ; # 204
209 PLANT.LOOP1.RHO(83) := 0.809747 ; # 205
210 PLANT.LOOP1.RHO(84) := 0.815419 ; # 206
211 PLANT.LOOP1.RHO(85) := 0.821618 ; # 207
212 PLANT.LOOP1.RHO(86) := 0.828396 ; # 208
213 PLANT.LOOP1.RHO(87) := 0.835814 ; # 209
214 PLANT.LOOP1.RHO(88) := 0.843939 ; # 210
215 PLANT.LOOP1.RHO(89) := 0.852847 ; # 211
216 PLANT.LOOP1.RHO(90) := 0.862626 ; # 212
217 PLANT.LOOP1.RHO(91) := 0.873377 ; # 213
218 PLANT.LOOP1.RHO(92) := 0.885216 ; # 214
219 PLANT.LOOP1.RHO(93) := 0.898277 ; # 215
220 PLANT.LOOP1.RHO(94) := 0.912717 ; # 216
221 PLANT.LOOP1.RHO(95) := 0.928718 ; # 217
222 PLANT.LOOP1.RHO(96) := 0.946498 ; # 218
223 PLANT.LOOP1.RHO(97) := 0.966314 ; # 219
224 PLANT.LOOP1.RHO(98) := 0.988474 ; # 220
225 PLANT.LOOP1.RHO(99) := 1.01335 ; # 221
226 PLANT.LOOP1.RHO(100) := 1.0414 ; # 222
227 PLANT.LOOP1.PEXTRA(1) := 2.04197e+006 ; # 223
228 PLANT.LOOP1.PEXTRA(2) := 2.04197e+006 ; # 223
229 PLANT.LOOP1.P(1) := 2.04197e+006 ; # 223
230 PLANT.LOOP1.P(2) := 2.03301e+006 ; # 224
231 PLANT.LOOP1.P(3) := 2.02702e+006 ; # 225
232 PLANT.LOOP1.P(4) := 2.02101e+006 ; # 226
233 PLANT.LOOP1.P(5) := 2.01499e+006 ; # 227
234 PLANT.LOOP1.P(6) := 2.00895e+006 ; # 228
235 PLANT.LOOP1.P(7) := 2.0029e+006 ; # 229
236 PLANT.LOOP1.P(8) := 1.99683e+006 ; # 230
237 PLANT.LOOP1.P(9) := 1.99074e+006 ; # 231
238 PLANT.LOOP1.P(10) := 1.98464e+006 ; # 232
239 PLANT.LOOP1.P(11) := 2.00285e+006 ; # 233
240 PLANT.LOOP1.P(12) := 2.00049e+006 ; # 234
241 PLANT.LOOP1.P(13) := 1.99745e+006 ; # 235
242 PLANT.LOOP1.P(14) := 1.99437e+006 ; # 236

```

```

243 PLANT.LOOP1.P(15) := 1.99125e+006 ; # 237
244 PLANT.LOOP1.P(16) := 1.98809e+006 ; # 238
245 PLANT.LOOP1.P(17) := 1.9849e+006 ; # 239
246 PLANT.LOOP1.P(18) := 1.98166e+006 ; # 240
247 PLANT.LOOP1.P(19) := 1.9784e+006 ; # 241
248 PLANT.LOOP1.P(20) := 1.97509e+006 ; # 242
249 PLANT.LOOP1.P(21) := 1.97176e+006 ; # 243
250 PLANT.LOOP1.P(22) := 1.96838e+006 ; # 244
251 PLANT.LOOP1.P(23) := 1.96498e+006 ; # 245
252 PLANT.LOOP1.P(24) := 1.96154e+006 ; # 246
253 PLANT.LOOP1.P(25) := 1.95806e+006 ; # 247
254 PLANT.LOOP1.P(26) := 1.95456e+006 ; # 248
255 PLANT.LOOP1.P(27) := 1.95102e+006 ; # 249
256 PLANT.LOOP1.P(28) := 1.94745e+006 ; # 250
257 PLANT.LOOP1.P(29) := 1.94385e+006 ; # 251
258 PLANT.LOOP1.P(30) := 1.94021e+006 ; # 252
259 PLANT.LOOP1.P(31) := 1.93655e+006 ; # 253
260 PLANT.LOOP1.P(32) := 1.93286e+006 ; # 254
261 PLANT.LOOP1.P(33) := 1.92913e+006 ; # 255
262 PLANT.LOOP1.P(34) := 1.92538e+006 ; # 256
263 PLANT.LOOP1.P(35) := 1.9216e+006 ; # 257
264 PLANT.LOOP1.P(36) := 1.91778e+006 ; # 258
265 PLANT.LOOP1.P(37) := 1.91394e+006 ; # 259
266 PLANT.LOOP1.P(38) := 1.91007e+006 ; # 260
267 PLANT.LOOP1.P(39) := 1.90617e+006 ; # 261
268 PLANT.LOOP1.P(40) := 1.90225e+006 ; # 262
269 PLANT.LOOP1.P(41) := 1.8983e+006 ; # 263
270 PLANT.LOOP1.P(42) := 1.89432e+006 ; # 264
271 PLANT.LOOP1.P(43) := 1.89031e+006 ; # 265
272 PLANT.LOOP1.P(44) := 1.88627e+006 ; # 266
273 PLANT.LOOP1.P(45) := 1.88221e+006 ; # 267
274 PLANT.LOOP1.P(46) := 1.87813e+006 ; # 268
275 PLANT.LOOP1.P(47) := 1.87401e+006 ; # 269
276 PLANT.LOOP1.P(48) := 1.86987e+006 ; # 270
277 PLANT.LOOP1.P(49) := 1.86571e+006 ; # 271
278 PLANT.LOOP1.P(50) := 1.86152e+006 ; # 272
279 PLANT.LOOP1.P(51) := 1.83045e+006 ; # 273
280 PLANT.LOOP1.P(52) := 1.82419e+006 ; # 274
281 PLANT.LOOP1.P(53) := 1.81794e+006 ; # 275
282 PLANT.LOOP1.P(54) := 1.81169e+006 ; # 276
283 PLANT.LOOP1.P(55) := 1.80541e+006 ; # 277
284 PLANT.LOOP1.P(56) := 1.79911e+006 ; # 278
285 PLANT.LOOP1.P(57) := 1.7928e+006 ; # 279
286 PLANT.LOOP1.P(58) := 1.78646e+006 ; # 280
287 PLANT.LOOP1.P(59) := 1.78011e+006 ; # 281
288 PLANT.LOOP1.P(60) := 1.77374e+006 ; # 282
289 PLANT.LOOP1.P(61) := 1.7945e+006 ; # 283
290 PLANT.LOOP1.P(62) := 1.793e+006 ; # 284
291 PLANT.LOOP1.P(63) := 1.7914e+006 ; # 285
292 PLANT.LOOP1.P(64) := 1.78981e+006 ; # 286
293 PLANT.LOOP1.P(65) := 1.78821e+006 ; # 287
294 PLANT.LOOP1.P(66) := 1.78662e+006 ; # 288
295 PLANT.LOOP1.P(67) := 1.78503e+006 ; # 289
296 PLANT.LOOP1.P(68) := 1.78345e+006 ; # 290
297 PLANT.LOOP1.P(69) := 1.78187e+006 ; # 291
298 PLANT.LOOP1.P(70) := 1.78029e+006 ; # 292
299 PLANT.LOOP1.P(71) := 1.77872e+006 ; # 293
300 PLANT.LOOP1.P(72) := 1.77715e+006 ; # 294
301 PLANT.LOOP1.P(73) := 1.77559e+006 ; # 295
302 PLANT.LOOP1.P(74) := 1.77404e+006 ; # 296
303 PLANT.LOOP1.P(75) := 1.77249e+006 ; # 297
304 PLANT.LOOP1.P(76) := 1.77095e+006 ; # 298
305 PLANT.LOOP1.P(77) := 1.76942e+006 ; # 299
306 PLANT.LOOP1.P(78) := 1.76789e+006 ; # 300
307 PLANT.LOOP1.P(79) := 1.76638e+006 ; # 301
308 PLANT.LOOP1.P(80) := 1.76487e+006 ; # 302
309 PLANT.LOOP1.P(81) := 1.76337e+006 ; # 303
310 PLANT.LOOP1.P(82) := 1.76189e+006 ; # 304
311 PLANT.LOOP1.P(83) := 1.76042e+006 ; # 305
312 PLANT.LOOP1.P(84) := 1.75896e+006 ; # 306
313 PLANT.LOOP1.P(85) := 1.75751e+006 ; # 307
314 PLANT.LOOP1.P(86) := 1.75608e+006 ; # 308
315 PLANT.LOOP1.P(87) := 1.75467e+006 ; # 309
316 PLANT.LOOP1.P(88) := 1.75327e+006 ; # 310
317 PLANT.LOOP1.P(89) := 1.75189e+006 ; # 311
318 PLANT.LOOP1.P(90) := 1.75054e+006 ; # 312
319 PLANT.LOOP1.P(91) := 1.7492e+006 ; # 313
320 PLANT.LOOP1.P(92) := 1.74789e+006 ; # 314
321 PLANT.LOOP1.P(93) := 1.7466e+006 ; # 315
322 PLANT.LOOP1.P(94) := 1.74534e+006 ; # 316
323 PLANT.LOOP1.P(95) := 1.7441e+006 ; # 317
324 PLANT.LOOP1.P(96) := 1.7429e+006 ; # 318
325 PLANT.LOOP1.P(97) := 1.74173e+006 ; # 319
326 PLANT.LOOP1.P(98) := 1.74059e+006 ; # 320
327 PLANT.LOOP1.P(99) := 1.73949e+006 ; # 321
328 PLANT.LOOP1.P(100) := 1.73843e+006 ; # 322
329 PLANT.LOOP1.P_OUT := 1.73785e+006 ; # 323
330 PLANT.LOOP1.HEXTRA(1) := 2.90016e+006 ; # 324
331 PLANT.LOOP1.HEXTRA(2) := 2.90016e+006 ; # 324
332 PLANT.LOOP1.H(1) := 2.90016e+006 ; # 324
333 PLANT.LOOP1.H(2) := 2.89803e+006 ; # 325
334 PLANT.LOOP1.H(3) := 2.8959e+006 ; # 326

```



```

335 PLANT.LOOP1.H(4) := 2.89378e+006 ; # 327
336 PLANT.LOOP1.H(5) := 2.89166e+006 ; # 328
337 PLANT.LOOP1.H(6) := 2.88954e+006 ; # 329
338 PLANT.LOOP1.H(7) := 2.88742e+006 ; # 330
339 PLANT.LOOP1.H(8) := 2.8853e+006 ; # 331
340 PLANT.LOOP1.H(9) := 2.88318e+006 ; # 332
341 PLANT.LOOP1.H(10) := 2.88106e+006 ; # 333
342 PLANT.LOOP1.H(11) := 2.93911e+006 ; # 334
343 PLANT.LOOP1.H(12) := 2.99572e+006 ; # 335
344 PLANT.LOOP1.H(13) := 3.05105e+006 ; # 336
345 PLANT.LOOP1.H(14) := 3.10513e+006 ; # 337
346 PLANT.LOOP1.H(15) := 3.15799e+006 ; # 338
347 PLANT.LOOP1.H(16) := 3.20966e+006 ; # 339
348 PLANT.LOOP1.H(17) := 3.26016e+006 ; # 340
349 PLANT.LOOP1.H(18) := 3.30952e+006 ; # 341
350 PLANT.LOOP1.H(19) := 3.35777e+006 ; # 342
351 PLANT.LOOP1.H(20) := 3.40492e+006 ; # 343
352 PLANT.LOOP1.H(21) := 3.45102e+006 ; # 344
353 PLANT.LOOP1.H(22) := 3.49607e+006 ; # 345
354 PLANT.LOOP1.H(23) := 3.54011e+006 ; # 346
355 PLANT.LOOP1.H(24) := 3.58315e+006 ; # 347
356 PLANT.LOOP1.H(25) := 3.62522e+006 ; # 348
357 PLANT.LOOP1.H(26) := 3.66634e+006 ; # 349
358 PLANT.LOOP1.H(27) := 3.70654e+006 ; # 350
359 PLANT.LOOP1.H(28) := 3.74582e+006 ; # 351
360 PLANT.LOOP1.H(29) := 3.78422e+006 ; # 352
361 PLANT.LOOP1.H(30) := 3.82175e+006 ; # 353
362 PLANT.LOOP1.H(31) := 3.85844e+006 ; # 354
363 PLANT.LOOP1.H(32) := 3.8943e+006 ; # 355
364 PLANT.LOOP1.H(33) := 3.92935e+006 ; # 356
365 PLANT.LOOP1.H(34) := 3.9636e+006 ; # 357
366 PLANT.LOOP1.H(35) := 3.99709e+006 ; # 358
367 PLANT.LOOP1.H(36) := 4.02981e+006 ; # 359
368 PLANT.LOOP1.H(37) := 4.0618e+006 ; # 360
369 PLANT.LOOP1.H(38) := 4.09307e+006 ; # 361
370 PLANT.LOOP1.H(39) := 4.12363e+006 ; # 362
371 PLANT.LOOP1.H(40) := 4.15351e+006 ; # 363
372 PLANT.LOOP1.H(41) := 4.1827e+006 ; # 364
373 PLANT.LOOP1.H(42) := 4.21124e+006 ; # 365
374 PLANT.LOOP1.H(43) := 4.23914e+006 ; # 366
375 PLANT.LOOP1.H(44) := 4.2664e+006 ; # 367
376 PLANT.LOOP1.H(45) := 4.29305e+006 ; # 368
377 PLANT.LOOP1.H(46) := 4.3191e+006 ; # 369
378 PLANT.LOOP1.H(47) := 4.34456e+006 ; # 370
379 PLANT.LOOP1.H(48) := 4.36944e+006 ; # 371
380 PLANT.LOOP1.H(49) := 4.39377e+006 ; # 372
381 PLANT.LOOP1.H(50) := 4.41751e+006 ; # 373
382 PLANT.LOOP1.H(51) := 4.41348e+006 ; # 374
383 PLANT.LOOP1.H(52) := 4.40946e+006 ; # 375
384 PLANT.LOOP1.H(53) := 4.40545e+006 ; # 376
385 PLANT.LOOP1.H(54) := 4.40144e+006 ; # 377
386 PLANT.LOOP1.H(55) := 4.39743e+006 ; # 378
387 PLANT.LOOP1.H(56) := 4.39343e+006 ; # 379
388 PLANT.LOOP1.H(57) := 4.38943e+006 ; # 380
389 PLANT.LOOP1.H(58) := 4.38543e+006 ; # 381
390 PLANT.LOOP1.H(59) := 4.38144e+006 ; # 382
391 PLANT.LOOP1.H(60) := 4.37745e+006 ; # 383
392 PLANT.LOOP1.H(61) := 4.3678e+006 ; # 384
393 PLANT.LOOP1.H(62) := 4.35751e+006 ; # 385
394 PLANT.LOOP1.H(63) := 4.34653e+006 ; # 386
395 PLANT.LOOP1.H(64) := 4.33483e+006 ; # 387
396 PLANT.LOOP1.H(65) := 4.32236e+006 ; # 388
397 PLANT.LOOP1.H(66) := 4.30905e+006 ; # 389
398 PLANT.LOOP1.H(67) := 4.29487e+006 ; # 390
399 PLANT.LOOP1.H(68) := 4.27974e+006 ; # 391
400 PLANT.LOOP1.H(69) := 4.26361e+006 ; # 392
401 PLANT.LOOP1.H(70) := 4.24641e+006 ; # 393
402 PLANT.LOOP1.H(71) := 4.22806e+006 ; # 394
403 PLANT.LOOP1.H(72) := 4.20851e+006 ; # 395
404 PLANT.LOOP1.H(73) := 4.18765e+006 ; # 396
405 PLANT.LOOP1.H(74) := 4.16541e+006 ; # 397
406 PLANT.LOOP1.H(75) := 4.1417e+006 ; # 398
407 PLANT.LOOP1.H(76) := 4.11641e+006 ; # 399
408 PLANT.LOOP1.H(77) := 4.08945e+006 ; # 400
409 PLANT.LOOP1.H(78) := 4.06069e+006 ; # 401
410 PLANT.LOOP1.H(79) := 4.03003e+006 ; # 402
411 PLANT.LOOP1.H(80) := 3.99734e+006 ; # 403
412 PLANT.LOOP1.H(81) := 3.96248e+006 ; # 404
413 PLANT.LOOP1.H(82) := 3.9253e+006 ; # 405
414 PLANT.LOOP1.H(83) := 3.88566e+006 ; # 406
415 PLANT.LOOP1.H(84) := 3.8434e+006 ; # 407
416 PLANT.LOOP1.H(85) := 3.79832e+006 ; # 408
417 PLANT.LOOP1.H(86) := 3.75026e+006 ; # 409
418 PLANT.LOOP1.H(87) := 3.69901e+006 ; # 410
419 PLANT.LOOP1.H(88) := 3.64436e+006 ; # 411
420 PLANT.LOOP1.H(89) := 3.58609e+006 ; # 412
421 PLANT.LOOP1.H(90) := 3.52395e+006 ; # 413
422 PLANT.LOOP1.H(91) := 3.45769e+006 ; # 414
423 PLANT.LOOP1.H(92) := 3.38703e+006 ; # 415
424 PLANT.LOOP1.H(93) := 3.31169e+006 ; # 416
425 PLANT.LOOP1.H(94) := 3.23135e+006 ; # 417
426 PLANT.LOOP1.H(95) := 3.14568e+006 ; # 418

```

```

427 PLANT.LOOP1.H(96) := 3.05433e+006 ; # 419
428 PLANT.LOOP1.H(97) := 2.95692e+006 ; # 420
429 PLANT.LOOP1.H(98) := 2.85305e+006 ; # 421
430 PLANT.LOOP1.H(99) := 2.74229e+006 ; # 422
431 PLANT.LOOP1.H(100) := 2.62419e+006 ; # 423
432 PLANT.LOOP1.HO := 2.90229e+006 ; # 424
433 PLANT.LOOP1.TEXTRA(1) := 856.26 ; # 425
434 PLANT.LOOP1.TEXTRA(2) := 856.26 ; # 425
435 PLANT.LOOP1.T(1) := 856.26 ; # 425
436 PLANT.LOOP1.T(2) := 855.85 ; # 426
437 PLANT.LOOP1.T(3) := 855.441 ; # 427
438 PLANT.LOOP1.T(4) := 855.032 ; # 428
439 PLANT.LOOP1.T(5) := 854.623 ; # 429
440 PLANT.LOOP1.T(6) := 854.215 ; # 430
441 PLANT.LOOP1.T(7) := 853.807 ; # 431
442 PLANT.LOOP1.T(8) := 853.399 ; # 432
443 PLANT.LOOP1.T(9) := 852.991 ; # 433
444 PLANT.LOOP1.T(10) := 852.584 ; # 434
445 PLANT.LOOP1.T(11) := 863.757 ; # 435
446 PLANT.LOOP1.T(12) := 874.654 ; # 436
447 PLANT.LOOP1.T(13) := 885.305 ; # 437
448 PLANT.LOOP1.T(14) := 895.715 ; # 438
449 PLANT.LOOP1.T(15) := 905.89 ; # 439
450 PLANT.LOOP1.T(16) := 915.836 ; # 440
451 PLANT.LOOP1.T(17) := 925.557 ; # 441
452 PLANT.LOOP1.T(18) := 935.058 ; # 442
453 PLANT.LOOP1.T(19) := 944.346 ; # 443
454 PLANT.LOOP1.T(20) := 953.423 ; # 444
455 PLANT.LOOP1.T(21) := 962.296 ; # 445
456 PLANT.LOOP1.T(22) := 970.968 ; # 446
457 PLANT.LOOP1.T(23) := 979.445 ; # 447
458 PLANT.LOOP1.T(24) := 987.731 ; # 448
459 PLANT.LOOP1.T(25) := 995.829 ; # 449
460 PLANT.LOOP1.T(26) := 1003.74 ; # 450
461 PLANT.LOOP1.T(27) := 1011.48 ; # 451
462 PLANT.LOOP1.T(28) := 1019.04 ; # 452
463 PLANT.LOOP1.T(29) := 1026.44 ; # 453
464 PLANT.LOOP1.T(30) := 1033.66 ; # 454
465 PLANT.LOOP1.T(31) := 1040.72 ; # 455
466 PLANT.LOOP1.T(32) := 1047.62 ; # 456
467 PLANT.LOOP1.T(33) := 1054.37 ; # 457
468 PLANT.LOOP1.T(34) := 1060.96 ; # 458
469 PLANT.LOOP1.T(35) := 1067.41 ; # 459
470 PLANT.LOOP1.T(36) := 1073.71 ; # 460
471 PLANT.LOOP1.T(37) := 1079.87 ; # 461
472 PLANT.LOOP1.T(38) := 1085.89 ; # 462
473 PLANT.LOOP1.T(39) := 1091.77 ; # 463
474 PLANT.LOOP1.T(40) := 1097.52 ; # 464
475 PLANT.LOOP1.T(41) := 1103.14 ; # 465
476 PLANT.LOOP1.T(42) := 1108.63 ; # 466
477 PLANT.LOOP1.T(43) := 1114 ; # 467
478 PLANT.LOOP1.T(44) := 1119.25 ; # 468
479 PLANT.LOOP1.T(45) := 1124.38 ; # 469
480 PLANT.LOOP1.T(46) := 1129.4 ; # 470
481 PLANT.LOOP1.T(47) := 1134.3 ; # 471
482 PLANT.LOOP1.T(48) := 1139.09 ; # 472
483 PLANT.LOOP1.T(49) := 1143.77 ; # 473
484 PLANT.LOOP1.T(50) := 1148.34 ; # 474
485 PLANT.LOOP1.T(51) := 1147.56 ; # 475
486 PLANT.LOOP1.T(52) := 1146.79 ; # 476
487 PLANT.LOOP1.T(53) := 1146.02 ; # 477
488 PLANT.LOOP1.T(54) := 1145.25 ; # 478
489 PLANT.LOOP1.T(55) := 1144.47 ; # 479
490 PLANT.LOOP1.T(56) := 1143.7 ; # 480
491 PLANT.LOOP1.T(57) := 1142.93 ; # 481
492 PLANT.LOOP1.T(58) := 1142.16 ; # 482
493 PLANT.LOOP1.T(59) := 1141.39 ; # 483
494 PLANT.LOOP1.T(60) := 1140.63 ; # 484
495 PLANT.LOOP1.T(61) := 1138.77 ; # 485
496 PLANT.LOOP1.T(62) := 1136.79 ; # 486
497 PLANT.LOOP1.T(63) := 1134.68 ; # 487
498 PLANT.LOOP1.T(64) := 1132.42 ; # 488
499 PLANT.LOOP1.T(65) := 1130.02 ; # 489
500 PLANT.LOOP1.T(66) := 1127.46 ; # 490
501 PLANT.LOOP1.T(67) := 1124.73 ; # 491
502 PLANT.LOOP1.T(68) := 1121.82 ; # 492
503 PLANT.LOOP1.T(69) := 1118.71 ; # 493
504 PLANT.LOOP1.T(70) := 1115.4 ; # 494
505 PLANT.LOOP1.T(71) := 1111.87 ; # 495
506 PLANT.LOOP1.T(72) := 1108.11 ; # 496
507 PLANT.LOOP1.T(73) := 1104.09 ; # 497
508 PLANT.LOOP1.T(74) := 1099.81 ; # 498
509 PLANT.LOOP1.T(75) := 1095.25 ; # 499
510 PLANT.LOOP1.T(76) := 1090.38 ; # 500
511 PLANT.LOOP1.T(77) := 1085.19 ; # 501
512 PLANT.LOOP1.T(78) := 1079.65 ; # 502
513 PLANT.LOOP1.T(79) := 1073.75 ; # 503
514 PLANT.LOOP1.T(80) := 1067.46 ; # 504
515 PLANT.LOOP1.T(81) := 1060.75 ; # 505
516 PLANT.LOOP1.T(82) := 1053.59 ; # 506
517 PLANT.LOOP1.T(83) := 1045.96 ; # 507
518 PLANT.LOOP1.T(84) := 1037.83 ; # 508

```

519 PLANT.LOOP1.T(85) := 1029.15 ; # 509
520 PLANT.LOOP1.T(86) := 1019.9 ; # 510
521 PLANT.LOOP1.T(87) := 1010.03 ; # 511
522 PLANT.LOOP1.T(88) := 999.513 ; # 512
523 PLANT.LOOP1.T(89) := 988.296 ; # 513
524 PLANT.LOOP1.T(90) := 976.334 ; # 514
525 PLANT.LOOP1.T(91) := 963.58 ; # 515
526 PLANT.LOOP1.T(92) := 949.979 ; # 516
527 PLANT.LOOP1.T(93) := 935.476 ; # 517
528 PLANT.LOOP1.T(94) := 920.011 ; # 518
529 PLANT.LOOP1.T(95) := 903.52 ; # 519
530 PLANT.LOOP1.T(96) := 885.936 ; # 520
531 PLANT.LOOP1.T(97) := 867.185 ; # 521
532 PLANT.LOOP1.T(98) := 847.191 ; # 522
533 PLANT.LOOP1.T(99) := 825.87 ; # 523
534 PLANT.LOOP1.T(100) := 803.137 ; # 524
535 PLANT.LOOP1.TO := 856.67 ; # 525
536 PLANT.LOOP1.TEXTRNL(1) := 291.15 ; # 526
537 PLANT.LOOP1.TEXTRNL(2) := 291.15 ; # 527
538 PLANT.LOOP1.TEXTRNL(3) := 291.15 ; # 528
539 PLANT.LOOP1.TEXTRNL(4) := 291.15 ; # 529
540 PLANT.LOOP1.TEXTRNL(5) := 291.15 ; # 530
541 PLANT.LOOP1.TEXTRNL(6) := 291.15 ; # 531
542 PLANT.LOOP1.TEXTRNL(7) := 291.15 ; # 532
543 PLANT.LOOP1.TEXTRNL(8) := 291.15 ; # 533
544 PLANT.LOOP1.TEXTRNL(9) := 291.15 ; # 534
545 PLANT.LOOP1.TEXTRNL(10) := 291.15 ; # 535
546 PLANT.LOOP1.TEXTRNL(11) := 889.835 ; # 536
547 PLANT.LOOP1.TEXTRNL(12) := 900.086 ; # 537
548 PLANT.LOOP1.TEXTRNL(13) := 910.162 ; # 538
549 PLANT.LOOP1.TEXTRNL(14) := 920.011 ; # 539
550 PLANT.LOOP1.TEXTRNL(15) := 929.638 ; # 540
551 PLANT.LOOP1.TEXTRNL(16) := 939.048 ; # 541
552 PLANT.LOOP1.TEXTRNL(17) := 948.245 ; # 542
553 PLANT.LOOP1.TEXTRNL(18) := 957.235 ; # 543
554 PLANT.LOOP1.TEXTRNL(19) := 966.021 ; # 544
555 PLANT.LOOP1.TEXTRNL(20) := 974.61 ; # 545
556 PLANT.LOOP1.TEXTRNL(21) := 983.004 ; # 546
557 PLANT.LOOP1.TEXTRNL(22) := 991.209 ; # 547
558 PLANT.LOOP1.TEXTRNL(23) := 999.229 ; # 548
559 PLANT.LOOP1.TEXTRNL(24) := 1007.07 ; # 549
560 PLANT.LOOP1.TEXTRNL(25) := 1014.73 ; # 550
561 PLANT.LOOP1.TEXTRNL(26) := 1022.22 ; # 551
562 PLANT.LOOP1.TEXTRNL(27) := 1029.54 ; # 552
563 PLANT.LOOP1.TEXTRNL(28) := 1036.69 ; # 553
564 PLANT.LOOP1.TEXTRNL(29) := 1043.69 ; # 554
565 PLANT.LOOP1.TEXTRNL(30) := 1050.52 ; # 555
566 PLANT.LOOP1.TEXTRNL(31) := 1057.2 ; # 556
567 PLANT.LOOP1.TEXTRNL(32) := 1063.73 ; # 557
568 PLANT.LOOP1.TEXTRNL(33) := 1070.12 ; # 558
569 PLANT.LOOP1.TEXTRNL(34) := 1076.36 ; # 559
570 PLANT.LOOP1.TEXTRNL(35) := 1082.45 ; # 560
571 PLANT.LOOP1.TEXTRNL(36) := 1088.41 ; # 561
572 PLANT.LOOP1.TEXTRNL(37) := 1094.24 ; # 562
573 PLANT.LOOP1.TEXTRNL(38) := 1099.93 ; # 563
574 PLANT.LOOP1.TEXTRNL(39) := 1105.5 ; # 564
575 PLANT.LOOP1.TEXTRNL(40) := 1110.94 ; # 565
576 PLANT.LOOP1.TEXTRNL(41) := 1116.26 ; # 566
577 PLANT.LOOP1.TEXTRNL(42) := 1121.45 ; # 567
578 PLANT.LOOP1.TEXTRNL(43) := 1126.53 ; # 568
579 PLANT.LOOP1.TEXTRNL(44) := 1131.5 ; # 569
580 PLANT.LOOP1.TEXTRNL(45) := 1136.35 ; # 570
581 PLANT.LOOP1.TEXTRNL(46) := 1141.1 ; # 571
582 PLANT.LOOP1.TEXTRNL(47) := 1145.73 ; # 572
583 PLANT.LOOP1.TEXTRNL(48) := 1150.27 ; # 573
584 PLANT.LOOP1.TEXTRNL(49) := 1154.7 ; # 574
585 PLANT.LOOP1.TEXTRNL(50) := 1159 ; # 575
586 PLANT.LOOP1.TEXTRNL(51) := 291.15 ; # 576
587 PLANT.LOOP1.TEXTRNL(52) := 291.15 ; # 577
588 PLANT.LOOP1.TEXTRNL(53) := 291.15 ; # 578
589 PLANT.LOOP1.TEXTRNL(54) := 291.15 ; # 579
590 PLANT.LOOP1.TEXTRNL(55) := 291.15 ; # 580
591 PLANT.LOOP1.TEXTRNL(56) := 291.15 ; # 581
592 PLANT.LOOP1.TEXTRNL(57) := 291.15 ; # 582
593 PLANT.LOOP1.TEXTRNL(58) := 291.15 ; # 583
594 PLANT.LOOP1.TEXTRNL(59) := 291.15 ; # 584
595 PLANT.LOOP1.TEXTRNL(60) := 291.15 ; # 585
596 PLANT.LOOP1.TEXTRNL(61) := 1132.12 ; # 586
597 PLANT.LOOP1.TEXTRNL(62) := 1129.7 ; # 587
598 PLANT.LOOP1.TEXTRNL(63) := 1127.12 ; # 588
599 PLANT.LOOP1.TEXTRNL(64) := 1124.36 ; # 589
600 PLANT.LOOP1.TEXTRNL(65) := 1121.43 ; # 590
601 PLANT.LOOP1.TEXTRNL(66) := 1118.29 ; # 591
602 PLANT.LOOP1.TEXTRNL(67) := 1114.96 ; # 592
603 PLANT.LOOP1.TEXTRNL(68) := 1111.4 ; # 593
604 PLANT.LOOP1.TEXTRNL(69) := 1107.6 ; # 594
605 PLANT.LOOP1.TEXTRNL(70) := 1103.55 ; # 595
606 PLANT.LOOP1.TEXTRNL(71) := 1099.23 ; # 596
607 PLANT.LOOP1.TEXTRNL(72) := 1094.63 ; # 597
608 PLANT.LOOP1.TEXTRNL(73) := 1089.72 ; # 598
609 PLANT.LOOP1.TEXTRNL(74) := 1084.49 ; # 599
610 PLANT.LOOP1.TEXTRNL(75) := 1078.91 ; # 600

```

611 PLANT.LOOP1.TEXTRNL(76) := 1072.96 ; # 601
612 PLANT.LOOP1.TEXTRNL(77) := 1066.61 ; # 602
613 PLANT.LOOP1.TEXTRNL(78) := 1059.84 ; # 603
614 PLANT.LOOP1.TEXTRNL(79) := 1052.63 ; # 604
615 PLANT.LOOP1.TEXTRNL(80) := 1044.93 ; # 605
616 PLANT.LOOP1.TEXTRNL(81) := 1036.73 ; # 606
617 PLANT.LOOP1.TEXTRNL(82) := 1027.98 ; # 607
618 PLANT.LOOP1.TEXTRNL(83) := 1018.65 ; # 608
619 PLANT.LOOP1.TEXTRNL(84) := 1008.7 ; # 609
620 PLANT.LOOP1.TEXTRNL(85) := 998.095 ; # 610
621 PLANT.LOOP1.TEXTRNL(86) := 986.784 ; # 611
622 PLANT.LOOP1.TEXTRNL(87) := 974.722 ; # 612
623 PLANT.LOOP1.TEXTRNL(88) := 961.86 ; # 613
624 PLANT.LOOP1.TEXTRNL(89) := 948.145 ; # 614
625 PLANT.LOOP1.TEXTRNL(90) := 933.521 ; # 615
626 PLANT.LOOP1.TEXTRNL(91) := 917.926 ; # 616
627 PLANT.LOOP1.TEXTRNL(92) := 901.297 ; # 617
628 PLANT.LOOP1.TEXTRNL(93) := 883.565 ; # 618
629 PLANT.LOOP1.TEXTRNL(94) := 864.657 ; # 619
630 PLANT.LOOP1.TEXTRNL(95) := 844.495 ; # 620
631 PLANT.LOOP1.TEXTRNL(96) := 822.996 ; # 621
632 PLANT.LOOP1.TEXTRNL(97) := 800.07 ; # 622
633 PLANT.LOOP1.TEXTRNL(98) := 775.624 ; # 623
634 PLANT.LOOP1.TEXTRNL(99) := 749.557 ; # 624
635 PLANT.LOOP1.TEXTRNL(100) := 721.768 ; # 625
636 PLANT.LOOP1.PSIEXTRA(1) := 1.28551e+006 ; # 626
637 PLANT.LOOP1.PSIEXTRA(2) := 1.28551e+006 ; # 626
638 PLANT.LOOP1.PSI(1) := 1.28551e+006 ; # 626
639 PLANT.LOOP1.PSI(2) := 1.27902e+006 ; # 627
640 PLANT.LOOP1.PSI(3) := 1.27441e+006 ; # 628
641 PLANT.LOOP1.PSI(4) := 1.26979e+006 ; # 629
642 PLANT.LOOP1.PSI(5) := 1.26517e+006 ; # 630
643 PLANT.LOOP1.PSI(6) := 1.26054e+006 ; # 631
644 PLANT.LOOP1.PSI(7) := 1.25591e+006 ; # 632
645 PLANT.LOOP1.PSI(8) := 1.25127e+006 ; # 633
646 PLANT.LOOP1.PSI(9) := 1.24663e+006 ; # 634
647 PLANT.LOOP1.PSI(10) := 1.24198e+006 ; # 635
648 PLANT.LOOP1.PSI(11) := 1.23734e+006 ; # 636
649 PLANT.LOOP1.PSI(12) := 1.23270e+006 ; # 637
650 PLANT.LOOP1.PSI(13) := 1.31449e+006 ; # 638
651 PLANT.LOOP1.PSI(14) := 1.33196e+006 ; # 639
652 PLANT.LOOP1.PSI(15) := 1.34847e+006 ; # 640
653 PLANT.LOOP1.PSI(16) := 1.36409e+006 ; # 641
654 PLANT.LOOP1.PSI(17) := 1.37885e+006 ; # 642
655 PLANT.LOOP1.PSI(18) := 1.39281e+006 ; # 643
656 PLANT.LOOP1.PSI(19) := 1.40601e+006 ; # 644
657 PLANT.LOOP1.PSI(20) := 1.4185e+006 ; # 645
658 PLANT.LOOP1.PSI(21) := 1.4303e+006 ; # 646
659 PLANT.LOOP1.PSI(22) := 1.44146e+006 ; # 647
660 PLANT.LOOP1.PSI(23) := 1.45201e+006 ; # 648
661 PLANT.LOOP1.PSI(24) := 1.46198e+006 ; # 649
662 PLANT.LOOP1.PSI(25) := 1.4714e+006 ; # 650
663 PLANT.LOOP1.PSI(26) := 1.4803e+006 ; # 651
664 PLANT.LOOP1.PSI(27) := 1.48869e+006 ; # 652
665 PLANT.LOOP1.PSI(28) := 1.49661e+006 ; # 653
666 PLANT.LOOP1.PSI(29) := 1.50407e+006 ; # 654
667 PLANT.LOOP1.PSI(30) := 1.5111e+006 ; # 655
668 PLANT.LOOP1.PSI(31) := 1.51772e+006 ; # 656
669 PLANT.LOOP1.PSI(32) := 1.52393e+006 ; # 657
670 PLANT.LOOP1.PSI(33) := 1.52977e+006 ; # 658
671 PLANT.LOOP1.PSI(34) := 1.53525e+006 ; # 659
672 PLANT.LOOP1.PSI(35) := 1.54038e+006 ; # 660
673 PLANT.LOOP1.PSI(36) := 1.54518e+006 ; # 661
674 PLANT.LOOP1.PSI(37) := 1.54965e+006 ; # 662
675 PLANT.LOOP1.PSI(38) := 1.55382e+006 ; # 663
676 PLANT.LOOP1.PSI(39) := 1.5577e+006 ; # 664
677 PLANT.LOOP1.PSI(40) := 1.56129e+006 ; # 665
678 PLANT.LOOP1.PSI(41) := 1.56461e+006 ; # 666
679 PLANT.LOOP1.PSI(42) := 1.56766e+006 ; # 667
680 PLANT.LOOP1.PSI(43) := 1.57047e+006 ; # 668
681 PLANT.LOOP1.PSI(44) := 1.57303e+006 ; # 669
682 PLANT.LOOP1.PSI(45) := 1.57536e+006 ; # 670
683 PLANT.LOOP1.PSI(46) := 1.57746e+006 ; # 671
684 PLANT.LOOP1.PSI(47) := 1.57935e+006 ; # 672
685 PLANT.LOOP1.PSI(48) := 1.58102e+006 ; # 673
686 PLANT.LOOP1.PSI(49) := 1.58249e+006 ; # 674
687 PLANT.LOOP1.PSI(50) := 1.58376e+006 ; # 675
688 PLANT.LOOP1.PSI(51) := 1.58483e+006 ; # 676
689 PLANT.LOOP1.PSI(52) := 1.58571e+006 ; # 677
690 PLANT.LOOP1.PSI(53) := 1.58643e+006 ; # 678
691 PLANT.LOOP1.PSI(54) := 1.58699e+006 ; # 679
692 PLANT.LOOP1.PSI(55) := 1.58747e+006 ; # 680
693 PLANT.LOOP1.PSI(56) := 1.58787e+006 ; # 681
694 PLANT.LOOP1.PSI(57) := 1.58819e+006 ; # 682
695 PLANT.LOOP1.PSI(58) := 1.58843e+006 ; # 683
696 PLANT.LOOP1.PSI(59) := 1.58859e+006 ; # 684
697 PLANT.LOOP1.PSI(60) := 1.58867e+006 ; # 685
698 PLANT.LOOP1.PSI(61) := 1.58867e+006 ; # 686
699 PLANT.LOOP1.PSI(62) := 1.58859e+006 ; # 687
700 PLANT.LOOP1.PSI(63) := 1.58843e+006 ; # 688
701 PLANT.LOOP1.PSI(64) := 1.58819e+006 ; # 689
702 PLANT.LOOP1.PSI(65) := 1.58787e+006 ; # 690

```

703 PLANT.LOOP1.PSI(66) := 1.49858e+006 ; # 691
704 PLANT.LOOP1.PSI(67) := 1.49439e+006 ; # 692
705 PLANT.LOOP1.PSI(68) := 1.49e+006 ; # 693
706 PLANT.LOOP1.PSI(69) := 1.48539e+006 ; # 694
707 PLANT.LOOP1.PSI(70) := 1.48056e+006 ; # 695
708 PLANT.LOOP1.PSI(71) := 1.47548e+006 ; # 696
709 PLANT.LOOP1.PSI(72) := 1.47014e+006 ; # 697
710 PLANT.LOOP1.PSI(73) := 1.46451e+006 ; # 698
711 PLANT.LOOP1.PSI(74) := 1.45857e+006 ; # 699
712 PLANT.LOOP1.PSI(75) := 1.45229e+006 ; # 700
713 PLANT.LOOP1.PSI(76) := 1.44565e+006 ; # 701
714 PLANT.LOOP1.PSI(77) := 1.43862e+006 ; # 702
715 PLANT.LOOP1.PSI(78) := 1.43116e+006 ; # 703
716 PLANT.LOOP1.PSI(79) := 1.42323e+006 ; # 704
717 PLANT.LOOP1.PSI(80) := 1.4148e+006 ; # 705
718 PLANT.LOOP1.PSI(81) := 1.40582e+006 ; # 706
719 PLANT.LOOP1.PSI(82) := 1.39623e+006 ; # 707
720 PLANT.LOOP1.PSI(83) := 1.38599e+006 ; # 708
721 PLANT.LOOP1.PSI(84) := 1.37502e+006 ; # 709
722 PLANT.LOOP1.PSI(85) := 1.36326e+006 ; # 710
723 PLANT.LOOP1.PSI(86) := 1.35062e+006 ; # 711
724 PLANT.LOOP1.PSI(87) := 1.33702e+006 ; # 712
725 PLANT.LOOP1.PSI(88) := 1.32234e+006 ; # 713
726 PLANT.LOOP1.PSI(89) := 1.30649e+006 ; # 714
727 PLANT.LOOP1.PSI(90) := 1.28931e+006 ; # 715
728 PLANT.LOOP1.PSI(91) := 1.27066e+006 ; # 716
729 PLANT.LOOP1.PSI(92) := 1.25037e+006 ; # 717
730 PLANT.LOOP1.PSI(93) := 1.22822e+006 ; # 718
731 PLANT.LOOP1.PSI(94) := 1.20397e+006 ; # 719
732 PLANT.LOOP1.PSI(95) := 1.17735e+006 ; # 720
733 PLANT.LOOP1.PSI(96) := 1.14802e+006 ; # 721
734 PLANT.LOOP1.PSI(97) := 1.11558e+006 ; # 722
735 PLANT.LOOP1.PSI(98) := 1.07957e+006 ; # 723
736 PLANT.LOOP1.PSI(99) := 1.03941e+006 ; # 724
737 PLANT.LOOP1.PSI(100) := 994398 ; # 725
738 PLANT.LOOP1.FEXTRA(1) := 27.6937 ; # 726
739 PLANT.LOOP1.FEXTRA(2) := 27.6937 ; # 726
740 PLANT.LOOP1.F(1) := 27.6937 ; # 726
741 PLANT.LOOP1.F(2) := 27.6937 ; # 727
742 PLANT.LOOP1.F(3) := 27.6937 ; # 728
743 PLANT.LOOP1.F(4) := 27.6937 ; # 729
744 PLANT.LOOP1.F(5) := 27.6937 ; # 730
745 PLANT.LOOP1.F(6) := 27.6937 ; # 731
746 PLANT.LOOP1.F(7) := 27.6937 ; # 732
747 PLANT.LOOP1.F(8) := 27.6937 ; # 733
748 PLANT.LOOP1.F(9) := 27.6937 ; # 734
749 PLANT.LOOP1.F(10) := 27.6937 ; # 735
750 PLANT.LOOP1.F(11) := 27.6937 ; # 736
751 PLANT.LOOP1.F(12) := 27.6937 ; # 737
752 PLANT.LOOP1.F(13) := 27.6937 ; # 738
753 PLANT.LOOP1.F(14) := 27.6937 ; # 739
754 PLANT.LOOP1.F(15) := 27.6937 ; # 740
755 PLANT.LOOP1.F(16) := 27.6937 ; # 741
756 PLANT.LOOP1.F(17) := 27.6937 ; # 742
757 PLANT.LOOP1.F(18) := 27.6937 ; # 743
758 PLANT.LOOP1.F(19) := 27.6937 ; # 744
759 PLANT.LOOP1.F(20) := 27.6937 ; # 745
760 PLANT.LOOP1.F(21) := 27.6937 ; # 746
761 PLANT.LOOP1.F(22) := 27.6937 ; # 747
762 PLANT.LOOP1.F(23) := 27.6937 ; # 748
763 PLANT.LOOP1.F(24) := 27.6937 ; # 749
764 PLANT.LOOP1.F(25) := 27.6937 ; # 750
765 PLANT.LOOP1.F(26) := 27.6937 ; # 751
766 PLANT.LOOP1.F(27) := 27.6937 ; # 752
767 PLANT.LOOP1.F(28) := 27.6937 ; # 753
768 PLANT.LOOP1.F(29) := 27.6937 ; # 754
769 PLANT.LOOP1.F(30) := 27.6937 ; # 755
770 PLANT.LOOP1.F(31) := 27.6937 ; # 756
771 PLANT.LOOP1.F(32) := 27.6937 ; # 757
772 PLANT.LOOP1.F(33) := 27.6937 ; # 758
773 PLANT.LOOP1.F(34) := 27.6937 ; # 759
774 PLANT.LOOP1.F(35) := 27.6937 ; # 760
775 PLANT.LOOP1.F(36) := 27.6937 ; # 761
776 PLANT.LOOP1.F(37) := 27.6937 ; # 762
777 PLANT.LOOP1.F(38) := 27.6937 ; # 763
778 PLANT.LOOP1.F(39) := 27.6937 ; # 764
779 PLANT.LOOP1.F(40) := 27.6937 ; # 765
780 PLANT.LOOP1.F(41) := 27.6937 ; # 766
781 PLANT.LOOP1.F(42) := 27.6937 ; # 767
782 PLANT.LOOP1.F(43) := 27.6937 ; # 768
783 PLANT.LOOP1.F(44) := 27.6937 ; # 769
784 PLANT.LOOP1.F(45) := 27.6937 ; # 770
785 PLANT.LOOP1.F(46) := 27.6937 ; # 771
786 PLANT.LOOP1.F(47) := 27.6937 ; # 772
787 PLANT.LOOP1.F(48) := 27.6937 ; # 773
788 PLANT.LOOP1.F(49) := 27.6937 ; # 774
789 PLANT.LOOP1.F(50) := 27.6937 ; # 775
790 PLANT.LOOP1.F(51) := 27.6937 ; # 776
791 PLANT.LOOP1.F(52) := 27.6937 ; # 777
792 PLANT.LOOP1.F(53) := 27.6937 ; # 778
793 PLANT.LOOP1.F(54) := 27.6937 ; # 779
794 PLANT.LOOP1.F(55) := 27.6937 ; # 780

795 PLANT.LOOP1.F(56) := 27.6937 ; # 781
796 PLANT.LOOP1.F(57) := 27.6937 ; # 782
797 PLANT.LOOP1.F(58) := 27.6937 ; # 783
798 PLANT.LOOP1.F(59) := 27.6937 ; # 784
799 PLANT.LOOP1.F(60) := 27.6937 ; # 785
800 PLANT.LOOP1.F(61) := 27.6937 ; # 786
801 PLANT.LOOP1.F(62) := 27.6937 ; # 787
802 PLANT.LOOP1.F(63) := 27.6937 ; # 788
803 PLANT.LOOP1.F(64) := 27.6937 ; # 789
804 PLANT.LOOP1.F(65) := 27.6937 ; # 790
805 PLANT.LOOP1.F(66) := 27.6937 ; # 791
806 PLANT.LOOP1.F(67) := 27.6937 ; # 792
807 PLANT.LOOP1.F(68) := 27.6937 ; # 793
808 PLANT.LOOP1.F(69) := 27.6937 ; # 794
809 PLANT.LOOP1.F(70) := 27.6937 ; # 795
810 PLANT.LOOP1.F(71) := 27.6937 ; # 796
811 PLANT.LOOP1.F(72) := 27.6937 ; # 797
812 PLANT.LOOP1.F(73) := 27.6937 ; # 798
813 PLANT.LOOP1.F(74) := 27.6937 ; # 799
814 PLANT.LOOP1.F(75) := 27.6937 ; # 800
815 PLANT.LOOP1.F(76) := 27.6937 ; # 801
816 PLANT.LOOP1.F(77) := 27.6937 ; # 802
817 PLANT.LOOP1.F(78) := 27.6937 ; # 803
818 PLANT.LOOP1.F(79) := 27.6937 ; # 804
819 PLANT.LOOP1.F(80) := 27.6937 ; # 805
820 PLANT.LOOP1.F(81) := 27.6937 ; # 806
821 PLANT.LOOP1.F(82) := 27.6937 ; # 807
822 PLANT.LOOP1.F(83) := 27.6937 ; # 808
823 PLANT.LOOP1.F(84) := 27.6937 ; # 809
824 PLANT.LOOP1.F(85) := 27.6937 ; # 810
825 PLANT.LOOP1.F(86) := 27.6937 ; # 811
826 PLANT.LOOP1.F(87) := 27.6937 ; # 812
827 PLANT.LOOP1.F(88) := 27.6937 ; # 813
828 PLANT.LOOP1.F(89) := 27.6937 ; # 814
829 PLANT.LOOP1.F(90) := 27.6937 ; # 815
830 PLANT.LOOP1.F(91) := 27.6937 ; # 816
831 PLANT.LOOP1.F(92) := 27.6937 ; # 817
832 PLANT.LOOP1.F(93) := 27.6937 ; # 818
833 PLANT.LOOP1.F(94) := 27.6937 ; # 819
834 PLANT.LOOP1.F(95) := 27.6937 ; # 820
835 PLANT.LOOP1.F(96) := 27.6937 ; # 821
836 PLANT.LOOP1.F(97) := 27.6937 ; # 822
837 PLANT.LOOP1.F(98) := 27.6937 ; # 823
838 PLANT.LOOP1.F(99) := 27.6937 ; # 824
839 PLANT.LOOP1.F(100) := 27.6937 ; # 825
840 PLANT.LOOP1.F_IN := 27.6937 ; # 826
841 PLANT.LOOP1.RHO_AVG := 0.919725 ; # 827
842 PLANT.LOOP1.TOTALMASS := 27.4149 ; # 828
843 PLANT.LOOP1.HT1.H2 := 17.344 ; # 829
844 PLANT.LOOP1.HT1.RHOPIPEHE := 1.13304 ; # 830
845 PLANT.LOOP1.HT1.VPIPE := 182.461 ; # 831
846 PLANT.LOOP1.HT1.HO := 1563 ; # 832
847 PLANT.LOOP1.HT1.U := 8.93635 ; # 833
848 PLANT.LOOP1.HT2.RHOPIPEHE := 0.915592 ; # 834
849 PLANT.LOOP1.HT2.VPIPE := 87.9967 ; # 835
850 PLANT.LOOP1.HT2.HO := 1665.62 ; # 836
851 PLANT.LOOP1.HT2.U := 1645.45 ; # 837
852 PLANT.LOOP1.HT3.H2 := 17.344 ; # 838
853 PLANT.LOOP1.HT3.RHOPIPEHE := 0.75785 ; # 839
854 PLANT.LOOP1.HT3.VPIPE := 236.032 ; # 840
855 PLANT.LOOP1.HT3.HO := 1372.09 ; # 841
856 PLANT.LOOP1.HT3.U := 10.3605 ; # 842
857 PLANT.LOOP1.HT4.RHOPIPEHE := 0.829069 ; # 843
858 PLANT.LOOP1.HT4.VPIPE := 83.9116 ; # 844
859 PLANT.LOOP1.HT4.U := 1299.78 ; # 845
860 PLANT.PIPEH.RHO(1) := 2.88031 ; # 846
861 PLANT.PIPEH.RHO(2) := 2.88987 ; # 847
862 PLANT.PIPEH.RHO(3) := 2.89973 ; # 848
863 PLANT.PIPEH.RHO(4) := 2.90991 ; # 849
864 PLANT.PIPEH.RHO(5) := 2.92042 ; # 850
865 PLANT.PIPEH.RHO(6) := 2.93127 ; # 851
866 PLANT.PIPEH.RHO(7) := 2.94248 ; # 852
867 PLANT.PIPEH.RHO(8) := 2.95405 ; # 853
868 PLANT.PIPEH.RHO(9) := 2.96601 ; # 854
869 PLANT.PIPEH.RHO(10) := 2.97836 ; # 855
870 PLANT.PIPEH.RHO(11) := 2.99112 ; # 856
871 PLANT.PIPEH.RHO(12) := 3.00432 ; # 857
872 PLANT.PIPEH.RHO(13) := 3.01796 ; # 858
873 PLANT.PIPEH.RHO(14) := 3.03206 ; # 859
874 PLANT.PIPEH.RHO(15) := 3.04666 ; # 860
875 PLANT.PIPEH.RHO(16) := 3.06175 ; # 861
876 PLANT.PIPEH.RHO(17) := 3.07737 ; # 862
877 PLANT.PIPEH.RHO(18) := 3.09354 ; # 863
878 PLANT.PIPEH.RHO(19) := 3.11029 ; # 864
879 PLANT.PIPEH.RHO(20) := 3.12763 ; # 865
880 PLANT.PIPEH.RHO(21) := 3.1456 ; # 866
881 PLANT.PIPEH.RHO(22) := 3.16422 ; # 867
882 PLANT.PIPEH.RHO(23) := 3.18352 ; # 868
883 PLANT.PIPEH.RHO(24) := 3.20354 ; # 869
884 PLANT.PIPEH.RHO(25) := 3.22431 ; # 870
885 PLANT.PIPEH.RHO(26) := 3.24587 ; # 871
886 PLANT.PIPEH.RHO(27) := 3.26824 ; # 872

887 PLANT.PIPEH.RHO(28) := 3.29149 ; # 873
888 PLANT.PIPEH.RHO(29) := 3.31563 ; # 874
889 PLANT.PIPEH.RHO(30) := 3.34074 ; # 875
890 PLANT.PIPEH.RHO(31) := 3.36684 ; # 876
891 PLANT.PIPEH.RHO(32) := 3.394 ; # 877
892 PLANT.PIPEH.RHO(33) := 3.42228 ; # 878
893 PLANT.PIPEH.RHO(34) := 3.45173 ; # 879
894 PLANT.PIPEH.RHO(35) := 3.48241 ; # 880
895 PLANT.PIPEH.RHO(36) := 3.5144 ; # 881
896 PLANT.PIPEH.RHO(37) := 3.54778 ; # 882
897 PLANT.PIPEH.RHO(38) := 3.58262 ; # 883
898 PLANT.PIPEH.RHO(39) := 3.61901 ; # 884
899 PLANT.PIPEH.RHO(40) := 3.65698 ; # 885
900 PLANT.PIPEH.P(1) := 6.9993e+006 ; # 886
901 PLANT.PIPEH.P(2) := 6.99792e+006 ; # 887
902 PLANT.PIPEH.P(3) := 6.99655e+006 ; # 888
903 PLANT.PIPEH.P(4) := 6.99518e+006 ; # 889
904 PLANT.PIPEH.P(5) := 6.99382e+006 ; # 890
905 PLANT.PIPEH.P(6) := 6.99246e+006 ; # 891
906 PLANT.PIPEH.P(7) := 6.9911e+006 ; # 892
907 PLANT.PIPEH.P(8) := 6.98976e+006 ; # 893
908 PLANT.PIPEH.P(9) := 6.98841e+006 ; # 894
909 PLANT.PIPEH.P(10) := 6.98708e+006 ; # 895
910 PLANT.PIPEH.P(11) := 6.98575e+006 ; # 896
911 PLANT.PIPEH.P(12) := 6.98442e+006 ; # 897
912 PLANT.PIPEH.P(13) := 6.9831e+006 ; # 898
913 PLANT.PIPEH.P(14) := 6.98179e+006 ; # 899
914 PLANT.PIPEH.P(15) := 6.98049e+006 ; # 900
915 PLANT.PIPEH.P(16) := 6.97919e+006 ; # 901
916 PLANT.PIPEH.P(17) := 6.9779e+006 ; # 902
917 PLANT.PIPEH.P(18) := 6.97661e+006 ; # 903
918 PLANT.PIPEH.P(19) := 6.97534e+006 ; # 904
919 PLANT.PIPEH.P(20) := 6.97407e+006 ; # 905
920 PLANT.PIPEH.P(21) := 6.97281e+006 ; # 906
921 PLANT.PIPEH.P(22) := 6.97155e+006 ; # 907
922 PLANT.PIPEH.P(23) := 6.97031e+006 ; # 908
923 PLANT.PIPEH.P(24) := 6.96907e+006 ; # 909
924 PLANT.PIPEH.P(25) := 6.96784e+006 ; # 910
925 PLANT.PIPEH.P(26) := 6.96662e+006 ; # 911
926 PLANT.PIPEH.P(27) := 6.9654e+006 ; # 912
927 PLANT.PIPEH.P(28) := 6.9642e+006 ; # 913
928 PLANT.PIPEH.P(29) := 6.96301e+006 ; # 914
929 PLANT.PIPEH.P(30) := 6.96182e+006 ; # 915
930 PLANT.PIPEH.P(31) := 6.96065e+006 ; # 916
931 PLANT.PIPEH.P(32) := 6.95948e+006 ; # 917
932 PLANT.PIPEH.P(33) := 6.95833e+006 ; # 918
933 PLANT.PIPEH.P(34) := 6.95718e+006 ; # 919
934 PLANT.PIPEH.P(35) := 6.95605e+006 ; # 920
935 PLANT.PIPEH.P(36) := 6.95493e+006 ; # 921
936 PLANT.PIPEH.P(37) := 6.95381e+006 ; # 922
937 PLANT.PIPEH.P(38) := 6.95271e+006 ; # 923
938 PLANT.PIPEH.P(39) := 6.95162e+006 ; # 924
939 PLANT.PIPEH.P(40) := 6.95055e+006 ; # 925
940 PLANT.PIPEH.H(1) := 4.52556e+006 ; # 926
941 PLANT.PIPEH.H(2) := 4.50427e+006 ; # 927
942 PLANT.PIPEH.H(3) := 4.4825e+006 ; # 928
943 PLANT.PIPEH.H(4) := 4.46023e+006 ; # 929
944 PLANT.PIPEH.H(5) := 4.43744e+006 ; # 930
945 PLANT.PIPEH.H(6) := 4.41412e+006 ; # 931
946 PLANT.PIPEH.H(7) := 4.39027e+006 ; # 932
947 PLANT.PIPEH.H(8) := 4.36587e+006 ; # 933
948 PLANT.PIPEH.H(9) := 4.3409e+006 ; # 934
949 PLANT.PIPEH.H(10) := 4.31535e+006 ; # 935
950 PLANT.PIPEH.H(11) := 4.28922e+006 ; # 936
951 PLANT.PIPEH.H(12) := 4.26248e+006 ; # 937
952 PLANT.PIPEH.H(13) := 4.23513e+006 ; # 938
953 PLANT.PIPEH.H(14) := 4.20714e+006 ; # 939
954 PLANT.PIPEH.H(15) := 4.17851e+006 ; # 940
955 PLANT.PIPEH.H(16) := 4.14921e+006 ; # 941
956 PLANT.PIPEH.H(17) := 4.11924e+006 ; # 942
957 PLANT.PIPEH.H(18) := 4.08858e+006 ; # 943
958 PLANT.PIPEH.H(19) := 4.05721e+006 ; # 944
959 PLANT.PIPEH.H(20) := 4.02511e+006 ; # 945
960 PLANT.PIPEH.H(21) := 3.99227e+006 ; # 946
961 PLANT.PIPEH.H(22) := 3.95868e+006 ; # 947
962 PLANT.PIPEH.H(23) := 3.92431e+006 ; # 948
963 PLANT.PIPEH.H(24) := 3.88914e+006 ; # 949
964 PLANT.PIPEH.H(25) := 3.85317e+006 ; # 950
965 PLANT.PIPEH.H(26) := 3.81636e+006 ; # 951
966 PLANT.PIPEH.H(27) := 3.7787e+006 ; # 952
967 PLANT.PIPEH.H(28) := 3.74017e+006 ; # 953
968 PLANT.PIPEH.H(29) := 3.70076e+006 ; # 954
969 PLANT.PIPEH.H(30) := 3.66043e+006 ; # 955
970 PLANT.PIPEH.H(31) := 3.61917e+006 ; # 956
971 PLANT.PIPEH.H(32) := 3.57696e+006 ; # 957
972 PLANT.PIPEH.H(33) := 3.53378e+006 ; # 958
973 PLANT.PIPEH.H(34) := 3.48959e+006 ; # 959
974 PLANT.PIPEH.H(35) := 3.44439e+006 ; # 960
975 PLANT.PIPEH.H(36) := 3.39814e+006 ; # 961
976 PLANT.PIPEH.H(37) := 3.35083e+006 ; # 962
977 PLANT.PIPEH.H(38) := 3.30242e+006 ; # 963
978 PLANT.PIPEH.H(39) := 3.2529e+006 ; # 964

```

979 PLANT.PIPEH.H(40) := 3.20232e+006 ; # 965
980 PLANT.PIPEH.H0 := 4.5464e+006 ; # 966
981 PLANT.PIPEH.T(1) := 1169.14 ; # 967
982 PLANT.PIPEH.T(2) := 1165.04 ; # 968
983 PLANT.PIPEH.T(3) := 1160.85 ; # 969
984 PLANT.PIPEH.T(4) := 1156.56 ; # 970
985 PLANT.PIPEH.T(5) := 1152.18 ; # 971
986 PLANT.PIPEH.T(6) := 1147.69 ; # 972
987 PLANT.PIPEH.T(7) := 1143.1 ; # 973
988 PLANT.PIPEH.T(8) := 1138.4 ; # 974
989 PLANT.PIPEH.T(9) := 1133.59 ; # 975
990 PLANT.PIPEH.T(10) := 1128.67 ; # 976
991 PLANT.PIPEH.T(11) := 1123.64 ; # 977
992 PLANT.PIPEH.T(12) := 1118.5 ; # 978
993 PLANT.PIPEH.T(13) := 1113.23 ; # 979
994 PLANT.PIPEH.T(14) := 1107.84 ; # 980
995 PLANT.PIPEH.T(15) := 1102.33 ; # 981
996 PLANT.PIPEH.T(16) := 1096.69 ; # 982
997 PLANT.PIPEH.T(17) := 1090.92 ; # 983
998 PLANT.PIPEH.T(18) := 1085.02 ; # 984
999 PLANT.PIPEH.T(19) := 1078.98 ; # 985
1000 PLANT.PIPEH.T(20) := 1072.8 ; # 986
1001 PLANT.PIPEH.T(21) := 1066.48 ; # 987
1002 PLANT.PIPEH.T(22) := 1060.02 ; # 988
1003 PLANT.PIPEH.T(23) := 1053.4 ; # 989
1004 PLANT.PIPEH.T(24) := 1046.63 ; # 990
1005 PLANT.PIPEH.T(25) := 1039.71 ; # 991
1006 PLANT.PIPEH.T(26) := 1032.62 ; # 992
1007 PLANT.PIPEH.T(27) := 1025.37 ; # 993
1008 PLANT.PIPEH.T(28) := 1017.96 ; # 994
1009 PLANT.PIPEH.T(29) := 1010.37 ; # 995
1010 PLANT.PIPEH.T(30) := 1002.61 ; # 996
1011 PLANT.PIPEH.T(31) := 994.665 ; # 997
1012 PLANT.PIPEH.T(32) := 986.539 ; # 998
1013 PLANT.PIPEH.T(33) := 978.227 ; # 999
1014 PLANT.PIPEH.T(34) := 969.722 ; # 1000
1015 PLANT.PIPEH.T(35) := 961.02 ; # 1001
1016 PLANT.PIPEH.T(36) := 952.118 ; # 1002
1017 PLANT.PIPEH.T(37) := 943.011 ; # 1003
1018 PLANT.PIPEH.T(38) := 933.692 ; # 1004
1019 PLANT.PIPEH.T(39) := 924.159 ; # 1005
1020 PLANT.PIPEH.T(40) := 914.423 ; # 1006
1021 PLANT.PIPEH.TEXTRNL(1) := 1159 ; # 1007
1022 PLANT.PIPEH.TEXTRNL(2) := 1154.7 ; # 1008
1023 PLANT.PIPEH.TEXTRNL(3) := 1150.27 ; # 1009
1024 PLANT.PIPEH.TEXTRNL(4) := 1145.73 ; # 1010
1025 PLANT.PIPEH.TEXTRNL(5) := 1141.1 ; # 1011
1026 PLANT.PIPEH.TEXTRNL(6) := 1136.35 ; # 1012
1027 PLANT.PIPEH.TEXTRNL(7) := 1131.5 ; # 1013
1028 PLANT.PIPEH.TEXTRNL(8) := 1126.53 ; # 1014
1029 PLANT.PIPEH.TEXTRNL(9) := 1121.45 ; # 1015
1030 PLANT.PIPEH.TEXTRNL(10) := 1116.26 ; # 1016
1031 PLANT.PIPEH.TEXTRNL(11) := 1110.94 ; # 1017
1032 PLANT.PIPEH.TEXTRNL(12) := 1105.5 ; # 1018
1033 PLANT.PIPEH.TEXTRNL(13) := 1099.93 ; # 1019
1034 PLANT.PIPEH.TEXTRNL(14) := 1094.24 ; # 1020
1035 PLANT.PIPEH.TEXTRNL(15) := 1088.41 ; # 1021
1036 PLANT.PIPEH.TEXTRNL(16) := 1082.45 ; # 1022
1037 PLANT.PIPEH.TEXTRNL(17) := 1076.36 ; # 1023
1038 PLANT.PIPEH.TEXTRNL(18) := 1070.12 ; # 1024
1039 PLANT.PIPEH.TEXTRNL(19) := 1063.73 ; # 1025
1040 PLANT.PIPEH.TEXTRNL(20) := 1057.2 ; # 1026
1041 PLANT.PIPEH.TEXTRNL(21) := 1050.52 ; # 1027
1042 PLANT.PIPEH.TEXTRNL(22) := 1043.69 ; # 1028
1043 PLANT.PIPEH.TEXTRNL(23) := 1036.69 ; # 1029
1044 PLANT.PIPEH.TEXTRNL(24) := 1029.54 ; # 1030
1045 PLANT.PIPEH.TEXTRNL(25) := 1022.22 ; # 1031
1046 PLANT.PIPEH.TEXTRNL(26) := 1014.73 ; # 1032
1047 PLANT.PIPEH.TEXTRNL(27) := 1007.07 ; # 1033
1048 PLANT.PIPEH.TEXTRNL(28) := 999.229 ; # 1034
1049 PLANT.PIPEH.TEXTRNL(29) := 991.209 ; # 1035
1050 PLANT.PIPEH.TEXTRNL(30) := 983.004 ; # 1036
1051 PLANT.PIPEH.TEXTRNL(31) := 974.61 ; # 1037
1052 PLANT.PIPEH.TEXTRNL(32) := 966.021 ; # 1038
1053 PLANT.PIPEH.TEXTRNL(33) := 957.235 ; # 1039
1054 PLANT.PIPEH.TEXTRNL(34) := 948.245 ; # 1040
1055 PLANT.PIPEH.TEXTRNL(35) := 939.048 ; # 1041
1056 PLANT.PIPEH.TEXTRNL(36) := 929.638 ; # 1042
1057 PLANT.PIPEH.TEXTRNL(37) := 920.011 ; # 1043
1058 PLANT.PIPEH.TEXTRNL(38) := 910.162 ; # 1044
1059 PLANT.PIPEH.TEXTRNL(39) := 900.086 ; # 1045
1060 PLANT.PIPEH.TEXTRNL(40) := 889.835 ; # 1046
1061 PLANT.PIPEH.F(1) := 32.4687 ; # 1047
1062 PLANT.PIPEH.F(2) := 32.4687 ; # 1048
1063 PLANT.PIPEH.F(3) := 32.4687 ; # 1049
1064 PLANT.PIPEH.F(4) := 32.4687 ; # 1050
1065 PLANT.PIPEH.F(5) := 32.4687 ; # 1051
1066 PLANT.PIPEH.F(6) := 32.4687 ; # 1052
1067 PLANT.PIPEH.F(7) := 32.4687 ; # 1053
1068 PLANT.PIPEH.F(8) := 32.4687 ; # 1054
1069 PLANT.PIPEH.F(9) := 32.4687 ; # 1055
1070 PLANT.PIPEH.F(10) := 32.4687 ; # 1056

```


1071 PLANT.PIPEH.F(11) := 32.4687 ; # 1057
1072 PLANT.PIPEH.F(12) := 32.4687 ; # 1058
1073 PLANT.PIPEH.F(13) := 32.4687 ; # 1059
1074 PLANT.PIPEH.F(14) := 32.4687 ; # 1060
1075 PLANT.PIPEH.F(15) := 32.4687 ; # 1061
1076 PLANT.PIPEH.F(16) := 32.4687 ; # 1062
1077 PLANT.PIPEH.F(17) := 32.4687 ; # 1063
1078 PLANT.PIPEH.F(18) := 32.4687 ; # 1064
1079 PLANT.PIPEH.F(19) := 32.4687 ; # 1065
1080 PLANT.PIPEH.F(20) := 32.4687 ; # 1066
1081 PLANT.PIPEH.F(21) := 32.4687 ; # 1067
1082 PLANT.PIPEH.F(22) := 32.4687 ; # 1068
1083 PLANT.PIPEH.F(23) := 32.4687 ; # 1069
1084 PLANT.PIPEH.F(24) := 32.4687 ; # 1070
1085 PLANT.PIPEH.F(25) := 32.4687 ; # 1071
1086 PLANT.PIPEH.F(26) := 32.4687 ; # 1072
1087 PLANT.PIPEH.F(27) := 32.4687 ; # 1073
1088 PLANT.PIPEH.F(28) := 32.4687 ; # 1074
1089 PLANT.PIPEH.F(29) := 32.4687 ; # 1075
1090 PLANT.PIPEH.F(30) := 32.4687 ; # 1076
1091 PLANT.PIPEH.F(31) := 32.4687 ; # 1077
1092 PLANT.PIPEH.F(32) := 32.4687 ; # 1078
1093 PLANT.PIPEH.F(33) := 32.4687 ; # 1079
1094 PLANT.PIPEH.F(34) := 32.4687 ; # 1080
1095 PLANT.PIPEH.F(35) := 32.4687 ; # 1081
1096 PLANT.PIPEH.F(36) := 32.4687 ; # 1082
1097 PLANT.PIPEH.F(37) := 32.4687 ; # 1083
1098 PLANT.PIPEH.F(38) := 32.4687 ; # 1084
1099 PLANT.PIPEH.F(39) := 32.4687 ; # 1085
1100 PLANT.PIPEH.F(40) := 32.4687 ; # 1086
1101 PLANT.PIPEH.F_IN := 32.4687 ; # 1087
1102 PLANT.PIPEH.PSI(1) := 6.03571e+006 ; # 1088
1103 PLANT.PIPEH.PSI(2) := 6.01884e+006 ; # 1089
1104 PLANT.PIPEH.PSI(3) := 6.00151e+006 ; # 1090
1105 PLANT.PIPEH.PSI(4) := 5.9837e+006 ; # 1091
1106 PLANT.PIPEH.PSI(5) := 5.96538e+006 ; # 1092
1107 PLANT.PIPEH.PSI(6) := 5.94655e+006 ; # 1093
1108 PLANT.PIPEH.PSI(7) := 5.92717e+006 ; # 1094
1109 PLANT.PIPEH.PSI(8) := 5.90723e+006 ; # 1095
1110 PLANT.PIPEH.PSI(9) := 5.88672e+006 ; # 1096
1111 PLANT.PIPEH.PSI(10) := 5.86559e+006 ; # 1097
1112 PLANT.PIPEH.PSI(11) := 5.84383e+006 ; # 1098
1113 PLANT.PIPEH.PSI(12) := 5.82142e+006 ; # 1099
1114 PLANT.PIPEH.PSI(13) := 5.79833e+006 ; # 1100
1115 PLANT.PIPEH.PSI(14) := 5.77452e+006 ; # 1101
1116 PLANT.PIPEH.PSI(15) := 5.74998e+006 ; # 1102
1117 PLANT.PIPEH.PSI(16) := 5.72466e+006 ; # 1103
1118 PLANT.PIPEH.PSI(17) := 5.69854e+006 ; # 1104
1119 PLANT.PIPEH.PSI(18) := 5.67158e+006 ; # 1105
1120 PLANT.PIPEH.PSI(19) := 5.64374e+006 ; # 1106
1121 PLANT.PIPEH.PSI(20) := 5.61499e+006 ; # 1107
1122 PLANT.PIPEH.PSI(21) := 5.58528e+006 ; # 1108
1123 PLANT.PIPEH.PSI(22) := 5.55457e+006 ; # 1109
1124 PLANT.PIPEH.PSI(23) := 5.52282e+006 ; # 1110
1125 PLANT.PIPEH.PSI(24) := 5.48997e+006 ; # 1111
1126 PLANT.PIPEH.PSI(25) := 5.45597e+006 ; # 1112
1127 PLANT.PIPEH.PSI(26) := 5.42078e+006 ; # 1113
1128 PLANT.PIPEH.PSI(27) := 5.38432e+006 ; # 1114
1129 PLANT.PIPEH.PSI(28) := 5.34653e+006 ; # 1115
1130 PLANT.PIPEH.PSI(29) := 5.30735e+006 ; # 1116
1131 PLANT.PIPEH.PSI(30) := 5.26672e+006 ; # 1117
1132 PLANT.PIPEH.PSI(31) := 5.22454e+006 ; # 1118
1133 PLANT.PIPEH.PSI(32) := 5.18075e+006 ; # 1119
1134 PLANT.PIPEH.PSI(33) := 5.13524e+006 ; # 1120
1135 PLANT.PIPEH.PSI(34) := 5.08794e+006 ; # 1121
1136 PLANT.PIPEH.PSI(35) := 5.03874e+006 ; # 1122
1137 PLANT.PIPEH.PSI(36) := 4.98752e+006 ; # 1123
1138 PLANT.PIPEH.PSI(37) := 4.93419e+006 ; # 1124
1139 PLANT.PIPEH.PSI(38) := 4.8786e+006 ; # 1125
1140 PLANT.PIPEH.PSI(39) := 4.82064e+006 ; # 1126
1141 PLANT.PIPEH.PSI(40) := 4.76024e+006 ; # 1127
1142 PLANT.PIPEH.HT.RHOPIPEH := 3.1094 ; # 1128
1143 PLANT.PIPEH.HT.VPIPE := 28.7014 ; # 1129
1144 PLANT.PIPEH.HT.HO := 1760.94 ; # 1130
1145 PLANT.PIPEH.HT.U := 1738.41 ; # 1131
1146 PLANT.HX2.TGASHOT(1) := 1136.77 ; # 1132
1147 PLANT.HX2.TGASHOT(2) := 1136.79 ; # 1133
1148 PLANT.HX2.TGASHOT(3) := 1134.68 ; # 1134
1149 PLANT.HX2.TGASHOT(4) := 1132.42 ; # 1135
1150 PLANT.HX2.TGASHOT(5) := 1130.02 ; # 1136
1151 PLANT.HX2.TGASHOT(6) := 1127.46 ; # 1137
1152 PLANT.HX2.TGASHOT(7) := 1124.73 ; # 1138
1153 PLANT.HX2.TGASHOT(8) := 1121.82 ; # 1139
1154 PLANT.HX2.TGASHOT(9) := 1118.71 ; # 1140
1155 PLANT.HX2.TGASHOT(10) := 1115.4 ; # 1141
1156 PLANT.HX2.TGASHOT(11) := 1111.87 ; # 1142
1157 PLANT.HX2.TGASHOT(12) := 1108.11 ; # 1143
1158 PLANT.HX2.TGASHOT(13) := 1104.09 ; # 1144
1159 PLANT.HX2.TGASHOT(14) := 1099.81 ; # 1145
1160 PLANT.HX2.TGASHOT(15) := 1095.25 ; # 1146
1161 PLANT.HX2.TGASHOT(16) := 1090.38 ; # 1147
1162 PLANT.HX2.TGASHOT(17) := 1085.19 ; # 1148

1163 PLANT.HX2.TGASHOT(18) := 1079.65 ; # 1149
1164 PLANT.HX2.TGASHOT(19) := 1073.75 ; # 1150
1165 PLANT.HX2.TGASHOT(20) := 1067.46 ; # 1151
1166 PLANT.HX2.TGASHOT(21) := 1060.75 ; # 1152
1167 PLANT.HX2.TGASHOT(22) := 1053.59 ; # 1153
1168 PLANT.HX2.TGASHOT(23) := 1045.96 ; # 1154
1169 PLANT.HX2.TGASHOT(24) := 1037.83 ; # 1155
1170 PLANT.HX2.TGASHOT(25) := 1029.15 ; # 1156
1171 PLANT.HX2.TGASHOT(26) := 1019.9 ; # 1157
1172 PLANT.HX2.TGASHOT(27) := 1010.03 ; # 1158
1173 PLANT.HX2.TGASHOT(28) := 999.513 ; # 1159
1174 PLANT.HX2.TGASHOT(29) := 988.296 ; # 1160
1175 PLANT.HX2.TGASHOT(30) := 976.334 ; # 1161
1176 PLANT.HX2.TGASHOT(31) := 963.58 ; # 1162
1177 PLANT.HX2.TGASHOT(32) := 949.979 ; # 1163
1178 PLANT.HX2.TGASHOT(33) := 935.476 ; # 1164
1179 PLANT.HX2.TGASHOT(34) := 920.011 ; # 1165
1180 PLANT.HX2.TGASHOT(35) := 903.52 ; # 1166
1181 PLANT.HX2.TGASHOT(36) := 885.936 ; # 1167
1182 PLANT.HX2.TGASHOT(37) := 867.185 ; # 1168
1183 PLANT.HX2.TGASHOT(38) := 847.191 ; # 1169
1184 PLANT.HX2.TGASHOT(39) := 825.87 ; # 1170
1185 PLANT.HX2.TGASHOT(40) := 803.137 ; # 1171
1186 PLANT.HX2.TGASCOLD(1) := 1126.15 ; # 1172
1187 PLANT.HX2.TGASCOLD(2) := 1123.33 ; # 1173
1188 PLANT.HX2.TGASCOLD(3) := 1120.32 ; # 1174
1189 PLANT.HX2.TGASCOLD(4) := 1117.12 ; # 1175
1190 PLANT.HX2.TGASCOLD(5) := 1113.7 ; # 1176
1191 PLANT.HX2.TGASCOLD(6) := 1110.06 ; # 1177
1192 PLANT.HX2.TGASCOLD(7) := 1106.17 ; # 1178
1193 PLANT.HX2.TGASCOLD(8) := 1102.03 ; # 1179
1194 PLANT.HX2.TGASCOLD(9) := 1097.61 ; # 1180
1195 PLANT.HX2.TGASCOLD(10) := 1092.9 ; # 1181
1196 PLANT.HX2.TGASCOLD(11) := 1087.88 ; # 1182
1197 PLANT.HX2.TGASCOLD(12) := 1082.52 ; # 1183
1198 PLANT.HX2.TGASCOLD(13) := 1076.81 ; # 1184
1199 PLANT.HX2.TGASCOLD(14) := 1070.72 ; # 1185
1200 PLANT.HX2.TGASCOLD(15) := 1064.23 ; # 1186
1201 PLANT.HX2.TGASCOLD(16) := 1057.3 ; # 1187
1202 PLANT.HX2.TGASCOLD(17) := 1049.92 ; # 1188
1203 PLANT.HX2.TGASCOLD(18) := 1042.04 ; # 1189
1204 PLANT.HX2.TGASCOLD(19) := 1033.65 ; # 1190
1205 PLANT.HX2.TGASCOLD(20) := 1024.69 ; # 1191
1206 PLANT.HX2.TGASCOLD(21) := 1015.15 ; # 1192
1207 PLANT.HX2.TGASCOLD(22) := 1004.97 ; # 1193
1208 PLANT.HX2.TGASCOLD(23) := 994.111 ; # 1194
1209 PLANT.HX2.TGASCOLD(24) := 982.535 ; # 1195
1210 PLANT.HX2.TGASCOLD(25) := 970.192 ; # 1196
1211 PLANT.HX2.TGASCOLD(26) := 957.03 ; # 1197
1212 PLANT.HX2.TGASCOLD(27) := 942.994 ; # 1198
1213 PLANT.HX2.TGASCOLD(28) := 928.028 ; # 1199
1214 PLANT.HX2.TGASCOLD(29) := 912.069 ; # 1200
1215 PLANT.HX2.TGASCOLD(30) := 895.052 ; # 1201
1216 PLANT.HX2.TGASCOLD(31) := 876.906 ; # 1202
1217 PLANT.HX2.TGASCOLD(32) := 857.556 ; # 1203
1218 PLANT.HX2.TGASCOLD(33) := 836.923 ; # 1204
1219 PLANT.HX2.TGASCOLD(34) := 814.921 ; # 1205
1220 PLANT.HX2.TGASCOLD(35) := 791.46 ; # 1206
1221 PLANT.HX2.TGASCOLD(36) := 766.443 ; # 1207
1222 PLANT.HX2.TGASCOLD(37) := 739.767 ; # 1208
1223 PLANT.HX2.TGASCOLD(38) := 711.321 ; # 1209
1224 PLANT.HX2.TGASCOLD(39) := 680.988 ; # 1210
1225 PLANT.HX2.TGASCOLD(40) := 648.643 ; # 1211
1226 PLANT.HX2.UHOT := 1299.78 ; # 1212
1227 PLANT.HX2.UCOLD := 1880.53 ; # 1213
1228 PLANT.HX2.THX(1) := 1132.12 ; # 1214
1229 PLANT.HX2.THX(2) := 1129.7 ; # 1215
1230 PLANT.HX2.THX(3) := 1127.12 ; # 1216
1231 PLANT.HX2.THX(4) := 1124.36 ; # 1217
1232 PLANT.HX2.THX(5) := 1121.43 ; # 1218
1233 PLANT.HX2.THX(6) := 1118.29 ; # 1219
1234 PLANT.HX2.THX(7) := 1114.96 ; # 1220
1235 PLANT.HX2.THX(8) := 1111.4 ; # 1221
1236 PLANT.HX2.THX(9) := 1107.6 ; # 1222
1237 PLANT.HX2.THX(10) := 1103.55 ; # 1223
1238 PLANT.HX2.THX(11) := 1099.23 ; # 1224
1239 PLANT.HX2.THX(12) := 1094.63 ; # 1225
1240 PLANT.HX2.THX(13) := 1089.72 ; # 1226
1241 PLANT.HX2.THX(14) := 1084.49 ; # 1227
1242 PLANT.HX2.THX(15) := 1078.91 ; # 1228
1243 PLANT.HX2.THX(16) := 1072.96 ; # 1229
1244 PLANT.HX2.THX(17) := 1066.61 ; # 1230
1245 PLANT.HX2.THX(18) := 1059.84 ; # 1231
1246 PLANT.HX2.THX(19) := 1052.63 ; # 1232
1247 PLANT.HX2.THX(20) := 1044.93 ; # 1233
1248 PLANT.HX2.THX(21) := 1036.73 ; # 1234
1249 PLANT.HX2.THX(22) := 1027.98 ; # 1235
1250 PLANT.HX2.THX(23) := 1018.65 ; # 1236
1251 PLANT.HX2.THX(24) := 1008.7 ; # 1237
1252 PLANT.HX2.THX(25) := 998.095 ; # 1238
1253 PLANT.HX2.THX(26) := 986.784 ; # 1239
1254 PLANT.HX2.THX(27) := 974.722 ; # 1240

1255 PLANT.HX2.THX(28) := 961.86 ; # 1241
1256 PLANT.HX2.THX(29) := 948.145 ; # 1242
1257 PLANT.HX2.THX(30) := 933.521 ; # 1243
1258 PLANT.HX2.THX(31) := 917.926 ; # 1244
1259 PLANT.HX2.THX(32) := 901.297 ; # 1245
1260 PLANT.HX2.THX(33) := 883.565 ; # 1246
1261 PLANT.HX2.THX(34) := 864.657 ; # 1247
1262 PLANT.HX2.THX(35) := 844.495 ; # 1248
1263 PLANT.HX2.THX(36) := 822.996 ; # 1249
1264 PLANT.HX2.THX(37) := 800.07 ; # 1250
1265 PLANT.HX2.THX(38) := 775.624 ; # 1251
1266 PLANT.HX2.THX(39) := 749.557 ; # 1252
1267 PLANT.HX2.THX(40) := 721.768 ; # 1253
1268 PLANT.PIPEC2.RHO(1) := 3.7063 ; # 1254
1269 PLANT.PIPEC2.RHO(2) := 3.52381 ; # 1255
1270 PLANT.PIPEC2.RHO(3) := 3.36718 ; # 1256
1271 PLANT.PIPEC2.RHO(4) := 3.2314 ; # 1257
1272 PLANT.PIPEC2.RHO(5) := 3.11269 ; # 1258
1273 PLANT.PIPEC2.RHO(6) := 3.0081 ; # 1259
1274 PLANT.PIPEC2.RHO(7) := 2.91535 ; # 1260
1275 PLANT.PIPEC2.RHO(8) := 2.83259 ; # 1261
1276 PLANT.PIPEC2.RHO(9) := 2.75835 ; # 1262
1277 PLANT.PIPEC2.RHO(10) := 2.69142 ; # 1263
1278 PLANT.PIPEC2.RHO(11) := 2.63081 ; # 1264
1279 PLANT.PIPEC2.RHO(12) := 2.5757 ; # 1265
1280 PLANT.PIPEC2.RHO(13) := 2.52539 ; # 1266
1281 PLANT.PIPEC2.RHO(14) := 2.47931 ; # 1267
1282 PLANT.PIPEC2.RHO(15) := 2.43696 ; # 1268
1283 PLANT.PIPEC2.RHO(16) := 2.39791 ; # 1269
1284 PLANT.PIPEC2.RHO(17) := 2.3618 ; # 1270
1285 PLANT.PIPEC2.RHO(18) := 2.32832 ; # 1271
1286 PLANT.PIPEC2.RHO(19) := 2.29719 ; # 1272
1287 PLANT.PIPEC2.RHO(20) := 2.26818 ; # 1273
1288 PLANT.PIPEC2.RHO(21) := 2.24106 ; # 1274
1289 PLANT.PIPEC2.RHO(22) := 2.21566 ; # 1275
1290 PLANT.PIPEC2.RHO(23) := 2.19182 ; # 1276
1291 PLANT.PIPEC2.RHO(24) := 2.16939 ; # 1277
1292 PLANT.PIPEC2.RHO(25) := 2.14823 ; # 1278
1293 PLANT.PIPEC2.RHO(26) := 2.12824 ; # 1279
1294 PLANT.PIPEC2.RHO(27) := 2.10932 ; # 1280
1295 PLANT.PIPEC2.RHO(28) := 2.09136 ; # 1281
1296 PLANT.PIPEC2.RHO(29) := 2.07429 ; # 1282
1297 PLANT.PIPEC2.RHO(30) := 2.05802 ; # 1283
1298 PLANT.PIPEC2.RHO(31) := 2.0425 ; # 1284
1299 PLANT.PIPEC2.RHO(32) := 2.02766 ; # 1285
1300 PLANT.PIPEC2.RHO(33) := 2.01345 ; # 1286
1301 PLANT.PIPEC2.RHO(34) := 1.99981 ; # 1287
1302 PLANT.PIPEC2.RHO(35) := 1.9867 ; # 1288
1303 PLANT.PIPEC2.RHO(36) := 1.97407 ; # 1289
1304 PLANT.PIPEC2.RHO(37) := 1.96189 ; # 1290
1305 PLANT.PIPEC2.RHO(38) := 1.95011 ; # 1291
1306 PLANT.PIPEC2.RHO(39) := 1.93872 ; # 1292
1307 PLANT.PIPEC2.RHO(40) := 1.92768 ; # 1293
1308 PLANT.PIPEC2.P(1) := 1.10918e+006 ; # 1294
1309 PLANT.PIPEC2.P(2) := 1.10715e+006 ; # 1295
1310 PLANT.PIPEC2.P(3) := 1.10506e+006 ; # 1296
1311 PLANT.PIPEC2.P(4) := 1.10291e+006 ; # 1297
1312 PLANT.PIPEC2.P(5) := 1.1007e+006 ; # 1298
1313 PLANT.PIPEC2.P(6) := 1.09844e+006 ; # 1299
1314 PLANT.PIPEC2.P(7) := 1.09613e+006 ; # 1300
1315 PLANT.PIPEC2.P(8) := 1.09377e+006 ; # 1301
1316 PLANT.PIPEC2.P(9) := 1.09136e+006 ; # 1302
1317 PLANT.PIPEC2.P(10) := 1.0889e+006 ; # 1303
1318 PLANT.PIPEC2.P(11) := 1.08641e+006 ; # 1304
1319 PLANT.PIPEC2.P(12) := 1.08387e+006 ; # 1305
1320 PLANT.PIPEC2.P(13) := 1.0813e+006 ; # 1306
1321 PLANT.PIPEC2.P(14) := 1.07869e+006 ; # 1307
1322 PLANT.PIPEC2.P(15) := 1.07604e+006 ; # 1308
1323 PLANT.PIPEC2.P(16) := 1.07336e+006 ; # 1309
1324 PLANT.PIPEC2.P(17) := 1.07065e+006 ; # 1310
1325 PLANT.PIPEC2.P(18) := 1.06791e+006 ; # 1311
1326 PLANT.PIPEC2.P(19) := 1.06513e+006 ; # 1312
1327 PLANT.PIPEC2.P(20) := 1.06233e+006 ; # 1313
1328 PLANT.PIPEC2.P(21) := 1.05951e+006 ; # 1314
1329 PLANT.PIPEC2.P(22) := 1.05665e+006 ; # 1315
1330 PLANT.PIPEC2.P(23) := 1.05377e+006 ; # 1316
1331 PLANT.PIPEC2.P(24) := 1.05087e+006 ; # 1317
1332 PLANT.PIPEC2.P(25) := 1.04794e+006 ; # 1318
1333 PLANT.PIPEC2.P(26) := 1.04499e+006 ; # 1319
1334 PLANT.PIPEC2.P(27) := 1.04201e+006 ; # 1320
1335 PLANT.PIPEC2.P(28) := 1.03902e+006 ; # 1321
1336 PLANT.PIPEC2.P(29) := 1.036e+006 ; # 1322
1337 PLANT.PIPEC2.P(30) := 1.03297e+006 ; # 1323
1338 PLANT.PIPEC2.P(31) := 1.02991e+006 ; # 1324
1339 PLANT.PIPEC2.P(32) := 1.02684e+006 ; # 1325
1340 PLANT.PIPEC2.P(33) := 1.02374e+006 ; # 1326
1341 PLANT.PIPEC2.P(34) := 1.02063e+006 ; # 1327
1342 PLANT.PIPEC2.P(35) := 1.0175e+006 ; # 1328
1343 PLANT.PIPEC2.P(36) := 1.01435e+006 ; # 1329
1344 PLANT.PIPEC2.P(37) := 1.01118e+006 ; # 1330
1345 PLANT.PIPEC2.P(38) := 1.008e+006 ; # 1331
1346 PLANT.PIPEC2.P(39) := 1.00479e+006 ; # 1332

1347 PLANT.PIPEC2.P(40) := 1.00158e+006 ; # 1333
1348 PLANT.PIPEC2.H(1) := 790991 ; # 1334
1349 PLANT.PIPEC2.H(2) := 863955 ; # 1335
1350 PLANT.PIPEC2.H(3) := 932380 ; # 1336
1351 PLANT.PIPEC2.H(4) := 996549 ; # 1337
1352 PLANT.PIPEC2.H(5) := 1.05673e+006 ; # 1338
1353 PLANT.PIPEC2.H(6) := 1.11316e+006 ; # 1339
1354 PLANT.PIPEC2.H(7) := 1.16608e+006 ; # 1340
1355 PLANT.PIPEC2.H(8) := 1.21572e+006 ; # 1341
1356 PLANT.PIPEC2.H(9) := 1.26226e+006 ; # 1342
1357 PLANT.PIPEC2.H(10) := 1.30591e+006 ; # 1343
1358 PLANT.PIPEC2.H(11) := 1.34685e+006 ; # 1344
1359 PLANT.PIPEC2.H(12) := 1.38523e+006 ; # 1345
1360 PLANT.PIPEC2.H(13) := 1.42123e+006 ; # 1346
1361 PLANT.PIPEC2.H(14) := 1.455e+006 ; # 1347
1362 PLANT.PIPEC2.H(15) := 1.48666e+006 ; # 1348
1363 PLANT.PIPEC2.H(16) := 1.51635e+006 ; # 1349
1364 PLANT.PIPEC2.H(17) := 1.54419e+006 ; # 1350
1365 PLANT.PIPEC2.H(18) := 1.57031e+006 ; # 1351
1366 PLANT.PIPEC2.H(19) := 1.59479e+006 ; # 1352
1367 PLANT.PIPEC2.H(20) := 1.61776e+006 ; # 1353
1368 PLANT.PIPEC2.H(21) := 1.6393e+006 ; # 1354
1369 PLANT.PIPEC2.H(22) := 1.65949e+006 ; # 1355
1370 PLANT.PIPEC2.H(23) := 1.67843e+006 ; # 1356
1371 PLANT.PIPEC2.H(24) := 1.6962e+006 ; # 1357
1372 PLANT.PIPEC2.H(25) := 1.71285e+006 ; # 1358
1373 PLANT.PIPEC2.H(26) := 1.72848e+006 ; # 1359
1374 PLANT.PIPEC2.H(27) := 1.74313e+006 ; # 1360
1375 PLANT.PIPEC2.H(28) := 1.75686e+006 ; # 1361
1376 PLANT.PIPEC2.H(29) := 1.76975e+006 ; # 1362
1377 PLANT.PIPEC2.H(30) := 1.78183e+006 ; # 1363
1378 PLANT.PIPEC2.H(31) := 1.79316e+006 ; # 1364
1379 PLANT.PIPEC2.H(32) := 1.80379e+006 ; # 1365
1380 PLANT.PIPEC2.H(33) := 1.81375e+006 ; # 1366
1381 PLANT.PIPEC2.H(34) := 1.8231e+006 ; # 1367
1382 PLANT.PIPEC2.H(35) := 1.83186e+006 ; # 1368
1383 PLANT.PIPEC2.H(36) := 1.84008e+006 ; # 1369
1384 PLANT.PIPEC2.H(37) := 1.84779e+006 ; # 1370
1385 PLANT.PIPEC2.H(38) := 1.85502e+006 ; # 1371
1386 PLANT.PIPEC2.H(39) := 1.8618e+006 ; # 1372
1387 PLANT.PIPEC2.H(40) := 1.86815e+006 ; # 1373
1388 PLANT.PIPEC2.H0 := 713180 ; # 1374
1389 PLANT.PIPEC2.T(1) := 648.643 ; # 1375
1390 PLANT.PIPEC2.T(2) := 680.988 ; # 1376
1391 PLANT.PIPEC2.T(3) := 711.321 ; # 1377
1392 PLANT.PIPEC2.T(4) := 739.767 ; # 1378
1393 PLANT.PIPEC2.T(5) := 766.443 ; # 1379
1394 PLANT.PIPEC2.T(6) := 791.46 ; # 1380
1395 PLANT.PIPEC2.T(7) := 814.921 ; # 1381
1396 PLANT.PIPEC2.T(8) := 836.923 ; # 1382
1397 PLANT.PIPEC2.T(9) := 857.556 ; # 1383
1398 PLANT.PIPEC2.T(10) := 876.906 ; # 1384
1399 PLANT.PIPEC2.T(11) := 895.052 ; # 1385
1400 PLANT.PIPEC2.T(12) := 912.069 ; # 1386
1401 PLANT.PIPEC2.T(13) := 928.028 ; # 1387
1402 PLANT.PIPEC2.T(14) := 942.994 ; # 1388
1403 PLANT.PIPEC2.T(15) := 957.03 ; # 1389
1404 PLANT.PIPEC2.T(16) := 970.192 ; # 1390
1405 PLANT.PIPEC2.T(17) := 982.535 ; # 1391
1406 PLANT.PIPEC2.T(18) := 994.111 ; # 1392
1407 PLANT.PIPEC2.T(19) := 1004.97 ; # 1393
1408 PLANT.PIPEC2.T(20) := 1015.15 ; # 1394
1409 PLANT.PIPEC2.T(21) := 1024.69 ; # 1395
1410 PLANT.PIPEC2.T(22) := 1033.65 ; # 1396
1411 PLANT.PIPEC2.T(23) := 1042.04 ; # 1397
1412 PLANT.PIPEC2.T(24) := 1049.92 ; # 1398
1413 PLANT.PIPEC2.T(25) := 1057.3 ; # 1399
1414 PLANT.PIPEC2.T(26) := 1064.23 ; # 1400
1415 PLANT.PIPEC2.T(27) := 1070.72 ; # 1401
1416 PLANT.PIPEC2.T(28) := 1076.81 ; # 1402
1417 PLANT.PIPEC2.T(29) := 1082.52 ; # 1403
1418 PLANT.PIPEC2.T(30) := 1087.88 ; # 1404
1419 PLANT.PIPEC2.T(31) := 1092.9 ; # 1405
1420 PLANT.PIPEC2.T(32) := 1097.61 ; # 1406
1421 PLANT.PIPEC2.T(33) := 1102.03 ; # 1407
1422 PLANT.PIPEC2.T(34) := 1106.17 ; # 1408
1423 PLANT.PIPEC2.T(35) := 1110.06 ; # 1409
1424 PLANT.PIPEC2.T(36) := 1113.7 ; # 1410
1425 PLANT.PIPEC2.T(37) := 1117.12 ; # 1411
1426 PLANT.PIPEC2.T(38) := 1120.32 ; # 1412
1427 PLANT.PIPEC2.T(39) := 1123.33 ; # 1413
1428 PLANT.PIPEC2.T(40) := 1126.15 ; # 1414
1429 PLANT.PIPEC2.TEXTRNL(1) := 721.768 ; # 1415
1430 PLANT.PIPEC2.TEXTRNL(2) := 749.557 ; # 1416
1431 PLANT.PIPEC2.TEXTRNL(3) := 775.624 ; # 1417
1432 PLANT.PIPEC2.TEXTRNL(4) := 800.07 ; # 1418
1433 PLANT.PIPEC2.TEXTRNL(5) := 822.996 ; # 1419
1434 PLANT.PIPEC2.TEXTRNL(6) := 844.495 ; # 1420
1435 PLANT.PIPEC2.TEXTRNL(7) := 864.657 ; # 1421
1436 PLANT.PIPEC2.TEXTRNL(8) := 883.565 ; # 1422
1437 PLANT.PIPEC2.TEXTRNL(9) := 901.297 ; # 1423
1438 PLANT.PIPEC2.TEXTRNL(10) := 917.926 ; # 1424

1439 PLANT.PIPEC2.TEXTRNL(11) := 933.521 ; # 1425
1440 PLANT.PIPEC2.TEXTRNL(12) := 948.145 ; # 1426
1441 PLANT.PIPEC2.TEXTRNL(13) := 961.86 ; # 1427
1442 PLANT.PIPEC2.TEXTRNL(14) := 974.722 ; # 1428
1443 PLANT.PIPEC2.TEXTRNL(15) := 986.784 ; # 1429
1444 PLANT.PIPEC2.TEXTRNL(16) := 998.095 ; # 1430
1445 PLANT.PIPEC2.TEXTRNL(17) := 1008.7 ; # 1431
1446 PLANT.PIPEC2.TEXTRNL(18) := 1018.65 ; # 1432
1447 PLANT.PIPEC2.TEXTRNL(19) := 1027.98 ; # 1433
1448 PLANT.PIPEC2.TEXTRNL(20) := 1036.73 ; # 1434
1449 PLANT.PIPEC2.TEXTRNL(21) := 1044.93 ; # 1435
1450 PLANT.PIPEC2.TEXTRNL(22) := 1052.63 ; # 1436
1451 PLANT.PIPEC2.TEXTRNL(23) := 1059.84 ; # 1437
1452 PLANT.PIPEC2.TEXTRNL(24) := 1066.61 ; # 1438
1453 PLANT.PIPEC2.TEXTRNL(25) := 1072.96 ; # 1439
1454 PLANT.PIPEC2.TEXTRNL(26) := 1078.91 ; # 1440
1455 PLANT.PIPEC2.TEXTRNL(27) := 1084.49 ; # 1441
1456 PLANT.PIPEC2.TEXTRNL(28) := 1089.72 ; # 1442
1457 PLANT.PIPEC2.TEXTRNL(29) := 1094.63 ; # 1443
1458 PLANT.PIPEC2.TEXTRNL(30) := 1099.23 ; # 1444
1459 PLANT.PIPEC2.TEXTRNL(31) := 1103.55 ; # 1445
1460 PLANT.PIPEC2.TEXTRNL(32) := 1107.6 ; # 1446
1461 PLANT.PIPEC2.TEXTRNL(33) := 1111.4 ; # 1447
1462 PLANT.PIPEC2.TEXTRNL(34) := 1114.96 ; # 1448
1463 PLANT.PIPEC2.TEXTRNL(35) := 1118.29 ; # 1449
1464 PLANT.PIPEC2.TEXTRNL(36) := 1121.43 ; # 1450
1465 PLANT.PIPEC2.TEXTRNL(37) := 1124.36 ; # 1451
1466 PLANT.PIPEC2.TEXTRNL(38) := 1127.12 ; # 1452
1467 PLANT.PIPEC2.TEXTRNL(39) := 1129.7 ; # 1453
1468 PLANT.PIPEC2.TEXTRNL(40) := 1132.12 ; # 1454
1469 PLANT.PIPEC2.F(1) := 43.1466 ; # 1455
1470 PLANT.PIPEC2.F(2) := 43.1466 ; # 1456
1471 PLANT.PIPEC2.F(3) := 43.1466 ; # 1457
1472 PLANT.PIPEC2.F(4) := 43.1466 ; # 1458
1473 PLANT.PIPEC2.F(5) := 43.1466 ; # 1459
1474 PLANT.PIPEC2.F(6) := 43.1466 ; # 1460
1475 PLANT.PIPEC2.F(7) := 43.1466 ; # 1461
1476 PLANT.PIPEC2.F(8) := 43.1466 ; # 1462
1477 PLANT.PIPEC2.F(9) := 43.1466 ; # 1463
1478 PLANT.PIPEC2.F(10) := 43.1466 ; # 1464
1479 PLANT.PIPEC2.F(11) := 43.1466 ; # 1465
1480 PLANT.PIPEC2.F(12) := 43.1466 ; # 1466
1481 PLANT.PIPEC2.F(13) := 43.1466 ; # 1467
1482 PLANT.PIPEC2.F(14) := 43.1466 ; # 1468
1483 PLANT.PIPEC2.F(15) := 43.1466 ; # 1469
1484 PLANT.PIPEC2.F(16) := 43.1466 ; # 1470
1485 PLANT.PIPEC2.F(17) := 43.1466 ; # 1471
1486 PLANT.PIPEC2.F(18) := 43.1466 ; # 1472
1487 PLANT.PIPEC2.F(19) := 43.1466 ; # 1473
1488 PLANT.PIPEC2.F(20) := 43.1466 ; # 1474
1489 PLANT.PIPEC2.F(21) := 43.1466 ; # 1475
1490 PLANT.PIPEC2.F(22) := 43.1466 ; # 1476
1491 PLANT.PIPEC2.F(23) := 43.1466 ; # 1477
1492 PLANT.PIPEC2.F(24) := 43.1466 ; # 1478
1493 PLANT.PIPEC2.F(25) := 43.1466 ; # 1479
1494 PLANT.PIPEC2.F(26) := 43.1466 ; # 1480
1495 PLANT.PIPEC2.F(27) := 43.1466 ; # 1481
1496 PLANT.PIPEC2.F(28) := 43.1466 ; # 1482
1497 PLANT.PIPEC2.F(29) := 43.1466 ; # 1483
1498 PLANT.PIPEC2.F(30) := 43.1466 ; # 1484
1499 PLANT.PIPEC2.F(31) := 43.1466 ; # 1485
1500 PLANT.PIPEC2.F(32) := 43.1466 ; # 1486
1501 PLANT.PIPEC2.F(33) := 43.1466 ; # 1487
1502 PLANT.PIPEC2.F(34) := 43.1466 ; # 1488
1503 PLANT.PIPEC2.F(35) := 43.1466 ; # 1489
1504 PLANT.PIPEC2.F(36) := 43.1466 ; # 1490
1505 PLANT.PIPEC2.F(37) := 43.1466 ; # 1491
1506 PLANT.PIPEC2.F(38) := 43.1466 ; # 1492
1507 PLANT.PIPEC2.F(39) := 43.1466 ; # 1493
1508 PLANT.PIPEC2.F(40) := 43.1466 ; # 1494
1509 PLANT.PIPEC2.F_IN := 43.1466 ; # 1495
1510 PLANT.PIPEC2.PSI(1) := 1.82247e+006 ; # 1496
1511 PLANT.PIPEC2.PSI(2) := 1.93726e+006 ; # 1497
1512 PLANT.PIPEC2.PSI(3) := 2.03443e+006 ; # 1498
1513 PLANT.PIPEC2.PSI(4) := 2.11734e+006 ; # 1499
1514 PLANT.PIPEC2.PSI(5) := 2.18855e+006 ; # 1500
1515 PLANT.PIPEC2.PSI(6) := 2.25006e+006 ; # 1501
1516 PLANT.PIPEC2.PSI(7) := 2.30342e+006 ; # 1502
1517 PLANT.PIPEC2.PSI(8) := 2.34986e+006 ; # 1503
1518 PLANT.PIPEC2.PSI(9) := 2.3904e+006 ; # 1504
1519 PLANT.PIPEC2.PSI(10) := 2.42585e+006 ; # 1505
1520 PLANT.PIPEC2.PSI(11) := 2.45689e+006 ; # 1506
1521 PLANT.PIPEC2.PSI(12) := 2.48407e+006 ; # 1507
1522 PLANT.PIPEC2.PSI(13) := 2.50788e+006 ; # 1508
1523 PLANT.PIPEC2.PSI(14) := 2.5287e+006 ; # 1509
1524 PLANT.PIPEC2.PSI(15) := 2.54688e+006 ; # 1510
1525 PLANT.PIPEC2.PSI(16) := 2.56271e+006 ; # 1511
1526 PLANT.PIPEC2.PSI(17) := 2.57643e+006 ; # 1512
1527 PLANT.PIPEC2.PSI(18) := 2.58827e+006 ; # 1513
1528 PLANT.PIPEC2.PSI(19) := 2.59842e+006 ; # 1514
1529 PLANT.PIPEC2.PSI(20) := 2.60703e+006 ; # 1515
1530 PLANT.PIPEC2.PSI(21) := 2.61426e+006 ; # 1516

```

1531 PLANT.PIPEC2.PSI(22) := 2.62023e+006 ; # 1517
1532 PLANT.PIPEC2.PSI(23) := 2.62506e+006 ; # 1518
1533 PLANT.PIPEC2.PSI(24) := 2.62884e+006 ; # 1519
1534 PLANT.PIPEC2.PSI(25) := 2.63167e+006 ; # 1520
1535 PLANT.PIPEC2.PSI(26) := 2.63363e+006 ; # 1521
1536 PLANT.PIPEC2.PSI(27) := 2.63479e+006 ; # 1522
1537 PLANT.PIPEC2.PSI(28) := 2.63522e+006 ; # 1523
1538 PLANT.PIPEC2.PSI(29) := 2.63496e+006 ; # 1524
1539 PLANT.PIPEC2.PSI(30) := 2.63409e+006 ; # 1525
1540 PLANT.PIPEC2.PSI(31) := 2.63263e+006 ; # 1526
1541 PLANT.PIPEC2.PSI(32) := 2.63064e+006 ; # 1527
1542 PLANT.PIPEC2.PSI(33) := 2.62816e+006 ; # 1528
1543 PLANT.PIPEC2.PSI(34) := 2.62522e+006 ; # 1529
1544 PLANT.PIPEC2.PSI(35) := 2.62186e+006 ; # 1530
1545 PLANT.PIPEC2.PSI(36) := 2.6181e+006 ; # 1531
1546 PLANT.PIPEC2.PSI(37) := 2.61397e+006 ; # 1532
1547 PLANT.PIPEC2.PSI(38) := 2.6095e+006 ; # 1533
1548 PLANT.PIPEC2.PSI(39) := 2.60471e+006 ; # 1534
1549 PLANT.PIPEC2.PSI(40) := 2.59962e+006 ; # 1535
1550 PLANT.PIPEC2.HT.RHOPIPEHE := 2.32481 ; # 1536
1551 PLANT.PIPEC2.HT.VPIPE := 65.9555 ; # 1537
1552 PLANT.PIPEC2.HT.U := 1880.53 ; # 1538

```

HTLNOPIPEHQSS_SS_OUT_INI.INITIAL

```

1 # Values for differential variables in computation HTLQSS_SS
2 # Saved at time 2120
3 PLANT.HX.THX(1) = 875.997 ; # 1
4 PLANT.HX.THX(2) = 887.105 ; # 2
5 PLANT.HX.THX(3) = 898.003 ; # 3
6 PLANT.HX.THX(4) = 908.635 ; # 4
7 PLANT.HX.THX(5) = 919.007 ; # 5
8 PLANT.HX.THX(6) = 929.126 ; # 6
9 PLANT.HX.THX(7) = 938.998 ; # 7
10 PLANT.HX.THX(8) = 948.629 ; # 8
11 PLANT.HX.THX(9) = 958.024 ; # 9
12 PLANT.HX.THX(10) = 967.19 ; # 10
13 PLANT.HX.THX(11) = 976.133 ; # 11
14 PLANT.HX.THX(12) = 984.857 ; # 12
15 PLANT.HX.THX(13) = 993.368 ; # 13
16 PLANT.HX.THX(14) = 1001.67 ; # 14
17 PLANT.HX.THX(15) = 1009.77 ; # 15
18 PLANT.HX.THX(16) = 1017.67 ; # 16
19 PLANT.HX.THX(17) = 1025.38 ; # 17
20 PLANT.HX.THX(18) = 1032.9 ; # 18
21 PLANT.HX.THX(19) = 1040.24 ; # 19
22 PLANT.HX.THX(20) = 1047.4 ; # 20
23 PLANT.HX.THX(21) = 1054.38 ; # 21
24 PLANT.HX.THX(22) = 1061.2 ; # 22
25 PLANT.HX.THX(23) = 1067.84 ; # 23
26 PLANT.HX.THX(24) = 1074.33 ; # 24
27 PLANT.HX.THX(25) = 1080.65 ; # 25
28 PLANT.HX.THX(26) = 1086.83 ; # 26
29 PLANT.HX.THX(27) = 1092.85 ; # 27
30 PLANT.HX.THX(28) = 1098.72 ; # 28
31 PLANT.HX.THX(29) = 1104.45 ; # 29
32 PLANT.HX.THX(30) = 1110.04 ; # 30
33 PLANT.HX.THX(31) = 1115.49 ; # 31
34 PLANT.HX.THX(32) = 1120.82 ; # 32
35 PLANT.HX.THX(33) = 1126.01 ; # 33
36 PLANT.HX.THX(34) = 1131.07 ; # 34
37 PLANT.HX.THX(35) = 1136.01 ; # 35
38 PLANT.HX.THX(36) = 1140.83 ; # 36
39 PLANT.HX.THX(37) = 1145.53 ; # 37
40 PLANT.HX.THX(38) = 1150.12 ; # 38
41 PLANT.HX.THX(39) = 1154.59 ; # 39
42 PLANT.HX.THX(40) = 1158.94 ; # 40
43 PLANT.LOOP1.PSI(1) = 1.21853e+006 ; # 41
44 PLANT.LOOP1.PSI(2) = 1.21407e+006 ; # 42
45 PLANT.LOOP1.PSI(3) = 1.2096e+006 ; # 43
46 PLANT.LOOP1.PSI(4) = 1.20513e+006 ; # 44
47 PLANT.LOOP1.PSI(5) = 1.20066e+006 ; # 45
48 PLANT.LOOP1.PSI(6) = 1.19618e+006 ; # 46
49 PLANT.LOOP1.PSI(7) = 1.1917e+006 ; # 47
50 PLANT.LOOP1.PSI(8) = 1.18721e+006 ; # 48
51 PLANT.LOOP1.PSI(9) = 1.18271e+006 ; # 49
52 PLANT.LOOP1.PSI(10) = 1.17821e+006 ; # 50
53 PLANT.LOOP1.PSI(11) = 1.21421e+006 ; # 51
54 PLANT.LOOP1.PSI(12) = 1.23642e+006 ; # 52
55 PLANT.LOOP1.PSI(13) = 1.25693e+006 ; # 53
56 PLANT.LOOP1.PSI(14) = 1.27623e+006 ; # 54
57 PLANT.LOOP1.PSI(15) = 1.2944e+006 ; # 55
58 PLANT.LOOP1.PSI(16) = 1.3115e+006 ; # 56

```

59 PLANT.LOOP1.PSI(17) = 1.32762e+006 ; # 57
60 PLANT.LOOP1.PSI(18) = 1.3428e+006 ; # 58
61 PLANT.LOOP1.PSI(19) = 1.35711e+006 ; # 59
62 PLANT.LOOP1.PSI(20) = 1.37059e+006 ; # 60
63 PLANT.LOOP1.PSI(21) = 1.38329e+006 ; # 61
64 PLANT.LOOP1.PSI(22) = 1.39525e+006 ; # 62
65 PLANT.LOOP1.PSI(23) = 1.40653e+006 ; # 63
66 PLANT.LOOP1.PSI(24) = 1.41714e+006 ; # 64
67 PLANT.LOOP1.PSI(25) = 1.42714e+006 ; # 65
68 PLANT.LOOP1.PSI(26) = 1.43655e+006 ; # 66
69 PLANT.LOOP1.PSI(27) = 1.4454e+006 ; # 67
70 PLANT.LOOP1.PSI(28) = 1.45372e+006 ; # 68
71 PLANT.LOOP1.PSI(29) = 1.46153e+006 ; # 69
72 PLANT.LOOP1.PSI(30) = 1.46887e+006 ; # 70
73 PLANT.LOOP1.PSI(31) = 1.47574e+006 ; # 71
74 PLANT.LOOP1.PSI(32) = 1.48219e+006 ; # 72
75 PLANT.LOOP1.PSI(33) = 1.48821e+006 ; # 73
76 PLANT.LOOP1.PSI(34) = 1.49385e+006 ; # 74
77 PLANT.LOOP1.PSI(35) = 1.4991e+006 ; # 75
78 PLANT.LOOP1.PSI(36) = 1.50399e+006 ; # 76
79 PLANT.LOOP1.PSI(37) = 1.50854e+006 ; # 77
80 PLANT.LOOP1.PSI(38) = 1.51275e+006 ; # 78
81 PLANT.LOOP1.PSI(39) = 1.51665e+006 ; # 79
82 PLANT.LOOP1.PSI(40) = 1.52024e+006 ; # 80
83 PLANT.LOOP1.PSI(41) = 1.52354e+006 ; # 81
84 PLANT.LOOP1.PSI(42) = 1.52657e+006 ; # 82
85 PLANT.LOOP1.PSI(43) = 1.52932e+006 ; # 83
86 PLANT.LOOP1.PSI(44) = 1.53181e+006 ; # 84
87 PLANT.LOOP1.PSI(45) = 1.53406e+006 ; # 85
88 PLANT.LOOP1.PSI(46) = 1.53607e+006 ; # 86
89 PLANT.LOOP1.PSI(47) = 1.53785e+006 ; # 87
90 PLANT.LOOP1.PSI(48) = 1.53941e+006 ; # 88
91 PLANT.LOOP1.PSI(49) = 1.54075e+006 ; # 89
92 PLANT.LOOP1.PSI(50) = 1.54188e+006 ; # 90
93 PLANT.LOOP1.PSI(51) = 1.5428e+006 ; # 91
94 PLANT.LOOP1.PSI(52) = 1.50808e+006 ; # 92
95 PLANT.LOOP1.PSI(53) = 1.50192e+006 ; # 93
96 PLANT.LOOP1.PSI(54) = 1.49574e+006 ; # 94
97 PLANT.LOOP1.PSI(55) = 1.48956e+006 ; # 95
98 PLANT.LOOP1.PSI(56) = 1.48336e+006 ; # 96
99 PLANT.LOOP1.PSI(57) = 1.47715e+006 ; # 97
100 PLANT.LOOP1.PSI(58) = 1.47093e+006 ; # 98
101 PLANT.LOOP1.PSI(59) = 1.46469e+006 ; # 99
102 PLANT.LOOP1.PSI(60) = 1.45845e+006 ; # 100
103 PLANT.LOOP1.PSI(61) = 1.47351e+006 ; # 101
104 PLANT.LOOP1.PSI(62) = 1.46929e+006 ; # 102
105 PLANT.LOOP1.PSI(63) = 1.46481e+006 ; # 103
106 PLANT.LOOP1.PSI(64) = 1.46016e+006 ; # 104
107 PLANT.LOOP1.PSI(65) = 1.45533e+006 ; # 105
108 PLANT.LOOP1.PSI(66) = 1.4503e+006 ; # 106
109 PLANT.LOOP1.PSI(67) = 1.44506e+006 ; # 107
110 PLANT.LOOP1.PSI(68) = 1.4396e+006 ; # 108
111 PLANT.LOOP1.PSI(69) = 1.4339e+006 ; # 109
112 PLANT.LOOP1.PSI(70) = 1.42795e+006 ; # 110
113 PLANT.LOOP1.PSI(71) = 1.42173e+006 ; # 111
114 PLANT.LOOP1.PSI(72) = 1.41522e+006 ; # 112
115 PLANT.LOOP1.PSI(73) = 1.4084e+006 ; # 113
116 PLANT.LOOP1.PSI(74) = 1.40125e+006 ; # 114
117 PLANT.LOOP1.PSI(75) = 1.39374e+006 ; # 115
118 PLANT.LOOP1.PSI(76) = 1.38585e+006 ; # 116
119 PLANT.LOOP1.PSI(77) = 1.37755e+006 ; # 117
120 PLANT.LOOP1.PSI(78) = 1.36881e+006 ; # 118
121 PLANT.LOOP1.PSI(79) = 1.35959e+006 ; # 119
122 PLANT.LOOP1.PSI(80) = 1.34986e+006 ; # 120
123 PLANT.LOOP1.PSI(81) = 1.33957e+006 ; # 121
124 PLANT.LOOP1.PSI(82) = 1.32868e+006 ; # 122
125 PLANT.LOOP1.PSI(83) = 1.31713e+006 ; # 123
126 PLANT.LOOP1.PSI(84) = 1.30488e+006 ; # 124
127 PLANT.LOOP1.PSI(85) = 1.29185e+006 ; # 125
128 PLANT.LOOP1.PSI(86) = 1.27797e+006 ; # 126
129 PLANT.LOOP1.PSI(87) = 1.26318e+006 ; # 127
130 PLANT.LOOP1.PSI(88) = 1.24738e+006 ; # 128
131 PLANT.LOOP1.PSI(89) = 1.23046e+006 ; # 129
132 PLANT.LOOP1.PSI(90) = 1.21233e+006 ; # 130
133 PLANT.LOOP1.PSI(91) = 1.19284e+006 ; # 131
134 PLANT.LOOP1.PSI(92) = 1.17186e+006 ; # 132
135 PLANT.LOOP1.PSI(93) = 1.14922e+006 ; # 133
136 PLANT.LOOP1.PSI(94) = 1.12472e+006 ; # 134
137 PLANT.LOOP1.PSI(95) = 1.09815e+006 ; # 135
138 PLANT.LOOP1.PSI(96) = 1.06925e+006 ; # 136
139 PLANT.LOOP1.PSI(97) = 1.03771e+006 ; # 137
140 PLANT.LOOP1.PSI(98) = 1.00319e+006 ; # 138
141 PLANT.LOOP1.PSI(99) = 965262 ; # 139
142 PLANT.LOOP1.PSI(100) = 923433 ; # 140
143 PLANT.LOOP1.PSIEXTRA(1) = 1.23448e+006 ; # 141
144 PLANT.LOOP1.PSIEXTRA(2) = 1.23448e+006 ; # 142
145 PLANT.HX2.THX(1) = 1127.77 ; # 264
146 PLANT.HX2.THX(2) = 1124.33 ; # 265
147 PLANT.HX2.THX(3) = 1120.69 ; # 266
148 PLANT.HX2.THX(4) = 1116.87 ; # 267
149 PLANT.HX2.THX(5) = 1112.85 ; # 268
150 PLANT.HX2.THX(6) = 1108.61 ; # 269

```

151 PLANT.HX2.THX(7) = 1104.16 ; # 270
152 PLANT.HX2.THX(8) = 1099.46 ; # 271
153 PLANT.HX2.THX(9) = 1094.52 ; # 272
154 PLANT.HX2.THX(10) = 1089.32 ; # 273
155 PLANT.HX2.THX(11) = 1083.85 ; # 274
156 PLANT.HX2.THX(12) = 1078.09 ; # 275
157 PLANT.HX2.THX(13) = 1072.03 ; # 276
158 PLANT.HX2.THX(14) = 1065.64 ; # 277
159 PLANT.HX2.THX(15) = 1058.92 ; # 278
160 PLANT.HX2.THX(16) = 1051.85 ; # 279
161 PLANT.HX2.THX(17) = 1044.4 ; # 280
162 PLANT.HX2.THX(18) = 1036.57 ; # 281
163 PLANT.HX2.THX(19) = 1028.32 ; # 282
164 PLANT.HX2.THX(20) = 1019.63 ; # 283
165 PLANT.HX2.THX(21) = 1010.49 ; # 284
166 PLANT.HX2.THX(22) = 1000.87 ; # 285
167 PLANT.HX2.THX(23) = 990.74 ; # 286
168 PLANT.HX2.THX(24) = 980.078 ; # 287
169 PLANT.HX2.THX(25) = 968.854 ; # 288
170 PLANT.HX2.THX(26) = 957.041 ; # 289
171 PLANT.HX2.THX(27) = 944.605 ; # 290
172 PLANT.HX2.THX(28) = 931.514 ; # 291
173 PLANT.HX2.THX(29) = 917.735 ; # 292
174 PLANT.HX2.THX(30) = 903.231 ; # 293
175 PLANT.HX2.THX(31) = 887.962 ; # 294
176 PLANT.HX2.THX(32) = 871.891 ; # 295
177 PLANT.HX2.THX(33) = 854.973 ; # 296
178 PLANT.HX2.THX(34) = 837.165 ; # 297
179 PLANT.HX2.THX(35) = 818.42 ; # 298
180 PLANT.HX2.THX(36) = 798.688 ; # 299
181 PLANT.HX2.THX(37) = 777.917 ; # 300
182 PLANT.HX2.THX(38) = 756.054 ; # 301
183 PLANT.HX2.THX(39) = 733.039 ; # 302
184 PLANT.HX2.THX(40) = 708.82 ; # 303
185 PLANT.PIPEC2.PSI(1) = 1.81868e+006 ; # 385
186 PLANT.PIPEC2.PSI(2) = 1.91901e+006 ; # 386
187 PLANT.PIPEC2.PSI(3) = 2.00606e+006 ; # 387
188 PLANT.PIPEC2.PSI(4) = 2.08199e+006 ; # 388
189 PLANT.PIPEC2.PSI(5) = 2.14854e+006 ; # 389
190 PLANT.PIPEC2.PSI(6) = 2.20709e+006 ; # 390
191 PLANT.PIPEC2.PSI(7) = 2.25877e+006 ; # 391
192 PLANT.PIPEC2.PSI(8) = 2.30451e+006 ; # 392
193 PLANT.PIPEC2.PSI(9) = 2.34506e+006 ; # 393
194 PLANT.PIPEC2.PSI(10) = 2.38106e+006 ; # 394
195 PLANT.PIPEC2.PSI(11) = 2.41306e+006 ; # 395
196 PLANT.PIPEC2.PSI(12) = 2.44149e+006 ; # 396
197 PLANT.PIPEC2.PSI(13) = 2.46677e+006 ; # 397
198 PLANT.PIPEC2.PSI(14) = 2.48921e+006 ; # 398
199 PLANT.PIPEC2.PSI(15) = 2.50911e+006 ; # 399
200 PLANT.PIPEC2.PSI(16) = 2.52672e+006 ; # 400
201 PLANT.PIPEC2.PSI(17) = 2.54225e+006 ; # 401
202 PLANT.PIPEC2.PSI(18) = 2.55591e+006 ; # 402
203 PLANT.PIPEC2.PSI(19) = 2.56786e+006 ; # 403
204 PLANT.PIPEC2.PSI(20) = 2.57824e+006 ; # 404
205 PLANT.PIPEC2.PSI(21) = 2.5872e+006 ; # 405
206 PLANT.PIPEC2.PSI(22) = 2.59485e+006 ; # 406
207 PLANT.PIPEC2.PSI(23) = 2.60129e+006 ; # 407
208 PLANT.PIPEC2.PSI(24) = 2.60662e+006 ; # 408
209 PLANT.PIPEC2.PSI(25) = 2.61094e+006 ; # 409
210 PLANT.PIPEC2.PSI(26) = 2.6143e+006 ; # 410
211 PLANT.PIPEC2.PSI(27) = 2.61679e+006 ; # 411
212 PLANT.PIPEC2.PSI(28) = 2.61846e+006 ; # 412
213 PLANT.PIPEC2.PSI(29) = 2.61938e+006 ; # 413
214 PLANT.PIPEC2.PSI(30) = 2.6196e+006 ; # 414
215 PLANT.PIPEC2.PSI(31) = 2.61915e+006 ; # 415
216 PLANT.PIPEC2.PSI(32) = 2.6181e+006 ; # 416
217 PLANT.PIPEC2.PSI(33) = 2.61647e+006 ; # 417
218 PLANT.PIPEC2.PSI(34) = 2.6143e+006 ; # 418
219 PLANT.PIPEC2.PSI(35) = 2.61163e+006 ; # 419
220 PLANT.PIPEC2.PSI(36) = 2.60848e+006 ; # 420
221 PLANT.PIPEC2.PSI(37) = 2.60489e+006 ; # 421
222 PLANT.PIPEC2.PSI(38) = 2.60088e+006 ; # 422
223 PLANT.PIPEC2.PSI(39) = 2.59648e+006 ; # 423
224 PLANT.PIPEC2.PSI(40) = 2.59171e+006 ; # 424

```

HTLNOPIPEHQSS_SS_OUT_PRE.PRESETS

```

1 # Values for computation HTLQSS_SS
2 # Saved at time 2120
3 PLANT.HX.TGASHOT(1) := 902.624 ; # 1
4 PLANT.HX.TGASHOT(2) := 913.125 ; # 2
5 PLANT.HX.TGASHOT(3) := 923.388 ; # 3
6 PLANT.HX.TGASHOT(4) := 933.4 ; # 4

```


7 PLANT.HX.TGASHOT(5) := 943.167 ; # 5
8 PLANT.HX.TGASHOT(6) := 952.696 ; # 6
9 PLANT.HX.TGASHOT(7) := 961.993 ; # 7
10 PLANT.HX.TGASHOT(8) := 971.062 ; # 8
11 PLANT.HX.TGASHOT(9) := 979.91 ; # 9
12 PLANT.HX.TGASHOT(10) := 988.542 ; # 10
13 PLANT.HX.TGASHOT(11) := 996.962 ; # 11
14 PLANT.HX.TGASHOT(12) := 1005.18 ; # 12
15 PLANT.HX.TGASHOT(13) := 1013.19 ; # 13
16 PLANT.HX.TGASHOT(14) := 1021.01 ; # 14
17 PLANT.HX.TGASHOT(15) := 1028.64 ; # 15
18 PLANT.HX.TGASHOT(16) := 1036.08 ; # 16
19 PLANT.HX.TGASHOT(17) := 1043.34 ; # 17
20 PLANT.HX.TGASHOT(18) := 1050.42 ; # 18
21 PLANT.HX.TGASHOT(19) := 1057.33 ; # 19
22 PLANT.HX.TGASHOT(20) := 1064.07 ; # 20
23 PLANT.HX.TGASHOT(21) := 1070.65 ; # 21
24 PLANT.HX.TGASHOT(22) := 1077.07 ; # 22
25 PLANT.HX.TGASHOT(23) := 1083.33 ; # 23
26 PLANT.HX.TGASHOT(24) := 1089.43 ; # 24
27 PLANT.HX.TGASHOT(25) := 1095.39 ; # 25
28 PLANT.HX.TGASHOT(26) := 1101.2 ; # 26
29 PLANT.HX.TGASHOT(27) := 1106.87 ; # 27
30 PLANT.HX.TGASHOT(28) := 1112.4 ; # 28
31 PLANT.HX.TGASHOT(29) := 1117.8 ; # 29
32 PLANT.HX.TGASHOT(30) := 1123.06 ; # 30
33 PLANT.HX.TGASHOT(31) := 1128.2 ; # 31
34 PLANT.HX.TGASHOT(32) := 1133.21 ; # 32
35 PLANT.HX.TGASHOT(33) := 1138.1 ; # 33
36 PLANT.HX.TGASHOT(34) := 1142.87 ; # 34
37 PLANT.HX.TGASHOT(35) := 1147.52 ; # 35
38 PLANT.HX.TGASHOT(36) := 1152.06 ; # 36
39 PLANT.HX.TGASHOT(37) := 1156.48 ; # 37
40 PLANT.HX.TGASHOT(38) := 1160.8 ; # 38
41 PLANT.HX.TGASHOT(39) := 1165.02 ; # 39
42 PLANT.HX.TGASHOT(40) := 1169.13 ; # 40
43 PLANT.HX.TGASCOLD(1) := 847.757 ; # 41
44 PLANT.HX.TGASCOLD(2) := 859.616 ; # 42
45 PLANT.HX.TGASCOLD(3) := 871.186 ; # 43
46 PLANT.HX.TGASCOLD(4) := 882.472 ; # 44
47 PLANT.HX.TGASCOLD(5) := 893.484 ; # 45
48 PLANT.HX.TGASCOLD(6) := 904.226 ; # 46
49 PLANT.HX.TGASCOLD(7) := 914.706 ; # 47
50 PLANT.HX.TGASCOLD(8) := 924.93 ; # 48
51 PLANT.HX.TGASCOLD(9) := 934.904 ; # 49
52 PLANT.HX.TGASCOLD(10) := 944.635 ; # 50
53 PLANT.HX.TGASCOLD(11) := 954.128 ; # 51
54 PLANT.HX.TGASCOLD(12) := 963.39 ; # 52
55 PLANT.HX.TGASCOLD(13) := 972.425 ; # 53
56 PLANT.HX.TGASCOLD(14) := 981.239 ; # 54
57 PLANT.HX.TGASCOLD(15) := 989.838 ; # 55
58 PLANT.HX.TGASCOLD(16) := 998.228 ; # 56
59 PLANT.HX.TGASCOLD(17) := 1006.41 ; # 57
60 PLANT.HX.TGASCOLD(18) := 1014.4 ; # 58
61 PLANT.HX.TGASCOLD(19) := 1022.19 ; # 59
62 PLANT.HX.TGASCOLD(20) := 1029.79 ; # 60
63 PLANT.HX.TGASCOLD(21) := 1037.2 ; # 61
64 PLANT.HX.TGASCOLD(22) := 1044.43 ; # 62
65 PLANT.HX.TGASCOLD(23) := 1051.49 ; # 63
66 PLANT.HX.TGASCOLD(24) := 1058.37 ; # 64
67 PLANT.HX.TGASCOLD(25) := 1065.09 ; # 65
68 PLANT.HX.TGASCOLD(26) := 1071.64 ; # 66
69 PLANT.HX.TGASCOLD(27) := 1078.03 ; # 67
70 PLANT.HX.TGASCOLD(28) := 1084.27 ; # 68
71 PLANT.HX.TGASCOLD(29) := 1090.35 ; # 69
72 PLANT.HX.TGASCOLD(30) := 1096.28 ; # 70
73 PLANT.HX.TGASCOLD(31) := 1102.07 ; # 71
74 PLANT.HX.TGASCOLD(32) := 1107.72 ; # 72
75 PLANT.HX.TGASCOLD(33) := 1113.23 ; # 73
76 PLANT.HX.TGASCOLD(34) := 1118.61 ; # 74
77 PLANT.HX.TGASCOLD(35) := 1123.85 ; # 75
78 PLANT.HX.TGASCOLD(36) := 1128.97 ; # 76
79 PLANT.HX.TGASCOLD(37) := 1133.96 ; # 77
80 PLANT.HX.TGASCOLD(38) := 1138.83 ; # 78
81 PLANT.HX.TGASCOLD(39) := 1143.58 ; # 79
82 PLANT.HX.TGASCOLD(40) := 1148.21 ; # 80
83 PLANT.HX.UHOT := 1738.41 ; # 81
84 PLANT.HX.UCOLD := 1645.45 ; # 82
85 PLANT.HX.TH(1) := 875.997 ; # 83
86 PLANT.HX.TH(2) := 887.105 ; # 84
87 PLANT.HX.TH(3) := 898.003 ; # 85
88 PLANT.HX.TH(4) := 908.635 ; # 86
89 PLANT.HX.TH(5) := 919.007 ; # 87
90 PLANT.HX.TH(6) := 929.126 ; # 88
91 PLANT.HX.TH(7) := 938.998 ; # 89
92 PLANT.HX.TH(8) := 948.629 ; # 90
93 PLANT.HX.TH(9) := 958.024 ; # 91
94 PLANT.HX.TH(10) := 967.19 ; # 92
95 PLANT.HX.TH(11) := 976.133 ; # 93
96 PLANT.HX.TH(12) := 984.857 ; # 94
97 PLANT.HX.TH(13) := 993.368 ; # 95
98 PLANT.HX.TH(14) := 1001.67 ; # 96

99 PLANT.HX.THX(15) := 1009.77 ; # 97
 100 PLANT.HX.THX(16) := 1017.67 ; # 98
 101 PLANT.HX.THX(17) := 1025.38 ; # 99
 102 PLANT.HX.THX(18) := 1032.9 ; # 100
 103 PLANT.HX.THX(19) := 1040.24 ; # 101
 104 PLANT.HX.THX(20) := 1047.4 ; # 102
 105 PLANT.HX.THX(21) := 1054.38 ; # 103
 106 PLANT.HX.THX(22) := 1061.2 ; # 104
 107 PLANT.HX.THX(23) := 1067.84 ; # 105
 108 PLANT.HX.THX(24) := 1074.33 ; # 106
 109 PLANT.HX.THX(25) := 1080.65 ; # 107
 110 PLANT.HX.THX(26) := 1086.83 ; # 108
 111 PLANT.HX.THX(27) := 1092.85 ; # 109
 112 PLANT.HX.THX(28) := 1098.72 ; # 110
 113 PLANT.HX.THX(29) := 1104.45 ; # 111
 114 PLANT.HX.THX(30) := 1110.04 ; # 112
 115 PLANT.HX.THX(31) := 1115.49 ; # 113
 116 PLANT.HX.THX(32) := 1120.82 ; # 114
 117 PLANT.HX.THX(33) := 1126.01 ; # 115
 118 PLANT.HX.THX(34) := 1131.07 ; # 116
 119 PLANT.HX.THX(35) := 1136.01 ; # 117
 120 PLANT.HX.THX(36) := 1140.83 ; # 118
 121 PLANT.HX.THX(37) := 1145.53 ; # 119
 122 PLANT.HX.THX(38) := 1150.12 ; # 120
 123 PLANT.HX.THX(39) := 1154.59 ; # 121
 124 PLANT.HX.THX(40) := 1158.94 ; # 122
 125 PLANT.LOOP1.RHO(1) := 1.14186 ; # 123
 126 PLANT.LOOP1.RHO(2) := 1.13901 ; # 124
 127 PLANT.LOOP1.RHO(3) := 1.13615 ; # 125
 128 PLANT.LOOP1.RHO(4) := 1.13328 ; # 126
 129 PLANT.LOOP1.RHO(5) := 1.13039 ; # 127
 130 PLANT.LOOP1.RHO(6) := 1.1275 ; # 128
 131 PLANT.LOOP1.RHO(7) := 1.12458 ; # 129
 132 PLANT.LOOP1.RHO(8) := 1.12166 ; # 130
 133 PLANT.LOOP1.RHO(9) := 1.11873 ; # 131
 134 PLANT.LOOP1.RHO(10) := 1.11578 ; # 132
 135 PLANT.LOOP1.RHO(11) := 1.10995 ; # 133
 136 PLANT.LOOP1.RHO(12) := 1.09332 ; # 134
 137 PLANT.LOOP1.RHO(13) := 1.07711 ; # 135
 138 PLANT.LOOP1.RHO(14) := 1.06165 ; # 136
 139 PLANT.LOOP1.RHO(15) := 1.04688 ; # 137
 140 PLANT.LOOP1.RHO(16) := 1.03275 ; # 138
 141 PLANT.LOOP1.RHO(17) := 1.01923 ; # 139
 142 PLANT.LOOP1.RHO(18) := 1.00627 ; # 140
 143 PLANT.LOOP1.RHO(19) := 0.993839 ; # 141
 144 PLANT.LOOP1.RHO(20) := 0.981903 ; # 142
 145 PLANT.LOOP1.RHO(21) := 0.970434 ; # 143
 146 PLANT.LOOP1.RHO(22) := 0.959403 ; # 144
 147 PLANT.LOOP1.RHO(23) := 0.948785 ; # 145
 148 PLANT.LOOP1.RHO(24) := 0.938555 ; # 146
 149 PLANT.LOOP1.RHO(25) := 0.928692 ; # 147
 150 PLANT.LOOP1.RHO(26) := 0.919175 ; # 148
 151 PLANT.LOOP1.RHO(27) := 0.909986 ; # 149
 152 PLANT.LOOP1.RHO(28) := 0.901106 ; # 150
 153 PLANT.LOOP1.RHO(29) := 0.89252 ; # 151
 154 PLANT.LOOP1.RHO(30) := 0.884211 ; # 152
 155 PLANT.LOOP1.RHO(31) := 0.876165 ; # 153
 156 PLANT.LOOP1.RHO(32) := 0.868369 ; # 154
 157 PLANT.LOOP1.RHO(33) := 0.860811 ; # 155
 158 PLANT.LOOP1.RHO(34) := 0.853477 ; # 156
 159 PLANT.LOOP1.RHO(35) := 0.846358 ; # 157
 160 PLANT.LOOP1.RHO(36) := 0.839443 ; # 158
 161 PLANT.LOOP1.RHO(37) := 0.832722 ; # 159
 162 PLANT.LOOP1.RHO(38) := 0.826186 ; # 160
 163 PLANT.LOOP1.RHO(39) := 0.819826 ; # 161
 164 PLANT.LOOP1.RHO(40) := 0.813634 ; # 162
 165 PLANT.LOOP1.RHO(41) := 0.807602 ; # 163
 166 PLANT.LOOP1.RHO(42) := 0.801723 ; # 164
 167 PLANT.LOOP1.RHO(43) := 0.795989 ; # 165
 168 PLANT.LOOP1.RHO(44) := 0.790396 ; # 166
 169 PLANT.LOOP1.RHO(45) := 0.784935 ; # 167
 170 PLANT.LOOP1.RHO(46) := 0.779602 ; # 168
 171 PLANT.LOOP1.RHO(47) := 0.774391 ; # 169
 172 PLANT.LOOP1.RHO(48) := 0.769296 ; # 170
 173 PLANT.LOOP1.RHO(49) := 0.764313 ; # 171
 174 PLANT.LOOP1.RHO(50) := 0.759442 ; # 172
 175 PLANT.LOOP1.RHO(51) := 0.746737 ; # 173
 176 PLANT.LOOP1.RHO(52) := 0.744574 ; # 174
 177 PLANT.LOOP1.RHO(53) := 0.74242 ; # 175
 178 PLANT.LOOP1.RHO(54) := 0.740254 ; # 176
 179 PLANT.LOOP1.RHO(55) := 0.738076 ; # 177
 180 PLANT.LOOP1.RHO(56) := 0.735886 ; # 178
 181 PLANT.LOOP1.RHO(57) := 0.733685 ; # 179
 182 PLANT.LOOP1.RHO(58) := 0.731471 ; # 180
 183 PLANT.LOOP1.RHO(59) := 0.729245 ; # 181
 184 PLANT.LOOP1.RHO(60) := 0.727007 ; # 182
 185 PLANT.LOOP1.RHO(61) := 0.737706 ; # 183
 186 PLANT.LOOP1.RHO(62) := 0.738969 ; # 184
 187 PLANT.LOOP1.RHO(63) := 0.740294 ; # 185
 188 PLANT.LOOP1.RHO(64) := 0.741736 ; # 186
 189 PLANT.LOOP1.RHO(65) := 0.7433 ; # 187
 190 PLANT.LOOP1.RHO(66) := 0.744995 ; # 188

191 PLANT.LOOP1.RHO(67) := 0.74683 ; # 189
192 PLANT.LOOP1.RHO(68) := 0.748813 ; # 190
193 PLANT.LOOP1.RHO(69) := 0.750955 ; # 191
194 PLANT.LOOP1.RHO(70) := 0.753266 ; # 192
195 PLANT.LOOP1.RHO(71) := 0.755759 ; # 193
196 PLANT.LOOP1.RHO(72) := 0.758444 ; # 194
197 PLANT.LOOP1.RHO(73) := 0.761337 ; # 195
198 PLANT.LOOP1.RHO(74) := 0.764452 ; # 196
199 PLANT.LOOP1.RHO(75) := 0.767805 ; # 197
200 PLANT.LOOP1.RHO(76) := 0.771413 ; # 198
201 PLANT.LOOP1.RHO(77) := 0.775295 ; # 199
202 PLANT.LOOP1.RHO(78) := 0.779473 ; # 200
203 PLANT.LOOP1.RHO(79) := 0.783969 ; # 201
204 PLANT.LOOP1.RHO(80) := 0.788809 ; # 202
205 PLANT.LOOP1.RHO(81) := 0.79402 ; # 203
206 PLANT.LOOP1.RHO(82) := 0.799632 ; # 204
207 PLANT.LOOP1.RHO(83) := 0.805679 ; # 205
208 PLANT.LOOP1.RHO(84) := 0.812199 ; # 206
209 PLANT.LOOP1.RHO(85) := 0.819233 ; # 207
210 PLANT.LOOP1.RHO(86) := 0.826828 ; # 208
211 PLANT.LOOP1.RHO(87) := 0.835034 ; # 209
212 PLANT.LOOP1.RHO(88) := 0.843911 ; # 210
213 PLANT.LOOP1.RHO(89) := 0.853523 ; # 211
214 PLANT.LOOP1.RHO(90) := 0.863944 ; # 212
215 PLANT.LOOP1.RHO(91) := 0.875257 ; # 213
216 PLANT.LOOP1.RHO(92) := 0.887559 ; # 214
217 PLANT.LOOP1.RHO(93) := 0.900957 ; # 215
218 PLANT.LOOP1.RHO(94) := 0.915576 ; # 216
219 PLANT.LOOP1.RHO(95) := 0.931562 ; # 217
220 PLANT.LOOP1.RHO(96) := 0.949081 ; # 218
221 PLANT.LOOP1.RHO(97) := 0.968833 ; # 219
222 PLANT.LOOP1.RHO(98) := 0.989539 ; # 220
223 PLANT.LOOP1.RHO(99) := 1.01298 ; # 221
224 PLANT.LOOP1.RHO(100) := 1.03897 ; # 222
225 PLANT.LOOP1.P(1) := 1.99164e+006 ; # 223
226 PLANT.LOOP1.P(2) := 1.98572e+006 ; # 224
227 PLANT.LOOP1.P(3) := 1.97979e+006 ; # 225
228 PLANT.LOOP1.P(4) := 1.97384e+006 ; # 226
229 PLANT.LOOP1.P(5) := 1.96788e+006 ; # 227
230 PLANT.LOOP1.P(6) := 1.9619e+006 ; # 228
231 PLANT.LOOP1.P(7) := 1.9559e+006 ; # 229
232 PLANT.LOOP1.P(8) := 1.94989e+006 ; # 230
233 PLANT.LOOP1.P(9) := 1.94386e+006 ; # 231
234 PLANT.LOOP1.P(10) := 1.93782e+006 ; # 232
235 PLANT.LOOP1.P(11) := 1.93177e+006 ; # 233
236 PLANT.LOOP1.P(12) := 1.92572e+006 ; # 234
237 PLANT.LOOP1.P(13) := 1.91967e+006 ; # 235
238 PLANT.LOOP1.P(14) := 1.91362e+006 ; # 236
239 PLANT.LOOP1.P(15) := 1.90757e+006 ; # 237
240 PLANT.LOOP1.P(16) := 1.90152e+006 ; # 238
241 PLANT.LOOP1.P(17) := 1.89547e+006 ; # 239
242 PLANT.LOOP1.P(18) := 1.88942e+006 ; # 240
243 PLANT.LOOP1.P(19) := 1.88337e+006 ; # 241
244 PLANT.LOOP1.P(20) := 1.87732e+006 ; # 242
245 PLANT.LOOP1.P(21) := 1.87127e+006 ; # 243
246 PLANT.LOOP1.P(22) := 1.86522e+006 ; # 244
247 PLANT.LOOP1.P(23) := 1.85917e+006 ; # 245
248 PLANT.LOOP1.P(24) := 1.85312e+006 ; # 246
249 PLANT.LOOP1.P(25) := 1.84707e+006 ; # 247
250 PLANT.LOOP1.P(26) := 1.84102e+006 ; # 248
251 PLANT.LOOP1.P(27) := 1.83497e+006 ; # 249
252 PLANT.LOOP1.P(28) := 1.82892e+006 ; # 250
253 PLANT.LOOP1.P(29) := 1.82287e+006 ; # 251
254 PLANT.LOOP1.P(30) := 1.81682e+006 ; # 252
255 PLANT.LOOP1.P(31) := 1.81077e+006 ; # 253
256 PLANT.LOOP1.P(32) := 1.80472e+006 ; # 254
257 PLANT.LOOP1.P(33) := 1.79867e+006 ; # 255
258 PLANT.LOOP1.P(34) := 1.79262e+006 ; # 256
259 PLANT.LOOP1.P(35) := 1.78657e+006 ; # 257
260 PLANT.LOOP1.P(36) := 1.78052e+006 ; # 258
261 PLANT.LOOP1.P(37) := 1.77447e+006 ; # 259
262 PLANT.LOOP1.P(38) := 1.76842e+006 ; # 260
263 PLANT.LOOP1.P(39) := 1.76237e+006 ; # 261
264 PLANT.LOOP1.P(40) := 1.75632e+006 ; # 262
265 PLANT.LOOP1.P(41) := 1.75027e+006 ; # 263
266 PLANT.LOOP1.P(42) := 1.74422e+006 ; # 264
267 PLANT.LOOP1.P(43) := 1.73817e+006 ; # 265
268 PLANT.LOOP1.P(44) := 1.73212e+006 ; # 266
269 PLANT.LOOP1.P(45) := 1.72607e+006 ; # 267
270 PLANT.LOOP1.P(46) := 1.72002e+006 ; # 268
271 PLANT.LOOP1.P(47) := 1.71397e+006 ; # 269
272 PLANT.LOOP1.P(48) := 1.70792e+006 ; # 270
273 PLANT.LOOP1.P(49) := 1.70187e+006 ; # 271
274 PLANT.LOOP1.P(50) := 1.69582e+006 ; # 272
275 PLANT.LOOP1.P(51) := 1.68977e+006 ; # 273
276 PLANT.LOOP1.P(52) := 1.68372e+006 ; # 274
277 PLANT.LOOP1.P(53) := 1.67767e+006 ; # 275
278 PLANT.LOOP1.P(54) := 1.67162e+006 ; # 276
279 PLANT.LOOP1.P(55) := 1.66557e+006 ; # 277
280 PLANT.LOOP1.P(56) := 1.65952e+006 ; # 278
281 PLANT.LOOP1.P(57) := 1.65347e+006 ; # 279
282 PLANT.LOOP1.P(58) := 1.64742e+006 ; # 280

283 PLANT.LOOP1.P(59) := 1.72979e+006 ; # 281
284 PLANT.LOOP1.P(60) := 1.72331e+006 ; # 282
285 PLANT.LOOP1.P(61) := 1.74441e+006 ; # 283
286 PLANT.LOOP1.P(62) := 1.74289e+006 ; # 284
287 PLANT.LOOP1.P(63) := 1.74128e+006 ; # 285
288 PLANT.LOOP1.P(64) := 1.73966e+006 ; # 286
289 PLANT.LOOP1.P(65) := 1.73806e+006 ; # 287
290 PLANT.LOOP1.P(66) := 1.73645e+006 ; # 288
291 PLANT.LOOP1.P(67) := 1.73485e+006 ; # 289
292 PLANT.LOOP1.P(68) := 1.73326e+006 ; # 290
293 PLANT.LOOP1.P(69) := 1.73167e+006 ; # 291
294 PLANT.LOOP1.P(70) := 1.73009e+006 ; # 292
295 PLANT.LOOP1.P(71) := 1.72851e+006 ; # 293
296 PLANT.LOOP1.P(72) := 1.72694e+006 ; # 294
297 PLANT.LOOP1.P(73) := 1.72538e+006 ; # 295
298 PLANT.LOOP1.P(74) := 1.72383e+006 ; # 296
299 PLANT.LOOP1.P(75) := 1.72228e+006 ; # 297
300 PLANT.LOOP1.P(76) := 1.72075e+006 ; # 298
301 PLANT.LOOP1.P(77) := 1.71922e+006 ; # 299
302 PLANT.LOOP1.P(78) := 1.7177e+006 ; # 300
303 PLANT.LOOP1.P(79) := 1.7162e+006 ; # 301
304 PLANT.LOOP1.P(80) := 1.7147e+006 ; # 302
305 PLANT.LOOP1.P(81) := 1.71322e+006 ; # 303
306 PLANT.LOOP1.P(82) := 1.71175e+006 ; # 304
307 PLANT.LOOP1.P(83) := 1.71029e+006 ; # 305
308 PLANT.LOOP1.P(84) := 1.70885e+006 ; # 306
309 PLANT.LOOP1.P(85) := 1.70742e+006 ; # 307
310 PLANT.LOOP1.P(86) := 1.70601e+006 ; # 308
311 PLANT.LOOP1.P(87) := 1.70462e+006 ; # 309
312 PLANT.LOOP1.P(88) := 1.70324e+006 ; # 310
313 PLANT.LOOP1.P(89) := 1.70189e+006 ; # 311
314 PLANT.LOOP1.P(90) := 1.70055e+006 ; # 312
315 PLANT.LOOP1.P(91) := 1.69924e+006 ; # 313
316 PLANT.LOOP1.P(92) := 1.69795e+006 ; # 314
317 PLANT.LOOP1.P(93) := 1.69668e+006 ; # 315
318 PLANT.LOOP1.P(94) := 1.69543e+006 ; # 316
319 PLANT.LOOP1.P(95) := 1.69422e+006 ; # 317
320 PLANT.LOOP1.P(96) := 1.69303e+006 ; # 318
321 PLANT.LOOP1.P(97) := 1.69187e+006 ; # 319
322 PLANT.LOOP1.P(98) := 1.69075e+006 ; # 320
323 PLANT.LOOP1.P(99) := 1.68965e+006 ; # 321
324 PLANT.LOOP1.P(100) := 1.6886e+006 ; # 322
325 PLANT.LOOP1.P_OUT := 1.68802e+006 ; # 323
326 PLANT.LOOP1.H(1) := 2.81134e+006 ; # 324
327 PLANT.LOOP1.H(2) := 2.80926e+006 ; # 325
328 PLANT.LOOP1.H(3) := 2.80719e+006 ; # 326
329 PLANT.LOOP1.H(4) := 2.80511e+006 ; # 327
330 PLANT.LOOP1.H(5) := 2.80304e+006 ; # 328
331 PLANT.LOOP1.H(6) := 2.80097e+006 ; # 329
332 PLANT.LOOP1.H(7) := 2.7989e+006 ; # 330
333 PLANT.LOOP1.H(8) := 2.79683e+006 ; # 331
334 PLANT.LOOP1.H(9) := 2.79476e+006 ; # 332
335 PLANT.LOOP1.H(10) := 2.7927e+006 ; # 333
336 PLANT.LOOP1.H(11) := 2.85599e+006 ; # 334
337 PLANT.LOOP1.H(12) := 2.9176e+006 ; # 335
338 PLANT.LOOP1.H(13) := 2.9777e+006 ; # 336
339 PLANT.LOOP1.H(14) := 3.03633e+006 ; # 337
340 PLANT.LOOP1.H(15) := 3.09354e+006 ; # 338
341 PLANT.LOOP1.H(16) := 3.14934e+006 ; # 339
342 PLANT.LOOP1.H(17) := 3.20379e+006 ; # 340
343 PLANT.LOOP1.H(18) := 3.2569e+006 ; # 341
344 PLANT.LOOP1.H(19) := 3.30872e+006 ; # 342
345 PLANT.LOOP1.H(20) := 3.35927e+006 ; # 343
346 PLANT.LOOP1.H(21) := 3.40859e+006 ; # 344
347 PLANT.LOOP1.H(22) := 3.4567e+006 ; # 345
348 PLANT.LOOP1.H(23) := 3.50364e+006 ; # 346
349 PLANT.LOOP1.H(24) := 3.54943e+006 ; # 347
350 PLANT.LOOP1.H(25) := 3.5941e+006 ; # 348
351 PLANT.LOOP1.H(26) := 3.63768e+006 ; # 349
352 PLANT.LOOP1.H(27) := 3.6802e+006 ; # 350
353 PLANT.LOOP1.H(28) := 3.72168e+006 ; # 351
354 PLANT.LOOP1.H(29) := 3.76215e+006 ; # 352
355 PLANT.LOOP1.H(30) := 3.80163e+006 ; # 353
356 PLANT.LOOP1.H(31) := 3.84014e+006 ; # 354
357 PLANT.LOOP1.H(32) := 3.87771e+006 ; # 355
358 PLANT.LOOP1.H(33) := 3.91437e+006 ; # 356
359 PLANT.LOOP1.H(34) := 3.95013e+006 ; # 357
360 PLANT.LOOP1.H(35) := 3.98502e+006 ; # 358
361 PLANT.LOOP1.H(36) := 4.01905e+006 ; # 359
362 PLANT.LOOP1.H(37) := 4.05226e+006 ; # 360
363 PLANT.LOOP1.H(38) := 4.08465e+006 ; # 361
364 PLANT.LOOP1.H(39) := 4.11626e+006 ; # 362
365 PLANT.LOOP1.H(40) := 4.14709e+006 ; # 363
366 PLANT.LOOP1.H(41) := 4.17717e+006 ; # 364
367 PLANT.LOOP1.H(42) := 4.20651e+006 ; # 365
368 PLANT.LOOP1.H(43) := 4.23514e+006 ; # 366
369 PLANT.LOOP1.H(44) := 4.26306e+006 ; # 367
370 PLANT.LOOP1.H(45) := 4.29031e+006 ; # 368
371 PLANT.LOOP1.H(46) := 4.31689e+006 ; # 369
372 PLANT.LOOP1.H(47) := 4.34282e+006 ; # 370
373 PLANT.LOOP1.H(48) := 4.36812e+006 ; # 371
374 PLANT.LOOP1.H(49) := 4.3928e+006 ; # 372

```

375 PLANT.LOOP1.H(50) := 4.41684e+006 ; # 373
376 PLANT.LOOP1.H(51) := 4.41279e+006 ; # 374
377 PLANT.LOOP1.H(52) := 4.40875e+006 ; # 375
378 PLANT.LOOP1.H(53) := 4.4047e+006 ; # 376
379 PLANT.LOOP1.H(54) := 4.40067e+006 ; # 377
380 PLANT.LOOP1.H(55) := 4.39663e+006 ; # 378
381 PLANT.LOOP1.H(56) := 4.3926e+006 ; # 379
382 PLANT.LOOP1.H(57) := 4.38857e+006 ; # 380
383 PLANT.LOOP1.H(58) := 4.38455e+006 ; # 381
384 PLANT.LOOP1.H(59) := 4.38053e+006 ; # 382
385 PLANT.LOOP1.H(60) := 4.37651e+006 ; # 383
386 PLANT.LOOP1.H(61) := 4.36206e+006 ; # 384
387 PLANT.LOOP1.H(62) := 4.34684e+006 ; # 385
388 PLANT.LOOP1.H(63) := 4.33083e+006 ; # 386
389 PLANT.LOOP1.H(64) := 4.31397e+006 ; # 387
390 PLANT.LOOP1.H(65) := 4.29622e+006 ; # 388
391 PLANT.LOOP1.H(66) := 4.27754e+006 ; # 389
392 PLANT.LOOP1.H(67) := 4.25788e+006 ; # 390
393 PLANT.LOOP1.H(68) := 4.23718e+006 ; # 391
394 PLANT.LOOP1.H(69) := 4.21539e+006 ; # 392
395 PLANT.LOOP1.H(70) := 4.19246e+006 ; # 393
396 PLANT.LOOP1.H(71) := 4.16832e+006 ; # 394
397 PLANT.LOOP1.H(72) := 4.14291e+006 ; # 395
398 PLANT.LOOP1.H(73) := 4.11616e+006 ; # 396
399 PLANT.LOOP1.H(74) := 4.088e+006 ; # 397
400 PLANT.LOOP1.H(75) := 4.05836e+006 ; # 398
401 PLANT.LOOP1.H(76) := 4.02716e+006 ; # 399
402 PLANT.LOOP1.H(77) := 3.99432e+006 ; # 400
403 PLANT.LOOP1.H(78) := 3.95975e+006 ; # 401
404 PLANT.LOOP1.H(79) := 3.92336e+006 ; # 402
405 PLANT.LOOP1.H(80) := 3.88505e+006 ; # 403
406 PLANT.LOOP1.H(81) := 3.84473e+006 ; # 404
407 PLANT.LOOP1.H(82) := 3.80228e+006 ; # 405
408 PLANT.LOOP1.H(83) := 3.75761e+006 ; # 406
409 PLANT.LOOP1.H(84) := 3.71058e+006 ; # 407
410 PLANT.LOOP1.H(85) := 3.66107e+006 ; # 408
411 PLANT.LOOP1.H(86) := 3.60896e+006 ; # 409
412 PLANT.LOOP1.H(87) := 3.55411e+006 ; # 410
413 PLANT.LOOP1.H(88) := 3.49637e+006 ; # 411
414 PLANT.LOOP1.H(89) := 3.43559e+006 ; # 412
415 PLANT.LOOP1.H(90) := 3.37161e+006 ; # 413
416 PLANT.LOOP1.H(91) := 3.30426e+006 ; # 414
417 PLANT.LOOP1.H(92) := 3.23337e+006 ; # 415
418 PLANT.LOOP1.H(93) := 3.15875e+006 ; # 416
419 PLANT.LOOP1.H(94) := 3.0802e+006 ; # 417
420 PLANT.LOOP1.H(95) := 2.99751e+006 ; # 418
421 PLANT.LOOP1.H(96) := 2.91047e+006 ; # 419
422 PLANT.LOOP1.H(97) := 2.81886e+006 ; # 420
423 PLANT.LOOP1.H(98) := 2.72242e+006 ; # 421
424 PLANT.LOOP1.H(99) := 2.6209e+006 ; # 422
425 PLANT.LOOP1.H(100) := 2.51405e+006 ; # 423
426 PLANT.LOOP1.HO := 2.81342e+006 ; # 424
427 PLANT.LOOP1.T(1) := 839.163 ; # 425
428 PLANT.LOOP1.T(2) := 838.763 ; # 426
429 PLANT.LOOP1.T(3) := 838.363 ; # 427
430 PLANT.LOOP1.T(4) := 837.964 ; # 428
431 PLANT.LOOP1.T(5) := 837.565 ; # 429
432 PLANT.LOOP1.T(6) := 837.166 ; # 430
433 PLANT.LOOP1.T(7) := 836.767 ; # 431
434 PLANT.LOOP1.T(8) := 836.369 ; # 432
435 PLANT.LOOP1.T(9) := 835.971 ; # 433
436 PLANT.LOOP1.T(10) := 835.574 ; # 434
437 PLANT.LOOP1.T(11) := 847.757 ; # 435
438 PLANT.LOOP1.T(12) := 859.616 ; # 436
439 PLANT.LOOP1.T(13) := 871.186 ; # 437
440 PLANT.LOOP1.T(14) := 882.472 ; # 438
441 PLANT.LOOP1.T(15) := 893.484 ; # 439
442 PLANT.LOOP1.T(16) := 904.226 ; # 440
443 PLANT.LOOP1.T(17) := 914.706 ; # 441
444 PLANT.LOOP1.T(18) := 924.93 ; # 442
445 PLANT.LOOP1.T(19) := 934.904 ; # 443
446 PLANT.LOOP1.T(20) := 944.635 ; # 444
447 PLANT.LOOP1.T(21) := 954.128 ; # 445
448 PLANT.LOOP1.T(22) := 963.39 ; # 446
449 PLANT.LOOP1.T(23) := 972.425 ; # 447
450 PLANT.LOOP1.T(24) := 981.239 ; # 448
451 PLANT.LOOP1.T(25) := 989.838 ; # 449
452 PLANT.LOOP1.T(26) := 998.228 ; # 450
453 PLANT.LOOP1.T(27) := 1006.41 ; # 451
454 PLANT.LOOP1.T(28) := 1014.4 ; # 452
455 PLANT.LOOP1.T(29) := 1022.19 ; # 453
456 PLANT.LOOP1.T(30) := 1029.79 ; # 454
457 PLANT.LOOP1.T(31) := 1037.2 ; # 455
458 PLANT.LOOP1.T(32) := 1044.43 ; # 456
459 PLANT.LOOP1.T(33) := 1051.49 ; # 457
460 PLANT.LOOP1.T(34) := 1058.37 ; # 458
461 PLANT.LOOP1.T(35) := 1065.09 ; # 459
462 PLANT.LOOP1.T(36) := 1071.64 ; # 460
463 PLANT.LOOP1.T(37) := 1078.03 ; # 461
464 PLANT.LOOP1.T(38) := 1084.27 ; # 462
465 PLANT.LOOP1.T(39) := 1090.35 ; # 463
466 PLANT.LOOP1.T(40) := 1096.28 ; # 464

```

```

467 PLANT.LOOP1.T(41) := 1102.07 ; # 465
468 PLANT.LOOP1.T(42) := 1107.72 ; # 466
469 PLANT.LOOP1.T(43) := 1113.23 ; # 467
470 PLANT.LOOP1.T(44) := 1118.61 ; # 468
471 PLANT.LOOP1.T(45) := 1123.85 ; # 469
472 PLANT.LOOP1.T(46) := 1128.97 ; # 470
473 PLANT.LOOP1.T(47) := 1133.96 ; # 471
474 PLANT.LOOP1.T(48) := 1138.83 ; # 472
475 PLANT.LOOP1.T(49) := 1143.58 ; # 473
476 PLANT.LOOP1.T(50) := 1148.21 ; # 474
477 PLANT.LOOP1.T(51) := 1147.43 ; # 475
478 PLANT.LOOP1.T(52) := 1146.65 ; # 476
479 PLANT.LOOP1.T(53) := 1145.87 ; # 477
480 PLANT.LOOP1.T(54) := 1145.1 ; # 478
481 PLANT.LOOP1.T(55) := 1144.32 ; # 479
482 PLANT.LOOP1.T(56) := 1143.54 ; # 480
483 PLANT.LOOP1.T(57) := 1142.77 ; # 481
484 PLANT.LOOP1.T(58) := 1141.99 ; # 482
485 PLANT.LOOP1.T(59) := 1141.22 ; # 483
486 PLANT.LOOP1.T(60) := 1140.45 ; # 484
487 PLANT.LOOP1.T(61) := 1137.66 ; # 485
488 PLANT.LOOP1.T(62) := 1134.74 ; # 486
489 PLANT.LOOP1.T(63) := 1131.65 ; # 487
490 PLANT.LOOP1.T(64) := 1128.41 ; # 488
491 PLANT.LOOP1.T(65) := 1124.99 ; # 489
492 PLANT.LOOP1.T(66) := 1121.4 ; # 490
493 PLANT.LOOP1.T(67) := 1117.61 ; # 491
494 PLANT.LOOP1.T(68) := 1113.63 ; # 492
495 PLANT.LOOP1.T(69) := 1109.43 ; # 493
496 PLANT.LOOP1.T(70) := 1105.02 ; # 494
497 PLANT.LOOP1.T(71) := 1100.37 ; # 495
498 PLANT.LOOP1.T(72) := 1095.48 ; # 496
499 PLANT.LOOP1.T(73) := 1090.33 ; # 497
500 PLANT.LOOP1.T(74) := 1084.91 ; # 498
501 PLANT.LOOP1.T(75) := 1079.2 ; # 499
502 PLANT.LOOP1.T(76) := 1073.2 ; # 500
503 PLANT.LOOP1.T(77) := 1066.88 ; # 501
504 PLANT.LOOP1.T(78) := 1060.22 ; # 502
505 PLANT.LOOP1.T(79) := 1053.22 ; # 503
506 PLANT.LOOP1.T(80) := 1045.84 ; # 504
507 PLANT.LOOP1.T(81) := 1038.08 ; # 505
508 PLANT.LOOP1.T(82) := 1029.91 ; # 506
509 PLANT.LOOP1.T(83) := 1021.31 ; # 507
510 PLANT.LOOP1.T(84) := 1012.26 ; # 508
511 PLANT.LOOP1.T(85) := 1002.73 ; # 509
512 PLANT.LOOP1.T(86) := 992.699 ; # 510
513 PLANT.LOOP1.T(87) := 982.14 ; # 511
514 PLANT.LOOP1.T(88) := 971.025 ; # 512
515 PLANT.LOOP1.T(89) := 959.325 ; # 513
516 PLANT.LOOP1.T(90) := 947.01 ; # 514
517 PLANT.LOOP1.T(91) := 934.046 ; # 515
518 PLANT.LOOP1.T(92) := 920.4 ; # 516
519 PLANT.LOOP1.T(93) := 906.036 ; # 517
520 PLANT.LOOP1.T(94) := 890.915 ; # 518
521 PLANT.LOOP1.T(95) := 874.999 ; # 519
522 PLANT.LOOP1.T(96) := 858.245 ; # 520
523 PLANT.LOOP1.T(97) := 840.609 ; # 521
524 PLANT.LOOP1.T(98) := 822.045 ; # 522
525 PLANT.LOOP1.T(99) := 802.504 ; # 523
526 PLANT.LOOP1.T(100) := 781.936 ; # 524
527 PLANT.LOOP1.TO := 839.563 ; # 525
528 PLANT.LOOP1.TEXTRNL(1) := 291.15 ; # 526
529 PLANT.LOOP1.TEXTRNL(2) := 291.15 ; # 527
530 PLANT.LOOP1.TEXTRNL(3) := 291.15 ; # 528
531 PLANT.LOOP1.TEXTRNL(4) := 291.15 ; # 529
532 PLANT.LOOP1.TEXTRNL(5) := 291.15 ; # 530
533 PLANT.LOOP1.TEXTRNL(6) := 291.15 ; # 531
534 PLANT.LOOP1.TEXTRNL(7) := 291.15 ; # 532
535 PLANT.LOOP1.TEXTRNL(8) := 291.15 ; # 533
536 PLANT.LOOP1.TEXTRNL(9) := 291.15 ; # 534
537 PLANT.LOOP1.TEXTRNL(10) := 291.15 ; # 535
538 PLANT.LOOP1.TEXTRNL(11) := 875.997 ; # 536
539 PLANT.LOOP1.TEXTRNL(12) := 887.105 ; # 537
540 PLANT.LOOP1.TEXTRNL(13) := 898.003 ; # 538
541 PLANT.LOOP1.TEXTRNL(14) := 908.635 ; # 539
542 PLANT.LOOP1.TEXTRNL(15) := 919.007 ; # 540
543 PLANT.LOOP1.TEXTRNL(16) := 929.126 ; # 541
544 PLANT.LOOP1.TEXTRNL(17) := 938.998 ; # 542
545 PLANT.LOOP1.TEXTRNL(18) := 948.629 ; # 543
546 PLANT.LOOP1.TEXTRNL(19) := 958.024 ; # 544
547 PLANT.LOOP1.TEXTRNL(20) := 967.19 ; # 545
548 PLANT.LOOP1.TEXTRNL(21) := 976.133 ; # 546
549 PLANT.LOOP1.TEXTRNL(22) := 984.857 ; # 547
550 PLANT.LOOP1.TEXTRNL(23) := 993.368 ; # 548
551 PLANT.LOOP1.TEXTRNL(24) := 1001.67 ; # 549
552 PLANT.LOOP1.TEXTRNL(25) := 1009.77 ; # 550
553 PLANT.LOOP1.TEXTRNL(26) := 1017.67 ; # 551
554 PLANT.LOOP1.TEXTRNL(27) := 1025.38 ; # 552
555 PLANT.LOOP1.TEXTRNL(28) := 1032.9 ; # 553
556 PLANT.LOOP1.TEXTRNL(29) := 1040.24 ; # 554
557 PLANT.LOOP1.TEXTRNL(30) := 1047.4 ; # 555
558 PLANT.LOOP1.TEXTRNL(31) := 1054.38 ; # 556

```

```

559 PLANT.LOOP1.TEXTRNL(32) := 1061.2 ; # 557
560 PLANT.LOOP1.TEXTRNL(33) := 1067.84 ; # 558
561 PLANT.LOOP1.TEXTRNL(34) := 1074.33 ; # 559
562 PLANT.LOOP1.TEXTRNL(35) := 1080.65 ; # 560
563 PLANT.LOOP1.TEXTRNL(36) := 1086.83 ; # 561
564 PLANT.LOOP1.TEXTRNL(37) := 1092.85 ; # 562
565 PLANT.LOOP1.TEXTRNL(38) := 1098.72 ; # 563
566 PLANT.LOOP1.TEXTRNL(39) := 1104.45 ; # 564
567 PLANT.LOOP1.TEXTRNL(40) := 1110.04 ; # 565
568 PLANT.LOOP1.TEXTRNL(41) := 1115.49 ; # 566
569 PLANT.LOOP1.TEXTRNL(42) := 1120.82 ; # 567
570 PLANT.LOOP1.TEXTRNL(43) := 1126.01 ; # 568
571 PLANT.LOOP1.TEXTRNL(44) := 1131.07 ; # 569
572 PLANT.LOOP1.TEXTRNL(45) := 1136.01 ; # 570
573 PLANT.LOOP1.TEXTRNL(46) := 1140.83 ; # 571
574 PLANT.LOOP1.TEXTRNL(47) := 1145.53 ; # 572
575 PLANT.LOOP1.TEXTRNL(48) := 1150.12 ; # 573
576 PLANT.LOOP1.TEXTRNL(49) := 1154.59 ; # 574
577 PLANT.LOOP1.TEXTRNL(50) := 1158.94 ; # 575
578 PLANT.LOOP1.TEXTRNL(51) := 291.15 ; # 576
579 PLANT.LOOP1.TEXTRNL(52) := 291.15 ; # 577
580 PLANT.LOOP1.TEXTRNL(53) := 291.15 ; # 578
581 PLANT.LOOP1.TEXTRNL(54) := 291.15 ; # 579
582 PLANT.LOOP1.TEXTRNL(55) := 291.15 ; # 580
583 PLANT.LOOP1.TEXTRNL(56) := 291.15 ; # 581
584 PLANT.LOOP1.TEXTRNL(57) := 291.15 ; # 582
585 PLANT.LOOP1.TEXTRNL(58) := 291.15 ; # 583
586 PLANT.LOOP1.TEXTRNL(59) := 291.15 ; # 584
587 PLANT.LOOP1.TEXTRNL(60) := 291.15 ; # 585
588 PLANT.LOOP1.TEXTRNL(61) := 1127.77 ; # 586
589 PLANT.LOOP1.TEXTRNL(62) := 1124.33 ; # 587
590 PLANT.LOOP1.TEXTRNL(63) := 1120.69 ; # 588
591 PLANT.LOOP1.TEXTRNL(64) := 1116.87 ; # 589
592 PLANT.LOOP1.TEXTRNL(65) := 1112.85 ; # 590
593 PLANT.LOOP1.TEXTRNL(66) := 1108.61 ; # 591
594 PLANT.LOOP1.TEXTRNL(67) := 1104.16 ; # 592
595 PLANT.LOOP1.TEXTRNL(68) := 1099.46 ; # 593
596 PLANT.LOOP1.TEXTRNL(69) := 1094.52 ; # 594
597 PLANT.LOOP1.TEXTRNL(70) := 1089.32 ; # 595
598 PLANT.LOOP1.TEXTRNL(71) := 1083.85 ; # 596
599 PLANT.LOOP1.TEXTRNL(72) := 1078.09 ; # 597
600 PLANT.LOOP1.TEXTRNL(73) := 1072.03 ; # 598
601 PLANT.LOOP1.TEXTRNL(74) := 1065.64 ; # 599
602 PLANT.LOOP1.TEXTRNL(75) := 1058.92 ; # 600
603 PLANT.LOOP1.TEXTRNL(76) := 1051.85 ; # 601
604 PLANT.LOOP1.TEXTRNL(77) := 1044.4 ; # 602
605 PLANT.LOOP1.TEXTRNL(78) := 1036.57 ; # 603
606 PLANT.LOOP1.TEXTRNL(79) := 1028.32 ; # 604
607 PLANT.LOOP1.TEXTRNL(80) := 1019.63 ; # 605
608 PLANT.LOOP1.TEXTRNL(81) := 1010.49 ; # 606
609 PLANT.LOOP1.TEXTRNL(82) := 1000.87 ; # 607
610 PLANT.LOOP1.TEXTRNL(83) := 990.74 ; # 608
611 PLANT.LOOP1.TEXTRNL(84) := 980.078 ; # 609
612 PLANT.LOOP1.TEXTRNL(85) := 968.854 ; # 610
613 PLANT.LOOP1.TEXTRNL(86) := 957.041 ; # 611
614 PLANT.LOOP1.TEXTRNL(87) := 944.605 ; # 612
615 PLANT.LOOP1.TEXTRNL(88) := 931.514 ; # 613
616 PLANT.LOOP1.TEXTRNL(89) := 917.735 ; # 614
617 PLANT.LOOP1.TEXTRNL(90) := 903.231 ; # 615
618 PLANT.LOOP1.TEXTRNL(91) := 887.962 ; # 616
619 PLANT.LOOP1.TEXTRNL(92) := 871.891 ; # 617
620 PLANT.LOOP1.TEXTRNL(93) := 854.973 ; # 618
621 PLANT.LOOP1.TEXTRNL(94) := 837.165 ; # 619
622 PLANT.LOOP1.TEXTRNL(95) := 818.42 ; # 620
623 PLANT.LOOP1.TEXTRNL(96) := 798.688 ; # 621
624 PLANT.LOOP1.TEXTRNL(97) := 777.917 ; # 622
625 PLANT.LOOP1.TEXTRNL(98) := 756.054 ; # 623
626 PLANT.LOOP1.TEXTRNL(99) := 733.039 ; # 624
627 PLANT.LOOP1.TEXTRNL(100) := 708.82 ; # 625
628 PLANT.LOOP1.PSI(1) := 1.21853e+006 ; # 626
629 PLANT.LOOP1.PSI(2) := 1.21407e+006 ; # 627
630 PLANT.LOOP1.PSI(3) := 1.2096e+006 ; # 628
631 PLANT.LOOP1.PSI(4) := 1.20513e+006 ; # 629
632 PLANT.LOOP1.PSI(5) := 1.20066e+006 ; # 630
633 PLANT.LOOP1.PSI(6) := 1.19618e+006 ; # 631
634 PLANT.LOOP1.PSI(7) := 1.1917e+006 ; # 632
635 PLANT.LOOP1.PSI(8) := 1.18721e+006 ; # 633
636 PLANT.LOOP1.PSI(9) := 1.18271e+006 ; # 634
637 PLANT.LOOP1.PSI(10) := 1.17821e+006 ; # 635
638 PLANT.LOOP1.PSI(11) := 1.21421e+006 ; # 636
639 PLANT.LOOP1.PSI(12) := 1.23642e+006 ; # 637
640 PLANT.LOOP1.PSI(13) := 1.25693e+006 ; # 638
641 PLANT.LOOP1.PSI(14) := 1.27623e+006 ; # 639
642 PLANT.LOOP1.PSI(15) := 1.2944e+006 ; # 640
643 PLANT.LOOP1.PSI(16) := 1.3115e+006 ; # 641
644 PLANT.LOOP1.PSI(17) := 1.32762e+006 ; # 642
645 PLANT.LOOP1.PSI(18) := 1.3428e+006 ; # 643
646 PLANT.LOOP1.PSI(19) := 1.35711e+006 ; # 644
647 PLANT.LOOP1.PSI(20) := 1.37059e+006 ; # 645
648 PLANT.LOOP1.PSI(21) := 1.38329e+006 ; # 646
649 PLANT.LOOP1.PSI(22) := 1.39525e+006 ; # 647
650 PLANT.LOOP1.PSI(23) := 1.40653e+006 ; # 648

```

```

651 PLANT.LOOP1.PSI(24) := 1.41714e+006 ; # 649
652 PLANT.LOOP1.PSI(25) := 1.42714e+006 ; # 650
653 PLANT.LOOP1.PSI(26) := 1.43655e+006 ; # 651
654 PLANT.LOOP1.PSI(27) := 1.4454e+006 ; # 652
655 PLANT.LOOP1.PSI(28) := 1.45372e+006 ; # 653
656 PLANT.LOOP1.PSI(29) := 1.46153e+006 ; # 654
657 PLANT.LOOP1.PSI(30) := 1.46887e+006 ; # 655
658 PLANT.LOOP1.PSI(31) := 1.47574e+006 ; # 656
659 PLANT.LOOP1.PSI(32) := 1.48219e+006 ; # 657
660 PLANT.LOOP1.PSI(33) := 1.48821e+006 ; # 658
661 PLANT.LOOP1.PSI(34) := 1.49385e+006 ; # 659
662 PLANT.LOOP1.PSI(35) := 1.4991e+006 ; # 660
663 PLANT.LOOP1.PSI(36) := 1.50399e+006 ; # 661
664 PLANT.LOOP1.PSI(37) := 1.50854e+006 ; # 662
665 PLANT.LOOP1.PSI(38) := 1.51275e+006 ; # 663
666 PLANT.LOOP1.PSI(39) := 1.51665e+006 ; # 664
667 PLANT.LOOP1.PSI(40) := 1.52024e+006 ; # 665
668 PLANT.LOOP1.PSI(41) := 1.52354e+006 ; # 666
669 PLANT.LOOP1.PSI(42) := 1.52657e+006 ; # 667
670 PLANT.LOOP1.PSI(43) := 1.52932e+006 ; # 668
671 PLANT.LOOP1.PSI(44) := 1.53181e+006 ; # 669
672 PLANT.LOOP1.PSI(45) := 1.53406e+006 ; # 670
673 PLANT.LOOP1.PSI(46) := 1.53607e+006 ; # 671
674 PLANT.LOOP1.PSI(47) := 1.53785e+006 ; # 672
675 PLANT.LOOP1.PSI(48) := 1.53941e+006 ; # 673
676 PLANT.LOOP1.PSI(49) := 1.54075e+006 ; # 674
677 PLANT.LOOP1.PSI(50) := 1.54188e+006 ; # 675
678 PLANT.LOOP1.PSI(51) := 1.5428e+006 ; # 676
679 PLANT.LOOP1.PSI(52) := 1.50808e+006 ; # 677
680 PLANT.LOOP1.PSI(53) := 1.50192e+006 ; # 678
681 PLANT.LOOP1.PSI(54) := 1.49574e+006 ; # 679
682 PLANT.LOOP1.PSI(55) := 1.48956e+006 ; # 680
683 PLANT.LOOP1.PSI(56) := 1.48336e+006 ; # 681
684 PLANT.LOOP1.PSI(57) := 1.47715e+006 ; # 682
685 PLANT.LOOP1.PSI(58) := 1.47093e+006 ; # 683
686 PLANT.LOOP1.PSI(59) := 1.46469e+006 ; # 684
687 PLANT.LOOP1.PSI(60) := 1.45845e+006 ; # 685
688 PLANT.LOOP1.PSI(61) := 1.47351e+006 ; # 686
689 PLANT.LOOP1.PSI(62) := 1.46929e+006 ; # 687
690 PLANT.LOOP1.PSI(63) := 1.46481e+006 ; # 688
691 PLANT.LOOP1.PSI(64) := 1.46016e+006 ; # 689
692 PLANT.LOOP1.PSI(65) := 1.45533e+006 ; # 690
693 PLANT.LOOP1.PSI(66) := 1.4503e+006 ; # 691
694 PLANT.LOOP1.PSI(67) := 1.44506e+006 ; # 692
695 PLANT.LOOP1.PSI(68) := 1.4396e+006 ; # 693
696 PLANT.LOOP1.PSI(69) := 1.4339e+006 ; # 694
697 PLANT.LOOP1.PSI(70) := 1.42795e+006 ; # 695
698 PLANT.LOOP1.PSI(71) := 1.42173e+006 ; # 696
699 PLANT.LOOP1.PSI(72) := 1.41522e+006 ; # 697
700 PLANT.LOOP1.PSI(73) := 1.4084e+006 ; # 698
701 PLANT.LOOP1.PSI(74) := 1.40125e+006 ; # 699
702 PLANT.LOOP1.PSI(75) := 1.39374e+006 ; # 700
703 PLANT.LOOP1.PSI(76) := 1.38585e+006 ; # 701
704 PLANT.LOOP1.PSI(77) := 1.37755e+006 ; # 702
705 PLANT.LOOP1.PSI(78) := 1.36881e+006 ; # 703
706 PLANT.LOOP1.PSI(79) := 1.35959e+006 ; # 704
707 PLANT.LOOP1.PSI(80) := 1.34986e+006 ; # 705
708 PLANT.LOOP1.PSI(81) := 1.33957e+006 ; # 706
709 PLANT.LOOP1.PSI(82) := 1.32868e+006 ; # 707
710 PLANT.LOOP1.PSI(83) := 1.31713e+006 ; # 708
711 PLANT.LOOP1.PSI(84) := 1.30488e+006 ; # 709
712 PLANT.LOOP1.PSI(85) := 1.29185e+006 ; # 710
713 PLANT.LOOP1.PSI(86) := 1.27797e+006 ; # 711
714 PLANT.LOOP1.PSI(87) := 1.26318e+006 ; # 712
715 PLANT.LOOP1.PSI(88) := 1.24738e+006 ; # 713
716 PLANT.LOOP1.PSI(89) := 1.23046e+006 ; # 714
717 PLANT.LOOP1.PSI(90) := 1.21233e+006 ; # 715
718 PLANT.LOOP1.PSI(91) := 1.19284e+006 ; # 716
719 PLANT.LOOP1.PSI(92) := 1.17186e+006 ; # 717
720 PLANT.LOOP1.PSI(93) := 1.14922e+006 ; # 718
721 PLANT.LOOP1.PSI(94) := 1.12472e+006 ; # 719
722 PLANT.LOOP1.PSI(95) := 1.09815e+006 ; # 720
723 PLANT.LOOP1.PSI(96) := 1.06925e+006 ; # 721
724 PLANT.LOOP1.PSI(97) := 1.03771e+006 ; # 722
725 PLANT.LOOP1.PSI(98) := 1.00319e+006 ; # 723
726 PLANT.LOOP1.PSI(99) := 965262 ; # 724
727 PLANT.LOOP1.PSI(100) := 923433 ; # 725
728 PLANT.LOOP1.F(1) := 27.5042 ; # 726
729 PLANT.LOOP1.F(2) := 27.5042 ; # 727
730 PLANT.LOOP1.F(3) := 27.5042 ; # 728
731 PLANT.LOOP1.F(4) := 27.5042 ; # 729
732 PLANT.LOOP1.F(5) := 27.5042 ; # 730
733 PLANT.LOOP1.F(6) := 27.5042 ; # 731
734 PLANT.LOOP1.F(7) := 27.5042 ; # 732
735 PLANT.LOOP1.F(8) := 27.5042 ; # 733
736 PLANT.LOOP1.F(9) := 27.5042 ; # 734
737 PLANT.LOOP1.F(10) := 27.5042 ; # 735
738 PLANT.LOOP1.F(11) := 27.5042 ; # 736
739 PLANT.LOOP1.F(12) := 27.5042 ; # 737
740 PLANT.LOOP1.F(13) := 27.5042 ; # 738
741 PLANT.LOOP1.F(14) := 27.5042 ; # 739
742 PLANT.LOOP1.F(15) := 27.5042 ; # 740

```



```

743 PLANT.LOOP1.F(16) := 27.5042 ; # 741
744 PLANT.LOOP1.F(17) := 27.5042 ; # 742
745 PLANT.LOOP1.F(18) := 27.5042 ; # 743
746 PLANT.LOOP1.F(19) := 27.5042 ; # 744
747 PLANT.LOOP1.F(20) := 27.5042 ; # 745
748 PLANT.LOOP1.F(21) := 27.5042 ; # 746
749 PLANT.LOOP1.F(22) := 27.5042 ; # 747
750 PLANT.LOOP1.F(23) := 27.5042 ; # 748
751 PLANT.LOOP1.F(24) := 27.5042 ; # 749
752 PLANT.LOOP1.F(25) := 27.5042 ; # 750
753 PLANT.LOOP1.F(26) := 27.5042 ; # 751
754 PLANT.LOOP1.F(27) := 27.5042 ; # 752
755 PLANT.LOOP1.F(28) := 27.5042 ; # 753
756 PLANT.LOOP1.F(29) := 27.5042 ; # 754
757 PLANT.LOOP1.F(30) := 27.5042 ; # 755
758 PLANT.LOOP1.F(31) := 27.5042 ; # 756
759 PLANT.LOOP1.F(32) := 27.5042 ; # 757
760 PLANT.LOOP1.F(33) := 27.5042 ; # 758
761 PLANT.LOOP1.F(34) := 27.5042 ; # 759
762 PLANT.LOOP1.F(35) := 27.5042 ; # 760
763 PLANT.LOOP1.F(36) := 27.5042 ; # 761
764 PLANT.LOOP1.F(37) := 27.5042 ; # 762
765 PLANT.LOOP1.F(38) := 27.5042 ; # 763
766 PLANT.LOOP1.F(39) := 27.5042 ; # 764
767 PLANT.LOOP1.F(40) := 27.5042 ; # 765
768 PLANT.LOOP1.F(41) := 27.5042 ; # 766
769 PLANT.LOOP1.F(42) := 27.5042 ; # 767
770 PLANT.LOOP1.F(43) := 27.5042 ; # 768
771 PLANT.LOOP1.F(44) := 27.5042 ; # 769
772 PLANT.LOOP1.F(45) := 27.5042 ; # 770
773 PLANT.LOOP1.F(46) := 27.5042 ; # 771
774 PLANT.LOOP1.F(47) := 27.5042 ; # 772
775 PLANT.LOOP1.F(48) := 27.5042 ; # 773
776 PLANT.LOOP1.F(49) := 27.5042 ; # 774
777 PLANT.LOOP1.F(50) := 27.5042 ; # 775
778 PLANT.LOOP1.F(51) := 27.5042 ; # 776
779 PLANT.LOOP1.F(52) := 27.5042 ; # 777
780 PLANT.LOOP1.F(53) := 27.5042 ; # 778
781 PLANT.LOOP1.F(54) := 27.5042 ; # 779
782 PLANT.LOOP1.F(55) := 27.5042 ; # 780
783 PLANT.LOOP1.F(56) := 27.5042 ; # 781
784 PLANT.LOOP1.F(57) := 27.5042 ; # 782
785 PLANT.LOOP1.F(58) := 27.5042 ; # 783
786 PLANT.LOOP1.F(59) := 27.5042 ; # 784
787 PLANT.LOOP1.F(60) := 27.5042 ; # 785
788 PLANT.LOOP1.F(61) := 27.5042 ; # 786
789 PLANT.LOOP1.F(62) := 27.5042 ; # 787
790 PLANT.LOOP1.F(63) := 27.5042 ; # 788
791 PLANT.LOOP1.F(64) := 27.5042 ; # 789
792 PLANT.LOOP1.F(65) := 27.5042 ; # 790
793 PLANT.LOOP1.F(66) := 27.5042 ; # 791
794 PLANT.LOOP1.F(67) := 27.5042 ; # 792
795 PLANT.LOOP1.F(68) := 27.5042 ; # 793
796 PLANT.LOOP1.F(69) := 27.5042 ; # 794
797 PLANT.LOOP1.F(70) := 27.5042 ; # 795
798 PLANT.LOOP1.F(71) := 27.5042 ; # 796
799 PLANT.LOOP1.F(72) := 27.5042 ; # 797
800 PLANT.LOOP1.F(73) := 27.5042 ; # 798
801 PLANT.LOOP1.F(74) := 27.5042 ; # 799
802 PLANT.LOOP1.F(75) := 27.5042 ; # 800
803 PLANT.LOOP1.F(76) := 27.5042 ; # 801
804 PLANT.LOOP1.F(77) := 27.5042 ; # 802
805 PLANT.LOOP1.F(78) := 27.5042 ; # 803
806 PLANT.LOOP1.F(79) := 27.5042 ; # 804
807 PLANT.LOOP1.F(80) := 27.5042 ; # 805
808 PLANT.LOOP1.F(81) := 27.5042 ; # 806
809 PLANT.LOOP1.F(82) := 27.5042 ; # 807
810 PLANT.LOOP1.F(83) := 27.5042 ; # 808
811 PLANT.LOOP1.F(84) := 27.5042 ; # 809
812 PLANT.LOOP1.F(85) := 27.5042 ; # 810
813 PLANT.LOOP1.F(86) := 27.5042 ; # 811
814 PLANT.LOOP1.F(87) := 27.5042 ; # 812
815 PLANT.LOOP1.F(88) := 27.5042 ; # 813
816 PLANT.LOOP1.F(89) := 27.5042 ; # 814
817 PLANT.LOOP1.F(90) := 27.5042 ; # 815
818 PLANT.LOOP1.F(91) := 27.5042 ; # 816
819 PLANT.LOOP1.F(92) := 27.5042 ; # 817
820 PLANT.LOOP1.F(93) := 27.5042 ; # 818
821 PLANT.LOOP1.F(94) := 27.5042 ; # 819
822 PLANT.LOOP1.F(95) := 27.5042 ; # 820
823 PLANT.LOOP1.F(96) := 27.5042 ; # 821
824 PLANT.LOOP1.F(97) := 27.5042 ; # 822
825 PLANT.LOOP1.F(98) := 27.5042 ; # 823
826 PLANT.LOOP1.F(99) := 27.5042 ; # 824
827 PLANT.LOOP1.F(100) := 27.5042 ; # 825
828 PLANT.LOOP1.F_IN := 27.5042 ; # 826
829 PLANT.LOOP1.TOTALMASS := 27.0521 ; # 827
830 PLANT.LOOP1.RHOEXTRA(1) := 1.15546 ; # 828
831 PLANT.LOOP1.RHOEXTRA(2) := 1.15546 ; # 829
832 PLANT.LOOP1.PEXTRA(1) := 2.01632e+006 ; # 830
833 PLANT.LOOP1.PEXTRA(2) := 2.01632e+006 ; # 831
834 PLANT.LOOP1.HEXTRA(1) := 2.81342e+006 ; # 832

```

835 PLANT.LOOP1.HEXTRA(2) := 2.81342e+006 ; # 833
836 PLANT.LOOP1.TEXTRA(1) := 839.563 ; # 834
837 PLANT.LOOP1.TEXTRA(2) := 839.563 ; # 835
838 PLANT.LOOP1.PSIEXTRA(1) := 1.23448e+006 ; # 836
839 PLANT.LOOP1.PSIEXTRA(2) := 1.23448e+006 ; # 837
840 PLANT.LOOP1.FEXTRA(1) := 27.5042 ; # 838
841 PLANT.LOOP1.FEXTRA(2) := 27.5042 ; # 839
842 PLANT.LOOP1.HT1.H2 := 17.344 ; # 840
843 PLANT.LOOP1.HT1.RHOPIPEHE := 1.12889 ; # 841
844 PLANT.LOOP1.HT1.VPIPE := 181.878 ; # 842
845 PLANT.LOOP1.HT1.HO := 1554.44 ; # 843
846 PLANT.LOOP1.HT1.U := 8.93607 ; # 844
847 PLANT.LOOP1.HT2.RHOPIPEHE := 0.898512 ; # 845
848 PLANT.LOOP1.HT2.VPIPE := 89.1714 ; # 846
849 PLANT.LOOP1.HT2.HO := 1665.62 ; # 847
850 PLANT.LOOP1.HT2.U := 1645.45 ; # 848
851 PLANT.LOOP1.HT3.H2 := 17.344 ; # 849
852 PLANT.LOOP1.HT3.RHOPIPEHE := 0.736935 ; # 850
853 PLANT.LOOP1.HT3.VPIPE := 241.071 ; # 851
854 PLANT.LOOP1.HT3.HO := 1364.58 ; # 852
855 PLANT.LOOP1.HT3.U := 10.3601 ; # 853
856 PLANT.LOOP1.HT4.RHOPIPEHE := 0.821936 ; # 854
857 PLANT.LOOP1.HT4.VPIPE := 84.1899 ; # 855
858 PLANT.LOOP1.HT4.U := 1299.78 ; # 856
859 PLANT.HX2.TGASHOT(1) := 1137.66 ; # 1143
860 PLANT.HX2.TGASHOT(2) := 1134.74 ; # 1144
861 PLANT.HX2.TGASHOT(3) := 1131.65 ; # 1145
862 PLANT.HX2.TGASHOT(4) := 1128.41 ; # 1146
863 PLANT.HX2.TGASHOT(5) := 1124.99 ; # 1147
864 PLANT.HX2.TGASHOT(6) := 1121.4 ; # 1148
865 PLANT.HX2.TGASHOT(7) := 1117.61 ; # 1149
866 PLANT.HX2.TGASHOT(8) := 1113.63 ; # 1150
867 PLANT.HX2.TGASHOT(9) := 1109.43 ; # 1151
868 PLANT.HX2.TGASHOT(10) := 1105.02 ; # 1152
869 PLANT.HX2.TGASHOT(11) := 1100.37 ; # 1153
870 PLANT.HX2.TGASHOT(12) := 1095.48 ; # 1154
871 PLANT.HX2.TGASHOT(13) := 1090.33 ; # 1155
872 PLANT.HX2.TGASHOT(14) := 1084.91 ; # 1156
873 PLANT.HX2.TGASHOT(15) := 1079.2 ; # 1157
874 PLANT.HX2.TGASHOT(16) := 1073.2 ; # 1158
875 PLANT.HX2.TGASHOT(17) := 1066.88 ; # 1159
876 PLANT.HX2.TGASHOT(18) := 1060.22 ; # 1160
877 PLANT.HX2.TGASHOT(19) := 1053.22 ; # 1161
878 PLANT.HX2.TGASHOT(20) := 1045.84 ; # 1162
879 PLANT.HX2.TGASHOT(21) := 1038.08 ; # 1163
880 PLANT.HX2.TGASHOT(22) := 1029.91 ; # 1164
881 PLANT.HX2.TGASHOT(23) := 1021.31 ; # 1165
882 PLANT.HX2.TGASHOT(24) := 1012.26 ; # 1166
883 PLANT.HX2.TGASHOT(25) := 1002.73 ; # 1167
884 PLANT.HX2.TGASHOT(26) := 992.699 ; # 1168
885 PLANT.HX2.TGASHOT(27) := 982.14 ; # 1169
886 PLANT.HX2.TGASHOT(28) := 971.025 ; # 1170
887 PLANT.HX2.TGASHOT(29) := 959.325 ; # 1171
888 PLANT.HX2.TGASHOT(30) := 947.01 ; # 1172
889 PLANT.HX2.TGASHOT(31) := 934.046 ; # 1173
890 PLANT.HX2.TGASHOT(32) := 920.4 ; # 1174
891 PLANT.HX2.TGASHOT(33) := 906.036 ; # 1175
892 PLANT.HX2.TGASHOT(34) := 890.915 ; # 1176
893 PLANT.HX2.TGASHOT(35) := 874.999 ; # 1177
894 PLANT.HX2.TGASHOT(36) := 858.245 ; # 1178
895 PLANT.HX2.TGASHOT(37) := 840.609 ; # 1179
896 PLANT.HX2.TGASHOT(38) := 822.045 ; # 1180
897 PLANT.HX2.TGASHOT(39) := 802.504 ; # 1181
898 PLANT.HX2.TGASHOT(40) := 781.936 ; # 1182
899 PLANT.HX2.TGASCOLD(1) := 1118.89 ; # 1183
900 PLANT.HX2.TGASCOLD(2) := 1114.97 ; # 1184
901 PLANT.HX2.TGASCOLD(3) := 1110.85 ; # 1185
902 PLANT.HX2.TGASCOLD(4) := 1106.51 ; # 1186
903 PLANT.HX2.TGASCOLD(5) := 1101.94 ; # 1187
904 PLANT.HX2.TGASCOLD(6) := 1097.13 ; # 1188
905 PLANT.HX2.TGASCOLD(7) := 1092.07 ; # 1189
906 PLANT.HX2.TGASCOLD(8) := 1086.74 ; # 1190
907 PLANT.HX2.TGASCOLD(9) := 1081.13 ; # 1191
908 PLANT.HX2.TGASCOLD(10) := 1075.22 ; # 1192
909 PLANT.HX2.TGASCOLD(11) := 1069.01 ; # 1193
910 PLANT.HX2.TGASCOLD(12) := 1062.47 ; # 1194
911 PLANT.HX2.TGASCOLD(13) := 1055.58 ; # 1195
912 PLANT.HX2.TGASCOLD(14) := 1048.33 ; # 1196
913 PLANT.HX2.TGASCOLD(15) := 1040.7 ; # 1197
914 PLANT.HX2.TGASCOLD(16) := 1032.67 ; # 1198
915 PLANT.HX2.TGASCOLD(17) := 1024.21 ; # 1199
916 PLANT.HX2.TGASCOLD(18) := 1015.31 ; # 1200
917 PLANT.HX2.TGASCOLD(19) := 1005.94 ; # 1201
918 PLANT.HX2.TGASCOLD(20) := 996.081 ; # 1202
919 PLANT.HX2.TGASCOLD(21) := 985.7 ; # 1203
920 PLANT.HX2.TGASCOLD(22) := 974.772 ; # 1204
921 PLANT.HX2.TGASCOLD(23) := 963.27 ; # 1205
922 PLANT.HX2.TGASCOLD(24) := 951.162 ; # 1206
923 PLANT.HX2.TGASCOLD(25) := 938.417 ; # 1207
924 PLANT.HX2.TGASCOLD(26) := 925.001 ; # 1208
925 PLANT.HX2.TGASCOLD(27) := 910.879 ; # 1209
926 PLANT.HX2.TGASCOLD(28) := 896.013 ; # 1210

927 PLANT.HX2.TGASCOLD(29) := 880.365 ; # 1211
928 PLANT.HX2.TGASCOLD(30) := 863.894 ; # 1212
929 PLANT.HX2.TGASCOLD(31) := 846.555 ; # 1213
930 PLANT.HX2.TGASCOLD(32) := 828.304 ; # 1214
931 PLANT.HX2.TGASCOLD(33) := 809.093 ; # 1215
932 PLANT.HX2.TGASCOLD(34) := 788.87 ; # 1216
933 PLANT.HX2.TGASCOLD(35) := 767.582 ; # 1217
934 PLANT.HX2.TGASCOLD(36) := 745.175 ; # 1218
935 PLANT.HX2.TGASCOLD(37) := 721.587 ; # 1219
936 PLANT.HX2.TGASCOLD(38) := 696.759 ; # 1220
937 PLANT.HX2.TGASCOLD(39) := 670.623 ; # 1221
938 PLANT.HX2.TGASCOLD(40) := 643.112 ; # 1222
939 PLANT.HX2.UHOT := 1299.78 ; # 1223
940 PLANT.HX2.UCOLD := 1880.53 ; # 1224
941 PLANT.HX2.THX(1) := 1127.77 ; # 1225
942 PLANT.HX2.THX(2) := 1124.33 ; # 1226
943 PLANT.HX2.THX(3) := 1120.69 ; # 1227
944 PLANT.HX2.THX(4) := 1116.87 ; # 1228
945 PLANT.HX2.THX(5) := 1112.85 ; # 1229
946 PLANT.HX2.THX(6) := 1108.61 ; # 1230
947 PLANT.HX2.THX(7) := 1104.16 ; # 1231
948 PLANT.HX2.THX(8) := 1099.46 ; # 1232
949 PLANT.HX2.THX(9) := 1094.52 ; # 1233
950 PLANT.HX2.THX(10) := 1089.32 ; # 1234
951 PLANT.HX2.THX(11) := 1083.85 ; # 1235
952 PLANT.HX2.THX(12) := 1078.09 ; # 1236
953 PLANT.HX2.THX(13) := 1072.03 ; # 1237
954 PLANT.HX2.THX(14) := 1065.64 ; # 1238
955 PLANT.HX2.THX(15) := 1058.92 ; # 1239
956 PLANT.HX2.THX(16) := 1051.85 ; # 1240
957 PLANT.HX2.THX(17) := 1044.4 ; # 1241
958 PLANT.HX2.THX(18) := 1036.57 ; # 1242
959 PLANT.HX2.THX(19) := 1028.32 ; # 1243
960 PLANT.HX2.THX(20) := 1019.63 ; # 1244
961 PLANT.HX2.THX(21) := 1010.49 ; # 1245
962 PLANT.HX2.THX(22) := 1000.87 ; # 1246
963 PLANT.HX2.THX(23) := 990.74 ; # 1247
964 PLANT.HX2.THX(24) := 980.078 ; # 1248
965 PLANT.HX2.THX(25) := 968.854 ; # 1249
966 PLANT.HX2.THX(26) := 957.041 ; # 1250
967 PLANT.HX2.THX(27) := 944.605 ; # 1251
968 PLANT.HX2.THX(28) := 931.514 ; # 1252
969 PLANT.HX2.THX(29) := 917.735 ; # 1253
970 PLANT.HX2.THX(30) := 903.231 ; # 1254
971 PLANT.HX2.THX(31) := 887.962 ; # 1255
972 PLANT.HX2.THX(32) := 871.891 ; # 1256
973 PLANT.HX2.THX(33) := 854.973 ; # 1257
974 PLANT.HX2.THX(34) := 837.165 ; # 1258
975 PLANT.HX2.THX(35) := 818.42 ; # 1259
976 PLANT.HX2.THX(36) := 798.688 ; # 1260
977 PLANT.HX2.THX(37) := 777.917 ; # 1261
978 PLANT.HX2.THX(38) := 756.054 ; # 1262
979 PLANT.HX2.THX(39) := 733.039 ; # 1263
980 PLANT.HX2.THX(40) := 708.82 ; # 1264
981 PLANT.PIPEC2.RHO(1) := 3.77479 ; # 1265
982 PLANT.PIPEC2.RHO(2) := 3.61285 ; # 1266
983 PLANT.PIPEC2.RHO(3) := 3.47031 ; # 1267
984 PLANT.PIPEC2.RHO(4) := 3.34393 ; # 1268
985 PLANT.PIPEC2.RHO(5) := 3.23116 ; # 1269
986 PLANT.PIPEC2.RHO(6) := 3.12995 ; # 1270
987 PLANT.PIPEC2.RHO(7) := 3.03864 ; # 1271
988 PLANT.PIPEC2.RHO(8) := 2.95586 ; # 1272
989 PLANT.PIPEC2.RHO(9) := 2.8805 ; # 1273
990 PLANT.PIPEC2.RHO(10) := 2.81162 ; # 1274
991 PLANT.PIPEC2.RHO(11) := 2.74842 ; # 1275
992 PLANT.PIPEC2.RHO(12) := 2.69025 ; # 1276
993 PLANT.PIPEC2.RHO(13) := 2.63652 ; # 1277
994 PLANT.PIPEC2.RHO(14) := 2.58675 ; # 1278
995 PLANT.PIPEC2.RHO(15) := 2.54053 ; # 1279
996 PLANT.PIPEC2.RHO(16) := 2.49748 ; # 1280
997 PLANT.PIPEC2.RHO(17) := 2.45729 ; # 1281
998 PLANT.PIPEC2.RHO(18) := 2.41967 ; # 1282
999 PLANT.PIPEC2.RHO(19) := 2.38439 ; # 1283
1000 PLANT.PIPEC2.RHO(20) := 2.35122 ; # 1284
1001 PLANT.PIPEC2.RHO(21) := 2.31998 ; # 1285
1002 PLANT.PIPEC2.RHO(22) := 2.29049 ; # 1286
1003 PLANT.PIPEC2.RHO(23) := 2.2626 ; # 1287
1004 PLANT.PIPEC2.RHO(24) := 2.23618 ; # 1288
1005 PLANT.PIPEC2.RHO(25) := 2.2111 ; # 1289
1006 PLANT.PIPEC2.RHO(26) := 2.18725 ; # 1290
1007 PLANT.PIPEC2.RHO(27) := 2.16453 ; # 1291
1008 PLANT.PIPEC2.RHO(28) := 2.14286 ; # 1292
1009 PLANT.PIPEC2.RHO(29) := 2.12215 ; # 1293
1010 PLANT.PIPEC2.RHO(30) := 2.10233 ; # 1294
1011 PLANT.PIPEC2.RHO(31) := 2.08332 ; # 1295
1012 PLANT.PIPEC2.RHO(32) := 2.06508 ; # 1296
1013 PLANT.PIPEC2.RHO(33) := 2.04754 ; # 1297
1014 PLANT.PIPEC2.RHO(34) := 2.03064 ; # 1298
1015 PLANT.PIPEC2.RHO(35) := 2.01436 ; # 1299
1016 PLANT.PIPEC2.RHO(36) := 1.99863 ; # 1300
1017 PLANT.PIPEC2.RHO(37) := 1.98342 ; # 1301
1018 PLANT.PIPEC2.RHO(38) := 1.96869 ; # 1302

1019 PLANT.PIPEC2.RHO(39) := 1.95441 ; # 1303
1020 PLANT.PIPEC2.RHO(40) := 1.94055 ; # 1304
1021 PLANT.PIPEC2.P(1) := 1.12004e+006 ; # 1305
1022 PLANT.PIPEC2.P(2) := 1.11785e+006 ; # 1306
1023 PLANT.PIPEC2.P(3) := 1.11559e+006 ; # 1307
1024 PLANT.PIPEC2.P(4) := 1.11327e+006 ; # 1308
1025 PLANT.PIPEC2.P(5) := 1.11089e+006 ; # 1309
1026 PLANT.PIPEC2.P(6) := 1.10845e+006 ; # 1310
1027 PLANT.PIPEC2.P(7) := 1.10596e+006 ; # 1311
1028 PLANT.PIPEC2.P(8) := 1.10341e+006 ; # 1312
1029 PLANT.PIPEC2.P(9) := 1.10081e+006 ; # 1313
1030 PLANT.PIPEC2.P(10) := 1.09816e+006 ; # 1314
1031 PLANT.PIPEC2.P(11) := 1.09547e+006 ; # 1315
1032 PLANT.PIPEC2.P(12) := 1.09272e+006 ; # 1316
1033 PLANT.PIPEC2.P(13) := 1.08994e+006 ; # 1317
1034 PLANT.PIPEC2.P(14) := 1.0871e+006 ; # 1318
1035 PLANT.PIPEC2.P(15) := 1.08423e+006 ; # 1319
1036 PLANT.PIPEC2.P(16) := 1.08132e+006 ; # 1320
1037 PLANT.PIPEC2.P(17) := 1.07837e+006 ; # 1321
1038 PLANT.PIPEC2.P(18) := 1.07538e+006 ; # 1322
1039 PLANT.PIPEC2.P(19) := 1.07235e+006 ; # 1323
1040 PLANT.PIPEC2.P(20) := 1.06929e+006 ; # 1324
1041 PLANT.PIPEC2.P(21) := 1.06619e+006 ; # 1325
1042 PLANT.PIPEC2.P(22) := 1.06306e+006 ; # 1326
1043 PLANT.PIPEC2.P(23) := 1.05989e+006 ; # 1327
1044 PLANT.PIPEC2.P(24) := 1.0567e+006 ; # 1328
1045 PLANT.PIPEC2.P(25) := 1.05347e+006 ; # 1329
1046 PLANT.PIPEC2.P(26) := 1.05022e+006 ; # 1330
1047 PLANT.PIPEC2.P(27) := 1.04693e+006 ; # 1331
1048 PLANT.PIPEC2.P(28) := 1.04361e+006 ; # 1332
1049 PLANT.PIPEC2.P(29) := 1.04027e+006 ; # 1333
1050 PLANT.PIPEC2.P(30) := 1.0369e+006 ; # 1334
1051 PLANT.PIPEC2.P(31) := 1.0335e+006 ; # 1335
1052 PLANT.PIPEC2.P(32) := 1.03008e+006 ; # 1336
1053 PLANT.PIPEC2.P(33) := 1.02662e+006 ; # 1337
1054 PLANT.PIPEC2.P(34) := 1.02315e+006 ; # 1338
1055 PLANT.PIPEC2.P(35) := 1.01965e+006 ; # 1339
1056 PLANT.PIPEC2.P(36) := 1.01612e+006 ; # 1340
1057 PLANT.PIPEC2.P(37) := 1.01257e+006 ; # 1341
1058 PLANT.PIPEC2.P(38) := 1.00899e+006 ; # 1342
1059 PLANT.PIPEC2.P(39) := 1.00539e+006 ; # 1343
1060 PLANT.PIPEC2.P(40) := 1.00177e+006 ; # 1344
1061 PLANT.PIPEC2.H(1) := 778513 ; # 1345
1062 PLANT.PIPEC2.H(2) := 840573 ; # 1346
1063 PLANT.PIPEC2.H(3) := 899531 ; # 1347
1064 PLANT.PIPEC2.H(4) := 955540 ; # 1348
1065 PLANT.PIPEC2.H(5) := 1.00875e+006 ; # 1349
1066 PLANT.PIPEC2.H(6) := 1.0593e+006 ; # 1350
1067 PLANT.PIPEC2.H(7) := 1.10732e+006 ; # 1351
1068 PLANT.PIPEC2.H(8) := 1.15294e+006 ; # 1352
1069 PLANT.PIPEC2.H(9) := 1.19627e+006 ; # 1353
1070 PLANT.PIPEC2.H(10) := 1.23745e+006 ; # 1354
1071 PLANT.PIPEC2.H(11) := 1.27656e+006 ; # 1355
1072 PLANT.PIPEC2.H(12) := 1.31372e+006 ; # 1356
1073 PLANT.PIPEC2.H(13) := 1.34901e+006 ; # 1357
1074 PLANT.PIPEC2.H(14) := 1.38255e+006 ; # 1358
1075 PLANT.PIPEC2.H(15) := 1.41441e+006 ; # 1359
1076 PLANT.PIPEC2.H(16) := 1.44467e+006 ; # 1360
1077 PLANT.PIPEC2.H(17) := 1.47342e+006 ; # 1361
1078 PLANT.PIPEC2.H(18) := 1.50073e+006 ; # 1362
1079 PLANT.PIPEC2.H(19) := 1.52668e+006 ; # 1363
1080 PLANT.PIPEC2.H(20) := 1.55133e+006 ; # 1364
1081 PLANT.PIPEC2.H(21) := 1.57475e+006 ; # 1365
1082 PLANT.PIPEC2.H(22) := 1.597e+006 ; # 1366
1083 PLANT.PIPEC2.H(23) := 1.61813e+006 ; # 1367
1084 PLANT.PIPEC2.H(24) := 1.63821e+006 ; # 1368
1085 PLANT.PIPEC2.H(25) := 1.65728e+006 ; # 1369
1086 PLANT.PIPEC2.H(26) := 1.6754e+006 ; # 1370
1087 PLANT.PIPEC2.H(27) := 1.69261e+006 ; # 1371
1088 PLANT.PIPEC2.H(28) := 1.70897e+006 ; # 1372
1089 PLANT.PIPEC2.H(29) := 1.7245e+006 ; # 1373
1090 PLANT.PIPEC2.H(30) := 1.73926e+006 ; # 1374
1091 PLANT.PIPEC2.H(31) := 1.75328e+006 ; # 1375
1092 PLANT.PIPEC2.H(32) := 1.7666e+006 ; # 1376
1093 PLANT.PIPEC2.H(33) := 1.77926e+006 ; # 1377
1094 PLANT.PIPEC2.H(34) := 1.79128e+006 ; # 1378
1095 PLANT.PIPEC2.H(35) := 1.8027e+006 ; # 1379
1096 PLANT.PIPEC2.H(36) := 1.81355e+006 ; # 1380
1097 PLANT.PIPEC2.H(37) := 1.82385e+006 ; # 1381
1098 PLANT.PIPEC2.H(38) := 1.83364e+006 ; # 1382
1099 PLANT.PIPEC2.H(39) := 1.84294e+006 ; # 1383
1100 PLANT.PIPEC2.H(40) := 1.85178e+006 ; # 1384
1101 PLANT.PIPEC2.H0 := 713180 ; # 1385
1102 PLANT.PIPEC2.T(1) := 643.112 ; # 1386
1103 PLANT.PIPEC2.T(2) := 670.623 ; # 1387
1104 PLANT.PIPEC2.T(3) := 696.759 ; # 1388
1105 PLANT.PIPEC2.T(4) := 721.587 ; # 1389
1106 PLANT.PIPEC2.T(5) := 745.175 ; # 1390
1107 PLANT.PIPEC2.T(6) := 767.582 ; # 1391
1108 PLANT.PIPEC2.T(7) := 788.87 ; # 1392
1109 PLANT.PIPEC2.T(8) := 809.093 ; # 1393
1110 PLANT.PIPEC2.T(9) := 828.304 ; # 1394

1111 PLANT.PIPEC2.T(10) := 846.555 ; # 1395
1112 PLANT.PIPEC2.T(11) := 863.894 ; # 1396
1113 PLANT.PIPEC2.T(12) := 880.365 ; # 1397
1114 PLANT.PIPEC2.T(13) := 896.013 ; # 1398
1115 PLANT.PIPEC2.T(14) := 910.879 ; # 1399
1116 PLANT.PIPEC2.T(15) := 925.001 ; # 1400
1117 PLANT.PIPEC2.T(16) := 938.417 ; # 1401
1118 PLANT.PIPEC2.T(17) := 951.162 ; # 1402
1119 PLANT.PIPEC2.T(18) := 963.27 ; # 1403
1120 PLANT.PIPEC2.T(19) := 974.772 ; # 1404
1121 PLANT.PIPEC2.T(20) := 985.7 ; # 1405
1122 PLANT.PIPEC2.T(21) := 996.081 ; # 1406
1123 PLANT.PIPEC2.T(22) := 1005.94 ; # 1407
1124 PLANT.PIPEC2.T(23) := 1015.31 ; # 1408
1125 PLANT.PIPEC2.T(24) := 1024.21 ; # 1409
1126 PLANT.PIPEC2.T(25) := 1032.67 ; # 1410
1127 PLANT.PIPEC2.T(26) := 1040.7 ; # 1411
1128 PLANT.PIPEC2.T(27) := 1048.33 ; # 1412
1129 PLANT.PIPEC2.T(28) := 1055.58 ; # 1413
1130 PLANT.PIPEC2.T(29) := 1062.47 ; # 1414
1131 PLANT.PIPEC2.T(30) := 1069.01 ; # 1415
1132 PLANT.PIPEC2.T(31) := 1075.22 ; # 1416
1133 PLANT.PIPEC2.T(32) := 1081.13 ; # 1417
1134 PLANT.PIPEC2.T(33) := 1086.74 ; # 1418
1135 PLANT.PIPEC2.T(34) := 1092.07 ; # 1419
1136 PLANT.PIPEC2.T(35) := 1097.13 ; # 1420
1137 PLANT.PIPEC2.T(36) := 1101.94 ; # 1421
1138 PLANT.PIPEC2.T(37) := 1106.51 ; # 1422
1139 PLANT.PIPEC2.T(38) := 1110.85 ; # 1423
1140 PLANT.PIPEC2.T(39) := 1114.97 ; # 1424
1141 PLANT.PIPEC2.T(40) := 1118.89 ; # 1425
1142 PLANT.PIPEC2.TEXTRNL(1) := 708.82 ; # 1426
1143 PLANT.PIPEC2.TEXTRNL(2) := 733.039 ; # 1427
1144 PLANT.PIPEC2.TEXTRNL(3) := 756.054 ; # 1428
1145 PLANT.PIPEC2.TEXTRNL(4) := 777.917 ; # 1429
1146 PLANT.PIPEC2.TEXTRNL(5) := 798.688 ; # 1430
1147 PLANT.PIPEC2.TEXTRNL(6) := 818.42 ; # 1431
1148 PLANT.PIPEC2.TEXTRNL(7) := 837.165 ; # 1432
1149 PLANT.PIPEC2.TEXTRNL(8) := 854.973 ; # 1433
1150 PLANT.PIPEC2.TEXTRNL(9) := 871.891 ; # 1434
1151 PLANT.PIPEC2.TEXTRNL(10) := 887.962 ; # 1435
1152 PLANT.PIPEC2.TEXTRNL(11) := 903.231 ; # 1436
1153 PLANT.PIPEC2.TEXTRNL(12) := 917.735 ; # 1437
1154 PLANT.PIPEC2.TEXTRNL(13) := 931.514 ; # 1438
1155 PLANT.PIPEC2.TEXTRNL(14) := 944.605 ; # 1439
1156 PLANT.PIPEC2.TEXTRNL(15) := 957.041 ; # 1440
1157 PLANT.PIPEC2.TEXTRNL(16) := 968.854 ; # 1441
1158 PLANT.PIPEC2.TEXTRNL(17) := 980.078 ; # 1442
1159 PLANT.PIPEC2.TEXTRNL(18) := 990.74 ; # 1443
1160 PLANT.PIPEC2.TEXTRNL(19) := 1000.87 ; # 1444
1161 PLANT.PIPEC2.TEXTRNL(20) := 1010.49 ; # 1445
1162 PLANT.PIPEC2.TEXTRNL(21) := 1019.63 ; # 1446
1163 PLANT.PIPEC2.TEXTRNL(22) := 1028.32 ; # 1447
1164 PLANT.PIPEC2.TEXTRNL(23) := 1036.57 ; # 1448
1165 PLANT.PIPEC2.TEXTRNL(24) := 1044.4 ; # 1449
1166 PLANT.PIPEC2.TEXTRNL(25) := 1051.85 ; # 1450
1167 PLANT.PIPEC2.TEXTRNL(26) := 1058.92 ; # 1451
1168 PLANT.PIPEC2.TEXTRNL(27) := 1065.64 ; # 1452
1169 PLANT.PIPEC2.TEXTRNL(28) := 1072.03 ; # 1453
1170 PLANT.PIPEC2.TEXTRNL(29) := 1078.09 ; # 1454
1171 PLANT.PIPEC2.TEXTRNL(30) := 1083.85 ; # 1455
1172 PLANT.PIPEC2.TEXTRNL(31) := 1089.32 ; # 1456
1173 PLANT.PIPEC2.TEXTRNL(32) := 1094.52 ; # 1457
1174 PLANT.PIPEC2.TEXTRNL(33) := 1099.46 ; # 1458
1175 PLANT.PIPEC2.TEXTRNL(34) := 1104.16 ; # 1459
1176 PLANT.PIPEC2.TEXTRNL(35) := 1108.61 ; # 1460
1177 PLANT.PIPEC2.TEXTRNL(36) := 1112.85 ; # 1461
1178 PLANT.PIPEC2.TEXTRNL(37) := 1116.87 ; # 1462
1179 PLANT.PIPEC2.TEXTRNL(38) := 1120.69 ; # 1463
1180 PLANT.PIPEC2.TEXTRNL(39) := 1124.33 ; # 1464
1181 PLANT.PIPEC2.TEXTRNL(40) := 1127.77 ; # 1465
1182 PLANT.PIPEC2.F(1) := 46.175 ; # 1466
1183 PLANT.PIPEC2.F(2) := 46.175 ; # 1467
1184 PLANT.PIPEC2.F(3) := 46.175 ; # 1468
1185 PLANT.PIPEC2.F(4) := 46.175 ; # 1469
1186 PLANT.PIPEC2.F(5) := 46.175 ; # 1470
1187 PLANT.PIPEC2.F(6) := 46.175 ; # 1471
1188 PLANT.PIPEC2.F(7) := 46.175 ; # 1472
1189 PLANT.PIPEC2.F(8) := 46.175 ; # 1473
1190 PLANT.PIPEC2.F(9) := 46.175 ; # 1474
1191 PLANT.PIPEC2.F(10) := 46.175 ; # 1475
1192 PLANT.PIPEC2.F(11) := 46.175 ; # 1476
1193 PLANT.PIPEC2.F(12) := 46.175 ; # 1477
1194 PLANT.PIPEC2.F(13) := 46.175 ; # 1478
1195 PLANT.PIPEC2.F(14) := 46.175 ; # 1479
1196 PLANT.PIPEC2.F(15) := 46.175 ; # 1480
1197 PLANT.PIPEC2.F(16) := 46.175 ; # 1481
1198 PLANT.PIPEC2.F(17) := 46.175 ; # 1482
1199 PLANT.PIPEC2.F(18) := 46.175 ; # 1483
1200 PLANT.PIPEC2.F(19) := 46.175 ; # 1484
1201 PLANT.PIPEC2.F(20) := 46.175 ; # 1485
1202 PLANT.PIPEC2.F(21) := 46.175 ; # 1486

```

1203 PLANT.PIPEC2.F(22) := 46.175 ; # 1487
1204 PLANT.PIPEC2.F(23) := 46.175 ; # 1488
1205 PLANT.PIPEC2.F(24) := 46.175 ; # 1489
1206 PLANT.PIPEC2.F(25) := 46.175 ; # 1490
1207 PLANT.PIPEC2.F(26) := 46.175 ; # 1491
1208 PLANT.PIPEC2.F(27) := 46.175 ; # 1492
1209 PLANT.PIPEC2.F(28) := 46.175 ; # 1493
1210 PLANT.PIPEC2.F(29) := 46.175 ; # 1494
1211 PLANT.PIPEC2.F(30) := 46.175 ; # 1495
1212 PLANT.PIPEC2.F(31) := 46.175 ; # 1496
1213 PLANT.PIPEC2.F(32) := 46.175 ; # 1497
1214 PLANT.PIPEC2.F(33) := 46.175 ; # 1498
1215 PLANT.PIPEC2.F(34) := 46.175 ; # 1499
1216 PLANT.PIPEC2.F(35) := 46.175 ; # 1500
1217 PLANT.PIPEC2.F(36) := 46.175 ; # 1501
1218 PLANT.PIPEC2.F(37) := 46.175 ; # 1502
1219 PLANT.PIPEC2.F(38) := 46.175 ; # 1503
1220 PLANT.PIPEC2.F(39) := 46.175 ; # 1504
1221 PLANT.PIPEC2.F(40) := 46.175 ; # 1505
1222 PLANT.PIPEC2.F_IN := 46.175 ; # 1506
1223 PLANT.PIPEC2.PSI(1) := 1.81868e+006 ; # 1507
1224 PLANT.PIPEC2.PSI(2) := 1.91901e+006 ; # 1508
1225 PLANT.PIPEC2.PSI(3) := 2.00606e+006 ; # 1509
1226 PLANT.PIPEC2.PSI(4) := 2.08199e+006 ; # 1510
1227 PLANT.PIPEC2.PSI(5) := 2.14854e+006 ; # 1511
1228 PLANT.PIPEC2.PSI(6) := 2.20709e+006 ; # 1512
1229 PLANT.PIPEC2.PSI(7) := 2.25877e+006 ; # 1513
1230 PLANT.PIPEC2.PSI(8) := 2.30451e+006 ; # 1514
1231 PLANT.PIPEC2.PSI(9) := 2.34506e+006 ; # 1515
1232 PLANT.PIPEC2.PSI(10) := 2.38106e+006 ; # 1516
1233 PLANT.PIPEC2.PSI(11) := 2.41306e+006 ; # 1517
1234 PLANT.PIPEC2.PSI(12) := 2.44149e+006 ; # 1518
1235 PLANT.PIPEC2.PSI(13) := 2.46677e+006 ; # 1519
1236 PLANT.PIPEC2.PSI(14) := 2.48921e+006 ; # 1520
1237 PLANT.PIPEC2.PSI(15) := 2.50911e+006 ; # 1521
1238 PLANT.PIPEC2.PSI(16) := 2.52672e+006 ; # 1522
1239 PLANT.PIPEC2.PSI(17) := 2.54225e+006 ; # 1523
1240 PLANT.PIPEC2.PSI(18) := 2.55591e+006 ; # 1524
1241 PLANT.PIPEC2.PSI(19) := 2.56786e+006 ; # 1525
1242 PLANT.PIPEC2.PSI(20) := 2.57824e+006 ; # 1526
1243 PLANT.PIPEC2.PSI(21) := 2.5872e+006 ; # 1527
1244 PLANT.PIPEC2.PSI(22) := 2.59485e+006 ; # 1528
1245 PLANT.PIPEC2.PSI(23) := 2.60129e+006 ; # 1529
1246 PLANT.PIPEC2.PSI(24) := 2.60662e+006 ; # 1530
1247 PLANT.PIPEC2.PSI(25) := 2.61094e+006 ; # 1531
1248 PLANT.PIPEC2.PSI(26) := 2.6143e+006 ; # 1532
1249 PLANT.PIPEC2.PSI(27) := 2.61679e+006 ; # 1533
1250 PLANT.PIPEC2.PSI(28) := 2.61846e+006 ; # 1534
1251 PLANT.PIPEC2.PSI(29) := 2.61938e+006 ; # 1535
1252 PLANT.PIPEC2.PSI(30) := 2.6196e+006 ; # 1536
1253 PLANT.PIPEC2.PSI(31) := 2.61915e+006 ; # 1537
1254 PLANT.PIPEC2.PSI(32) := 2.6181e+006 ; # 1538
1255 PLANT.PIPEC2.PSI(33) := 2.61647e+006 ; # 1539
1256 PLANT.PIPEC2.PSI(34) := 2.6143e+006 ; # 1540
1257 PLANT.PIPEC2.PSI(35) := 2.61163e+006 ; # 1541
1258 PLANT.PIPEC2.PSI(36) := 2.60848e+006 ; # 1542
1259 PLANT.PIPEC2.PSI(37) := 2.60489e+006 ; # 1543
1260 PLANT.PIPEC2.PSI(38) := 2.60088e+006 ; # 1544
1261 PLANT.PIPEC2.PSI(39) := 2.59648e+006 ; # 1545
1262 PLANT.PIPEC2.PSI(40) := 2.59171e+006 ; # 1546
1263 PLANT.PIPEC2.HT.RHOPIPEHE := 2.39784 ; # 1547
1264 PLANT.PIPEC2.HT.VPIPE := 68.6177 ; # 1548
1265 PLANT.PIPEC2.HT.U := 1880.53 ; # 1549

```

SIMULATIONS_CH3_LOOPONLY_FULLDYN.JAC

```

1 INCLUDE MODELS_PHYSICALPROPERTIES
2 INCLUDE MODELS_HEATEXCHANGERS
3 INCLUDE MODELS_PIPEMODELS
4 INCLUDE MODELS_HEATTRANSFERLOOP
5 #####
6 SIMULATION HTLFullDyn_SS
7 #####
8 OPTIONS
9   INIT_PRINT_LEVEL:=0;
10  DYNAMIC_PRINT_LEVEL:=1;
11  DYNAMIC_REPORTING_INTERVAL:=10;
12  CSVOUTPUT:=TRUE;
13  DYNAMIC_BOUNDS := TRUE;
14  INIT_BLOCK_SOLVE:= TRUE;
15  INIT_RELATIVE_TOLERANCE := 1e-9;
16  INIT_ABSOLUTE_TOLERANCE := 1e-8;
17  REINIT_RELATIVE_TOLERANCE:= 1e-7;

```

```

18 REINIT_ABSOLUTE_TOLERANCE:= 1e-7;
19 DYNAMIC_RELATIVE_TOLERANCE:= 1e-6;
20 DYNAMIC_ABSOLUTE_TOLERANCE:= 1e-8;
21 REINIT_MAX_ITERATIONS:= 1000;
22 REINIT_PRINT_LEVEL:= 0;
23 CHECK_MATH_EXCEPTIONS:= FALSE;
24 DYNAMIC_SCALING:= TRUE;
25 INITIALIZE_SENSITIVITIES := TRUE;
26 UNIT
27 Plant AS HeatTransferLoopFullDynPipesFullDyn
28 SET
29 #Plant.Loop1
30 Plant.Loop1.InitDeltaP:=500.0;
31 Plant.Loop1.MaxDeltaP:= 304125;
32 # Plant.PipeH
33 Plant.PipeH.InitP:=6.95e6;
34 Plant.PipeH.InitT:= 273.15 + 530;
35 Plant.PipeC2.InitP:=1.00e6;
36 Plant.InitT:= 273.15+18;
37 INTERMEDIATE
38 INPUT
39 #Loop1
40 Plant.Loop1.DeltaP:= 304125;
41 Plant.Loop1.AdaptFactor1:=1;
42 Plant.Loop1.AdaptFactor2:=1;
43 Plant.Loop1.ModifyFlow := 0.00;
44 Plant.Loop1.comp_leak := 0.0;
45 # PipeH
46 WITHIN Plant DO
47 PipeH.TO:=1173.1500244140625; #PipeH.InitT;
48 PipeH.P_In:= 7000000.0; #PipeH.InitP + 100;
49 PipeH.P_Out:=6950000.0;#PipeH.InitP;
50 END # within
51 # PipeC2
52 WITHIN Plant DO
53 PipeC2.TO:= 614.15;#InitT;
54 PipeC2.P_In:=1110000.0; #PipeC2.InitP+100;
55 PipeC2.P_Out:=1000000.0; #PipeC2.InitP;
56 END # within
57 PRESET
58 INCLUDE ..\input\HTLFULLDYN_SS_IN_PRE
59 INITIAL
60 INCLUDE ..\input\HTLFULLDYN_SS_IN_INI
61 SCHEDULE
62 SEQUENCE
63 CONTINUE FOR 100
64 RESET
65 Plant.PipeC2.P_In:= 1110000.0 + 10950.0*(TIME-OLD(TIME))/10;
66 Plant.Loop1.DeltaP:= 304125 + (331300 - 304125)*(TIME - OLD(TIME))/10;
67 END # reset
68 CONTINUE FOR 10
69 RESET
70 Plant.PipeC2.P_In:=1110000.0 + 10950.0;
71 Plant.Loop1.DeltaP:= 331300;
72 END # reset
73 CONTINUE FOR 1000
74 RESET
75 Plant.Loop1.ModifyFlow:= -0.01;
76 END # reset
77 CONTINUE FOR 38.55
78 RESET
79 Plant.Loop1.ModifyFlow:= 0.0;
80 END # reset
81 CONTINUE FOR 1000
82 DISPLAY TIME, "seg" END
83 SAVE PRESETS HTLFullDyn_SS_Out_PRE
84 SAVE INITIAL HTLFullDyn_SS_Out_INI
85 END # sequence
86 END # simulation
87 *****
88
89 *****
90
91 SIMULATION HTLFullDyn_QStepDecrFPHX_Event30s
92 *****
93 OPTIONS
94 INIT_PRINT_LEVEL:=0;
95 DYNAMIC_PRINT_LEVEL:=0;
96 DYNAMIC_REPORTING_INTERVAL:=0.1;
97 CSVOUTPUT:=TRUE;
98 DYNAMIC_BOUNDS := TRUE;
99 INIT_BLOCK_SOLVE:= TRUE;
100 INIT_RELATIVE_TOLERANCE := 1e-9;
101 INIT_ABSOLUTE_TOLERANCE := 1e-8;
102 REINIT_RELATIVE_TOLERANCE:= 1e-7;
103 REINIT_ABSOLUTE_TOLERANCE:= 1e-7;
104 DYNAMIC_RELATIVE_TOLERANCE:= 1e-6;
105 DYNAMIC_ABSOLUTE_TOLERANCE:= 1e-8;
106 REINIT_MAX_ITERATIONS:= 1000;
107 REINIT_PRINT_LEVEL:= 0;
108 CHECK_MATH_EXCEPTIONS:= FALSE;
109 DYNAMIC_SCALING:= TRUE;

```

```

110     INITIALIZE_SENSITIVITIES := TRUE;
111 UNIT
112 Plant AS HeatTransferLoopFullDynPipesFullDyn
113 SET
114     #Plant.Loop1
115     Plant.Loop1.InitDeltaP:=500.0;
116     Plant.Loop1.MaxDeltaP:= 304125;
117     # Plant.PipeH
118     Plant.PipeH.InitP:=6.95e6;
119     Plant.PipeH.InitT:= 273.15 + 530;
120     Plant.PipeC2.InitP:=1.00e6;
121     Plant.InitT:= 273.15+18;
122 INTERMEDIATE
123 INPUT
124     #Loop1
125     Plant.Loop1.DeltaP:= 331300;
126     Plant.Loop1.AdaptFactor1:=1;
127     Plant.Loop1.AdaptFactor2:=1;
128     Plant.Loop1.ModifyFlow := 0.00;
129     Plant.Loop1.comp_leak := 0.0;
130     # PipeH
131     WITHIN Plant DO
132         PipeH.TO:=1173.15; #PipeH.InitT;
133         PipeH.P_In:= 7000000.0; #PipeH.InitP + 100;
134         PipeH.P_Out:=6950000.0;#PipeH.InitP;
135     END # within
136     # PipeC2
137     WITHIN Plant DO
138         PipeC2.TO:= 614.15;#InitT;
139         PipeC2.P_In:=1120950.0; #PipeC2.InitP+100;
140         PipeC2.P_Out:=1000000.0; #PipeC2.InitP;
141     END # within
142 PRESET
143 INCLUDE ..\HTLFullDyn_SS_sout\HTLFullDyn_SS_Out_PRE
144 INITIAL
145 INCLUDE ..\HTLFullDyn_SS_sout\HTLFullDyn_SS_Out_INI
146 SCHEDULE
147 SEQUENCE
148     CONTINUE FOR 10
149     DISPLAY Plant.PipeC2.F(1) END
150     RESET
151     Plant.PipeC2.P_In:= 1120950.0 - (1120950.0 - 1000000.0)*0.658*(TIME - OLD(TIME))/0.2;
152     END # reset
153     CONTINUE FOR 0.2
154     RESET
155     Plant.PipeC2.P_In:= 1120950.0 - (1120950.0 - 1000000.0)*0.658;
156     END # reset
157     CONTINUE FOR 19.8 #20
158     DISPLAY TIME, "seg" END
159     DISPLAY Plant.PipeC2.F(1) END
160     SAVE PRESETS HTLFullDyn_QStepDecrFPHX_Event30s_Out_PRE
161     SAVE INITIAL HTLFullDyn_QStepDecrFPHX_Event30s_Out_INI
162     END # sequence
163 END # simulation
164 #####
165
166
167 #####
168 SIMULATION HTLFullDyn_QStepDecrFPHX_PostEvent1000s
169 #####
170 OPTIONS
171     INIT_PRINT_LEVEL:=0;
172     DYNAMIC_PRINT_LEVEL:=0;
173     DYNAMIC_REPORTING_INTERVAL:=1.0;
174     CSVOUTPUT:=TRUE;
175     DYNAMIC_BOUNDS := TRUE;
176     INIT_BLOCK_SOLVE:= TRUE;
177     INIT_RELATIVE_TOLERANCE := 1e-9;
178     INIT_ABSOLUTE_TOLERANCE := 1e-8;
179     REINIT_RELATIVE_TOLERANCE:= 1e-9;
180     REINIT_ABSOLUTE_TOLERANCE:= 1e-9;
181     DYNAMIC_RELATIVE_TOLERANCE:= 1e-6;
182     DYNAMIC_ABSOLUTE_TOLERANCE:= 1e-8;
183     REINIT_MAX_ITERATIONS:= 1000;
184     REINIT_PRINT_LEVEL:= 0;
185     CHECK_MATH_EXCEPTIONS:= FALSE;
186     DYNAMIC_SCALING:= TRUE;
187     INITIALIZE_SENSITIVITIES := TRUE;
188 UNIT
189 Plant AS HeatTransferLoopFullDynPipesFullDyn
190 SET
191     #Plant.Loop1
192     Plant.Loop1.InitDeltaP:=500.0;
193     Plant.Loop1.MaxDeltaP:= 304125;
194     # Plant.PipeH
195     Plant.PipeH.InitP:=6.95e6;
196     Plant.PipeH.InitT:= 273.15 + 530;
197     Plant.PipeC2.InitP:=1.00e6;
198     Plant.InitT:= 273.15+18;
199 INTERMEDIATE
200 INPUT
201     #Loop1

```



```

202 Plant.Loop1.DeltaP:= 331300;
203 Plant.Loop1.AdaptFactor1:=1;
204 Plant.Loop1.AdaptFactor2:=1;
205 Plant.Loop1.ModifyFlow := 0.00;
206 Plant.Loop1.comp_leak := 0.0;
207 # PipeH
208 WITHIN Plant DO
209 PipeH.TO:=1173.1500; #PipeH.InitT;
210 PipeH.P_In:= 7000000.0; #PipeH.InitP + 100;
211 PipeH.P_Out:=6950000.0;#PipeH.InitP;
212 END # within
213 # PipeC2
214 WITHIN Plant DO
215 PipeC2.TO:= 614.15;#InitT;
216 PipeC2.P_In:=1120950.0 - (1120950.0 - 1000000.0 )*0.658; # 1110000.0; #PipeC2.InitP+100;
217 PipeC2.P_Out:=1000000.0; #PipeC2.InitP;
218 END # within
219 PRESET
220 INCLUDE ..\HTLFullDyn_QStepDecrFPHX_Event30s_sout\HTLFullDyn_QStepDecrFPHX_Event30s_Out_PRE
221 INITIAL
222 INCLUDE ..\HTLFullDyn_QStepDecrFPHX_Event30s_sout\HTLFullDyn_QStepDecrFPHX_Event30s_Out_INI
223 SCHEDULE
224 SEQUENCE
225 CONTINUE FOR 1000
226 DISPLAY TIME, "seg" END
227 DISPLAY Plant.PipeC2.F(1) END
228 SAVE PRESETS HTLFullDyn_QStepDecrFPHX_PostEvent1000s_Out_PRE
229 SAVE INITIAL HTLFullDyn_QStepDecrFPHX_PostEvent1000s_Out_INI
230 END # sequence
231 END # simulation
232 #####
233
234
235 #####
236 SIMULATION HTLFullDyn_QStepIncDPLoopComp_Event160sToTime
237 #####
238 OPTIONS
239 INIT_PRINT_LEVEL:=0;
240 DYNAMIC_PRINT_LEVEL:=0;
241 DYNAMIC_REPORTING_INTERVAL:=0.01;
242 CSVOUTPUT:=TRUE;
243 DYNAMIC_BOUNDS := TRUE;
244 INIT_BLOCK_SOLVE:= TRUE;
245 INIT_RELATIVE_TOLERANCE := 1e-9;
246 INIT_ABSOLUTE_TOLERANCE := 1e-8;
247 REINIT_RELATIVE_TOLERANCE:= 1e-7;
248 REINIT_ABSOLUTE_TOLERANCE:= 1e-7;
249 DYNAMIC_RELATIVE_TOLERANCE:= 1e-6;
250 DYNAMIC_ABSOLUTE_TOLERANCE:= 1e-8;
251 REINIT_MAX_ITERATIONS:= 1000;
252 REINIT_PRINT_LEVEL:= 0;
253 CHECK_MATH_EXCEPTIONS:= FALSE;
254 DYNAMIC_SCALING:= TRUE;
255 INITIALIZE_SENSITIVITIES := TRUE;
256 UNIT
257 Plant AS HeatTransferLoopFullDynPipesFullDyn
258 SET
259 #Plant.Loop1
260 Plant.Loop1.InitDeltaP:=500.0;
261 Plant.Loop1.MaxDeltaP:= 304125;
262 # Plant.PipeH
263 Plant.PipeH.InitP:=6.95e6;
264 Plant.PipeH.InitT:= 273.15 + 530;
265 Plant.PipeC2.InitP:=1.00e6;
266 Plant.InitT:= 273.15+18;
267 INTERMEDIATE
268 INPUT
269 #Loop1
270 Plant.Loop1.DeltaP:= 331300;
271 Plant.Loop1.AdaptFactor1:=1;
272 Plant.Loop1.AdaptFactor2:=1;
273 Plant.Loop1.ModifyFlow := 0.00;
274 Plant.Loop1.comp_leak := 0.0;
275 # PipeH
276 WITHIN Plant DO
277 PipeH.TO:=1173.15; #PipeH.InitT;
278 PipeH.P_In:= 7000000.0; #PipeH.InitP + 100;
279 PipeH.P_Out:=6950000.0;#PipeH.InitP;
280 END # within
281 # PipeC2
282 WITHIN Plant DO
283 PipeC2.TO:= 614.15;#InitT;
284 PipeC2.P_In:=1120950.0; #PipeC2.InitP+100;
285 PipeC2.P_Out:=1000000.0; #PipeC2.InitP;
286 END # within
287 PRESET
288 INCLUDE ..\HTLFullDyn_SS_sout\HTLFullDyn_SS_Out_PRE
289 INITIAL
290 INCLUDE ..\HTLFullDyn_SS_sout\HTLFullDyn_SS_Out_INI
291 SCHEDULE
292 SEQUENCE
293 CONTINUE FOR 10

```

```

294     RESET
295     Plant.Loop1.DeltaP:= 331300 + 47515*(TIME-10)/0.2;
296     END # reset
297     CONTINUE FOR 0.2
298     RESET
299     Plant.Loop1.DeltaP:= 331300 + 47515;
300     END # reset
301     CONTINUE FOR 149.8 #20
302     DISPLAY TIME, "seg" END
303     DISPLAY Plant.PipeC2.F(1) END
304     SAVE PRESETS HTLFullDyn_QStepDecrFPHX_Event160s_Out_PRE
305     SAVE INITIAL HTLFullDyn_QStepDecrFPHX_Event160s_Out_INI
306     END # sequence
307 END # simulation
308 #####
309
310
311 #####
312 SIMULATION HTLFullDyn_QStepIncDPLoopComp_Event30s
313 #####
314 OPTIONS
315     INIT_PRINT_LEVEL:=0;
316     DYNAMIC_PRINT_LEVEL:=0;
317     DYNAMIC_REPORTING_INTERVAL:=0.005;
318     CSVOUTPUT:=TRUE;
319     DYNAMIC_BOUNDS := TRUE;
320     INIT_BLOCK_SOLVE:= TRUE;
321     INIT_RELATIVE_TOLERANCE := 1e-9;
322     INIT_ABSOLUTE_TOLERANCE := 1e-8;
323     REINIT_RELATIVE_TOLERANCE:= 1e-7;
324     REINIT_ABSOLUTE_TOLERANCE:= 1e-7;
325     DYNAMIC_RELATIVE_TOLERANCE:= 1e-6;
326     DYNAMIC_ABSOLUTE_TOLERANCE:= 1e-8;
327     REINIT_MAX_ITERATIONS:= 1000;
328     REINIT_PRINT_LEVEL:= 0;
329     CHECK_MATH_EXCEPTIONS:= FALSE;
330     DYNAMIC_SCALING:= TRUE;
331     INITIALIZE_SENSITIVITIES := TRUE;
332
333 UNIT
334 Plant AS HeatTransferLoopFullDynPipesFullDyn
335 SET
336     #Plant.Loop1
337     Plant.Loop1.InitDeltaP:=500.0;
338     Plant.Loop1.MaxDeltaP:= 304125;
339     # Plant.PipeH
340     Plant.PipeH.InitP:=6.95e6;
341     Plant.PipeH.InitT:= 273.15 + 530;
342     Plant.PipeC2.InitP:=1.00e6;
343     Plant.InitT:= 273.15+18;
344 INTERMEDIATE
345 INPUT
346     #Loop1
347     Plant.Loop1.DeltaP:= 331300;
348     Plant.Loop1.AdaptFactor1:=1;
349     Plant.Loop1.AdaptFactor2:=1;
350     Plant.Loop1.ModifyFlow := 0.00;
351     Plant.Loop1.comp_leak := 0.0;
352     # PipeH
353     WITHIN Plant DO
354     PipeH.TO:=1173.1500244140625; #PipeH.InitT;
355     PipeH.P_In:= 7000000.0; #PipeH.InitP + 100;
356     PipeH.P_Out:=6950000.0;#PipeH.InitP;
357     END # within
358     # PipeC2
359     WITHIN Plant DO
360     PipeC2.TO:= 614.15;#InitT;
361     PipeC2.P_In:=1110000.0 + 10950.0; # 1110000.0; #PipeC2.InitP+100;
362     PipeC2.P_Out:=1000000.0; #PipeC2.InitP;
363     END # within
364 PRESET
365     INCLUDE ..\HTLFullDyn_SS_sout\HTLFullDyn_SS_Out_PRE
366 INITIAL
367     INCLUDE ..\HTLFullDyn_SS_sout\HTLFullDyn_SS_Out_INI
368 SCHEDULE
369 SEQUENCE
370     CONTINUE FOR 10
371     RESET
372     Plant.Loop1.DeltaP:= 331300 + 47515*(TIME-10)/0.2;
373     END # reset
374     CONTINUE FOR 0.2
375     RESET
376     Plant.Loop1.DeltaP:= 331300 + 47515;
377     END # reset
378     CONTINUE FOR 19.8# 20
379     DISPLAY TIME, "seg" END
380     DISPLAY Plant.Loop1.F(1) END
381     SAVE PRESETS HTLFullDyn_QStepIncDPLoopComp_Event30s_Out_PRE
382     SAVE INITIAL HTLFullDyn_QStepIncDPLoopComp_Event30s_Out_INI
383     END # sequence
384 END # simulation
385 #####
386

```

```

386
387 *****
388 SIMULATION HTLFullDyn_QStepIncDPLoopComp_PostEvent1000s
389 *****
390 OPTIONS
391   INIT_PRINT_LEVEL:=0;
392   DYNAMIC_PRINT_LEVEL:=0;
393   DYNAMIC_REPORTING_INTERVAL:=1.0;
394   CSVOUTPUT:=TRUE;
395   DYNAMIC_BOUNDS := TRUE;
396   INIT_BLOCK_SOLVE:= TRUE;
397   INIT_RELATIVE_TOLERANCE := 1e-9;
398   INIT_ABSOLUTE_TOLERANCE := 1e-8;
399   REINIT_RELATIVE_TOLERANCE:= 1e-7;
400   REINIT_ABSOLUTE_TOLERANCE:= 1e-7;
401   DYNAMIC_RELATIVE_TOLERANCE:= 1e-6;
402   DYNAMIC_ABSOLUTE_TOLERANCE:= 1e-8;
403   REINIT_MAX_ITERATIONS:= 1000;
404   REINIT_PRINT_LEVEL:= 0;
405   CHECK_MATH_EXCEPTIONS:= FALSE;
406   DYNAMIC_SCALING:= TRUE;
407   INITIALIZE_SENSITIVITIES := TRUE;
408 UNIT
409   Plant AS HeatTransferLoopFullDynPipesFullDyn
410 SET
411   #Plant.Loop1
412   Plant.Loop1.InitDeltaP:=500.0;
413   Plant.Loop1.MaxDeltaP:= 304125;
414   # Plant.PipeH
415   Plant.PipeH.InitP:=6.95e6;
416   Plant.PipeH.InitT:= 273.15 + 530;
417   Plant.PipeC2.InitP:=1.00e6;
418   Plant.InitT:= 273.15+18;
419 INTERMEDIATE
420 INPUT
421   #Loop1
422   Plant.Loop1.DeltaP:= 331300 + 47515;
423   Plant.Loop1.AdaptFactor1:=1;
424   Plant.Loop1.AdaptFactor2:=1;
425   Plant.Loop1.ModifyFlow := 0.00;
426   Plant.Loop1.comp_leak := 0.0;
427   # PipeH
428   WITHIN Plant D0
429     PipeH.T0:=1173.1500244140625; #PipeH.InitT;
430     PipeH.P_In:= 7000000.0; #PipeH.InitP + 100;
431     PipeH.P_Out:=6950000.0;#PipeH.InitP;
432   END # within
433   # PipeC2
434   WITHIN Plant D0
435     PipeC2.T0:= 614.15;#InitT;
436     PipeC2.P_In:=1110000.0 + 10950.0; #PipeC2.InitP+100;
437     PipeC2.P_Out:=1000000.0; #PipeC2.InitP;
438   END # within
439 PRESET
440   INCLUDE ..\HTLFullDyn_QStepIncDPLoopComp_Event30s_sout\HTLFullDyn_QStepIncDPLoopComp_Event30s_Out_PRE
441 INITIAL
442   INCLUDE ..\HTLFullDyn_QStepIncDPLoopComp_Event30s_sout\HTLFullDyn_QStepIncDPLoopComp_Event30s_Out_INI
443 SCHEDULE
444 SEQUENCE
445   CONTINUE FOR 1000
446   DISPLAY TIME, "seg" END
447   DISPLAY Plant.Loop1.F(1) END
448   SAVE PRESETS HTLFullDyn_StepIncDPLoopComp_QPostEvent1000s_Out_PRE
449   SAVE INITIAL HTLFullDyn_StepIncDPLoopComp_QPostEvent1000s_Out_INI
450 END # sequence
451 END # simulation
452 *****

```

SIMULATIONS_CH3_LOOPONLY_0MACH.JAC

```

1 INCLUDE MODELS_PHYSICALPROPERTIES
2 INCLUDE MODELS_HEATEXCHANGERS
3 INCLUDE MODELS_PIPEMODELS
4 INCLUDE MODELS_HEATTRANSFERLOOP
5 *****
6 SIMULATION HTLOMach_SS
7 *****
8 OPTIONS
9   INIT_PRINT_LEVEL:=0;
10  DYNAMIC_PRINT_LEVEL:=1;
11  DYNAMIC_REPORTING_INTERVAL:=10;
12  CSVOUTPUT:=TRUE;
13  DYNAMIC_BOUNDS := TRUE;

```

```

14 INIT_BLOCK_SOLVE:= TRUE;
15 INIT_RELATIVE_TOLERANCE := 1e-9;
16 INIT_ABSOLUTE_TOLERANCE := 1e-8;
17 REINIT_RELATIVE_TOLERANCE:= 1e-8;
18 REINIT_ABSOLUTE_TOLERANCE:= 1e-8;
19 DYNAMIC_RELATIVE_TOLERANCE:= 1e-8;
20 DYNAMIC_ABSOLUTE_TOLERANCE:= 1e-8;
21 REINIT_MAX_ITERATIONS:= 2000;
22 REINIT_PRINT_LEVEL:= 0;
23 CHECK_MATH_EXCEPTIONS:= FALSE;
24 DYNAMIC_SCALING:= TRUE;
25 INITIALIZE_SENSITIVITIES := TRUE;
26 UNIT
27 Plant AS HeatTransferLoop0MachPipesFullDyn
28 SET
29 #Plant.Loop1
30 Plant.Loop1.InitDeltaP:=500.0;
31 Plant.Loop1.MaxDeltaP:= 304125;
32 # Plant.PipeH
33 Plant.PipeH.InitP:=6.95e6;
34 Plant.PipeH.InitT:= 273.15 + 530;
35 Plant.PipeC2.InitP:=1.00e6;
36 Plant.InitT:= 273.15+18;
37 INTERMEDIATE
38 INPUT
39 #Loop1
40 Plant.Loop1.DeltaP:= 304125;
41 Plant.Loop1.AdaptFactor1:=1;
42 Plant.Loop1.AdaptFactor2:=1;
43 Plant.Loop1.ModifyFlow := 0.00;
44 Plant.Loop1.comp_leak := 0.0;
45 # PipeH
46 WITHIN Plant DO
47 PipeH.TO:=1173.1500244140625; #PipeH.InitT;
48 PipeH.P_In:= 7000000.0; #PipeH.InitP + 100;
49 PipeH.P_Out:=6950000.0;#PipeH.InitP;
50 END # within
51 # PipeC2
52 WITHIN Plant DO
53 PipeC2.TO:= 614.15;#InitT;
54 PipeC2.P_In:=1110000.0; #PipeC2.InitP+100;
55 PipeC2.P_Out:=1000000.0; #PipeC2.InitP;
56 END # within
57 PRESET
58 INCLUDE ..\input\HTLOMACH_SS_IN_PRE
59 INITIAL
60 INCLUDE ..\input\HTLOMACH_SS_IN_INI
61 SCHEDULE
62 SEQUENCE
63 CONTINUE FOR 100
64 RESET
65 Plant.PipeC2.P_In:= 1110000.0 + 10950.0*(TIME-OLD(TIME))/10;
66 Plant.Loop1.DeltaP:= 304125 + (331300 - 304125)*(TIME - OLD(TIME))/10;
67 END # reset
68 CONTINUE FOR 10
69 RESET
70 Plant.PipeC2.P_In:=1110000.0 + 10950.0;
71 Plant.Loop1.DeltaP:= 331300;
72 END # reset
73 CONTINUE FOR 1000
74 RESET
75 Plant.Loop1.ModifyFlow:= -0.01;
76 END # reset
77 CONTINUE FOR 38.55
78 RESET
79 Plant.Loop1.ModifyFlow:= 0.0;
80 END # reset
81 CONTINUE FOR 1000
82 DISPLAY TIME, "seg" END
83 SAVE PRESETS HTLOMACH_SS_OUT_PRE
84 SAVE INITIAL HTLOMACH_SS_OUT_INI END # sequence
85 END # simulation
86 #####
87
88
89 #####
90 SIMULATION HTLOMach_QStepDecrFPHX_Event30s
91 #####
92 OPTIONS
93 INIT_PRINT_LEVEL:=0;
94 DYNAMIC_PRINT_LEVEL:=0;
95 DYNAMIC_REPORTING_INTERVAL:=0.1;
96 CSVOUTPUT:=TRUE;
97 DYNAMIC_BOUNDS := TRUE;
98 INIT_BLOCK_SOLVE:= TRUE;
99 INIT_RELATIVE_TOLERANCE := 1e-9;
100 INIT_ABSOLUTE_TOLERANCE := 1e-8;
101 REINIT_RELATIVE_TOLERANCE:= 1e-8;
102 REINIT_ABSOLUTE_TOLERANCE:= 1e-8;
103 DYNAMIC_RELATIVE_TOLERANCE:= 1e-6;
104 DYNAMIC_ABSOLUTE_TOLERANCE:= 1e-8;
105 REINIT_MAX_ITERATIONS:= 2000;

```

```

106 REINIT_PRINT_LEVEL:= 0;
107 CHECK_MATH_EXCEPTIONS:= FALSE;
108 DYNAMIC_SCALING:= TRUE;
109 INITIALIZE_SENSITIVITIES := TRUE;
110 UNIT
111 Plant AS HeatTransferLoop0MachPipesFullDyn
112 SET
113 #Plant.Loop1
114 Plant.Loop1.InitDeltaP:=500.0;
115 Plant.Loop1.MaxDeltaP:= 304125;
116 # Plant.PipeH
117 Plant.PipeH.InitP:=6.95e6;
118 Plant.PipeH.InitT:= 273.15 + 530;
119 Plant.PipeC2.InitP:=1.00e6;
120 Plant.InitT:= 273.15+18;
121 INTERMEDIATE
122 INPUT
123 #Loop1
124 Plant.Loop1.DeltaP:= 331300;
125 Plant.Loop1.AdaptFactor1:=1;
126 Plant.Loop1.AdaptFactor2:=1;
127 Plant.Loop1.ModifyFlow := 0.00;
128 Plant.Loop1.comp_leak := 0.0;
129 # PipeH
130 WITHIN Plant DO
131 PipeH.TO:=1173.1500; #PipeH.InitT;
132 PipeH.P_In:= 7000000.0; #PipeH.InitP + 100;
133 PipeH.P_Out:=6950000.0;#PipeH.InitP;
134 END # within
135 # PipeC2
136 WITHIN Plant DO
137 PipeC2.TO:= 614.15;#InitT;
138 PipeC2.P_In:=1120950.0; #PipeC2.InitP+100;
139 PipeC2.P_Out:=1000000.0; #PipeC2.InitP;
140 END # within
141 PRESET
142 INCLUDE ..\HTLOMach_SS_sout\HTLOMach_SS_Out_PRE
143 INITIAL
144 INCLUDE ..\HTLOMach_SS_sout\HTLOMach_SS_Out_INI
145 SCHEDULE
146 SEQUENCE
147 CONTINUE FOR 10
148 DISPLAY Plant.PipeC2.F(1) END
149 RESET
150 Plant.PipeC2.P_In:= 1120950.0 - (1120950.0 - 1000000.0)*0.658*(TIME - OLD(TIME))/0.2;
151 END # reset
152 CONTINUE FOR 0.2
153 RESET
154 Plant.PipeC2.P_In:= 1120950.0 - (1120950.0 - 1000000.0)*0.658;
155 END # reset
156 CONTINUE FOR 19.8 #20
157 DISPLAY TIME, "seg" END
158 DISPLAY Plant.PipeC2.F(1) END
159 SAVE PRESETS HTLOMach_QStepDecrFPHX_Event30s_Out_PRE
160 SAVE INITIAL HTLOMach_QStepDecrFPHX_Event30s_Out_INI
161 END # sequence
162 END # simulation
163 #####
164
165
166 #####
167 SIMULATION HTLOMach_QStepDecrFPHX_PostEvent1000s
168 #####
169 OPTIONS
170 INIT_PRINT_LEVEL:=0;
171 DYNAMIC_PRINT_LEVEL:=0;
172 DYNAMIC_REPORTING_INTERVAL:=1.0;
173 CSVOUTPUT:=TRUE;
174 DYNAMIC_BOUNDS := TRUE;
175 INIT_BLOCK_SOLVE:= TRUE;
176 INIT_RELATIVE_TOLERANCE := 1e-9;
177 INIT_ABSOLUTE_TOLERANCE := 1e-8;
178 REINIT_RELATIVE_TOLERANCE:= 1e-8;
179 REINIT_ABSOLUTE_TOLERANCE:= 1e-8;
180 DYNAMIC_RELATIVE_TOLERANCE:= 1e-6;
181 DYNAMIC_ABSOLUTE_TOLERANCE:= 1e-8;
182 REINIT_MAX_ITERATIONS:= 2000;
183 REINIT_PRINT_LEVEL:= 0;
184 CHECK_MATH_EXCEPTIONS:= FALSE;
185 DYNAMIC_SCALING:= TRUE;
186 INITIALIZE_SENSITIVITIES := TRUE;
187 UNIT
188 Plant AS HeatTransferLoop0MachPipesFullDyn
189 SET
190 #Plant.Loop1
191 Plant.Loop1.InitDeltaP:=500.0;
192 Plant.Loop1.MaxDeltaP:= 304125;
193 # Plant.PipeH
194 Plant.PipeH.InitP:=6.95e6;
195 Plant.PipeH.InitT:= 273.15 + 530;
196 Plant.PipeC2.InitP:=1.00e6;
197 Plant.InitT:= 273.15+18;

```

```

198 INTERMEDIATE
199 INPUT
200 #Loop1
201 Plant.Loop1.DeltaP:= 331300;
202 Plant.Loop1.AdaptFactor1:=1;
203 Plant.Loop1.AdaptFactor2:=1;
204 Plant.Loop1.ModifyFlow := 0.00;
205 Plant.Loop1.comp_leak := 0.0;
206 # PipeH
207 WITHIN Plant DO
208   PipeH.TO:=1173.1500; #PipeH.InitT;
209   PipeH.P_In:= 7000000.0; #PipeH.InitP + 100;
210   PipeH.P_Out:=6950000.0;#PipeH.InitP;
211 END # within
212 # PipeC2
213 WITHIN Plant DO
214   PipeC2.TO:= 614.15;#InitT;
215   PipeC2.P_In:=1120950.0 - (1120950.0 - 1000000.0 )*0.658; # 1110000.0; #PipeC2.InitP+100;
216   PipeC2.P_Out:=1000000.0; #PipeC2.InitP;
217 END # within
218 PRESET
219 INCLUDE ..\HTLOMach_QStepDecrFPHX_Event30s_sout\HTLOMach_QStepDecrFPHX_Event30s_Out_PRE
220 INITIAL
221 INCLUDE ..\HTLOMach_QStepDecrFPHX_Event30s_sout\HTLOMach_QStepDecrFPHX_Event30s_Out_INI
222 SCHEDULE
223 SEQUENCE
224 CONTINUE FOR 1000
225 DISPLAY TIME, "seg" END
226 SAVE PRESETS HTLOMach_QStepDecrFPHX_PostEvent1000s_Out_PRE
227 SAVE INITIAL HTLOMach_QStepDecrFPHX_PostEvent1000s_Out_INI
228 END # sequence
229 END # simulation
230 #####
231
232
233 #####
234 SIMULATION HTLOMach_QStepIncDPLoopComp_Event160sToTime
235 #####
236 OPTIONS
237 INIT_PRINT_LEVEL:=0;
238 DYNAMIC_PRINT_LEVEL:=0;
239 DYNAMIC_REPORTING_INTERVAL:=0.01;
240 CSVOUTPUT:=TRUE;
241 DYNAMIC_BOUNDS := TRUE;
242 INIT_BLOCK_SOLVE:= TRUE;
243 INIT_RELATIVE_TOLERANCE := 1e-9;
244 INIT_ABSOLUTE_TOLERANCE := 1e-8;
245 REINIT_RELATIVE_TOLERANCE:= 1e-8;
246 REINIT_ABSOLUTE_TOLERANCE:= 1e-8;
247 DYNAMIC_RELATIVE_TOLERANCE:= 1e-6;
248 DYNAMIC_ABSOLUTE_TOLERANCE:= 1e-8;
249 REINIT_MAX_ITERATIONS:= 2000;
250 REINIT_PRINT_LEVEL:= 0;
251 CHECK_MATH_EXCEPTIONS:= FALSE;
252 DYNAMIC_SCALING:= TRUE;
253 INITIALIZE_SENSITIVITIES := TRUE;
254 UNIT
255 Plant AS HeatTransferLoop0MachPipesFullDyn
256 SET
257 #Plant.Loop1
258 Plant.Loop1.InitDeltaP:=500.0;
259 Plant.Loop1.MaxDeltaP:= 304125;
260 # Plant.PipeH
261 Plant.PipeH.InitP:=6.95e6;
262 Plant.PipeH.InitT:= 273.15 + 530;
263 Plant.PipeC2.InitP:=1.00e6;
264 Plant.InitT:= 273.15+18;
265 INTERMEDIATE
266 INPUT
267 #Loop1
268 Plant.Loop1.DeltaP:= 331300;
269 Plant.Loop1.AdaptFactor1:=1;
270 Plant.Loop1.AdaptFactor2:=1;
271 Plant.Loop1.ModifyFlow := 0.00;
272 Plant.Loop1.comp_leak := 0.0;
273 # PipeH
274 WITHIN Plant DO
275   PipeH.TO:=1173.1500; #PipeH.InitT;
276   PipeH.P_In:= 7000000.0; #PipeH.InitP + 100;
277   PipeH.P_Out:=6950000.0;#PipeH.InitP;
278 END # within
279 # PipeC2
280 WITHIN Plant DO
281   PipeC2.TO:= 614.15;#InitT;
282   PipeC2.P_In:=1120950.0; #PipeC2.InitP+100;
283   PipeC2.P_Out:=1000000.0; #PipeC2.InitP;
284 END # within
285 PRESET
286 INCLUDE ..\HTLOMach_SS_sout\HTLOMACH_SS_OUT_PRE
287 INITIAL
288 INCLUDE ..\HTLOMach_SS_sout\HTLOMACH_SS_OUT_INI
289 SCHEDULE

```

```

290 SEQUENCE
291 CONTINUE FOR 10
292 RESET
293 Plant.Loop1.DeltaP:= 331300 + 47515*(TIME-10)/0.2;
294 END # reset
295 CONTINUE FOR 0.2
296 RESET
297 Plant.Loop1.DeltaP:= 331300 + 47515;
298 END # reset
299 CONTINUE FOR 149.8 #20
300 DISPLAY TIME, "seg" END
301 SAVE PRESETS HTLOMach_QStepDecrFPHX_Event160s_Out_PRE
302 SAVE INITIAL HTLOMach_QStepDecrFPHX_Event160s_Out_INI
303 END # sequence
304 END # simulation
305 *****
306
307
308
309
310
311
312
313
314
315
316 *****
317 SIMULATION HTLOMach_QStepIncDPLoopComp_Event30s
318 *****
319 OPTIONS
320 INIT_PRINT_LEVEL:=0;
321 DYNAMIC_PRINT_LEVEL:=0;
322 DYNAMIC_REPORTING_INTERVAL:= 0.005; # 0.1;
323 CSVOUTPUT:=TRUE;
324 DYNAMIC_BOUNDS := TRUE;
325 INIT_BLOCK_SOLVE:= TRUE;
326 INIT_RELATIVE_TOLERANCE := 1e-9;
327 INIT_ABSOLUTE_TOLERANCE := 1e-8;
328 REINIT_RELATIVE_TOLERANCE:= 1e-8;
329 REINIT_ABSOLUTE_TOLERANCE:= 1e-8;
330 DYNAMIC_RELATIVE_TOLERANCE:= 1e-6;
331 DYNAMIC_ABSOLUTE_TOLERANCE:= 1e-8;
332 REINIT_MAX_ITERATIONS:= 2000;
333 REINIT_PRINT_LEVEL:= 0;
334 CHECK_MATH_EXCEPTIONS:= FALSE;
335 DYNAMIC_SCALING:= TRUE;
336 INITIALIZE_SENSITIVITIES := TRUE;
337 UNIT
338 Plant AS HeatTransferLoop0MachPipesFullDyn
339 SET
340 #Plant.Loop1
341 Plant.Loop1.InitDeltaP:=500.0;
342 Plant.Loop1.MaxDeltaP:= 304125;
343 # Plant.PipeH
344 Plant.PipeH.InitP:=6.95e6;
345 Plant.PipeH.InitT:= 273.15 + 530;
346 Plant.PipeC2.InitP:=1.00e6;
347 Plant.InitT:= 273.15+18;
348 INTERMEDIATE
349 INPUT
350 #Loop1
351 Plant.Loop1.DeltaP:= 331300;
352 Plant.Loop1.AdaptFactor1:=1;
353 Plant.Loop1.AdaptFactor2:=1;
354 Plant.Loop1.ModifyFlow := 0.00;
355 Plant.Loop1.comp_leak := 0.0;
356 # PipeH
357 WITHIN Plant D0
358 PipeH.TO:=1173.1500244140625; #PipeH.InitT;
359 PipeH.P_In:= 7000000.0; #PipeH.InitP + 100;
360 PipeH.P_Out:=6950000.0;#PipeH.InitP;
361 END # within
362 # PipeC2
363 WITHIN Plant D0
364 PipeC2.TO:= 614.15;#InitT;
365 PipeC2.P_In:=1110000.0 + 10950.0; # 1110000.0; #PipeC2.InitP+100;
366 PipeC2.P_Out:=1000000.0; #PipeC2.InitP;
367 END # within
368 PRESET
369 INCLUDE ..\HTLOMach_SS_sout\HTLOMach_SS_Out_PRE
370 INITIAL
371 INCLUDE ..\HTLOMach_SS_sout\HTLOMach_SS_Out_INI
372 SCHEDULE
373 SEQUENCE
374 CONTINUE FOR 10
375 RESET
376 Plant.Loop1.DeltaP:= 331300 + 47515*(TIME-10)/0.2;
377 END # reset
378 CONTINUE FOR 0.2
379 RESET
380 Plant.Loop1.DeltaP:= 331300 + 47515;
381 END # reset

```

```

382     CONTINUE FOR 19.8# 20
383     DISPLAY TIME, "seg" END
384     DISPLAY Plant.Loop1.F(1) END
385     SAVE PRESETS HTLOMach_QStepIncDPLoopComp_Event30s_Out_PRE
386     SAVE INITIAL HTLOMach_QStepIncDPLoopComp_Event30s_Out_INI
387     END # sequence
388 END # simulation
389 #####
390
391
392 #####
393 SIMULATION HTLOMach_QStepIncDPLoopComp_PostEvent1000s
394 #####
395 OPTIONS
396     INIT_PRINT_LEVEL:=0;
397     DYNAMIC_PRINT_LEVEL:=0;
398     DYNAMIC_REPORTING_INTERVAL:= 1.0; # 0.1;
399     CSVOUTPUT:=TRUE;
400     DYNAMIC_BOUNDS := TRUE;
401     INIT_BLOCK_SOLVE:= TRUE;
402     INIT_RELATIVE_TOLERANCE := 1e-9;
403     INIT_ABSOLUTE_TOLERANCE := 1e-8;
404     REINIT_RELATIVE_TOLERANCE:= 1e-8;
405     REINIT_ABSOLUTE_TOLERANCE:= 1e-8;
406     DYNAMIC_RELATIVE_TOLERANCE:= 1e-6;
407     DYNAMIC_ABSOLUTE_TOLERANCE:= 1e-8;
408     REINIT_MAX_ITERATIONS:= 2000;
409     REINIT_PRINT_LEVEL:= 0;
410     CHECK_MATH_EXCEPTIONS:= FALSE;
411     DYNAMIC_SCALING:= TRUE;
412     INITIALIZE_SENSITIVITIES := TRUE;
413 UNIT
414     Plant AS HeatTransferLoop0MachPipesFullDyn
415 SET
416     #Plant.Loop1
417     Plant.Loop1.InitDeltaP:=500.0;
418     Plant.Loop1.MaxDeltaP:= 304125;
419     # Plant.PipeH
420     Plant.PipeH.InitP:=6.95e6;
421     Plant.PipeH.InitT:= 273.15 + 530;
422     Plant.PipeC2.InitP:=1.00e6;
423     Plant.InitT:= 273.15+18;
424 INTERMEDIATE
425 INPUT
426     #Loop1
427     Plant.Loop1.DeltaP:= 331300 + 47515;
428     Plant.Loop1.AdaptFactor1:=1;
429     Plant.Loop1.AdaptFactor2:=1;
430     Plant.Loop1.ModifyFlow := 0.00;
431     Plant.Loop1.comp_leak := 0.0;
432     # PipeH
433     WITHIN Plant DO
434         PipeH.TO:=1173.1500244140625; #PipeH.InitT;
435         PipeH.P_In:= 7000000.0; #PipeH.InitP + 100;
436         PipeH.P_Out:=6950000.0;#PipeH.InitP;
437     END # within
438     # PipeC2
439     WITHIN Plant DO
440         PipeC2.TO:= 614.15;#InitT;
441         PipeC2.P_In:=1110000.0 + 10950.0; #PipeC2.InitP+100;
442         PipeC2.P_Out:=1000000.0; #PipeC2.InitP;
443     END # within
444 PRESET
445     INCLUDE ..\HTLOMach_QStepIncDPLoopComp_Event30s_sout\HTLOMach_QStepIncDPLoopComp_Event30s_Out_PRE
446 INITIAL
447     INCLUDE ..\HTLOMach_QStepIncDPLoopComp_Event30s_sout\HTLOMach_QStepIncDPLoopComp_Event30s_Out_INI
448 SCHEDULE
449     SEQUENCE
450         CONTINUE FOR 1000
451         DISPLAY TIME, "seg" END
452         DISPLAY Plant.Loop1.F(1) END
453         SAVE PRESETS HTLOMach_QStepIncDPLoopComp_PostEvent1000s_Out_PRE
454         SAVE INITIAL HTLOMach_QStepIncDPLoopComp_PostEvent1000s_Out_PREs_Out_INI
455     END # sequence
456 END # simulation
457 #####

```

SIMULATIONS_CH3_LOOPONLY_QSS.JAC

```

1 INCLUDE MODELS_PHYSICALPROPERTIES
2 INCLUDE MODELS_HEATEXCHANGERS
3 INCLUDE MODELS_PIPEMODELS
4 INCLUDE MODELS_HEATTRANSFERLOOP

```



```

5 *****
6 SIMULATION HTLQSS_SS
7 *****
8 OPTIONS
9   INIT_PRINT_LEVEL:=0;
10  DYNAMIC_PRINT_LEVEL:=1;
11  DYNAMIC_REPORTING_INTERVAL:=10;
12  CSVOUTPUT:=TRUE;
13  DYNAMIC_BOUNDS := TRUE;
14  INIT_BLOCK SOLVE:= TRUE;
15  INIT_RELATIVE_TOLERANCE := 1e-9;
16  INIT_ABSOLUTE_TOLERANCE := 1e-8;
17  REINIT_RELATIVE_TOLERANCE:= 1e-8;
18  REINIT_ABSOLUTE_TOLERANCE:= 1e-8;
19  DYNAMIC_RELATIVE_TOLERANCE:= 1e-6;
20  DYNAMIC_ABSOLUTE_TOLERANCE:= 1e-8;
21  REINIT_MAX_ITERATIONS:= 2000;
22  REINIT_PRINT_LEVEL:= 0;
23  CHECK_MATH_EXCEPTIONS:= FALSE;
24  DYNAMIC_SCALING:= TRUE;
25  INITIALIZE_SENSITIVITIES := TRUE;
26 UNIT
27   Plant AS HeatTransferLoopQSSPipesFullDyn
28 SET
29   #Plant.Loop1
30   Plant.Loop1.InitDeltaP:=500.0;
31   Plant.Loop1.MaxDeltaP:=0.321e6;
32   # Plant.PipeH
33   Plant.PipeH.InitP:=6.95e6;
34   Plant.PipeH.InitT:= 273.15 + 530;
35   Plant.PipeC2.InitP:=1.00e6;
36   Plant.InitT:= 273.15+18;
37 INTERMEDIATE
38 INPUT
39   #Loop1
40   Plant.Loop1.DeltaP:= 304125;
41   Plant.Loop1.AdaptFactor1:=1;
42   Plant.Loop1.AdaptFactor2:=1;
43   Plant.Loop1.ModifyFlow := 0.00;
44   Plant.Loop1.rho_avg := 0.919725239276886;
45   # PipeH
46   WITHIN Plant DO
47     PipeH.TO:=1173.1500244140625; #PipeH.InitT;
48     PipeH.P_In:= 7000000.0; #PipeH.InitP + 100;
49     PipeH.P_Out:=6950000.0;#PipeH.InitP;
50   END # within
51   # PipeC2
52   WITHIN Plant DO
53     PipeC2.TO:= 614.15;#InitT;
54     PipeC2.P_In:=1110000.0; #PipeC2.InitP+100;
55     PipeC2.P_Out:=1000000.0; #PipeC2.InitP;
56   END # within
57 PRESET
58   INCLUDE ..\input\HTLQSS_SS_IN_PRE
59 INITIAL
60   INCLUDE ..\input\HTLQSS_SS_IN_INI
61 SCHEDULE
62 SEQUENCE
63   CONTINUE FOR 100
64   RESET
65     Plant.PipeC2.P_In:= 1110000.0 + 10950.0*(TIME-OLD(TIME))/10;
66     Plant.Loop1.DeltaP:= 304125 + (331300 - 304125)*(TIME - OLD(TIME))/10;
67   END # reset
68   CONTINUE FOR 10
69   RESET
70     Plant.PipeC2.P_In:=1110000.0 + 10950.0;
71     Plant.Loop1.DeltaP:=331300;
72   END # reset
73   CONTINUE FOR 1000
74   RESET
75     Plant.Loop1.rho_avg:= 0.919725239276886 - 0.0140*0.919725239276886*(TIME-OLD(TIME))/10;
76   END # reset
77   CONTINUE FOR 10
78   RESET
79     Plant.Loop1.rho_avg:= (1.0 - 0.0140)*0.919725239276886;
80   END
81   CONTINUE FOR 1000
82   DISPLAY TIME, "seg" END
83   SAVE PRESETS HTLQSS_SS_Out_PRE
84   SAVE INITIAL HTLQSS_SS_Out_INI
85 END # sequence
86 END # simulation
87 *****
88
89
90 *****
91 SIMULATION HTLQSS_QStepDecrFPHX_Event30s
92 *****
93 OPTIONS
94   INIT_PRINT_LEVEL:=0;
95   DYNAMIC_PRINT_LEVEL:=0;
96   DYNAMIC_REPORTING_INTERVAL:=0.01;

```

```

97     CSVOUTPUT:=TRUE;
98     DYNAMIC_BOUNDS := TRUE;
99     INIT_BLOCK_SOLVE:= TRUE;
100    INIT_RELATIVE_TOLERANCE := 1e-9;
101    INIT_ABSOLUTE_TOLERANCE := 1e-8;
102    REINIT_RELATIVE_TOLERANCE:= 1e-8;
103    REINIT_ABSOLUTE_TOLERANCE:= 1e-8;
104    DYNAMIC_RELATIVE_TOLERANCE:= 1e-6;
105    DYNAMIC_ABSOLUTE_TOLERANCE:= 1e-8;
106    REINIT_MAX_ITERATIONS := 2000;
107    REINIT_PRINT_LEVEL:= 0;
108    CHECK_MATH_EXCEPTIONS:= FALSE;
109    DYNAMIC_SCALING:= TRUE;
110    INITIALIZE_SENSITIVITIES := TRUE;
111    UNIT
112    Plant AS HeatTransferLoopQSSPipesFullDyn
113    SET
114    #Plant.Loop1
115    Plant.Loop1.InitDeltaP:=500.0;
116    Plant.Loop1.MaxDeltaP:=0.321e6;
117    # Plant.PipeH
118    Plant.PipeH.InitP:=6.95e6;
119    Plant.PipeH.InitT:= 273.15 + 530;
120    Plant.PipeC2.InitP:=1.00e6;
121    Plant.InitT:= 273.15+18;
122    INTERMEDIATE
123    INPUT
124    #Loop1
125    Plant.Loop1.DeltaP:= 331300;
126    Plant.Loop1.AdaptFactor1:=1;
127    Plant.Loop1.AdaptFactor2:=1;
128    Plant.Loop1.ModifyFlow := 0.00;
129    Plant.Loop1.rho_avg := (1.0 - 0.0140)*0.919725239276886;
130    # PipeH
131    WITHIN Plant DO
132    PipeH.TO:=1173.1500244140625; #PipeH.InitT;
133    PipeH.P_In:= 700000.0; #PipeH.InitP + 100;
134    PipeH.P_Out:=6950000.0;#PipeH.InitP;
135    END # within
136    # PipeC2
137    WITHIN Plant DO
138    PipeC2.TO:= 614.15;#InitT;
139    PipeC2.P_In:=1120950.0; #PipeC2.InitP+100;
140    PipeC2.P_Out:=1000000.0; #PipeC2.InitP;
141    END # within
142    PRESET
143    INCLUDE ..\HTLQSS_SS_sout\HTLQSS_SS_OUT_PRE
144    INITIAL
145    INCLUDE ..\HTLQSS_SS_sout\HTLQSS_SS_OUT_INI
146    SCHEDULE
147    SEQUENCE
148    CONTINUE FOR 10 #10
149    DISPLAY Plant.PipeC2.F(1) END
150    RESET
151    Plant.PipeC2.P_In:= 1120950.0 - (1120950.0 - 1000000.0)*0.658*(TIME - OLD(TIME))/0.2;
152    END # reset
153    CONTINUE FOR 0.2
154    RESET
155    Plant.PipeC2.P_In:= 1120950.0 - (1120950.0 - 1000000.0)*0.658;
156    END # reset
157    CONTINUE FOR 19.8 #20
158    DISPLAY TIME, "seg" END
159    DISPLAY Plant.PipeC2.F(1) END
160    SAVE PRESETS HTLQSS_QStepDecrFPHX_Event30s_Out_PRE
161    SAVE INITIAL HTLQSS_QStepDecrFPHX_Event30s_Out_INI
162    END # sequence
163    END # simulation
164    #####
165
166
167    #####
168    SIMULATION HTLQSS_QStepDecrFPHX_PostEvent1000s
169    #####
170    OPTIONS
171    INIT_PRINT_LEVEL:=0;
172    DYNAMIC_PRINT_LEVEL:=0;
173    DYNAMIC_REPORTING_INTERVAL:=1.0;
174    CSVOUTPUT:=TRUE;
175    DYNAMIC_BOUNDS := TRUE;
176    INIT_BLOCK_SOLVE:= TRUE;
177    INIT_RELATIVE_TOLERANCE := 1e-9;
178    INIT_ABSOLUTE_TOLERANCE := 1e-8;
179    REINIT_RELATIVE_TOLERANCE:= 1e-8;
180    REINIT_ABSOLUTE_TOLERANCE:= 1e-8;
181    DYNAMIC_RELATIVE_TOLERANCE:= 1e-6;
182    DYNAMIC_ABSOLUTE_TOLERANCE:= 1e-8;
183    REINIT_MAX_ITERATIONS := 2000;
184    REINIT_PRINT_LEVEL:= 0;
185    CHECK_MATH_EXCEPTIONS:= FALSE;
186    DYNAMIC_SCALING:= TRUE;
187    INITIALIZE_SENSITIVITIES := TRUE;
188    UNIT

```

```

189     Plant AS HeatTransferLoopQSSPipesFullDyn
190 SET
191     #Plant.Loop1
192     Plant.Loop1.InitDeltaP:=500.0;
193     Plant.Loop1.MaxDeltaP:= 304125;
194     # Plant.PipeH
195     Plant.PipeH.InitP:=6.95e6;
196     Plant.PipeH.InitT:= 273.15 + 530;
197     Plant.PipeC2.InitP:=1.00e6;
198     Plant.InitT:= 273.15+18;
199 INTERMEDIATE
200 INPUT
201     #Loop1
202     Plant.Loop1.DeltaP:= 331300;
203     Plant.Loop1.AdaptFactor1:=1;
204     Plant.Loop1.AdaptFactor2:=1;
205     Plant.Loop1.ModifyFlow := 0.00;
206     Plant.Loop1.rho_avg := (1.0 - 0.0140)*0.919725239276886;
207     # PipeH
208     WITHIN Plant DO
209         PipeH.TO:=1173.1500; #PipeH.InitT;
210         PipeH.P_In:= 7000000.0; #PipeH.InitP + 100;
211         PipeH.P_Out:=6950000.0;#PipeH.InitP;
212     END # within
213     # PipeC2
214     WITHIN Plant DO
215         PipeC2.TO:= 614.15;#InitT;
216         PipeC2.P_In:=1120950.0 - (1120950.0 - 1000000.0 )*0.658;      # 1110000.0; #PipeC2.InitP+100;
217         PipeC2.P_Out:=1000000.0; #PipeC2.InitP;
218     END # within
219 PRESET
220     INCLUDE ..\HTLQSS_QStepDecrFPHX_Event30s_sout\HTLQSS_QStepDecrFPHX_Event30s_Out_PRE
221 INITIAL
222     INCLUDE ..\HTLQSS_QStepDecrFPHX_Event30s_sout\HTLQSS_QStepDecrFPHX_Event30s_Out_INI
223 SCHEDULE
224     SEQUENCE
225         CONTINUE FOR 1000
226         DISPLAY TIME, "seg" END
227         DISPLAY Plant.PipeC2.F(1) END
228         SAVE PRESETS HTLQSS_QStepDecrFPHX_PostEvent1000s_Out_PRE
229         SAVE INITIAL HTLQSS_QStepDecrFPHX_PostEvent1000s_Out_INI
230     END # sequence
231 END # simulation
232 #####
233
234
235 #####
236 SIMULATION HTLQSS_QStepIncDPLoopComp_Event160sToTime
237 #####
238 OPTIONS
239     INIT_PRINT_LEVEL:=0;
240     DYNAMIC_PRINT_LEVEL:=0;
241     DYNAMIC_REPORTING_INTERVAL:=0.01;
242     CSVOUTPUT:=TRUE;
243     DYNAMIC_BOUNDS := TRUE;
244     INIT_BLOCK_SOLVE:= TRUE;
245     INIT_RELATIVE_TOLERANCE := 1e-9;
246     INIT_ABSOLUTE_TOLERANCE := 1e-8;
247     REINIT_RELATIVE_TOLERANCE:= 1e-8;
248     REINIT_ABSOLUTE_TOLERANCE:= 1e-8;
249     DYNAMIC_RELATIVE_TOLERANCE:= 1e-6;
250     DYNAMIC_ABSOLUTE_TOLERANCE:= 1e-8;
251     REINIT_MAX_ITERATIONS:= 2000;
252     REINIT_PRINT_LEVEL:= 0;
253     CHECK_MATH_EXCEPTIONS:= FALSE;
254     DYNAMIC_SCALING:= TRUE;
255     INITIALIZE_SENSITIVITIES := TRUE;
256 UNIT
257     Plant AS HeatTransferLoopQSSPipesFullDyn
258 SET
259     #Plant.Loop1
260     Plant.Loop1.InitDeltaP:=500.0;
261     Plant.Loop1.MaxDeltaP:=0.321e6;
262     # Plant.PipeH
263     Plant.PipeH.InitP:=6.95e6;
264     Plant.PipeH.InitT:= 273.15 + 530;
265     Plant.PipeC2.InitP:=1.00e6;
266     Plant.InitT:= 273.15+18;
267 INTERMEDIATE
268 INPUT
269     #Loop1
270     Plant.Loop1.DeltaP:= 331300;
271     Plant.Loop1.AdaptFactor1:=1;
272     Plant.Loop1.AdaptFactor2:=1;
273     Plant.Loop1.ModifyFlow := 0.00;
274     Plant.Loop1.rho_avg := (1.0 - 0.0140)*0.919725239276886;
275     # PipeH
276     WITHIN Plant DO
277         PipeH.TO:=1173.1500244140625; #PipeH.InitT;
278         PipeH.P_In:= 7000000.0; #PipeH.InitP + 100;
279         PipeH.P_Out:=6950000.0;#PipeH.InitP;
280     END # within

```

```

281 # PipeC2
282 WITHIN Plant DO
283   PipeC2.TO:= 614.15;#InitT;
284   PipeC2.P_In:=1120950.0; #PipeC2.InitP+100;
285   PipeC2.P_Out:=1000000.0; #PipeC2.InitP;
286 END # within
287 PRESET
288   INCLUDE ..\HTLQSS_SS_sout\HTLQSS_SS_Out_PRE
289 INITIAL
290   INCLUDE ..\HTLQSS_SS_sout\HTLQSS_SS_Out_INI
291 SCHEDULE
292 SEQUENCE
293   CONTINUE FOR 10 #10
294   RESET
295     Plant.Loop1.DeltaP:= 331300 + 47515*(TIME-10)/0.2;
296   END # reset
297   CONTINUE FOR 0.2
298   RESET
299     Plant.Loop1.DeltaP:= 331300 + 47515;
300   END # reset
301   CONTINUE FOR 149.8 #20
302   DISPLAY TIME, "seg" END
303   DISPLAY Plant.PipeC2.F(1) END
304   SAVE PRESETS HTLQSS_QStepDecrFPHX_Event160s_Out_PRE
305   SAVE INITIAL HTLQSS_QStepDecrFPHX_Event160s_Out_INI
306 END # sequence
307 END # simulation
308 #####
309
310
311 #####
312 SIMULATION HTLQSS_QStepIncDPLoopComp_Event30s
313 #####
314 OPTIONS
315   INIT_PRINT_LEVEL:=0;
316   DYNAMIC_PRINT_LEVEL:=0;
317   DYNAMIC_REPORTING_INTERVAL:= 0.005; # 0.1;
318   CSVOUTPUT:=TRUE;
319   DYNAMIC_BOUNDS := TRUE;
320   INIT_BLOCK SOLVE:= TRUE;
321   INIT_RELATIVE_TOLERANCE := 1e-9;
322   INIT_ABSOLUTE_TOLERANCE := 1e-8;
323   REINIT_RELATIVE_TOLERANCE:= 1e-8;
324   REINIT_ABSOLUTE_TOLERANCE:= 1e-8;
325   DYNAMIC_RELATIVE_TOLERANCE:= 1e-6;
326   DYNAMIC_ABSOLUTE_TOLERANCE:= 1e-8;
327   REINIT_MAX_ITERATIONS:= 2000;
328   REINIT_PRINT_LEVEL:= 0;
329   CHECK_MATH_EXCEPTIONS:= FALSE;
330   DYNAMIC_SCALING:= TRUE;
331   INITIALIZE_SENSITIVITIES := TRUE;
332 UNIT
333   Plant AS HeatTransferLoopQSSPipesFullDyn
334 SET
335   #Plant.Loop1
336   Plant.Loop1.InitDeltaP:=-500.0;
337   Plant.Loop1.MaxDeltaP:=304125;
338   # Plant.PipeH
339   Plant.PipeH.InitP:=6.95e6;
340   Plant.PipeH.InitT:= 273.15 + 530;
341   Plant.PipeC2.InitP:=1.00e6;
342   Plant.InitT:= 273.15+18;
343 INTERMEDIATE
344 INPUT
345   #Loop1
346   Plant.Loop1.DeltaP:= 331300;
347   Plant.Loop1.AdaptFactor1:=1;
348   Plant.Loop1.AdaptFactor2:=1;
349   Plant.Loop1.ModifyFlow := 0.00;
350   Plant.Loop1.rho_avg := (1.0 - 0.0140)*0.919725239276886;
351   # PipeH
352   WITHIN Plant DO
353     PipeH.TO:=1173.1500244140625; #PipeH.InitT;
354     PipeH.P_In:= 7000000.0; #PipeH.InitP + 100;
355     PipeH.P_Out:=6950000.0;#PipeH.InitP;
356   END # within
357   # PipeC2
358   WITHIN Plant DO
359     PipeC2.TO:= 614.15;#InitT;
360     PipeC2.P_In:=1110000.0 + 10950.0; #PipeC2.InitP+100;
361     PipeC2.P_Out:=1000000.0; #PipeC2.InitP;
362   END # within
363 PRESET
364   INCLUDE ..\HTLQSS_SS_sout\HTLQSS_SS_Out_PRE
365 INITIAL
366   INCLUDE ..\HTLQSS_SS_sout\HTLQSS_SS_Out_INI
367 SCHEDULE
368 SEQUENCE
369   CONTINUE FOR 10
370   RESET
371     Plant.Loop1.DeltaP:= 331300 + 47515*(TIME-10)/0.2;
372   END # reset

```

```

373     CONTINUE FOR 0.2
374     RESET
375         Plant.Loop1.DeltaP:= 331300 + 47515;
376     END # reset
377     CONTINUE FOR 19.9# 20
378     DISPLAY TIME, "seg" END
379     DISPLAY Plant.Loop1.F(1) END
380     SAVE PRESETS HTLQSS_QStepIncDPLoopComp_Event30s_Out_PRE
381     SAVE INITIAL HTLQSS_QStepIncDPLoopComp_Event30s_Out_INI
382     END # sequence
383 END # simulation
384 *****
385
386 *****
387 *****
388 SIMULATION HTLQSS_QStepIncDPLoopComp_PostEvent1000s
389 *****
390     OPTIONS
391         INIT_PRINT_LEVEL:=0;
392         DYNAMIC_PRINT_LEVEL:=0;
393         DYNAMIC_REPORTING_INTERVAL:= 1.0; # 0.1;
394         CSVOUTPUT:=TRUE;
395         DYNAMIC_BOUNDS := TRUE;
396         INIT_BLOCK_SOLVE:= TRUE;
397         INIT_RELATIVE_TOLERANCE := 1e-9;
398         INIT_ABSOLUTE_TOLERANCE := 1e-8;
399         REINIT_RELATIVE_TOLERANCE:= 1e-8;
400         REINIT_ABSOLUTE_TOLERANCE:= 1e-8;
401         DYNAMIC_RELATIVE_TOLERANCE:= 1e-6;
402         DYNAMIC_ABSOLUTE_TOLERANCE:= 1e-8;
403         REINIT_MAX_ITERATIONS:= 2000;
404         REINIT_PRINT_LEVEL:= 0;
405         CHECK_MATH_EXCEPTIONS:= FALSE;
406         DYNAMIC_SCALING:= TRUE;
407         INITIALIZE_SENSITIVITIES := TRUE;
408     UNIT
409     Plant AS HeatTransferLoopQSSPipesFullDyn
410     SET
411     #Plant.Loop1
412     Plant.Loop1.InitDeltaP:=500.0;
413     Plant.Loop1.MaxDeltaP:=304125;
414     # Plant.PipeH
415     Plant.PipeH.InitP:=6.95e6;
416     Plant.PipeH.InitT:= 273.15 + 530;
417     Plant.PipeC2.InitP:=1.00e6;
418     Plant.InitT:= 273.15+18;
419     INTERMEDIATE
420     INPUT
421     #Loop1
422     Plant.Loop1.DeltaP:= 331300 + 47515;
423     Plant.Loop1.AdaptFactor1:=1;
424     Plant.Loop1.AdaptFactor2:=1;
425     Plant.Loop1.ModifyFlow := 0.00;
426     Plant.Loop1.rho_avg := (1.0 - 0.0140)*0.919725239276886;
427     # PipeH
428     WITHIN Plant DO
429     PipeH.TO:=1173.1500244140625; #PipeH.InitT;
430     PipeH.P_In:= 7000000.0; #PipeH.InitP + 100;
431     PipeH.P_Out:=6950000.0;#PipeH.InitP;
432     END # within
433     # PipeC2
434     WITHIN Plant DO
435     PipeC2.TO:= 614.15;#InitT;
436     PipeC2.P_In:=1110000.0 + 10950.0; #PipeC2.InitP+100;
437     PipeC2.P_Out:=1000000.0; #PipeC2.InitP;
438     END # within
439     PRESET
440     INCLUDE ..\HTLQSS_QStepIncDPLoopComp_Event30s_sout\HTLQSS_QStepIncDPLoopComp_Event30s_Out_PRE
441     INITIAL
442     INCLUDE ..\HTLQSS_QStepIncDPLoopComp_Event30s_sout\HTLQSS_QStepIncDPLoopComp_Event30s_Out_INI
443     SCHEDULE
444     SEQUENCE
445     CONTINUE FOR 1000
446     DISPLAY TIME, "seg" END
447     DISPLAY Plant.Loop1.F(1) END
448     SAVE PRESETS HTLQSS_QStepIncDPLoopComp_PostEvent1000s_Out_PRE
449     SAVE INITIAL HTLQSS_QStepIncDPLoopComp_PostEvent1000s_Out_INI
450     END # sequence
451 END # simulation
452 *****

```

SIMULATIONS_CH4_HTLANDNUCLEARREACTOR_QSS.JAC

```

1  INCLUDE MODELS_PHYSICALPROPERTIES
2  INCLUDE MODELS_HEATEXCHANGERS
3  INCLUDE MODELS_NUCLEARREACTORPROPERTIES
4  INCLUDE MODELS_NUCLEARREACTORANDAUXS
5  INCLUDE MODELS_NUCLEARREACTORLOOP
6  INCLUDE MODELS_PIPEMODELS
7  INCLUDE MODELS_HEATTRANSFERLOOP
8  #####
9  SIMULATION NuclearReactorAndHTLQSS_ULOF_FullEvent
10 #####
11  OPTIONS
12    INIT_PRINT_LEVEL:=0; DYNAMIC_PRINT_LEVEL:=0;
13    DYNAMIC_REPORTING_INTERVAL:=1; CSVOUTPUT:=TRUE;
14    DYNAMIC_BOUNDS := TRUE;
15    INIT_BLOCK_SOLVE:= TRUE; INIT_RELATIVE_TOLERANCE := 1e-9;
16    INIT_ABSOLUTE_TOLERANCE := 1e-8; REINIT_RELATIVE_TOLERANCE:= 1e-7;
17    REINIT_ABSOLUTE_TOLERANCE:= 1e-8; DYNAMIC_RELATIVE_TOLERANCE:= 1e-7;
18    DYNAMIC_ABSOLUTE_TOLERANCE:= 1e-8; REINIT_MAX_ITERATIONS:= 1000;
19    REINIT_PRINT_LEVEL:= 0; CHECK_MATH_EXCEPTIONS:= FALSE;
20    DYNAMIC_SCALING:= TRUE; INITIALIZE_SENSITIVITIES := TRUE;
21  PARAMETER
22    # Loop2
23    QFission_K0 AS REAL
24    CO AS REAL
25    TTrans AS REAL
26    TCoreOut_SetPoint AS REAL
27    Xe0 AS REAL
28    IConc0 AS REAL
29  UNIT
30    # Loop2
31    Plant2 AS PlantNR
32    #HeatTransferLoopQSSNoPipeH
33    Plant AS HeatTransferLoopQSSNoPipeH
34  VARIABLE
35    TCoreOutGas As Temperature
36    TFuelAvg AS Temperature
37    TFuelMax AS Temperature
38  SET
39    # Simulation
40    #SET
41    QFission_K0:= 250e6/1e8*1/100;
42    CO:= 5.3510274e10/1e8*1/100;
43    TTrans:= 300; # s? ### fix this
44    TCoreOut_SetPoint := 900 + 273.16; # L1530
45    #CALCULATED
46    IConc0:= Plant2.NR.Poison.gamma_I*Plant2.NR.Poison.sigma_total/Plant2.NR.Poison.lambda_I*Plant2.NR.Poison.
      phi0;
47    Xe0:= (Plant2.NR.Poison.gamma_xe+Plant2.NR.Poison.gamma_I)*
48    Plant2.NR.Poison.sigma_total/(Plant2.NR.Poison.lambda_xe+Plant2.NR.Poison.sigma_xe+Plant2.NR.Poison.phi0)
      *Plant2.NR.Poison.phi0;
49    # Loop2
50    Plant2.NR.WPrim0 := 126.6;
51    Plant2.NR.Poison.phi0 := 1e18;
52    Plant2.PipeH.InitP:=6.95e6;
53    Plant2.PipeH.rho:= 3.93;
54    # Plant2
55    Plant2.InitDeltaP := 100;
56    Plant2.MaxDeltaP := 0.29e6;
57    Plant2.InitT:= 300; # 273.15+530;
58    Plant2.WpcupipeRatio:=3.18;
59    # HeatTransferLoopQSSNoPipeH
60    Plant.Loop1.InitDeltaP:=500.0;
61    Plant.Loop1.MaxDeltaP:=0.321e6;
62    Plant.PipeC2.InitP:=1.00e6;
63    Plant.InitT:= 273.15+18;
64  INTERMEDIATE
65    # Loop2
66    # PIPEH
67    i_UH:= Plant2.PipeH.HT.U;
68    i_r0H:= Plant2.PipeH.r0;
69    i_VH2:= Plant2.PipeH.Vol;
70    # heat calculation
71    QH:= sigma(4*i_UH/(2*i_r0H))*(Plant2.PipeH.TExtrnl(1:Plant2.PipeH.NG)
72    -Plant2.PipeH.T(1:Plant2.PipeH.NG))*i_VH2);
73    QHdiff:= Plant2.PipeH.A*Plant2.PipeH.rho(Plant2.PipeH.NG)*Plant2.PipeH.v(Plant2.PipeH.NG)*Plant2.PipeH.h(
      Plant2.PipeH.NG) -
74    Plant2.PipeH.A*Plant2.PipeH.rho(1)*Plant2.PipeH.v(1)*Plant2.PipeH.h(1);
75    mdotH:= Plant2.PipeH.rho(1)*Plant2.PipeH.v(1)*Plant2.PipeH.A;
76  EQUATION
77    # Loop2
78    FOR I:=1 TO Plant2.PipeH.NG DO
79      Plant2.PipeH.TExtrnl(Plant2.PipeH.NG+1-I) = Plant.HX.THX(I); ###
80    END # for
81    # Dummy variables for reporting
82    TCoreOutGas = Plant2.NR.Thyd.TCoreOut - 273.16;
83    TFuelAvg = Plant2.NR.Thyd.T_FuelAvg - 273.16;
84    TFuelMax = Plant2.NR.Thyd.TSolid(10,2) - 273.16;
85    # HeatTransferLoopQSSNoPipeH
86    Plant.HX.UHot = Plant2.PipeH.HT.U;
87    FOR I:= 1 TO Plant.HX.NGHX DO
88      Plant.HX.TGasHot(I) = Plant2.PipeH.T(Plant2.PipeH.NG + 1 - I);
89    END # for

```

```

90 INPUT
91 # Loop2
92 Plant2.NR.PhoControl := 0.0; # 0.0001;
93 Plant2.NR.wPhoExtra1 := 1.0;
94 Plant2.NR.PhoExtra2 := 0.0;
95 Plant2.Comp.P2:= 7.0e6;
96 Plant2.Comp.PR:= 1.0001; # we start at a low number
97 # HeatTransferLoopQSSNoPipeH
98 Plant.Loop1.DeltaP:= 331300;
99 Plant.Loop1.AdaptFactor1:=1;
100 Plant.Loop1.AdaptFactor2:=1;
101 Plant.Loop1.ModifyFlow := 0.00;
102 Plant.Loop1.rho_avg := (1.0 - 0.0140)*0.919725239276886;
103 WITHIN Plant DO
104 PipeC2.TO:= 614.15;#InitT;
105 PipeC2.P_In:=1120950.0; #PipeC2.InitP+100;
106 PipeC2.P_Out:=1000000.0; #PipeC2.InitP;
107 END # within
108 PRESET
109 # Loop2
110 WITHIN Plant2 DO
111 FOR I:= 1 TO PipeH.NG DO
112 PipeH.P(I):= PipeH.InitP;
113 PipeH.T(I):= PipeH.Temp;
114 Comp.P1:= PipeH.InitP;
115 END # for
116 END # within
117 # HeatTransferLoopQSSNoPipeH
118 INCLUDE ..\input\HTLNOPIPEHQSS_SS_OUT_PRE
119 INITIAL
120 # Loop2
121 WITHIN Plant2 DO
122 FOR I:=2 TO PipeH.NG DO
123 PipeH.$rho_E(I)= 0;
124 END # for
125 END # within
126 Plant2.NR.Thyd.TSolid = 600;
127 Plant2.NR.Kinetics.QFission_K = QFission_K0;
128 Plant2.NR.Kinetics.C = C0;
129 Plant2.NR.Poison.IConc = IConc0;
130 Plant2.NR.Poison.Xe = Xe0;
131 INCLUDE ..\input\HTLNOPIPEHQSS_SS_OUT_INI
132 SCHEDULE
133 SEQUENCE
134 CONTINUE FOR 10*60
135 # Loop2: start compressor 2 until reaching target speed in coolant loop
136 RESET
137 Plant2.Comp.PR := 1.0001 + 0.03*(TIME - OLD(TIME))/(6*60);
138 END # reset
139 CONTINUE UNTIL mdoth > 32.0 # Plant2.NR.Thyd.WPrim > 124
140 RESET
141 Plant2.Comp.PR := OLD(Plant2.Comp.PR);
142 END # reset
143 CONTINUE FOR 1*60
144 # Loop2: increase reactivity power reaches 250e6 W
145 RESET
146 Plant2.NR.PhoControl := 0.0001*(TIME-OLD(TIME))/(5*60);
147 END # reset
148 CONTINUE FOR 5*60
149 RESET
150 Plant2.NR.PhoControl := OLD(Plant2.NR.PhoControl);
151 END # reset
152 CONTINUE UNTIL Plant2.NR.Thyd.QFission > 250e6
153 CONTINUE FOR 17.1 # this extra time lets QFission reach the right value.
154 RESET
155 Plant2.NR.PhoControl := 0.0;
156 END # reset
157 CONTINUE FOR 1*60
158 DISPLAY Plant2.NR.Thyd.QFission END
159 DISPLAY "17.1" END
160 CONTINUE FOR 800*60
161 SAVE PRESETS PRESETS_NuclearReactorOperating
162 SAVE INITIAL INITIAL_NuclearReactorOperating
163 # Insert Temperature Reactivity
164 RESET
165 Plant2.NR.wPhoExtra1:= 0;
166 Plant2.NR.PhoExtra2:=OLD(Plant2.NR.PhoExtra1);
167 END # reset
168 CONTINUE FOR 1*60
169 DISPLAY TIME END
170 RESET
171 Plant2.NR.PhoExtra2:=OLD(Plant2.NR.PhoExtra2); # trick to eliminate problems of phoextra2 jumping during
transient
172 END
173 CONTINUE FOR 1*60
174 DISPLAY Plant.Loop1.F(1) END
175 DISPLAY Plant.Loop1.DeltaP END
176 DISPLAY "This is QH", QH, "This is QHdiff", QHdiff END
177 # This is the new transient. I will stop the flow in the intermediate loop.
178 RESET
179 Plant.Loop1.DeltaP := 328300 - (328300 - 2500.0)*(TIME - OLD(TIME))/5;
180 END # reset

```

```

181     CONTINUE FOR 5
182     RESET
183     Plant.Loop1.DeltaP := 2500.0;
184     END # reset
185     CONTINUE FOR 100*60
186     DISPLAY Plant.Loop1.F(1) END
187     DISPLAY "This is QH", QH, "This is QHdiff", QHdiff END
188     END # sequence
189     END # simulation
190     #####
191
192
193     #####
194     SIMULATION NuclearReactorAndHTLQSS_HTLLeak_FullEvent
195     #####
196     OPTIONS
197     INIT_PRINT_LEVEL:=0; DYNAMIC_PRINT_LEVEL:=0;
198     DYNAMIC_REPORTING_INTERVAL:=1; CSVOUTPUT:=TRUE;
199     DYNAMIC_BOUNDS := TRUE;
200     INIT_BLOCK_SOLVE:= TRUE; INIT_RELATIVE_TOLERANCE := 1e-9;
201     INIT_ABSOLUTE_TOLERANCE := 1e-8; REINIT_RELATIVE_TOLERANCE:= 1e-7;
202     REINIT_ABSOLUTE_TOLERANCE:= 1e-8; DYNAMIC_RELATIVE_TOLERANCE:= 1e-7;
203     DYNAMIC_ABSOLUTE_TOLERANCE:= 1e-8; REINIT_MAX_ITERATIONS:= 1000;
204     REINIT_PRINT_LEVEL:= 0; CHECK_MATH_EXCEPTIONS:= FALSE;
205     DYNAMIC_SCALING:= TRUE; INITIALIZE_SENSITIVITIES := TRUE;
206     PARAMETER
207     # Loop2
208     QFission_K0 AS REAL
209     CO AS REAL
210     TTrans AS REAL
211     TCoreOut_SetPoint AS REAL
212     Xe0 AS REAL
213     IConc0 AS REAL
214     UNIT
215     # Loop2
216     Plant2 AS PlantNR
217     #HeatTransferLoopQSSNoPipeH
218     Plant AS HeatTransferLoopQSSNoPipeH
219     VARIABLE
220     TCoreOutGas As Temperature
221     TFuelAvg AS Temperature
222     TFuelMax AS Temperature
223     SET
224     # Simulation
225     #SET
226     QFission_K0:= 250e6/1e8*1/100;
227     CO:= 5.3510274e10/1e8*1/100;
228     TTrans:= 300; # s? ### fix this
229     TCoreOut_SetPoint := 900 + 273.16; # L1530
230     #CALCULATED
231     IConc0:= Plant2.NR.Poison.gamma_I*Plant2.NR.Poison.sigma_total/Plant2.NR.Poison.lambda_I*Plant2.NR.Poison.
        phi0;
232     Xe0:= (Plant2.NR.Poison.gamma_xe+Plant2.NR.Poison.gamma_I)*
233     Plant2.NR.Poison.sigma_total/(Plant2.NR.Poison.lambda_xe+Plant2.NR.Poison.sigma_xe*Plant2.NR.Poison.phi0)
        *Plant2.NR.Poison.phi0;
234
235     # Loop2
236     Plant2.NR.WPrim0 := 126.6;
237     Plant2.NR.Poison.phi0 := 1e18;
238     Plant2.PipeH.InitP:=6.95e6;
239     Plant2.PipeH.rho:= 3.93;
240     # Plant2
241     Plant2.InitDeltaP := 100;
242     Plant2.MaxDeltaP := 0.29e6;
243     Plant2.InitT:= 300; # 273.15+530;
244     Plant2.WcupPipeRatio:=3.17;
245     # HeatTransferLoopQSSNoPipeH
246     Plant.Loop1.InitDeltaP:=500.0;
247     Plant.Loop1.MaxDeltaP:=0.321e6;
248     Plant.PipeC2.InitP:=1.00e6;
249     Plant.InitT:= 273.15+18;
250     INTERMEDIATE
251     # Loop2
252     # PIPEH
253     i_UH:= Plant2.PipeH.HT.U;
254     i_rOH:= Plant2.PipeH.r0;
255     i_VH2:= Plant2.PipeH.Vol;
256     # heat calculation
257     QH:= sigma(4*i_UH/(2*i_rOH))*(Plant2.PipeH.TExtrnl(1:Plant2.PipeH.NG)
258     -Plant2.PipeH.T(1:Plant2.PipeH.NG))*i_VH2);
259     QHdiff:= Plant2.PipeH.A*Plant2.PipeH.rho(Plant2.PipeH.NG)*Plant2.PipeH.v(Plant2.PipeH.NG)*Plant2.PipeH.h(
260     Plant2.PipeH.NG) -
261     Plant2.PipeH.A*Plant2.PipeH.rho(1)*Plant2.PipeH.v(1)*Plant2.PipeH.h(1);
262     mdotH:= Plant2.PipeH.rho(1)*Plant2.PipeH.v(1)*Plant2.PipeH.A;
263     EQUATION
264     # Loop2
265     FOR I:=1 TO Plant2.PipeH.NG DO
266     Plant2.PipeH.TExtrnl(Plant2.PipeH.NG+1-I) = Plant.HX.THX(I); ###
267     END # for
268     # Dummy variables for reporting
269     TCoreOutGas = Plant2.NR.Thyd.TCoreOut - 273.16;
270     TFuelAvg = Plant2.NR.Thyd.T_FuelAvg - 273.16;
271     TFuelMax = Plant2.NR.Thyd.TSolid(10,2) - 273.16;

```



```

270 # HeatTransferLoopQSSNoPipeH
271 Plant.HX.UHot = Plant2.PipeH.HT.U;
272 FOR I:= 1 TO Plant.HX.NGHX DO
273   Plant.HX.TGasHot(I) = Plant2.PipeH.T(Plant2.PipeH.NG + 1 - I);
274 END # for
275 INPUT
276 # Loop2
277 Plant2.NR.PhoControl := 0.0; # 0.0001;
278 Plant2.NR.wPhoExtra1 := 1.0;
279 Plant2.NR.PhoExtra2 := 0.0;
280 Plant2.Comp.P2:= 7.0e6;
281 Plant2.Comp.PR:= 1.0001; # we start at a low number
282 # HeatTransferLoopQSSNoPipeH
283 Plant.Loop1.DeltaP:= 328300;
284 Plant.Loop1.AdaptFactor1:=1;
285 Plant.Loop1.AdaptFactor2:=1;
286 Plant.Loop1.ModifyFlow := 0.00;
287 Plant.Loop1.rho_avg := (1.0 - 0.0140)*0.919725239276886;
288 WITHIN Plant DO
289   PipeC2.TO:= 614.15;#InitT;
290   PipeC2.P_In:=1120950.0; #PipeC2.InitP+100;
291   PipeC2.P_Out:=1000000.0; #PipeC2.InitP;
292 END # within
293 PRESET
294 # Loop2
295 WITHIN Plant2 DO
296   FOR I:= 1 TO PipeH.NG DO
297     PipeH.P(I):= PipeH.InitP;
298     PipeH.T(I):= PipeH.Temp;
299     Comp.P1:= PipeH.InitP;
300   END # for
301 END # within
302 # HeatTransferLoopQSSNoPipeH
303 INCLUDE ..\input\HTLNOPIPEHQSS_SS_OUT_PRE
304 INITIAL
305 # Loop2
306 WITHIN Plant2 DO
307   FOR I:=2 TO PipeH.NG DO
308     PipeH.rho_E(I)= 0;
309   END # for
310 END # within
311 Plant2.NR.Thyd.TSolid = 600;
312 Plant2.NR.Kinetics.QFission_K = QFission_K0;
313 Plant2.NR.Kinetics.C = C0;
314 Plant2.NR.Poison.IConc = IConc0;
315 Plant2.NR.Poison.Xe = Xe0;
316 INCLUDE ..\input\HTLNOPIPEHQSS_SS_OUT_INI
317 SCHEDULE
318 SEQUENCE
319 CONTINUE FOR 10*60
320 # Loop2: start compressor 2 until reaching target speed in coolant loop
321 RESET
322 Plant2.Comp.PR := 1.0001 + 0.03*(TIME - OLD(TIME))/(6*60);
323 END # reset
324 CONTINUE UNTIL mdotH > 32.0 # Plant2.NR.Thyd.WPrim > 124
325 RESET
326 Plant2.Comp.PR := OLD(Plant2.Comp.PR);
327 END # reset
328 CONTINUE FOR 1*60
329 # Loop2: increase reactivity power reaches 250e6 W
330 RESET
331 Plant2.NR.PhoControl := 0.0001*(TIME-OLD(TIME))/(5*60);
332 END # reset
333 CONTINUE FOR 5*60
334 RESET
335 Plant2.NR.PhoControl := OLD(Plant2.NR.PhoControl);
336 END # reset
337 CONTINUE UNTIL Plant2.NR.Thyd.QFission > 250e6
338 CONTINUE FOR 17.1 # this extra time lets QFission reach the right value.
339 RESET
340 Plant2.NR.PhoControl := 0.0;
341 END # reset
342 CONTINUE FOR 1*60
343 DISPLAY Plant2.NR.Thyd.QFission END
344 DISPLAY "17.1" END
345 CONTINUE FOR 800*60
346 SAVE PRESETS PRESETS_NuclearReactorOperating
347 SAVE INITIAL INITIAL_NuclearReactorOperating
348 # Insert Temperature Reactivity
349 RESET
350 Plant2.NR.wPhoExtra1:= 0;
351 Plant2.NR.PhoExtra2:=OLD(Plant2.NR.PhoExtra1);
352 END # reset
353 CONTINUE FOR 1*60
354 DISPLAY TIME END
355 RESET
356 Plant2.NR.PhoExtra2:=OLD(Plant2.NR.PhoExtra2); # trick to eliminate problems of phoextra2 jumping during
    transient
357 END
358 CONTINUE FOR 1*60
359 DISPLAY Plant.Loop1.F(1) END
360 DISPLAY Plant.Loop1.DeltaP END

```

```

361      # This is the new transient. 50% decrease in helium mass in loop
362      RESET
363      Plant.Loop1.rho_avg := (1.0 - 0.0140)*0.919725239276886 - 0.50* (1.0 - 0.0140)*0.919725239276886*(TIME-
      OLD(TIME))/60;
364      END
365      CONTINUE FOR 60
366      RESET
367      Plant.Loop1.rho_avg := 0.50* (1.0 - 0.0140)*0.919725239276886;
368      END # reset
369      CONTINUE FOR 100*60
370      DISPLAY "This is QH", QH, "This is QHdiff", QHdiff END
371      DISPLAY "This is mdotH", mdotH END
372      DISPLAY "Thotout", (Plant2.PipeH.T(Plant2.PipeH.NG) - 273.15) END
373      DISPLAY Plant2.NR.Thyd.TSolid, Plant2.NR.Thyd.TGas END
374      DISPLAY "This is QC2", QC2, "This is QC2diff", QC2diff END
375      DISPLAY "This is mdotC2", mdotC2 END
376      DISPLAY "This is mdotH", mdotH END
377      DISPLAY "This is mdotC2", mdotC2 END
378      END # sequence
379      END # simulation
380      #####
381
382
383      #####
384      SIMULATION NuclearReactorAndHTLQSS_LossHeatSink_FullEvent
385      #####
386      OPTIONS
387      INIT_PRINT_LEVEL:=0; DYNAMIC_PRINT_LEVEL:=0;
388      DYNAMIC_REPORTING_INTERVAL:=1; CSVOUTPUT:=TRUE;
389      DYNAMIC_BOUNDS := TRUE;
390      INIT_BLOCK_SOLVE:= TRUE; INIT_RELATIVE_TOLERANCE := 1e-9;
391      INIT_ABSOLUTE_TOLERANCE := 1e-8; REINIT_RELATIVE_TOLERANCE:= 1e-7;
392      REINIT_ABSOLUTE_TOLERANCE:= 1e-8; DYNAMIC_RELATIVE_TOLERANCE:= 1e-7;
393      DYNAMIC_ABSOLUTE_TOLERANCE:= 1e-8; REINIT_MAX_ITERATIONS:= 1000;
394      REINIT_PRINT_LEVEL:= 0; CHECK_MATH_EXCEPTIONS:= FALSE;
395      DYNAMIC_SCALING:= TRUE; INITIALIZE_SENSITIVITIES := TRUE;
396      PARAMETER
397      # Loop2
398      QFission_K0 AS REAL
399      CO AS REAL
400      TTrans AS REAL
401      TCoreOut_SetPoint AS REAL
402      Xe0 AS REAL
403      IConc0 AS REAL
404      UNIT
405      # Loop2
406      Plant2 AS PlantNR
407      #HeatTransferLoopQSSNoPipeH
408      Plant AS HeatTransferLoopQSSNoPipeH
409      VARIABLE
410      TCoreOutGas AS Temperature
411      TFuelAvg AS Temperature
412      TFuelMax AS Temperature
413      SET
414      # Simulation
415      #SET
416      QFission_K0:= 250e6/1e8*1/100;
417      CO:= 5.3510274e10/1e8*1/100;
418      TTrans:= 300; # s? ### fix this
419      TCoreOut_SetPoint := 900 + 273.16; # L1530
420      #CALCULATED
421      IConc0:= Plant2.NR.Poison.gamma_I*Plant2.NR.Poison.sigma_total/Plant2.NR.Poison.lambda_I*Plant2.NR.Poison.
      phi0;
422      Xe0:= (Plant2.NR.Poison.gamma_xe*Plant2.NR.Poison.gamma_I)*
423      Plant2.NR.Poison.sigma_total/(Plant2.NR.Poison.lambda_xe*Plant2.NR.Poison.sigma_xe*Plant2.NR.Poison.phi0)
      *Plant2.NR.Poison.phi0;
424      # Loop2
425      Plant2.NR.WPrim0 := 126.6;
426      Plant2.NR.Poison.phi0 := 1e18;
427      Plant2.PipeH.InitP:=6.95e6;
428      Plant2.PipeH.rho:= 3.93;
429      # Plant2
430      Plant2.InitDeltaP := 100;
431      Plant2.MaxDeltaP := 0.29e6;
432      Plant2.InitT:= 300; # 273.15+530;
433      Plant2.WcupipeRatio:=3.17;
434      # HeatTransferLoopQSSNoPipeH
435      Plant.Loop1.InitDeltaP:=500.0;
436      Plant.Loop1.MaxDeltaP:=0.321e6;
437      Plant.PipeC2.InitP:=1.00e6;
438      Plant.InitT:= 273.15+18;
439      INTERMEDIATE
440      # Loop2
441      # PIPEH
442      i_UH:= Plant2.PipeH.HT.U;
443      i_r0H:= Plant2.PipeH.r0;
444      i_VH2:= Plant2.PipeH.Vol;
445      # heat calculation
446      QH:= sigma(4*i_UH/(2*i_r0H)*(Plant2.PipeH.TExtrnl(1:Plant2.PipeH.NG)
447      -Plant2.PipeH.T(1:Plant2.PipeH.NG))*i_VH2);
448      QHdiff:= Plant2.PipeH.A*Plant2.PipeH.rho(Plant2.PipeH.NG)*Plant2.PipeH.v(Plant2.PipeH.NG)*Plant2.PipeH.h(
      Plant2.PipeH.NG) -

```

```

449     Plant2.PipeH.A*Plant2.PipeH.rho(1)*Plant2.PipeH.v(1)*Plant2.PipeH.h(1);
450     mdotH:= Plant2.PipeH.rho(1)*Plant2.PipeH.v(1)*Plant2.PipeH.A;
451 EQUATION
452 # Loop2
453 FOR I:=1 TO Plant2.PipeH.NG DO
454     Plant2.PipeH.TExtrnl(Plant2.PipeH.NG+1-I) = Plant.HX.THX(I); ###
455 END # for
456 # Dummy variables for reporting
457 TCoreOutGas = Plant2.NR.Thyd.TCoreOut - 273.16;
458 TFuelAvg = Plant2.NR.Thyd.T_FuelAvg - 273.16;
459 TFuelMax = Plant2.NR.Thyd.TSolid(10,2) - 273.16;
460 # HeatTransferLoopQSSNoPipeH
461 Plant.HX.UHot = Plant2.PipeH.HT.U;
462 FOR I:= 1 TO Plant.HX.NGHX DO
463     Plant.HX.TGasHot(I) = Plant2.PipeH.T(Plant2.PipeH.NG + 1 - I);
464 END # for
465 INPUT
466 # Loop2
467 Plant2.NR.PhoControl := 0.0; # 0.0001;
468 Plant2.NR.wPhoExtra1 := 1.0;
469 Plant2.NR.PhoExtra2 := 0.0;
470 Plant2.Comp.P2:= 7.0e6;
471 Plant2.Comp.PR:= 1.0001; # we start at a low number
472 # HeatTransferLoopQSSNoPipeH
473 Plant.Loop1.DeltaP:= 328300;
474 Plant.Loop1.AdaptFactor1:=1;
475 Plant.Loop1.AdaptFactor2:=1;
476 Plant.Loop1.ModifyFlow := 0.00;
477 Plant.Loop1.rho_avg := (1.0 - 0.0140)*0.919725239276886;
478 WITHIN Plant DO
479     PipeC2.TO:= 614.15;#InitT;
480     PipeC2.P_In:=1120950.0; #PipeC2.InitP+100;
481     PipeC2.P_Out:=1000000.0; #PipeC2.InitP;
482 END # within
483 PRESET
484 # Loop2
485 WITHIN Plant2 DO
486     FOR I:= 1 TO PipeH.NG DO
487         PipeH.P(I):= PipeH.InitP;
488         PipeH.T(I):= PipeH.Temp;
489         Comp.P1:= PipeH.InitP;
490     END # for
491 END # within
492 # HeatTransferLoopQSSNoPipeH
493 INCLUDE ..\input\HTLNOPIPEHQSS_SS_OUT_PRE
494 INITIAL
495 # Loop2
496 WITHIN Plant2 DO
497     FOR I:=2 TO PipeH.NG DO
498         PipeH.$rho_E(I)= 0;
499     END # for
500 END # within
501     Plant2.NR.Thyd.TSolid = 600;
502     Plant2.NR.Kinetics.QFission_K = QFission_K0;
503     Plant2.NR.Kinetics.C = C0;
504     Plant2.NR.Poison.IConc = IConc0;
505     Plant2.NR.Poison.Ie = Ie0;
506     INCLUDE ..\input\HTLNOPIPEHQSS_SS_OUT_INI
507 SCHEDULE
508 SEQUENCE
509     CONTINUE FOR 10*60
510 # Loop2: start compressor 2 until reaching target speed in coolant loop
511 RESET
512     Plant2.Comp.PR := 1.0001 + 0.03*(TIME - OLD(TIME))/(6*60);
513 END # reset
514 CONTINUE UNTIL mdotH > 32.0 # Plant2.NR.Thyd.WPrim > 124
515 RESET
516     Plant2.Comp.PR := OLD(Plant2.Comp.PR);
517 END # reset
518 CONTINUE FOR 1*60
519 # Loop2: increase reactivity power reaches 250e6 W
520 RESET
521     Plant2.NR.PhoControl := 0.0001*(TIME-OLD(TIME))/(5*60);
522 END # reset
523 CONTINUE FOR 5*60
524 RESET
525     Plant2.NR.PhoControl := OLD(Plant2.NR.PhoControl);
526 END # reset
527 CONTINUE UNTIL Plant2.NR.Thyd.QFission > 250e6
528 CONTINUE FOR 17.1 # this extra time lets QFission reach the right value.
529 RESET
530     Plant2.NR.PhoControl := 0.0;
531 END # reset
532 CONTINUE FOR 1*60
533 DISPLAY Plant2.NR.Thyd.QFission END
534 DISPLAY "17.1" END
535 CONTINUE FOR 800*60
536 SAVE PRESETS PRESETS_NuclearReactorOperating
537 SAVE INITIAL INITIAL_NuclearReactorOperating
538 # Insert Temperature Reactivity
539 RESET
540     Plant2.NR.wPhoExtra1:= 0;

```

```

541     Plant2.NR.PhoExtra2:=OLD(Plant2.NR.PhoExtra1);
542     END # reset
543     CONTINUE FOR 1*60
544     DISPLAY TIME END
545     RESET
546     Plant2.NR.PhoExtra2:=OLD(Plant2.NR.PhoExtra2); # trick to eliminate problems of phoextra2 jumping during
        transient
547     END
548     CONTINUE FOR 1*60
549     DISPLAY Plant.Loop1.F(1) END
550     DISPLAY Plant.Loop1.DeltaP END
551     # This is the new transient. 50% decrease in helium mass in loop
552     RESET
553     Plant.PipeC2.P_In:= 1120950.0 - 120894.0*(TIME-OLD(TIME))/15;
554     END
555     CONTINUE FOR 15
556     RESET
557     Plant.PipeC2.P_In:= 1120950.0 - 120894.0;
558     END # reset
559     CONTINUE FOR 100*60
560     DISPLAY "This is QH", QH, "This is QHdiff", QHdiff END
561     END # sequence
562     END # simulation
563     #####

```

Bibliography

- [1] Energy Information Administration. International energy outlook 2009. Technical report, U.S. Department of Energy, Washington, DC, 2009.
- [2] R. Agrawal, N. R. Singh, F. H. Ribeiro, and W. N. Delgass. Sustainable fuel for the transportation sector. *Proceedings of the National Academy of Sciences*, 104(12):4828, 2007.
- [3] U. M. Ascher and L. R. Petzold. *Computer Methods for Ordinary Differential Equations and Differential-Algebraic Equations*. Society for Industrial & Applied Mathematics, Philadelphia, PA, USA, 1998.
- [4] P. I. Barton. Dyanmic modeling and simulation notes. Class notes, M.I.T, 1997.
- [5] P. I. Barton and C. C. Pantelides. Modeling of combined discrete/continuous processes. *AIChE Journal*, 40(6):966–979, 1994.
- [6] BP. BP Statistical Review of World Energy June 2010. bp.com/statisticalreview.
- [7] R. S. Cherry and R. A. Wood. Use of a nuclear high temperature gas reactor in a coal-to-liquids process. Technical Report INL/EXT-06-11667, Idaho National Laboratory, 2006.
- [8] C. B. Davis, R. B. Barner, S. R. Sherman, and D. F. Wilson. Thermal-hydraulic analyses of heat transfer fluid requirements and characteristics for coupling a hydrogen product plant to a high-temperature nuclear reactor. Technical Report INL/EXT-05-00453, Idaho National Laboratory, 2005.
- [9] I. S. Duff, A. M. Erisman, and J. K. Reid. *Direct Methods for Sparse Matrices*. Oxford University Press, 1986.
- [10] R. Elder and R. Allen. Nuclear heat for hydrogen production: Coupling a very high/high temperature reactor to a hydrogen production plant. *Progress in Nuclear Energy*, 51(3):500–525, 2009.
- [11] A. E. Finan and A. C. Kadak. Integration of Nuclear Energy Into Oil Sands Projects. *Journal of Engineering for Gas Turbines and Power-Transactions of the ASME*, 132(4):042902–1–8, 2010.

- [12] C. W. Forsberg. Nuclear energy for a low-carbon-dioxide-emission transportation system with liquid fuels. *Nuclear Technology*, 164(3):348–367, 2008.
- [13] C. W. Forsberg. Sustainability by combining nuclear, fossil, and renewable energy sources. *Progress in nuclear energy*, 51(1):192–200, 2009.
- [14] R. O. Gauntt. *MELCOR Computer Code Manuals, Vol. 1: Primer and Users' Guide Version 1.8.6*. Sandia National Laboratories, 2005.
- [15] C. W. Gear. The automatic integration of ordinary differential equations. *Communications of the ACM*, 14(3):179, 1971.
- [16] A. Griewank and A. Walther. *Evaluating derivatives: principles and techniques of algorithmic differentiation*. Society for Industrial and Applied Mathematics (SIAM), 2nd edition, 2008.
- [17] M. Hanke, K. Henrik, A. Olsson, and M. Strömngren. Stability analysis of a degenerate hyperbolic system modelling a heat exchanger. *Mathematics and Computers in Simulation*, 74(1):8–19, 2007.
- [18] E. A. Harvego, M. G. McKellar, J. E. O'Brien, and J. S. Herring. Parametric evaluation of large-scale high-temperature electrolysis hydrogen production using different advanced nuclear reactor heat sources. *Nuclear Engineering and Design*, 239:1571–1580, Sep 2009.
- [19] E. A. Harvego, M. G. McKellar, M. S. Sohal, J. E. O'Brien, and J. S. Herring. Economic analysis of a nuclear reactor powered high-temperature electrolysis hydrogen production plant. In *ES2008: Proceedings of the 2nd International Conference on Energy Sustainability - 2008*, pages 549–558. Amer. Soc. Mechanical Engineers, 2009.
- [20] A. Hauch, S. D. Ebbesen, S. H. Jensen, and M. Mogensen. Highly efficient high temperature electrolysis. *Journal of Materials Chemistry*, 18(20):2331–2340, May 2008.
- [21] A. F. Henry. *Nuclear Reactor Analysis*. MIT Press, 1975.
- [22] A. C. Kadak. A future for nuclear energy: pebble bed reactors. *Int. J. Critical Infrastructures*, 1(4):330–345, 2005.
- [23] A. C. Kadak. MIT pebble bed reactor projects. *Nuclear Engineering and Technology*, 39:95–102, 2007.
- [24] J. F. Kikstra and A. H. M. Verkooijen. Dynamic Modeling of a Cogenerating Nuclear Gas Turbine Plant - Part I: Modeling and Validation. *Journal of Engineering for Gas Turbines and Power*, 124:725, 2002.
- [25] R. J. Leveque. *Finite Volume Methods for Hyperbolic Problems*. Cambridge University Press, Cambridge, UK, 2002.

- [26] Pebble Bed Modular Reactor Limited. Photo gallery—fuel composition. <http://www.pbmr.co.za/index.asp?Content=213>.
- [27] W. Malalasekera and H. K. Versteeg. *An introduction to computational fluid dynamics*. Longman Scientific & Technical, 1995.
- [28] J. J. Marano and J. P. Ciferno. Life-cycle greenhouse-gas emissions inventory for Fischer-Tropsch fuels. Technical report, Energy and Environmental Solutions, LLC for the U.S. Department of Energy, National Energy Laboratory, 2001.
- [29] W. E. Martinson and P. I. Barton. A differentiation index for partial differential-algebraic equations. *SIAM Journal on Scientific Computing*, 21(6):2295–2315, 2000.
- [30] S. E. Mattsson. On modelling and differential/algebraic systems. *Simulation*, 52(1):24, 1989.
- [31] T. McCann and P. Magee. Crude oil greenhouse gas life cycle analysis helps assign values for CO₂ emissions trading. *Oil & Gas J.*, 97:38–44, Feb. 22 1999.
- [32] M. G. McKellar, J. E. O’Brien, E. A. Harvego, and J. S. Herring. Optimized flow sheet for a reference commercial-scale nuclear-driven high-temperature electrolysis hydrogen production plant. Technical Report INL/EXT-07-13573, Idaho National Laboratory, November 2007.
- [33] Special Metals. Incoloy alloy 800. <http://www.specialmetals.com/products/incoloyalloy800h&ht.php>, May 2010.
- [34] National Energy Board (NEB). Canada’s oil sands: Opportunities and challenges to 2015: An energy market assessment. Technical report, NEB, Calgary, Alta., May 2004.
- [35] Numerica Technology, Cambridge, MA, U.S.A. *JACOBIAN User Guide*, 2006.
- [36] J. O’Brien, C. Stoots, J. S. Herring, and G. L. Hawkes. Hydrogen production from nuclear energy via high temperature electrolysis. Technical Report INL/CON-06-01375, INL, 2006.
- [37] U.S. Department of Energy Research Advisory Committee and the Generation IV International Forum. A technology roadmap for generation IV nuclear energy systems. Technical report, 2002.
- [38] C. H. Oh, E. S. Kim, S. R. Sherman, and R. Vilim. HyPEP FY-07 Report: System Integration Model Development. Technical Report INL/EXT-07-12470, Idaho National Laboratory, 2007.
- [39] S. V. Patankar. *Numerical heat transfer and fluid flow*. Taylor & Francis, 1980.
- [40] A. Pothen and C. J. Fan. Computing the block triangular form of a sparse matrix. *ACM Trans. Math. Software*, 16(4):303–324, 1990.

- [41] Process System Enterprise Ltd. *gPROMS Introductory User Guide*, 2004.
- [42] M. Richards, A. Shenoy, K. Schultz, L. Brown, E. Harvego, M. McKellar, J. P. Coupey, S. M. M. Reza, F. Okamoto, and N. Handa. H₂-MHR conceptual designs based on the sulphur-iodine process and high-temperature electrolysis. *International Journal of Nuclear Hydrogen Production and Applications*, 1(1):36–50, 2006.
- [43] S. B. Rodriguez, R. O. Gauntt, R. Cole, F. Gelbard, K. Mcfadden, T. Drennen, B. Martin, D. Louie, L. Archuleta, M. El-Genk, J. Tournier, F. Espinoza, S.T. Revankar, and K. Vierow. Transient analysis of Sulfur-Iodine cycle experiments and very high temperature reactor simulations using MELCOR-H₂. *Nuclear Technology*, 166(1):76–85, Apr 2009.
- [44] D. K. Ryland, H. Li, and R. R. Sadhankar. Electrolytic hydrogen generation using CANDU nuclear reactors. *International Journal of Energy Research*, 31(12):1142–1155, 2007.
- [45] D. Saphier. HTGR Transient Analysis with the DSNP Simulation Language. Technical Report RASG-111-84, Soreq Nuclear Research Center, Israel, December 1984.
- [46] M.G. Savage. A one-dimensional modeling of radial heat removal during depressurized heatup transients in modular pebble-bed and prismatic high temperature gas-cooled reactors. Technical Report ORNL/TM-9215, Oak Ridge National Laboratory, July 1984.
- [47] W. E. Schiesser. *The numerical method of lines: integration of partial differential equations*. Academic Press San Diego, 1991.
- [48] M. Schipper. Energy-related carbon dioxide emissions in U. S. manufacturing. Technical Report DOE/EIA-0573, Energy Information Administration, 2006.
- [49] D. Sedes. Modelling, simulation and process safety analysis. A case study: The formaldehyde process. Technical report, Massachusetts Institute of Technology, 1994.
- [50] P. L. Spath and M. K. Mann. Life cycle assessment of hydrogen production via natural gas steam reforming. Technical report, National Renewable Energy Laboratory, 2001.
- [51] C. Stoots, J. O’Brien, S. Herring, K. Condie, L. Moore-McAteer, J. J. Hartvigsen, and D. Larsen. High Temperature Solid-Oxide Electrolyzer 2500 Hour Test Results At The Idaho National Laboratory. In *2009 AIChE Annual Meeting, Conference Proceedings*. INL/CON-09-16888, Idaho National Laboratory (INL), 2009.
- [52] The RELAP5-3D Code Development Team. *RELAP-3D Code Manual*. Idaho National Laboratory, Idaho Falls, Idaho, U.S.A., 2005.

- [53] Aspen Tech. *Aspen Custom Modeler User Manuals*, 2005.
- [54] J. E. Tolsma and P. I. Barton. On computational differentiation. *Computers & Chemical Engineering*, 22(4/5):475–490, 1998.
- [55] U.S. Environmental Protection Agency, Office of Air and Radiation. Technical support document for hydrogen production: Proposed rule for mandatory reporting of greenhouse gases. Technical report, 2008.
- [56] U.S. Nuclear Regulatory Commission, Washington, DC 20555-0001. *Nuclear Power Plant Licensing Process*, nureg/br-0298, rev. 2 edition, July 2004.
- [57] K. Vierow, Y. Liao, J. Johnson, M. Kenton, and R. Gauntt. Severe accident analysis of a PWR station blackout with the MELCOR, MAAP4 and SCDAP/RELAP5 codes. *Nuclear Engineering and Design*, 234(1-3):129–145, 2004.
- [58] R. B. Vilim. Dynamic modeling efforts for system interface studies. Technical Report ANL-07/16, Argonne National Laboratory, December 2006.
- [59] R. B. Vilim. Initial Assessment of the Operability of the VHTR-HTSE Nuclear-Hydrogen Plant. Technical Report ANL-08/01, Nuclear Engineering Division, Argonne National Laboratory, September 2007.
- [60] C. Wang. *Design, Analysis and Optimization of the Power Conversion System for the Modular Pebble Bed Reactor Systems*. Ph.D. Thesis, Massachusetts Institute of Technology, 2003.
- [61] M. Wang, M. Wu, and H. Huo. Life-cycle energy and greenhouse gas emission impacts of different corn ethanol plant types. *Environmental Research Letters*, 2:024001, 2007.
- [62] M. Q. Wang. Estimation of energy efficiencies of U. S. petroleum refineries. Technical report, Argonne National Laboratory, Argonne, IL, 2008.
- [63] B. Yildiz and M. S. Kazimi. Efficiency of hydrogen production systems using alternative nuclear energy technologies. *International Journal of Hydrogen Energy*, 31:77–92, 2006.
- [64] B. Yildiz, M. C. Petri, G. Conzelmann, and C. W. Forsberg. Configuration and technology implications of potential nuclear hydrogen system applications. Technical Report ANL-05/30, Argonne National Laboratory, 2005.
- [65] Z. Zhang, Z. Wu, D. Wang, Y. Xu, Y. Sun, F. Li, and Y. Dong. Current status and technical description of Chinese 2 x 250 MWth HTR-PM demonstration plant. *Nuclear Engineering and Design*, 239(7):1212–1219, Jul 2009.